

Personalisation of dexamethasone in childhood acute lymphoblastic leukaemia

Rosanna Katharine Jackson

Thesis submitted in part requirement for the degree of Doctor of Philosophy (PhD)

September 2017

Northern Institute for Cancer Research

Faculty of Medical Sciences

Newcastle University

Newcastle upon Tyne

September 2017



Abstract

Dexamethasone (dex) is a key treatment for childhood acute lymphoblastic leukaemia (ALL), but is associated with significant variability in terms of toxicity and efficacy. In this project, the following variables were assessed to better understand how dex personalisation may be achieved: pharmacokinetics, intracellular dex accumulation, glucocorticoid receptor (GR) posttranslational modifications and B-cell maturation state.

For pharmacokinetic studies, samples were collected from 154 patients randomised to short (10mg/m² x 14 days) or standard (6mg/m² x 28 days) dex induction therapy, as part of the UKALL 2011 trial, and analysed using a validated LC/MS method. Wide pharmacokinetic variability was observed, with AUC_{0-12h} and C_{max} significantly higher on the short compared to standard arm. However there was substantial overlap between the two arms, with a number of patients on the standard arm exhibiting higher exposures than those on short therapy. The UKALL 2011 trial found no statistical difference in terms of steroid-related toxicity or MRD response between short and standard dosing. These data suggest that the considerable dex pharmacokinetic variation identified may be a more important factor than variation in dosing regimen.

For cellular pharmacology experiments, cell lines, primagraft and primary patient samples were studied. Dex sensitivity was assessed using Alamar Blue assays and GI₅₀ values ranged from 2-1000nM. Western blotting indicated wildtype GR in all samples. Dex accumulation was assessed by LC/MS and flow cytometric analysis of dex-FITC. While patient samples exhibited large variability, dex accumulation was not significantly different between sensitive and resistant cells. Differential dex sensitivity was not accounted for by differences in GR posttranslational modifications, assessed using capillary isoelectric focusing. However, assessment of B-cell maturation using mass cytometry revealed a relationship with dex resistance. Importantly, >50% of patient cell samples had dex GI₅₀ values greater than plasma concentrations observed on either arm of the UKALL 2011 trial. A combined approach incorporating pharmacokinetic assessments and cellular response in ALL cells may allow a more comprehensive understanding of dex pharmacology to optimise its clinical utility.

Acknowledgements

Firstly, I would like to thank my supervisors, Dr. Gareth Veal and Prof. Julie Irving for all their help and guidance over the last four years. I feel very lucky to have had such supportive supervisors, who helped me gain confidence in my ability and scientific skills during my time in the NICR. I am also extremely privileged to have been part of two such kind and friendly lab groups, who have made my PhD so enjoyable. There are too many people to name in person, but particular thanks need to go to Phil Berry for all his help and enthusiasm with LC/MS problems, QlikSense, and chromatography, and to Julie Errington for showing me the ropes with the GCLP, and sitting through hours of data verification with me. Thanks to Liz Matheson for teaching me all my tissue culture and western blotting, it was a privilege to learn from the Queen of westerns herself! Thanks also to Marian, Lynne, Zach, and Ali for all their help with my many, many, questions.

Thanks to Tony Whetton for hosting me at the Wolfson Molecular Imaging Centre, Manchester University, and Rognvald Blance for all his help in taming Peggy Sue. I am also very grateful to the Newcastle Flow Cytometry Core Facility, particularly Dr. Rachel Queen and Dr. David MacDonald, for all their time, help and advice with Wanderlust. Thanks to my progression panel, Prof. Christine Harrison and Prof. Ann Daly for their guidance over the course of this project.

My time in the NICR has been full of fun and experiences which I will never forget. Mostly, these revolve around cake, an essential part of any PhD. From Friday cakes with the LLR group, to the numerous cake sales to raise money for the National AND Yorkshire Three Peak Challenges, and not forgetting *finally* winning the CRUK bake off. Thanks to the core five, team CyTOF, and L.A.R.S. for all the laughs and also being so enthusiastic about nautical Tuesdays. A huge thanks to Rich and my family and friends for encouraging me when I doubted myself and for their continued support over the years. It has helped immensely.

I am extremely grateful to Cancer Research UK, for funding my project, and to Children with Cancer UK, the ECMC and NECCR for the funds they provided. Thank you to the patients and their families for providing the samples, which are essential for ongoing scientific progress in fighting ALL and improving the lives of future children with ALL.

Statement of work undertaken

Data generated as part of the UKALL 2011 dex sub-study was verified with help from Julie Errington.

All primagrafts used in Chapters 4-6 were created and tracked by Ali Alhammer, Zach Dixon, Marian Case, and Liz Matheson.

Some of the data used to generate Table 4.2 and Figure 4.11 was submitted as part of my Masters by Research degree (Newcastle University, 2014).

The vincristine data from Figure 4.6 - Figure 4.9 was generated by Charlotte Lecour, a pharmacy student from Toulouse University who did a summer project at the Northern Institute for Cancer Research.

GR posttranslational modification work was carried out at the Wolfson Molecular Imaging Centre at Manchester University, with the support of Prof. Tony Whetton, Dr. Andrew Pierce and Rognvald Blance. Rognvald helped set up the assay on the Peggy Sue capillary isoelectric focusing machine and generated the data used to make Figure 5.4B.

Support for the Mass cytometry experiments in Chapter 6 was provided by the Flow Cytometry Core Facility at Newcastle University, in particular, Dr. Andrew Filby, Dr. David McDonald and Dr. Andrew Fuller. Bioinformatic analyses for this project were performed by Dr. Rachel Queen.

All other work and data analysis were performed by myself.

Table of contents

Abstract	iii
Acknowledgements	v
Statement of work undertaken	vii
Table of contents	ix
List of figures	xiv
List of tables	xx
List of abbreviations	xxii
Chapter 1. Introduction	1
1.1 Cancer	3
1.1.1 Paediatric cancer.....	3
1.2 Acute lymphoblastic leukaemia	3
1.2.1 Aetiology	4
1.2.2 Epidemiology.....	5
1.2.3 Classification	5
1.2.4 Prognosis	11
1.3 Therapy	11
1.3.1 UKALL group trial history	12
1.3.2 Therapy today – UKALL 2011 trial.....	15
1.4 Dexamethasone	18
1.4.1 The glucocorticoids	18
1.4.2 Glucocorticoid mechanism of action in ALL.....	18
1.4.3 Choice of glucocorticoid.....	19
1.4.4 Optimisation of dex.....	20
1.5 Dex pharmacokinetics	21
1.5.1 Source of pharmacokinetic variation	22
1.6 Dex pharmacogenetics	23
1.6.1 The Glucocorticoid Receptor	24
1.6.2 Cytochromes P450 (CYP450).....	24
1.6.3 MDR1.....	25

1.6.4	Glutathione S-transferases	26
1.6.5	BCL2 family.....	27
1.6.6	Genes associated with asparaginase and steroid toxicity	27
1.7	Dex at the level of the cell.....	30
1.8	Mechanisms of dex resistance.....	30
1.8.1	The glucocorticoid receptor.....	32
1.8.2	Post-GR mechanisms of resistance.....	32
1.8.3	Pre-GR mechanisms of resistance	33
1.8.4	The GR interactome	33
1.8.5	Intracellular dex accumulation	34
1.8.6	B cell developmental stage	35
1.9	Models of ALL	35
1.9.1	Cell lines	36
1.9.2	Patient and primagraft models	36
1.10	Project summary.....	37
1.11	Aims and Objectives.....	38
Chapter 2.	Materials and methods.....	39
2.1	UKALL 2011 trial.....	41
2.1.1	UKALL 2011 study details.....	41
2.1.2	Patients and treatment regimen	41
2.1.3	Sample collection	42
2.1.4	Bioanalytical method validation	42
2.1.5	Reverse phase liquid chromatography and tandem mass spectrometry (LC/MS).....	43
2.1.6	Pharmacokinetic analysis.....	45
2.1.7	Determination of plasma dex concentrations – extraction method.....	46
2.1.8	Measurement of dex concentrations in cerebrospinal fluid (CSF)	48
2.2	Cell Culture	49
2.2.1	Tissue culture reagents and equipment	49
2.2.2	Cell culture media	49
2.2.3	Cell lines	50
2.2.4	Primary derived xenograft (primagraft) samples	51
2.2.5	Patient samples.....	55

2.2.6 Cell line maintenance and culture	58
2.3 Drug sensitivity assessment using Alamar Blue	59
2.4 Intracellular accumulation of dex measured by LC/MS.....	60
2.4.1 Optimisation of LC/MS assay for small cell numbers	62
2.5 Intracellular accumulation measured by fluorescence activated cell sorting (FACS).....	62
2.5.1 FACSCalibur calibration	63
2.5.2 Method development	64
2.5.3 Final flow cytometry method.....	64
2.6 Capillary-based isoelectric focusing immunoassays	65
2.6.1 Cell lysis	65
2.6.2 Protein concentration determination.....	66
2.6.3 Western blotting	67
2.6.4 Western blotting under non denaturing conditions.....	71
2.6.5 ProteinSimple Peggy Sue analysis of the GR posttranslational modifications	71
2.7 Mass cytometry.....	75
2.7.1 Mass cytometry panel.....	77
2.7.2 Metal labelling with antibodies	80
2.7.3 Cell staining with antibodies	83
2.7.4 Wanderlust algorithm	87
2.8 Statistical analysis	89
Chapter 3. Pharmacokinetics of dexamethasone in acute lymphoblastic leukaemia	91
3.1 Introduction	93
3.2 Chapter specific aims.....	95
3.3 Results	96
3.3.1 Patient characteristics.....	96
3.3.2 Dex pharmacokinetics.....	98
3.3.3 Interpatient pharmacokinetic variability	99
3.3.4 Inpatient variability and asparaginase effect.....	111
3.3.5 Covariate analysis: pharmacokinetics and patient characteristics.....	120
3.3.6 Covariate analysis: pharmacokinetics and concomitant medication	123
3.3.7 Relationship between dex pharmacokinetics and toxicity	129

3.3.8 The effect of variable dex pharmacokinetics on outcome	136
3.3.9 Cerebrospinal fluid pharmacokinetics	138
3.4 Discussion.....	143
Chapter 4. Intracellular dexamethasone accumulation	151
4.1 Introduction.....	153
4.2 Chapter specific aims	154
4.3 Results.....	155
4.3.1 Method validation.....	155
4.3.2 Assessment of MDR1 dex transporter status	162
4.3.3 Dex sensitivity in cell lines	168
4.3.4 Intracellular accumulation of dex in cell lines	170
4.3.5 Viability of cryopreserved cells	172
4.3.6 Dex sensitivity of primagraft and patient samples.	174
4.3.7 Dex accumulation in primagraft and patient samples.....	183
4.4 Discussion.....	193
Chapter 5. GR post translational modifications and GC sensitivity	199
5.1 Introduction.....	201
5.2 Chapter specific aims	202
5.3 Results.....	203
5.3.1 Assessment of GR by western blot	203
5.3.2 Peggy Sue Antibody selection	205
5.3.3 Antibody Validation	210
5.3.4 Analysis of the GR by cIEF in ALL cell lines.....	217
5.3.5 Analysis of the GR by cIEF in primagraft ALL cells	220
5.3.6 Investigation into reduced signal in untreated samples	226
5.4 Discussion.....	228
Chapter 6. B cell maturation and GC sensitivity.....	237
6.1 Introduction.....	239
6.2 Chapter specific aims:	241
6.3 Results.....	242
6.3.1 Gating strategy.....	242
6.3.2 Panel design	243
6.3.3 Validation of antibody-metal conjugation.....	243
6.3.4 Antibody panel validation	247

6.3.5 Remission bone marrow samples	251
6.3.6 Cell Lines.....	257
6.3.7 Primagraft samples	259
6.3.8 Patient samples.....	262
6.3.9 Total event number acquired on the Helios mass cytometer	263
6.3.10 Pre Wanderlust analysis.....	264
6.3.11 Selection of Wanderlust start cell.....	268
6.3.12 Wanderlust.....	271
6.3.13 Post Wanderlust analysis	277
6.4 Discussion	279
Chapter 7. General discussion.....	285
Bibliography	297
Appendices.....	329

List of figures

Figure 1.1 Lymphoid cell development. ALL can arise in Pre-B, Mature B, or T cells.....	4
Figure 1.2 Frequencies of ALL cytogenetic subtypes, adapted from (Inaba <i>et al.</i> , 2013).	7
Figure 1.3 Outcome of patients with acute lymphoblastic leukemia (ALL) by genetic risk group.....	8
Figure 1.4 Chemical structures of glucocorticoids: cortisol, prednisolone, prednisone and dex.....	18
Figure 1.5 Schematic of possible dex resistance mechanisms.	31
Figure 1.6 Project summary.	37
Figure 2.1 Sampling days for the dex pharmacokinetic study.....	42
Figure 2.2 Schematic illustrating tandem mass spectrometry.	44
Figure 2.3 Example layout of ProteinSimple plate.....	73
Figure 2.4 Schematic of mass cytometry taken from (Bendall <i>et al.</i> , 2012).....	76
Figure 2.5 Wanderlust developmental trajectory method, adapted from Bendall <i>et al.</i> (2014).	88
Figure 3.1 Variation in dex plasma concentration-time profiles observed in patients on both short therapy (10mg/m ² x 14 days, blue) and standard therapy (6mg/m ² x 28 days, red).....	101
Figure 3.2 Variation in dex plasma concentration-time profiles observed in patients on (A and B) short therapy (10mg/m ² x 14 days, blue) and (C and D) standard therapy (6mg/m ² x 28 days, red). Patients are separated into NCI standard risk (A and C) and standard risk (B and D).....	105
Figure 3.3 Interpatient variation in dex pharmacokinetic parameters obtained at the beginning of treatment.....	107
Figure 3.4 Variation in plasma dex area under the curve in patients on both short therapy and standard therapy, calculated following a single drug exposure (A), adjusted to exposure per 1mg/m ² (B) and when extrapolated to total induction therapy exposure (C).....	108
Figure 3.5: Dex concentration time profiles for patients with extreme dex pharmacokinetics.....	110
Figure 3.6 Inpatient variation in pharmacokinetic profiles and albumin concentrations between the beginning and end of induction chemotherapy.	113
Figure 3.7 Correlation between dex clearance and albumin concentrations pre- and post-asparaginase therapy.....	114

Figure 3.8 Asparaginase trough levels in patients on the dex pharmacokinetic sub-study at day 16 and day 30.	116
Figure 3.9 Correlation between trough asparaginase levels, and albumin and dex clearance.	117
Figure 3.10 Inpatient variation in dex pharmacokinetic parameters and albumin levels in patients receiving one or two doses of asparaginase between dex sampling days.	119
Figure 3.11 Effect of treatment regimen on dex AUC _{0-12h} and clearance.....	121
Figure 3.12 Relationship between patient characteristics and dex clearance at the beginning and end of induction therapy.	122
Figure 3.13 Relationship between concomitant medication administration and dex pharmacokinetic parameters at the beginning (A) and end (B) of induction therapy.	128
Figure 3.14 Relationship between incidence of grade 3-4 toxicity and patient age and surface area.....	132
Figure 3.15 Relationship between incidence of grade 3-4 toxicity and dex pharmacokinetic parameters.....	133
Figure 3.16 Relationship between incidence of grade 3-4 toxicity and treatment regimen.	134
Figure 3.17 Association between dex exposure and outcome, defined by MRD.....	137
Figure 3.18 Typical chromatograms for 100ng/ml dex and beclomethasone in spiked water, mobile phase and artificial CSF.....	139
Figure 3.19 Initial quantification of dex in CSF samples from children with ALL.....	140
Figure 3.20 CSF dex concentrations in day 8 patient samples on the UKALL 2011 trial.	142
Figure 4.1 Example LC/MS chromatograms showing the minimum number of cells needed to obtain a quantifiable dex peak after incubation with 500nM dex.....	156
Figure 4.2 Mean fluorescence intensity of dex-FITC after incubation periods of 5 – 60 minutes.	158
Figure 4.3 Mean fluorescence intensity of PreB697 cells, R3D11 and REH cells after 45minutes of incubation with dex-FITC.	159
Figure 4.4 Effect of the number of washes on dex FITC fluorescence.	160
Figure 4.5 Example flow cytometry dot plots showing different clustering of cells when incubated with dex-FITC at 4°C and 37°C.	161

Figure 4.6 Sensitivity of CCRF CEM and CEM VCR cells to dex (A) and vincristine (B) generated using alamar blue.	163
Figure 4.7 Accumulation of dex (A) and vincristine (B) in CCRF CEM and CEM VCR cells.	164
Figure 4.8 Sensitivities of MDCKII-WT and MDCKII-MDR1 cell lines to vincristine (A) and act D (B).	166
Figure 4.9 Accumulation of dex (A) act D (B) and vincristine (C) in MDCKII-WT and MDCKII-MDR1 cells.	167
Figure 4.10 Sensitivity of PreB697 cell lines and REH to dex <i>in vitro</i> with Alamar Blue after a 96h incubation with 0.1-1000nM dex.	169
Figure 4.11 Intracellular dex accumulation in PreB697 and selected dex resistant sub lines.	171
Figure 4.12: <i>In vitro</i> dex sensitivity of L779 primagraft samples pre- and post-cryopreservation, measured using Alamar blue.	172
Figure 4.13 Intracellular dex accumulation in L779 primagraft samples pre- and post-cryopreservation.	173
Figure 4.14 Dex sensitivity of primagraft samples.	178
Figure 4.15 Dex sensitivity of primary samples.	180
Figure 4.16. Intracellular accumulation of dex in primagraft cells assessed using LC/MS.	185
Figure 4.17 Dex accumulation in primary patient samples after incubation with 500nM dex.	186
Figure 4.18 Comparison of dex accumulation measured by LC/MS between patient cells and cell lines.	186
Figure 4.19 Intracellular dex accumulation measured by LC/MS in dex sensitive and dex resistant cells after incubation with 500nM dex.	187
Figure 4.20 Intracellular accumulation of dex-FITC in primagraft samples (A) and primary patient samples (B) measured by flow cytometry.	189
Figure 4.21 Comparison of dex accumulation measured by flow cytometry between patient cells and cell lines.	191
Figure 4.22 Intracellular dex-FITC accumulation measured by flow cytometry in dex sensitive and dex resistant cells after incubation with 500nM dex-FITC.	191
Figure 4.23 Correlation of LC/MS and flow cytometry methods for the assessment of intracellular dex concentrations in ALL cell lysates.	192

Figure 5.1 Example western blots of lysates probed for GR and phosphorylated GR (s211).....	204
Figure 5.2 Comparison of Santa Cruz NR3C1 antibody (E-20, left) with Sigma NR3C1 antibody (HPA004248, middle) on the Peggy Sue and Sigma NR3C1 (HPA004248, right) on the NanoPro1000.....	206
Figure 5.3 GR analysis using Santa Cruz E-20 antibody by cIEF and western blot.....	207
Figure 5.4 Testing of GR antibodies by western blot and cIEF.	209
Figure 5.5 Peggy Sue lysate freeze thaw stability.....	210
Figure 5.6 Peggy Sue D8H2 (Cell Signalling) antibody titration in PreB697 dex treated lysates.....	212
Figure 5.7 Peggy Sue lysate titration in PreB697 dex treated lysates probed with D8H2 (Cell Signalling) GR antibody.	214
Figure 5.8 Variation between technical and biological replicates.....	216
Figure 5.9 Electropherograms generated by cIEF of PreB697, R3F9, R3D11 and REH cell lines with D8H2 (Cell Signalling) GR antibody.....	218
Figure 5.10 Proportion of total electropherogram area under the curve comprised of individual electropherogram peaks for PreB697, R3F9 and R3D11 cell lines.....	219
Figure 5.11 Electropherograms of primagraft lysates by cIEF probed with D8H2 (Cell Signalling) GR antibody.	221
Figure 5.12 Electropherogram peak areas displayed relative to the total area under the curve of the GR profile for control vehicle and dex treated primagraft samples.	223
Figure 5.13 Comparison of peak composition of GR profiles between sensitive and resistant primagraft samples.	225
Figure 5.14 Analysis of GR lysates by western blot under non-denaturing conditions.	227
Figure 5.15 NR3C1 alpha amino function domain.	230
Figure 5.16 Position of NR3C1 post translational modifications.	231
Figure 6.1 Gating strategy for all samples to isolate live, single cells in all cell lines, primagraft and patient samples.....	242
Figure 6.2 Antibody conjugation validation with BD beads.....	244
Figure 6.3 Titration of conjugated antibodies CD34 and IgH and staining index values.	246
Figure 6.4 Full Wanderlust antibody panel with PreB697 cells.	249

Figure 6.5 Contour plots indicating potential spill over from 167Er into 166Er, and 169Er into 168Er.	250
Figure 6.6 Mass Minus Many experiment to determine spillover.	250
Figure 6.7 Gating strategy to isolate different B cell populations in remission bone marrow samples using mass cytometry.	252
Figure 6.8 Comparison of Wanderlust antibody panel data generated by mass cytometry to historical flow cytometry data; CD34 positive cells.....	253
Figure 6.9 Comparison of Wanderlust antibody panel data generated by mass cytometry to historical flow cytometry data; CD34 negative cells.....	254
Figure 6.10 Comparison of data generated using the metal-altered Wanderlust panel across B cells of different maturation stages to that published in Bendall <i>et al.</i> (2014).	256
Figure 6.11 Histograms of T-ALL patient samples stained with the Wanderlust Panel.	257
Figure 6.12 Histograms of Wanderlust markers for PreB697 and GC resistant sub lines.	258
Figure 6.13 Histograms of primagraft samples, stained with the Wanderlust panel, derived from the same patient.	260
Figure 6.14 Histograms of primagraft samples from L919 first relapse and second relapse, stained with the Wanderlust panel, show differences in key markers.	261
Figure 6.15 Histograms of patient samples stained with the Wanderlust panel.	262
Figure 6.16 Number of events in each sample after gating.	263
Figure 6.17 Heat map showing expression of all the Wanderlust markers.....	264
Figure 6.18 MDS plot of all of all cell samples colour coded by date (A) and primagraft samples (B).	266
Figure 6.19 MDS plot displaying all samples after removal of cell lines acquired on the 24 th May.	267
Figure 6.20 Start cell selection, adapted from Bendall <i>et al.</i> (2014) (A) and trajectories created in this project (B).	270
Figure 6.21 Wanderlust trajectories resulting from four individual remission bone marrow samples.....	272
Figure 6.22 Summary of Wanderlust marker expression throughout B cell development as ordered by the Wanderlust trajectory.	274
Figure 6.23 Cluster dendrogram of primagraft samples.	275

Figure 6.24 Wanderlust trajectories created after the addition of all ALL samples (A),
dex sensitive ALL samples (B) and dex resistant ALL samples (C).....276

Figure 6.25 Density plot showing the normalised maturation of cells in remission,
resistant, and sensitive cells.278

Figure 6.26 Average Wanderlust maturation value of cells in each patient sample....278

List of tables

Table 1.1 Outcomes of contemporary trials involving children and adolescents with ALL in North America and Western Europe.	14
Table 1.2 Drugs administered to ALL patients in the different phases of the UKALL 2011 trial.	16
Table 1.3 Genetic variation associated with adverse outcome with asparaginase therapy and risk of steroid induced osteonecrosis.....	29
Table 2.1 Gradient profile of mobile phases for the two chromatography methods used.....	45
Table 2.2 Details of primagraft samples.	54
Table 2.3 Details of patient samples.....	57
Table 2.4 LC/MS details for intracellular accumulation experiments.	61
Table 2.5: Antibodies and probing conditions.	70
Table 2.6 Peggy Sue machine settings for glucocorticoid receptor analysis.	74
Table 2.7 Panel of antibodies used in mass cytometry experiment to imitate Wanderlust panel.....	79
Table 2.8 Fluidigm antibody preparation guide.....	84
Table 3.1 Characteristics of patients sampled at the beginning of treatment time point, end of treatment time point, and patients studied on both sampling days.	98
Table 3.2 Comparison of pharmacokinetic parameters between short (10mg/m ²) and standard (6mg/m ²) groups after a single dose of dex.	106
Table 3.3 Pharmacokinetic parameters in patients with extreme profiles after a single dose of 5mg/m ² (841, 1259, 1453) or 3mg/m ² (567, 808).....	109
Table 3.4 Relationship between concomitant drug administration and dex pharmacokinetic parameters.....	127
Table 3.5 Grade 3-4 toxicities experienced during induction phase in patients on the dex pharmacokinetic sub-study of the UKALL 2011 trial.....	131
Table 3.6 Steroid specific adverse events in patients on the UKALL 2011 dex pharmacokinetic sub-study and their relationship with dex pharmacokinetic parameters.....	135
Table 4.1 Lowest number of PreB697 cells that gave a quantifiable dex peak, on three separate days.	157
Table 4.2 Cell line sensitivity to dex assessed using Alamar Blue assay.	170

Table 4.3 Primagraft and patient sample dex sensitivity status.....	182
Table 5.1 Identification of samples in outlier groups shown in Figure 5.12.....	224

List of abbreviations

11-BOHSD	11 β -hydroxysteroid dehydrogenase enzymes
AEIOP	Italian Association of Pediatric Hematology and Oncology
ALL	Acute lymphoblastic leukaemia
AUC	Area under the curve
ANOVA	Analysis of variance
BCA	Bicinchoninic acid
BCP-ALL	B cell precursor acute lymphoblastic leukaemia
BCRP	Breast cancer resistant protein
BFM	Berlin-Frankfurt- Münster
CCG	Children's Cancer Group
CD	Cluster of differentiation
cIEF	Capillary isoelectric focussing
C _{max}	Maximum drug concentration
COG	Children's Oncology Group
CSF	Cerebrospinal fluid
CNS	Central nervous system
CRF	Case report form
CV	Control vehicle
CYP450	Cytochrome P450
CyTOF	Cytometry by Time of Flight
DCOG	Dutch Childhood Oncology Group
Dex	Dexamethasone
DCFI	Dana-Faber Cancer Institute
DI	Delayed intensification
DNA	Deoxyribonucleic acid
EFS	Event free survival
EMA	European Medicines Agency
EORTC CLG	European Organization for Research and Treatment of Cancer- Children's Leukemia Group
FACS	Fluorescence activated cell sorting
FISH	Fluorescence in situ hybridisation
FITC	Fluorescein isothiocyanate
GC	Glucocorticoid
GI ₅₀	Concentration required to cause growth inhibition in 50% of cells
GR	Glucocorticoid receptor
GRE	Glucocorticoid receptor element

GSH	Glutathione
GST	Glutathione s-transferase
HR	High risk
HRP	Horseradish peroxidase
HSP	Heat shock protein
iAMP21	Intrachromosomal amplification of chromosome 21
ICP-MS	Inductively coupled plasma mass spectrometry
IS	Internal standard
LC/MS	Tandem liquid chromatography - mass spectrometry
LD	Linkage disequilibrium
LDL-C	Low density lipoprotein C
LOD	Limit of detection
LOQ	Limit of quantitation
MDR	Multi drug resistance
MFI	Mean fluorescence intensity
MLL	Mixed lineage leukaemia gene
MLPA	Multiplex ligation-probe amplification
MMI	Mean mass intensity
MMM	Mass minus many
MMR	Mismatch repair
MP	Mobile phase
MRC	Medical research council
MRD	Minimal residual disease
MRP	Multidrug resistance-associated protein
MTT	3-(4,5-dimethylthiazol-2-yl)-2,5-diphenyltetrazolium
m/z	Mass to charge ratio
N/A	Not applicable
NCI	National Cancer Institute
NCRI	National Cancer Research Institute
NICR	Northern Institute for Cancer Research
NOPHO	Nordic Society of Paediatric Haematology and Oncology
NR112	Nuclear receptor subfamily 1 group I member 2
OS	Overall survival
PBS	Phosphate buffered saline
PVDF	Polyvinylidene fluoride
PXR	Pregnane X Receptor
QC	Quality control

QoL	Quality of life
R1	Randomisation 1
rcf	Relative centrifugal force
SAE	Serious adverse event
SD	Standard deviation
SDS	Sodium dodecyl sulphate
SEM	Standard error of the mean
SBP	Steroid binding protein
SJCRH	St. Jude Children's Research Hospital
T_{1/2}	Half life
T-ALL	T cell precursor acute lymphoblastic leukaemia
TDM	Therapeutic dose monitoring
T_{max}	Time to maximum drug concentration
TPMT	Thiopurine methyltransferase
TRM	Treatment related mortality
TTR	Time to relapse
TBS-T	Tris buffered saline with Tween 20
TOF	Time of flight
UKALL	United Kingdom National Randomised Trial for Children and Young Adults with Acute Lymphoblastic Leukaemia and Lymphoma
v/v	Volume per volume
WCC	White blood cell count
WT	Wild type
w/v	Weight per volume
w/w	Weight per weight

Chapter 1. Introduction

1.1 Cancer

The development of cancer is caused by dysregulated cell function resulting in sustained cell proliferation. The hallmarks of cancer were first published in 2000 by Hanahan and Weinberg (2000) and illustrate how normal, healthy cells are able to evolve into a malignant state. They include sustained proliferative signalling, evading growth suppressors, resisting cell death, inducing angiogenesis, enabling replicative immortality and activating invasion and metastasis. More recently, these hallmarks have been updated to also include two 'emerging hallmarks' and two 'enabling characteristics' (Hanahan and Weinberg, 2011).

In the UK, there are over 350,000 new cases of cancer every year, of which half are diagnosed in the over 70s. These cancers are primarily a result of lifestyle factors and environmental exposures that accumulate throughout life.

1.1.1 Paediatric cancer

Paediatric cancer accounts for less than 1% of all cancer cases. However, it still accounts for a significant proportion of non-accidental childhood deaths. Paediatric cancers are predominantly different in origin to adult cancers, with poorly defined risk factors. This is because there are considerably fewer cases than in adults and cancer type is more diverse. However paediatric cancer is, in general, more chemosensitive than adult cancer (Burke *et al.*, 1999).

With around 400 new cases per year in the UK, acute lymphoblastic leukaemia (ALL) is the most common cancer of childhood, accounting for approximately a quarter of all childhood cancers and 78% of childhood leukaemia (Cancer Research UK; Pui *et al.*, 2008).

1.2 Acute lymphoblastic leukaemia

Over the past few decades, therapy and prognosis in ALL have improved dramatically, and a once fatal disease is now curable in the majority of cases. This has been possible due to many years of multifaceted research which has led to the development of a clearer understanding of the disease.

1.2.1 Aetiology

ALL results from the abnormal expansion of lymphoid progenitor cells. Clonal rearrangements in T-cell receptor or immunoglobulin genes, or expression of cell surface glycoproteins and differentiation-linked molecules, alter the cell's ability for self-renewal, differentiation, and response to growth and death signals (Pui *et al.*, 2004; Armstrong and Look, 2005; Pui *et al.*, 2008). This is illustrated in Figure 1.1.

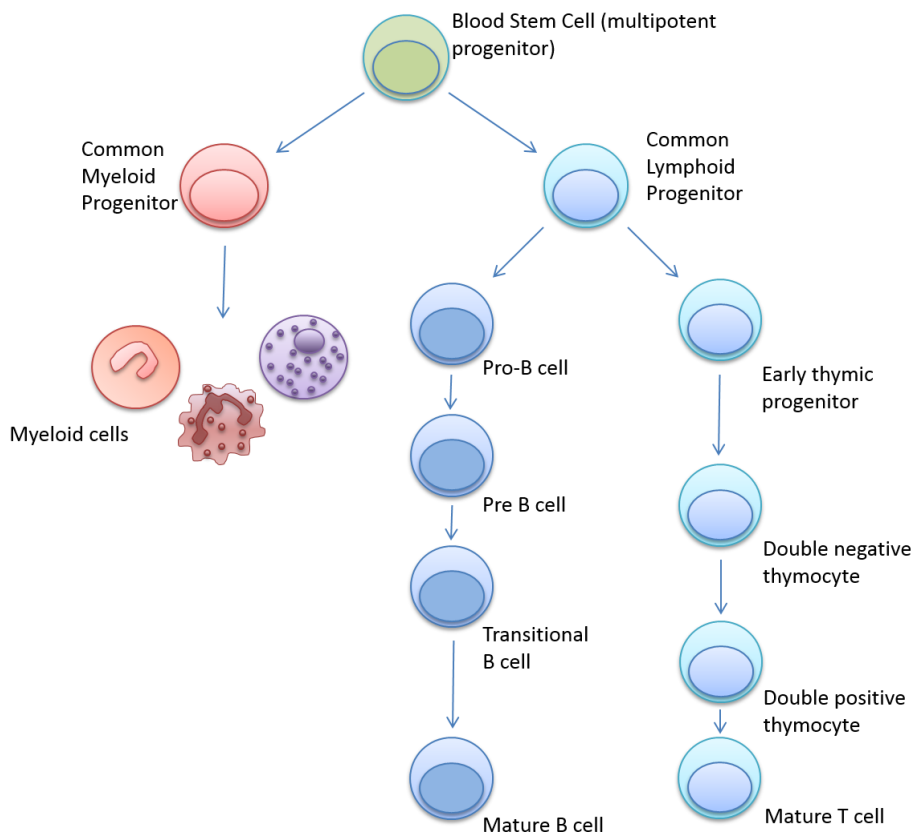


Figure 1.1 Lymphoid cell development. ALL can arise in Pre-B, Mature B, or T cells.

In the vast majority of ALL cases, a genetic change can be identified (Pui *et al.*, 2011). Such changes include structural and numerical chromosomal changes, gene mutation and amplification at the molecular level, and loss of heterozygosity (Pui *et al.*, 2004; Pui *et al.*, 2008; Inaba *et al.*, 2013). These genetic changes affect various pathways in the cell, for example the activation of tyrosine kinases or formation of chimeric transcription factors. These aberrations are also used to subdivide ALL into a number of groups, which have different prognoses (Inaba *et al.*, 2013; Moorman *et al.*, 2014). These will be further discussed in 1.2.3.

1.2.2 Epidemiology

The cause of ALL is largely unexplained. While a small proportion can be attributed to inherited conditions such as Down's syndrome (Hasle *et al.*, 2000; Pui *et al.*, 2004; Pui *et al.*, 2008; Li *et al.*, 2014), or exposure to chemotherapeutic agents or radiation, most epidemiological studies have not found convincing associations between supposed 'risk' factors and ALL incidence (Pui *et al.*, 2008; Inaba *et al.*, 2013).

There have been two hypotheses relating to the development of ALL; Greaves' delayed infection hypothesis and Kinlen's population mixing hypothesis (Kinlen and Petridou, 1995; Greaves, 2006). The former highlights a role for delayed exposure to common pathogens following underexposure as an infant, and the latter places emphasis on unusual mixing of populations causing exposures to novel viruses. Both hypotheses have the common theme that a lack of exposure to pathogens in early life can lead to abnormal development of the immune system, and a subsequent predisposition to the development of a haematological malignancy.

Both pre- and post-natal events are involved in the development of ALL (Gale *et al.*, 1997; Wiemels *et al.*, 1999; Greaves, 2005), evidenced through the study of Guthrie cards and monozygotic twins. A number of leukaemia-associated genetic changes have been detected at birth (Wiemels *et al.*, 1999; Wiemels *et al.*, 2002; McHale *et al.*, 2003a; McHale *et al.*, 2003b). Interestingly, a study by Mori *et al.* (2002) showed that the ETV6-RUNX1 fusion was present in cord blood at an incidence 100 fold higher than the incidence of ETV6-RUNX1 ALL in children, meaning that only 1% with the fusion at birth went on to develop ALL. This highlights the role of postnatal events in the development of childhood ALL, such as the deletion of wildtype RUNX1 (Mori *et al.*, 2002; Wiemels, 2012). Twin studies also provided evidence for a prenatal origin of ALL, as pre-leukaemic clones have been shown to transfer between monozygotic twins *in utero* through the monochorionic placenta. Nonetheless, it is still hypothesised that further events are required for disease development (Greaves *et al.*, 2003; Maia *et al.*, 2003).

1.2.3 Classification

ALL is a heterogeneous group of diseases which can be classified according to immunophenotype, cytogenetics or submicroscopic genetic changes.

1.2.3.1 Immunophenotype

Cells express surface markers which compose the immunophenotype of the cell and its differentiation stage. These are named cluster of differentiation (CD) markers. In ALL, the immunophenotype of the cell is indicative of the cell maturation state when it became malignant.

B cell precursor ALL (BCP-ALL) makes up approximately 85% of all ALL cases, and can be subdivided into pro-B, pre-B, transitional B, and mature B cell ALL based on the differentiation stage of the cell (Onciu, 2009). The first markers of B cell lineage have historically been thought to be CD19 and CD22, however a recent study has identified early expression of CD24 and TdT (terminal deoxynucleotidyl transferase) (Bendall *et al.*, 2014). CD markers used in the diagnosis and classification of BCP-ALL are CD19, CD20, CD22, CD24 and CD79a (Chiaretti *et al.*, 2014). T cell ALL (T-ALL) represents a smaller proportion of ALL (around 15%) (Onciu, 2009). Immunophenotypic markers important in the diagnosis and classification of T-ALL include CD1a, CD2, CD3, CD4, CD5, CD7 and CD8 (Chiaretti *et al.*, 2014).

1.2.3.2 Cytogenetics

The cytogenetics of ALL are defined by genetic alterations at the level of the chromosome. Changes can either be ploidy (numerical) or structural, such as deletions and fusions in chromosomes. The cytogenetic subgroup is an important prognostic factor in ALL, illustrated in Figure 1.2. Modern therapy is stratified based on some cytogenetic subgroupings, with targeted therapies such as imatinib used where possible and poorer prognosis subgroups treated on more intensive protocols.

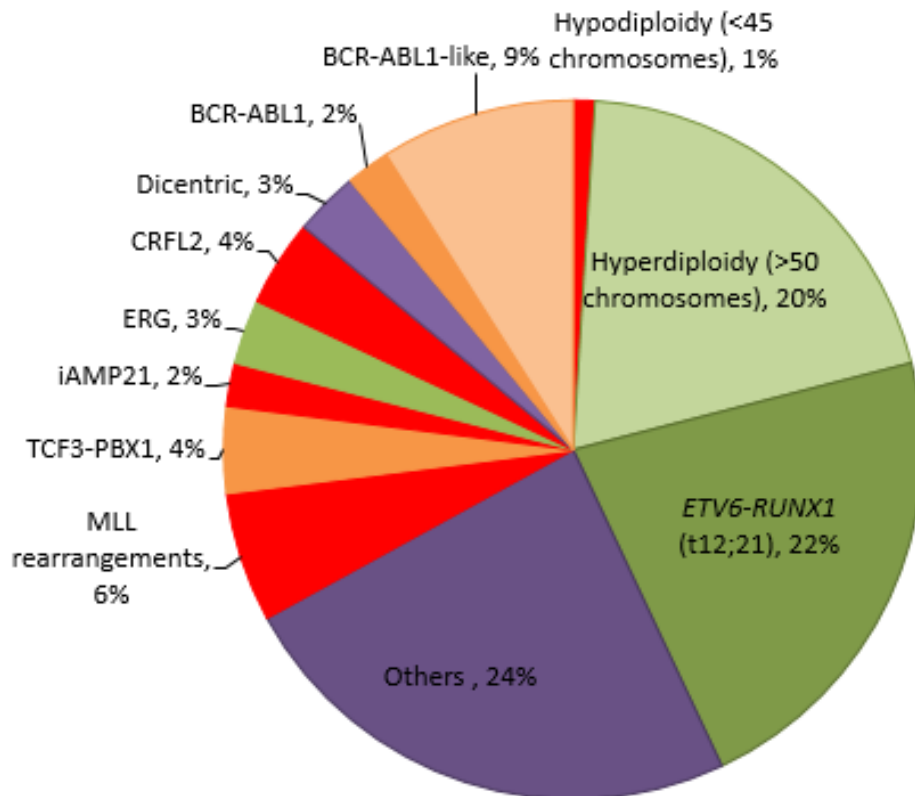


Figure 1.2 Frequencies of ALL cytogenetic subtypes, adapted from (Inaba *et al.*, 2013).

Shading – green: good prognosis; orange: poorer prognosis but may be abrogated with specific therapy; red: poor prognosis; purple: varying prognosis.

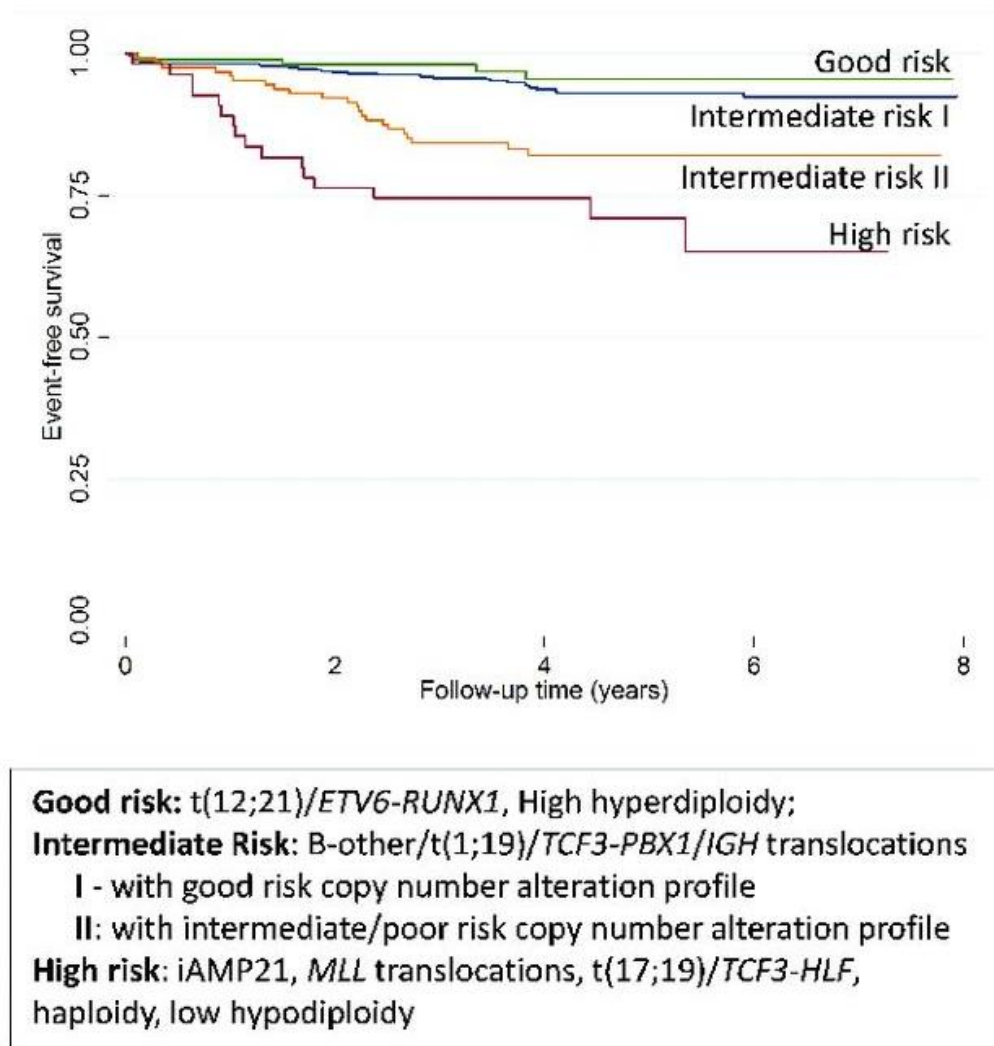


Figure 1.3 Outcome of patients with acute lymphoblastic leukemia (ALL) by genetic risk group.

Event-free survival of children and adolescents with B-cell precursor ALL treated on UKALL 2003 and stratified by cytogenetics and copy number alterations profile. Taken from Moorman *et al.* (2016).

High hyperdiploidy accounts for 20% of ALL cases and is defined by a non-random gain of at least five chromosomes, with a total chromosome number of >50. It has a good prognosis, with a 5 year survival of >90% (Moorman *et al.*, 2010). Hypodiploidy, which only accounts for about 1% of cases, has a much poorer prognosis. ALL hypodiploidy is defined by <44 chromosomes (Inaba *et al.*, 2013).

Chromosomal structural abnormalities affect a number of different genes. The most common is a fusion at t(12;21)(p13;q22), leading to the *ETV6-RUNX1* fusion gene. It

accounts for approximately 25% of ALL cases, and mainly occurs in children between the ages of 2-9 years (Kanerva *et al.*, 2004; Rubnitz *et al.*, 2008). The affected genes have roles in haematopoiesis and lymphoid cell development, and consequently the fusion gene leads to ALL development. *ETV6-RUNX1* ALL has a good prognosis (Mullighan, 2012), although this can be altered by other major risk factors such as white blood cell count (WCC) and initial response to therapy (Loh *et al.*, 2006; Bhojwani *et al.*, 2012).

MLL (mixed lineage leukaemia) rearrangements account for 6% of ALL, with the *MLL* gene having the potential to create fusions with different gene partners. In all cases *MLL* rearrangements are aggressive with a poor prognosis, and tend to have an early age of onset (Johansson *et al.*, 1998; Harrison *et al.*, 2005).

Although more common in chronic myeloid leukaemia, *BCR-ABL1* also accounts for a small number of ALL cases. The fusion at t(9;22)(q34;q11) results in the Philadelphia chromosome, which gives rise to a constitutively activated tyrosine kinase affecting signalling in the RAS/RAF/MEK/ERK pathway, which has roles in cell survival, proliferation and differentiation. Historically, this subgroup had a poor prognosis, but this has been greatly improved by the development of imatinib and other tyrosine kinase inhibitors (Schultz *et al.*, 2009; Ravandi *et al.*, 2010; Schultz *et al.*, 2014). Additionally, there is a subgroup known as *BCR-ABL1*-like (Den Boer *et al.*, 2009; Roberts *et al.*, 2014). Despite having no *BCR-ABL1* fusion, *BCR-ABL1*-like patients display a similar genetic expression profile to *BCR-ABL1* patients in all other respects, and some have kinase activating mutations. Although previously associated with a poor prognosis, it has been recently observed that the development of tyrosine kinase inhibitors may also improve outcome for these patients (Roberts *et al.*, 2014; Ishibashi *et al.*, 2016).

Other common cytogenetic subgroups include *TCF3-PBX1* and intrachromosomal amplification of chromosome 21 (iAMP21). The *TCF3-PBX1* fusion t(1; 19) is found in 4% of ALL, resulting in the abnormal activation of *PBX1* in lymphoblasts leading to lymphoblast transformation (Hunger, 1996; Kamps, 1997). This subgroup has been associated with a higher incidence of Central Nervous System (CNS) relapse. In iAMP21, there are complex rearrangements in chromosome 21. Patients with iAMP21

are often older, with a median age of onset of 9 years of age (Harrison, 2015). Intensive therapy can minimise the high relapse rate seen in this subgroup with standard therapy (Anthony *et al.*, 2013; Nyla *et al.*, 2013).

1.2.3.3 Submicroscopic genetic changes

There are a wide range of submicroscopic genetic alterations in ALL. These broadly affect genes involved in lymphoid cell differentiation, cell cycle regulation, proliferation and cell survival and lymphoid cell development (Mullighan *et al.*, 2007). There is often an association between the primary chromosomal abnormality and secondary genetic mutations. For example, *MLL* gene fusions typical have less than one additional event, reflected by its early age of onset. Conversely, patients with an *ETV6-RUNX1* translocation, which has an median age of onset of four years, normally have around 6-8 cooperating mutations (Sun *et al.*, 2017). Of note, genes commonly affected in ALL include *PAX5*, *IKZF1*, *JAK1/2* and *CRLF2*.

PAX5 and Ikaros are both transcription factors involved in B lymphoid cell development. Mutations in *PAX5* specifically affect DNA binding and have been detected in 31.7% of BCP-ALL (Kuiper *et al.*, 2007; Mullighan *et al.*, 2007; Mullighan *et al.*, 2008a). Mutations and deletions in *IKZF1*, which codes for Ikaros, result in a loss of function of the gene, leading to stalled maturation. *IKZF1* mutations are present in 15% of all BCP-ALL, but are seen at a much higher rate of 80% of *BCR-ABL1* ALL (Mullighan *et al.*, 2007; Mullighan *et al.*, 2008a; Martinelli *et al.*, 2009; Mullighan, 2012).

The JAK-STAT pathway is important for the proliferation of ALL cells. Mutations in *JAK1* and *JAK2* are common in Down syndrome ALL and high risk ALL patients with no *BCR-ABL1* translocation, resulting in constitutive activation of the JAK-STAT pathway (Bercovich *et al.*, 2008; Mullighan *et al.*, 2009b). Similarly, *CRLF2*, which is also involved in activation of the JAK-STAT pathway, is mutated in approximately 15% of ALL cases (Mullighan *et al.*, 2009a; Russell *et al.*, 2009; Cario *et al.*, 2010).

Finally, the RAS genes are frequently mutated in ALL at presentation and relapse (Case *et al.*, 2008; Irving *et al.*, 2014; Irving, 2016), with a greater incidence in high risk ALL.

Mutations affect signalling in the RAS/RAF/MEK/ERK pathway, leading to altered cell survival, proliferation and differentiation (Zhang *et al.*, 2011).

1.2.4 Prognosis

A number of factors are known to influence prognosis in children with ALL. Firstly, as previously discussed, cytogenetic and genetic subgroups affect outcome, with high hyperdiploidy and *ETV6-RUNX1* associated with a good prognosis, and hypodiploidy, *MLL* rearrangements, *BCR-ABL1*, *BCR-ABL1*-like and *iAMP21* being associated with a poorer prognosis. Genomic features such as mutations in *IKFZ1* are also linked to poor outcome.

Secondly, patient characteristics have a bearing on prognosis. Positive prognostic factors are an age of between 1-10 years, female sex, and white or asian ethnicity. In contrast, infants or older children do worse, along with males and patients of black or Hispanic race. A WCC of $>50 \times 10^9$ cells/l is also indicative of a poor prognosis.

Glucocorticoid (GC) response is a crucial prognostic factor in ALL. The Berlin-Frankfurt-Münster (BFM) group has shown that a good response to 7-day GC monotherapy correlated with a better patient outcome in three separate trials (Dordelmann *et al.*, 1999; Schrappe *et al.*, 2000).

Recently, a number of studies have also highlighted the prognostic significance of early treatment response, measured by MRD status (minimal residual disease, the sub-clinical level of leukaemic cells present after induction therapy). It was observed that MRD status was the most important predictive prognostic variable when comparing children with a similar risk on the same therapy (Cave *et al.*, 1998; van Dongen *et al.*, 1998; Vora *et al.*, 2013a). Furthermore, the UKALL 2003 trial also showed that children who received post induction stratification of therapy based on MRD status had an improved EFS (event free survival) (Goulden, 2012).

1.3 Therapy

Chemotherapy for ALL is broken down into a number of phases with different objectives. Initially, induction therapy aims to reduce the leukaemic burden on the body and restore normal haematopoiesis. Subsequently, consolidation and delayed

intensification phases eliminate residual ALL cells. Finally, maintenance therapy aims to prevent relapse (Pui *et al.*, 2004; Pui and Evans, 2006).

Over the last few decades, the MRC-NCRI (Medical Research Council-National Cancer Institute) group have coordinated a series of clinical trials (United Kingdom National Randomised Trial for Children and Young Adults with Acute Lymphoblastic Leukaemia and Lymphoma) which have contributed substantially to the improved prognosis of children in the UK with ALL. Accrual to UKALL trials has been excellent, enabling improvement to treatment protocols and consequently survival. This is evidenced by the UKALL 2003 trial, which recruited more than 97% of eligible patients (Goulden, 2012).

1.3.1 UKALL group trial history

In 1972, 5 year EFS was 35% for children with ALL in the UK. The first UKALL trials, UKALL I–XI (1970-1997), primarily aimed to improve outcome through intensification of therapy. Trials I-VII failed to demonstrate significant improvement in outcome for patients (Working Party on Leukaemia, 1986). UKALL VIII to XI, however, enhanced prognosis for ALL patients, with five year EFS at the end of this time at 63.1% (Eden *et al.*, 1991; Chessells *et al.*, 1995; Hill *et al.*, 2004). Key modifications during this period included the introduction of more than one delayed intensification therapy block, and the replacement of cranial irradiation with intrathecal chemotherapy as CNS directed treatment.

The following trial, UKALL 97 (1997-1999), only ran for two years before modification to a US CCG (Children's Cancer Group) style protocol (UKALL 97/99, 1999-2003), as the outcomes of UKALL X and UKALL XI were inferior to US (CCG) and European (BFM) trials (Chessells *et al.*, 2002).

In UKALL97/99, therapy was also stratified by NCI (National Cancer Institute) risk and early response to induction therapy for the first time. The trial additionally investigated the selection of GC used in treatment. Dex was compared to prednisolone for induction and maintenance therapy at doses of 6.5 and 40mg/m² respectively. A one third reduction in CNS and systemic relapse was observed in patients treated with dex. Furthermore, 5 year EFS was 80%, an increase of 12%

compared to UKALLXI (Mitchell *et al.*, 2005; Mitchell *et al.*, 2010). The choice of GC used in ALL protocols is discussed further in 1.4.3.

The main focus of UKALL 2003, the most recently completed UK trial (2003-2011), was improved treatment stratification. In UKALL 97/99, a number of patients who relapsed had not been randomised as high risk and therefore had not received the most intensive therapy. MRD had also been recently determined as the best predictor of outcome in children on the same treatment. As such, UKALL 2003 randomised patients with a day 29 MRD of less than 0.01% at day 29 and a negative week 11 MRD result to one delayed intensification block. All other patients received standard therapy with two delayed intensification blocks.

The 5 year EFS of UKALL 2003 was 87.2%, with an overall survival of 91.5%. This was comparable to other major trials worldwide (Table 1.1). Furthermore, the trial showed that there was no significant difference between patients who had received one delayed intensification compared to two in terms of EFS (94.4% vs. 95.5% respectively), supporting the stratification of therapy by MRD (Vora *et al.*, 2013b; Vora *et al.*, 2014).

Research Group	Trial	Region	Dates	No. Patients	EFS	OS	Reference
MRC-NCRI	UKALL 2003	United Kingdom	2003-2011	3126	87.2	91.5	(Vora <i>et al.</i> , 2013b)
COG	Many	US, Canada, Australia, New Zealand	2000-2005	6994	N/A	91.3	(Hunger <i>et al.</i> , 2012)
SJCRH	Total Therapy Study XV	US	2000-2007	498	85.6	93.5	(Pui <i>et al.</i> , 2009)
DFCI	DFCI ALL Consortium Protocol 00-01	US, Canada	200-2004	492	80.0	91.0	(Vrooman <i>et al.</i> , 2013)
AEIOP-BFM	AEIOP-BFM ALL 2000	Western Europe	2000-2006	4480	80.3	91.1	(Conter <i>et al.</i> , 2010)
DCOG	DCOG Protocol ALL-9	The Netherlands	1997-2004	859	81	86	(Veerman <i>et al.</i> , 2009)
EORTC CLG	EORTC CLG 58591	Belgium, France	1998-2008	1940	82.6	89.7	(Domenech <i>et al.</i> , 2014)
NOPHO	ALL-2000	Denmark, Finland, Iceland, Norway, Sweden	2000-2007	1023	79	89	(Schmiegelow <i>et al.</i> , 2010)

Table 1.1 Outcomes of contemporary trials involving children and adolescents with ALL in North America and Western Europe.

Adapted From Hunger and Mullighan (2015) AIEOP: Italian Association of Pediatric Hematology and Oncology, BFM: Berlin–Frankfurt–Münster, DCOG: Dutch Childhood Oncology Group, DFCI: Dana–Farber Cancer Institute, EORTC CLG: European Organization for Research and Treatment of Cancer–Children’s Leukemia Group, MRC-NCRI: Medical Research Council–National Cancer Research Institute, N/A not available, NOPHO Nordic Society of Paediatric Haematology and Oncology, SJCRH St. Jude Children’s Research Hospital. EFS: Event free survival. OS: Overall survival. Survival percentages shown rates at 5 years except AIEOP-BFM trial, which were reported at 7 years.

1.3.2 Therapy today – UKALL 2011 trial

As previously noted, current therapy is initially stratified based on a number of 'risk groups', including cytogenetic subgroup, white blood cell count and age, then further stratified based on MRD (Pui *et al.*, 2008). However, it has been suggested these groupings are still not comprehensive enough, as relapse still occurs in all risk groups (Asselin, 2012; Vora *et al.*, 2013b). Furthermore, many children experience potentially unnecessary severe toxicity associated with the first phase of treatment, and there also remains a percentage of children who do not achieve remission (Vora *et al.*, 2013b) (Jackson *et al.*, 2016). The chemotherapy regimen of the current UKALL trial (UKALL 2011) is shown in Table 1.2.

Treatment Phase	Drugs administered
Induction therapy	Dex Vincristine Pegaspargase (Daunorubicin for Regimen B patients)
Consolidation	Methotrexate Mercaptopurine Cyclophosphamide Cytarabine Vincristine (Pegaspargase for high risk patients)
Delayed intensification	Dex Vincristine Doxorubicin Pegaspargase Methotrexate Cyclophosphamide Mercaptopurine Cytarabine
Maintenance	Mecaptopurine Methotrexate

Table 1.2 Drugs administered to ALL patients in the different phases of the UKALL 2011 trial.

Adapted from (Goulden, 2012).

Despite reporting a 5 year EFS of 87.2% and an overall survival (OS) of 91.5% , UKALL 2003 also reported a significant decrease in quality of life (QoL), along with a 3% risk of treatment-related mortality and non-haematological serious adverse events (SAEs) in approximately a quarter of patients. (Vora *et al.*, 2013b). This high level of toxicity is seen as unacceptable in a treatment with such a high EFS (Goulden, 2012); with survival rates approaching 90% (higher for low risk groups), treatment related mortality accounts for a significant proportion of those who do not survive their disease. Furthermore, the necessity of a decreased QoL in all patients is questionable, when in fact, the intensified protocol only benefits 40% of patients. 50% of patients were cured on the less intensive protocols of the 1980s, and a further 10% would not have been cured on either protocol.

As a result, the ongoing UKALL 2011 trial was designed to maintain the current good prognosis whilst reducing the burden of treatment. As dex is responsible for pronounced toxicity during the induction phase of chemotherapy, the trial was planned to investigate the effects of a modification of dex dosing. This will be further discussed in 1.4.4.

1.4 Dexamethasone

Due to its ability to induce apoptosis in cells of lymphoid lineage, the GC dex plays a key role in the treatment of ALL.

1.4.1 The glucocorticoids

GCs are synthetic analogues of the stress hormone cortisol, differing by minor changes to their chemical structure which alter their pharmacokinetic properties and biological activity, shown in Figure 1.4.

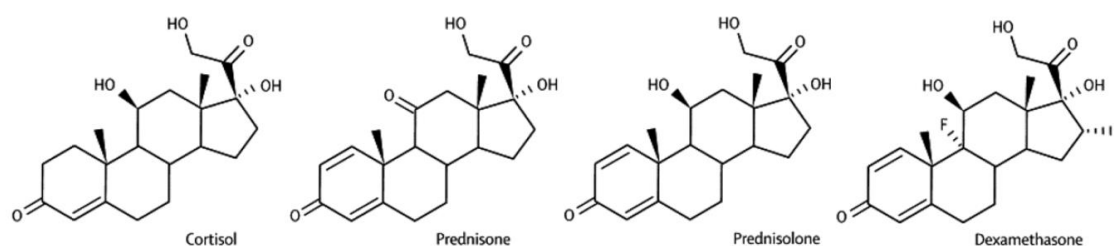


Figure 1.4 Chemical structures of glucocorticoids: cortisol, prednisolone, prednisone and dex.

Taken from (Inaba and Pui, 2010).

GCs are known to have roles in a wide range of biological processes (Nicolaidis *et al.*, 2010). Amongst these, immunosuppressive and anti-inflammatory properties have led to frequent prescription of GCs for a variety of illnesses including allergies and autoimmune diseases (Kofler, 2000; Nicolaidis *et al.*, 2010). However, this wide range of clinical effects also accounts for many of the adverse events experienced by ALL patients receiving dex, such as osteonecrosis and life-threatening infection.

1.4.2 Glucocorticoid mechanism of action in ALL

The antileukaemic effects of dex are moderated by the glucocorticoid receptor (GR), also known as NR3C1 (Kofler, 2000). When not bound to ligand, the GR is held in the cytoplasm by a heterocomplex with several proteins (Nicolaidis *et al.*, 2010). Dex can enter the cell passively, due to its small size and lipophilicity. Upon binding dex, the GR dissociates from the heterocomplex and the resulting dex-GR complex exerts its effects in two ways. Firstly, as a dimer, it interacts with glucocorticoid response

elements (GREs) and transactivates gene expression (Schaaf and Cidlowski, 2002; Tissing *et al.*, 2003; Tissing *et al.*, 2006). Secondly, as a monomer, the dex-GR complex indirectly causes transrepression of genes. This occurs through interference with the activity of transcription factors such as NFκB and AP-1 via protein-protein interactions, prevention of DNA binding, and competition for coactivators (Kofler, 2000; Schaaf and Cidlowski, 2002; Tissing *et al.*, 2003; Inaba and Pui, 2010). It is a combination of gene transactivation and transrepression which results in a change in expression of oncogenes and inhibition of cytokine production, ultimately causing cell-cycle arrest and cell death (Inaba and Pui, 2010).

1.4.3 Choice of glucocorticoid

Historically, prednisolone was the steroid of choice in ALL protocols. However, over the last two decades, dex has been increasingly used due to its superior CNS penetration, discussed below (Inaba and Pui, 2010).

The two glucocorticoids have differing pharmacokinetic properties, which may influence efficacy in ALL. Dex has a longer half-life than prednisolone, which is thought to be due to the fluorine present on ring B of the chemical structure (Meikle and Tyler, 1977; Rose and Saccar, 1978) (Figure 1.4). Dex has also been shown to be 70% protein bound over a wide concentration range, however prednisolone protein binding is concentration dependent (60% at 10µM to 95% at <0.5µM) (Balis *et al.*, 1987). This may affect the amount of free drug available for clearance in different body compartments. There are varying reports regarding the bioequivalence of dex and prednisolone, with 1mg of dex reported to be equivalent to 5 – 15.2mg of prednisolone in ALL cells *in vitro*, including when grown on a bone marrow feeder layer (Ito *et al.*, 1996; Kaspers *et al.*, 1996).

The ability to cross the blood brain barrier is an important property of GCs. Due to the elimination of cranial irradiation from treatment protocols, GCs play a vital role in eliminating and preventing CNS leukaemia (Pui and Howard, 2008; Pui *et al.*, 2009). There have been no studies investigating the pharmacokinetics of dex and prednisolone in the cerebrospinal fluid (CSF) in humans, however Balis *et al.* (1987) found that prednisolone had a shorter CSF half-life than dex (2.9 vs. 4h) in a non-human primate model, after intravenous administration of 6 or 40mg/m² of

prednisolone or dex, respectively. This was likely attributable to the variable protein binding of prednisolone at CNS concentrations. Such differences in CNS exposure between GCs may affect the length of time CNS leukaemic blasts are exposed to cytotoxic concentrations of drug. This important observation led to clinical trials investigating the efficacy of dex and prednisolone in ALL, both in terms of outcome and CNS relapse.

The majority of trials used dex and prednisolone at a ratio of 1:6.67, equivalent to 6 and 40mg/m² respectively. In trials at this dose, and others where the dex-prednisolone dose ratio was less than 7 (dex dose 6-18mg), patients had a better 5 year EFS and fewer CNS relapses when treated with dex (Jones *et al.*, 1991; Veerman *et al.*, 1996; Silverman *et al.*, 2001; Bostrom *et al.*, 2003; Mitchell *et al.*, 2005; Vrooman *et al.*, 2013). However, this enhanced prognosis was observed in parallel with an increase in toxicity incidence. In trials where the dose ratio was greater than 7, there was no difference in efficacy observed between dex and prednisolone (Igarashi *et al.*, 2005b; Domenech *et al.*, 2014), indicating that the benefit is dose dependent (Inaba and Pui, 2010). However, a meta-analysis looking at all randomised ALL trials comparing GC selection found that overall, dex was more efficacious than prednisolone (Teuffel *et al.*, 2011).

In UK protocols, the substantial benefit of dex in terms of EFS and reduction of CNS and bone marrow relapse shown in the UKALL97/99 trial, has resulted in dex becoming established as the steroid of choice. Different strategies for optimisation of GC dosing in this project will therefore focus on dex.

1.4.4 Optimisation of dex

Problems associated with both under-treatment and over-exposure of dex reinforce the need for further ways to individualise patient treatment, to reduce any unnecessary burden of therapy whilst giving the best possible chance of survival (Pui *et al.*, 2011). The challenge lies in selecting patients who could benefit from a reduction in therapy, and equally patients for which further treatment intensification is necessary.

However, adjusting a potentially life threatening therapy is not a simple task. Investigations into future patient stratification should consider both the molecular and clinical pharmacology of dex. Areas to consider include pharmacokinetics, pharmacogenetics and the action of dex at the level of the ALL cell. A review on this topic has been published in the British Journal of Haematology, and can be found in appendix H (Jackson *et al.*, 2016).

1.5 Dex pharmacokinetics

Pharmacokinetics is a valuable tool that is already being utilised in a number of other cancer therapies to guide dosing (Burke *et al.*, 1999; Veal *et al.*, 2013; Paci *et al.*, 2014). In ALL therapy, the St Jude Total XV protocol utilised pharmacokinetics to adjust the dosing of methotrexate and mercaptopurine to avoid sub-optimal exposures and needless toxicity in individual patients (Pui *et al.*, 2012).

However, despite the extensive clinical use of dex, and the successful application of therapeutic dose monitoring with drugs such as methotrexate, there is a remarkably limited amount of information regarding dex pharmacokinetics, particularly in children. An American study showed substantial inter-patient variability in dex pharmacokinetics in children with ALL, with a greater than ten-fold variability in systemic drug exposure observed at a dose of 8 mg/m²/day (Yang *et al.*, 2008). The extent of pharmacokinetic variation reflects that seen in one other non-ALL paediatric study (Richter *et al.*, 1983) and in healthy adult volunteers (Loew *et al.*, 1986; O'Sullivan *et al.*, 1997; Queckenberg *et al.*, 2011).

Although the impact of this variation has not been extensively studied, an initial follow up analysis of the study found that risk of haematological and CNS relapse was affected by interpatient variability in dex exposure, in conjugation with the presence of anti-asparaginase antibodies. Furthermore, an association was also observed between grade 3/4 osteonecrosis and lower dex clearance (Kawedia *et al.*, 2012). While these observations require validation in independent clinical trials, they highlight the need for further study in this area.

It is important to clarify the relationship between dex pharmacokinetics, clinical response and toxicity for two main reasons. Firstly, it may be possible to further

stratify ALL therapy by adjustment of dex dose. Secondly, variability in dex pharmacokinetics may impact studies aiming to optimise dex dosing. A number of protocols are investigating dose changes of 2-4mg/m² in an attempt to improve outcome. However, if inter-patient variability in dex pharmacokinetics is as large as that reported, pharmacokinetic variability may mask any potential benefits of such a change. For this reason, a UKALL 2011 sub-study is seeking to resolve these problems by investigating how dose changes impact on dex pharmacokinetics. This sub-study is being undertaken as part of this project and involves the characterisation of dex pharmacokinetics following contrasting doses and duration of dex treatment in a randomised study.

1.5.1 Source of pharmacokinetic variation

Data from Yang *et al.* (2008) suggest that apparent dex clearance is influenced by serum albumin concentration, age, and concurrent use of drugs. It will be important to verify these findings independently. This is a complicated area when the number of other drugs that are administered alongside dex in ALL therapy are also considered (Jackson *et al.*, 2016).

1.5.1.1 Asparaginase

The observed correlation between albumin concentration and dex clearance is unusual, as it is not thought to be a direct result of protein binding. Instead, Yang *et al.* (2008) hypothesised that this relationship is the result of concomitant administration of asparaginase during induction chemotherapy.

Asparaginase is known to decrease hepatic synthesis of proteins, which could affect the production of both albumin and cytochrome P450 enzymes involved in the metabolism of dex. Therefore a reduction in albumin would be exhibited in patients in parallel to a decreased dex clearance. The clinical consequences of an interaction between asparaginase and dex pharmacokinetics needs to be investigated further. In some cases, patients develop antibodies to asparaginase, causing asparaginase insensitivity (Woo *et al.*, 1998). Children may therefore not only lose the antileukaemic benefit of asparaginase, but may also have a lower exposure to dex, as

they will not experience the lowered dex clearance (and therefore higher exposure) associated with asparaginase activity.

While these findings need to be independently investigated, if inpatient variation was attributed to concomitant administration of asparaginase, the decrease in dex clearance associated with asparaginase treatment would need to be factored into any proposed dex dose adjustment approach utilised for individual patients (Jackson *et al.*, 2016).

1.5.1.2 Age effect

Yang *et al.* (2008) reported a lower dex clearance in older children. This finding is consistent with clinical observations, as older children tend to experience more toxicity than younger children. The lower clearance would cause an increased exposure to dex and thus a higher incidence of toxicity.

Importantly, despite causing an increase in toxicity, the comparably higher exposure to dex observed in older children does not translate to a better clinical outcome. This may be due to a higher prevalence in older children of poor prognosis subtypes (Plasschaert *et al.*, 2004) and highlights the complexity of dealing with a heterogeneous disease. The therapeutic window for dex may well differ between patient subpopulations, based on known risk factors including cytogenetics and microscopic genetic alterations, as well as additional unknown factors (Jackson *et al.*, 2016; McNeil *et al.*, 2016).

1.6 Dex pharmacogenetics

There are a number of well documented examples where pharmacogenetic information has been utilised to personalise dosing of anticancer drugs. One example is the administration of azathioprine and 6-mercaptopurine in relation to TPMT (thiopurine methyltransferase) genotype (McLeod *et al.*, 2000; Relling *et al.*, 2013). A number of the genes involved in both the pharmacokinetics and mechanism of action of dex exhibit polymorphisms, making it an important avenue of investigation for the personalisation of dex therapy.

1.6.1 The Glucocorticoid Receptor

The mechanism of action of dex is mediated by the GR. Therefore polymorphisms in *NR3C1* have the potential to alter dex response in ALL patients. In particular, mutations affecting the expression and/or function may not only affect the therapeutic benefits of dex treatment, but also impact on experience of toxicity. There are a number of documented polymorphisms *NR3C1*. The *bclI* restriction fragment length polymorphism has been associated with increased GC sensitivity regarding high blood pressure and hyperinsulinaemia (Buemann *et al.*, 1997; Rosmond *et al.*, 2000), however another study found it was associated with a decreased GC response, measured by white blood cell lysozyme release (Panarelli *et al.*, 1998). Of interest, the variant was associated with a worse overall survival in 222 children with ALL (Fleury *et al.*, 2004), so it is possible that this polymorphism affects GC in a tissue specific manner. Furthermore, a GR haplotype including this variant (along with -627A and 9bT polymorphisms) were associated with a reduced EFS in 310 children with ALL (Labuda *et al.*, 2010). However, these associations need confirming in an independent study.

Another polymorphism of interest is the amino acid change N363S. There are a number of studies highlighting a role for the variant allele in increased sensitivity to glucocorticoids with regards to insulin response, weight and response to exogenous cortisol (Huizenga *et al.*, 1998; Dobson *et al.*, 2001; Roussel *et al.*, 2003). Fleury *et al.* (2004) did not find any association with outcome in children with ALL. However, this study did not look at experience of toxicity. It is important to further investigate the role of variants affecting GC response, as an altered sensitivity to GCs may mean that patients with the variant allele may be more susceptible to toxicity.

1.6.2 Cytochromes P450 (CYP450)

The main cytochrome P450 enzyme involved in the metabolism of dex is CYP3A4, which is responsible for the 6 α - and 6 β -hydroxylation of dex. CYP17 is involved to a lesser extent in the metabolism of dex, and is thought to be responsible for the generation of side chain cleaved dex (Tomlinson *et al.*, 1997).

Basal expression of CYP3A4 varies greatly between individuals. There are a number of variant alleles in CYP3A4, however most of these are present at low frequencies, and

appear to have little functional significance (Plant, 2007; Amacher, 2012). It is thought that much of the variation may be due to genetic variation in transcriptional regulators, however apart from the PXR (Lamba *et al.*, 2010), few polymorphisms have been identified (King *et al.*, 2003). One polymorphism in CYP3A4 which has been shown to have functional consequences in the metabolism of CYP3A substrates, is the intron C>T polymorphism, CYP3A4*22. Carriers of CYP3A4*22 have been found to have reduced CYP3A4 activity in several studies (Elens *et al.*, 2013a; Elens *et al.*, 2013b; Kitzmiller *et al.*, 2014). For example Elens *et al.* (2013a) found a 20% decrease in midazolam activity compared to patients with CYP3A4*1/*1.

There is an additional CYP3A enzyme present in 10-20% of the population called CYP3A5 (Daly, 2003). CYP3A5 has a comparable substrate specificity to CYP3A4, and in individuals with CYP3A5 expression, could be responsible for up to 50% of CYP3A activity (Andrews and Daly, 2008). Homozygotes for the CYP3A5*3 polymorphism, a loss of function mutation, have also been shown to have reduced CYP3A activity compared to those with CYP3A5*1/*1 (Kitzmiller *et al.*, 2014).

There are no data currently available in children with cancer concerning the effects of variation in CYP3A4/5 expression on dex pharmacokinetics or treatment outcome. However, differential CYP3A4 levels have been associated with altered outcome in adult cancers (Miyoshi *et al.*, 2002; Dhaini *et al.*, 2003). As such, investigation of the effect of CYP3A expression in ALL could provide useful data to support the future stratification of dex therapy.

1.6.3 MDR1

The body possesses a number of transporter proteins which actively pump endogenous and exogenous compounds in and out of cells. These include multidrug resistance protein 1 (MDR1, also termed ABCB1) and multidrug resistance-associated protein (MRP1 or ABCC1). Altered transporter protein expression can potentially impact on drug disposition through differences in absorption of orally administered drugs, ability to cross the blood brain barrier and drug elimination and excretion.

There is well characterised inter-individual variation in the expression of MDR1, encoded by the *ABCB1* gene (Leschziner *et al.*, 2006). Such variation in MDR1

expression may well affect dex pharmacokinetics, as it is thought to be a substrate for MDR1 (Cole *et al.*, 1992). Indeed, a study in healthy volunteers found that exposure to dex was increased upon concomitant administration of the MDR1 inhibitor, valsopodar (Kovarik *et al.*, 1998). However, studies regarding the effect of MDR1 expression in ALL cells cast doubt on the substrate specificity of dex, as many studies have found no effect of ALL cell MRD1 expression on outcome (Kakihara *et al.*, 1999; Plasschaert *et al.*, 2003; Balamurugan *et al.*, 2007).

The *ABCB1* gene harbours a number of polymorphisms including two which are relatively common, an amino acid change at position 2677, and a silent mutation at position 3435. There are limited data concerning the effects of these polymorphisms in ALL, however the wildtype form of the C3435T mutation has been associated with a poorer outcome in two studies (Jamroziak *et al.*, 2004; Gregers *et al.*, 2015). This association is similar to that observed in other cancers (van den Heuvel-Eibrink *et al.*, 2001; Lal *et al.*, 2008). Further work is needed to ascertain whether dex is a substrate for MDR1, and the subsequent effect polymorphisms could have on patient outcome.

1.6.4 Glutathione S-transferases

The glutathione S-transferases (GSTs) are involved in a number of cellular processes, such as the neutralisation of oxidative stress and phase II metabolism of xenobiotics. It has been suggested that sensitivity to GCs may be affected by changes in GST expression, possible due to better neutralisation of oxidative stress or increased excretion of drug following conjugation to reduced glutathione (Iwata *et al.*, 1997; Den Boer *et al.*, 1999). Polymorphisms in all four major subfamilies (GST α , GST μ , GST θ and GST π) have been reported. Of particular note, polymorphisms in *GSTM1* and *GSTT1* can result in a null phenotype, and have been reported in 50% and 15–38% of Caucasians, respectively (Chen *et al.*, 1997).

The effect of GST genotype on dex response is not clear, with conflicting reports in the literature. A number of groups found an association between both *GSTT1* and *GSTM1* null genotype and decreased risk of relapse (Hall *et al.*, 1994; Anderer *et al.*, 2000; Takanashi *et al.*, 2003), however these were not statistically significant. Conversely, several other studies, including one of 710 ALL patients (Davies *et al.*, 2002a), have not found any association between GST genotype and outcome in ALL (Krajinovic *et al.*,

2002). These contradictory data may be due to limited knowledge regarding the contribution to GC metabolism of different GST isoforms. Similarly, data concerning the influence of GST genotype in individual subgroups of ALL may help to resolve these contradictory findings (Jackson *et al.*, 2016).

1.6.5 BCL2 family

The BCL2 family is crucially involved in the apoptotic response of GCs. A number of genes in this family exhibit polymorphisms (Wang *et al.*, 2003; Tissing *et al.*, 2007), which have been implicated in studies investigating outcome in ALL. A decrease in overall survival has been associated with variants in *BCL2L11* (29201 C>T) and *MCL1* (-486 G>T) (Gagne *et al.*, 2013; Sanchez *et al.*, 2014). In combination, variants in both genes potentiated the effect on overall survival, which was more noticeable when patients received higher doses of GCs (Gagne *et al.*, 2013).

The (-938 C>A) promotor polymorphism in the *BCL2* gene has also been associated with GC response. The single nucleotide polymorphism (SNP) was correlated with a higher expression of BCL2, resulting in children experiencing a poor initial GC response and consequently being risk stratified to the high risk arm (Kunkele *et al.*, 2013). Additional studies need to be carried out to ascertain the validity of the currently published data, due to the important roles played by these genes in the mechanism of ALL cell death, which is further discussed in 1.8.2.

1.6.6 Genes associated with asparaginase and steroid toxicity

There have been a number of reports highlighting the significance of various genes on the likelihood of developing asparaginase antibodies and similarly experiencing steroid related toxicities, such as osteonecrosis. Most of these genes have only been identified in a single cohort of patients, so further investigation is needed in an independent cohort of patients to establish the significance of these genes. Genes of interest are shown in Table 1.3.

	Group	Gene	Implications	Reference
Osteonecrosis	CRHR1	<i>CRHR1</i>	May impact the risk of bone density deficits in patients treated with GCs and antimetabolites in a sex-specific manner.	(Jones <i>et al.</i> , 2008)
	Vitamin D Receptor	<i>VDR Fok I</i>	Variation associated with lower bone marrow density in paediatric non ALL patients, therefore might identify patients at higher risk of osteonecrosis.	(Relling <i>et al.</i> , 2004; Jakubowska-Pietkiewicz <i>et al.</i> , 2012)
	Plasminogen and fibrinolysis	<i>PAI-1</i>	Inhibition of fibrinolysis via suppression of promotion of thrombosis and inhibition of tissue plasminogen activator may cause raised intraosseous venous pressure stopping blood flow to bones.	(French <i>et al.</i> , 2008)
	Glutamate receptor	<i>GRIN3A</i>	Minor allele associated with osteonecrosis in ALL patients.	(Karol <i>et al.</i> , 2015; Karol <i>et al.</i> , 2016)
		<i>GRID2</i>	Associated with osteonecrosis in ALL patients of <10 years.	
	Fat and cholesterol metabolism genes	<i>ACP1</i>	Regulates lipid levels and osteoblast differentiation. Associated with risk of osteonecrosis, lower albumin and higher cholesterol.	(Kawedia <i>et al.</i> , 2011)
<i>SH3YL1</i>				
<i>BMP7</i>		Causes altered bone formation and metabolism before and during therapy for ALL, also plays a role in osteonecrosis through effects to local bone vasculature.	(Karol <i>et al.</i> , 2016)	
<i>PROX1</i>	Variants cause altered lipid trafficking in bone marrow and/or increase plasma lipids.			

(Continued overleaf)

	Group	Gene	Implications	Reference
Asparaginase	Human Leucocyte antigen genes	HLA-DRB1*07:01	Altered binding affinity for asparaginase epitopes may lead to higher incidence of asparaginase allergy.	(Fernandez <i>et al.</i> , 2014)
	G protein signalling	SGSM2	Age dependent association of SGSM2 and LDL-C cause altered lipid levels.	(Dumitrescu <i>et al.</i> , 2011)

Table 1.3 Genetic variation associated with adverse outcome with asparaginase therapy and risk of steroid induced osteonecrosis.

LDL-C: low density lipoprotein C. LD: linkage disequilibrium.

1.7 Dex at the level of the cell

In parallel to studying the clinical pharmacology of dex, it is also important to consider the activity of dex at the level of the individual cancer cell, as this is what results in ALL cytotoxicity and disease reduction. For example, plasma levels of dex may not be of clinical importance if a patient's ALL cells are resistant to the drug. In this clinical situation, even a high exposure to dex as measured by plasma pharmacokinetics is unlikely to lead to therapeutic benefit, but the patient may be more likely to experience an increase in treatment associated toxicities.

As previously discussed in 1.2.4, GC response is an important prognostic factor in ALL. Furthermore, despite the observed improvements in survival in ALL, relapse still occurs in 20% of patients, for which therapy resistance is often the cause (Pui and Evans, 2006). A study by Klumper *et al.* found that GC response *in vitro* in relapsed ALL samples was significantly less than at presentation (1995). However, the mechanisms of action and resistance of dex are still not clear. Given the shortage of therapeutic options for relapsed ALL, an improved understanding of resistance mechanisms may enable further stratification of dex to prevent unnecessary toxicity, and aid the development of novel therapeutics for this group of patients.

1.8 Mechanisms of dex resistance

Mechanisms of dex resistance within the cell can be broadly grouped into pre-GC receptor mechanisms and post-GC mechanisms (Figure 1.5)(Kofler *et al.*, 2003). Pre-receptor mechanisms include factors such as a change in intracellular dex concentration due to increased levels of steroid binding protein, a change in uptake or efflux by multidrug transporters or altered expression of the 11 β -hydroxysteroid dehydrogenase enzymes (11- β OHSD). Similarly mutation or deletion of the GR and altered levels of GR-related proteins in the cytoplasm and nucleus can also be classed as pre receptor mechanisms. Post-GC receptor mechanisms include defects in the response pathway and inhibitory cross talk or other mechanisms interfering with GC response. Some of these mechanisms are discussed in greater detail below.

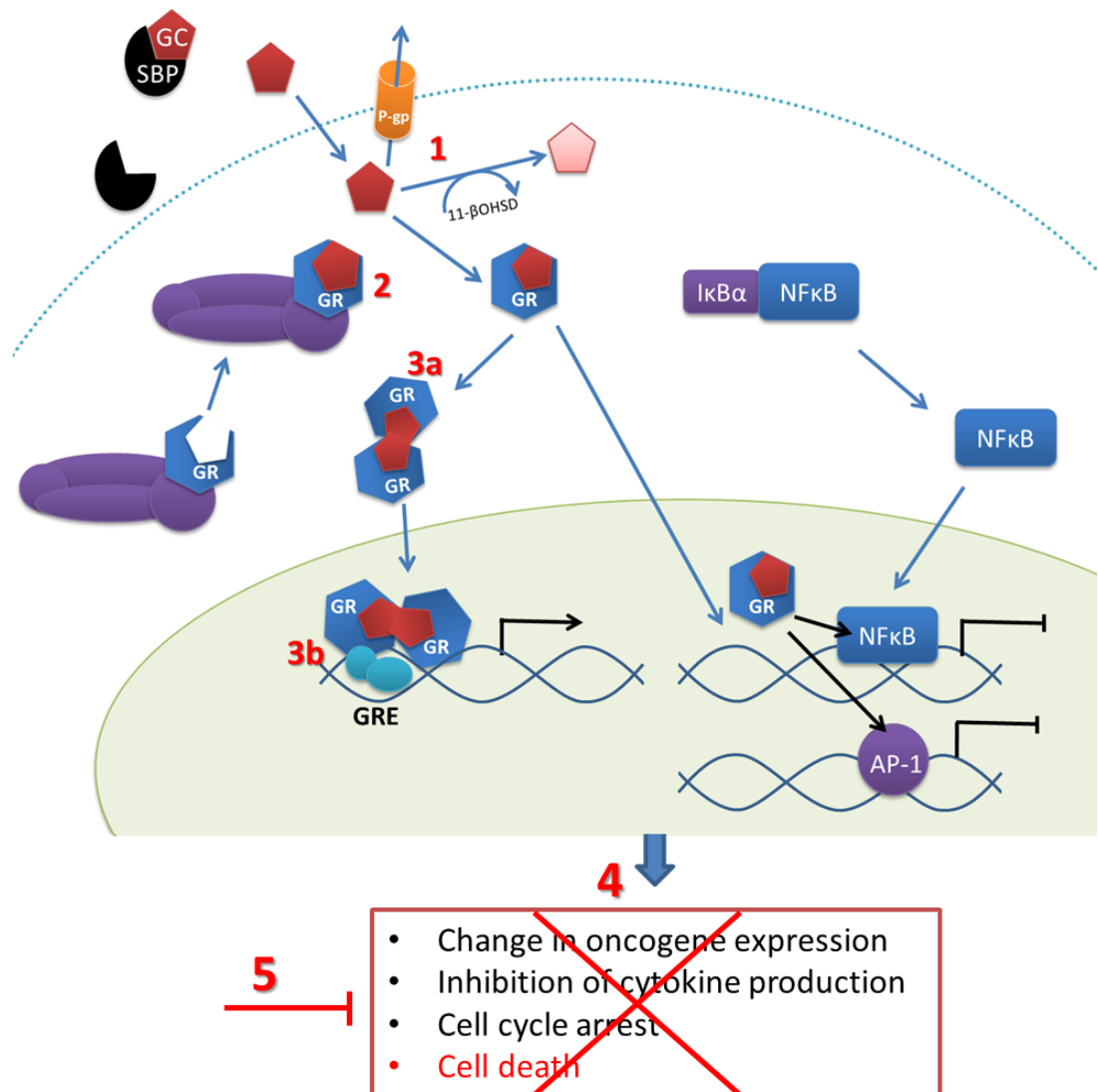


Figure 1.5 Schematic of possible dex resistance mechanisms.

Pre-GC receptor mechanisms: (1) change in intracellular dex concentration due to a) increased levels of steroid binding protein (SBP) b) change in uptake or efflux by multidrug transporters or c) altered expression of 11β-hydroxysteroid dehydrogenase enzymes (11-βOHS). (2) Mutation/deletion of the GR. (3) Altered levels of GR-related proteins in a) the cytoplasm or b) the nucleus. Post-GC receptor mechanisms: (4) defects in the response pathway and (5) inhibitory cross talk or other mechanisms interfering with GC response. Taken from (Jackson *et al.*, 2016).

1.8.1 The glucocorticoid receptor

It has been shown that small reductions in GR protein levels can significantly alter GC response (Costlow *et al.*, 1982; Gruber *et al.*, 2009). Consequently, the effect of GR expression levels on GC sensitivity has been extensively studied. While some studies have reported an association between ligand binding on GC sensitivity and quantitative GR expression (Mastrangelo *et al.*, 1980; Marchetti *et al.*, 1981; Pui *et al.*, 1984; Tissing *et al.*, 2005b), others have not seen such a relationship (Homo *et al.*, 1980; Lauten *et al.*, 2003b). However, it may be that a threshold GR level is needed for GC response and therefore higher levels would confer no increased GC sensitivity. Conversely, a higher GC dose may be able to compensate for a low GR expression, however it is uncertain whether this would be achievable therapeutically (Jackson *et al.*, 2016).

GR levels can be affected by a number of mechanisms, including somatic mutation of *NR3C1*. Although GC resistant cell lines often harbour sequence mutations in *NR3C1*, mutations are rare in patient samples (Irving *et al.*, 2005a; Tissing *et al.*, 2005b). However, at relapse, *NR3C1* deletions have been identified (Hogan *et al.*, 2011; Kuster *et al.*, 2011; Bokemeyer *et al.*, 2014). Approximately 8% of BCP-ALL patients were found to have *NR3C1* deletions in the UKALLR3 trial for relapsed ALL and these were associated with poor outcome (Irving *et al.*, 2016). Interestingly, it was possible to identify an *NR3C1* deletion in the corresponding diagnostic samples of some patients.

Somatic epigenetic changes have been identified in GC resistant ALL cells which may alter GR activity. For example, overexpression of *NLRP3* and *CASP1* have been shown to affect *CASP1*-mediated GR cleavage and consequently GC response (Paugh *et al.*, 2015). GC resistance has been reversed by *CASP1* inhibition in some models, and thus the development of *CASP1* inhibitors may represent an approach for GC re-sensitisation in ALL (Jackson *et al.*, 2016).

1.8.2 Post-GR mechanisms of resistance

The BCL-2 pathway has an important role in apoptotic response of ALL cells following GC exposure, which has prompted its investigation in GC resistance. The pro-apoptotic BCL2L11 (BIM) protein has been shown to be an important mediator of GC-induced apoptosis (Abrams *et al.*, 2004; Lu *et al.*, 2006; Bachmann *et al.*, 2007). BCL2 and MCL1 are important anti-apoptotic proteins which have also been found to be dysregulated

in GC resistance (Miyashita and Reed, 1993; Inoue *et al.*, 2002; Holleman *et al.*, 2004; Ploner *et al.*, 2005; Wei *et al.*, 2006; Stam *et al.*, 2010). BCL2 antagonists have also been shown to re-sensitise T-ALL cells to dex (Bonapace *et al.*, 2010). The role of this family in GC response is exemplified in a recent study, which showed that GC-induced apoptosis was controlled by opposing regulation of BIM and BCL2 in GC sensitive and resistant primary derived ALL cells (Jing *et al.*, 2015).

1.8.3 Pre-GR mechanisms of resistance

The role of proteins associated with the GR as a GC resistance mechanism has also been investigated. Some groups found that in certain GC resistant cell lines, the GC-GR complex failed to translocate to the nucleus (Antakly *et al.*, 1990). However, many others showed no difference in GC-GR nuclear translocation between GC-sensitive and resistant cells in both patient samples and cell lines (Pui and Costlow, 1986).

Importantly, there are a number of potential GC resistance mechanisms that remain unexplored. These include intracellular accumulation of dex, the GR interactome, the developmental stage of leukaemic cells, and whether these differ in sensitive and resistant cells. These will be discussed in the following sections.

1.8.4 The GR interactome

There has been evidence for GR related proteins affecting GR function and therefore causing GC resistance. Some resistant ALL samples have been shown to have deletions in *BTG1* and *TBL1XR1*, which reduced GR signalling (van Galen *et al.*, 2010; Jones *et al.*, 2014). Similarly, activation of AKT1 in T-ALL has been shown to block GR nuclear translocation through direct phosphorylation of the GR (Piovan *et al.*, 2013). However, Bachmann *et al.* (2007) found that in a primary derived xenograft model, GC-sensitive and resistant samples showed analogous GR nuclear translocation, suggesting in the majority of cases that GC resistance is not caused by a lack of nuclear translocation.

However, there is evidence to suggest that the GR posttranslational modifications may be altered in GC resistant ALL cells. The GR interactome comprises of both proteins interacting with the GR, and also post-translational modifications of the GR.

Unpublished data from J. Irving's lab, has shown differences in GR isoelectric point profiles using capillary isoelectric focussing (cIEF, detailed in Appendix E). The

differences were seen in an ALL cell line model of GC resistance, which retains many aspects of primary cells such as GC-induced GR nuclear translocation and up-regulation of transcriptional targets, but does not undergo apoptosis (Nicholson *et al.*, 2010).

Differences in the GR interactome could be attributed to a number of factors. Several studies have identified that changes in, or modulation of, heat shock protein HSP90 (also known as HSP90AA1) affects GR activity (Picard *et al.*, 1990; Cadepond *et al.*, 1991; Cadepond *et al.*, 1993; Segnitz and Gehring, 1997; Lauten *et al.*, 2003a; Shen *et al.*, 2010). Similarly, the ratio of FKBP51 (FKBP5) to FKBP52 (FKBP4), complex immunophilins which play a role in GR signalling, has been implicated in GC resistance in primates (Denny *et al.*, 2000; Davies *et al.*, 2002b). However, other studies found no evidence that HSP90, FKBP51 or FKBP52 are implicated in GC resistance (Lauten *et al.*, 2003a; Tissing *et al.*, 2005a). As most of these studies are well over 10 years old, with recent advances in proteomic technology it would be beneficial to investigate this discrepancy further, as it may uncover novel ways to re-sensitise patients to GCs.

1.8.5 Intracellular dex accumulation

One area of investigation into dex resistance that remains relatively unexplored is whether concentrations of intracellular dex differ between sensitive and resistant ALL cells. This is an important complementary investigation to dex pharmacokinetic studies, as it defines the applicability of the plasma concentration of dex to the leukaemic cells.

Intracellular levels of dex could be affected by several factors. A well-documented mechanism of drug resistance is expression of MDR proteins. Investigation into the effect of expression of MDR1 on outcome in ALL cells have revealed contrasting results. Expression of MDR1 in ALL cells has been associated with a more unfavourable outcome (Dhooge *et al.*, 2002), increased risk of relapse (Goasguen *et al.*, 1996) and lower survival (Casale *et al.*, 2004). However, a number of other groups found no effect of MDR1 expression on outcome (Kakihara *et al.*, 1999; Plasschaert *et al.*, 2003; Balamurugan *et al.*, 2007). There are also other multidrug transporters such as multidrug resistance-associated protein 1 (MRP1) and lung resistance protein (LRP). However, there are limited studies regarding the effect of such transporters in ALL which report contrasting results (Beck *et al.*, 1996; Kakihara *et al.*, 1999)

A change in intracellular dex concentration could also be caused by events such as increased steroid binding protein, or a change in 11 β -hydroxysteroid dehydrogenase enzyme expression (intracellular enzymes which can activate and deactivate dex), which have been shown to be altered in ALL cells *ex vivo* (Sai *et al.*, 2009). Therefore, investigating whether intracellular dex levels differ in GC-sensitive and resistance cells represents an interesting and novel approach that may aid further stratification of dex therapy.

1.8.6 B cell developmental stage

The potential importance of B cell maturation as a mechanism of dex resistance has been highlighted in several papers, including a study by Rhein *et al.* and more recently by Nicholson *et al.* (2007; 2015). Rhein *et al.* used genome wide gene expression analysis of ALL samples and found that persisting blasts following dex exposure had differential expression of genes such as CD11b and CD119, indicating a shift to more mature B cells (2007). Nicholson *et al.* showed that GC resistant cell lines had reduced levels of PAX5 compared to the GC sensitive parent line, PreB697. Furthermore, increasing GC resistance was associated using gene set enrichment analysis to a more mature cell stage. PAX5 mutations are commonly seen in patients with pre-B ALL (Mullighan *et al.*, 2007; Mullighan *et al.*, 2008b; Nebral *et al.*, 2009), although it is not known how this affects their sensitivity to dex.

Cellular development is a highly orchestrated process with single cells maturing into different diverse cell types. Although often thought as comprising of distinct cell types, cell development is a continuum of different cell states, many of which have not yet been identified. A deeper comprehension of cell development, including B cell lymphopoiesis, will enable us to understand better how it is involved in therapy resistance in cancer, but also about cancer development (Bendall *et al.*, 2012).

1.9 Models of ALL

The study of dex resistance can be carried out using a variety of different models. Investigations utilising patient samples is often challenging due to small sample volumes and inability to maintain long term cultures. Two alternative models often used are cell lines and primagraft models.

1.9.1 Cell lines

CCRF-CEM and Jurkat cell lines are commonly used in the study of GC resistance, however these often show a deletion or mutation of the GR as a primary resistance mechanism. This is most likely the result of a mutation in the *MLH1* gene, causing defective mismatch repair (MMR). This leads to increased basal mutation rate, and thus under GC selection, GR mutation commonly occurs (Schmidt *et al.*, 2006b). However, both GR mutation/deletion and deficiencies in MMR are rarely found in patient samples (Matheson and Hall, 2003; Irving *et al.*, 2005a; Tissing *et al.*, 2005c), making the study of resistance in these cell lines only applicable to the few patients cases whose ALL does not exhibit wild type (WT) GR. However, the GC resistant sub clones of the ALL cell line, PreB697, contain two WT GR alleles. This similarity to patient samples makes them an ideal model for the study of dex resistance (Schmidt *et al.*, 2006b).

1.9.2 Patient and primagraft models

Although patient bone marrow samples would be optimal for research, it is often not possible to obtain enough ALL cells to undertake extensive experiments. Primagraft models are popular for the study of GC resistance as it is possible to generate a large number of cells of primary origin, allowing more comprehensive studies to be performed (Schmidt *et al.*, 2006b; Bachmann *et al.*, 2007; Samuels *et al.*, 2014; Jing *et al.*, 2015). Primagraft samples are created by tail vein or intra-femoral injection of primary patient material in immunocompromised mice. Once human cell engraftment is high enough, mice are sacrificed, and ALL cells are harvested from the spleen. Primagraft models are also clinically applicable, as the *in vitro* sensitivity of primagraft samples has also been shown to reflect the clinical outcome of the patients from which they were derived (Jing *et al.*, 2015). They have also been shown to closely resemble the immunophenotype and genetics of the original patient sample (Woiterski *et al.*, 2013).

1.10 Project summary

A variety of approaches are needed to investigate the stratification of dex therapy. It is important to consider systemic dex concentrations, to define the exposure of both cancer cells and normal cells to dex, which can be affected by a number of factors including pharmacogenetics. However, it is also important to define the availability and action of dex within the cancer cell to achieve the best chance of survival. Undefined areas include the effect of intracellular dex, alterations in the GR posttranslational modifications and the B cell maturation state on the sensitivity of ALL cells to dex (Figure 1.6).

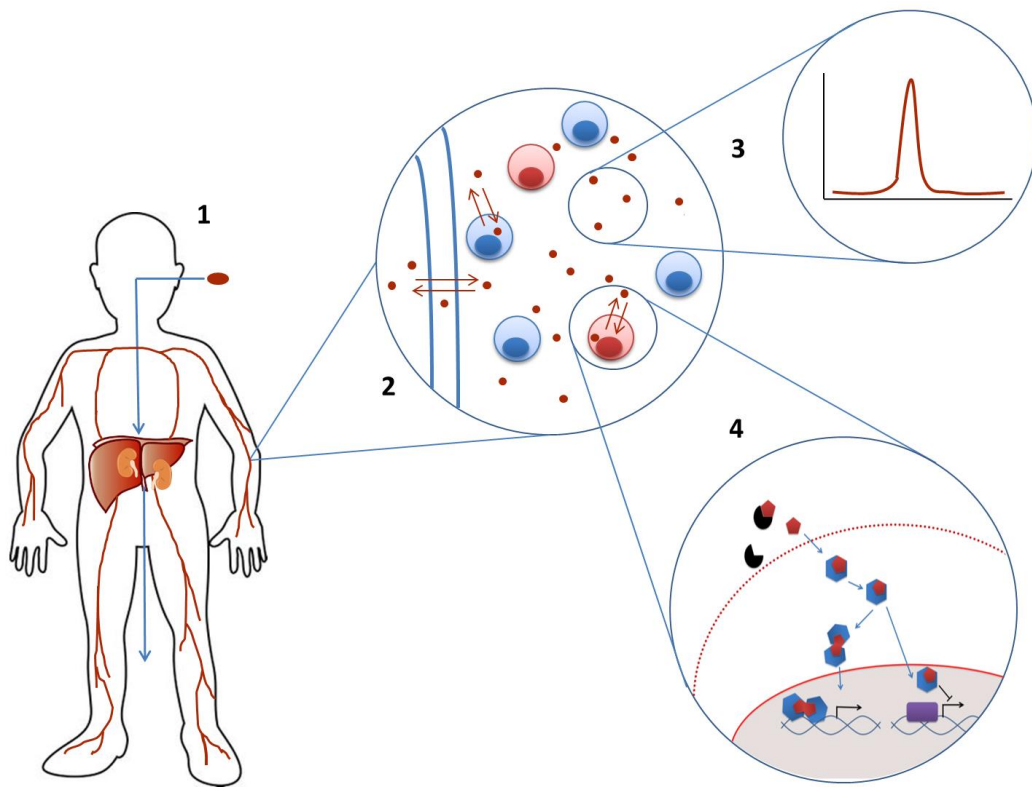


Figure 1.6 Project summary.

1. Dex is taken orally and is metabolised by the liver before it reaches the systemic circulation. Dex is also eliminated renally once in the systemic circulation.
2. Magnification of blood vessel - dex is able to passively diffuse into normal (blue) and cancer (red) cells from the plasma. Dex is also able to diffuse out of the blood vessels into other tissues, causing toxicity.
3. Pharmacokinetic analysis is performed on plasma dex concentrations. This measures the circulating concentration of dex that cells are exposed to, but not how much is in the cancer cells or their sensitivity to dex.
4. Studies are also needed to investigate intracellular levels of dex, and the sensitivity of the cancer cells to this drug. Areas which require further investigation include GR posttranslational modifications and B cell maturation state.

1.11 Aims and Objectives

The main focus of this project is to identify and investigate potential ways to personalise and optimise dex therapy in childhood ALL patients, to ensure optimal exposure whilst limiting unnecessary side effects.

1. To characterise dex pharmacokinetics following short (10mg/m² x 14 days) and standard (6mg/m² x 28 days) treatment, investigating differences in key parameters between the two groups and the effect of age on dex clearance in patients enrolled in the UKALL2011 trial.
2. To investigate differences in dex uptake in GC sensitive and resistant cells *in vitro* and *in vivo*.
3. To investigate whether the GR posttranslational modifications differ between GC sensitive and resistant cells using the novel proteomic technique, capillary isoelectric focussing coupled to immunoassay.
4. To establish whether cell developmental stage affects GC sensitivity, using a combination of mass cytometry and the Wanderlust algorithm.

Chapter 2. Materials and methods

2.1 UKALL 2011 trial

2.1.1 UKALL 2011 study details

The United Kingdom National Trial for Children and Young Adults with Acute Lymphoblastic Leukaemia and Lymphoma 2011 (UKALL 2011) is a national multicentre, phase III, randomised control trial looking to refine treatment for children and young adults diagnosed with acute lymphoblastic leukaemia or acute lymphoblastic lymphoma. The investigation into dex pharmacokinetics being undertaken in this project, forms a sub-study of the UKALL 2011 trial, 'Dexamethasone pharmacokinetic study', detailed in appendix 15 of the UKALL 2011 protocol version 5.0. The National Research Ethics Service Committee (London) approved all study protocols. Informed written consent was taken from all parents, or patients where appropriate.

Clinical trials authorisation number: 2010 – 020924 – 22

Sponsor Protocol Number: RG_09-072

CAS CODE: HM3009

Eudract Number: 2010-020924-22

ISRCTN Reference Number: ISRCTN64515327

2.1.2 Patients and treatment regimen

Patients were recruited to the dex pharmacokinetic sub-study at first diagnosis of ALL upon recruitment to the main UKALL 2011 trial. Patients between the ages of one and 24 years 364 days were eligible for the study. Full exclusion criteria is detailed in Appendix 2. Patients were assigned to a risk category based on factors including age, white blood cell count and cytogenetic subgroup, and were then randomised to receive dex as either short (10mg/m² x 14 days; total dose 140mg/m²) or standard (6mg/m² x 28 days; total dose 168mg/m²) treatment. Dex was administered orally split into two doses per day.

Patient characteristics and clinical parameters were recorded on case report forms (CRFs) on each pharmacokinetic sampling day. Concomitant drugs administered up to seven days before and on sampling days, were also recorded on CRFs. Toxicity and MRD data were gathered centrally by the clinical trial sponsor.

2.1.3 Sample collection

Blood samples (approximately 3ml) were obtained before administration of dex and at 1, 2, 4 and 8 hours post-administration, with the actual time each sample was taken accurately recorded. Samples were taken on one of the first three days (beginning of treatment), and one of the last three days (end of treatment) of induction therapy. Duration of therapy varied between different cohorts, therefore end of treatment sampling day differed between the groups, as shown in Figure 2.1. Plasma was separated by centrifugation for 5 minutes at 2,000 g and 4°C of the whole blood samples at the hospital site and stored at -20°C until transport to Newcastle for analysis. Samples were transported on dry ice by next day delivery.

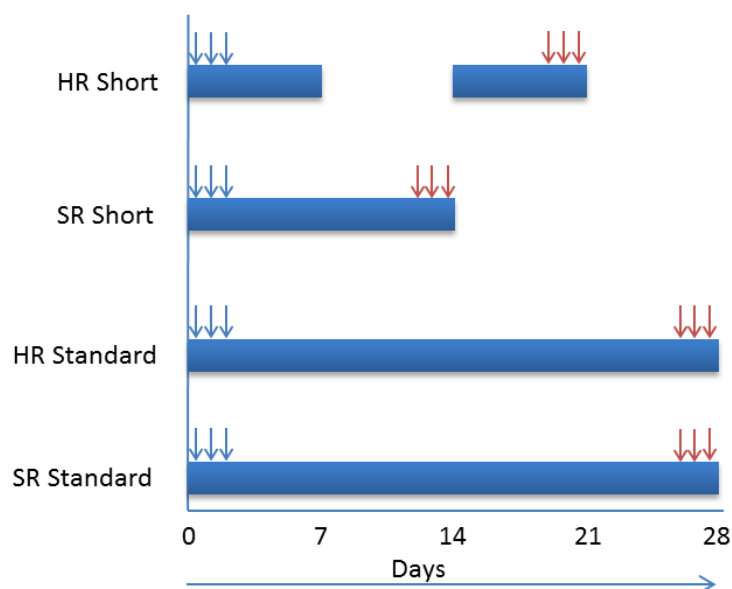


Figure 2.1 Sampling days for the dex pharmacokinetic study.

Samples were taken on one of the first three days of induction therapy (blue arrow) or one of the last three days of induction therapy (red arrow). HR = high risk SR = standard risk.

2.1.4 Bioanalytical method validation

All method validation was performed in accordance with the European Medicines Agency (EMA) 2011 guidelines (reference number: EMEA/CHMP/EWP/192217/2009 Rev.1 Corr.2**) on bioanalytical method validation and is reported as part of my Masters by Research thesis 'Investigating the Clinical Pharmacology of Dexamethasone in Acute Lymphoblastic Leukaemia', Newcastle University, 2014.

2.1.5 Reverse phase liquid chromatography and tandem mass spectrometry (LC/MS)

Chromatography is a technique used for the separation of components in a mixture. In reverse phase liquid chromatography, this is achieved using the hydrophobic characteristics of the compounds. Samples bind to a stationary phase consisting of immobilised hydrophobic ligands, to varying extents depending on their hydrophobicity. The concentration gradient of organic in the mobile phases can then be increased to elute compounds in order of hydrophobicity. The aqueous mobile phase often contains a weak acid to provide ions for the ionisation step in the subsequent mass spectrometry.

After separation, mass spectrometry is used to detect and quantitate compounds, through the measurement of the mass to charge ratio (m/z). In tandem mass spectrometry, compounds are fragmented using collision gas. The mass to charge ratio of both the parent compound and fragments are measured, allowing greater sensitivity. A current is produced, which is turned into a voltage pulse that can be detected by an appropriate software. The data is displayed as a chromatogram. A schematic of this process is displayed in Figure 2.2.

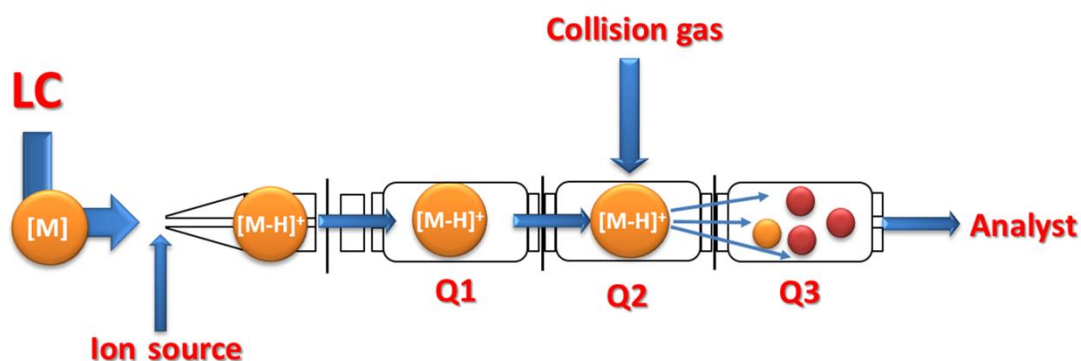


Figure 2.2 Schematic illustrating tandem mass spectrometry.

Compounds separated by reverse-phase liquid chromatography (LC) enter the mass spectrometer and are ionised before being focused into the first module (Q1), where the m/z of the parent compound is measured. The compounds are then fragmented by collision gas in the second module (Q2), before the m/z of the fragments is measured in the third module (Q3). The resultant current is converted into a voltage pulse which is detected by Analyst software.

Equipment:

Perkin Elmer Series 200 system comprising of a micropump, autosampler and peltier column oven	Perkin Elmer (Massachusetts, USA)
API Q Trap 3200 LC/MS	Applied Biosystems (Massachusetts, USA)
Agilent 1260 Infinity system comprising of a column oven, pump, and multi sampler	Agilent (Naldbonn, Germany)
API 4000 LC/MS	Applied Biosystems
Gemini 3 μ C18 110A column (50x3mm)	Phenomenex (Macclesfield, UK)
Guard column with 4x2mm C18 cartridge	Phenomenex

LC/MS conditions:

For experiments up until June 2016, The LC/MS analysis was performed using an API Q Trap 3200 LC/MS attached to a Perkin Elmer Series 200 system. Further LC/MS parameters can be found in Appendix C. After this time, an API4000 LC/MS attached to an Agilent 1260 Infinity system was used. Due to the differences in LC/MS systems, it was necessary to alter the chromatographic method and perform a revalidation. The full LC/MS parameters and validation report can be found in Appendix C and Appendix B, respectively. The flow rate for both systems was 0.3 ml/min. The gradient profile used for both LC/MS systems is shown in Table 2.1.

For all LC/MS analyses, a Gemini 3 μ C18 110A column (50x3mm) fitted with a 4x2mm C18 cartridge was used. Equilibration of either machine was ensured using 10 system suitability sample injections of 1 μ g/ml dex and beclomethasone in a mobile phase mixture of 70% 0.1% formic acid: 30% acetonitrile before each run.

API Q Trap 3200			API 4000		
Total Time (min)	A (%)	B (%)	Total Time (min)	A (%)	B (%)
0.0	60.0	40.0	0.0	100	0
0.5	60.0	40.0	0.5	100	0
1.5	0.0	100.0	7.0	30.0	70.0
2.0	60.0	40.0	9.0	30.0	70.0
5.0	60.0	40.0	10.0	100.0	0
			13	100.0	0

Table 2.1 Gradient profile of mobile phases for the two chromatography methods used.

Mobile phase A: 0.1% (w/w) formic acid. Mobile phase B: 100% Acetonitrile.

2.1.6 Pharmacokinetic analysis

Data were verified independently, and a non-compartmental pharmacokinetic analysis was performed using Phoenix WinNonLin v6.0 (Certara, New Jersey, USA). A non-compartmental analysis was used as it requires fewer assumptions regarding the number of compartments in the physiological system. The use of a compartmental model was also not appropriate given the number of sampling points, as too few

sampling points can lead to reduced accuracy in pharmacokinetic parameters estimates. A population pharmacokinetic model would be of use; because it takes the whole population rather than the individual into account, it enables better predictions to be made about pharmacokinetics in an individual. However, population pharmacokinetic modelling is computationally complex. As recruitment to the dex pharmacokinetic sub-study is still ongoing, the data generated up to this point have been analysed using a non-compartmental analysis with a view to perform a population pharmacokinetic analysis once patient recruitment and sample analysis is completed.

The concentration data were log transformed and the area under the curve (AUC) of the concentration time profile of plasma dex was estimated using the linear trapezoidal rule and extrapolated to 12 hours (AUC_{0-12h}). This length of time was used because the patients are administered dex twice daily. Clearance was estimated using dose, and normalised to patient surface area.

2.1.7 Determination of plasma dex concentrations – extraction method

Analyte sample extraction for LC/MS analysis is an essential process as interfering matrix elements can affect accuracy, precision, limit of detection, and variability of the assay. Occasionally matrix elements can also co elute with the analyte resulting in an inability to integrate the analyte peak. In addition to purifying the samples, the extraction process also leaves the analyte of interest in an aqueous/organic solution appropriate for analysis and solution at a concentration appropriate for detection by LC/MS.

Liquid-liquid extraction was used to separate dex from plasma. Liquid-liquid extraction, sometimes referred to as solvent extraction, uses the difference in solubility of a compound in immiscible liquids. Since dex is lipophilic, addition of a solvent (methyl-butyl-tert-ether) draws the dex into the solvent. This can then be separated from the aqueous plasma liquid containing impurities. An internal standard (beclomethasone) with similar physico-chemical properties to the analyte was used to adjust for variability in the extraction method and measurement by LC/MS.

Reagents and Equipment:

Human plasma	Blood Transfusion Service (Newcastle, UK)
Dexamethasone	Sigma Aldrich (Gillingham, UK)
Beclomethasone	Sigma Aldrich
25% Ammonium hydroxide	FSA laboratory supplies (Loughborough, UK). Diluted in house 1:4 to 6% formic acid
Formic acid	FSA laboratory supplies. 0.1% (w/w) solution prepared in house and filtered using SolVac Filtration apparatus.
Pressure Plus Duran Bottles	FSA laboratory supplies
12ml Pyrex screw-capped centrifuge tubes	FSA laboratory supplies
Borosilicate disposable tubes (10ml)	FSA laboratory supplies
Autosampler inserts 200µl	Jaytee (Kent, UK)
SolVac® Filtration Apparatus	VWR international (Leicestershire, UK)
GHP filter membrane, 0.45µm, 47mm	VWR international
TurboVap LV Evaporator	Zymark, (UK)
Multitube vortexer	Janke and Kuntel, IKA laboratechnik, (Germany)
FLUOStar Omega Plate Reader	BMG Labtech (Aylesbury, UK)

Protocol:

Stock solutions of both dex and the internal standard beclomethasone were prepared in methanol at 1mg/ml and stored at 4°C. The exact concentrations of the dex stocks were determined using the Molar Extinction Coefficient of dex on the Omega FLUOStar microplate reader at 239 nanometers.

Dex calibration curve standards were prepared in blank plasma using the standard stock solution at concentrations of 1- 250ng/ml on the QTrap and 1-100ng/ml on the API4000. Quality control (QC) samples were prepared independently at concentrations of 5, 50 and 250ng/ml on the QTrap, or 2, 45 and 90ng/ml on the API4000. Aliquots were stored at -20°C for use for up to 6 months. The extraction method was adapted from a previously published method by Chen *et al.* (2002) with a change of injection volume from 20µl to 50µl to enhance LC/MS sensitivity. All patient samples were

extracted alongside calibration curve standards in duplicate, and QC samples were included at the beginning and end of each run to ensure intra-assay consistency.

Briefly, standards were processed in duplicate, QCs in triplicate and patient samples were processed once. Plasma samples (500µl) were added to screw-capped tubes and 25µl 400ng/ml internal standard was added to each tube, followed by 0.1ml 6% ammonium hydroxide to alkalise the sample. Methyl-t-butyl ether (3ml) was then added to each tube and samples were vortexed for 3 minutes using the multi-tube vortexer. Tubes were centrifuged for 6 minutes at 3000 g at 15°C to ensure separation of the organic and aqueous layers. The aqueous layer was then flash frozen in a bath of dry ice and methanol, before the organic layer was separated into a fresh labelled borosilicate tube. The samples were then evaporated to dryness at 30°C under nitrogen gas. Samples were stored at this point for up to two weeks at 4°C, or were analysed straight away.

To analyse samples, samples were reconstituted in 200µl of a 30:70 ratio of acetonitrile/0.1% formic acid by vortexing for approximately 20 seconds before being transferred to labelled eppendorf tubes. The eppendorfs were centrifuged at 10,000 g for 3 minutes and 150µl of the supernatant was transferred to an insert. The inserts were placed in the LC/MS and 50µl was injected for analysis as described in 2.1.5. Analyst software (Sciex, Chesire, UK) was used to analyse and quantify chromatograms.

2.1.8 Measurement of dex concentrations in cerebrospinal fluid (CSF)

CSF samples were collected by Dr. Christina Halsey in Glasgow. As CSF is a relatively clean matrix, no extraction was needed. CSF samples were injected onto the API4000 alongside a dex standard curve prepared in artificial CSF (Harvard Apparatus, Cambridge, UK) using the same LC/MS method as described in 2.1.5.

2.2 Cell Culture

2.2.1 Tissue culture reagents and equipment

Media, including RPMI 1640 and Dulbecco's Modified Eagle Medium	Sigma Aldrich (Dorset, UK)
Foetal Bovine Serum (FBS)	Invitrogen Life Technologies (Paisley, UK)
Trypsin	Sigma Aldrich
L-Glutamine	Sigma Aldrich
Penicillin Streptomycin	Sigma Aldrich
Phosphate Buffered Saline	Invitrogen Life Technologies
Trypan Blue	Invitrogen Life Technologies
Neubauer Counting Chamber	Hawksley (Sussex, UK)
Analogue Tube Roller SRT9	Stuart Scientific (Staffordshire, UK)
Bead Bath	Gallenkamp/Weiss (Loughborough, UK)
Class II microbiological safety cabinet	Medical Air Technology Ltd. (Manchester, UK)
FLUOStar Omega Microplate Reader	BMG Labtech
Olympus transmitted light microscope	Olympus (Japan)
Zeiss transmitted light microscope	Carl Zeiss Ltd. (Hertfordshire, UK)

2.2.2 Cell culture media

Cells	Medium	Supplements
PreB697, PreB697 sub lines, REH, CCRF-CEM, CCRF-VCR	RPMI 1640	2mM L-Glutamine 10% v/v foetal bovine serum
Primary patient and primagraft cells	RPMI 1640	2mM L-Glutamine 15% v/v foetal bovine serum 2mM Penicillin streptomycin
MDCKII-WT MDCKII-MDR1 MDCKII-BCRP	Dulbecco's Modified Eagle's Medium	2mM L-Glutamine 10% v/v foetal bovine serum

2.2.3 Cell lines

All cell lines were available from the NICR central cell bank.

Cell line	Origin	Reference
PreB697	Precursor B cell ALL Created from the bone marrow of a 12 year old male at relapse in 1979.	(Findley et al., 1982)
R3F9, R3D11, R3G7, R3C3, R4C10	GC resistant sublines of PreB69. Originally created though limiting dilution in the lab of Prof. R. Kofler. University of Innsbrück, Austria. In brief, cells were cultured in the presence of 10^{-7} M dex for 3-4 weeks of selection culture before individual clones were selected and expanded.	(Schmidt <i>et al.</i> , 2006a)
CCRF-CEM	T cell ALL Created from the peripheral blood of a three year old female at relapse in 1964.	(Foley et al., 1965)
CCRF-VCR	Subline of CCRF-CEM cells express p glycoprotein receptor due to limiting stepwise exposure to vincristine.	(Haber et al., 1989)
REH	Non-B non-T acute lymphocytic leukaemia Created from the peripheral blood of a 15 year old female at relapse.	ATCC website
MDCKII-WT	Wild type polarised Madin-Darby canine kidney cell line.	
MDCKII-MDR1	Wild type polarised Madin-Darby canine kidney cell line transfected with MDR1.	(Schinkel <i>et al.</i> , 1993; Schinkel <i>et al.</i> , 1995a)
MDCKII-BCRP	Wild type polarised Madin-Darby canine kidney cell line transfected with BCRP.	(Pavek et al., 2005)
Kasumi	Acute myeloblastic leukaemia cell line from a 7 year old Japanese male. CD34 positive.	ATCC website
Ramos	B lymphocyte cell line originating from a 3 year old Caucasian male with Burkitt's lymphoma. Expresses IgM strongly.	ATCC website

2.2.4 Primary derived xenograft (primagraft) samples

Primagraft models have been used by a number of groups for the study of GC resistance (Schmidt *et al.*, 2006a; Bachmann *et al.*, 2007; Samuels *et al.*, 2014; Jing *et al.*, 2015) as they provide a high yield of cells from a primary origin, allowing more expansive investigations to be carried out. Primagraft models are also clinically applicable, as cells from primagraft samples closely resemble the leukaemic profile of the sample they were derived from. They have also been shown to reflect the clinical outcome of the original patient (Woiterski *et al.*, 2013; Jing *et al.*, 2015).

Primagrafts used in this work were generated, monitored and euthanised by Ali Alhammer, Zach Dixon, Elizabeth Matheson and Marian Case, who were all trained and held a home office license at the time of this work. NSG (IL-2R common gamma chain null) mice were used as they provide the best platform for leukaemic cell engraftment (Shultz *et al.*, 2005; Shultz *et al.*, 2007). Mice were injected intra-femorally with 1×10^6 patient or primagraft cells. Engraftment was monitored in the peripheral blood of the animals using tail bleeds of around 50 μ l using flow cytometry. Once engraftment of the peripheral blood was greater than 40%, mice were euthanised. The spleens were removed and spleen engraftment was assessed by flow cytometry using anti-human CD10, CD19 and CD34 and anti-mouse CD45 antibodies on a FACSCanto II. The full methods have been previously detailed (Irving *et al.*, 2014). Cells were resuspended in growth media and then used in this project for downstream analyses. Table 2.2 contains details of the primagraft samples used.

Patient	Disease Stage	Gender	Age	Immuno-phenotype	Trial	Current Status	Pres WCC	Initial response	Cytogenetics	Mouse	Date sacrificed	Created by
LK196	2nd Relapse	M	16	BCP-ALL	UKALL 2011	Died post relapse TTR 5 m	315.5	MRD D28 low risk	HeH	JM271	12/07/2016	M.C.
										JM272	12/07/2016	
L578	2nd Relapse	F	3	BCP-ALL	UKALL 97	Died post relapse TTR 44 m	4.1	NK	HeH	AZ7	06/01/2016	A.A. and Z.D.
										AZ9	08/01/2016	
										AZ8	11/01/2016	
L779	Pres	M	5	BCP-ALL	UKALL 2003	DLS 2013	28.1	NK	HeH	JM 151	16/10/2014	E.M.
										JM 150	23/10/2014	
										JM 152	30/10/2014	
										AZ13	18/03/2016	A.A.
L824	Pres	F	16	BCP-ALL	UKALL 2003	Died post relapse TTR 38 m	20	MRD D28 Positive	Failed	AZ21	03/08/2016	A.A.
										AZ22	10/08/2016	
										AZ26	09/06/2016	

Patient	Disease Stage	Gender	Age	Immuno-phenotype	Trial	Current Status	Pres WCC	Initial response	Cytogenetics	Mouse	Date sacrificed	Created by
L825	Pres	F	14	BCP-ALL	UKALL 2003	Died post infection	100	MRD D28 Positive	Failed	JM156	07/11/2014	E.M.
										JM158	28/11/2014	
										JM157	04/12/2014	
										AZ12	09/11/2015	A.A. and
										AZ10	11/11/2015	Z.D.
										AZ17	01/03/2016	A.A.
L829	Pres 1 st Relapse	F	3	BCP-ALL	UKALL 2003	Died post relapse TTR 19 m	11.7	MRD D28 Negative	HeH	AZ2	16/12/2015	A.A and
										AZ3	10/12/2015	Z.D.
										JM254	16/10/2015	E.M.
										JM251	16/10/2015	
										AZ16	24/02/2016	A.A.
										AZ15	02/03/2016	
L897	Pres	M	16	BCP-ALL	UKALL 2003	Died post relapse TTR 19 m	110	MRD High Risk	B-Other	JM149	25/09/2014	E.M.
										JM148	02/10/2014	

Patient	Disease Stage	Gender	Age	Immuno-phenotype	Trial	Current Status	Pres WCC	Initial response	Cytogenetics	Mouse	Date sacrificed	Created by
L910	Pres	F	1	BCP-ALL	UKALL 2003	DLS-2013	35.8	NK	t(1;19)	AZ28	29/04/2016	A.A.
										AZ27	05/05/2016	
L914	Pres	F	7	BCP-ALL	UKALL 2003	DLS-2013	32.3	High MRD D8	HeH	AZ6	21/10/2015	A.A and
										AZ4	04/11/2015	Z.D.
										AZ5	05/11/2015	
L919	1st Relapse	M	2	BCP-ALL	UKALL 2003	TTR 34 m DLS-2014	1.8	NK	B-Other	JM267	05/08/2016	M.C
										JM268	05/08/2016	
	2nd Relapse									AZ20	14/07/2016	A.A.
L920	Pres	F	4	BCP-ALL	UKALL 2003	DLS 2013	NK	Indeterminate	Failed	AZ23	13/07/2016	
										AZ24	21/07/2016	
L4951	Pres	NK	NK	NK	NK	NK	NK	NK	Philadelphia Chromosome positive	AZ25	17/05/2016	
										AZ26	09/06/2016	

Table 2.2 Details of primagraft samples.

Pres=presentation; M=male; F=female; BCP-ALL = B cell precursor ALL; DLS= Date last seen in hospital; TTR=time to relapse; WCC= White cell count at presentation, x 10⁹/L; NK = not known; MRD= minimal residual disease; D8=day 8; D28=day 28; HeH=high hyperdiploidy. Created by: M.C.=Marian Case, A.A.= Ali Alhammer, Z.D.= Zach Dixon, E.M. = Elizabeth Matheson.

2.2.5 Patient samples

Patient bone marrow samples were obtained from children with ALL undergoing treatment at the Royal Victoria Infirmary (Newcastle upon Tyne, UK) through the Bloodwise biobank after project approval. Local ethical guidelines were followed when acquiring parental consent and obtaining samples. Patient details are found in Table 2.3.

Separation of white cells

Separation of white cells was carried out on the day of bone marrow aspiration by Marian Case, Elizabeth Matheson and Lynne Minto using Lymphoprep™ (Nycomed, Oslo, Norway). Briefly, bone marrow aspirates were diluted in a 1:1 ratio with PBS. This mixture was layered over 8ml of lymphoprep before centrifugation at 800 g for 15 minutes with no brake. The mononuclear cell layer was removed and washed twice in PBS. Cells were either used immediately, or cryopreserved for later experimentation.

Patient ID	Sex	Age at pres	Immuno-phenotype	Treatment protocol	Current Status	Pres WCC	Day 8 blast count	Cytogenetics (If available)
LK203	m	4.3	T ALL	UKALL 2011	No relapse/alive	760.3	Not known	Fail
LK209	m	9.2	BCP ALL	UKALL 2011	CNS relapse/alive TTR: 20 months	7.6	0.04 %	t(12;21)
LK213	f	5.3	BCP ALL	UKALL 2011	No relapse/alive	7.4	6.89 %	fail
LK220	m	10.8	BCP ALL	UKALL 2011	No relapse/alive	28.9	Not known	normal
LK221	f	1.7	BCP ALL	UKALL 2011	No relapse/alive	77.8	0.45 %	normal
LK96R	f	1.9	BCP ALL		Relapsed/Alive TTR: 28 months	4.5	0.16 % (day 15)	t(12;21)
L926	f	10.8	BCP ALL	Interim	No relapse/alive	Not known	0.49 %	Not known
L943	m	2.6	BCP ALL	Interim	No relapse/alive	Not known	0.12 %	Not known
L919	m	2.7	BCP ALL	UKALL 2003	Relapsed/Alive TTR: 1 st 23 months, 2 nd 21 months after 1 st)	1.5	Not known	B other
L890	m	5.8	BCP ALL	UKALL 2003	No relapse/alive	25	18.71 %	HeH
L705	m	10.8	T ALL	UKALL 2003	Relapse/alive TTR: 14 months	733	1 %	HeH

Patient ID	Sex	Age at pres	Immuno-phenotype	Treatment protocol	Current Status	Pres WCC	Day 8 blast count	Cytogenetics (If available)
L715	m	14.3	BCP ALL	UKALL 2003	No relapse/alive	153	>90 %	HeH
L723	f	12.0	BCP ALL	UKALL 2003	No relapse/alive	53.3	Reduced blast count	46,XX,del(6)(q1?),add(19)(p13)
L733	f	2.4	BCP ALL	UKALL 2003	No relapse/alive	9	<5 %	46,XX,del(12)(p1?2)
L809	m	16.7	T ALL	UKALL 2003	No relapse/alive	319	74 %	46,XY,del(6)(q13q23)
L826	m	0.7	BCP ALL	Not on trial	No relapse/alive	346	Not known	t(4;11)
L837	f	6.0	Pre-B ALL	UKALL 2003	Relapse/alive TTR: 54 months	125	40 %	t(12;21)
L835	m	4.8	Pre-B ALL	UKALL 2003	No relapse/alive	7.8	Not known	HeH
L940	m	2.6	BCP ALL	Interim	No relapse/alive	Not known	Not known	Not known
LK268	m	6.6	BCP ALL	UKALL 2011	No relapse/alive	5.6	3.73 %	t(12;21)
LK269	m	18.3	BCP ALL	UKALL 2011	No relapse/alive	8.4	0.83 %	HeH

57

Table 2.3 Details of patient samples.

M=male F=female; TTR = time to relapse; HeH = high hyperdiploidy; WCC = $\times 10^9/L$.

2.2.6 Cell line maintenance and culture

2.2.6.1 Thawing viable cells

Vials were removed from the liquid nitrogen and rapidly thawed at 37°C. The appropriate medium (5ml) was added slowly to the cells before centrifugation at 230 g for 5 minutes. The medium was aspirated, and the cell pellet was resuspended in the appropriate medium and placed in a tissue culture flask.

2.2.6.2 Cell counting and viability assessment

Trypan Blue exclusion was used to enumerate cells and assess viability. Cells were mixed in a 1:1 ratio with 0.4% trypan blue and were then counted with the aid of an Improved Neubauer counting chamber. Trypan blue can enter dead or damaged cells whereas healthy cells exclude the dye, therefore non-viable cells are blue and viable cells are not blue. Viability was calculated as a percentage of non-blue cells of the total number of cells (blue and non-blue).

2.2.6.3 Cell culture

All suspension cells were grown in suspension at a density of $0.5-2 \times 10^6$ /ml. Adherent cells were cultured as a monolayer and were passaged at around 80% confluence, using 1 x trypsin-EDTA. Primagraft cells were cultured in suspension culture.

Cells were kept in a humidified tissue culture incubator at 37°C, 5% CO₂ and all cell lines were regularly screen for mycoplasma using MycoAlert® (Lonza, UK). All cell lines were authenticated externally by short tandem repeat profiling at LCG.

2.2.6.4 Cryopreservation of cells

Frozen stocks were made from cells that were in the exponential growth phase. Cells were counted and viability assessed, as described above. Cells were pelleted and resuspended at a concentration of 5×10^6 cells/ ml in freeze mix (10% (v/v) DMSO in FBS) and then aliquoted in 1ml volumes into cryovials. The cryovials were placed in a polystyrene box filled with cotton wool and placed in the -80°C freezer for slow freezing, before being transferred to liquid nitrogen after 2-14 days.

2.3 Drug sensitivity assessment using Alamar Blue

The cytotoxicities of various drugs were determined using Alamar Blue (rezasurin) assays. In these assays, rezasurin (non-fluorescent blue) is reduced in viable cells to resorufin (fluorescent red) (Nakayama *et al.*, 1997). Fluorescence is therefore proportional to the number of metabolically active cells.

Reagents

Alamar Blue	Thermofisher Scientific
Dexamethsone	Sigma Aldrich
Vincristine	RVI Pharmacy (Newcastle, UK)
Actinomycin D (act D)	Sigma Aldrich

Protocol

Stocks of drugs were prepared in ethanol (dex and vincristine) or methanol (act D). Subsequent dilutions were made with control vehicle (CV, RF10 at 0.1% ethanol/methanol) to give final concentrations ranging from 0.1nM to 10,000 nM.

100µl of cells at a density of 3×10^5 cells/ml for suspension cell lines, 6×10^4 for adherent cells, or 4×10^6 cells/ml for primagraft/patient cells, were dispensed into each well of a 96 well plate. Suspension cell lines, primagraft and patient cells were incubated in triplicate with drug concentrations or CV for 96 hours. This incubation length was chosen as it is approximately three doubling times for the cell lines (mean doubling time 33.9 ± 5.3 (SD), data from L. Nicholson's PhD thesis). This incubation time is also the most appropriate for primary cells, as several studies in independent patient groups have shown that incubation of primary cells for 96 hours with dex *in vitro* is predictive of the patient's clinical outcome (Kaspers *et al.*, 1996; Hongo *et al.*, 1997; Kaspers *et al.*, 1997; Den Boer *et al.*, 2003; Frost *et al.*, 2003). Adherent cell lines were incubated for 24 hours prior to the addition of drug to allow cells to adhere to the 96 well plate, before also being incubated in triplicate with drug concentrations or CV for 96 hours. Dex stability in RF10 over 96 hours in a humidified incubator (37°C 5% CO₂) was confirmed using LC/MS. Dex peak area of three replicates for each time point was consistent from 0-96 hours with a coefficient of variation of 4.7%. 20µl of

Alamar blue was then added to each well, and left for a further 3-4 hours for cell lines, or 5-6 hours for primagraft/patient cells. Plates were read at 570nm excitation and 585nm emission using a FLOUstar Omega plate reader and quantified using Omega data analysis software. Results were reported as a percentage of the CV treated cells. Non-linear regression curves were used to calculate GI₅₀ (dose causing 50% growth inhibition) values using GraphPad Prism software.

2.4 Intracellular accumulation of dex measured by LC/MS

Protocol

Suspensions cells lines and primagraft cells were seeded at 1×10^6 cells/ml. 6.5 ml cells were then treated with CV or clinically relevant concentrations of dex, vincristine or act D ranging from 100-1,000nM over 4 hours. Adherent cell lines were seeded at 1×10^5 cells/well in 6 well plates and left for 24 hours to allow cells to adhere to the plates. Cells were then treated with drug as detailed for suspension cells.

After 4 hours, the media was removed and cells were washed twice with ice cold PBS. In the case of the dex assays, cells were lysed with methanol spiked with 4ng/ml beclomethasone, as an internal standard. In the case of vincristine and act D, methanol was used without beclomethasone. Centrifugation at 16,000 g ensured removal of cell debris and complete cell lysis. Samples were then evaporated to dryness using TurboVap LV evaporator and reconstituted in a mixture of mobile phase for analysis. Dex: 70:30 0.1% formic acid and acetonitrile. Vincristine: 50:50 0.02M ammonium acetate and methanol. Act D: 50:50 1% acetic acid pH4, and methanol.

Calibration curves were prepared in duplicate in the same mobile phase mixture ranging from 0 to 100ng/ml for dex 0-20ng/ml for act D and vincristine, and run at the start of each assay. Low, medium and high standards were also included at the end of the run. The LC/MS method was the same as described in 2.1.7 with adaptations shown in Table 2.4. The equation of the standard curve was calculated in Microsoft Excel, using linear through zero regression. Data were normalised using the internal standard, if used, and drug concentrations in cell lysates were back calculated using the linear regression standard curve equation.

	Dex	Act D	Vincristine
LC/MS	API4000 LC/MS (Applied Biosystems, California, US) attached to a series 200 micropump, autosampler and peltier column oven (All Perkin Elmer, Beckonsfield, UK)	API4000 LC/MS (Applied Biosystems, California, US) attached to a series 200 micropump, autosampler and peltier column oven (All Perkin Elmer, Beckonsfield, UK)	API4000 LC/MS (Applied Biosystems, California, US) attached to a series 200 micropump, autosampler and peltier column oven (All Perkin Elmer, Beckonsfield, UK)
Column and Guard Column	Gemini 3 μ C ₁₈ 110A column (50 x 3mm) fitted with a C ₁₈ (4 x 2mm) security guard cartridge (Phenomenex, Cheshire, UK)	Luna 3 μ C ₈ Mercury column (20 x 4mm) fitted with a C ₈ (4 x 2mm) security guard cartridge (Phenomenex)	Luna 3 μ C ₈ (2), (50 x 2mm) fitted with a C ₈ (4 x 2mm) security guard cartridge (Phenomenex)
Mobile Phase A	0.1% (w/w) formic acid	1% acetic acid pH4	0.2M Ammonium Acetate pH 5
Mobile Phase B	100% Acetonitrile	100% Methanol	100% Methanol
Flow Rate	0.3ml/min	0.5ml/min	0.4ml/min
Injection Volume	50 μ l	50 μ l	50 μ l

Table 2.4 LC/MS details for intracellular accumulation experiments.

2.4.1 Optimisation of LC/MS assay for small cell numbers

As there are a limited number of cells available for experimentation in patient samples, the method was optimised for use with small cell numbers. Optimisation was performed using PreB697 cells. Cells were seeded at decreasing densities ranging from 2.2×10^6 cells/ml to 0.1×10^6 cells/ml (total of 14×10^6 and 0.65×10^6 cells respectively) before incubation with 500nM dex for 4 h at 37°C. Extraction was performed as described above.

2.5 Intracellular accumulation measured by fluorescence activated cell sorting (FACS)

Flow cytometry allows analysis of multiple aspects of single cells, such as size, cell type and complexity. It consists of three main systems; the fluidics, lasers and optics, and electronics systems. The fluidics system controls the flow of particles or cells through the laser beam using hydrodynamic focusing, and the removal of waste. The optics system uses lasers and detectors to determine certain physical characteristics of the cell and generate fluorescence. For example, beams of lasers directed at the flow of cells scatter when they hit the cells. This is measured to give forward scatter, a measure of the size of the cell, and side scatter, a measure of the granularity of the cell. These measurements allow differentiation between different cell types in a heterogeneous population.

Fluorophores such as fluorescein isothiocyanate (FITC) can be conjugated to antibodies and compounds to further differentiate between cells, or assess different characteristics of the cell. When these fluorescent markers are excited by lasers, they emit light at specific wavelengths. Multiparametric analysis can be achieved by using different fluorophores with different excitation and emission wavelengths. However, compensation is required to adjust for overlap of emission spectra. Optical filters and beam splitters direct the fluorescent and scattered light to detectors, where it is converted into an electrical signal.

Reagents and equipment

Dexamethasone-fluorescein (Dex-FITC)	Thermo Fisher Scientific. Powder diluted to 10mM solution in ethanol in house and stored at 4°C.
Dulbeccos PBS 10x concentrated without Ca and Mg (diluted in house)	Sigma Aldrich
Bovine Serum Albumin Fraction V (BSA) 0.2% PBSA	Sigma Aldrich 0.2% BSA (w/v) in 1 x Dulbecco's PBS, prepared in house, and sterile filtered.
BD FACStow™ Sheath Fluid, BD FACSRinse Solution, BD FACS Clean solution.	BD Biosciences (Oxford, UK)
BD CaliBRITE™ 3 beads (containing unlabelled beads, FITC labelled beads and PerCP labelled beads.	BD Biosciences
BD CaliBRITE™ APC beads	
BD Cytometer Setup and Tracking beads	BD Biosciences
Falcon tubes (5ml capped)	Scientific laboratory supplies ltd, (Nottingham, UK)
FACSCalibur™	BD Biosciences
FACSCanto™	BD Biosciences
BD CellQuest Pro™ Software	BD Biosciences
BD FACSDiva™ Software	BD Biosciences
BD FACSComp™ software	BD Biosciences

2.5.1 FACSCalibur calibration

The FACSCalibur™ was calibrated once a week using BD CaliBRITE™ beads with FACSComp™ software. One drop of unlabelled beads and one drop of APC beads were added to a 5ml Falcon tube containing 1ml FACSFlow™. The tube was mixed by inversion and then installed on the machine for the first stage of calibration. A further 2ml FACSFlow™ was added to the tube, along with one drop of PerCP, one drop of FITC, and one drop of PE labelled beads. The tube was once again mixed by inversion and installed onto the machine. FACSComp™ results were saved as electronic files.

2.5.2 Method development

An assay published by Kowalik et al. (2013) for the quantification of GR levels in mouse thymocytes using dex-FITC was optimised for use in ALL cells.

First, the incubation time to give optimal fluorescence intensity was investigated. PreB697 cells (5×10^5) were incubated with 500nM dex-FITC or CV for 5-60 minutes at 4°C, before washing twice and analysis on FACScalibur. From this, an incubation time of 45 minutes was chosen. The method was then tested on REH and PreB697 cell lines, and was deemed to be a measure of intracellular dex rather than GR levels, as REH cells, which do not express GR (Grausenburger *et al.*, 2016), had an intracellular FITC signal. Therefore further optimisation was performed.

The effect of temperature was measured by incubating 5×10^5 PreB697 cells with dex-FITC for 45 minutes at 4 or 37°C. The number of washes for optimal removal of extracellular dex was studied; cells were washed once, twice or three times with ice cold PBS after incubation with dex-FITC or CV before analysis on FACScalibur.

2.5.3 Final flow cytometry method

Two aliquots of 5×10^5 cells were transferred to falcon tubes. Both aliquots were pelleted; one was resuspended in 500nM dex-FITC in PBS, and the other in CV to discount any solvent effect (0.05% ethanol in PBS). Cells were incubated in the dark at 37°C in a humidified incubator for 45 minutes. Cells were then washed twice in ice cold PBS before being resuspended in 500µl fresh ice cold PBS for immediate analysis on the FACScalibur machine. The geometric mean of the control vehicle and dex-FITC treated cells was assessed. The ratio of the geometric means was assessed to determine the mean fluorescence intensity (MFI).

2.6 Capillary-based isoelectric focusing immunoassays

2.6.1 Cell lysis

In a living cell, post translational modifications are an essential way of governing how the cell functions and responds to exogenous stimuli, including drug responses. It is important to maintain protein modifications during cell lysis to enable analysis of cellular responses.

Reagents

Bicine/CHAPS lysis buffer (1ml)	952µl Bicine/CHAPS buffer	ProteinSimple (Oxford, UK)
	8µl Benzoylase nuclease	Merck (Watford, UK)
	10µl Phosphatase inhibitor buffer 2	Sigma Aldrich
	10µl Phosphatase inhibitor buffer 3	Sigma Aldrich
	10µl Protease inhibitor cocktail	Sigma Aldrich
	10µl 100mM Sodium orthovanadate	Sigma Aldrich
	1µl 500mM NaF	Sigma Aldrich
Bicine/sucrose wash buffer	20mM Bicine	Sigma Aldrich
	200mM Sucrose.	Sigma Aldrich

Protocol

Approximately 1.5×10^7 cells were centrifuged at 500 g for 5 minutes. The cells were washed once in 5 ml bicine/sucrose wash buffer. 50µL of bicine/CHAPS lysis buffer was added to each pellet on ice. Pellets were incubated on ice with bicine/CHAPS lysis buffer for one hour, with regular vortexing.

Cell debris was removed by centrifugation at 20,000 g for 15 minutes at 4°C. The supernatant was then transferred immediately to two clean, cold microfuge tubes and snap frozen on dry ice. Aliquots were stored at -80°C until analysis. One aliquot was thawed and used for protein determination concentration and the other was used for charge analysis (detailed in 2.6.5).

2.6.2 Protein concentration determination

It is important to determine the protein concentration of samples so that an equal amount of protein can be analysed in size and charge assays. Lysate protein concentrations were determined using the Pierce BCA (bicinchoninic acid) Protein Assay Kit (Thermo-Fisher).

The assay uses the principle that proteins cause reduction of Cu^{2+} to Cu^+ in an alkaline environment. The Cu^+ reacts with the BCA to generate a purple complex, which has a linear absorbance at 562nm. This colour change is proportional to the amount of protein in the sample.

Reagents

Reagent A	Sodium carbonate, sodium bicarbonate, bicinchonic acid and sodium tartrate in 0.1M sodium hydroxide
Reagent B	4% cupric sulphate
Working Reagent	Reagents A and B in a ratio of 50:1
Bovine Serum Albumin	Diluted in house with dH_2O to form a standard curve

Protocol

The BCA assay was executed according to manufacturer's instructions. Lysates were diluted 1:10 in dH_2O . 10 μl of each diluted sample and standards were loaded into a 96 well flat bottomed plate in quadruplicate. 190 μl of working reagent was then added to each well of the plate before incubation at 37°C for 30 minutes. The absorbance was measure on a FLUOStar Omega Microplate Reader. A standard curve was constructed using Omega software and protein concentrations were determined.

2.6.3 Western blotting

Western blotting is a technique that allows qualitative and semi-quantitative analysis of protein expression. Cell lysates are denatured through the addition of beta mercaptoethanol and sodium dodecyl sulphate (SDS) to the loading buffer and heating. Denatured cell lysate samples in Laemmli buffer are first separated using gel electrophoresis, which separates macromolecules based on their size. The pore size in the gel regulate how quickly proteins travel through the gel. Proteins subsequently need to be transferred to a membrane (PVDF or nitrocellulose), with a high protein affinity, to allow immunodetection of proteins. This process is achieved through sandwiching the gel with the membrane between layers of filter paper and sponge. An electric field is then applied across the gel and the membrane, allowing the protein to move from the gel to the membrane.

Proteins are then detected by immunodetection. As the membrane has a high capacity for protein binding, empty sites on the membrane need to be blocked using a buffer with a high protein content (5% w/v skimmed milk powder in TBS-Tween (TBS-T)). A primary antibody is used that is specific for the protein of interest. The primary antibody is followed by a secondary antibody raised against the immunoglobulins the primary antibody is produced in. The secondary antibody is conjugated to horseradish peroxidase (HRP). A chemiluminescence reaction is then performed using Amersham ECL prime. In a multistep reaction, the oxidation of luminol is catalysed by HRP, which produces intermediates such as luminol endoperoxide. Peroxide interacts with these intermediates to produce aminophthalate and chemiluminescence. Light emission is proportional to the amount of protein and can detected by exposure to x-ray film.

Reagents and Equipment

Precision Plus Protein™ Dual Color Standard	BioRad (Hertfordshire, UK)
10% Tris-Glycine Gels	BioRad
PVDF Membrane	Biorad
3mm Filter Card	Thermo Fisher (Paisley, UK)
Amersham ECL Prime	Amersham Life Sciences (Buckinghamshire, UK)
BioRad Power Pac 200	BioRad
Fujifilm corporation RX MIF sheet X-Ray film	FSA laboratory supplies
Fuji X-Ray film processor RG11	Fuji Photo Film co. Ltd. (Tokyo, Japan)
Gyro-Rocker SRT9	Fisher Scientific (Loughborough, UK)
Mini-PROTEAN 11 Electrophoresis Cell	BioRad
Mini Trans-Blot Electrophoretic Transfer Cell	BioRad
Stirrer UC151	Bibby Scientific Limited (Staffordshire, UK)

Buffers (all chemicals from Sigma (Dorset, UK) unless otherwise stated)

Laemmli Buffer	62.5mM Tris-HCL, pH 6.8 4% SDS 20% (v/v) glycerol 5% 2 mercaptoethanol 0.0005% bromophenol blue
Electrode Buffer	41.2mM Tris 192mM Glycine 0.1% (w/v) SDS
Transfer Buffer	10mM CAPS, 10% (v/v) methanol
Tris-Buffered Saline with Tween (TBS-T)	0.154M NaCl 0.05M Tris 0.5% (v/v) Tween-20
Blocking Buffer	5% (w/v) dried skimmed milk powder (Marvel, Lincolnshire, UK), in TBS- T

Protocol

Protein samples were prepared to a concentration of 1mg/ml in laemmli buffer and denatured by heating to 100°C for 5 minutes. In each BioRad mini gel, 5µl of marker was loaded into the first well followed by 12µl of each sample in subsequent wells. An empty well was left between primagraft and patient samples to account for variation in accuracy of the protein estimation due to red cell contamination. Proteins were separated for 30 minutes at a constant voltage of 220V.

Mini-blot equipment was used for electroblotting. All components of the electroblotting sandwich were soaked in transfer buffer prior to assembly. The PVDF membrane was soaked in methanol for 20 seconds before transfer buffer. The sandwich was constructed in cassettes in the following order: sponge, two filter cards, gel, membrane, two filter cards and a final sponge. Bubbles were removed using a stripette as a rolling pin. Proteins were transferred for 1 hour at 100V. An ice pack and stirrer were placed in the tank, and the tank was placed on a stirrer to prevent the tank overheating.

The PVDF membrane was then blocked for 40 minutes in blocking buffer. Primary antibody probing was performed as per Table 2.5 on a rocking platform. Three rinses of the membrane were then performed in TBS-T followed by a 12 minute wash in TBS-T on a rocking platform. Next, the membrane was incubated with the relevant secondary antibody for 30 minutes at room temperature on a rocking platform. The membrane was then washed 4 times for 5 minutes in TBS-T.

ECL prime western blotting detection reagents were used to detect membrane HRP, following manufacturer's instructions. Reagent A and reagent B were mixed in a ratio of 1:1 and applied to the membrane. The membrane was incubated with this mixture for 5 minutes at room temperature. Excess ECL reagent was removed by blotting on paper towel before the membrane was wrapped in Saran Wrap (Thermo Fisher). The membranes were then exposed to x-ray film in an autoradiography cassette for an appropriate duration to give visible bands. The x-ray films were developed using the Fuji X Ray film processor.

	Protein	Molecular Weight (kDa)	Catalogue Number	Species and clonality	Supplier	Probing Conditions	Dilution	Dilution of Secondary Ab
Primary	GR	~95	Sc-1003	Rabbit	Santa Cruz	1 hour, RT	1:500	1:2500
	GR	~95	Ab3579	Rabbit	Abcam	1 hour, RT	5µg/ml	1:2500
	GR	~95	D8H2	Rabbit	Cell Signalling	Overnight, 4 °C	1:1000	1:2500
	GR	~95	D6H2L	Rabbit	Cell Signalling	Overnight, 4 °C	1:1000	1:2500
	pGR (s211)	~95	4161S	Rabbit	Cell Signalling	Overnight, 4 °C	1:2000	1:2500
	Alpha tubulin	50	T6074	Mouse	Sigma-Aldrich	1 hour, RT	1:500,000	1:4,000
Secondary	Rabbit-Ig	-	P0448	Goat	Dako (Glosturp, Denmark)	30 minutes, RT	-	-
	Mouse-Ig	-	P0447	Goat	Dako	30 minutes, RT	-	-

Table 2.5: Antibodies and probing conditions.

Dilutions were made in blocking buffer except GR (Santa Cruz) which was diluted in 5% bovine serum albumin (w/v) in TBS-T. RT=room temperature.

2.6.4 Western blotting under non denaturing conditions

A western blot under non denaturing conditions assesses protein in their native state. The original protein conformation is maintained by avoiding denaturation of proteins in the sample preparation stage. For example beta mercaptoethanol and SDS are not used and samples are not heated prior to separation on the polyacrylamide gel.

Reagents

All equipment and reagents used were the same as in the western blot detailed in 2.6.3. The sample buffer and running buffer differed, and are detailed below.

Sample buffer	6.06 Tris Base in 100ml di H ₂ O pHd to 6.8 5ml Tris-HCl 4 ml Glycerol 11 ml DiH ₂ O Per ml add 50ul bromophenol blue
Running Buffer	3.0g Tris Base 14.4g glycine 1L H ₂ O

Protocol

The protocol was as detailed in 2.6.3, with a difference in gel separation conditions; 12.5µg protein was loaded onto the gel and the gel was run for 40 minutes at 200V.

2.6.5 ProteinSimple Peggy Sue analysis of the GR posttranslational modifications

NanoPro Technology has been developed by ProteinSimple, and comprises automated capillary-based immunoassays. In these experiments, separation by charge has been used, although size separation is also possible. Proteins are separated by isoelectric focussing in capillaries; voltage is applied across the capillary and proteins and standards concentrate at their isoelectric points (PI), the pH where net electrical charge is neutral. Ultraviolet light activates photoactive capture chemistry which is coated on the walls of the capillaries, cross linking the samples to the capillary wall. Proteins are washed and probed with primary, secondary and tertiary antibodies. Addition of luminol and peroxidase causes a chemiluminescent reaction which is captured by a camera within the machine. The data is collected in Compass Software

(ProteinSimple) and can be displayed as an electropherogram or a digital image of the capillaries.

This work was done in the Whetton Lab in the Wolfson Molecular Imaging Unit at Manchester University. Support was kindly provided by Rognvald Blance, also from Manchester University.

Reagents

All reagents were purchased from ProteinSimple (Oxford, UK).

Protocol

For each run, the volumes of reagents were calculated based on the number of samples and the initial and desired protein concentration of each sample.

The DMSO inhibitor mix was first mixed with the sample diluent. Following this, the ladder (pI standard ladder 3) and premix (5-8 nested, cat number 040-972) were combined, and mixed by pipetting. The DMSO and sample diluent mixture were added to the lysate to dilute the sample to the desired concentration. The lysate mixture was then combined with the ladder and premix and mixed by pipetting.

The antibodies (primary, secondary and tertiary) were diluted using antibody diluent to achieve the desired concentrations. The luminol and peroxidase were mixed in a ratio of 1:1 and all components were pipetted into the ProteinSimple plate. An example of the plate layout can be seen in Figure 2.3. All samples were run in duplicate for the assay validation and in triplicate for sample analysis.

	1	2	3	4	5	6	7	8	9	10	11	12
A	Sample 1			Sample 2			Sample 3			Sample 4		
B	Sample 5			Sample 6			Sample 7			Sample 8		
C												
D	Biotinylated anti-Protein Simple, 1:100											
E	streptavidin-HRP Protein Simple, 041-106 1:100											
J	luminol/oxidase 1:1											

Figure 2.3 Example layout of ProteinSimple plate.

Samples were run in duplicate for validation, and triplicate for sample analysis. Up to 8 rows of samples can be run simultaneously. The blue row contains the primary antibody. The dark green row contains the secondary antibody, which was always diluted 1:100 in sample diluent. The light green row contains the tertiary antibody (streptavidin-HRP), which was always diluted 1:100 in sample diluent. The yellow row contains the luminol and peroxidase, mixed in a ratio of 1:1. This must always be at least 2 rows away from the tertiary antibody.

The final primary antibody concentration used was 1:25 and the lysate concentration was between 0.3 and 0.8mg/ml depending on sample type and availability of sample for patient and primagraft samples. The machine settings for all runs can be found in Table 2.6.

Sample:	Load time (secs)	25	
Separation:	Separation profile	Power 1 Step	
	Power (μ W)	21000	
	Time (mins)	40	
	Standards exposure time (secs)	1	
Immobilisation:	Time (secs)	100	
	Washes	2	
	Wash load time (secs)	20	
	Wash soak time (secs)	150	
Primary antibody:	Time (mins)	120	
	Load time (secs)	2	
	Washes	2	
	Wash load time (secs)	20	
	Wash soak time (secs)	150	
Secondary antibody:	Time (mins)	60	
	Load time (secs)	2	
	Washes	2	
	Wash load time (secs)	20	
	Wash soak time (secs)	150	
Streptavidin-HRP:	Time (mins)	10	
	Load time (secs)	2	
	Washes	2	
	Wash load time (secs)	20	
	Wash soak time (secs)	150	
Detection:	Wash load time (secs)	2	
	Detection profile	6 exposures	30 secs
			60 secs
			120 secs
			240 secs
			480 secs
			960 secs

Table 2.6 Peggy Sue machine settings for glucocorticoid receptor analysis.

2.7 Mass cytometry

Mass cytometry is a new technique that allows measurement of more than 40 parameters in a single cell simultaneously, a feat not possible with techniques such as flow cytometry. Mass cytometry is inductively coupled plasma mass spectrometry (ICP-MS) coupled to single cell analysis (Bandura *et al.*, 2009). Cells are labelled with antibodies conjugated to rare earth metals such as lanthanides as reporters (Lou *et al.*, 2007; Majonis *et al.*, 2010). The unconjugated antibodies are the same as those used in flow cytometry (Bendall *et al.*, 2012; Takahashi *et al.*, 2017). Although it is not currently possible to measure light parameters such as forward and side scatter, rhodium or iridium can be used to provide information about DNA content (Ornatsky *et al.*, 2008b) and chelated metals or platinum metals for viability (Ornatsky *et al.*, 2006; Bendall *et al.*, 2011; Fienberg *et al.*, 2012; Newell *et al.*, 2012). Furthermore, the addition of normalisation beads can reduce the impact of fluctuation in machine performance and also improve quantitative analysis between instruments (Finck *et al.*, 2013; Tricot *et al.*, 2015). This process is illustrated in Figure 2.4.

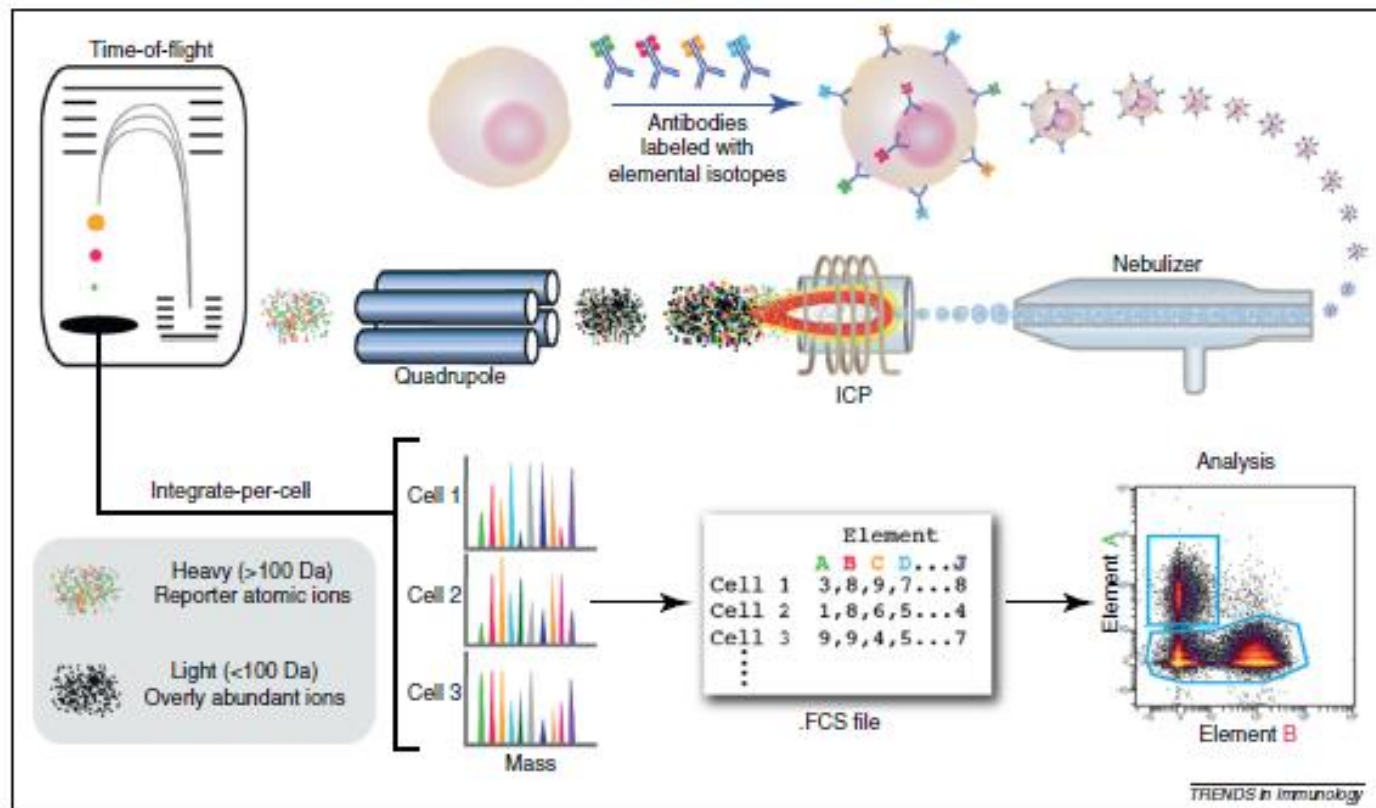


Figure 2.4 Schematic of mass cytometry taken from (Bendall *et al.*, 2012).

Antibodies tagged with metal isotopes bind to cellular epitopes. The cell passes through a nebuliser and where it is vaporised before being introduced to the argon plasma (ICP). This causes cells to be ionised and atomised. The quadrupole removes overly abundant ions, before the elemental composition of remaining heavy elements is determined by time of flight (TOF) mass cytometry. This information is displayed in .FCS files which can be analysed by cytometry platforms, such as Cytobank or FCsexpress.

2.7.1 Mass cytometry panel

This experiment was designed using the Wanderlust panel published in (Bendall *et al.*, 2014). The panel used a series of markers to identify the development trajectory of human B lymphocytes. In the project, the panel has been imitated to study the developmental stage of malignant B cells. The antibodies and clones have been kept the same, with the exception of the CD34 clone. The metal tags were altered, explained below.

The original panel used the CD34, clone 8G12. It was not possible to source this antibody commercially in a carrier free format at a concentration suitable for metal conjugation. CD34 clone 581 was therefore used which was evaluated by (Arseniev *et al.*, 1999) and shown to be comparable to 8G12.

The metal markers used in the Wanderlust panel were altered, due to the commercial availability of metal conjugated antibodies. By changing the metal tags, only two antibodies needed in house conjugation, significantly reducing the cost of the experiment. The panel metal design was achieved using the MAXPAR panel designer and support from Nina Lane (Field Applications Scientist, Fluidigm). The full panel used is shown in Table 2.7.

Reactivity	Company	Metal label	Target	Clone	Expressed by (cell type)	Functional significance in B cell development
Human	Fluidigm	162Dy	CD79B	CB3-1	B cells	(IG beta) Subunit of B cell receptor. Required for initiation of B cell signal transduction.
Human	Fluidigm	173Yb	HLA-DR	L243	B cells	MHC class II cell surface receptor. Involved in increasing production of IgM (heavy chain).
Human	Fluidigm	146Nd	IgD	IA6-2	Transitional B cells, immature B cells	Roles in B cell receptor signalling (negative).
Human	Bio-technie	176Yb*	IgM heavy chain	polyclonal	Pro B - PreB cells	Part of PreB Cell receptor complex.
Human	Fluidigm	160Gd	Ig kappa (light chain)	MHK-49	Immature B cells	Light chain of B cell receptor complex.
Human	Fluidigm	151Eu	Ig lambda (light chain)	MHL-38	Immature B cells	Light chain of B cell receptor complex.
Human	Fluidigm	156Gd	CD10	HI10a	B and T cell precursors	Neutral endopeptidase that inactivate several peptide hormones.
Human	Fluidigm	168Er	Ki-67	B56	N/A	Cellular marker of proliferation.
Human	Fluidigm	141Pr	CD45	HI30	Hematopoietic cells	Regulator of T-and B-cell antigen receptor signalling.
Human	Fluidigm	167Er	CD38	HIT2	Early B and T cells	Cell adhesion and signal transduction.
Human	Fluidigm	147Sm	CD20	2H7	T and B cell subsets	Development and differentiation of B cells into plasma cells.
Human	Fluidigm	169Tm	CD19	HIB19	B Cells (not plasma cells)	Regulates B cell development, activation and differentiation.

Human	Fluidigm	158Gd	CD179b	HSL11	PreB Cells	(lambda V) Part of PreB cell receptor complex. B-cell proliferation and differentiation.
Human	BioLegend	164Dy*	CD34	581 **	Haematopoietic stem cells and progenitors	Cell adhesion. Possible role in early haematopoiesis by mediating the attachment of stem cells to the bone marrow or directly to stromal cells.
Human	Fluidigm	166Er	CD24	ML5	B-cells, granulocytes, epithelial cells and monocytes.	Regulation of B-cell proliferation and maturation.
Human	Fluidigm	143Nd	CD117 (ckit)	104D2	Haematopoietic stem cells and progenitors	(c-KIT) Receptor tyrosine kinase important for proliferation, activation, and chemotaxis.
Human	Fluidigm	149Sm	CD179a	HSL96	PreB Cells	(vPreB). Part of PreB cell receptor complex. Roles in early B cell differentiation.
Human	Fluidigm	144Nd	CD72	3F3	B-cells (not plasma B-cells)	B cell proliferation.

Table 2.7 Panel of antibodies used in mass cytometry experiment to imitate Wanderlust panel.

*Metals conjugated in house using MAXPAR® labelling kits: 176Yb;164Dy. **Clone different to that of Wanderlust panel. See 2.7.1 for explanation.

2.7.2 Metal labelling with antibodies

It was not possible to commercially source all antibodies conjugated to the required metals. Therefore two antibodies were conjugated in house: IgM heavy chain (IgH) and CD34. Antibodies for conjugation must be in a carrier free format (no BSA) to allow for successful conjugation of the metal. The MAXPAR® Metal conjugation protocol was followed with minor adaptations.

Reagents

MAXPAR® antibody labelling kit	R-Buffer C-Buffer L-Buffer W-Buffer MAXPAR® polymer Lanthanide solution	Fluidigm
Centrifugal Filter Unit: 3 kDa Amicon Ultra- 500 µL V bottom		Merck
Centrifugal Filter Unit: 50 kDa Amicon Ultra- 500 µL V bottom		Merck
Pierce™ 0.5M TCEP: Bond-Breaker TCEP (tris (2-carboxyethyl) phosphine) solution		VWR International
PBS – based antibody stabilization solution		Candor Biosciences (Wangen, Germany)
BD CompBeads anti mouse Ig κ		BD Biosciences

Protocol

The polymer was first pre-loaded with the lanthanide metal. To achieve this, the polymer was resuspended in 95µl L-Buffer and mixed by pipetting. The lanthanide metal solution (3µl) was added to the tube to achieve a final concentration of 2.5mM. This mixture was then incubated at 37°C for 30 minutes.

During this time, the buffer exchange and partial reduction of the antibody was performed. The 0.5M TCEP stock was diluted to 4mM in R-Buffer to achieve a total of 100µl per antibody being conjugated. Simultaneously, 300µl of R-Buffer was added to a 50kDa filter. The antibody was then added to the filter and the tube was centrifuged

for 10 minutes at 12,000 g at room temperature. The flow through was discarded and 100µl of the 4mM TCEP-R-Buffer was added to each antibody, mixed by pipetting and incubated at 37°C for 30 minutes. Next, the lanthanide loaded polymer was purified. L-Buffer (200µl) was added to a 3kDa filter, followed by the metal-loaded polymer mixture. The filter was centrifuged for 25 minutes at 12,000 g at room temperature.

The partially reduced antibody was then purified. C-Buffer (300µl) was added to the 50kDa filter, followed by centrifugation at 12,000 g for 10 minutes at room temperature. The flow through was discarded and 400µl C-Buffer was added to the filter, followed by a further 10 minute centrifuge at 12,000 g. Following this, the antibody was conjugated with the lanthanide-loaded polymer. The flow through from both the 3kDa filter containing the lanthanide loaded polymer and the 50kDa filter containing the partially reduced antibody was discarded. The lanthanide-loaded polymer was resuspended in 100µl C-Buffer, and this was transferred to the corresponding partially reduced antibody in the 50kDa filter, mixed briefly by pipetting, and incubated at 37°C for 60 minutes.

The metal conjugated antibody was then washed by adding 300µl W-Buffer and centrifugation at 12,000 g for 5 minutes. The flow through was discarded and this process was repeated three more times with 400µl W-Buffer to make a total of four washes. Recovery of the antibody was achieved by adding 100µl of W-Buffer to the walls of the filter followed by inversion of the filter into a fresh collection tube. The inverted filter was centrifuged at 1000 g for 2 minutes. A further 100µl W-Buffer was added to the filter and the centrifugation step repeated.

To determine the yield of the metal conjugated antibody, the absorbance was measured at 280 nanometers against a blank of W-Buffer using the NanoDrop. The antibody was diluted to a final concentration of 0.1mg/ml in the commercially available antibody stabilisation buffer.

Validation of antibody conjugation

The validation of the antibody conjugation involves two steps; first to ensure there is metal present on the antibody, and second to check that the antibody still recognises its specified antigen. To validate that the metal is on the antibody BD CompBeads

(anti-mouse Ig κ) were used. These beads are polystyrene microparticles which contain anti-mouse Ig κ particles, and therefore bind any mouse κ light chain antibody. If signal is generated in a metal channel when using these beads, it shows the metal has conjugated successfully to the antibody. The antibody (1 μ l) was added to 1ml PBS containing 2 drops BD CompBeads and incubated for 30 minutes at room temperature. The beads were then washed twice in PBS followed by three washes in MAXPAR[®] water before acquisition on the Helios mass cytometer.

To ensure the antibody still recognised the target antigen, cell lines were used that were known to express the antigen of interest. Kasumi and Ramos cells were used which are positive for CD34 and IgH, respectively. The cells were used in a 1:1 ratio so each tube had a negative and positive population for each marker. The antibodies were titrated in MAXPAR[®] cell staining buffer to achieve a final antibody dilution of 1:250, 1:500, 1:1000, 1:2000 and 1:5000. The cell staining protocol outlined in 2.7.3 was then followed.

2.7.3 Cell staining with antibodies

Reagents

Benzonase nuclease	Sigma Aldrich
Dulbecco's phosphate buffered saline (10x)	Sigma Aldrich
RF10	As per 2.2.2
MAXPAR® Water	Fluidigm (London, UK)
Cell staining buffer	Fluidigm
Fluidigm (London, UK)	Fluidigm
Methanol	FSA laboratory supplies
Pierce 16% formaldehyde	Thermofisher
Cisplatin 5mM	Fluidigm
Iridium	Fluidigm

Equipment

Polypropylene FACS tubes	Laboratory supplies
3µm filter caps	Sysmex Partec (Goerlitz, Germany)
BD Accuri C6 Cytometer	BD Biosciences
Helios™	Fluidigm

Solutions

RF10-benzonase media	50U/ml RF10
3.2% formaldehyde	10ml 16% formaldehyde and 40ml dH ₂ O
Intercalation solution (per sample)	1ml Fix and Perm, 1µl iridium

(a) Number of Samples	(d) Volume of Antibody (μ l)	(c) Vol Cell Staining Buffer (μ l)	(b) Number of Antibodies																			
			1	2	3	4	5	6	7	8	9	10	11	12	13	14	15	16	17	18	19	20
1	1.1		53.9	52.8	51.7	50.6	49.5	48.4	47.3	46.2	45.1	44	42.9	41.8	40.7	39.6	38.5	37.4	36.3	35.2	34.1	33
2	2.2		108	106	103	101	99	96.8	94.6	92.4	90.2	88	85.8	83.6	81.4	79.2	77	74.8	72.6	70.4	68.2	66
3	3.3		162	158	155	152	149	145	142	139	135	132	129	125	122	119	116	112	109	106	102	99
4	4.4		216	211	207	202	198	194	189	185	180	176	172	167	163	158	154	150	145	141	136	132
5	5.5		270	264	259	253	248	242	237	231	226	220	215	209	204	198	193	187	182	176	171	165
6	6.6		323	317	310	304	297	290	284	277	271	264	257	251	244	238	231	224	218	211	205	198
7	7.7		377	370	362	354	347	339	331	323	316	308	300	293	285	277	270	262	254	246	239	231
8	8.8		431	422	414	405	396	387	378	370	361	352	343	334	326	317	308	299	290	282	273	264
9	9.9		485	475	465	455	446	436	426	416	406	396	386	376	366	356	347	337	327	317	307	297
10	11		539	528	517	506	495	484	473	462	451	440	429	418	407	396	385	374	363	352	341	330
11	12.1		593	581	569	557	545	532	520	508	496	484	472	460	448	436	424	411	399	387	375	363
12	13.2		647	634	620	607	594	581	568	554	541	528	515	502	488	475	462	449	436	422	409	396

Table 2.8 Fluidigm antibody preparation guide.

To use the table: find the row matching the number of samples that need to be processed (a) and the column for the number of antibodies used in the staining (b). The number where the row and column meet in (c) is the total volume of Cell staining buffer needed. The volume of each antibody is indicated in column (d). A volume of 50 μ l of the final solution is added to each sample stained.

During the antibody staining procedure, no glassware was utilised that had already been through the laboratory wash. Laboratory soaps can contain barium, which is often still present on glassware even after several washes. Barium contamination leads to a huge signal in the 138 channel, which can not only damage the detector, but also cause spill over into other channels including the +16 channel, 154. All buffers were therefore stored in new plastic ware that had not been through the laboratory wash.

To produce the antibody cocktail, cell staining buffer was added to an eppendorf followed by each of the antibodies. The volume of cell staining buffer and antibodies was determined using the Fluidigm Antibody Preparation Guide, (Table 2.7).

Thawed cryopreserved cell lines and primagraft cells, and cell lines in culture were used. Cryopreserved cells were thawed quickly in a water bath at 37°C. Cells were added to 1ml warmed benzoylase medium, and vials were rinsed with medium to retrieve all cells. Cells were then centrifuged at 473g for 8 minutes. The supernatant was removed and 9ml of warmed benzoylase medium was added to each tube. Cells were once again centrifuged at 473g for 8 minutes before being resuspended in 1ml PBS. Cells were counted using trypan blue and adjusted to a total cell number of approximately 3×10^6 cells. For cell lines in culture, cells were counted using trypan blue and adjusted to a total cell number of 1×10^6 cells.

Cisplatin staining

Incubation with cisplatin concentrations is performed to identify viable and non-viable cells after analysis by mass cytometry. Low concentration cisplatin is more readily taken up by dead or dying cells after short incubations. Therefore live cells will have low cisplatin levels, allowing differentiation between viable and non-viable cells.

Cells were washed in 1ml pre-warmed PBS and resuspended in 1ml PBS. A 1.25M concentration of cisplatin was achieved by diluting the cisplatin stock 1:4 in PBS to produce a 5mM solution, before a 1:1,000 dilution on addition to the cells (1µL in 1ml). The cells were incubated at room temperature for 4 minutes before the staining was quenched by addition of 5ml warm RF10. The tubes were centrifuged for 5 minutes at

3,000 g and then resuspended in 700µL RF10 and left to rest in culture conditions for 15 minutes.

Antibody staining

Cells were washed with 3.5ml MAXPAR® cell staining buffer and the supernatant was discarded, leaving approximately 50µl per tube. 50µl of the surface antibody cocktail was then added to each tube to make a total staining volume of 100µl per tube. The samples were vortexed and incubated at room temperature for 30 minutes. Following this, samples were washed in 2ml of MAXPAR® cell staining buffer, and cells were resuspended in 50µl of the supernatant.

Cells were chilled on ice for 10 minutes before 1ml of methanol at 4°C was added to each tube to permeabilise the cells. The cells were left to incubate on ice for a further 15 minutes. Cells were then washed twice with 2ml MAXPAR® cell staining buffer. Following the second wash, cells were resuspended in 50µl of the supernatant. To this, 50µl of intracellular staining antibodies were added to make a total staining volume of 100µl. Cells were gently vortexed and left to incubate for 30 minutes at room temperature.

Following this incubation, cells were washed twice in 2ml MAXPAR® cell staining buffer, and cells were resuspended in the residual volume after the second wash. To each tube, 1ml intercalation solution was then added and gently vortexed. At this point, cells were left for 12-48 hours at 4°C. To fix the cells, 1ml 3.2% formaldehyde was added to each sample and incubated for 30 minutes at room temperature.

Samples were then washed in 1ml MAXPAR® water, followed by a wash with 2ml MAXPAR® water. Cell pellets were resuspended in 300µl MAXPAR® water and filtered through 3µM filter caps into new, labelled tubes.

The number of cells was measured on the BD Accuri Cytometer. The volume of the cell suspension was then adjusted with MAXPAR® to achieve a concentration of 5×10^5 cells/ml including EQ beads. The data were then acquired on the Helios by a member of the Flow Cytometry Core Facility. Data were normalised using EQ beads and analysed using FCS express 6 (De Novo Software, California, US).

2.7.4 Wanderlust algorithm

The Wanderlust algorithm is a graph based trajectory that orders cells based on their maturity. The algorithm makes several assumptions: firstly that the sample used to generate the algorithm contain cells from the whole developmental process; secondly that the development is linear (i.e. non-branching) and thirdly, that protein expression changes occur gradually throughout development (Bendall *et al.*, 2014).

The graph based algorithm overcomes previous problems associated with cell ordering according to developmental hierarchy (Bendall *et al.*, 2011; Qiu *et al.*, 2011). These include false assumptions of linearity, and also the loss of single cell resolution and directionality through cells grouping into overly coarse clusters (Bendall *et al.*, 2014).

The algorithm is described in more detail in Figure 2.5.

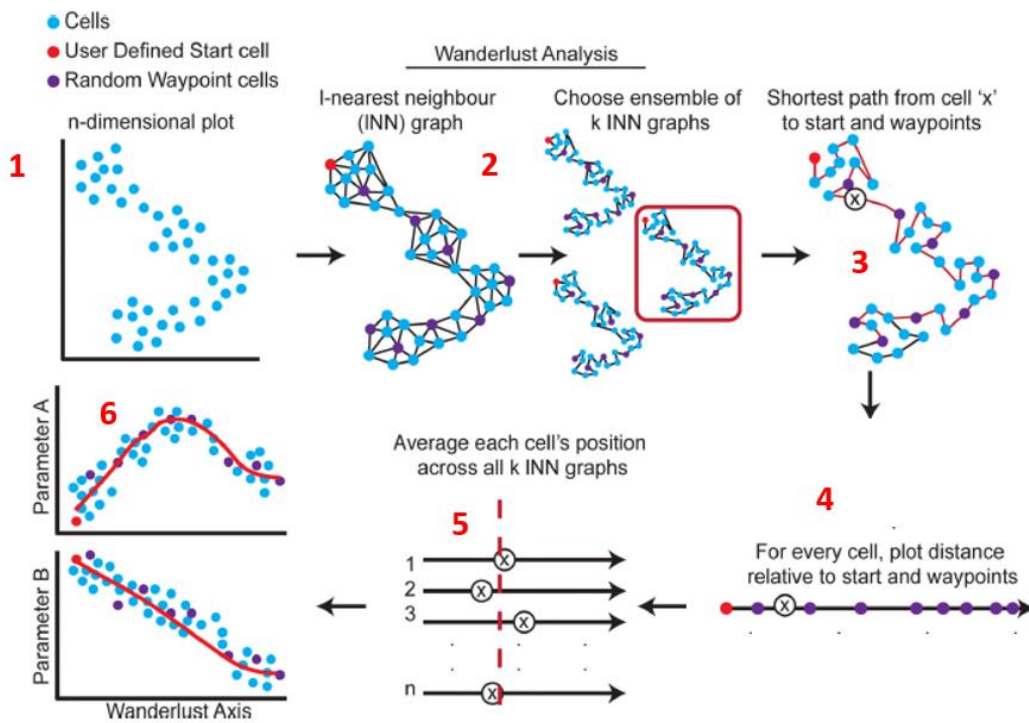


Figure 2.5 Wanderlust developmental trajectory method, adapted from Bendall *et al.* (2014).

1. Cells are mapped onto an n-dimensional plot, each dot represents a single cell.
2. A start cell is selected by the user, which defines where the algorithm will begin the trajectory. Waypoint cells are additionally selected at random by the algorithm, which aids the algorithm later on. The algorithm then generates a path based on each cell's nearest neighbour on the n dimensional plot. This step is done hundreds of times.
3. The shortest path through the cells is measured. This is done for each graph.
4. The distance of each cell relative to the start of the trajectory and waypoint cells is calculated.
5. The positions for each cell generated by the individual graphs are averaged. This means that the impact of any noise and short circuits generated by the algorithm on individual graphs will be reduced.
6. The final trajectory is the average of all the graphs. The expression of individual markers can be plotted against the wanderlust position to examine the expression of that marker over cell development.

Protocol

All analyses described in this section were performed by Dr. Rachel Queen.

Multidimensional scaling (MDS) plots and heat maps were generated using R software. This was to check there was no batch effect, for example by date or sample type. It was also possible to ensure at this point that replicates clustered together.

The wanderlust algorithm is available as a MATLAB (Mathworks, Massachusetts, US) tool. The default parameters for the algorithm were kept, which were all the same as detailed in Bendall *et al.* (2014) except for 'k', the part of the algorithm that defines the number of clusters in the graph based algorithm. The default setting for k in MATLAB is 8, however the Bendall paper use a value of 5. In the analysis performed here, a value of 5 would not generate the trajectory and therefore the programmes default value of 8 was kept. Once the algorithm had been run in MATLAB, results were exported to R for further analysis.

The details of the samples used in the trajectory is described in Chapter 6. Briefly, four remission bone marrow cells were run with the ALL samples. A group of approximately 20 start cells were chosen. The choice of start cell was optimised and is described in more detail in Chapter 6.

2.8 Statistical analysis

All statistical analyses were performed using GraphPad Prism, version 6.07 (California, USA) unless otherwise stated in the results.

Chapter 3. Pharmacokinetics of dexamethasone in acute lymphoblastic leukaemia

3.1 Introduction

The GC, dex, is a key component of therapy in childhood ALL. While the use of dex has undoubtedly contributed to the improvements in outcome in ALL seen over the past decades, it also makes a major contribution to a variety of short and long-term side effects, which may negate its antileukaemic benefit. The toxicity observed in the recently completed UKALL 2003 trial is seen as being unacceptably high in the context of a trial with such high disease free survival, with a >3% risk of treatment related mortality reported, and approximately a quarter of patients suffering at least one non-haematological serious adverse event (Bartram *et al.*, 2016; Eiser *et al.*, 2017). As such, the ongoing UKALL 2011 trial has investigated whether a shorter, more intense, dose of dex (10mg/m² x 14 days, 'short') would reduce toxicity associated with long term steroid exposure, compared to the UKALL 2003 dosing schedule (6mg/m² x 28 days, 'standard').

Despite its widespread successful use in a number of cancers, very limited information is available concerning dex pharmacokinetics in children. A study in this area showed substantial interpatient variability following treatment of children with ALL, with a >10-fold variability in systemic drug exposure observed at a dose of 8 mg/m²/day (Yang *et al.*, 2008). Variability was correlated with a number of covariates including serum albumin concentration, concurrent use of other drugs and age. As a result, it is important to further investigate these findings, as a 10-fold variation in dex pharmacokinetics may mask any potential benefit of a <2-fold dose change in the UKALL 2011 trial. In this chapter, the impact of pharmacokinetic variation on drug scheduling, i.e. standard versus short dex within the current UKALL 2011 trial, and on clinical outcome was therefore investigated, see 3.2 for more detail.

It is also important to investigate the potential effect of asparaginase, a drug concomitantly administered during induction therapy, on dex pharmacokinetics. Yang *et al.* showed that asparaginase caused a reduction in dex clearance. This is of significance, as a number of patients do not have adequate levels of asparaginase; in the UKALL 2003 trial this comprised 11% and 20% of standard risk and high risk patients, respectively. These patients will not only fail to gain any clinical benefit from asparaginase, but may also experience lower exposures to dex, as they will not

experience the reported asparaginase associated reduction in dex clearance. Therefore, as part of the UKALL 2011 trial, the relationship between dex and asparaginase will be investigated. Vaskar Saha's group in Manchester are performing a UKALL 2011 sub-study measuring asparaginase trough levels in patients. Therefore, where patients are enrolled on both sub studies, it will be possible to investigate the potential synergy previously reported between dex and asparaginase. Importantly, patients receive dex both pre- and post-asparaginase, thus allowing the impact of asparaginase on dex pharmacokinetics to be appropriately assessed.

In addition to studying plasma dex pharmacokinetics, a pilot study investigating variation in CSF dex concentrations was also performed in a small number of patients. The UKALL 2003 trial reported Kaplan-Meier estimates for any CNS relapse at 5 years to be 3%, with isolated CNS relapse at 1.9% (Vora *et al.*, 2013b). Dex has replaced prednisolone as steroid of choice in the UK as it showed fewer CNS relapses in the UKALL 97/99 trial (Mitchell *et al.*, 2005). However, as patients do not receive cranial irradiation, steroids play a major role in combatting CNS disease. Dex CSF pharmacokinetics have not been previously described in humans. However, a study investigating plasma dex pharmacokinetics found that higher dex clearance was associated with CNS relapse (Kawedia *et al.*, 2012). It will be interesting to determine whether this effect is, in part, related to variability in CSF dex concentrations similar to that seen in the systemic circulation.

In summary, clarification of the relationship between dex pharmacokinetics, clinical response and toxicity may enable further stratification of ALL therapy to maintain good outcomes whilst reducing the adverse effects of treatment (Jackson *et al.*, 2016).

3.2 Chapter specific aims

- Characterise dex pharmacokinetics in patients on the UKALL 2011 trial following short ($10\text{mg}/\text{m}^2 \times 14$ days) and standard ($6\text{mg}/\text{m}^2 \times 28$ days) treatment, investigating differences in key parameters between the two groups.
- Determine the effect of covariates such as age and concomitant medication on dex pharmacokinetic parameters.
- Establish whether variation in dex pharmacokinetics affects experience of toxicity and early indicators of outcome such as MRD results.
- Investigate the effect of asparaginase administration on dex pharmacokinetics.
- Evaluate whether dex pharmacokinetics in CSF are variable in a small number of patients.

3.3 Results

3.3.1 Patient characteristics

A total of 166 patients were recruited from 12 centres across the UK to the dex pharmacokinetic sub-study, between June 2013 and November 2016, for the current analysis. Samples were received from 154 patients; 10 patients withdrew consent prior to pharmacokinetic sampling, and samples from two patients were not received. Of the 154 patients for whom dex samples were received in Newcastle, extraction of dex for pharmacokinetic analysis was performed in 149 patients. The remaining five patients were not included in the current analyses due to time constraints but will be included in a later analysis incorporating additional pharmacokinetic study patients.

Samples from four patients were excluded from analysis due to deviations from the sample collection protocol. Two patients did not receive a full dose of dex and one patient was administered an incorrect dose of dex. One patient was administered dex orally on the first sampling day, but was administered dex intravenously at the end of induction therapy sampling time point. The second day of sampling was therefore removed from analysis. Hence, the total number of patients used for analysis was 146 patients; 83 were on 'short' treatment and 63 were on 'standard' treatment. The median age of patients studied was 6.7 years on the short arm and 6.4 years on the standard arm. Full patient characteristics are detailed in Table 3.1.

		Total	Short	Standard
Beginning of treatment		139	80	59
Age	1-5	71	40	31
	5-10	37	20	17
	10-25	31	20	11
Gender	Female	67	35	32
	Male	72	45	27
SA (m ²)	<0.5	2	1	1
	0.5-1	99	56	43
	1-1.5	19	12	7
	>1.5	19	11	8
WCC	<50 x 10 ⁹ /l	135	78	57
	>50 x 10 ⁹ /l	4	2	2
End of treatment		71	43	28
Age	1-5	32	21	11
	5-10	24	12	12
	10-25	15	10	5
Gender	Female	35	21	14
	Male	36	22	14
SA (m ²)	<0.5	1	1	0
	0.5-1	50	32	18
	1-1.5	13	5	8
	>1.5	7	5	2
WCC *	<50 x 10 ⁹ /l	67	42	25
	>50 x 10 ⁹ /l	0	0	0

(Continued overleaf)

		Total	Short	Standard
Both sampling days		65	40	25
Age	1-5	30	21	9
	5-10	21	10	11
	10-25	14	9	5
Gender	Female	32	20	12
	Male	33	20	13
SA (m ²)	<0.5	1	1	0
	0.5-1	46	29	17
	1-1.5	12	5	7
	>1.5	6	5	1
WCC	<50 x 10 ⁹ /l	63	40	23
	>50 x 10 ⁹ /l	2	0	2

Table 3.1 Characteristics of patients sampled at the beginning of treatment time point, end of treatment time point, and patients studied on both sampling days.

*WCC characteristics for end of treatment sampling = 67 patients (4 patients did not have haematology results for end of treatment sampling).

3.3.2 Dex pharmacokinetics

A total of 139 patients underwent 'beginning of treatment' pharmacokinetic sampling, 71 underwent 'end of treatment' pharmacokinetic sampling and 65 patients were sampled at both time points. It was not possible to calculate plasma dex pharmacokinetics for the beginning and end of induction therapy in 14 and 7 patients respectively, as there were too few samples to ascertain a maximal concentration or clearance values. This was due to samples not being collected at all time points, for example no sample being taken at 4 or 8 hours. An incomplete sample set was most commonly attributed to physical problems with sampling, or lack of availability of the patient or research nurse. Thus, pharmacokinetic parameters were successfully calculated in 127 beginning of treatment samples and 64 end of treatment samples. Paired beginning and end of treatment pharmacokinetic data were obtained for 54 patients.

3.3.3 Interpatient pharmacokinetic variability

There was wide variability observed in dex pharmacokinetics, with AUC_{0-12h} and C_{max} values being significantly higher on the short compared to the standard arm; AUC : 584.6 hr*ng/ml (69.12-1,606) versus 404.2 hr*ng/ml (38.31-1,009), C_{max} : 115ng/ml (13.0-265) versus 78.6ng/ml (9.8-196) median (range), $p=0.0001$ for both, student's t-test (Figure 3.1, Figure 3.3, Figure 3.4A). However there was substantial overlap between the two arms, with a number of patients on the standard arm exhibiting higher exposures than those on short therapy. This equates to a >20-fold range after a single dex dose, despite there being a <2-fold difference in dose. For comparisons with cellular dex data in later chapters, C_{max} data equates to short: 293 nM (33.1 – 675.2) standard: 201.8 nM (24.9-449.4) median (range).

AUC was linear between patients receiving dex doses of 6 and 10 mg/m²/day. When AUC_{0-12h} data was normalised to exposure per dose of 1mg/m² dex, there was no significant difference between the two dex dosing arms (student's t test, $p=0.6$). This is important to establish when assessing a dose change.

The accuracy and therefore utility of pharmacokinetic parameters such as T_{max} and half-life were limited due to the small number of sampling points in the study. In particular, this is the case for patients with a T_{max} of later than 2h, or in patients with an incomplete set of samples. In this situation, half-life is calculated based on only two data points. For data shown here, half-life was calculated based on two data points in 18 patients, three points in 43 patients and four data points in 64 patients. Therefore while these data give an approximation of half-life, it is not highly accurate.

The limited number of sampling points is displayed in the trimodal distribution of the T_{max} data in Figure 3.3. The limited number of sampling points means that T_{max} will most commonly be at the sampling points of 1, 2 or 4 hours. However, from the collected data, there was no difference between the short and standard dex arms in terms of both parameters. The median T_{max} was 1.50h in the short arm and 1.16h in the standard arm. Dex half-life values were 2.56h and 3.20h for the short and standard arms, respectively (T_{max} $p=0.38$, half-life $p=0.81$, student's t test).

These parameters can be extrapolated to represent patient exposure over the duration of treatment, as patients on short therapy received 14 days of dex treatment and

patients on standard therapy received 28 days. When considering cumulative exposure, there was a significantly higher exposure of patients on the standard arm with a median of 22,634 hr*ng/ml (range: 2,146-56,480) compared to 16,370 hr*ng/ml (1,935-44,968) on the short arm ($p=0.0027$, student's t test, Figure 3.4B). Full pharmacokinetic parameters are shown in Table 3.2.

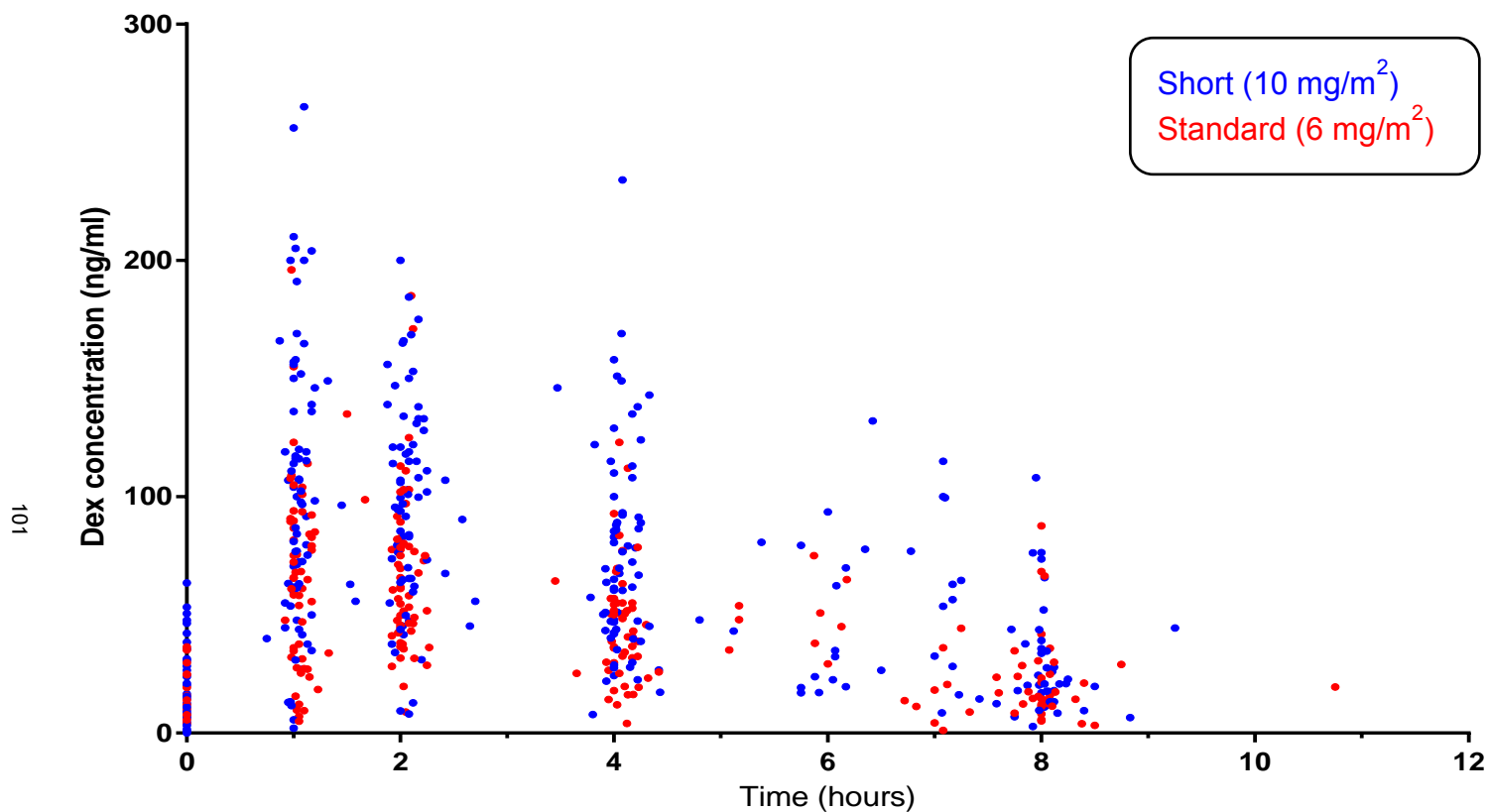
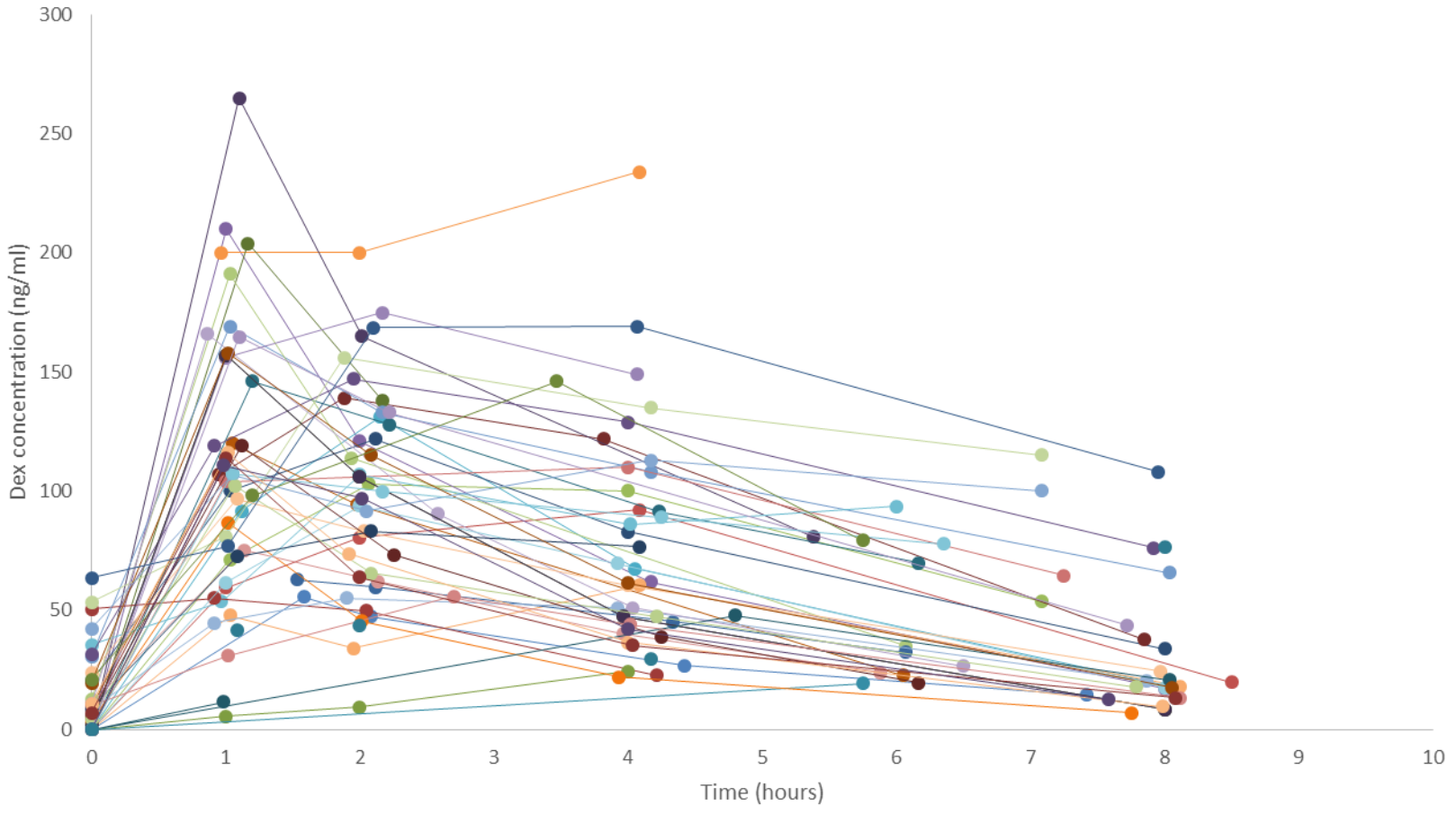


Figure 3.1 Variation in dex plasma concentration-time profiles observed in patients on both short therapy (10mg/m² x 14 days, blue) and standard therapy (6mg/m² x 28 days, red).

Blood samples were taken before, and between 1 and 8 hours, following oral administration of a single dex dose of either 3mg/m² (red) or 5mg/m² (blue). Plasma was separated from whole blood and dex concentrations quantified using a validated LC/MS method. Each dot represents a single sample from a single patient from the UKALL 2011 cohort.

A

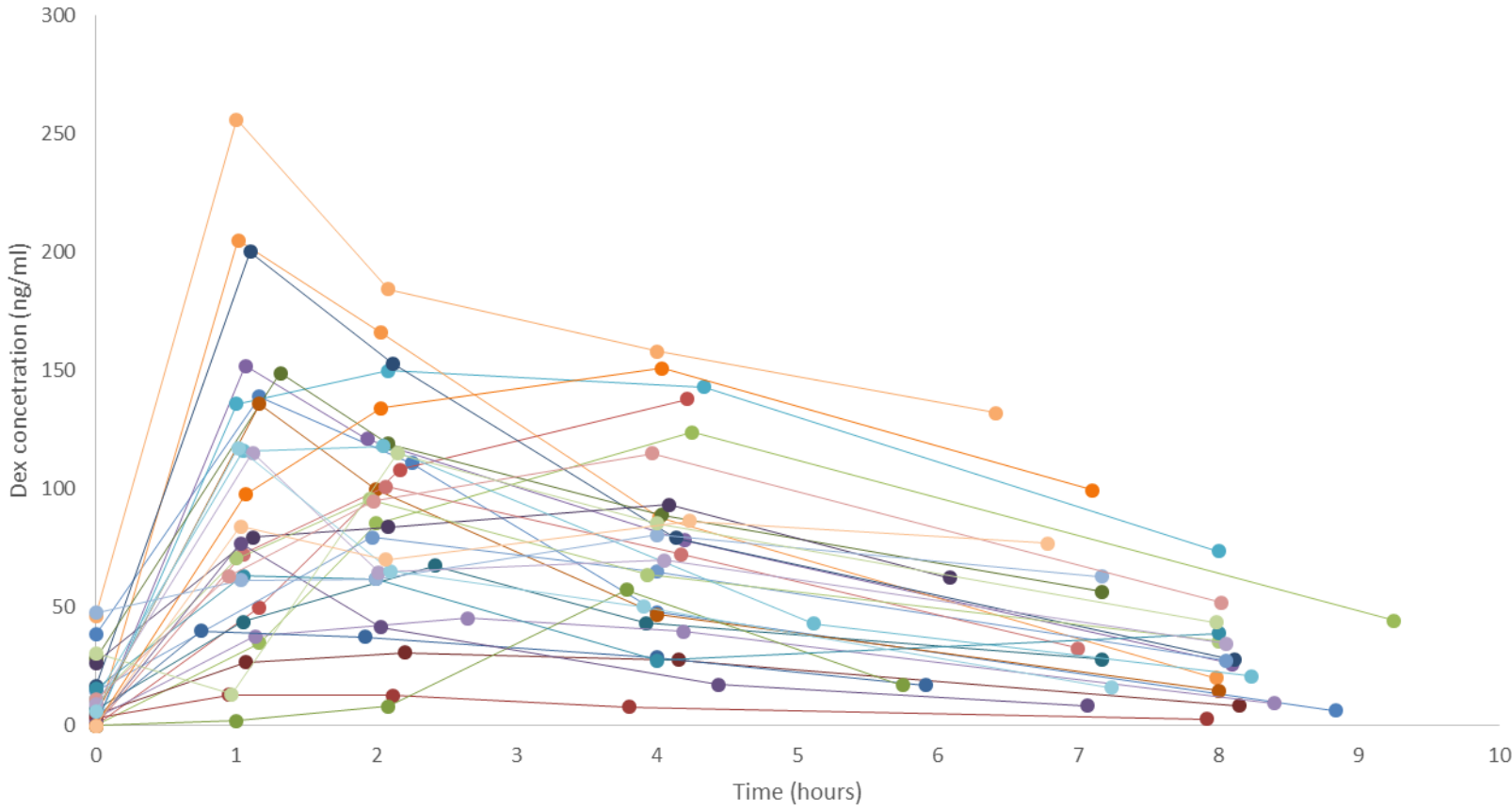
Short dex dosing, standard risk patients



102

Short dex dosing, high risk patients

B

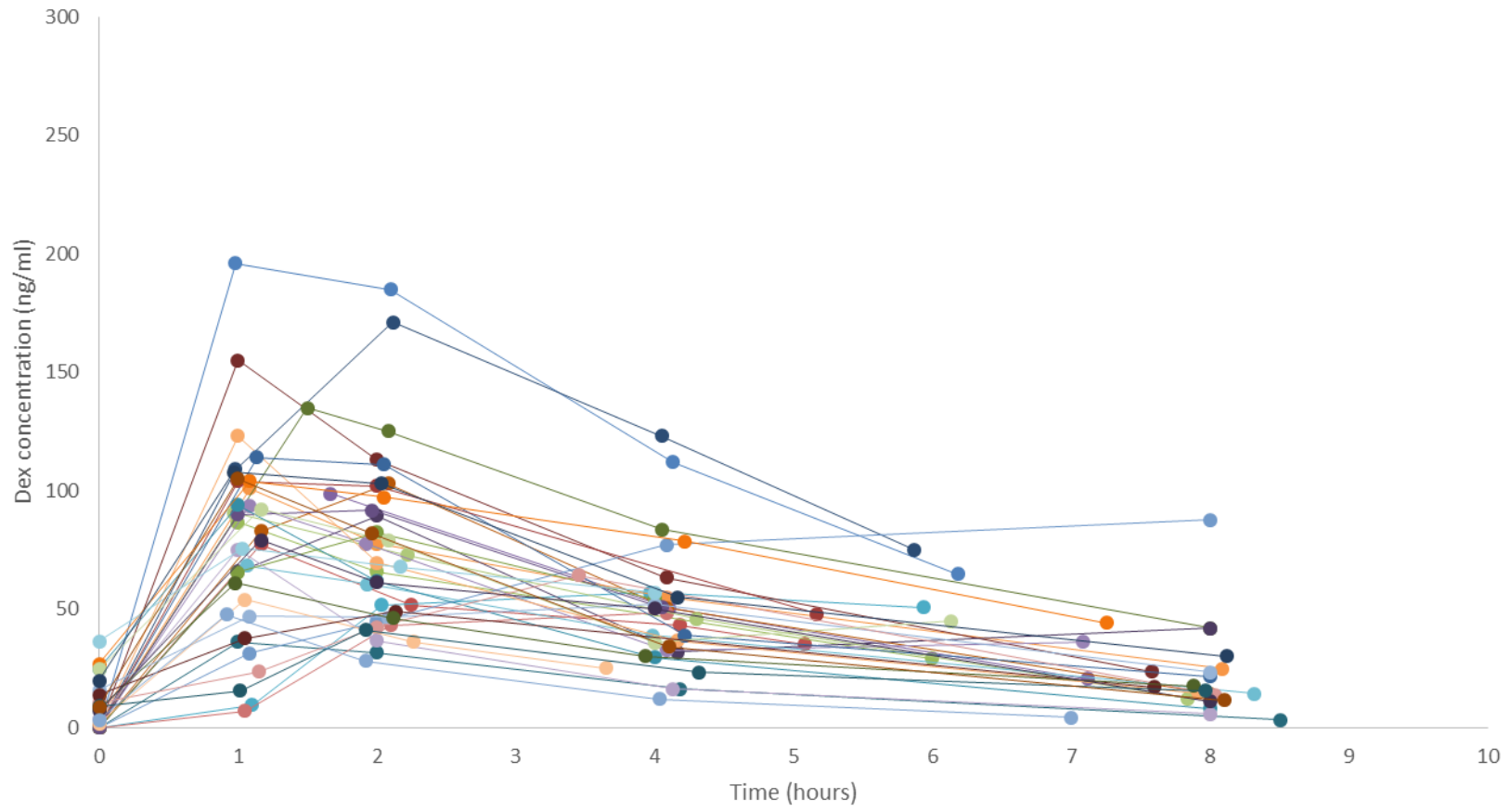


103

Standard dex dosing, standard risk patients

C

104



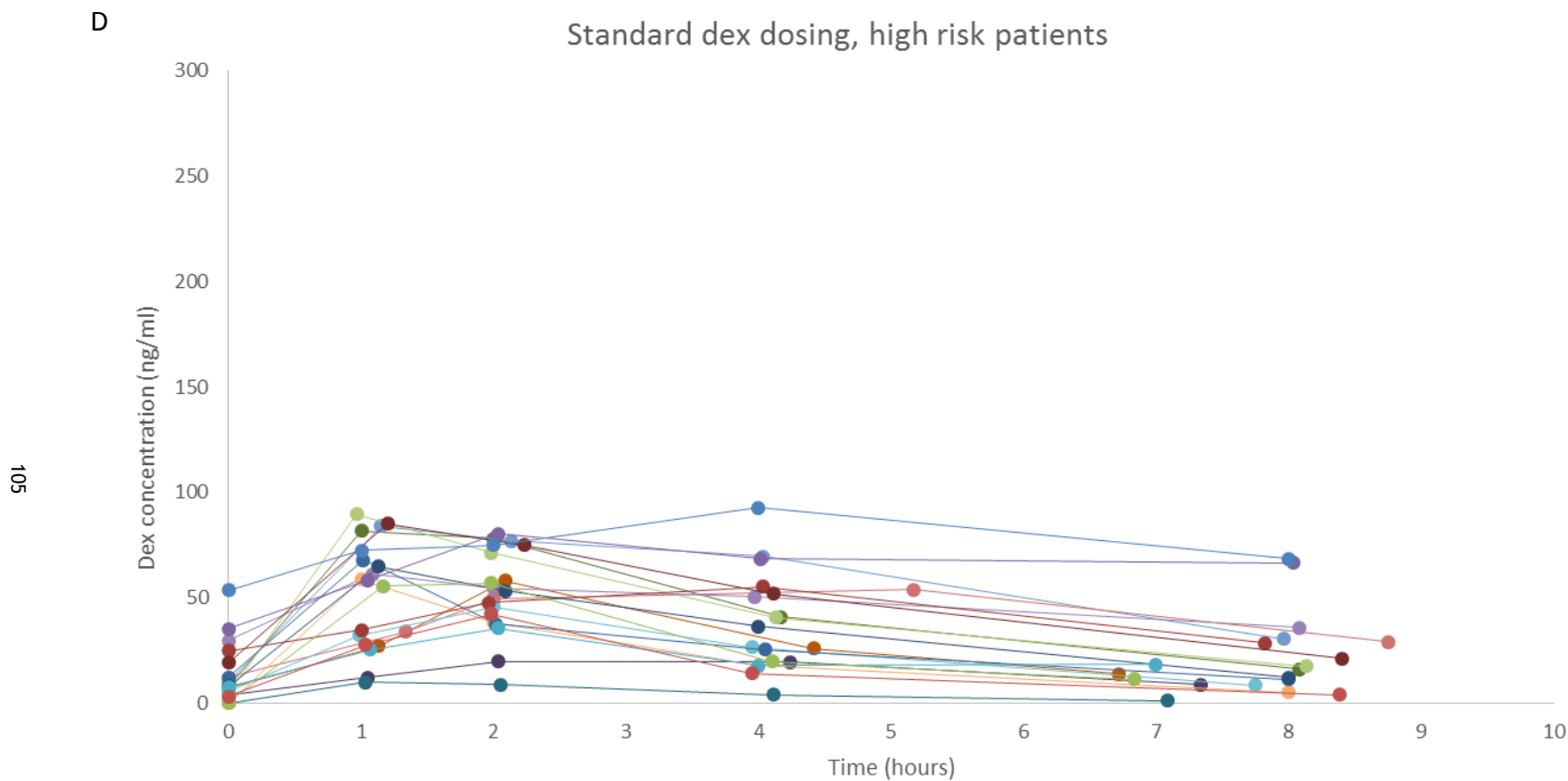


Figure 3.2 Variation in dex plasma concentration-time profiles observed in patients on (A and B) short therapy (10mg/m² x 14 days, blue) and (C and D) standard therapy (6mg/m² x 28 days, red). Patients are separated into NCI standard risk (A and C) and standard risk (B and D).

Blood samples were taken before, and between 1 and 8 hours, following oral administration of a single dex dose of either 3mg/m² or 5mg/m². Dex concentrations quantified using a validated LC/MS method. Each point represents a single sample from a single patient from the UKALL 2011 cohort.

Regimen	Short (n=73)			Standard (n=54)			P Value
	Median	Minimum	Maximum	Median	Minimum	Maximum	
Half-life (h)	2.91	1.12	17.3	3.20	1.78	25.0	0.81
T _{max} (h)	1.32	0.75	4.25	1.16	0.92	5.17	0.38
C _{max} (ng/ml)	116.2	13.0	265.0	79.2	9.76	196.0	<0.0001
AUC _{0-12h} (hr*ng/ml)	584.6	69.12	1606	404.2	38.31	1009	<0.0001
Clearance (l/h/m ²)	7.89	1.79	70.28	6.74	0.25	76.16	0.86
Volume of distribution (l)	25.88	11.6	384	28	7.16	126	0.34
Cumulative AUC (hr*ng/ml)	16,370	2,146	56,480	22,634	1,935	44,968	0.0027

Table 3.2 Comparison of pharmacokinetic parameters between short (10mg/m²) and standard (6mg/m²) groups after a single dose of dex.

Blood samples were taken before treatment and between 1 and 8 hours following oral administration on one of the first three days of dex induction chemotherapy. Cumulative AUC is taken from AUC₀₋₁₂ hour data extrapolated to duration of dex therapy (14 days for short, 28 days for standard). P values comparing pharmacokinetic parameters on short versus standard therapy were generated using unpaired student's t tests.

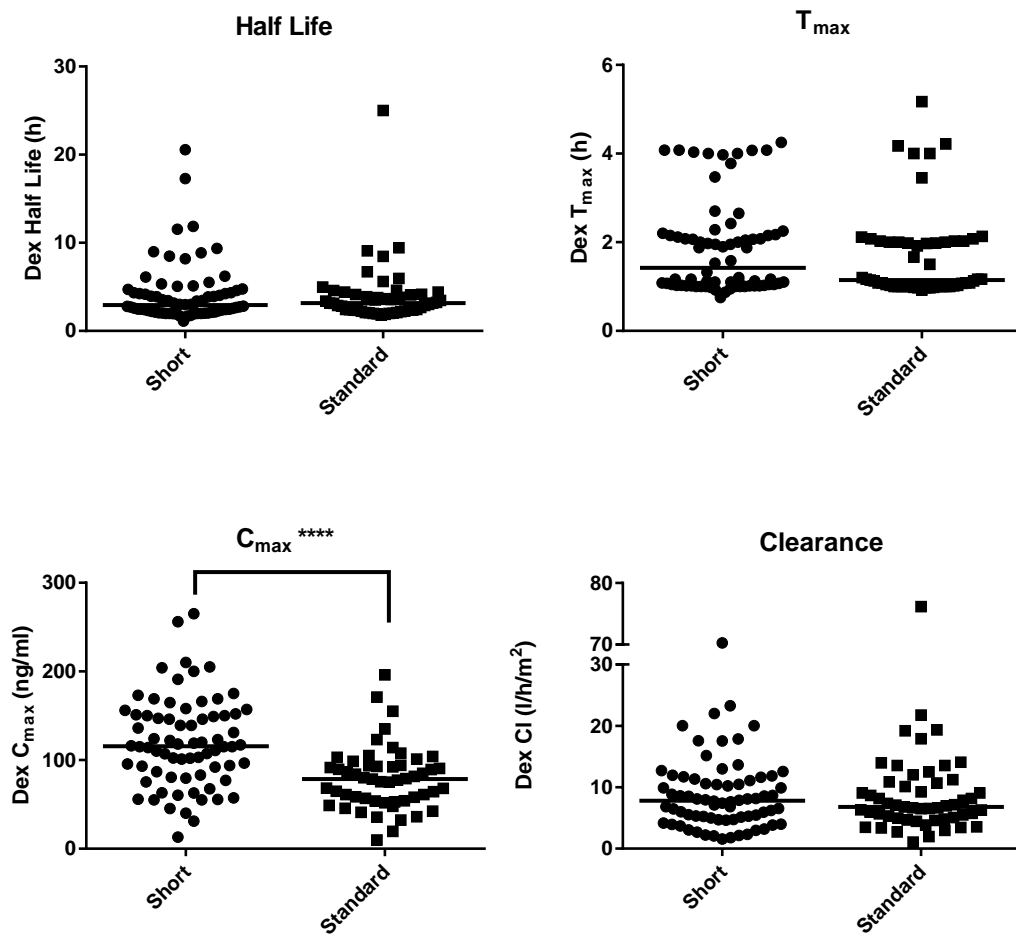


Figure 3.3 Interpatient variation in dex pharmacokinetic parameters obtained at the beginning of treatment.

Blood samples were taken before treatment and between 1 and 8 hours following oral administration on one of the first three days of dex induction chemotherapy. Short therapy (10mg/m² x 14 days), standard therapy (6mg/m² x 28 days). Horizontal bars represent median values. P values were generated using the unpaired student's t test (half-life and clearance data were log transformed to achieve a normal distribution prior to statistical analysis); half-life: p=0.81, T_{max}: p=0.88; C_{max}: p<0.0001; clearance: p=0.81.

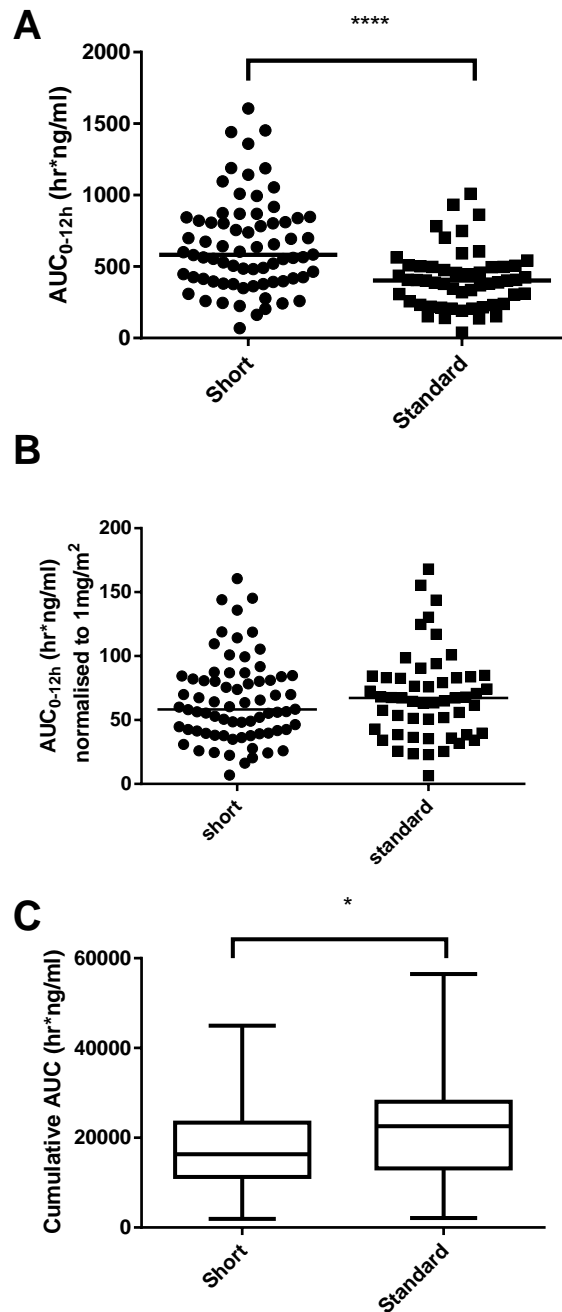


Figure 3.4 Variation in plasma dex area under the curve in patients on both short therapy and standard therapy, calculated following a single drug exposure (A), adjusted to exposure per 1mg/m² (B) and when extrapolated to total induction therapy exposure (C).

Short therapy (10mg/m² x 14 days), standard therapy (6mg/m² x 28 days). AUC was normalised to 1mg/m² by dividing short and standard AUC_{0-12h} data by 10 and 6 respectively. Cumulative AUC is taken from AUC_{0-12h} data extrapolated to duration of dex therapy (14 days for short, 28 days for standard). Horizontal bars represent median values. P values were generated using the unpaired student's t test. AUC_{0-12h} p<0.0001; normalised AUC_{0-12h} p=0.6; Cumulative AUC p=0.0027.

3.3.3.1 Patients with extreme dex pharmacokinetic profiles

In this study, several patients were identified that had extreme pharmacokinetic profiles. These mainly fell into two group; patients with extremely high clearance values (patient 808 and 1259), and patients in whom dexamethasone appears to be eliminated very slowly (patients 1453, 567 and 841). Concentration time profiles for these patients can be seen in Figure 3.3 and pharmacokinetic parameters are shown in Table 3.3.

	Patient ID				
	808	1259	1453	567	841
Half-life (h)	1.9	2.9	N/A	N/A	N/A
T _{max} (h)	1.03	0.95	4.17	3.97	2
C _{max} (ng/ml)	9.76	13.0	113	56.9	107
AUC _{0-12h} (hr*ng/ml)	38.3	69.11	1149	554.3	945.0
Clearance (l/h/m ²)	76.16	70.28	N/A	N/A	N/A
Volume of distribution (l)	126.2	384.0	N/A	N/A	N/A

Table 3.3 Pharmacokinetic parameters in patients with extreme profiles after a single dose of 5mg/m² (841, 1259, 1453) or 3mg/m² (567, 808).

Blood samples were taken before treatment and between 1 and 8 hours following oral administration on one of the first three days of dex induction chemotherapy. N/A = not applicable (it was not possible to calculate certain parameters in these patients).

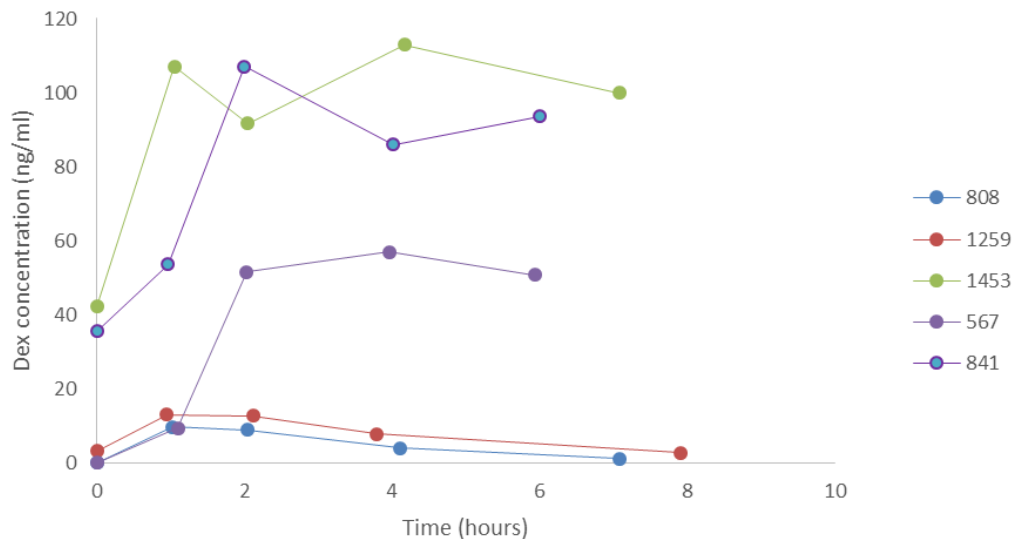


Figure 3.5: Dex concentration time profiles for patients with extreme dex pharmacokinetics.

Blood samples were taken before, and between 1 and 8 hours, following oral administration of a single dex dose of either 3mg/m² (patient 567, 808) or 5mg/m² (patient 841, 1259, 1453). Plasma dex concentrations quantified using a validated LC/MS method. Each point represents a single sample from a single patient from the UKALL 2011 cohort.

The two patients with an extremely high dex clearance both had very low exposures to dex (AUC_{0-12h} of 38.3 and 69.1 hr*ng/ml compared to the median values of 404.2 and 584.6 hr*ng/ml for the respective arms of therapy the patients were on).

There are two possible reasons for the high clearance; firstly that the patients have expression of an enzyme such as CYP3A5 that will increase metabolism of dex, or secondly that the patient has not been exposed to the full dose of dex. This may be due to reduced absorption in these patients, or that the patient has not taken the full dose of dex. It is important to investigate this further, as if the low exposure was caused by an increased dex metabolism, there may be a sub set of patients who will be exposed to potentially sub therapeutic levels of dex. This could be investigated further using a candidate gene analysis assessing variants of CYP3A4, the cytochrome P450 principally responsible for the metabolism of dex, and expression of CYP3A5, which has been reported to increase CYP3A activity (Kitzmiller *et al.*, 2014). Secondly, a dietary study could be performed. Dex is lipophilic, and as such the patient's diet may affect absorption, as absorption of

other lipophilic drugs has been shown to be reduced by increased dietary lipids (Persson *et al.*, 2008).

There were also patients who exhibited sustained dex concentrations after oral administration of the drug, with little perceivable dex elimination. It was not possible to calculate certain pharmacokinetic parameters for this drug, as there was no real decrease in plasma dex concentrations to calculate these. One potential cause for this is a prior administration of dex through the sampling line. However, as there is a much lower dex concentration in the pre dose sample, this is unlikely to be the case. Another explanation for sustained plasma dex concentrations could be a reduced CYP3A activity. For example, patients with CYP3A4*22 have been found to have reduced CYP3A4 activity in several studies (Elens *et al.*, 2013a; Elens *et al.*, 2013b; Kitzmiller *et al.*, 2014). This is important to investigate further, as these patients could be at risk of increased treatment related morbidity and mortality.

Although both these cases of extreme pharmacokinetic profiles may be due to problems with dex dosing or blood sampling, there may also be a physiological reason. It will be important to determine this, as if the observed differences were due to differences in dosing or sampling, it may be that variation in AUC is not as large as initially thought. However, if this variation has a physiological basis, the outcome of these patients should be monitored, to determine whether those with a low exposure have an increased chance of relapse, and similarly those with apparent poor elimination experience dex associated morbidities such as osteonecrosis. A candidate gene study assessing whether polymorphisms in CYP3A4 and 5 have a role in these extreme profiles may help to resolve this issue.

3.3.4 Inpatient variability and asparaginase effect

Dex has been reported to be both a substrate for, and inducer of, enzymes of drug metabolism and drug transporters (Jugert *et al.*, 1994; Demeule *et al.*, 1999; Rushmore and Kong, 2002; Xu *et al.*, 2005; Shou *et al.*, 2008). It is therefore important to assess inpatient variability to establish whether there is any auto-induction or inhibition of clearance during treatment. Furthermore, Yang *et al.* (2008) reported a possible association between asparaginase administration and

dex clearance. As patients in the current cohort received at least one dose of asparaginase between the two pharmacokinetic sampling days (Figure 2.1), the potential effect of asparaginase on dex pharmacokinetics was also assessed in this study.

There were 54 patients for whom complete beginning and end of treatment pharmacokinetic data were generated. C_{max} , clearance and AUC_{0-12h} were all significantly different within patients, as shown in Figure 3.6 (paired student's t test, C_{max} $p=0.0003$, clearance $p=0.0016$ and AUC_{0-12h} $p=0.0003$). However, despite these differences between the sampling days being statistically significant in the group overall, for some individuals the opposite change is seen. This makes the clinical use of the observation challenging. An overall increase in exposure cannot be assumed and incorporated into dosing protocols if this is not the case for some patients. If a therapeutic monitoring situation was adapted, sampling at two time points during induction therapy would be needed to ensure all patients had an appropriate exposure to the drug.

Whilst hypothesised to affect dex clearance through interfering with *de novo* synthesis of drug metabolising enzymes, asparaginase is also thought to inhibit the production of proteins such as albumin (Oettgen *et al.*, 1970; Cairo, 1982). Indeed, Yang *et al.* (2008) observed a drop in serum albumin levels following the addition of asparaginase to therapy, with a correlation between dex clearance and albumin levels. Likewise, in the current cohort of patients, a drop in albumin levels was observed upon the addition of asparaginase therapy ($n=46$, paired student's t test $p=0.0078$, Figure 3.6F). However, a correlation between dex clearance and albumin was not observed post-asparaginase treatment (pre-asparaginase: $p=0.03$; post-asparaginase: $p=0.81$, Figure 3.7).

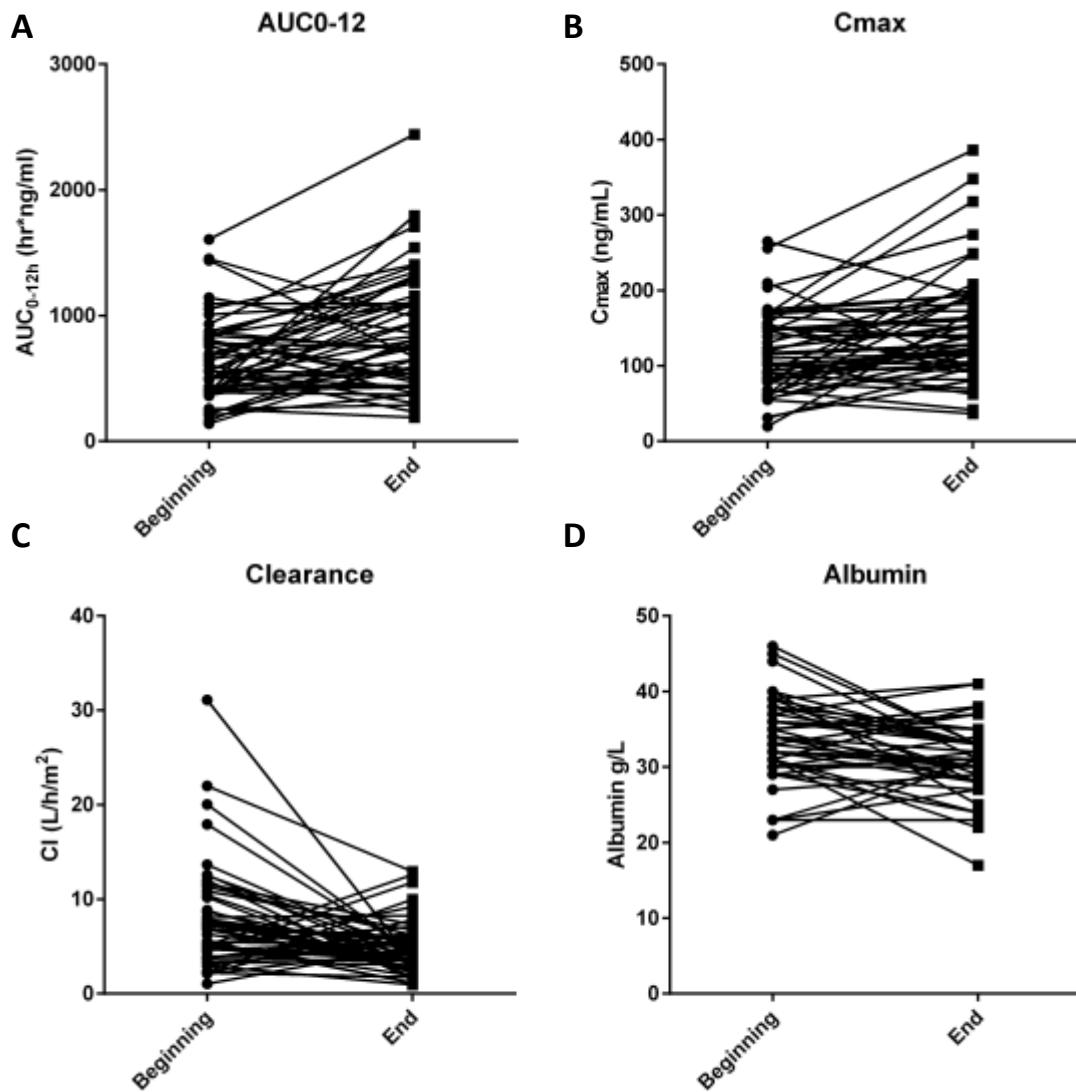


Figure 3.6 Intrapatient variation in pharmacokinetic profiles and albumin concentrations between the beginning and end of induction chemotherapy.

Pharmacokinetic parameters were calculated in WinNonlin and compared in patients who had undergone sampling at both the beginning and end of induction therapy using a paired student's t test. A: Area under the Curve between 0 and 12 hours, n=54, p=0.0003; B: Maximum plasma concentration, n=54, p=0.0003; C: Clearance, n=54, p=0.0016; D: Albumin concentration in blood, n=46, p=0.0078.

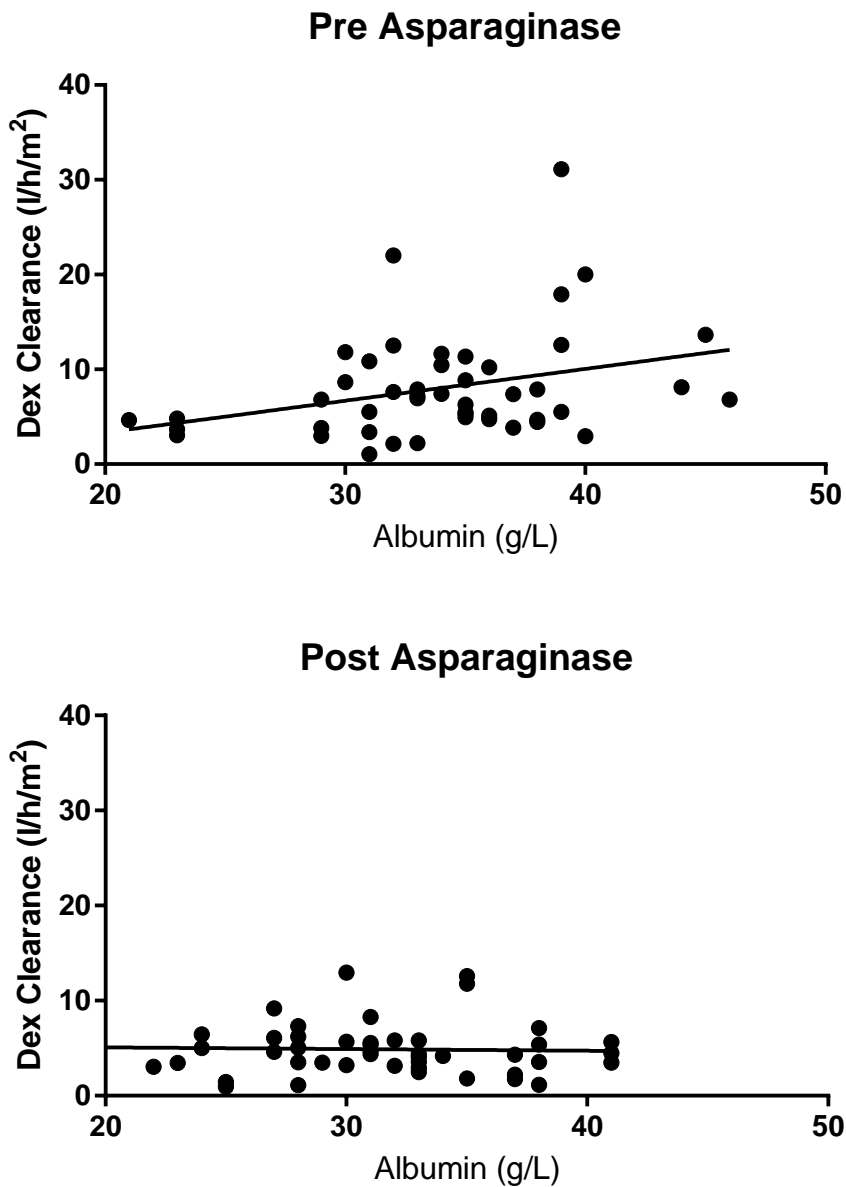


Figure 3.7 Correlation between dex clearance and albumin concentrations pre- and post-asparaginase therapy.

Taken from 47 patients who were analysed for dex pharmacokinetics on one of the first and one of the last three days of induction dex therapy, i.e. pre- and post-asparaginase administration. The correlation between the two parameters was assessed using a linear regression analysis (pre-asparaginase r^2 : 0.1, $p=0.03$; post-asparaginase r^2 : 0.001, $p=0.8$).

To further elucidate a potential interaction between asparaginase and dex, the relationship between asparaginase concentrations and dex pharmacokinetic values was assessed. If asparaginase does affect dex pharmacokinetics, low asparaginase levels may mean that patients not only have a reduced asparaginase antileukaemic action, but will also fail to exhibit the reduced dex clearance associated with asparaginase activity, which would be associated with higher drug exposure.

The asparaginase sub-study was performed by Vaskar Saha's group at Manchester University using a chromogenic assay to measure asparaginase trough levels on days 16 and 30 of treatment. However, there were only 15 patients, for whom valid dex pharmacokinetic parameters were calculated, who were also enrolled on the asparaginase sub-study. This low cross over between the two sub studies is likely due to a difference in hospital site recruitment.

For patients with both asparaginase and dex data available, there was marked interpatient variability in trough asparaginase levels, with a 3.7- and 3.0- fold range in levels observed on day 16 and day 30, respectively. There was also a significant increase in trough asparaginase levels from day 16 to day 30 (paired student's t test, $p < 0.0002$, Figure 3.8). It was not possible to assess the effect of asparaginase allergy on dex pharmacokinetics, as there were only 2 of the 16 patients who had experienced a hypersensitivity reaction. Furthermore, in both cases the hypersensitivity reaction occurred beyond the end of induction therapy.

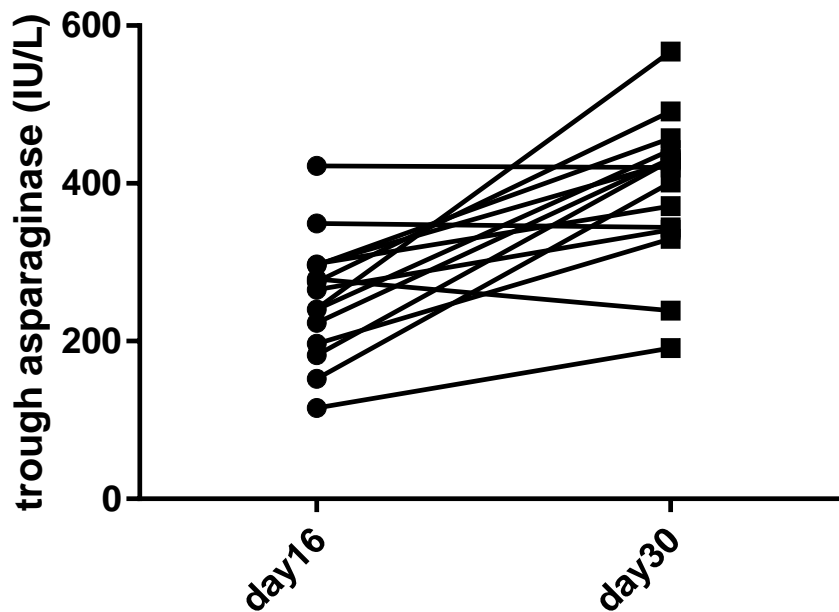


Figure 3.8 Asparaginase trough levels in patients on the dex pharmacokinetic sub-study at day 16 and day 30.

Asparaginase trough levels were measured by V. Saha’s group at Manchester University using a chromogenic assay. There was a significant increase in asparaginase trough levels from day 16 to day 30 (paired student’s t test, $p=0.0002$, $n=15$).

In patients with both asparaginase trough levels and dex pharmacokinetic data, a correlation analysis was performed to assess the relationships between asparaginase, albumin and dex clearance. As the end of induction treatment dex sampling was carried out on days 12-14 or 19-21 for short dex therapy patients, dex clearance values and albumin levels from short therapy were correlated with day 16 asparaginase levels. Similarly, end of induction dex sampling was carried out on days 26-28 for standard dex therapy patients, and therefore albumin levels were correlated with day 30 asparaginase levels (Figure 3.9). It was not possible to assess a correlation between dex clearance and asparaginase levels in those on standard dex, as there were only three standard dex patients who had clearance values and asparaginase trough concentrations. There was no correlation between asparaginase trough concentrations and albumin levels at the end of induction therapy (short dex: $r^2 = 0.2$, $p=0.13$, $n=14$; standard dex: $r^2 = 0.0008$, $p=0.9$, $n=8$). Similarly, there was no correlation between end of treatment dex clearance values in short dex patients and day 16 trough asparaginase levels ($r^2 = 0.03$, $p=0.5$, $n=16$).

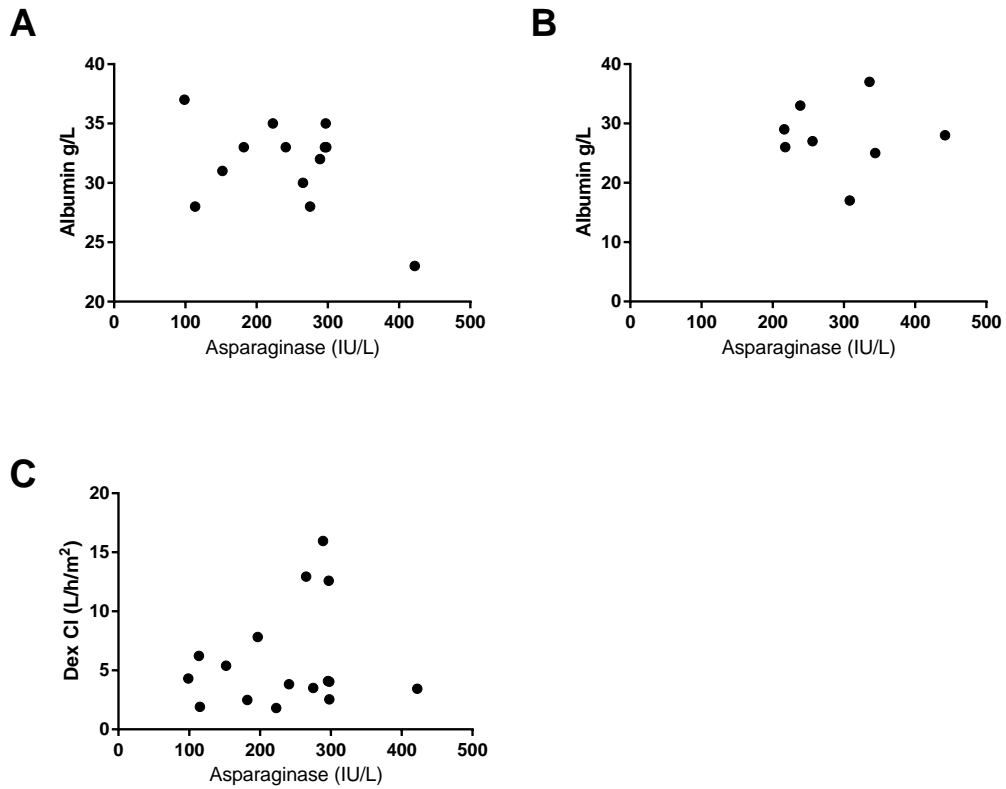


Figure 3.9 Correlation between trough asparaginase levels, and albumin and dex clearance.

The correlation between the two parameters was assessed using a linear regression analysis, r^2 values are shown below. (A) Patients on short dex dosing: end of treatment albumin concentrations correlated with day 16 trough asparaginase levels ($r^2 = 0.2$, $p=0.13$, $n=14$); (B) Patients on standard dex dosing: end of treatment albumin concentrations correlated with day 30 trough asparaginase levels ($r^2 = 0.0008$, $p=0.9$, $n=8$); (C) Patients on short dex dosing: end of treatment dex clearance value correlated with day 14 trough asparaginase levels ($r^2 = 0.03$, $p=0.5$, $n=16$).

To clarify the effect of asparaginase on dex treatment in a larger patient group, intrapatient pharmacokinetic differences were compared in patients who had received one dose of asparaginase versus two. Asparaginase is dosed on days 4 and 18 of induction therapy. Therefore, regimen A patients (NCI standard risk) on the short dex arm will have received one asparaginase dose between the two dex sampling days, whereas regimen B (NCI high risk) patients on the short dex arm and all standard dex arm patients will have received two doses of asparaginase between the dex sampling days. Changes in dex AUC_{0-12h}, clearance and albumin concentration between the beginning and end of induction therapy were compared in those who had been administered one dose of asparaginase vs those who had been administered two doses (Figure 3.10). There was a larger increase in AUC_{0-12h} and decrease in albumin concentrations in patients who had been administered two doses of asparaginase compared to those who had only had one ($p=0.006$ and 0.03 vs. 0.01 and 0.08 respectively, paired student's t test). However, this effect was not seen for dex clearance (2 doses: $p = 0.05$, 1 dose: $p=0.01$).

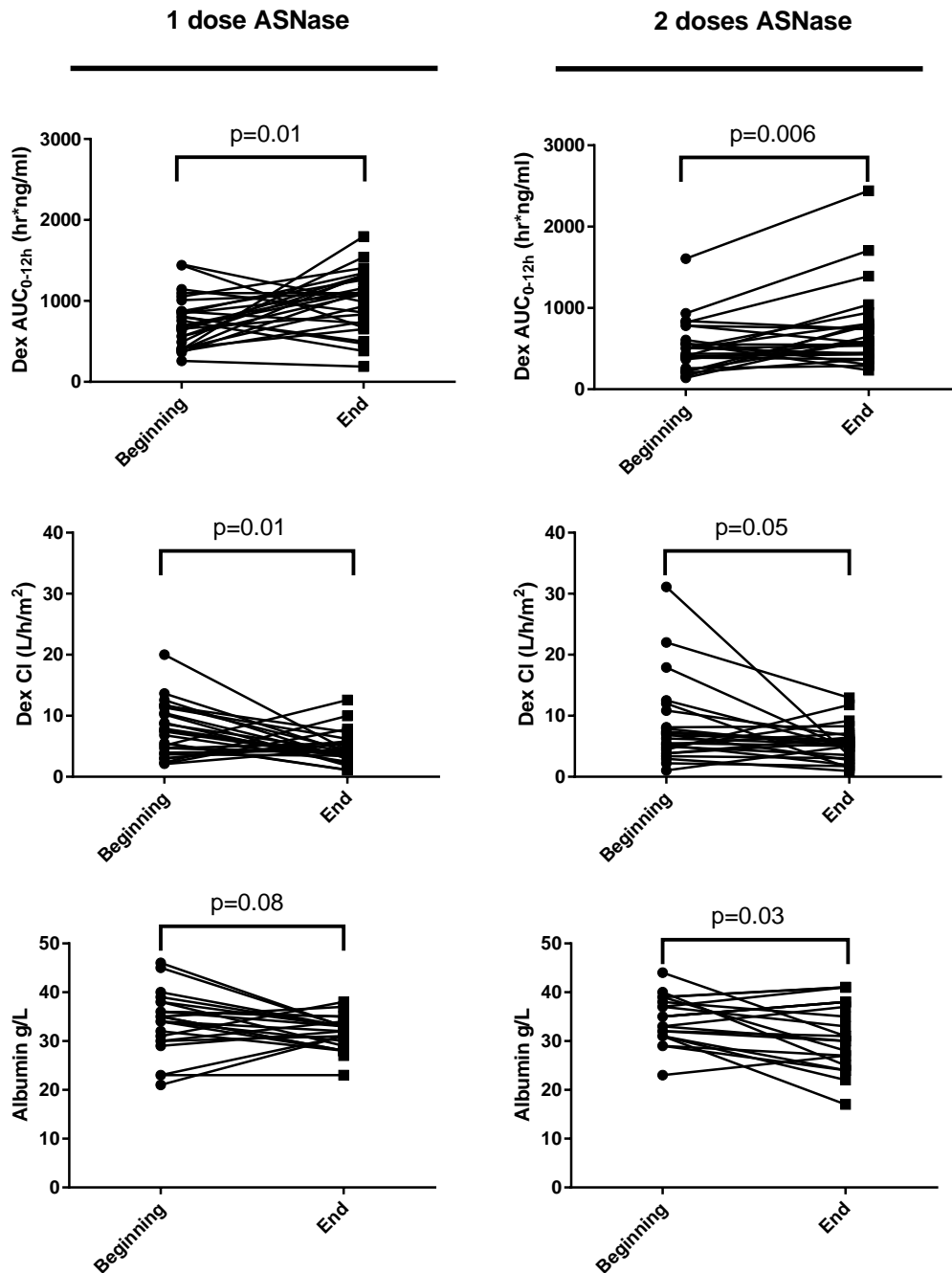


Figure 3.10 Inpatient variation in dex pharmacokinetic parameters and albumin levels in patients receiving one or two doses of asparaginase between dex sampling days.

Dex area under the curve between 0 and 12 hours, dex clearance and albumin concentrations were compared between the beginning and end of induction therapy. The left panel shows patients who had received one dose of asparaginase between dex sampling days. The right panel shows data for patients who had been administered two doses of asparaginase. P values were generated using the paired student's t test.

3.3.5 Covariate analysis: pharmacokinetics and patient characteristics

Regimen B patients receive daunorubicin in addition to the three drug induction given to regimen A patients. To assess whether the addition of daunorubicin, or other patient characteristics specific to this group of patients, may have affected dex pharmacokinetics, relationships between treatment regimen and dex AUC_{0-12h} and clearance were studied (Figure 3.11). There was a statistically significant difference in clearance values observed between NCI standard risk and NCI high risk patients ($p=0.02$), however this was likely to be a result of two outliers in the high risk group. When these patients were excluded from analysis, there was no longer a statistical difference in clearance between the risk groups ($p=0.19$). There was no effect of patient regimen on end of induction therapy clearance ($p=0.74$), or AUC_{0-12h}, both at the beginning and end of induction therapy ($p=0.21$ and 0.18 , respectively).

To determine whether variations in other patient characteristics could account for some of the variability seen in dex pharmacokinetics, relationships between dex clearance and patient surface area, age and gender were tested. However, no relationships were observed between clearance and any of these parameters, either at the beginning or end of induction therapy (Figure 3.12). For example, r^2 values for the correlation between surface area and dex clearance were 0.001 at the beginning and 0.01 at the end of induction therapy ($p=0.71$ and 0.44 , respectively). Similarly, r^2 squared values for the correlation between patient age and clearance were 0.003 at the beginning of induction therapy and 0.001 at the end of induction therapy ($p=0.49$ and $p=0.76$, respectively). This is in contrast to the findings of Yang *et al.* (2008), who reported an association between dex clearance and patient age, with older patients having a lower clearance and thus higher exposure to dex.

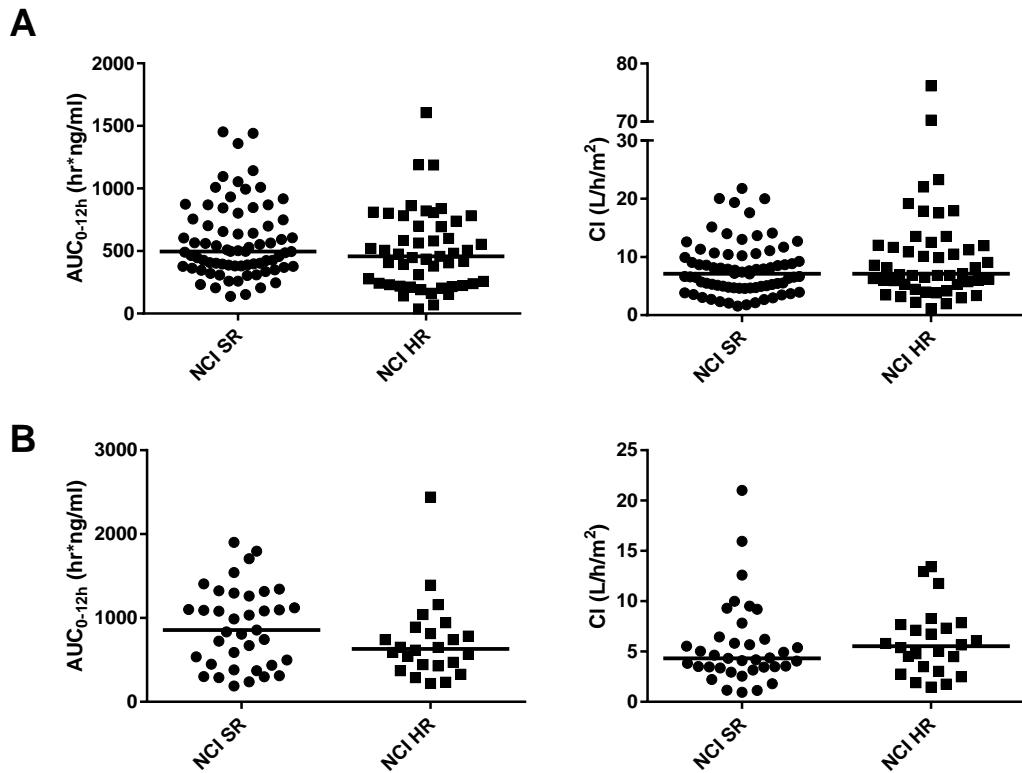


Figure 3.11 Effect of treatment regimen on dex AUC_{0-12h} and clearance.

SR = standard risk HR=high risk. Horizontal bars represent median values. (A) Beginning of induction therapy pharmacokinetic sampling point. Left: difference in area under the curve between 0 and 12 hours between standard and high risk patients at the beginning of induction therapy ($p=0.21$); right: difference in clearance between standard and high risk patients at the beginning of induction therapy ($p=0.02$; without outliers, $p = 0.19$). (B) End of induction therapy pharmacokinetic sampling point. Left: difference in area under the curve between 0 and 12 hours between standard and high risk patients at the end of induction therapy ($p=0.18$); right: difference in clearance between standard and high risk patients at the end of induction therapy ($p=0.74$). P values were generated using the unpaired student's t test (clearance data were transformed to achieve a log distribution before statistical analysis).

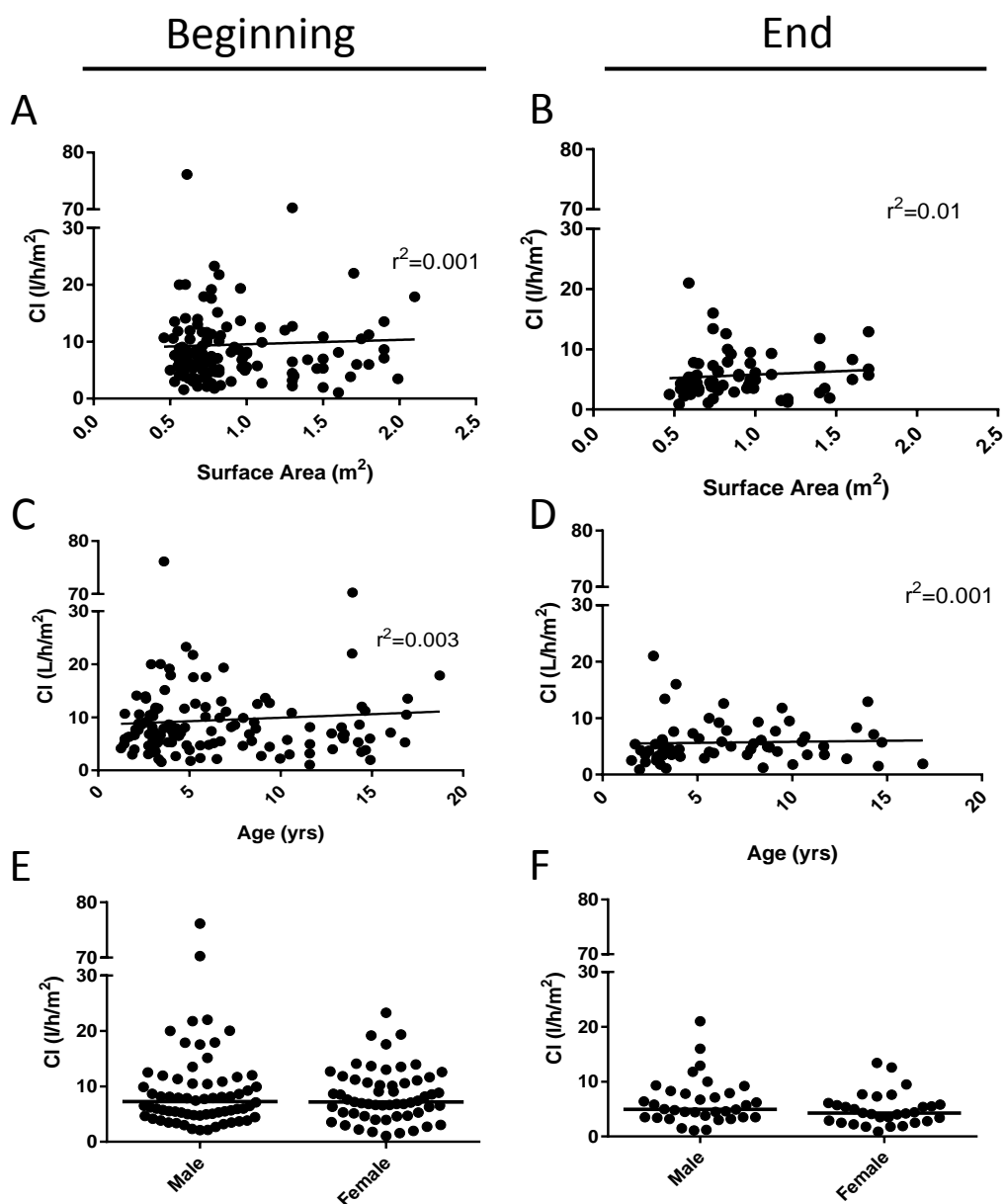


Figure 3.12 Relationship between patient characteristics and dex clearance at the beginning and end of induction therapy.

(A-D) Correlations between parameters were assessed using linear regression analysis, r^2 values are shown on the graph. (A) Correlation between surface area and clearance at the beginning of induction therapy ($n=125$, $p=0.71$) and (B) at the end of induction therapy ($n=64$, $p=0.44$). (C) Correlation between age and clearance at the beginning of induction therapy ($n=125$, $p=0.49$) and (D) at the end of induction therapy ($n=64$, $p=0.76$).

(E-F) Relationship between gender and clearance at the beginning (E) of induction therapy ($n=125$), 7.3 (2.09-76.16) vs. 7.2 (1.07-23.28) l/h/m² ($p=0.23$) and end (F) of induction therapy ($n=64$), 4.9 (1.1-21) vs. 4.25 (0.9-13.4) l/h/m² ($p=0.23$). Data is median (range), p values generated using an unpaired t test (data were log transformed to achieve a normal distribution before statistical analysis). Horizontal bars represent median values.

3.3.6 Covariate analysis: pharmacokinetics and concomitant medication

As patients are often prescribed multiple drugs in addition to the three or four drugs used in induction therapy, it is important to assess the effect of the administration of these additional drugs on dex pharmacokinetics. Firstly, a number of the drugs being administered are both substrates for, and inhibitors or inducers of, CYP3A4, the main cytochrome P450 enzyme responsible for the metabolism of dex. Examples include the proton pump inhibitor, omeprazole, prescribed to reduce gastric irritation, and the antifungal, fluconazole. Secondly, a number of drugs can affect passage through the digestive system which may lead to differences in absorption, thus affecting pharmacokinetics. For example, metoclopramide, an anti-emetic, increases the rate of gastric emptying.

To assess the impact of concomitant medication on dex pharmacokinetics, drugs administered seven days prior to dex until the day of pharmacokinetic sampling were documented. In total, 76 different drugs were recorded, however many of these were only administered to small numbers of patients. Drugs were only assessed if they had been administered to at least 10 patients, with pharmacokinetic parameters compared between patients who had received the drug and those who had not.

The full list of concomitant medications analysed is shown in Table 3.4. For the majority of medications, there was no difference in dex clearance or exposure, as defined by AUC_{0-12h} , between those who had taken the concomitant medication and those who had not. Bonferroni's correction was performed for multiple comparisons. Due to the large number of statistical tests performed on pharmacokinetic parameters, the p value at which significance was accepted was adjusted. As 13 tests were performed on beginning, and 12 tests were performed on end of induction therapy pharmacokinetics, p values of <0.0038 and 0.0042 respectively were accepted as significant. A small number of medications did appear to be associated with dex pharmacokinetics, although only one association was significant after correction for multiple testing.

Administration of rasburicase (n=23) for hyperuricaemia was associated with lower dex AUC_{0-12h} values at the beginning of induction therapy (rasburicase: 397.8

hr*ng/ml (38.31 - 1187), no rasburicase: 506.4 hr*ng/ml (137.2-1606), median (range), $p=0.0097$, student's t-test) and higher dex clearance values (rasburicase: 10.86 l/h/m² (3.46 - 76.2), no rasburicase: 6.81 l/h/m² (1.07 - 31.1), median (range), $p<0.0001$) (Figure 3.13A). There was only one patient taking rasburicase on or immediately before the end of induction therapy sampling, so it was not possible to ascertain whether it also affected end of treatment dex pharmacokinetics.

There was also a significant increase in dex exposure in patients being administered osmotic agents, although this was not reflected in the clearance values (osmotic agent AUC_{0-12h}: 591.9 hr*ng/ml (215.2-1452), clearance 4.69 l/h/m² (1.07 – 20.03) vs no osmotic agent AUC_{0-12h}: 424.9 hr*ng/ml (38.31 – 1606), clearance: 7.62 l/h/m² (1.55 – 76.16); $p=0.01$ and 0.08, respectively). However, this increase in dex exposure was not significant after correction for multiple testing. The altered exposure in this situation may be due to a change in bioavailability of the drug rather than altered drug elimination. Osmotic agents are prescribed to patients with constipation, so passage of gastric contents, including dex, through the gastrointestinal tract will be altered in these patients. The association between osmotic agents and dex exposure, however, was not seen at the second pharmacokinetic sampling point at the end of induction therapy ($p=0.5$, student's t test).

In contrast, despite not being correlated with pharmacokinetics at the start of induction therapy, administration of ranitidine was associated with dex AUC_{0-12h} and clearance at the end of induction therapy pharmacokinetic sampling point (ranitidine AUC_{0-12h}: 1102 hr*ng/ml (189-2441), clearance: 3.49 l/h/m² (0.95 – 6.75) vs no ranitidine AUC_{0-12h}: 741 hr*ng/ml (218 – 1902), clearance: 5.22 l/h/m² (1.16 – 21.0) $p=0.045$ and $p=0.001$, respectively), (Figure 3.13B). However, after adjustment for multiple testing using Bonferroni's correction, this was not statistically significant. Although ranitidine has been reported to be an inhibitor of CYP3A (U.S. Food and Drug Administration, 2017), a number of studies also found no inhibitory effect *in vivo* (Martinez *et al.*, 1999; Lemahieu *et al.*, 2005).

Drug	Class	Potential effect on dex pharmacokinetics	Sampling day	No Patients	AUC values (hr*ng/ml) drug vs no drug (median (range))	AUC p value	Clearance values (l/h/m ²) drug vs no drug (median (range))	Clearance p value
Any opiate	Opiates	May affect absorption	Beginning	57	491 (38.3-1606) vs 446 (69.1-1452)	0.44	6.82 (1.07-76.2) vs 7.43 (1.55-70.3)	0.779
			End	18	798 (239-2441) vs 743 (189-1707)	0.14	3.48 (1.13-21.0) vs 4.63 (0.95-15.9)	0.57
Metaclopramide	Antiemetic	Increases gastric emptying	Beginning	13	393 (205-839) vs 479 (38.3-1606)	0.19	8.17 (1.07-23.3) vs 7.07 (1.55-76.2)	0.88
			End	7	N/A			
Ondansetron	Antiemetic	CYP3A4 S, P-gp I-	Beginning	65	476 (38.3-1606) vs 506 (142-1440)	0.66	6.96 (1.07-76.2) vs 7.39 (1.79-20.0)	0.19
			End	25	742 (234-2441) vs 820 (189-1902)	0.97	4.93 (0.95-21.0) vs 4.27 (1.13-13.4)0-	0.47
Amikacin	Antibiotic	P-gp S	Beginning	20	585 (137-1452) vs 467 (38.3-1606)	0.24	5.64 (2.09-22.0) vs 7.41 (1.07-76.2)	0.42
			End	6	N/A			

(Continued overleaf)

Cotrimoxazole	Antibiotic	N/A	End	33	933 (189-2441) vs 603 (234-1902)	0.09	4.05 (0.95-15.9) vs 5.75 (1.13-21.0)	0.09
Gentamycin		CYP3A4 S P-gp S	Beginning	14	451 (162-839) vs 493 (38.3-1606)	0.54	7.95 (3.55-31.1) vs 7.09 (1.07-76.2)	0.94
Meropenam		CYP3A4 S P-gp S	Beginning	20	430 (142-1606) vs 493 (38.3-1452)	0.38	8.37 (1.55-17.9) vs 7.09 (1.07-76.2)	0.6
			End	9	N/A			
Piperacillin/ tazobactam		CYP3A4 S P-gp S	Beginning	69	503 (38.3-1452) vs 426 (142-1606)	0.52	6.96 (1.07-76.2) vs 7.72 (1.55-31.1)	0.68
			End	11	546 (189-1902) vs 795 (219-2441)	0.38	4.63 (1.13-21.0) vs 4.51 (0.95-15.9)	0.35
Teicoplanin	N/A	Beginning	28	498 (162-1606) vs 484 (38.3-1452)	0.63	6.48 (1.55-31.1) vs 7.28 (1.07-76.2)	0.44	
Rasburicase	Anti- hyperuricaemic	N/A	Beginning	23	398 (38.3-1187) vs 506 (137-1606)	0.0097	10.9 (3.46-76.2) vs 6.81 (1.07-31.1)	<0.0001*
			End	1	N/A			
Omeprazole	Antisecretory	CYP3A4 S/I-/I+ P-gp I-	Beginning	31	496 (206-839) vs 483 (38.3-1606)	0.22	7.88 (1.07-20.0) vs 7.07 (1.55-76.2)	0.42
			End	30	824 (219-2441) vs 723 (189-1405)	0.11	4.13 (0.95-15.9) vs 5.39 (1.13-21.0)	0.3

Ranitidine	Antisecretory	N/A	Beginning	25	486 (38.3-1359) vs 491 (69.1-1606)	0.49	7.07 (1.55-76.2) vs 7.17 (1.07-70.3)	0.38
			End	13	1102 (189-2441) vs 742 (219-1902)	0.045	3.49 (0.95-6.75) vs 5.21 (1.16-21.0)	0.01
Ambisome	Antifungal	CYP3A4 S	Beginning	16	421 (69.1-1189) vs 493 (38.3-1606)	0.4	8.66 (1.98-70.3) vs 7.14 (1.07-76.2)	0.11
			End	7	N/A			
Osmotic Agents	Laxative	May affect absorption	Beginning	27	592 (215-1452) vs 448 (38.3-1606)	0.0052	4.69 (1.07-20.0) vs 7.62 (1.55-76.2)	0.089
			End	17	933 (189-2441) vs 742 (219-1902)	0.51	4.36 (1.75-21.0) vs 4.86 (0.95-15.9)	0.87

Table 3.4 Relationship between concomitant drug administration and dex pharmacokinetic parameters.

P values were derived by comparing the means of pharmacokinetic parameters in those who had taken a drug versus those who had not using an unpaired student's t test. PK= pharmacokinetics; S=substrate; I- = inhibitor; I+ = inducer. N/A = fewer than 10 patients therefore statistical analysis not performed. Bonferroni's correction was performed for multiple comparisons. Due to the large number of statistical tests performed on pharmacokinetic parameters, the p value at which significance was accepted was adjusted. As 13 tests were performed on beginning, and 12 tests were performed on end of induction therapy pharmacokinetics, p values of <0.0038 and <0.0042 respectively were accepted as significant.

* denotes statistically significant result.

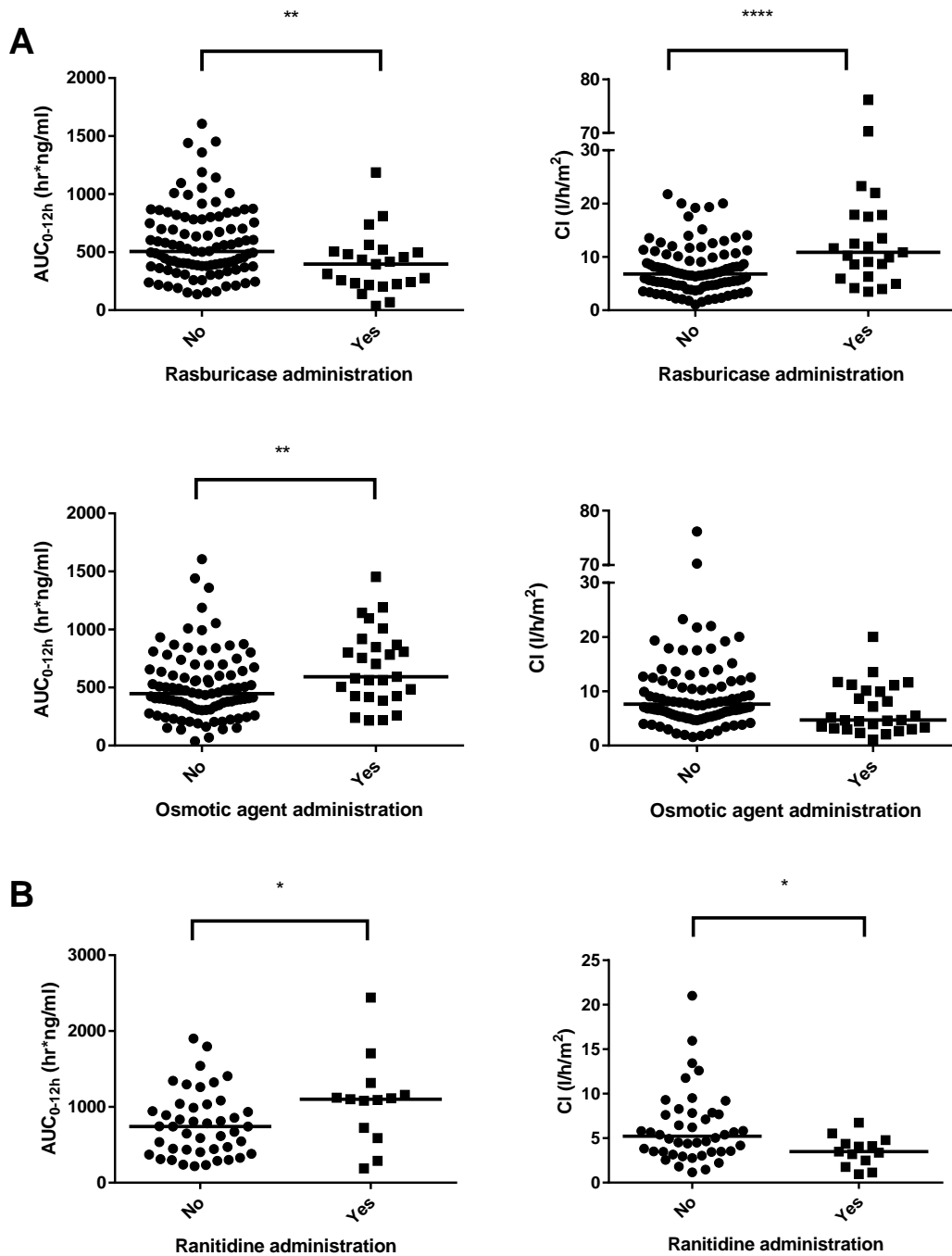


Figure 3.13 Relationship between concomitant medication administration and dex pharmacokinetic parameters at the beginning (A) and end (B) of induction therapy.

(A) Difference in AUC_{0-12h} and clearance between patients that had taken rasburicase or osmotic agent versus those who had not at the beginning of induction therapy (rasburicase: AUC $p=0.0097$, clearance $p<0.0001$; osmotic agent: AUC $p=0.0052$; clearance $p=0.089$). (B) Difference in AUC_{0-12h} and clearance between patients that had taken ranitidine versus those who had not at the end of induction therapy (ranitidine: AUC $p=0.045$, clearance $p=0.01$). Horizontal bars represent median values.

3.3.7 Relationship between dex pharmacokinetics and toxicity

In order to assess whether variation in dex pharmacokinetics affected incidence of toxicity, key pharmacokinetic parameters were compared between patients who had experienced at least one grade 3/4 adverse event and those who had not. Toxicity data were obtained for 120 patients who also had valid beginning of induction therapy dex pharmacokinetic data. In total, 68 patients were recorded as having experienced a grade 3/4 adverse event.

The most common category of adverse events experienced was infections and infestations, with 50 (42%) patients experiencing an infection. Device related infections and upper respiratory infections were the most common types of infections, experienced by 17 (12%) and 12 (9%) patients respectively. A full list of grade 3-4 toxicities is shown in Table 3.5.

There was a bimodal distribution for patient age or body surface area and experiencing a grade 3-4 toxicity (Figure 3.14). The relationships between age or body surface area and incidence of toxicity were assessed using a chi squared test. There was a trend towards a higher proportion of toxicity in patients of greater compared to less than 10 years of age, however this was not statistically significant ($p=0.058$). There was also a higher proportion of patients with a larger body surface area (greater than 1.25m^2 experiencing Grade 3/4 toxicities ($p=0.01$).

There were no associations between any dex pharmacokinetic parameter and the incidence of any grade 3-4 adverse event ($\text{AUC}_{0-12\text{h}}$ $p=0.6$, cumulative AUC $p=0.4$, C_{max} $p=0.9$, clearance $p=0.9$; one way ANOVA) (Figure 3.15). Similarly, there was no effect of treatment regimen or dex arm on the incidence of toxicity ($p=0.1$ and 0.7 respectively, chi squared test) (Figure 3.16). However, other chemotherapeutic agents are also used during induction therapy which contribute to toxicity, and this may confound the relationship between the incidence of toxicity and dex pharmacokinetic parameters.

In an attempt to limit the influence of other chemotherapeutic agents, several steroid-related toxicities were selected (with at least 10 incidences) and their relationship with dex pharmacokinetic parameters was assessed (Table 3.6). There was a trend towards an increased $\text{AUC}_{0-12\text{h}}$ being associated with haematological

events, however this was not statistically significant ($p=0.09$, student's t test). There were also no significant association with any of the other steroid-related toxicities and dex pharmacokinetic parameters (student's unpaired t test, Table 3.6).

	Number of Patients		
	Total* n (%)	Short dex n (%)	Standard dex n (%)
Blood and Lymphatic disorders	9 (7.5)	8 (11.6)	1 (2.0)
Gastrointestinal disorders	11 (9.2)	6 (8.7)	5 (9.8)
Hepatobiliary disorders	1 (0.8)	1 (1.4)	0 (0)
Infections and infestations	48 (40)	29 (42.0)	19 (37.3)
Injury, poisoning and procedural complications	2 (1.6)	2 (2.9)	0 (0)
Investigations	2 (1.6)	2 (2.9)	0 (0)
Metabolism and nutrition disorders	10 (8.3)	6 (8.7)	4 (7.8)
Musculoskeletal and connective tissue disorders	4 (3.3)	1 (1.4)	3 (5.9)
Nervous System disorders	3 (2.5)	2 (2.9)	1 (1.7)
Skin and subcutaneous tissue disorders	3 (2.5)	2 (2.9)	1 (1.7)
Vascular disorders	7 (5.8)	4 (5.8)	3 (5.9)
None	47 (39)	28 (40.6)	19 (37.2)

Table 3.5 Grade 3-4 toxicities experienced during induction phase in patients on the dex pharmacokinetic sub-study of the UKALL 2011 trial.

*Total = total number of patients with valid pharmacokinetic data at the beginning of treatment pharmacokinetic sampling day. Short n=69, standard n=51. 'None' includes patients who experienced grade one or two toxicity only.

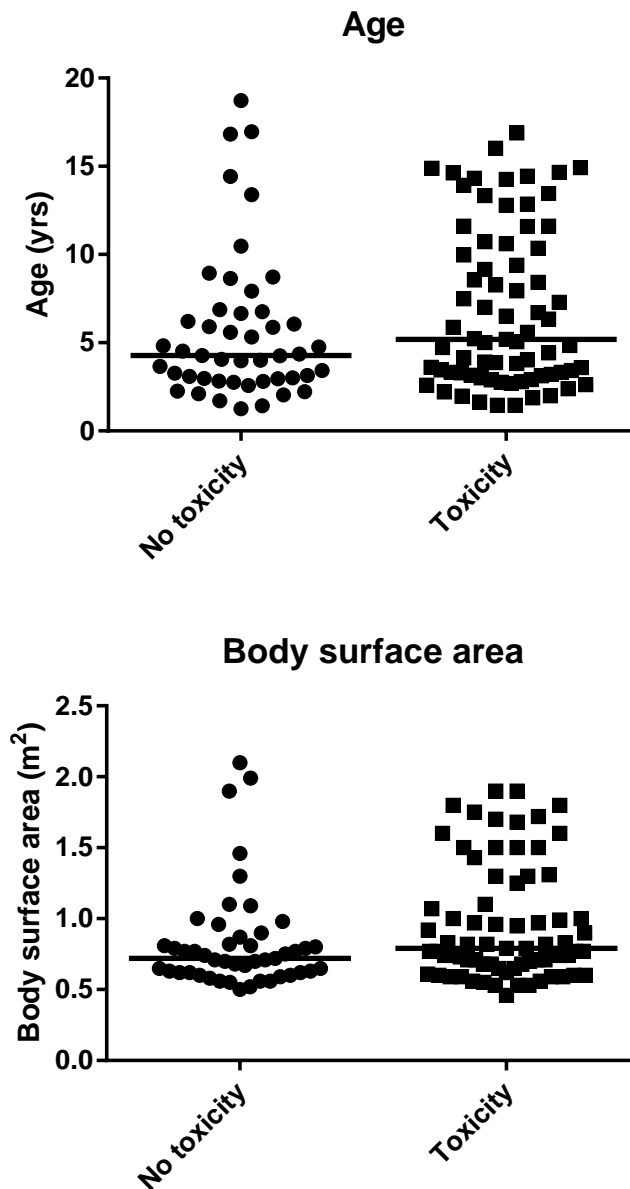


Figure 3.14 Relationship between incidence of grade 3-4 toxicity and patient age and surface area.

Due to the bimodal distribution for patient age or body surface area and experiencing a grade 3-4 toxicity, the relationships between age or body surface area and incidence of toxicity were assessed using a chi squared test. Age: incidence of toxicity was compared in patients of less than and greater than 10 years of age ($p=0.058$). Body surface area: incidence of toxicity was compared in patients of less than or greater than 1.25m^2 ($p=0.01$). Horizontal line shows median value.

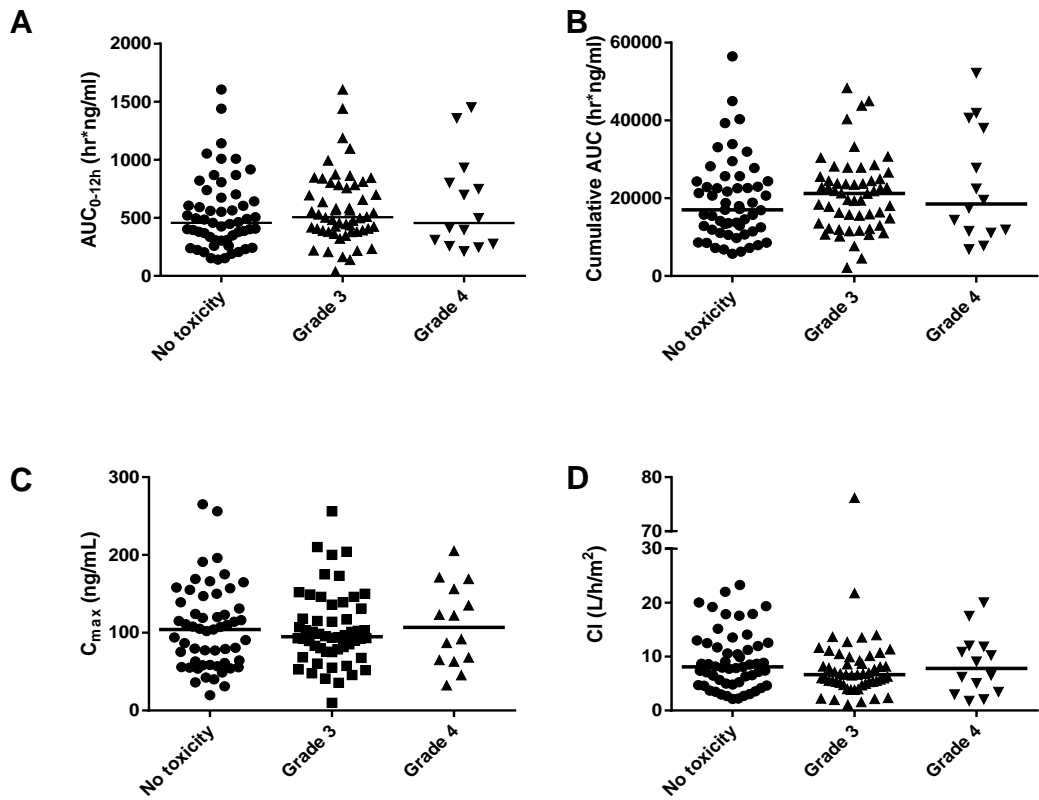
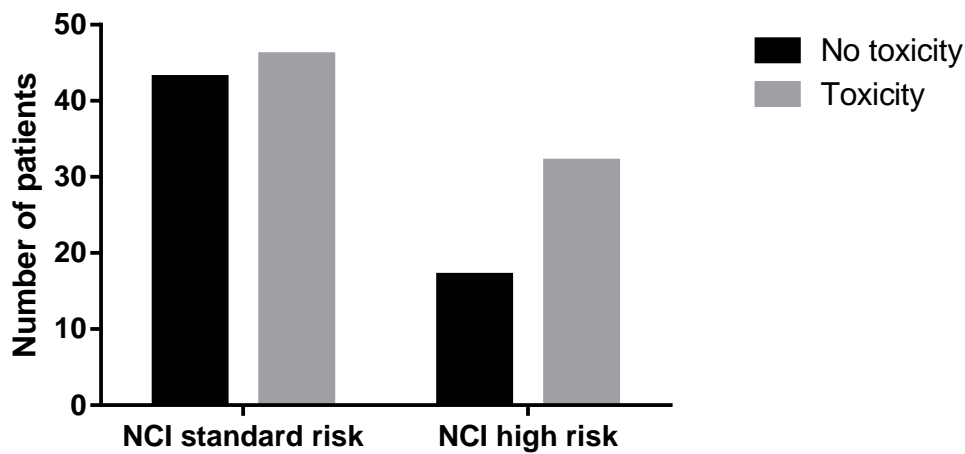


Figure 3.15 Relationship between incidence of grade 3-4 toxicity and dex pharmacokinetic parameters.

(A) Area under the curve between 0 and 12 hours after a single dose of dex; (B) Cumulative AUC (hr*ng/ml) extrapolated to exposure for duration of induction therapy; (C) Maximum plasma concentration reached; (D) Clearance normalised to body surface area. Horizontal bars represent median values. No toxicity includes patients with grade 1-2 toxicity.

A



B

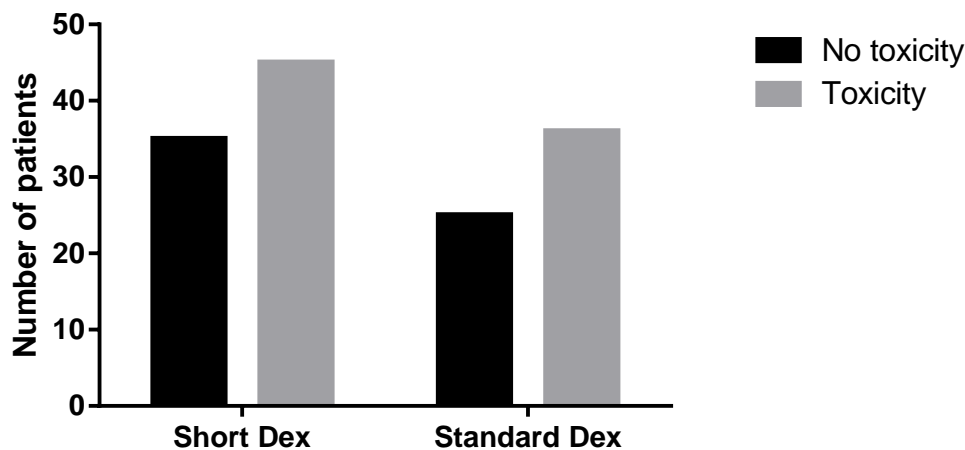


Figure 3.16 Relationship between incidence of grade 3-4 toxicity and treatment regimen.

(A) Incidence of toxicity in NCI standard risk (regimen A) versus NCI high risk (regimen B) patients. Despite an increase in toxicity cases in the NCI high risk group, this was not statistically significant ($p=0.1$, Chi-square test). (B) Incidence of toxicity in patients on short dex dosing versus those on standard dex dosing. There was no significant difference between the two in terms of the number of patients experiencing toxicity ($p=0.7$, Chi-square test).

	Number of Patients			Association with pharmacokinetic parameters (p-value)			
	Total* n (%)	Short dex n (%)	Standard dex n (%)	AUC _{0-12h} (hr*ng/ml)	Cumulative AUC (hr*ng/ml)	C _{max} (ng/ml)	Clearance (l/h/m ²)
Encephalopathy	3 (2.5)	2 (2.9)	1 (2.0)	N/A	N/A	N/A	N/A
Fracture	3 (2.5)	3 (4.3)	0 (0)	N/A	N/A	N/A	N/A
Glucose related	10 (8.3)	6 (8.7)	4 (7.8)	0.45	0.36	0.64	0.90
Hypertension	6 (5)	3 (4.3)	3 (5.9)	N/A	N/A	N/A	N/A
Infection	51 (42.5)	30 (43.5)	21 (4.1)	0.54	0.74	0.70	0.56
Muscle related	4 (3.3)	2 (2.9)	2 (3.9)	N/A	N/A	N/A	N/A
Osteoporosis	1 (0.83)	1 (1.4)	0 (0)	N/A	N/A	N/A	N/A
Psychosis	0 (0)	0 (0)	0 (0)	N/A	N/A	N/A	N/A
Thromboembolic events	1 (0.83)	1 (1.4)	0 (0)	N/A	N/A	N/A	N/A
Blood Disorders	9 (0.75)	8 (11.6)	1 (2.0)	N/A	N/A	N/A	N/A

Table 3.6 Steroid specific adverse events in patients on the UKALL 2011 dex pharmacokinetic sub-study and their relationship with dex pharmacokinetic parameters.

Steroid specific adverse events were assessed where there were at least ten incidences within patients on the dex pharmacokinetic sub-study. Pharmacokinetic parameters were compared between patients who had experienced a steroid related toxicity and those who had not. P values were generated using the unpaired student's t test. N/A = No statistical test performed due to low patient numbers for the individual steroid specific adverse event.

3.3.8 The effect of variable dex pharmacokinetics on outcome

Currently, there is no long term follow up data for patients on this trial. Therefore, day 8 response and MRD measurements were used as a surrogate marker of clinical response, as MRD measurements have been shown to be highly prognostic of patient outcome (Vora *et al.*, 2013b). All patients were assessed for blast count at day 8 and MRD at day 29 of therapy.

There was a significant difference in AUC_{0-12h} between patients with a day 8 bone marrow blast count of less, or greater than, 5%. A day 8 blast count of less than 5% was associated with a higher mean dex exposure ($p = 0.0007$, student's t test, Figure 3.17A). However, importantly there was no difference between the short and standard arm in terms of day 8 blast count ($p = 0.058$, student's t test, Figure 3.17B). This indicates that dex exposure may be more important than dose administered.

When extended to day 29 MRD, no associations were observed between any pharmacokinetic parameter and risk status ($p = 0.71$, student's t test, Figure 3.17C). A longer follow up time is needed to establish the significance of this rapid early response in patients with high dex exposures in this population.

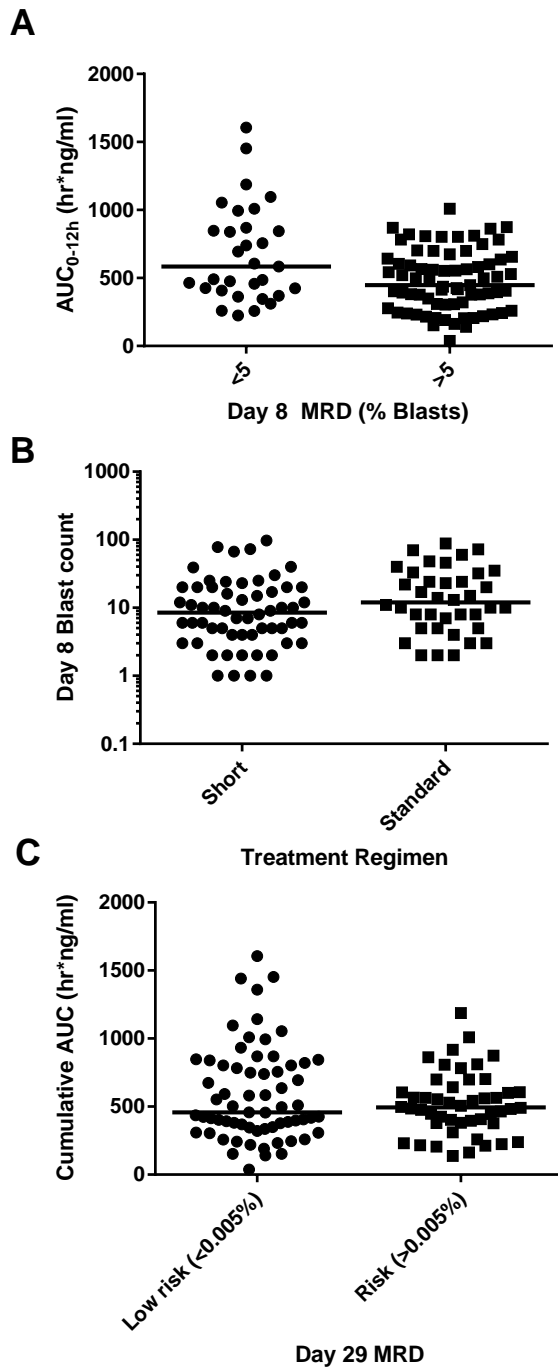


Figure 3.17 Association between dex exposure and outcome, defined by MRD.

(A) There was a significant difference in exposure, defined by AUC_{0-12h} between patients with a day 8 blast count of <5 or >5 ($p = 0.0007$) (B) There was no difference in day 8 blast count between patients on short and standard dex therapy ($p = 0.057$) (C) There was no difference in exposure between patients with < 0.005% or >0.005% MRD measurement ($p=0.71$). P values were generated using the student's t test. Data in (B) were log transformed to achieve a normal distribution before testing for significance. Horizontal bars represent median values.

3.3.9 Cerebrospinal fluid pharmacokinetics

CNS directed therapy is an important part of ALL treatment protocols, without which it has been shown that up to 75% of children relapse with CNS disease (Evans *et al.*, 1970). Dex is the steroid of choice in the UK due to its superior efficacy against CNS disease compared to prednisolone (Mitchell *et al.*, 2005). As dex pharmacokinetics are highly variable in plasma, the same may be true for CSF dex pharmacokinetics, which could affect risk of CNS relapse. Therefore a small pilot study was performed on retrospectively collected CSF samples to quantify dex concentrations, in collaboration with Dr. Christina Halsey at Glasgow University, who kindly provided CSF samples from children with ALL.

Initially, the LC/MS method used for the quantification of dex concentrations in plasma and cell lysates was assessed for its suitability for use with artificial CSF (aCSF). A number of ions are present in CSF and there was a concern that this may lead to ion suppression of the LC/MS signal. To test this, 100ng/ml dex was spiked in water, mobile phase (70% 0.1% formic acid, 30% acetonitrile) and aCSF, and chromatograms were compared. In all three matrices, dex had a comparable retention time of ~9.4 minutes. There was a slight reduction in signal in the aCSF sample, with a peak area of 6.4×10^5 compared to 7.6×10^5 in mobile phase. However, as this was only a 15% reduction, this would not affect quantification of CSF dex peaks, and the method was deemed acceptable for use with CSF samples.

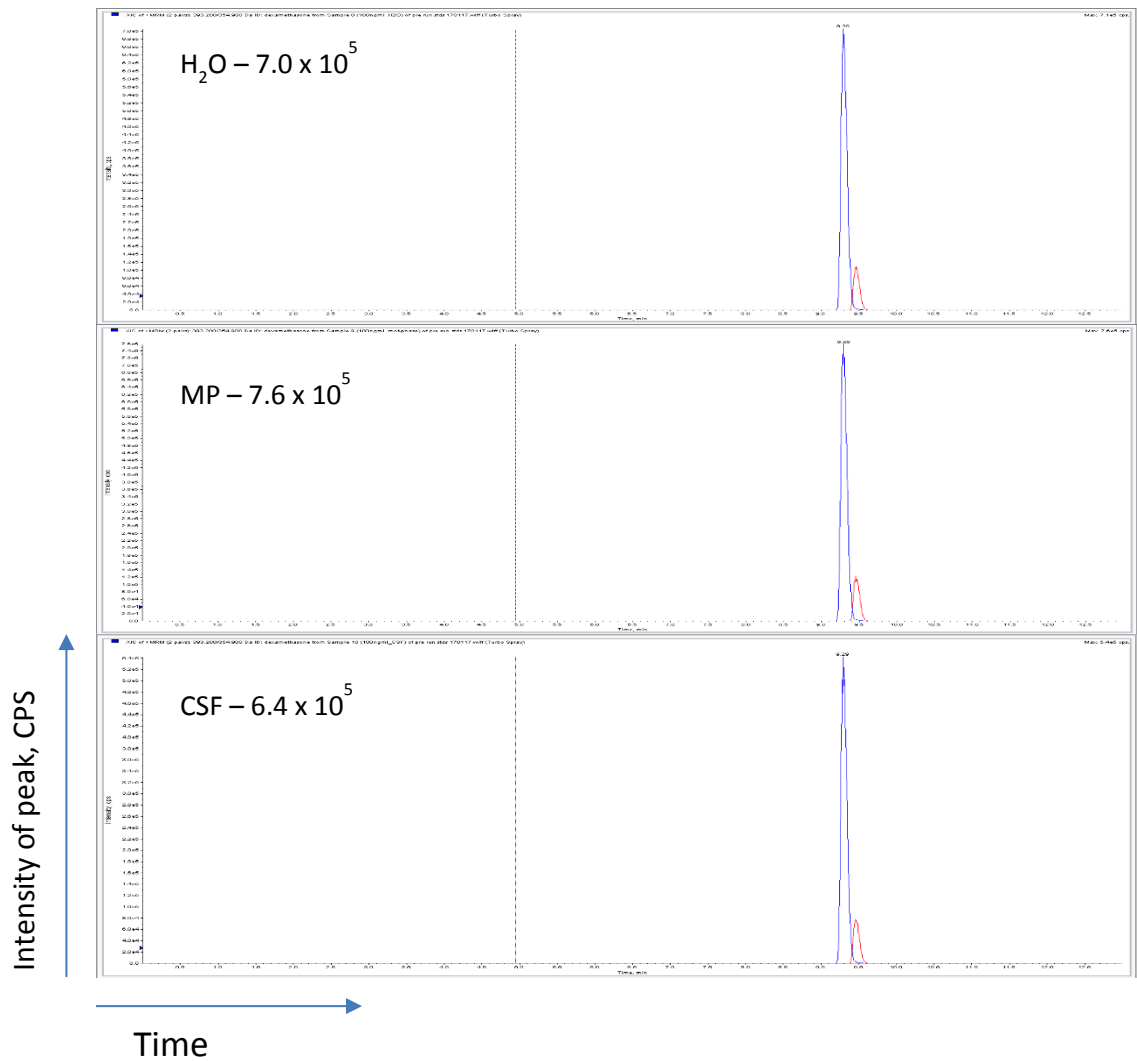


Figure 3.18 Typical chromatograms for 100ng/ml dex and beclomethasone in spiked water, mobile phase and artificial CSF.

Mobile phase consisted of 70% 0.1% formic acid and 30% acetonitrile. Dex (blue) and beclomethasone (red) peaks displayed a similar retention time in all matrices of approximately 9.4 minutes. There was a slightly reduced signal in the aCSF sample, however this would not affect the quantification of dex CSF peaks.

A total of 39 patient CSF samples were analysed from 36 patients. Samples were injected onto the LC/MS after a standard curve of dex prepared in aCSF. This included thirty-three day 8 CSF samples and six day 28 samples. Patients were receiving either short dex therapy (10mg/m² x 14 days, n=11) and or standard dex therapy (6mg/m² x 28 days, n=25) as part of the interim guidelines between UKALL 2003 and 2011, or the UKALL 2011 trial. Three day 8 patients had CSF dex concentrations below the limit of quantification and were therefore excluded from the analysis.

There was wide variation in CSF dex concentrations both at day 7 (6.5 ng/ml (1.4-17)) and day 28 (4.4 ng/ml (0.4-11.1), median (range)). However, detailed sampling time information was not recorded for these patients, hence differences in the length of time between dex dosing and CSF sampling may have contributed to the variation seen in CSF dex concentrations.

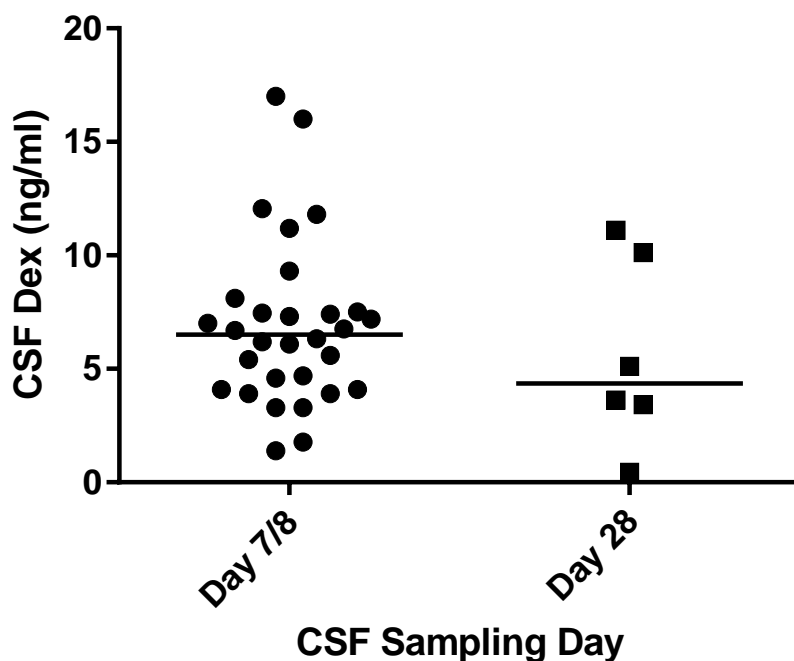


Figure 3.19 Initial quantification of dex in CSF samples from children with ALL.

CSF samples were provided by Dr Christina Halsey. Samples were taken at days 7, 8 and 28 of induction chemotherapy from patients enrolled on the interim guidelines prior to the UKALL 2011 trial, or the UKALL 2011 trial. Dex CSF concentrations were measure using LC/MS. Horizontal bars represent median values.

There was no significant relationship between age and CSF dex concentrations ($p=0.29$, one way ANOVA, Figure 3.20A). There was a statistically significant increase in CSF dex concentration in patients who had received $10\text{mg}/\text{m}^2$ per day compared to patients who had received $6\text{mg}/\text{m}^2$ per day (8.3 ng/ml (4.1-16) vs 6.3 ng/ml (1.4-8.1); median (range), $p=0.01$, unpaired student's t test). However, similar to plasma dex data, there was large variation within the arms in CSF dex concentrations and there was an overlap between the two arms (Figure 3.20B).

Of the thirty day 8 patients analysed, two patients experienced a CNS relapse and one patient experienced a bone marrow relapse. There were not enough patients with a CNS relapse to perform any statistical tests to assess a change in CSF dex concentrations in these patients, however Figure 3.20C shows that the two patients with a CNS relapse fall in the middle of the range of patients who did not relapse (CNS relapse: 3.9 and 7.3 ng/ml , no CNS relapse 6.5 ng/ml (1.4-12.1), median (range)). This may suggest that CNS dex concentration is not a factor in CNS relapse, however these are very small patient numbers. Furthermore, as previously noted, the time between dex administration and CSF sampling was not recorded for the patients. This may have affected all the results generated and therefore a study with increased patient numbers and more detailed sampling time records needs to be performed to expand on these preliminary findings.

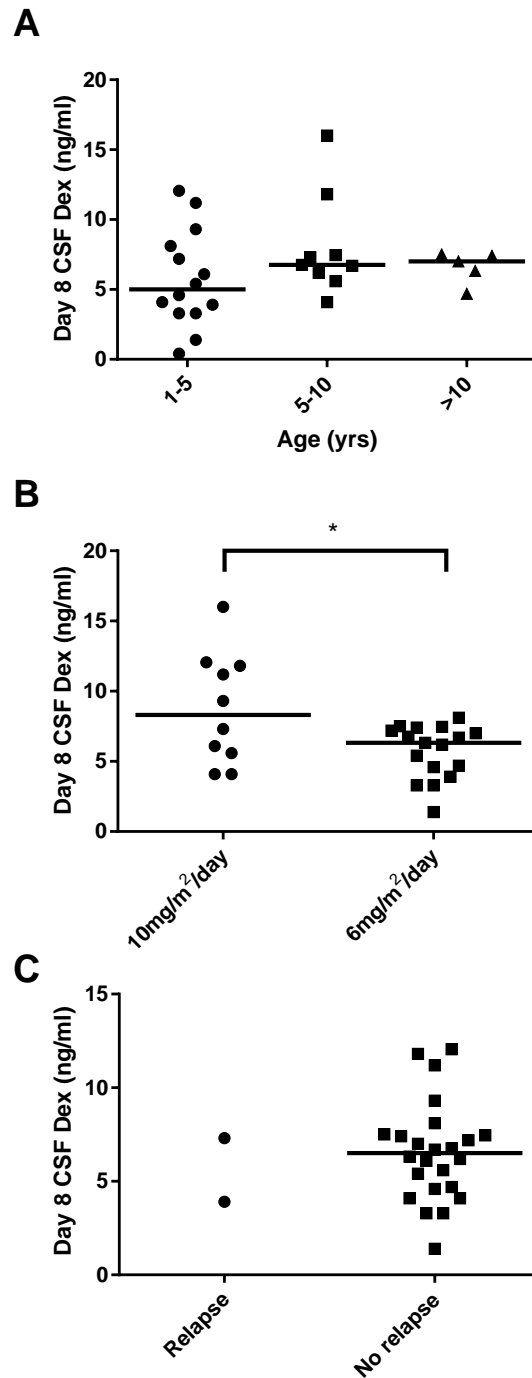


Figure 3.20 CSF dex concentrations in day 8 patient samples on the UKALL 2011 trial.

(A) CSF dex concentrations in different age groups in years ($p=0.29$, one way ANOVA); (B) CSF dex concentrations in patients who received 6mg/m^2 dex per day and $10\text{mg/m}^2/\text{day}$ ($p=0.008$, unpaired student's t test); (C) CSF dex concentrations in patients who relapsed in the CSF and patients who have not relapsed. No statistical text was performed due to small patient numbers in CSF relapse group. One patient was excluded as they had a bone marrow relapse. Horizontal bars represent median values.

3.4 Discussion

Over recent decades, survival for patients with ALL has increased dramatically. However, this is mainly due to augmentation and intensification of treatment, which has conversely also brought about a significant increase in toxicity and decreased quality of life. As such, the focus in paediatric ALL has shifted to reducing treatment related morbidity and mortality whilst maintaining current survival rates. Despite current stratification approaches, there is a need for further ways to personalise therapy to give patients the best chance of survival and the lowest chance of side effects. Dex pharmacokinetics have been reported to be highly variable (Yang *et al.*, 2008), and as such may provide an approach to stratify dex therapy. This project has therefore aimed to characterise the relationship between dex scheduling, pharmacokinetics and both clinical outcome and toxicity as part of the UKALL 2011 trial. Despite closure of the R1 arm of the trial, recruitment to the dex pharmacokinetic sub-study is still ongoing to generate equal patient numbers in the short and standard patient groups. The results discussed here therefore represent an interim analysis of the data generated to date.

Patient samples analysed to date have shown large interindividual variability in pharmacokinetics, with a >20-fold variation in AUC_{0-12h} values on both arms of therapy. This is larger than the level of variability previously reported in a US study; Yang *et al.* observed a 10-fold variation in dex exposure in a cohort of 214 patients. Similarly, the extent of dex pharmacokinetic variability in this trial is greater than that seen in one other non-ALL paediatric study (Richter *et al.*, 1983) and in healthy adult volunteers (Loew *et al.*, 1986; O'Sullivan *et al.*, 1997; Queckenberg *et al.*, 2011), however these sample groups were much smaller.

Parameters such as AUC_{0-12h} and C_{max} were significantly higher on the short compared to the standard dex arm of therapy, with a linear increase in AUC_{0-12h} between the two dex doses. However there was substantial overlap between the two patient groups. A number of patients on the standard arm exhibited higher exposures than those on short therapy, an important observation given the different durations of therapy on the two arms. Importantly, the UKALL 2011 R1 study found no statistical difference in terms of steroid related toxicity or MRD response between short and standard dex

dosing. This suggests that the considerable variation in dex pharmacokinetics shown here may mask any benefit of a change in dosing regimen on the two arms of the randomisation. Accordingly, a less than 2-fold difference in dose might not be a great enough modification to impact on patient outcome considering the 20-fold variation in pharmacokinetic exposure.

Furthermore, the significance of variation in dex exposure is reflected in the day 8 blast count results. Despite there being no statistical difference in day 8 blast count between the short and standard dex arms, patients with a blast count of <5% had a significantly higher exposure to dex than those with a blast count of >5%. This highlights the impact of variable dex exposure when assessing a dose change. Conversely, there was no difference in exposure at day 29 in patients within the 'low risk' (<0.005% blasts) and 'risk' (>0.005% blasts) group. This may be due to the differences in dex dosing durations. However, due to the important prognostic significance of early dex response, a longer follow up time is needed to assess the implication of a variable dex exposure on long term patient outcome.

In patients with paired beginning and end of induction therapy samples, pharmacokinetic profiles differed between the beginning and end of induction chemotherapy, with AUC_{0-12h} being significantly higher at the end of induction chemotherapy. A number of covariates were therefore analysed to find predictors likely to cause change within and between patients. Dex is reported to be an inducer of CYP3A4, which plays a major role in its metabolism (Moore and Kliewer, 2000). However, this would be expected to cause an increase in clearance from the beginning to the end of induction therapy, the opposite to what has been observed here. One possible explanation for this is the concomitant administration of asparaginase during induction chemotherapy, which has been suggested to influence dex pharmacokinetics (Yang *et al.*, 2008). This is thought to be due to asparaginase-mediated inhibition of protein production, such as albumin and dex metabolising enzymes. Furthermore, exposure to asparaginase has been shown to alter risk of dex induced osteonecrosis in both mice and humans (Kawedia *et al.*, 2011; Liu *et al.*, 2016).

Direct investigation of the relationship between dex and asparaginase in the current study was limited by the small number of patients who were enrolled on both the dex

and asparaginase sub-studies. However, it was possible to look at albumin levels and differences in dex pharmacokinetics in patients who had received one asparaginase dose versus two, as Yang *et al.* previously reported a correlation between albumin levels and dex clearance. In this study, despite a drop in albumin concentration post asparaginase being observed, in parallel to a decrease in dex clearance, no direct correlation between albumin and dex clearance was observed.

Differences seen in this study may be due to a difference in protocols between the two studies. In the Yang study, patients were sampled for dex and asparaginase analysis at week 7 and week 8 of therapy. Therefore the impact of 7 weeks of asparaginase therapy on *de novo* protein synthesis on albumin and dex metabolising enzymes may be more pronounced than the 1-3 weeks of patients analysed in this study.

Additionally, asparaginase concentrations in patients on this trial may not yet have reached steady state levels; as asparaginase trough concentrations were significantly greater after the second compared to the first dose of asparaginase.

Importantly, the number of asparaginase doses did appear to impact on inpatient variability in dex pharmacokinetics and albumin concentrations. A larger increase in dex AUC_{0-12h} and decrease in albumin was observed in patients who had received two doses of asparaginase compared to one, although the same relationship was not seen with dex clearance. To better understand these results and how they compare to those of Yang *et al.*, it would be beneficial to investigate this impact further with later dex and asparaginase sampling points.

Later dex pharmacokinetic and asparaginase sampling points and increased patient numbers would also enable further analysis of the effect of asparaginase allergy on dex pharmacokinetics. Yang *et al.* found that developing an asparaginase allergy affected both serum albumin concentrations and dex clearance. It was not possible to verify this effect in the current cohort of patients, as the two patients in this study (recruited to both sub-studies) who experienced asparaginase allergy, both developed asparaginase hypersensitivity after the end of induction therapy.

It is also important to consider other possible mechanisms leading to a reduction in clearance between the beginning and end of induction therapy. It is unlikely dex causes auto inhibition of its clearance although it is thought to be an inducer of CYP3A

(Moore and Kliewer, 2000). It is possible that the lipophilic nature of dex may contribute to the reduction of clearance seen throughout induction therapy. Dex may accumulate in the fat compartment of the patient after initial doses. When the fat compartment becomes saturated, subsequent administrations of dex remain in the systemic circulation. This will cause an increase in AUC, and as clearance is inversely proportional to AUC, a decrease in clearance. A similar situation has been described for cyclosporine. This hypothesis could be tested in the future by measuring percentage body fat and comparing this to the level of inpatient variability observed. This may also explain why some patients had larger inpatient variability than others and would help in the interpretation of inpatient variability data.

Previous studies have suggested that increased age is associated with a worse outcome and increased side effects (Plasschaert *et al.*, 2004; Yang *et al.*, 2008; Vora *et al.*, 2013b). Yang *et al.* saw an inverse correlation between age and dex clearance. As older children often have a poorer prognosis it was important to investigate altered pharmacokinetics in this high risk population further. The UKALL 2011 trial was open to patients aged between 1 and 25 years, allowing further investigations into the relationship between age and dex pharmacokinetics. However, in the dex pharmacokinetic sub-study, no association between age and dex clearance was observed. Similarly, there was no statistically significant effect of patient age on incidence of toxicity in patients on the dex sub-study.

A number of the concomitant medications administered during the induction phase of therapy are also CYP3A substrates, and therefore may explain some of the pharmacokinetic variability. Patients who had taken rasburicase, a drug used to prevent tumour lysis syndrome in patients with a high tumour burden, exhibited a lower mean dex AUC_{0-12h} and increase in drug clearance. Tumour lysis syndrome occurs when a large number of tumour cells are killed simultaneously as a result of therapy, releasing their contents into the bloodstream. This can result in several life threatening metabolic disturbances, including hyperuricaemia (Howard *et al.*, 2011). Rasburicase is a recombinant urate oxidase enzyme which has urolytic activity, reversing hyperuricaemia (Pession *et al.*, 2005). As rasburicase is given to patients with high tumour burden, these patients will be more commonly on regimen B, and will therefore have a four drug induction including daunorubicin.

Of the 23 patients in this trial taking rasburicase, 20 were on regimen B. As a result it was important to assess whether the observed pharmacokinetic differences may have been due to the concomitant administration of the anthracycline, daunorubicin, in these regimen B patients. Furthermore, Yang *et al.* found that doxorubicin, also an anthracycline antibiotic, affected dex clearance. However, in this study, no difference in AUC values or clearance were seen in patients on regimen B (Figure 3.11). This indicates that the decreased dex exposure in patients taking rasburicase is due to the rasburicase or the high tumour burden itself. In the latter situation, a higher number of blasts could mean a larger proportion of dex is intracellular. This would result in lower plasma dex concentrations which would be exhibited as a lower AUC and higher clearance. Importantly, the majority of these patients are high risk with an associated poorer prognosis. This association between rasburicase and AUC should therefore be investigated in an independent cohort of patients. If the decreased dex exposure is not due to greater intracellular dex levels, a lower exposure in a high risk patient group is potentially of concern.

There was also a correlation between the administration of ranitidine or osmotic laxatives and an increased exposure to dex. Although ranitidine is a weak inhibitor of CYP3A4, this is unlikely to fully explain the increase in dex AUC. Ranitidine and osmotic laxatives are administered to treat dex side effects. It is therefore likely that the association seen with administration of these drugs and an increased exposure resulting in increased side effects rather than a consequence of the drug on dex metabolism.

In patients analysed to date, there was no association seen between the experience of toxicity and pharmacokinetic parameters. Firstly, this may be because toxicity data is confounded by concomitant administration of other toxic chemotherapeutics. For example, vincristine, a drug also administered in induction therapy, is also immunosuppressive and may therefore contribute to the occurrence of therapy related infection. Secondly, despite an attempt to assess the relationship between steroid specific toxicities and dex pharmacokinetics, such as hypertension, the numbers of patients in these analyses were very low. Higher patient numbers would therefore enable analysis of individual toxicities with a strong association with GC therapy.

CSF dex concentrations were also assessed in a small number of patients. Results were comparable to plasma pharmacokinetic data; there was a significantly higher dex concentration in short compared to standard patients, however there was an overlap between the two arms. Of the patients analysed, there were only two patients who relapsed. These patients had CSF dex concentrations well within the range of patients who remained in remission. However, it is important to consider that the exact CSF sampling times were not recorded as the study was performed retrospectively, and variation in sampling times will have contributed to the variation seen between patients. Furthermore, without paired plasma and CSF sampled it is difficult to establish the relationship between plasma and CSF dex concentrations. However, these data have shown that it is possible to detect dex in CSF samples, which will be useful for future studies. Due to the important role of dex in eliminating CNS blasts, it may be worth investigating CSF dex pharmacokinetics with recorded sampling times and paired plasma samples in a larger patient group in a prospective study.

One of the problems with the traditional pharmacokinetic sampling approach used in this project was that it required patients to be in hospital and research nurses to be available to collect samples. This firstly meant that a number of patients had missing samples, and it was not possible to accurately calculate pharmacokinetic parameters for them and thus they were excluded from analysis. Secondly, a number of patients were not sampled at both the beginning and the end of induction therapy, limiting characterisation of inpatient variability.

To combat the former problem, a population pharmacokinetic approach could be used for the analysis of patient data. When the full cohort of patients have been recruited and all samples analysed, this is the approach that will be taken to analyse the data generated. A collaboration has been established with Martina Liebich (Munster, Germany), who has developed a population pharmacokinetic model for a reduced cohort of patients in this trial (n=107) using NONMEM 7.3. The model is a one-compartment model with first-order absorption and first-order elimination and also includes proportional residual variability and allometric scaling (presented at the PAGE 26 meeting (Lieblich *et al.*, 2017)). This approach will be able to better evaluate pharmacokinetic parameters in patients missing samples, and will therefore enable a more in depth analysis of the influence of covariates and comparisons between the

two dosing regimens. This type of modelling would also be used if a dex dose monitoring approach was taken into the clinic. The use of a population pharmacokinetic model would mean fewer samples would be needed to predict individual patient's exposure to dex.

To address the latter issue, future studies could explore a different sampling approach. Increasing sensitivity of LC/MS systems means that collection methods such as Guthrie card or other micro blood sampling methods, such as Mitra blood sampling tips, could be used. For example, one study has been able to accurately quantify dex in dried blood spots from 30µl of blood (Patel *et al.*, 2010). Although this approach would need extensive validation, it would enable patients to generate samples at home and thus recruitment and retention to pharmacokinetic studies may be improved.

In summary, high inter and inpatient variability has been observed. The UKALL 2011 trial aimed to investigate whether a shorter, more intense dex dose, would decrease toxicity whilst maintaining survival rates. However, a futility analysis in April 2017 demonstrated that there was no statistical difference between the dosing arms in terms of steroid related toxicity, MRD or relapse free survival. In this project, it has been seen that at day 8, dex exposure was more important than treatment arm, (short vs. standard), in terms of dex response. Furthermore, a significantly higher cumulative exposure to dex on the standard arm suggests that in a drug treatment with markedly variable pharmacokinetics, duration of therapy may be more important in terms of the likely impact on clinical response and toxicity

ALL is a heterogeneous disease and it may well be that the therapeutic index is different in different subtypes and this may account for some of the variability seen in response. A much larger study would need to be performed to assess this.

Incorporation of later sampling time points in the delayed intensification phase of therapy would also help to elucidate the relationships between dex pharmacokinetics and both asparaginase and individual steroid related toxicities.

Chapter 4. Intracellular dexamethasone accumulation

4.1 Introduction

In addition to studying the systemic pharmacokinetics of dex, the intracellular pharmacology of the drug should also be considered, as this is what ultimately results in ALL cytoreduction and clinical benefit. The GR is a ligand-activated transcription factor belonging to the nuclear receptor superfamily. Once bound to ligand, it translocates to the nucleus where it mediates GC-induced cell death, by transactivation or transrepression of target genes (Schaaf and Cidlowski, 2002; Inaba and Pui, 2010). In some cases, ALL cells can exhibit markedly reduced sensitivity to dex therapy. This results in a reduced clinical benefit from dex treatment whilst patients are still exposed to therapy-related toxicity. Studying dex pharmacokinetics alone may allow modulation of the drug concentrations that leukaemic cells are exposed to, but does not provide information regarding the drug- target interaction or downstream response of the ALL cells (Jackson *et al.*, 2016).

Despite playing a central role in the treatment of ALL for a number of decades, the mechanisms of action and resistance of dex are still not fully clear. An improved understanding of these mechanisms is not only needed to develop new therapies for patients with resistant disease, but also to identify patients who may not benefit clinically from dex therapy, or equally those who may benefit from a reduction or intensification of therapy.

An important area of investigation into dex resistance that remains relatively unexplored is whether concentrations of intracellular dex differ between sensitive and resistant ALL cells. This is a key complementary investigation to dex pharmacokinetic studies, as it defines the applicability of the plasma concentration of dex to the leukaemic cells.

Intracellular drug levels can potentially be affected by several factors, including variation in expression of membrane transporters. This has been shown to be an important factor for other commonly used cancer drugs such as actinomycin D (act D) (Hill *et al.*, 2013; Hill *et al.*, 2014). Substrate specificity of dex for MDR1 is debatable. Although dex has been reported to be a substrate for MDR1 (Cole *et al.*, 1992; Schinkel *et al.*, 1995b), investigations into the impact of MDR1 expression of ALL cells on outcome, although not GC response itself, have revealed contrasting results. For

example, expression of MDR1 in ALL cells has been associated with a more unfavourable course (Dhooge *et al.*, 2002), increased risk of relapse (Goasguen *et al.*, 1996), and lower survival (Casale *et al.*, 2004). However, a number of other groups found no effect of MDR1 expression on outcome (Kakihara *et al.*, 1999; Plasschaert *et al.*, 2003; Balamurugan *et al.*, 2007). Whether dex is an MDR1 substrate therefore needs further clarification.

A change in intracellular dex concentration could also be caused by events such as increased steroid binding protein, or a change in 11 β -hydroxysteroid dehydrogenase enzyme (11 β -HSD) expression. There are two forms of 11 β -HSD; 11 β -HSD1 which converts inactive 11 β -keto GC into active GC, and is expressed in GC target tissues, and 11 β -HSD2 which inactivates GC but is only has restricted expression (Seckl, 2004). Although there have been limited studies looking at 11 β -HSD, Sai *et al.* (2009) found that 11 β -HSD1 expression was decreased in GC resistant ALL cells *ex vivo* compared to GC-sensitive ALL cells. Therefore, investigating whether intracellular dex levels differ in GC-sensitive and resistance cells represents an interesting and novel avenue that may aid further stratification of dex therapy.

4.2 Chapter specific aims

- Assess whether dex is a substrate for the multi drug transporter MDR1.
- To assess dex accumulation in ALL cells and correlate with dex sensitivity.

4.3 Results

In order to assess intracellular accumulation in ALL cells, two methods were utilised. The first used LC/MS to measure dex concentrations and the second used flow cytometry to measure intracellular dex conjugated to the fluorochrome, fluorescein.

4.3.1 Method validation

4.3.1.1 Assessment of dex concentrations in cell lysates using LC/MS

The validation of the LC/MS method was performed in cell lines and was submitted as part of a Masters by Research Degree, awarded in 2012 (Jackson, 2014). The validation is detailed in Appendix D.

The LC/MS assay was optimised in this project to define the smallest number of cells necessary for successful extraction and sufficient signal on the LC/MS, to allow use with patient samples. Optimisation was performed with PreB697 cells. Cells were seeded at decreasing densities ranging from 2.2×10^6 cells/ml to 0.1×10^6 cells/ml (total of 14×10^6 and 0.6×10^6 cells respectively) before incubation with 500nM dex for 4h at 37°C. Extraction was then performed before quantification of dex peaks by LC/MS. Figure 4.1 shows examples of peaks from dilutions that were above and below the limit of quantitation (defined as 10 x baseline).

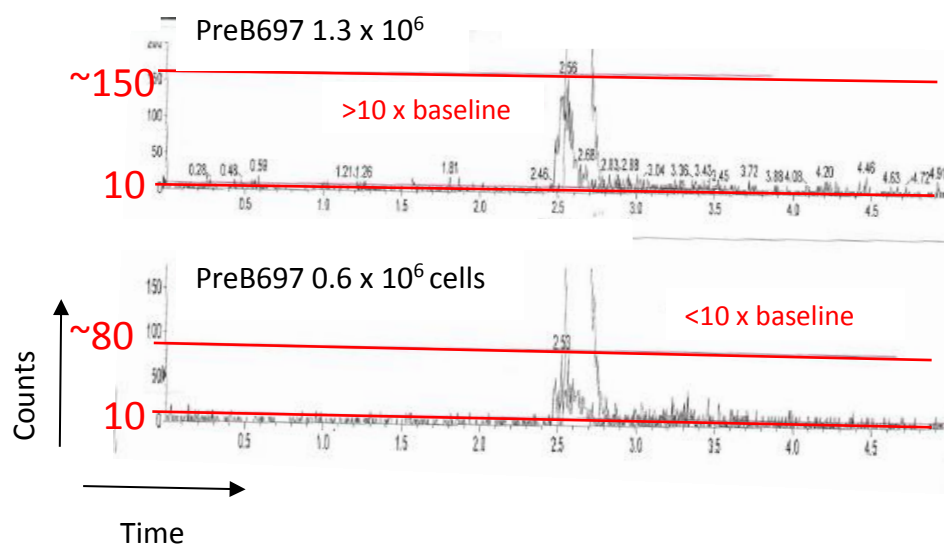


Figure 4.1 Example LC/MS chromatograms showing the minimum number of cells needed to obtain a quantifiable dex peak after incubation with 500nM dex.

PreB697 cells of differing densities were incubated with 500nM dex for 4 hours before cell lysis and measurement of intracellular dex concentrations. The lower limit of quantitation was defined at 10 x baseline reading. The top pane shows a total of 1.3×10^6 PreB697 cells. Dex peak (~150 counts) at ~2.6 minutes is > 10 x the baseline (~10 counts), to allow differentiation of peaks from baseline noise. The bottom pane shows a total of 0.6×10^6 PreB697 cells. Dex peak (~80 counts) at ~2.6 minutes is < 10 x the baseline (~10 counts).

There was some variation in the lowest defined number of cells between the three experiments performed. This was most likely due to daily variation in LC/MS sensitivity. A serial dilution was performed, resulting in cell number halving with each dilution. The natural daily variation in LC/MS sensitivity may have therefore caused the 1:16 dilution to have been above and below the quantitation limit, causing the variation in the lower limit of quantitation (Table 4.1).

	Lowest total number of cells that gave a quantifiable peak (x 10 ⁶)
Rep 1	0.6
Rep 2	1.6
Rep 3	1.3

Table 4.1 Lowest number of PreB697 cells that gave a quantifiable dex peak, on three separate days.

Cells were seeded at decreasing densities ranging from 2.2×10^6 cells/ml to 0.1×10^6 cells/ml (total of 14×10^6 and 0.6×10^6 cells respectively) before incubation with 500nM dex for 4h at 37°C. Extraction was then performed before quantification of dex peaks by LC/MS. A quantifiable peak was defined at >10x baseline.

To account for this variability, the assay with the least sensitivity was used to define the lowest total number of cells needed, which was 1.6×10^6 per sample. Therefore, for patient experiments, cells were resuspended at a concentration of 1×10^6 cells/ml with a total cell number of at least 1.6×10^6 .

4.3.1.2 Assessment of dex concentrations in cell lysates using flow cytometry

This method was adapted from a study using dex-FITC. The authors described the assay as a measure of dex-binding to the GR in human thymocytes (Kowalik *et al.*, 2013). Initially, the optimal incubation time was established to give the maximal fluorescence. PreB697 cells were incubated with 500nM dex-FITC or control vehicle (CV) for 5, 15, 30 or 60 minutes and then analysed by flow cytometry. All samples were gated on forward and side scatter to eliminate debris and isolate single cells. The ratio of mean fluorescence intensity (MFI) of the FITC channel for CV and dex-FITC treated cells was then calculated.

The MFI ratio increased in a time-dependent manner from 5 to 30 minutes incubation, but not between 30 and 60 minutes of incubation (Figure 4.2). An incubation time of 45 minutes was therefore chosen for further experiments.

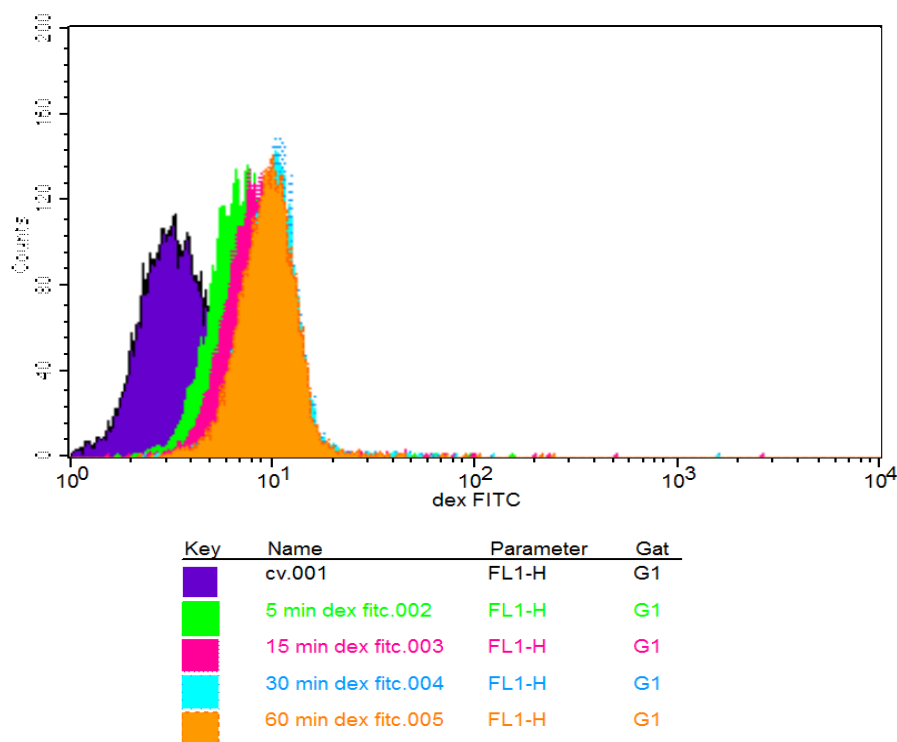


Figure 4.2 Mean fluorescence intensity of dex-FITC after incubation periods of 5 – 60 minutes.

There was no increase in MFI from 30 to 60 minutes.

The method was subsequently tested in PreB697 cells, dex resistant sub clones and REH cells. MFI values did not differ between PreB697 cell lines, resistant sub lines or REH cells ($p=0.9$, one way ANOVA) (Figure 4.3). Given that the method was designed to measure GR binding, this was surprising, as REH cells do not contain a functional GR (Grausenburger *et al.*, 2016). Furthermore, R3D11 has previously been shown to have a reduced level of GR (Nicholson *et al.*, 2010). It was therefore concluded that Kowalik's method does not measure GR level, but is actually a measure of intracellular dex accumulation.

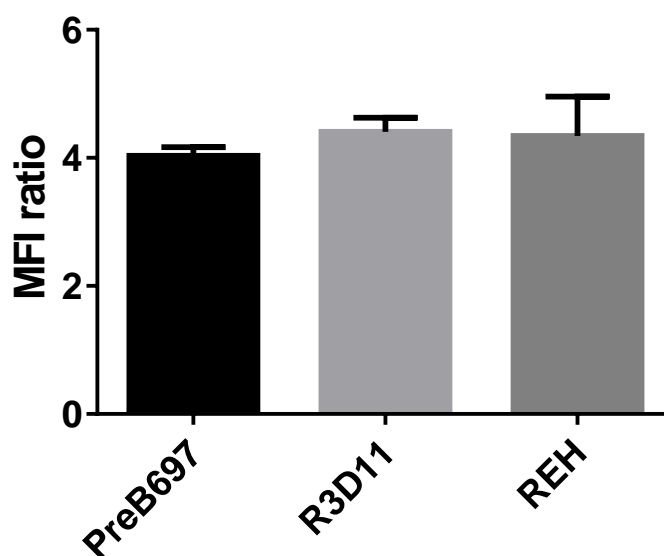


Figure 4.3 Mean fluorescence intensity of PreB697 cells, R3D11 and REH cells after 45minutes of incubation with dex-FITC.

There was no difference in MFI between any of the cell lines ($p=0.9$, one way ANOVA). MFI ratio is cells treated with CV:cells treated with dex-FITC. Results are mean \pm SEM of three independent replicates.

Due to the discrepancy with the method published by Kowalik *et al*, further method development work was performed. Firstly, the number of washes necessary to remove surface dex-FITC was determined. MFI decreased from one to two washes, but did not further greatly decrease from two to three washes (Figure 4.4). This indicated that one wash was not sufficient to remove extracellular dex-FITC, and therefore further experiments were performed with two washes.

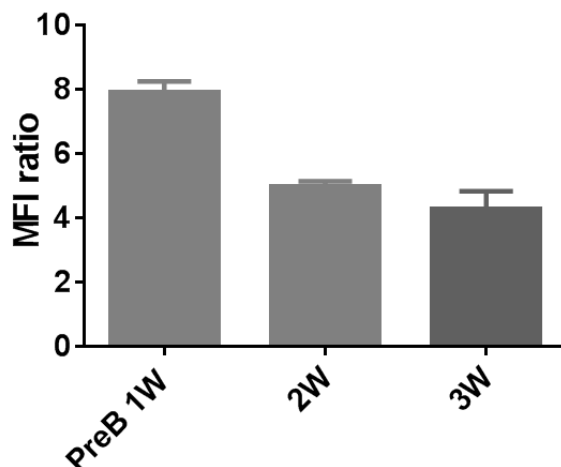


Figure 4.4 Effect of the number of washes on dex FITC fluorescence.

Mean fluorescence intensity of PreB697 cells after incubation with dex-FITC for 45 minutes, followed by one (1W), two (2W), or three washes (3W) in PBS before resuspension in fresh PBS for immediate analysis on the FACSCalibur. Results are mean \pm SEM of three experiments.

The effect of temperature on incubation was also investigated. The published method performed incubation steps at 4°C. However, as this experiment is a measure of intracellular accumulation, it is more physiologically relevant to incubate cells at 37°C.

The clustering of some cell lines on dot plots changed between 4°C and 37°C (Figure 4.5). This was characterised by an increase in size (shown by a change forward scatter) seen in PreB697 cells (A and B). In CEM VCR cells (C and D), there were also two distinct populations of cells observed when cells were incubated at 4°C. Therefore future incubations were performed at 37°C. The final method is detailed in 2.5.3.

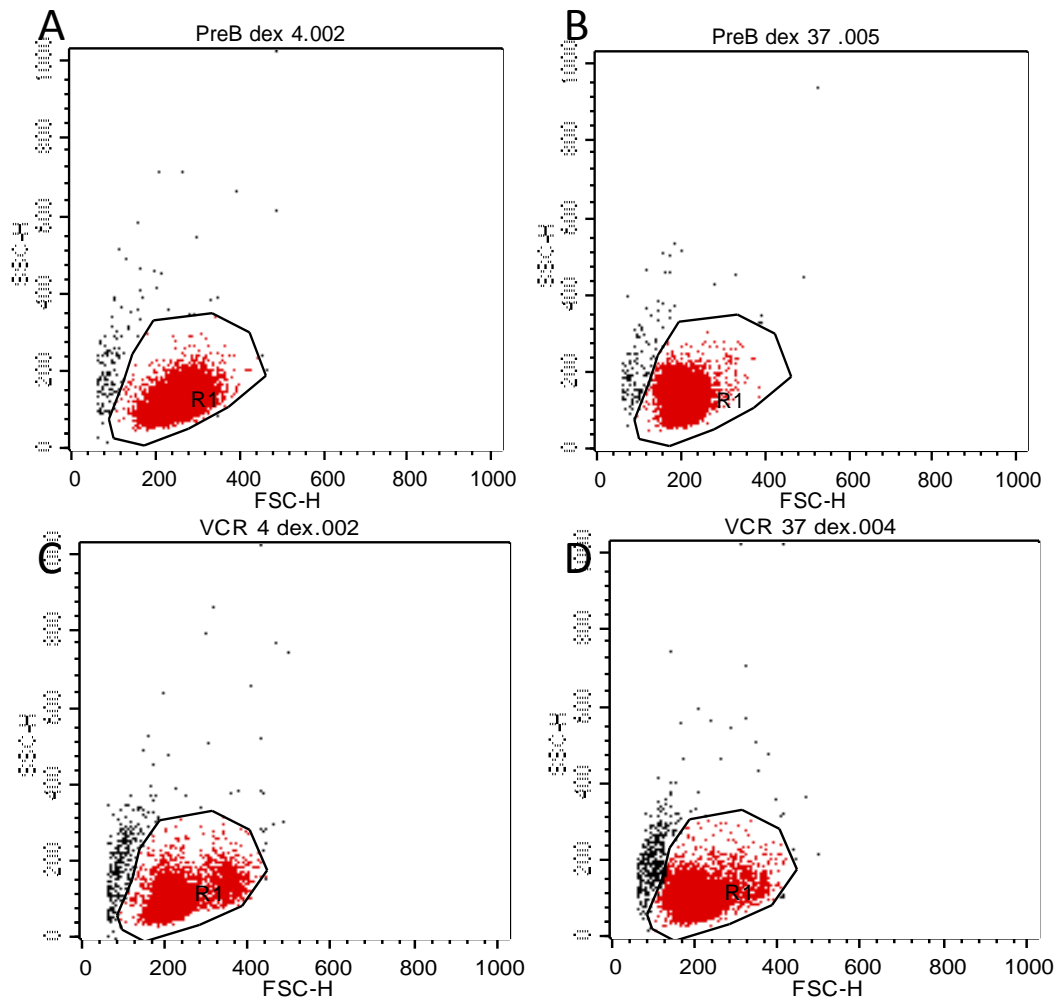


Figure 4.5 Example flow cytometry dot plots showing different clustering of cells when incubated with dex-FITC at 4°C and 37°C.

Each cell line experiment was performed simultaneously at each temperature. (A) PreB697 cells incubated at 4°C, (B) PreB697 cells incubated at 37°C, (C) CEM VCR cells incubated at 4°C, (D) CEM VCR cells incubated at 37°C. (Y axis: SSC-H = side scatter, X axis: FSC-H = forward scatter).

4.3.2 Assessment of MDR1 dex transporter status

Specificity of dex for the multidrug transporter, MDR1 was assessed using two paired wildtype and MDR-1 expressing cell lines. CCRF-CEM, a T-ALL cell line, has a MDR1 expressing sub-clone generated through exposure to vincristine (CCRF-VCR, (Haber *et al.*, 1989)). Madin-Darby canine kidney (MDCKII) wildtype cells do not express multi drug transporters, whereas MCKII-MDR1 have been created using gene transfection of human *MDR1*. In order to assess whether dex is an MDR1 substrate, drug sensitivity and intracellular accumulation assays were performed using dex alongside experiments with vincristine and act D, known substrates of multidrug transporter proteins (Cass *et al.*, 1989; Hill *et al.*, 2013). All vincristine data were generated by Charlotte Lecour, a placement student from Toulouse University.

There was a significant difference in vincristine GI_{50} between CCRF CEM and CEM VCR cell lines (CEM: $1.53\text{nM} \pm 0.13$, VCR: $3352\text{nM} \pm 754$ (mean \pm SEM), $p=0.01$, student's t-test), confirming the expression of MDR1 in the CEM VCR cells. In contrast, cell GI_{50} for dex (CEM: $290\text{nM} \pm 51$, VCR: $595\text{nM} \pm 265$) did not differ between the wild type and MDR1 expressing cells ($p=0.3$, Figure 4.6). These results are reflected in the drug accumulation experiments (Figure 4.7).

Vincristine accumulation in CCRF CEM cells was significantly higher than in CEM VCR cells (two-way ANOVA, $p<0.0001$). This is seen in the 26- and 18- fold higher vincristine accumulation at 100 and 500nM respectively, in CCRF CEM cells compared to CEM VCR cells. Conversely, dex accumulation was actually slightly greater in the CEM VCR cells ($p=0.02$, two-way ANOVA). Taken together, drug sensitivity and accumulation experiments suggest that dex is not a substrate for MDR1 in CCRF CEM cell lines.

A

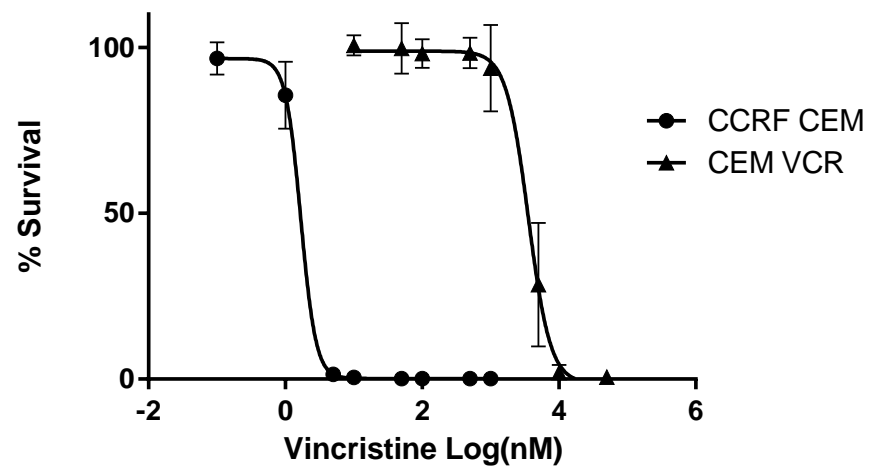
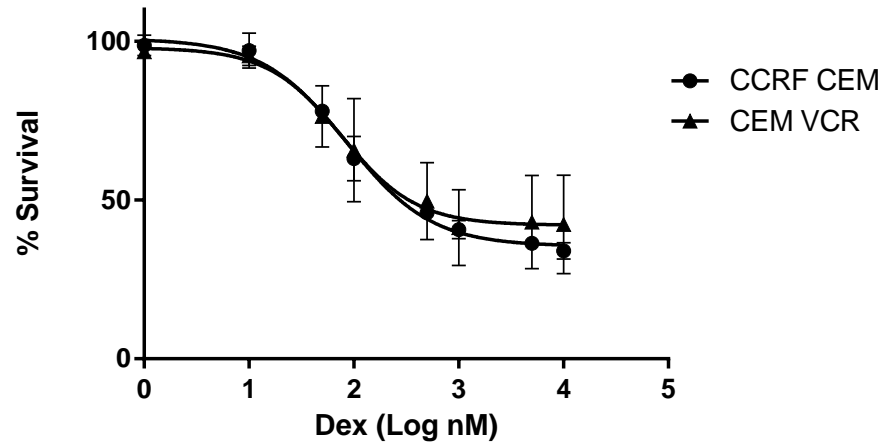


Figure 4.6 Sensitivity of CCRF CEM and CEM VCR cells to dex (A) and vincristine (B) generated using alamar blue.

Cells were incubated with concentrations of dex or vincristine for 96h before addition of Alamar Blue. Results reported as mean percentage survival from 3 experiments \pm SEM relative to cells treated with CV. GI₅₀ values were significantly different for vincristine but not dex between the two cell lines ($p=0.01$ and 0.3 respectively, student's t test).

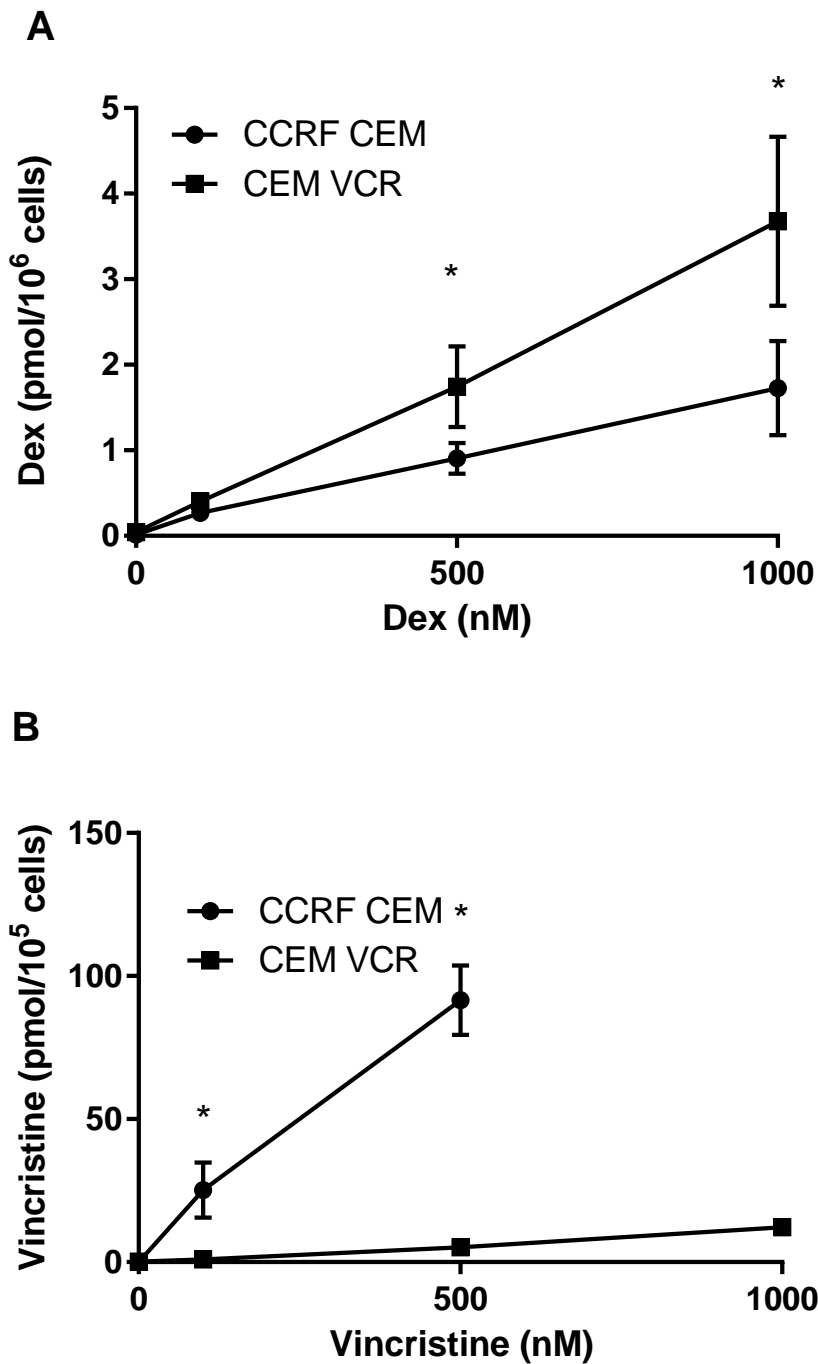


Figure 4.7 Accumulation of dex (A) and vincristine (B) in CCRF CEM and CEM VCR cells.

Concentrations measured by LC/MS after incubation with concentrations of dex or vincristine for 4 hours. Results presented are \pm SEM from at least 3 experiments. There was a significant difference in both dex and vincristine accumulation ($p=0.02$ and <0.0001 respectively, two way ANOVA with Sidaks correction for multiple comparisons).

To confirm this observation, accumulation was tested in paired MDCKII cell lines, MDCKII-WT and MDCKII-MDR1. Dex sensitivity was not assessed in these cell lines as they are not lymphoid cells, and therefore neither cell line would be sensitive to dex nevertheless it would have served as a negative control. Despite this, MDR1 expression and function in the MDCKII-MDR1 were verified through drug sensitivity assays using vincristine and act D. MDCKII cell line vincristine GI_{50} concentrations differed significantly (MDCKII-WT: 56.2 ± 5.0 and MDCKII-MDR1: 1228 ± 315.7 (mean \pm SEM), $p = 0.02$ t-test), as well as act D GI_{50} concentrations (MDCKII-WT: 9.1 ± 0.4 and MDCKII-MDR1: 21.62 ± 3.86 , $p = 0.0059$ t-test) (Figure 4.8). This confirms the expression of MDR1 in MDCKII-MDR1 cells.

As anticipated, MDCKII-WT also had a greater accumulation of both vincristine and act D than the MDR1 expressing MDCKII-MDR1 cells (Figure 4.9). With act D, there was a 1.9 fold higher accumulation in MDCKII-WT cells with 500 and 1000nM act D than MDCKII-MDR1 cells, with accumulation in the two cell lines being significantly different (two-way ANOVA, <0.0001). There was also 5.8-fold increase in vincristine accumulation at 500nM in MDCKII-WT compared to MDCKII-MDR. A two-way ANOVA performed on data from concentrations used in both cell lines (0, 100 and 500nM) revealed a significant difference in accumulation between the two cell lines ($p=0.01$). In contrast, there was no statistical difference in dex accumulation between MDCKII-WT and MDCKII-MDR1 cells ($p=0.8$, two-way ANOVA).

Collectively, drug sensitivity and accumulation experiments in both paired cell lines indicate that dex is not a substrate for MDR1.

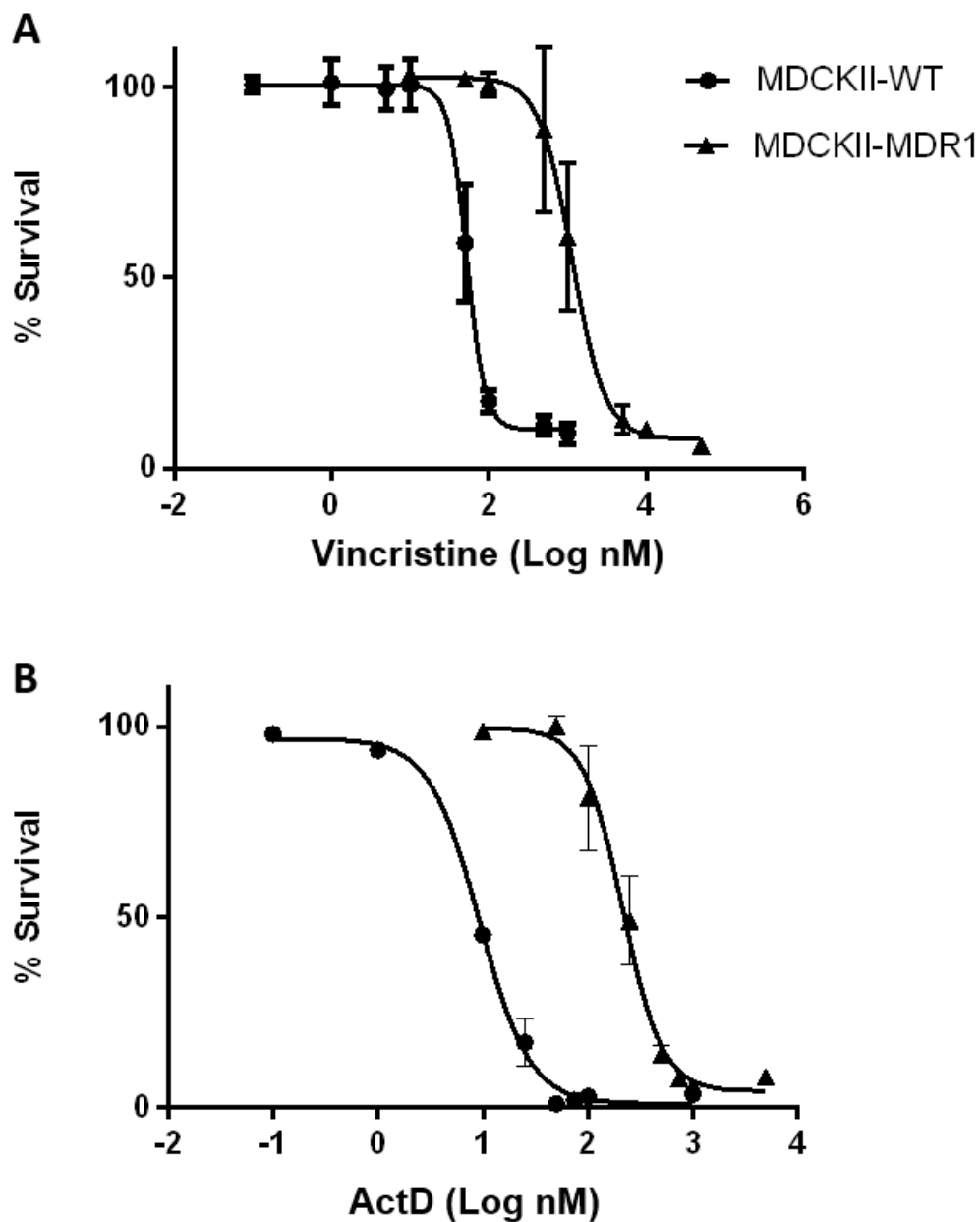


Figure 4.8 Sensitivities of MDCKII-WT and MDCKII-MDR1 cell lines to vincristine (A) and act D (B).

Cells were incubated with concentrations of vincristine or act D for 96h before addition of Alamar Blue. Results are reported as mean percentage survival from 3 experiments \pm SEM relative to cells treated with CV. GI₅₀ values were significantly different for vincristine and act D between the two cell lines ($p=0.02$, 0.0059 respectively, student's t test).

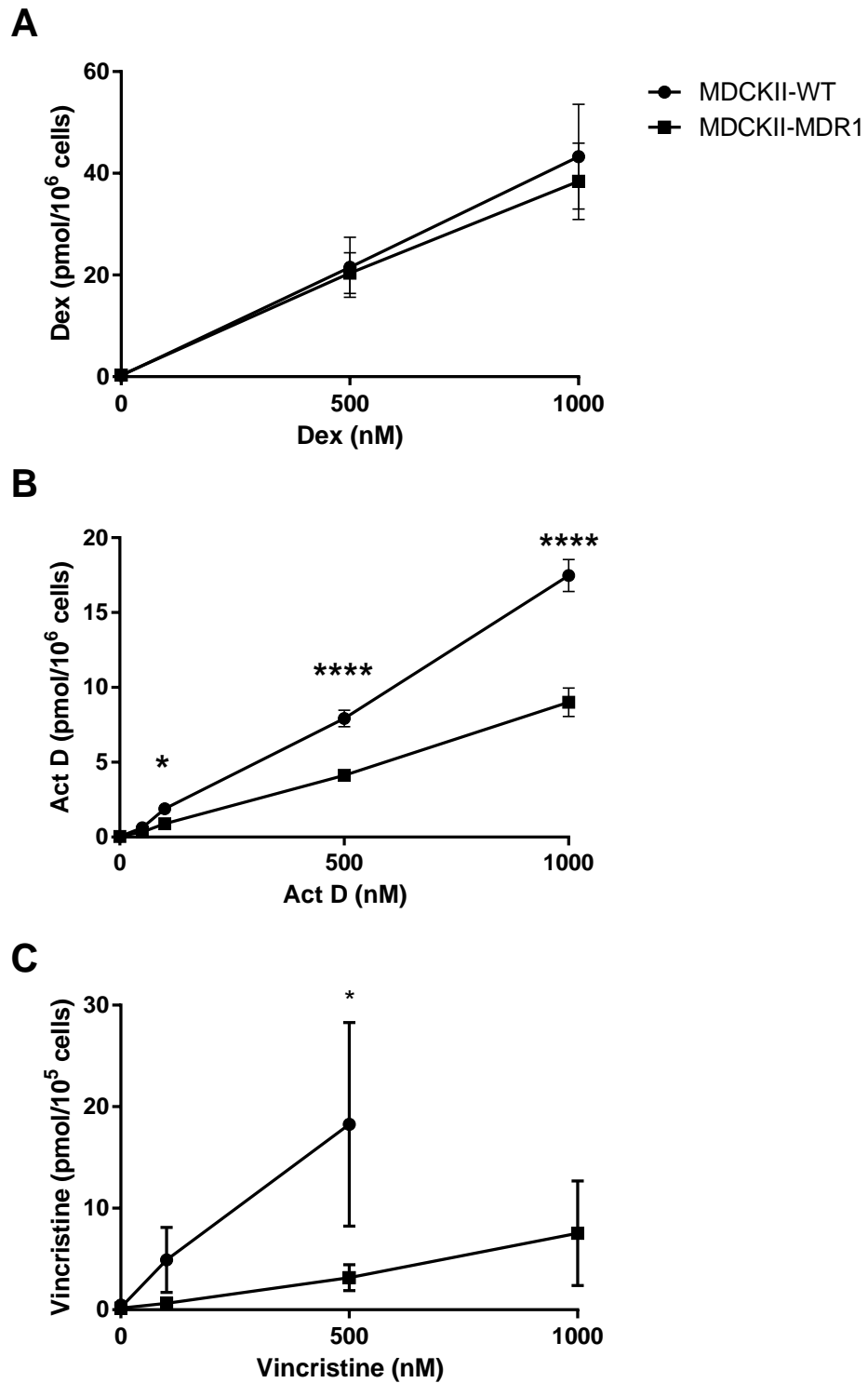


Figure 4.9 Accumulation of dex (A) act D (B) and vincristine (C) in MDCKII-WT and MDCKII-MDR1 cells.

Concentrations measured by LC/MS after incubation of cells with dex, act D or vincristine for 4 hours. Results presented are \pm SEM from 3 experiments. The accumulation did not differ between cell lines for dex but did for act D and vincristine ($p > 0.8$, < 0.0001 , 0.01 respectively, 2 way ANOVA, Sidaks correction for multiple comparisons).

4.3.3 Dex sensitivity in cell lines

Dex sensitivity experiments were performed in PreB697 cells and dex resistant sub lines R3F9, R3D11, R3C3, R3G7 and R4C10 and submitted as part of my MRes.

Resistant sub lines were created in the lab of R. Kofler using selection culture in the presence of dex for 3–4 weeks before individual clones were selected and expanded (Schmidt *et al.* 2006a). In addition, in this project, dex sensitivity on REH cells was performed. Cells were incubated with concentrations of dex for 96 hours before the assessment of viability using Alamar Blue.

Dose response curves generated using Alamar Blue are shown in Figure 4.10. PreB697 had a dex GI₅₀ of 37 ± 1.2 nM (SEM). REH cells and all PreB697 sub lines generated GI₅₀ values of >1000nM, except for R3C3 cells, which had a GI₅₀ of 191 ± 1.3 nM (Table 4.2). All sub lines differed significantly in their sensitivity to dex compared to PreB697 cells (two-way ANOVA $p < 0.0001$).

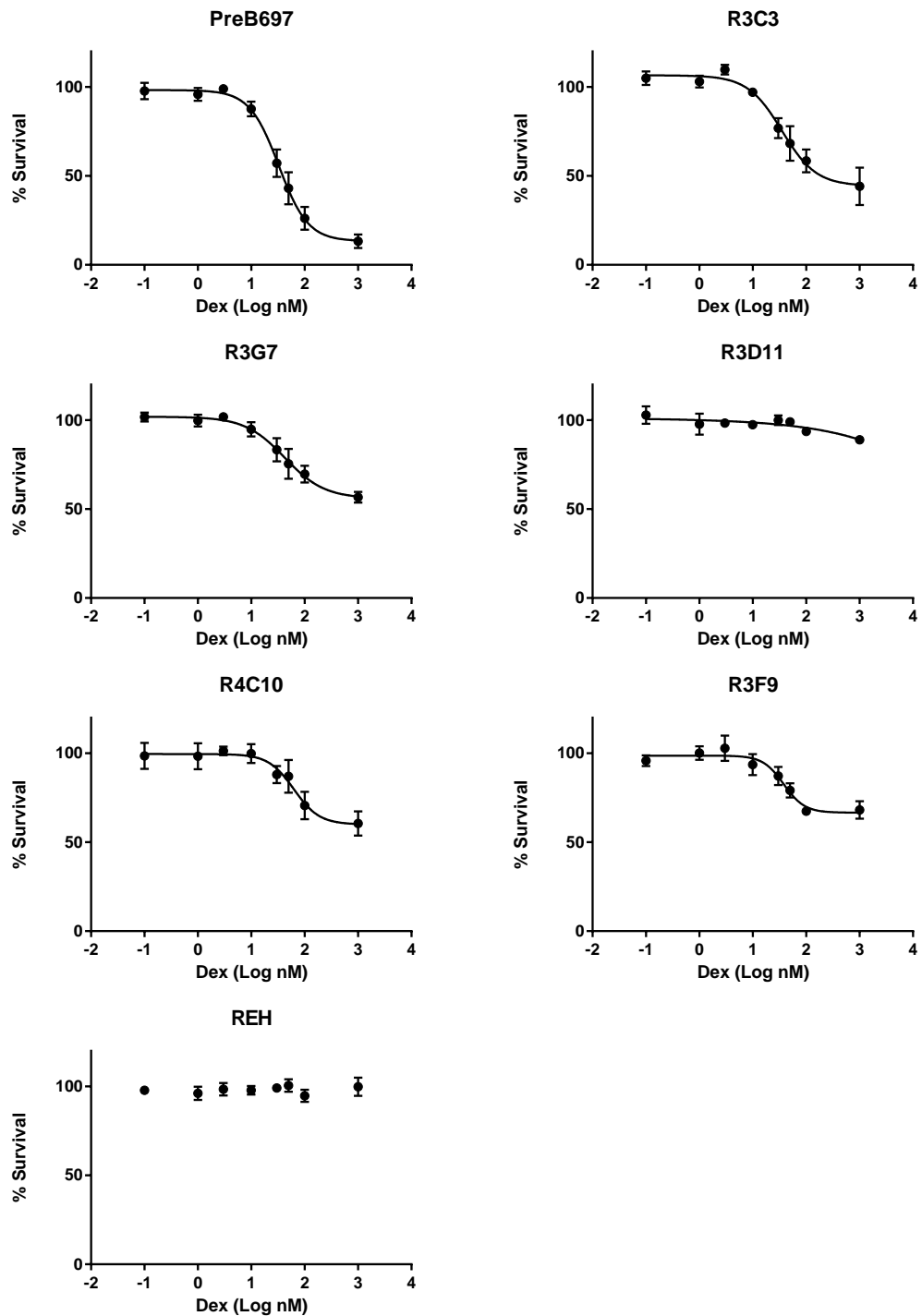


Figure 4.10 Sensitivity of PreB697 cell lines and REH to dex *in vitro* with Alamar Blue after a 96h incubation with 0.1-1000nM dex.

Results reported as mean percentage survival from 3 experiments \pm SEM relative to cells treated with CV. All sub lines differed significantly in their sensitivity to dex compared to PreB697 cells (two way ANOVA $p < 0.001$). Data submitted as part of MRes, REH data generated in this project.

Cell line	Dex GI ₅₀ (nM)	Cell viability at 1000nM (% relative to CV treated cells)
PreB697	37	13
R3D11	>1000	89
R3F9	>1000	61
R3C3	191	44
R3G7	>1000	57
R4C10	>1000	68
Reh	>1000	99.9

Table 4.2 Cell line sensitivity to dex assessed using Alamar Blue assay.

Sensitivity was assessed using Alamar blue after a 96h exposure to concentrations of dex ranging from 0.1-1000nM. Data is from 3 independent experiments. All sub lines differed significantly in their sensitivity to dex compared to PreB697 cells (two-way ANOVA $p < 0.0001$).

4.3.4 Intracellular accumulation of dex in cell lines

As part of the MRes project, dex accumulation was assessed in PreB697 and resistant sub lines (Figure 4.11). In all cell lines, intracellular dex levels increased in a concentration dependent manner. There was no difference in dex accumulation between R3C3, R3G7, R4C10 and R3F9 compared to PreB697 cells ($p > 0.15$, two way ANOVA with Sidak's correction for multiple comparisons). Finally, R3D11 displayed lower dex accumulation compared to parental 697 cells under the same experimental conditions ($p = 0.0122$, two way ANOVA). However, a difference in accumulation was only seen after incubation with 500 and 750nM dex, and not 1000nM dex (Figure 4.11).

These results are comparable to data obtained using flow cytometry to measure intracellular accumulation of dex-FITC, which showed no difference in dex-FITC accumulation between any cell line ($p = 0.89$, one way ANOVA). The difference in dex accumulation between PreB697 and R3D11 at 500 and 750nM is likely to be inconsequential as this difference was not seen 1000nM. Overall, as LC/MS data did not show a difference in accumulation at every concentration, and flow cytometry data showed no difference in intracellular accumulation of dex-FITC, it is likely that PreB697 and R3D11 do not differ in terms of dex accumulation.

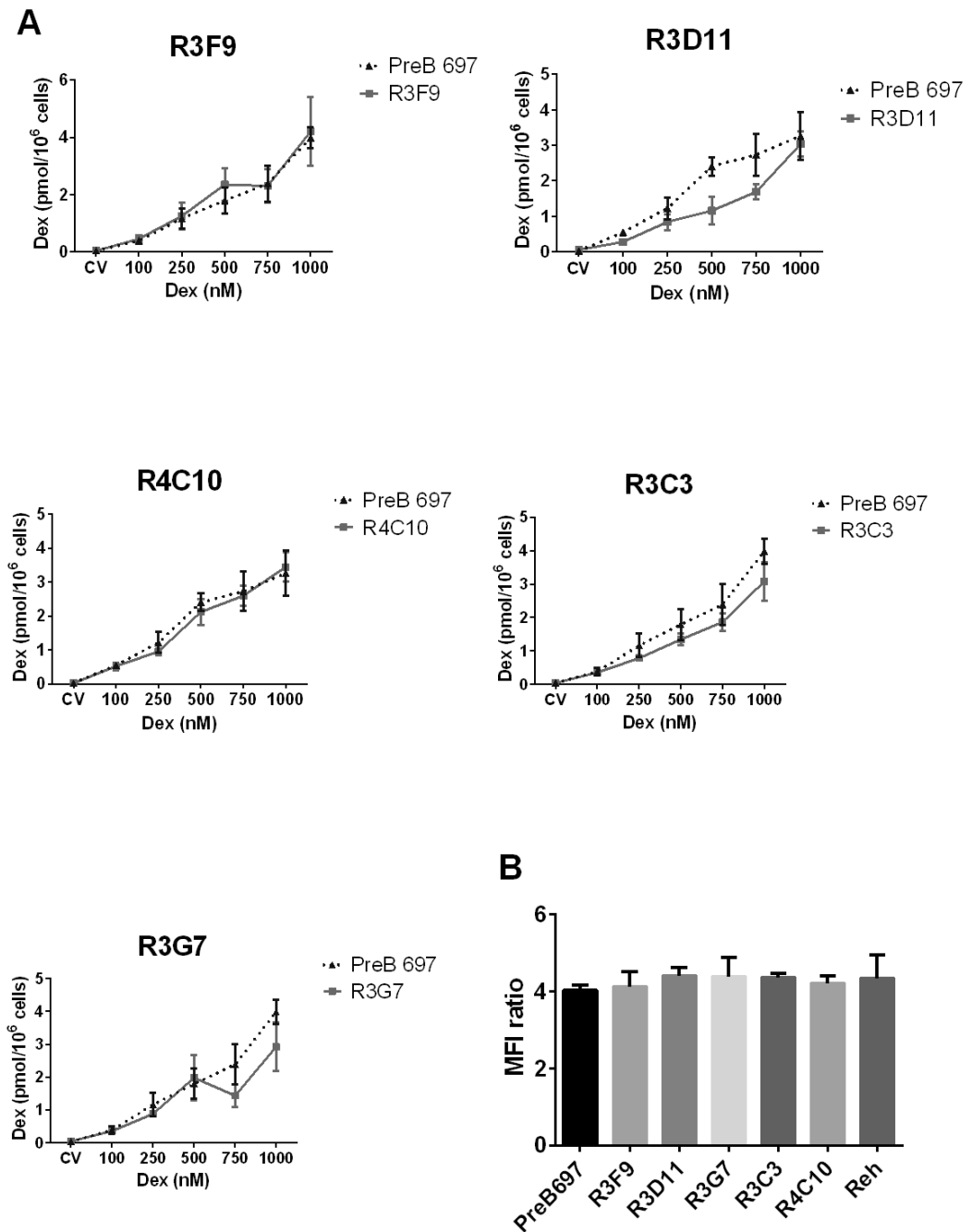


Figure 4.11 Intracellular dex accumulation in PreB697 and selected dex resistant sub lines.

(A) Concentrations measured by LC/MS after cell lines were incubated with dex for 4 hours. (B) Mean fluorescence intensity of Dex-FITC measured using flow cytometry. Results presented are \pm SEM from 3 experiments. There was no difference between any cell line and its PreB697 comparison (A: $p > 0.056$ two way ANOVA with Sidaks correction for multiple comparisons B: $p = 0.89$, one way ANOVA).

4.3.5 Viability of cryopreserved cells

To determine whether it was possible to analyse dex sensitivity and accumulation retrospectively in cryopreserved patient and primagraft samples, dex sensitivity assays and intracellular dex accumulation experiments were performed in L779 primagraft samples before and after they been cryopreserved in liquid nitrogen. In all primagraft samples, dex sensitivity was significantly different after cryopreservation (two-way ANOVA, $p < 0.001$ for all, Figure 4.12).

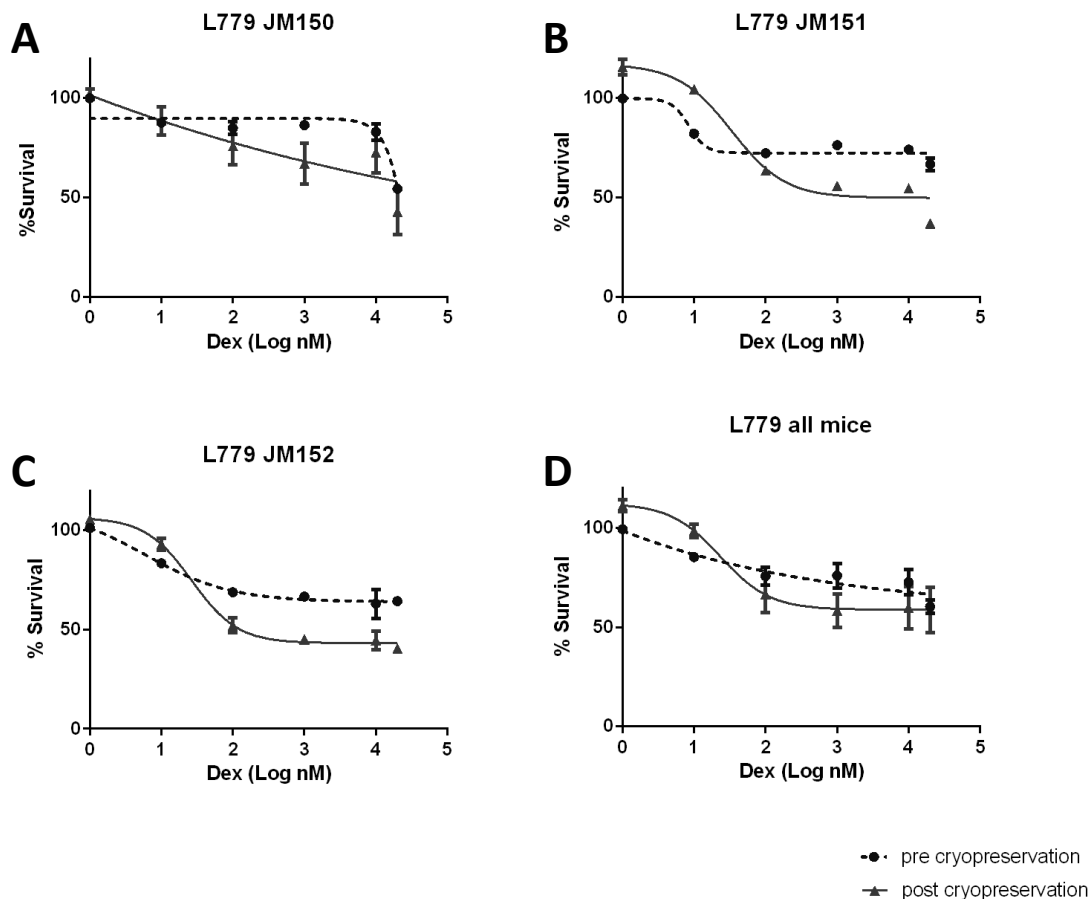


Figure 4.12: *In vitro* dex sensitivity of L779 primagraft samples pre- and post-cryopreservation, measured using Alamar blue.

Results are reported relative to cells treated with CV. A-C show results from individual mouse samples, each point is the mean of three wells \pm SEM. D shows the mean of all L779 primagraft samples.

A difference was also observed in intracellular dex accumulation between pre- and post-cryopreserved samples. The LC/MS data showed a drop in intracellular accumulation in two samples and an increase in accumulation in one sample. The FACS data also shows a drop in intracellular accumulation in the same two samples, with the third sample showing a similar level of accumulation (Figure 4.13). Neither difference was statistically significant. Due to the significant differences seen in dex sensitivity and non-significant differences in dex accumulation, subsequent studies were performed prospectively on all patient and primagraft samples.

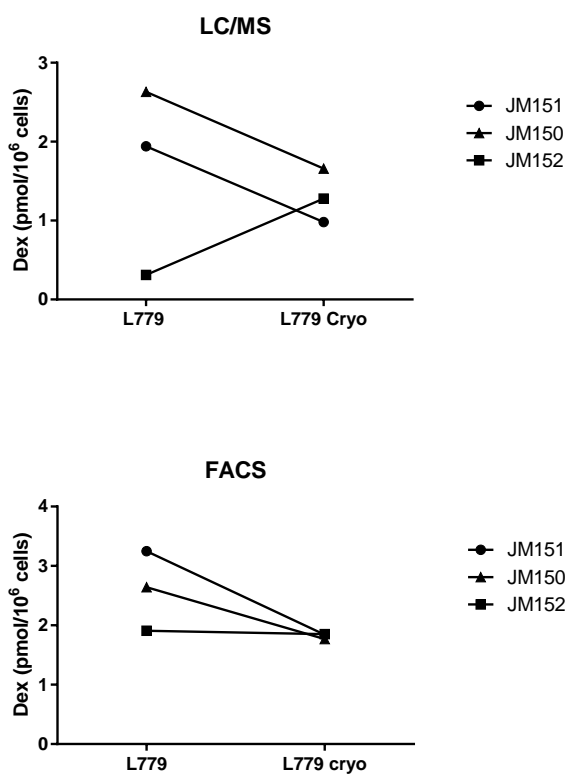


Figure 4.13 Intracellular dex accumulation in L779 primagraft samples pre- and post-cryopreservation.

Cells were incubated with 500nM dex-FITC before analysis by LC/MS or flow cytometry respectively, in primagraft samples derived from patient L779 before and after cryopreservation.

4.3.6 Dex sensitivity of primagraft and patient samples.

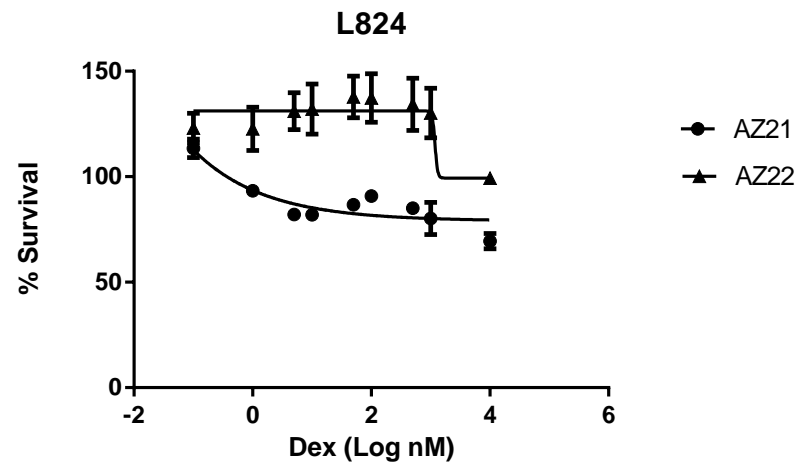
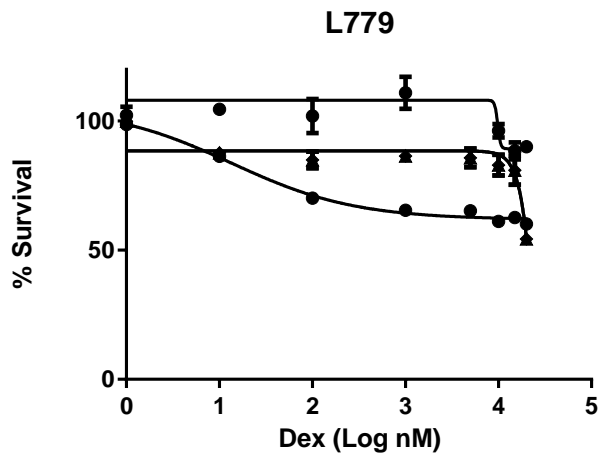
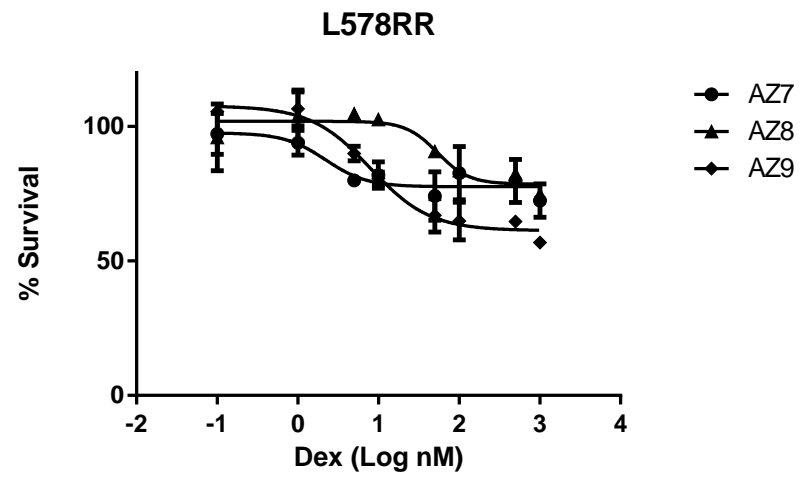
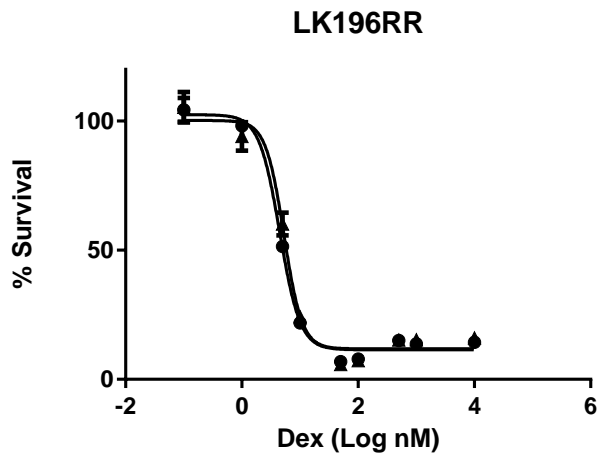
Dex sensitivity was assessed using the Alamar Blue assays. Depending on the number of cells available for analysis, cells were incubated with a range of concentrations of dex (0.1 – 10,000nM) for 96 hours, before the addition of Alamar Blue.

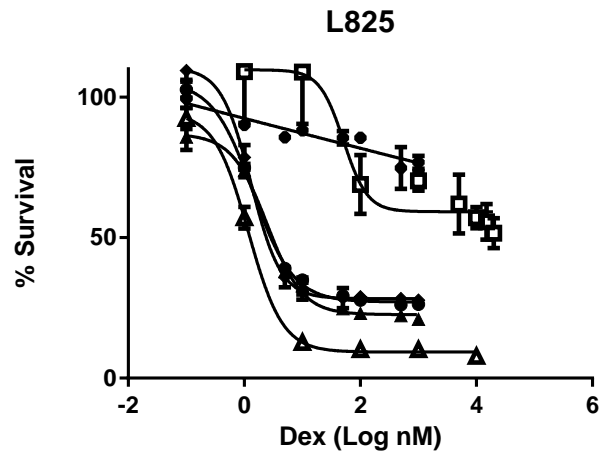
In total, dex sensitivity was assessed in 37 primagraft samples from 12 patients (Figure 4.14). In one patient (L829), there were matched presentation and relapse samples available. In another (L919), there were matched first and second relapse samples. Samples exhibited a range of dex GI₅₀ values from 1.3 to > 1000nM, with 11 primagraft samples displaying dex sensitivity, and 26 dex resistance. Dex sensitivity was defined as a GI₅₀ of < 500 nM. Generally, primagrafts derived from the same patient had similar GI₅₀ values. Samples from L825 and L914, however, displayed more variation in dex sensitivity (GI₅₀ values L825: JM156 and JM157 >1000nm vs JM158, AZ10, AZ12 and AZ17 1.3-3nM; L914: AZ4 and AZ5 >1000nM vs AZ6 4.6nM). This could be due to experimental difficulty assessing viability in primary cells, or a different leukaemic clone engrafting into the mouse.

In this project, eight primary patient samples were also assessed, shown in Figure 4.15. Primary patient cells also exhibited a range of dex sensitivities, with GI₅₀ values ranging from 2.4 to >1000nM. Five patients were dex sensitive and three were dex resistant.

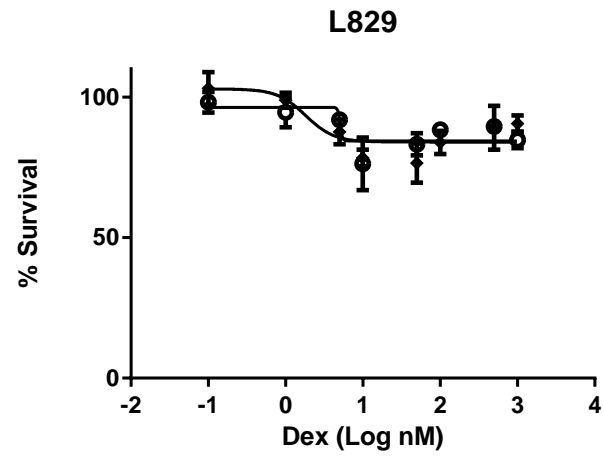
GI₅₀ values for all primagraft and primary patient samples are shown in Table 4.3. In addition, percentage survival of samples at 1000nM were also calculated and displayed in Table 4.3 to differentiate between samples which are strongly and weakly resistant. In some experiments, samples were used with previously defined dex sensitivities (Lindsay Nicholson). Details of dex sensitivity of these patients is also displayed in Table 4.3 and denoted by a '#’.

Overall, a wide range of dex sensitivities were observed in patient and primagraft cells. In addition, western blotting was performed to test for normal GR expression and function. All primagraft and patient samples displayed normal GR expression and phosphorylation at serine 211 upon stimulation with dex treatment (shown in Figure 5.1). This bank of primagraft and patient samples is a good resource which can be utilised for studies in this project into dex resistance mechanisms.

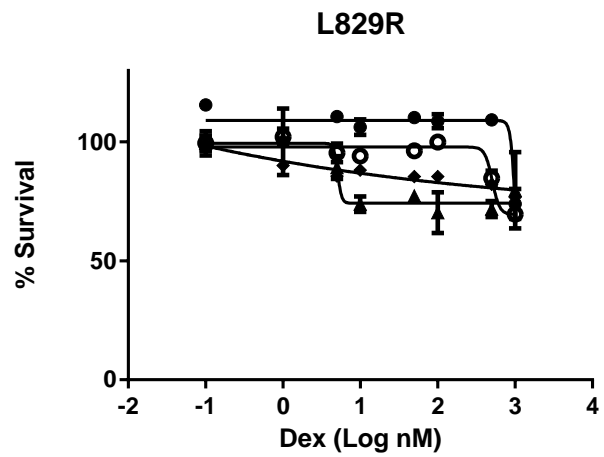




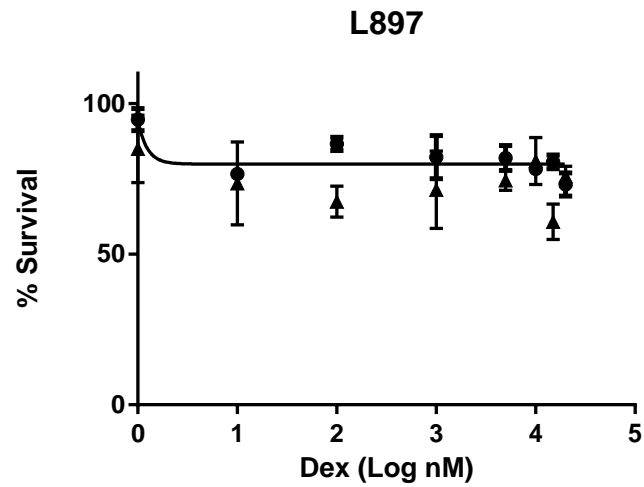
- AZ12
- ▲ AZ10
- ◆ AZ17
- ▲ JM158
- JM156
- JM157



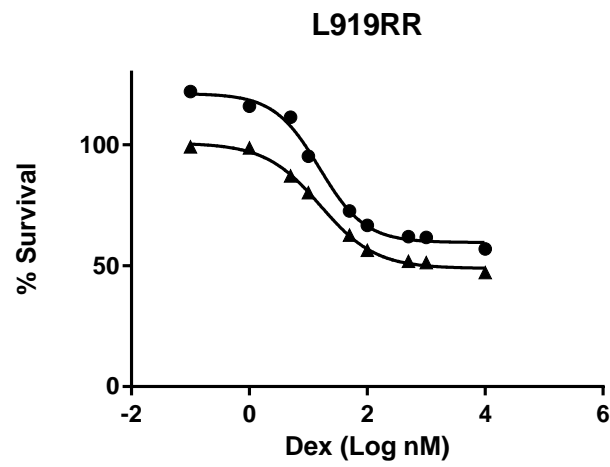
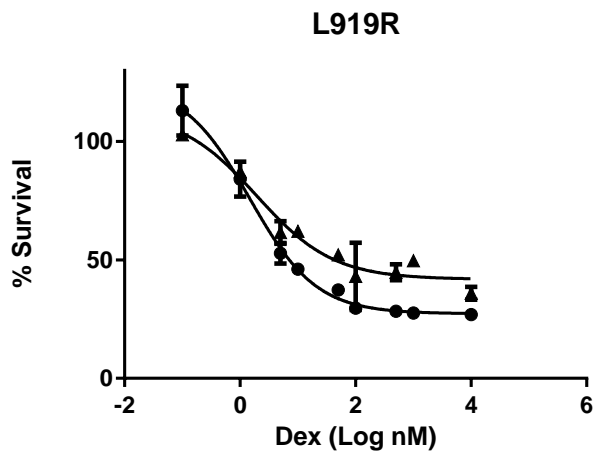
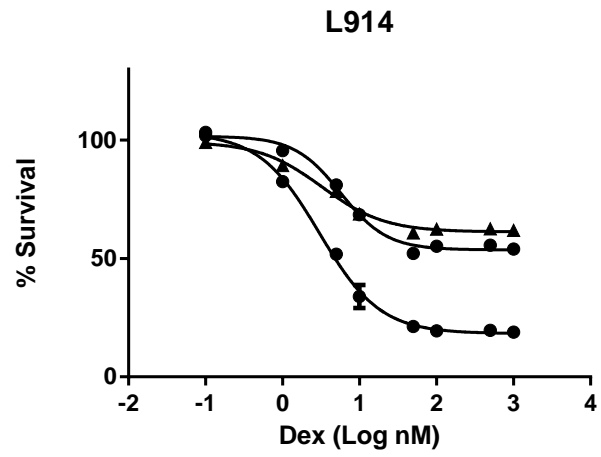
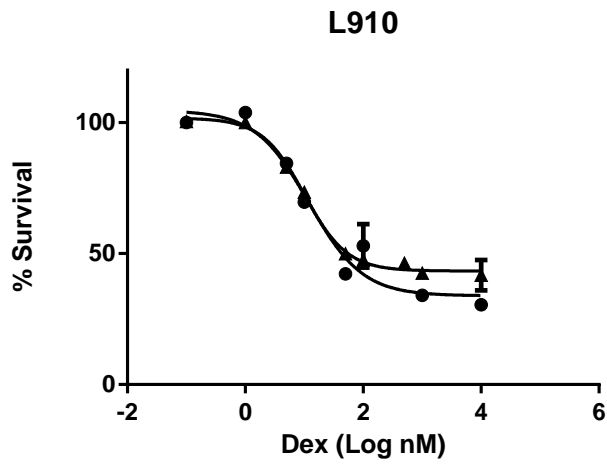
- AZ2
- ◆ AZ3



- AZ15
- ▲ AZ16
- ◆ JM251
- JM254



- JM148
- ▲ JM149



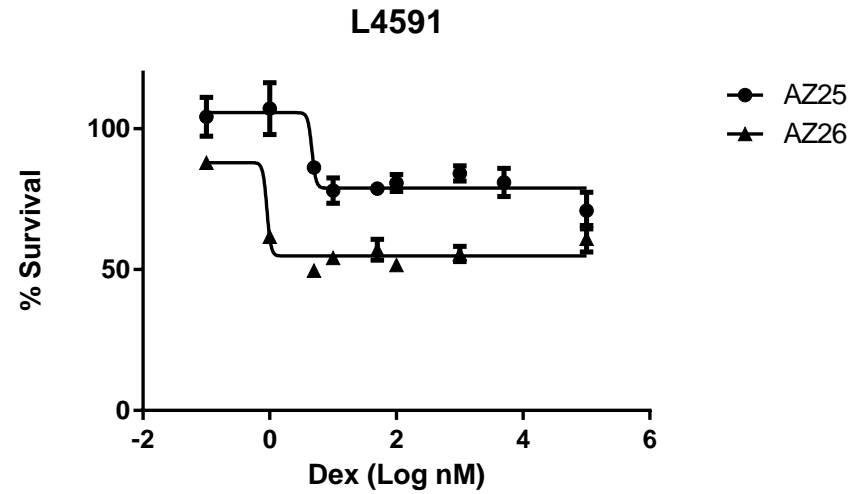
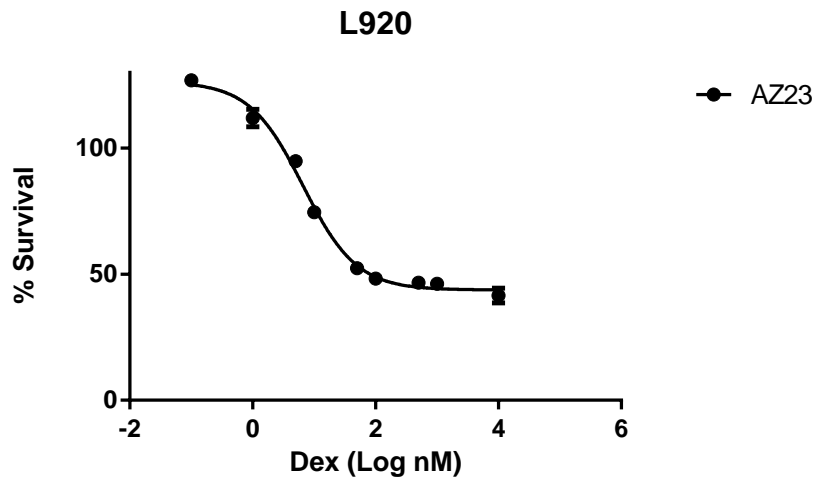
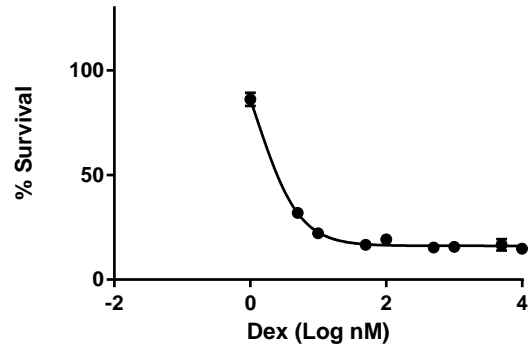


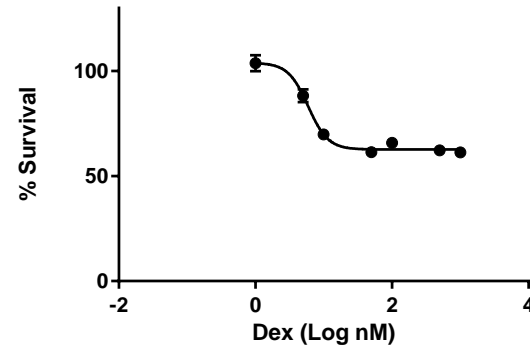
Figure 4.14 Dex sensitivity of primagraft samples.

Cells were incubated with concentrations of dex ranging from 0.1 – 10,000nM dex for 96 hours before addition of Alamar Blue. Each graph shows mice implanted with cells from the same patient, indicated in the heading of each graph. Results reported as mean percentage survival from 3 wells \pm SEM relative to cells treated with CV. R=first relapse RR=second relapse.

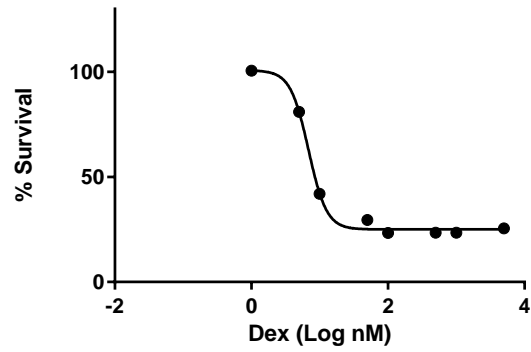
L96R



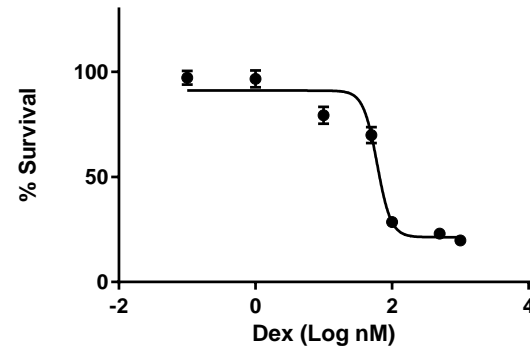
LK182



LK221



LK203



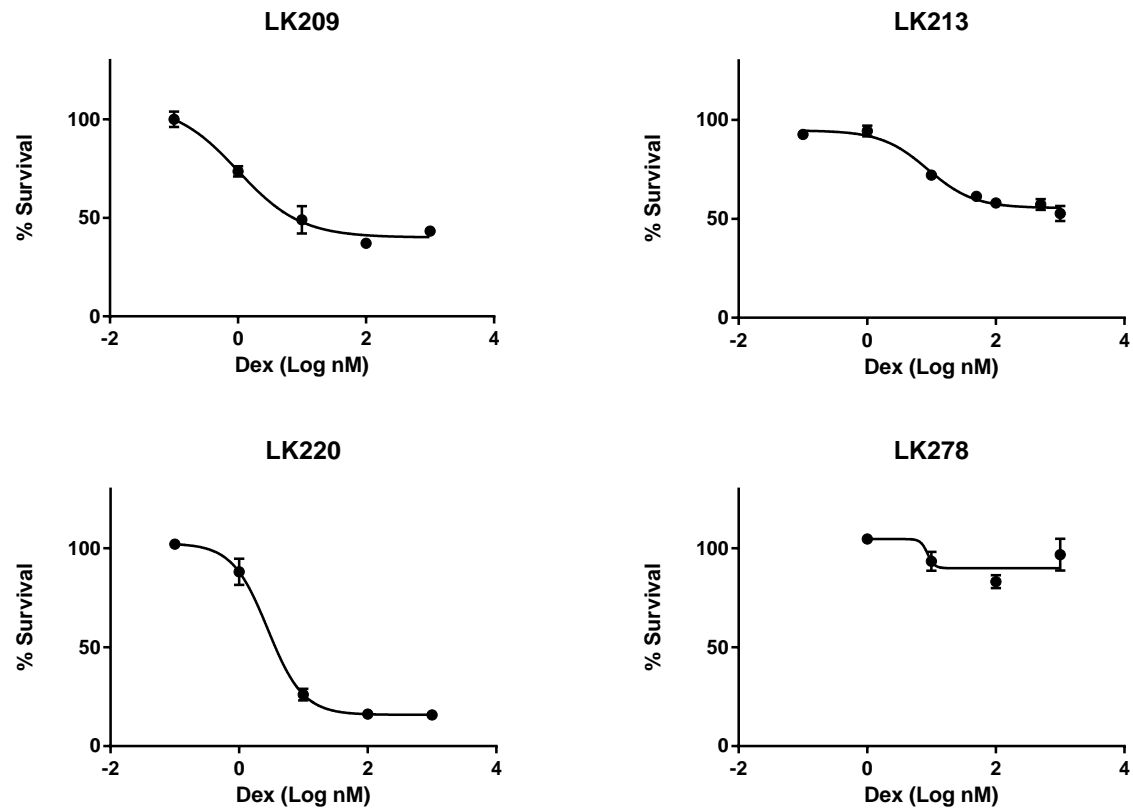


Figure 4.15 Dex sensitivity of primary samples.

Cells were incubated with concentrations of dex ranging from 0.1 – 10,000nM dex for 96 hours before addition of Alamar Blue. Each graph shows a single patient, indicated in the heading of each graph. Results reported as mean percentage survival from 3 wells \pm SEM relative to cells treated with CV.

Patient	Stage	Mouse number	Dex GI ₅₀ (nM)	Survival at 1000nM (%)	Broad class
LK196	2 nd Relapse	JM271	5	14	Sensitive
		JM271	5.8	15	Sensitive
L578	2 nd Relapse	AZ7	>1000	72	Resistant
		AZ8	>1000	75	Resistant
		AZ9	>1000	57	Resistant
L779	Presentation	JM150	>1000	83	Resistant
		JM151	>1000	83	Resistant
		JM152	>1000	61	Resistant
		AZ13	>1000	96	Resistant
L824	Presentation	AZ21	>1000	80	Resistant
		AZ22	>1000	130	Resistant
L825	Presentation	JM156	>1000	70	Resistant
		JM157	>1000	77	Resistant
		JM158	1.3	10	Sensitive
		AZ10	3	21	Sensitive
		AZ12	3	26	Sensitive
		AZ17	2.4	28	Sensitive
L829	Presentation	AZ2	>1000	85	Resistant
		AZ3	>1000	91	Resistant
L829	1 st Relapse	AZ15	>1000	74	Resistant
		AZ16	>1000	80	Resistant
		JM251	>1000	77	Resistant
		JM254	>1000	70	Resistant
L897	Presentation	JM148	>1000	78	Resistant
		JM149	>1000	81	Resistant
L910	Presentation	AZ27	42	34	Sensitive
		AZ28	55	43	Sensitive
L914	Presentation	AZ4	>1000	54	Resistant
		AZ5	>1000	62	Resistant
		AZ6	4.6	19	Sensitive

L919	1 st Relapse	JM267	44	28	Sensitive
		JM268	7.1	50	Sensitive
L919	2 nd Relapse	AZ19	>1000	57	Resistant
		AZ20	851	47	Resistant
L920	Presentation	AZ23	83	46	Sensitive
L4591	Presentation	AZ24	>1000	84	Resistant
		AZ25	>1000	56	Resistant
LK182	Presentation	N/A	>1000	61	Resistant
LK203	Presentation	N/A	71	20	Sensitive
LK209	Presentation	N/A	4	43	Sensitive
LK213	Presentation	N/A	>1000	53	Resistant
LK220	Presentation	N/A	4	16	Sensitive
LK221	Presentation	N/A	3.3	23	Sensitive
LK278	Presentation	N/A	>1000	97	Resistant
L96R	1 st Relapse	N/A	2.4	16	Sensitive
L705 #	Presentation	N/A	41.4	/	Sensitive
L715 #	Presentation	N/A	74.9	/	Sensitive
L733 #	Presentation	N/A	200	/	Sensitive
L809 #	Presentation	N/A	67.4	/	Sensitive

Table 4.3 Primagraft and patient sample dex sensitivity status.

Dex GI₅₀ values for primagraft and patient samples. Sensitivity was defined by a GI₅₀ value of <500nM. # Dex sensitivity assay performed previously by L. Nicholson.

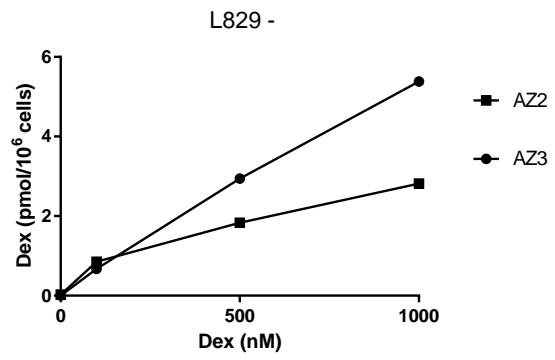
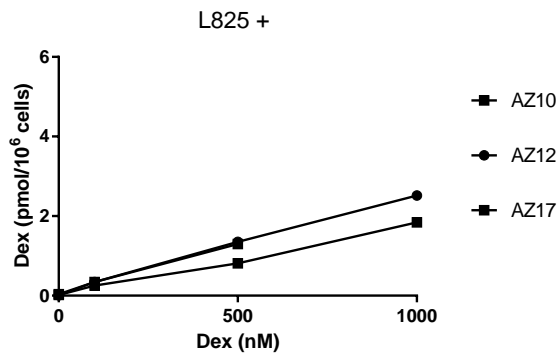
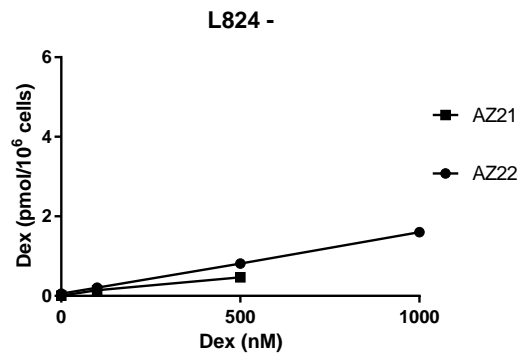
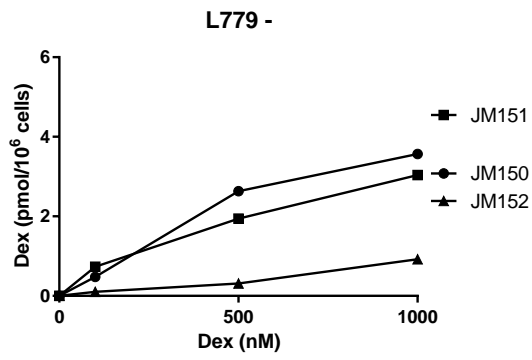
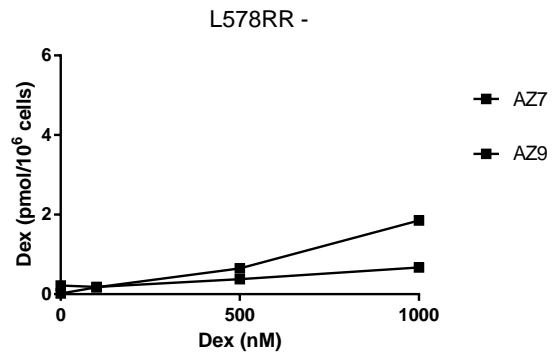
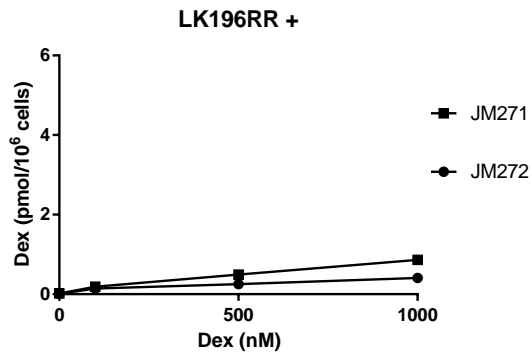
4.3.7 Dex accumulation in primagraft and patient samples

Intracellular dex levels were determined by LC/MS after incubation of primagraft and patient samples with varying concentrations of dex for 4 hours. In total, 24 primagraft (from 11 patients, Figure 4.16) and 6 patient samples (Figure 4.17) were assessed.

Primagraft samples showed a 20-fold variation in dex accumulation, with intracellular concentrations, after incubation with 500nM dex, ranging from 0.13 – 2.94 pmol/10⁶ cells. The mean intracellular accumulation was 1.15 ± 0.83 pmol dex/10⁶ cells (SD). There was a 3.7-fold difference in dex accumulation in patient samples after incubation with 500nM dex (range: 0.29-1.07) with a mean accumulation of 0.9 ± 0.6 pmol dex/10⁶ cells (SD).

In general, primagrafts derived from the same patient demonstrated comparable dex accumulation, particularly after incubation with a dex concentration of 500nM. Of exception were L779, where mouse JM152 displayed a lower intracellular accumulation, and L915 where AZ6 had a much lower accumulation than AZ4 and AZ5. The latter result is in keeping with the dex sensitivity data, where AZ6 produced a different GI₅₀ to AZ4 and AZ5 (Figure 4.12). This may be caused by engraftment of a different leukaemic clone in this mouse.

Intracellular dex accumulation in primagraft and patient samples was significantly lower than in PreB697 cell lines (p=0.03, student's t test, Figure 4.18). PreB697 cell lines had a mean accumulation of 1.83 ± 0.47 pmol dex/10⁶ cells compared to all patient and primagraft cells with a mean accumulation of 1.1 ± 0.79 pmol dex/10⁶ cells. Patient cells are, in general, smaller than PreB697 cell lines. This is apparent visually by microscopy, and also in flow cytometry where instrument setting have to be changed to account for size differences between patient samples and cell lines. Therefore, a lower accumulation in patient cells is in keeping with this observation, as the rate of diffusion of a substance into a cell is dependent on cell surface area.



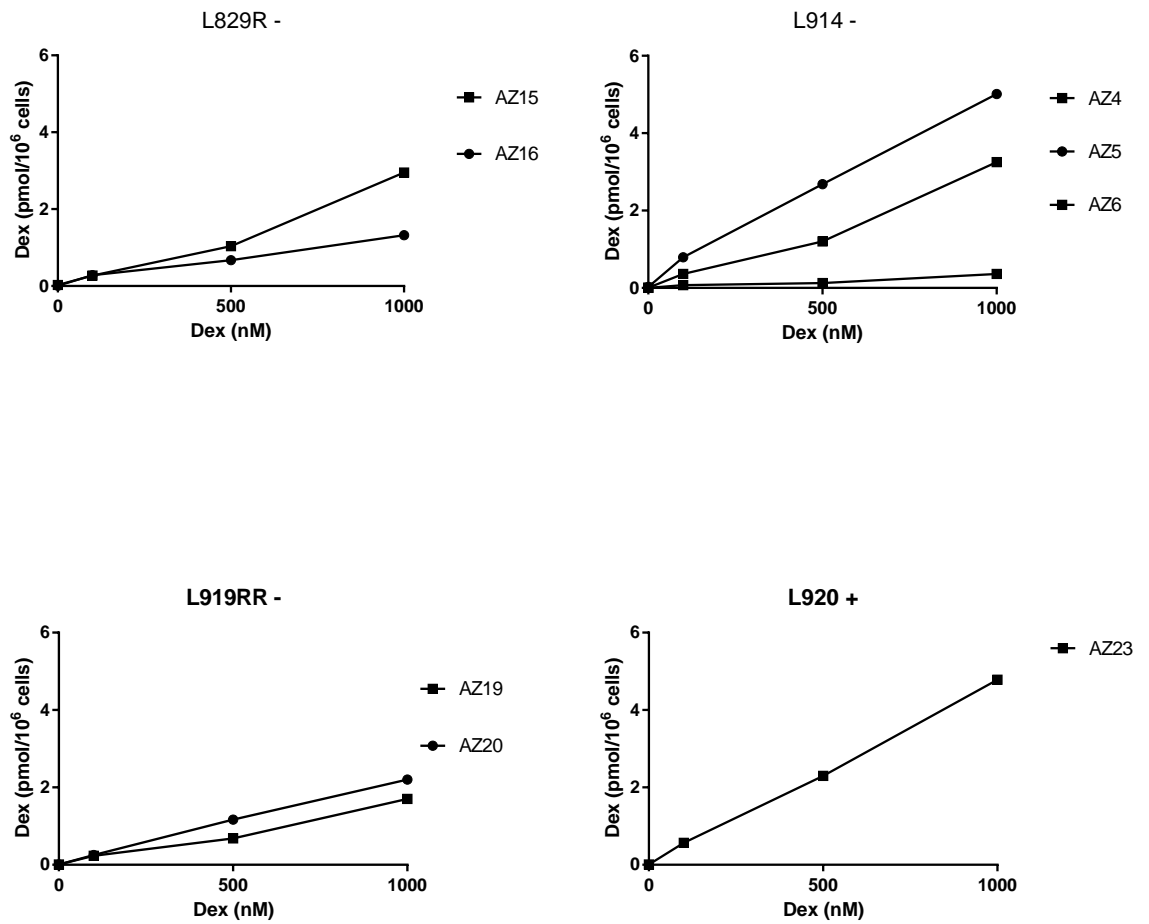


Figure 4.16. Intracellular accumulation of dex in primagraft cells assessed using LC/MS.

Dex concentrations measured by LC/MS after incubation with 100-1000nM dex for 4 hours. Dex sensitive and resistant samples are identified with a + and - respectively.

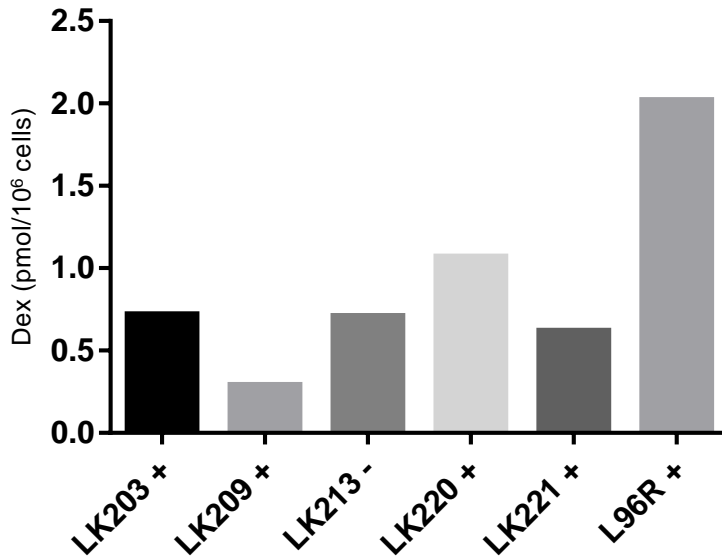


Figure 4.17 Dex accumulation in primary patient samples after incubation with 500nM dex.

Cells were incubated with 500nM dex for four hours before lysis with methanol and measurement of dex concentrations in cell lysates by LC/MS. Dex sensitive and resistant samples are shown by + and - respectively.

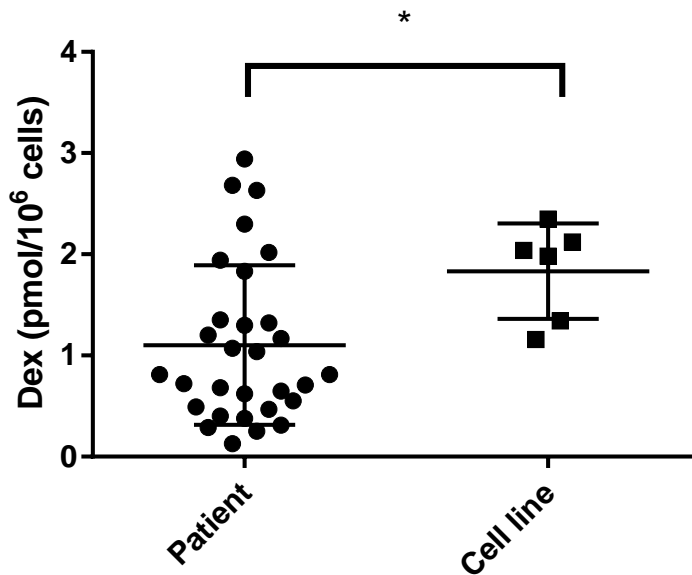


Figure 4.18 Comparison of dex accumulation measured by LC/MS between patient cells and cell lines.

Cells were incubated with 500nM dex for four hours and concentrations of dex in cell lysates was measured by LC/MS. Dex uptake in patient samples is significantly lower than in PreB697 cell lines ($p=0.03$, unpaired student's t test). Error bars are mean \pm SD.

One of the aims of this chapter was to establish whether dex accumulation differs between sensitive and resistant samples. When patient and primagraft cells were grouped together, despite there being a wide range in accumulation in sensitive and resistant samples, there was no difference in intracellular accumulation of dex ($p=0.67$, student's t test, Figure 4.19). Sensitive samples had a mean dex accumulation of 1.02 ± 0.67 pmol dex/ 10^6 cells, and for resistant samples this was 1.15 ± 0.86 pmol dex/ 10^6 cells (SD). This is in line with data generated in PreB697 cell lines, where no difference was seen in dex accumulation between dex-sensitive and resistant cells.

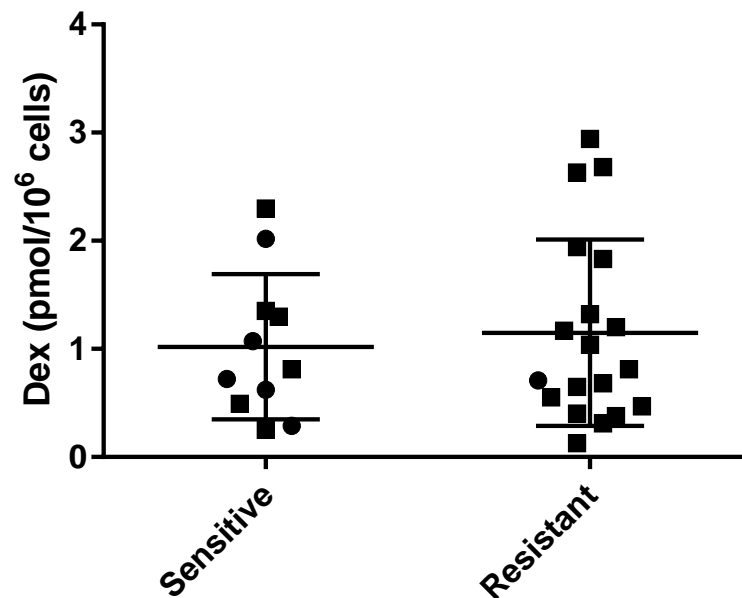


Figure 4.19 Intracellular dex accumulation measured by LC/MS in dex sensitive and dex resistant cells after incubation with 500nM dex.

There was no significant difference in intracellular accumulation of dex in sensitive and resistant samples ($p = 0.67$, unpaired student's t-test) Patient samples are circles, primagraft samples are squares. Error bars are mean \pm SD.

The wide variation in dex accumulation was also seen using a flow cytometry method measuring intracellular accumulation of dex-FITC. Samples were analysed after incubation with 500nM dex-FITC for 45 minutes at 37°C. Dex-FITC accumulation was assessed in 27 primagraft samples (derived from 12 patients) and 6 primary patient samples. Primagraft samples displayed a 15-fold variation in dex accumulation by flow cytometry, with intracellular dex accumulation after incubation with 500nM dex-FITC ranging from a mean MFI ratio of 0.67 – 10.24 (Figure 4.20A). The mean intracellular accumulation MFI was 4.23 ± 1.97 (SD). There was similarly a 3.1 fold difference in dex accumulation in patient samples (range: 3.7-11.5) with a mean accumulation of 6.44 ± 3.2 (SD) (Figure 4.20B).

Once again, primagrafts derived from the same patient demonstrated similar dex accumulation (Figure 4.20A). As with the LC/MS data, L779/JM152 displayed a lower intracellular accumulation of dex FITC although there did not appear to be a difference between L914/AZ6 compared to L914/AZ 4 and AZ5, as was observed in LC/MS data.

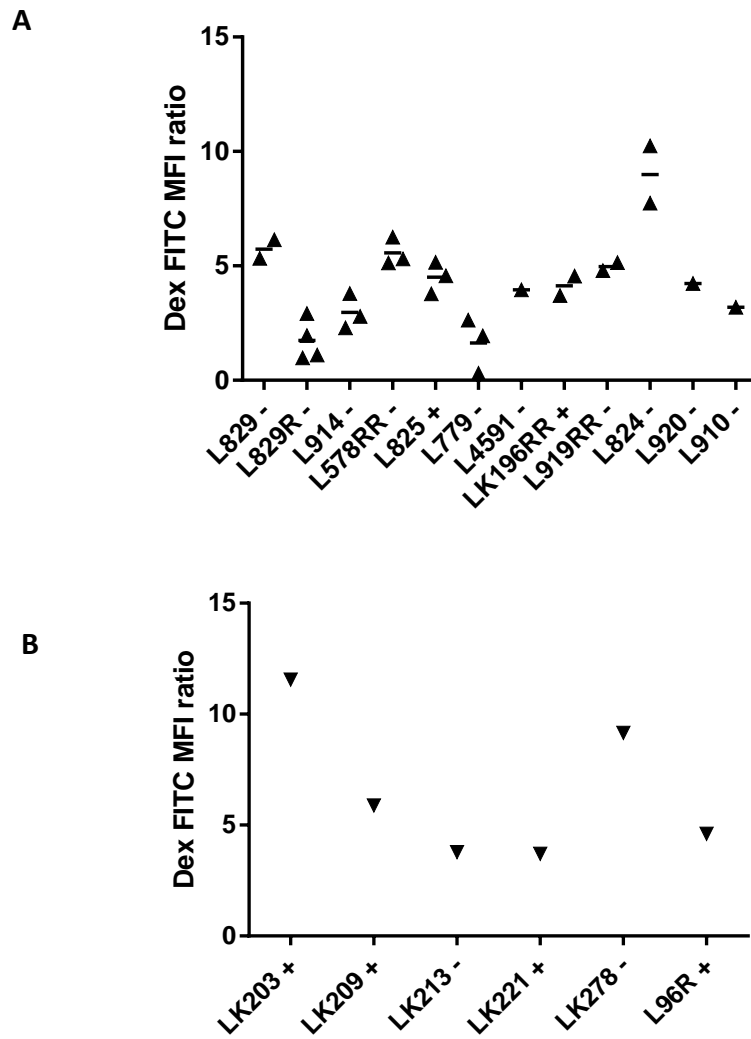


Figure 4.20 Intracellular accumulation of dex-FITC in primagraft samples (A) and primary patient samples (B) measured by flow cytometry.

All samples were incubated with dex-FITC for 45 minutes at 37°C, before FITC emission was measured in CV and dex-FITC treated samples. Data displayed is the MFI ratio of CV to dex-FITC treated samples. Dex sensitive and resistant samples are shown by + and - respectively.

In contrast to data generated by LC/MS, there was no significant difference in dex-FITC accumulation between PreB697 cell lines and patient samples (MFI ratios of 4.27 ± 0.15 , 4.63 ± 2.35 respectively, mean \pm SD, $p=0.69$, student's t-test, Figure 4.21).

However, when patient and primagraft cells were grouped together, there was a wide range in accumulation in sensitive and resistant samples, similar to the LC/MS data. There was also no difference in intracellular accumulation of dex between dex sensitive and resistant samples ($p=0.17$, student's t test, Figure 4.22).

A correlation could not be performed using all samples measured, as sample sets differed for LC/MS and flow cytometry experiments. Some samples were measured by LC/MS before the flow cytometry method had been developed. Similarly, in other cases, there were not enough cells for LC/MS analysis. Initially a correlation analysis was performed between the two methods at the validation stage of the flow cytometry method (Figure 4.23A). Both methods correlated well with a Pearson's r^2 value of 0.54 ($p=0.0027$). However, on analysis of the full sample set used in both methods, the correlation between the two methods decreased ($r^2 = 0.008$, Figure 4.23B). This may be due to differences between dex and dex-FITC, and how it is accumulated within cells. It is also possible that the stability of dex FITC reagent may have affected the correlation over time, which is discussed further in section 4.4. Nevertheless, the LC/MS method showed a wide range in dex accumulation and no difference in dex accumulation between dex sensitive and resistant samples.

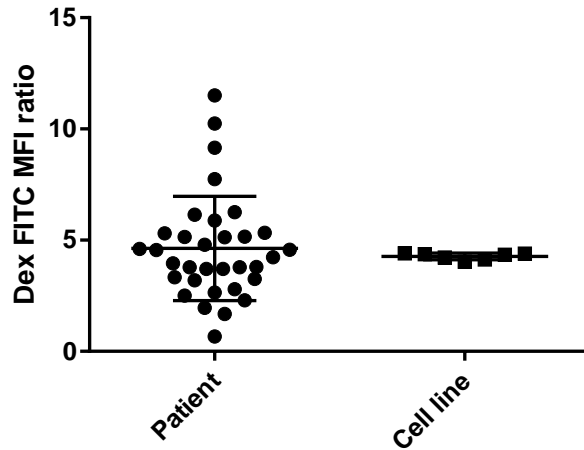


Figure 4.21 Comparison of dex accumulation measured by flow cytometry between patient cells and cell lines.

Cells were incubated with dex-FITC for 45 minutes at 37°C, before FITC emission was measured in control vehicle and dex-FITC treated samples. Data displayed is the MFI ratio of CV to dex-FITC treated samples. Error bars show mean \pm SD.

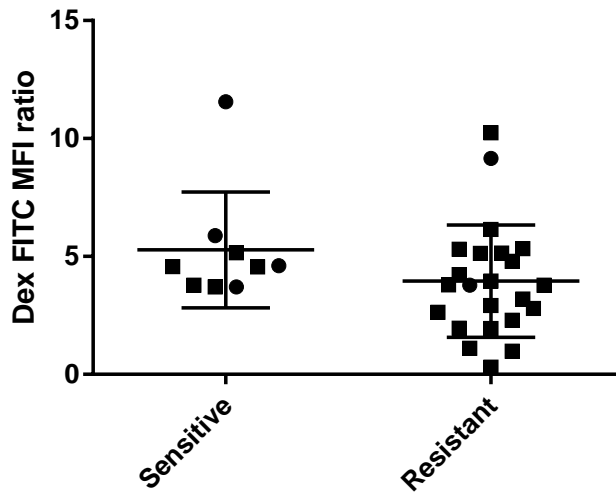


Figure 4.22 Intracellular dex-FITC accumulation measured by flow cytometry in dex sensitive and dex resistant cells after incubation with 500nM dex-FITC.

There was no significant difference in intracellular dex accumulation between dex sensitive and resistant samples ($p = 0.17$, unpaired student's t-test) Patient samples are circles, primagraft samples are squares. Error bars show mean \pm SD.

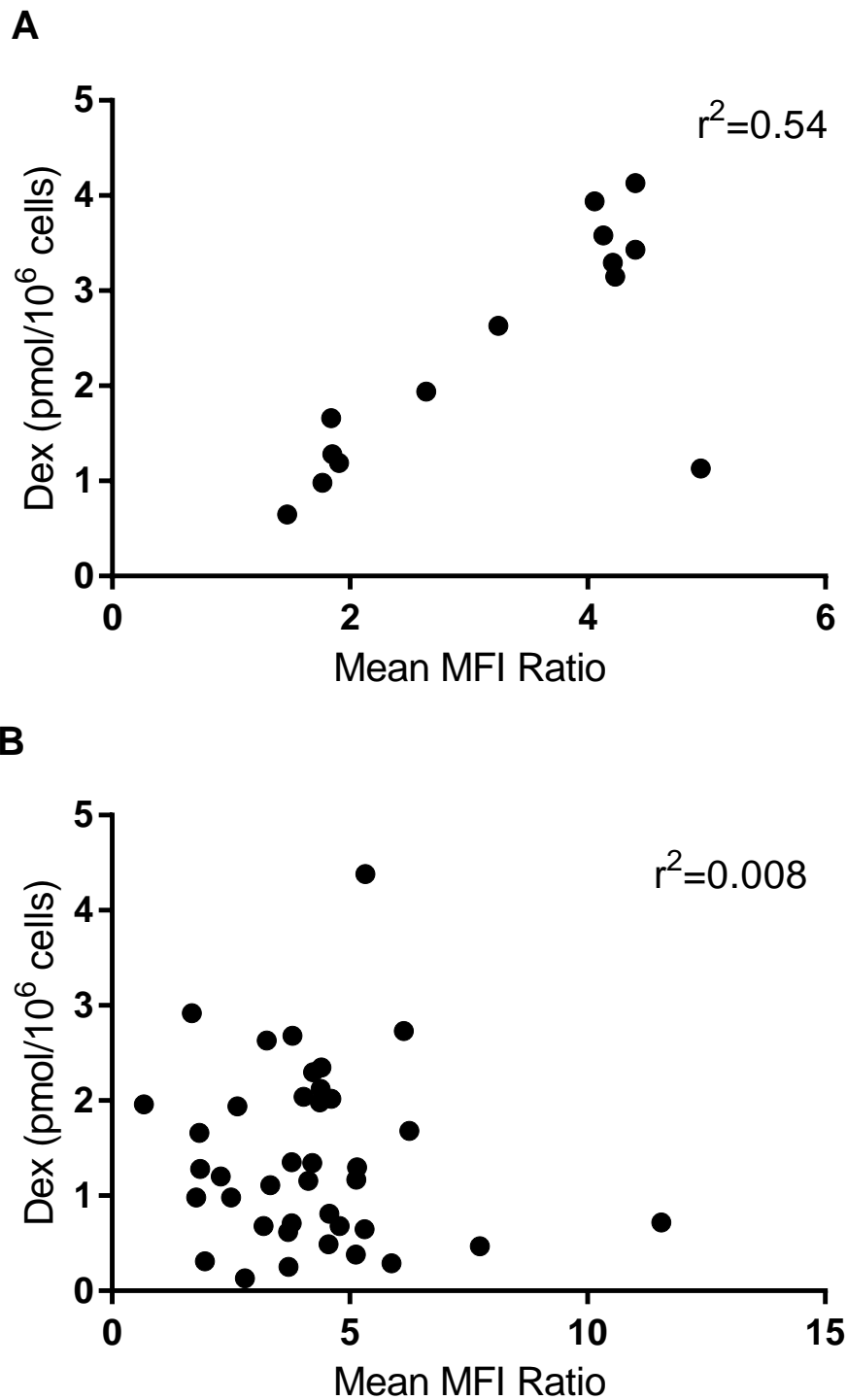


Figure 4.23 Correlation of LC/MS and flow cytometry methods for the assessment of intracellular dex concentrations in ALL cell lysates.

The correlation between the two methods was assessed using a linear regression analysis, r^2 values are shown on the graph. (A) Initial correlation of samples at the validation stage of the flow cytometry method. (B) Correlation of all samples analysed using both LC/MS and flow cytometry.

4.4 Discussion

Despite being used widely for a number of decades, the mechanisms of action and resistance of dex are still not fully elucidated. It is important that we deepen our understanding of these mechanisms, as relapsed ALLs are often GC resistant. Better knowledge surrounding these areas could lead to resensitisation or development of new therapies for dex resistant patients. A key area that remains unexplored is whether variations in intracellular dex accumulation influences dex response.

In this chapter, dex sensitivity was determined using Alamar blue assays, which assess metabolic activity of cells. The majority of the viability curves show a residual population of metabolically active cells. Even at dex concentrations of 1000nM in dex sensitive samples, there are residual cells. This is in contrast to the cell viability curves from vincristine and actinomycin D in Figure 4.8, where a near complete cell kill is seen. This phenomenon has also been seen in other studies assessing dex sensitivity by different methods (although still assessing metabolic activity) such as the MTT and MTS assays (Bachmann *et al.*, 2005; Bachmann *et al.*, 2007; Nicholson *et al.*, 2015). This incomplete cell kill is not due to a lack of stability of dex, as it was shown to be stable in culture conditions over 96h. The population of residual cells may be a result of the differing dosing schedule of *in vitro* assays compared to the clinical situation. As demonstrated by various clinical trials worldwide, the dose and schedule of GC is important in determining outcome. It may be that multiple doses of dex are needed to result in total cell kill, rather than a single exposure over 96h. It would be useful to investigate the effect of differing *in vitro* dex dosing schedules on cell proliferation and survival. However, these Alamar blue cell viability assays are still clinically relevant. Bachmann *et al.* (2005) found that *in vitro* assessment of dex sensitivity using MTT assays after a 96h exposure to dex, closely reflected the outcome of the patient samples from which they were derived. Furthermore, several studies from groups in Sweden and Holland have shown that the *in vitro* dex cytotoxicity results from 96h exposures to dex were predictive of clinical outcome (Hongo *et al.*, 1997; Kaspers *et al.*, 1997; Den Boer *et al.*, 2003; Frost *et al.*, 2003). Therefore using the outcome of these assays as an indicator of how the patient will respond to dex in the clinic is still relevant.

A number of well used anti-cancer drugs have been shown to be substrates for multidrug transporters such as MDR1, affecting intracellular concentrations of the drug. There have been mixed reports regarding the effect of MDR1 and dex (Cole *et al.*, 1992; Schinkel *et al.*, 1995b). Therefore, substrate specificity of dex for MDR1 was established in two paired cell lines with overexpression of MDR1. Despite showing a clear decrease in drug sensitivity and drug accumulation in MDR1 overexpressing lines for vincristine and act D, no difference was seen in dex sensitivity or accumulation.

There have been a number of clinical studies investigating the effect of MDR1 expression in ALL cells. Some studies associated MDR1 expression with a more unfavourable outcome (Goasguen *et al.*, 1996; Dhooge *et al.*, 2002; Casale *et al.*, 2004), however there was no link to GC response. The effect of MDR1 on outcome may be due to substrate specificity of other drugs administered to ALL patients, such as vincristine. The majority of studies, however, found no effect of MDR1 expression on outcome, which supports the findings in this chapter (den Boer *et al.*, 1998; Kanerva *et al.*, 1998; Kakiyama *et al.*, 1999; Kanerva *et al.*, 2001; Olson *et al.*, 2005). It should be noted, however, that these groups investigated childhood leukaemia patients being treated on protocols containing multiple chemotherapeutic agents.

There are limited single agent studies investigating substrate specificity for MDR1. Schinkel *et al.* found that dex accumulation in the brain was 2-fold higher in a *MDR1a* knock-out mice model, the mouse form of human MDR1, compared to wildtype mice (1995b). However, no difference was found in any other body compartment including the plasma, which supports the data generated in this chapter. The difference in brain accumulation in mice compared to data generated here may be due to differences between human MDR1 and mouse MDR1a.

The observation that dex is not an MDR1 substrate is also important when considering dex pharmacokinetics. Multidrug transporters including MDR1 are expressed in the liver, kidney and gastrointestinal tract (Fojo *et al.*, 1987). Therefore, MDR1 can affect pharmacokinetics of substrates due to decreased absorption in the gastrointestinal tract and increased secretion of substrates into urine and bile (Fojo *et al.*, 1987; Schinkel, 1998; Evans and McLeod, 2003; Sakaeda *et al.*, 2003). The indication that dex

is not a substrate for MDR1 suggests that observed pharmacokinetic dex variation is not likely to be due to genetic germline variation in MDR1.

In this chapter, dex accumulation was measured in ALL cells. The methods used were applicable to the small numbers of cells often obtained in patient samples. Dex concentrations were quantifiable in cell numbers of 1×10^6 after incubation with 500nM dex, allowing measurement of patient samples where limited numbers of cells are available.

The ability to use primagraft and patient samples in this project is a strength. In the past, many studies have made hypotheses for drug resistance mechanisms through cell line investigations, however these have rarely translated into the patient setting. It has been shown that investigations in primagraft samples have produced results that mirror the patient outcome from which they were derived (Jing *et al.*, 2015), and therefore provide a more appropriate model than cell lines. For example, in this project dex sensitivities of the primagraft samples reflected patients' MRD results, where available. Patient L897 was found to be resistant to dex, which is reflected in a high MRD result at day 28. Patients L914 and L825 also had high MRD at day 8 and 28 respectively. There was heterogeneity in dex sensitivity response in primagrafts derived from these patients, with some displaying sensitivity and some resistance. It is possible that they may be more than one leukaemic clone at presentation, with the resistant clone persevering causing high MRD. In contrast, patient L910 was found to be dex sensitive which was reflected in their low risk trial status.

Using LC/MS, a 20-fold variation was seen in intracellular dex accumulation in primagraft and patient samples. It has been established that this is not likely to be due to export via MDR1. There are also other multidrug transporters such as MRP1, BCRP (breast cancer resistance protein) and LRP. However, there are limited studies regarding the effect of such transporters in ALL which report contrasting results (Beck *et al.*, 1996; Kakiyama *et al.*, 1999; Robey *et al.*, 2007). It may be useful to further explore the contributions of these multidrug transporter proteins to intracellular dex accumulation. This could be achieved using the MDCKII cell line model, as there are MDCKII cell lines overexpressing MRP1, BCRP and LRP proteins.

This range in intracellular dex concentration could also be caused by events such as increased steroid binding protein, or a change in 11 β -hydroxysteroid dehydrogenase enzyme (11 β -HSD) expression. There are two forms of 11 β -HSD; 11 β -HSD1 which converts inactive 11 β -keto GC into active GC, and is expressed in GC target tissues, and 11 β -HSD2 which inactivates GC but is only has restricted expression (Seckl, 2004). Although there have been limited studies looking at 11 β -HSD, Sai *et al.* (2009) found that 11 β -HSD1 expression was decreased in GC resistant ALL cells *ex vivo* compared to GC-sensitive ALL cells. Therefore, investigating whether intracellular dex levels differ in GC-sensitive and resistance cells represents an interesting and novel avenue that may aid further stratification of dex therapy.

The physical properties of dex could affect its investigation. As dex is small and lipophilic (reported logP values of 1.95 and 1.83 (Hansch C., 1995; Thakur *et al.*, 2011)), it could passively diffuse out of cells during the washing steps of the experiment until a steady state is reached. However, act D and vincristine are also small and lipophilic (logP values 2.82 and 4.77 respectively (Hansch C., 1995; Walsh *et al.*, 2016)) and able to cross the plasma membrane passively. In this project, a clear difference was seen in accumulation of vincristine and act D in MDR1 expressing and wildtype cell lines, which would have been diminished if the washing steps caused passive efflux of small lipophilic drugs.

Intracellular dex accumulation results for some patients differed between the LC/MS and flow cytometry methods used. This may be due to differences in experimental procedure including differences between dex and dex-FITC. In LC/MS, the mass to charge ratio of dex and fragments are measured. This means only 'pure' dex will be measured, not dex in complex with other molecules or proteins, such as the GR or glutathione. In contrast, the flow cytometry method measures fluorescence of the fluorochrome, FITC, which is conjugated to dex. This will therefore still fluoresce when dex is bound to any other molecule. Therefore the differences observed between the two methods may be due to the difference in amounts of 'pure' dex and total dex within the cell.

However, the stability of dex-FITC was not assessed; differences observed between the two methods could also be caused by degradation of FITC. FITC is sensitive to

photobleaching, the effect of light on degradation of the fluorophore (Hama *et al.*, 2006; Mahmoudian *et al.*, 2011). Although the antibody was aliquoted into opaque tubes, fluorescence may have diminished over time causing samples analysed at the start of an aliquot to emit a brighter signal than those at the end. The stability of dex-FITC was not tested over time. This could have therefore affected the data and thus the correlation with the LC/MS results. Further work should be done to check this, to ascertain whether the poor correlation between the two methods is due to a difference in what is being assessed or photodegradation of dex-FITC.

Nonetheless, in LC/MS experiments, no difference was seen between sensitive and resistant patient cells in terms of intracellular dex accumulation. This suggests that other cellular mechanisms are more important in defining cellular sensitivity to dex. This will be investigated further in chapters 5 and 6.

Despite being able to relate intracellular dex levels to the *in vitro* dex response of the cell, directly establishing the effect of intracellular dex levels on signalling downstream of the GR would require additional experiments. However, as no relationship has been seen between intracellular dex levels and dex sensitivity, further investigations to analyse the down-stream consequences and how these relate to *in vitro* dex sensitivity may not be relevant.

These data suggest that while pharmacokinetics and cellular response are hugely variable, variations in drug accumulation do not appear to be caused by MDR1 substrate specificity, or play a key role in dex response in ALL cells. Importantly, 62% of patient cells had dex GI₅₀ values greater than plasma concentrations observed in any patient, on both arms on the UKALL 2011 trial. These patients exhibiting a high dex GI₅₀ values may be less likely to obtain a clinical benefit from dex at a dose equivalent to that used in the UKALL 2011 trial. A combined approach incorporating pharmacokinetic assessments and cellular response in ALL cells should be further investigated, to allow a comprehensive understanding of dex pharmacology with a view to optimising its clinical utility.

Chapter 5. GR post translational modifications and GC sensitivity

5.1 Introduction

Despite the observed improvements in survival in ALL, relapse still occurs in 20%, for which therapy resistance is often the cause (Pui and Evans, 2006). GC response *in vitro* has been found to be significantly less in relapsed ALL samples compared to presentation samples (Klumper *et al.*, 1995). However, the mechanisms of action and resistance of dex are still not clear. Given the shortage of therapeutic options for relapsed ALL, an improved understanding of resistance mechanisms may enable further stratification of dex to prevent unnecessary toxicity, and aid the development of novel therapeutics for this group of patients.

Studies into glucocorticoid resistance have shown that cells undergo GR-ligand nuclear translocation and GR binding, albeit to varying degrees, irrespective of GC sensitivity status (Bachmann *et al.*, 2005; Nicholson *et al.*, 2010). In order to produce a GC response, the GR must interact with specific proteins in a highly coordinated process for the inactive state in the cytosol to transform successfully to the fully transcriptionally active nuclear form.

These roles of proteins include trafficking GR to and from the nucleus and orchestrators of transcriptional machinery. In addition, phosphorylation and other post-translational modifications are also important regulatory events (Bodwell *et al.*, 1998). Phosphorylation of the GR by GCs can affect co factor interaction, strength and duration of signalling, and target promotor specificity (Manning *et al.*, 2002; Wang *et al.*, 2002). For example, serine 211 on the GR is phosphorylated upon stimulation with ligand and correlates with the transcriptional activity of the GR (Wang *et al.*, 2002). Therefore, characterising the roles of interacting proteins or post-translational modifications of the GR in both the active and inactive state, in dex sensitive and resistant cells, may reveal differences that potentially could lead to GC re-sensitising targets.

Groups have previously used transcriptome and bioinformatic approaches to identify novel regulators of GR function, however methods to study the GR interactome were based initially on large amounts (gram weight quantities) of material from animal models (Pierce *et al.*, 2012). One new technology which overcomes the requirement for large amounts of material is NanoPro technology (Protein Simple, Santa Clara,

California). This assay is based on capillary isoelectric focusing coupled to a fluorescence immunoassay (cIEF). In cIEF, proteins are separated by isoelectric focussing in capillaries where they concentrate at their pI. Proteins are then cross-linked to the capillary wall using ultraviolet light before being washed and probed with primary, secondary and tertiary antibodies. Addition of luminol and peroxidase causes a chemiluminescent reaction which is quantified by the machine.

Pilot studies using cIEF performed by Lindsay Nicholson (former member of J. Irving's group) showed differences in the GR pI profiles using a pan-specific GR antibody in an ALL cell line model of GC-resistance which recapitulates many features of primary cells, including GC-induced nuclear translocation, up-regulation of GR transcriptional targets, but no Bim induction or associated apoptosis (Pierce *et al.*, 1998; Nicholson *et al.*, 2010; Griaud *et al.*, 2012). This pilot data is detailed in Appendix E.

Therefore, advances in high end proteomics offer new approaches to gain insight into GR regulation and dex resistance that may lead to novel agents to enhance dex response and improve ALL outcome. Pilot data indicate that the GR posttranslational modifications differs in dex sensitive and resistant ALL cells but further characterisation is needed in a range of dex sensitive and resistant samples to establish the molecular basis of the change in GR pI. As part of this project (detailed in Chapter 4), the dex sensitivity of a range of cell lines and primagraft samples has been established, making further investigation into GR posttranslational modifications possible.

5.2 Chapter specific aims

- Establish GR expression and function in all samples.
- Validate HPA004248, or other GR pan specific antibody for cIEF on Peggy Sue machine (ProteinSimple).
- Investigate GR posttranslational modifications in primary ALL samples using cIEF (Peggy Sue).

5.3 Results

5.3.1 Assessment of GR by western blot

All samples were assessed by western blot for the expression of GR using a pan specific antibody (Santa Cruz), and GR phosphorylation at serine 211 (Cell Signalling), an indication that the GR has successfully translocated to the nucleus (Wang *et al.*, 2002). Lysates were also probed for α -tubulin to ensure equal protein loading.

Figure 5.1 shows representative western blots. In all samples, GR was evenly expressed in untreated lysates and lysates treated with control vehicle and 100nM dex for 3 hours. Only dex treated samples show a strong band for pGR at S211, indicating that upon dex treatment, the GR has been released from the heteromeric protein complex in the cytoplasm and has translocated to the nucleus. R3D11 and Reh cells serve as hemizygous and negative controls respectively. R3D11 has a reduced GR expression, and REH shows no GR or phosphorylated GR expression.

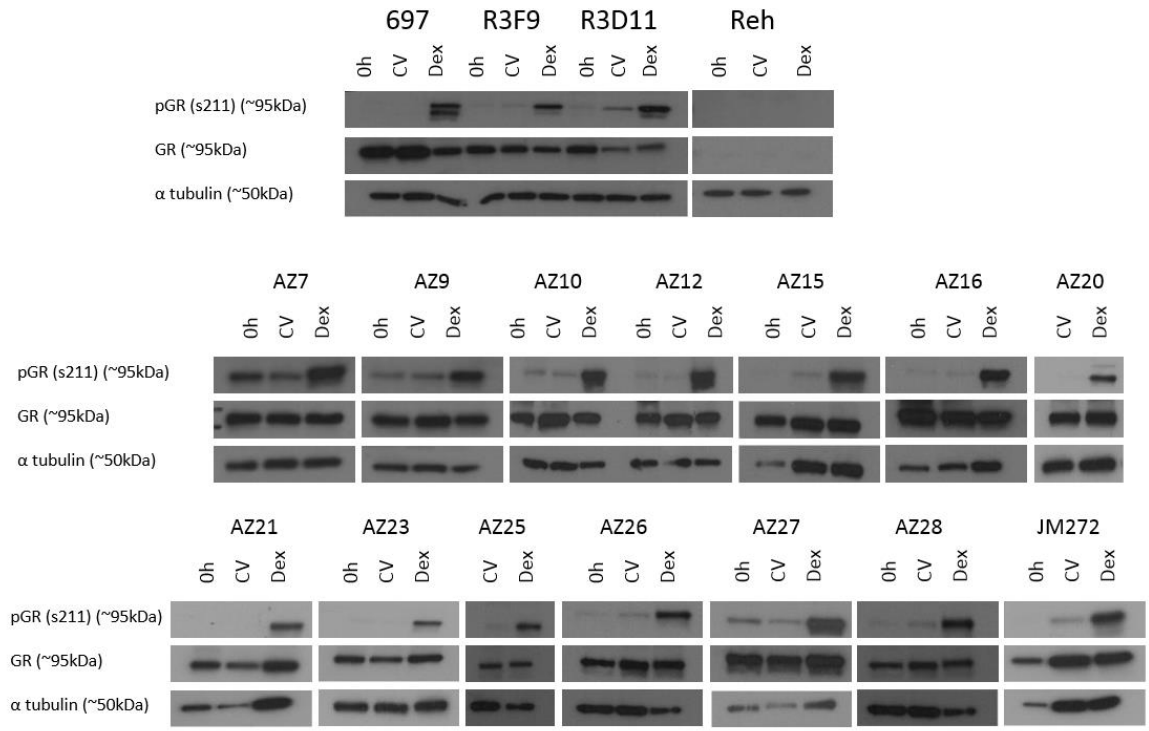


Figure 5.1 Example western blots of lysates probed for GR and phosphorylated GR (s211).

Lysates were generated after treatment with control vehicle or 100nM dex for 3 hours before lysis. Lysates were probed with a pan specific GR antibody (santa cruz sc-1003), and pGR (s211) antibody (cell signalling, 4161). 0h = untreated lysates. CV = control vehicle treated lysates. Dex = dex treated lysates.

5.3.2 Peggy Sue Antibody selection

The initial aim was to optimise the HPA004248 antibody (Sigma) for cIEF on the Peggy Sue machine, an upgrade from the ProteinSimple NanoPro 1000 machine used in the generation of the pilot data. The main differences between the two systems is that the Peggy Sue can carry out size assays in addition to charge assays. Unfortunately the cIEF assay did not transfer well to the new machine. In an preliminary signal strength test, the HPA004248 antibody was compared to a Santa Cruz GR E-20 antibody (Sc-1003), used in western blot analysis of lysates. Figure 5.2 shows electropherograms of R3F9 lysates probed with both antibodies. Lysates were treated with both control vehicle (top row) and 100nM dex (bottom row). The signal with the HPA004248 antibody was very low, with the chemiluminescence signal of 80 – 100 not rising much above the baseline of 20. This is in contrast with data generated on the NanoPro1000 using the same antibody (Figure 5.2). The Santa Cruz E-20 antibody, however, gave a much stronger chemiluminescence signal of 700 -1000, and was therefore selected for further optimisation.

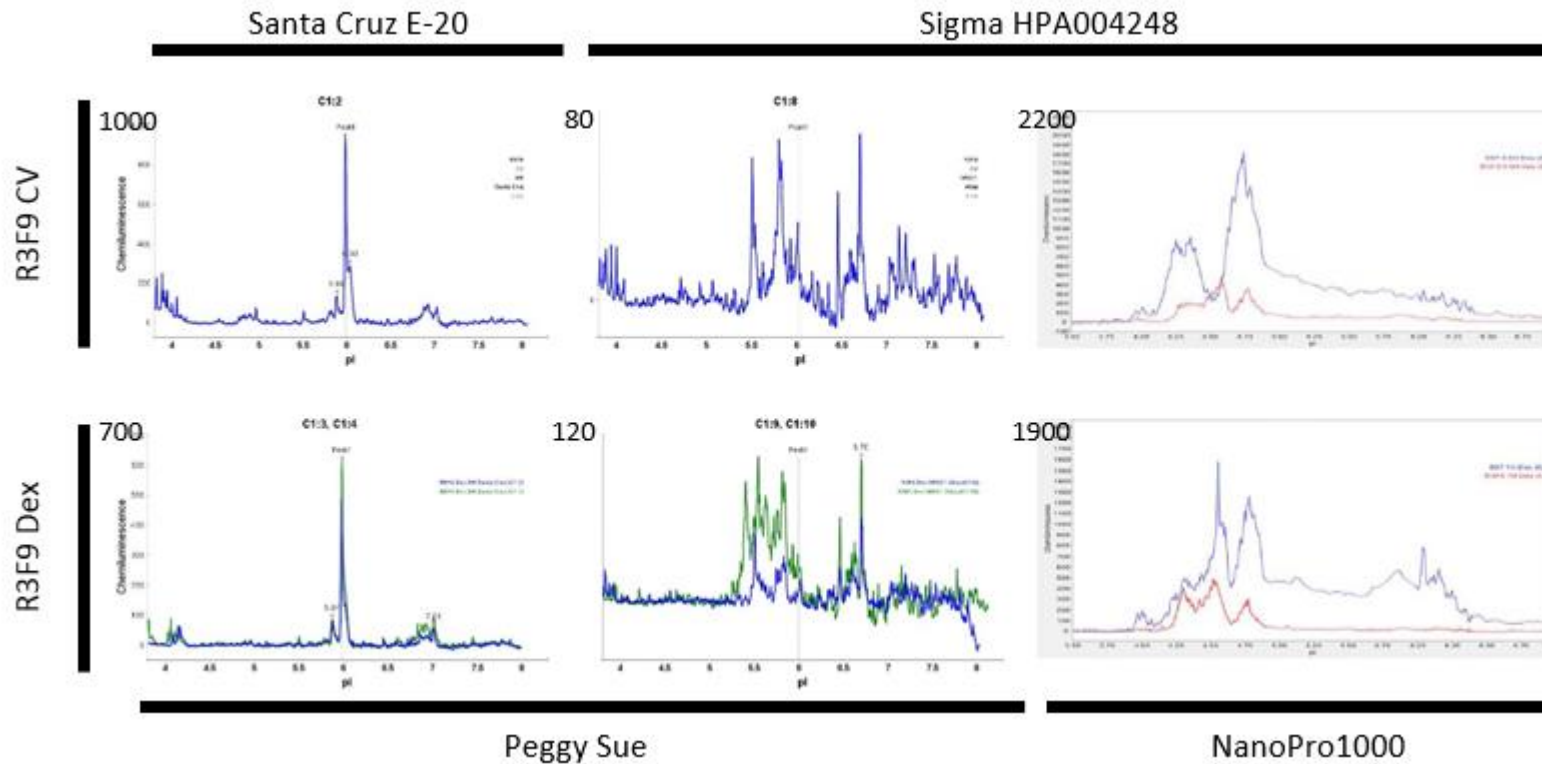


Figure 5.2 Comparison of Santa Cruz NR3C1 antibody (E-20, left) with Sigma NR3C1 antibody (HPA004248, middle) on the Peggy Sue and Sigma NR3C1 (HPA004248, right) on the NanoPro1000.

R3F9 lysates were treated with control vehicle (top row) and 100nM dex (bottom row) for 3 hours. Blue and green lines for Peggy Sue data in the dex treated samples show technical replicates. Red line on the NanoPro1000 data shows R3F9 results. The number on the Y axis (chemiluminescence) indicates the scale of the graph. X axis = pH.

Upon further optimisation, it was established that the E-20 antibody is not specific for the GR on the Peggy Sue platform.

Figure 5.3 shows R3D11 lysates (positive for the GR, and REH lysates, which do not express GR. In (A) Peggy Sue charge analysis on untreated lysates produces a strong signal in both cell lines, irrespective of GR status. In (B), however, western blot analysis of the same lysates probed with the same GR E-20 antibody showed a positive signal in the R3D11, but a negative signal with REH lysates. A new GR antibody was therefore selected.

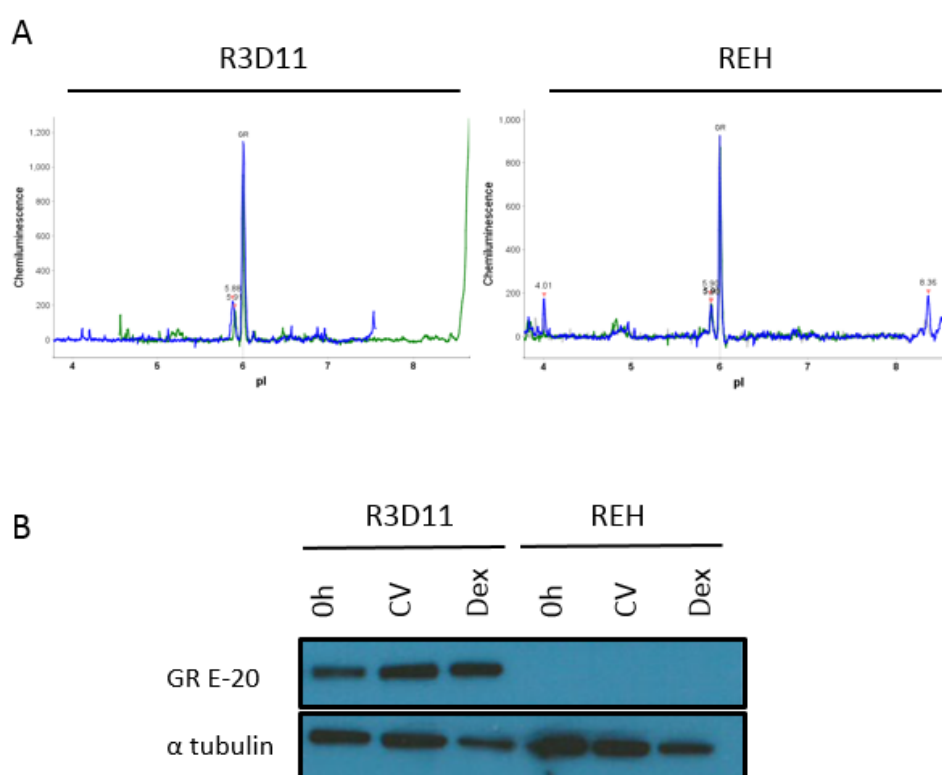


Figure 5.3 GR analysis using Santa Cruz E-20 antibody by cIEF and western blot.

(A) R3D11 and REH lysates measured on the Peggy Sue with E-20 antibody, both showing a strong positive result. Y axis = chemiluminescence. X axis = pI (B) The same lysates analysed by western blot using the E-20 antibody. REH is negative for GR. 0h = untreated lysate. CV = control vehicle treated lysate. Dex = 100nM dex treated lysate.

Three more commercially available GR antibodies were identified; Abcam (ab3579), and Cell Signalling D8H2 (#3660), and D6H2L (#12041). Western blot analysis of the three antibodies with PreB697 (GR positive cell line) and REH (GR negative cell line) revealed ab3579 to be non-specific for the GR. However, bands were displayed at the expected size of ~95kDa in the two Cell Signaling antibodies. The REH cells displayed a faint band at ~70kDa with all antibodies. Although often used as a negative control, REH cells have been shown to have one deleted allele, and one truncated allele of 528 amino acids. The full GR has 778 amino acids so the molecular weight of the faint band corresponds with the truncated GR allele. These antibodies were therefore tested on the Peggy Sue platform by Rognvald Blance (Manchester University). Both antibodies displayed a chemiluminescence signal above baseline, with the D8H2 exhibiting a slightly stronger signal of approximately 300 compared to 200 with the D6H2L antibody. D8H2 was therefore taken forward for further validation on the Peggy Sue.

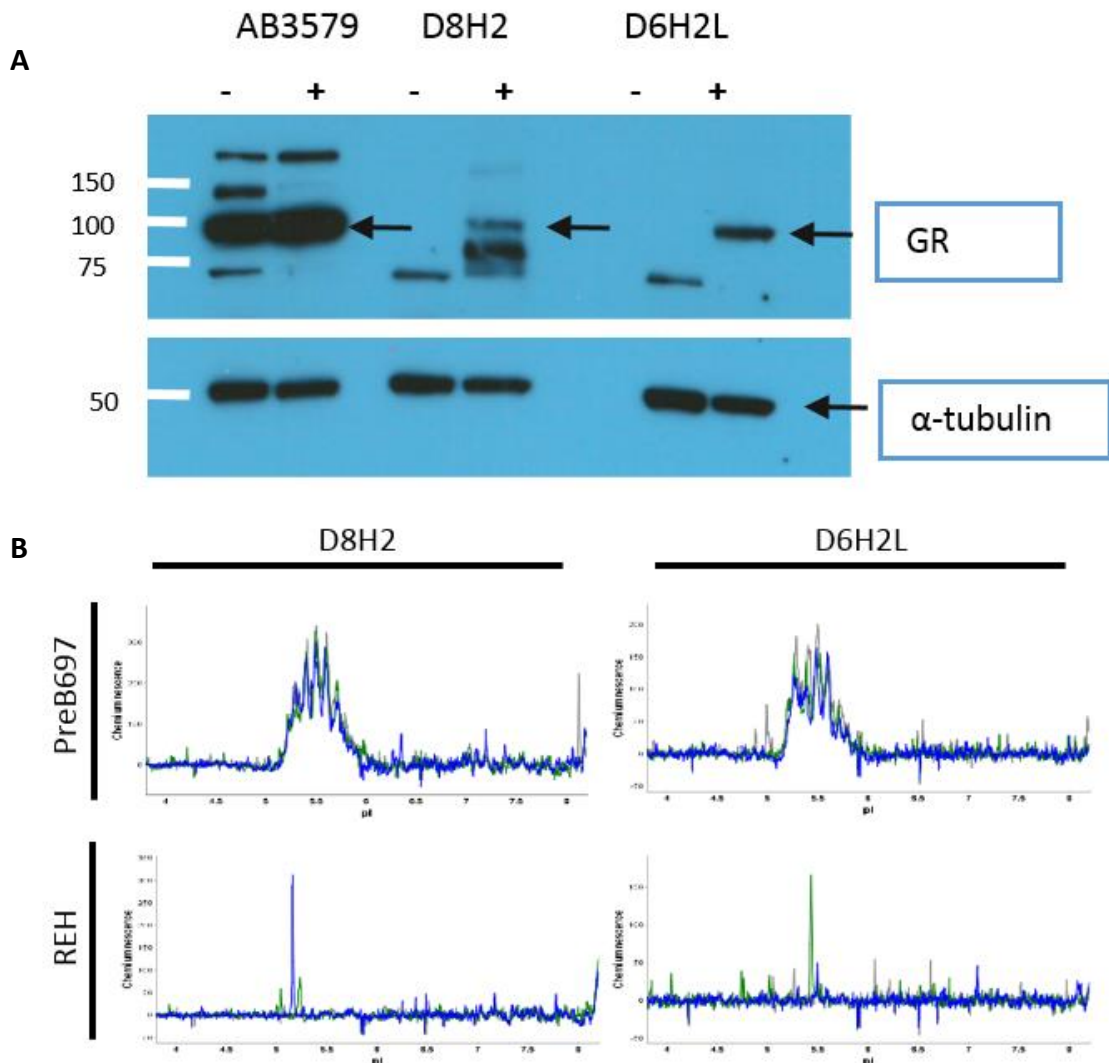


Figure 5.4 Testing of GR antibodies by western blot and cIEF.

(A) Shows three pan specific GR antibodies tested with GR negative cell line, REH, and GR positive cell line, PreB697, depicted by '-' and '+' respectively. Antibodies from left to right are Abcam 3579, Cell Signalling D8H2 and D6H2L. electropherograms generated on the Peggy Sue machine for PreB697 (top) and REH (bottom) lysates treated with 100nM dex, and probed with Cell Signalling antibodies D8H2 (left) and D6H2L (right). Blue, green and grey lines are technical replicates. Y axis = chemiluminescence. X axis = pI.

5.3.3 Antibody Validation

Freeze-Thaw Stability

As cIEF assesses the presence of post-translational modifications, which can be lost through freeze-thaw cycles, the freeze-thaw stability of the lysates was established. As can be seen in Figure 5.5, the samples did not have good freeze-thaw stability. A freshly thawed dex treated PreB697 lysate has a chemiluminescence value of around 130. However, after one freeze thaw cycle this drops to around 30, which is barely distinguishable from the baseline. All further validation and experiments were therefore performed with freshly thawed lysates.

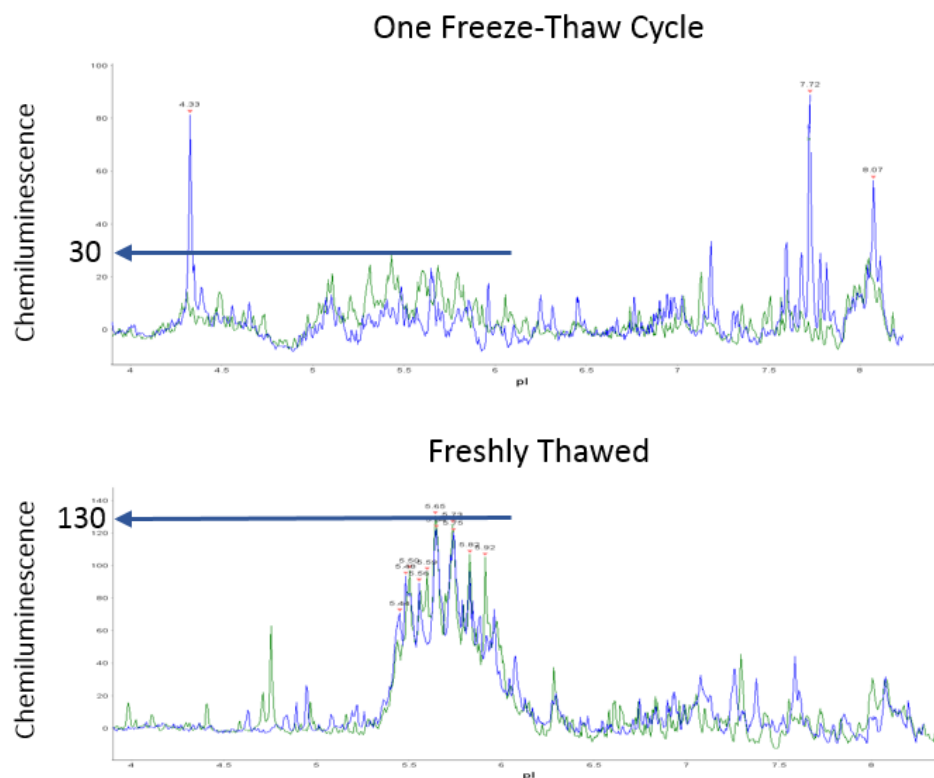


Figure 5.5 Peggy Sue lysate freeze thaw stability.

PreB697 lysates treated with 100nM dex are shown measured on the Peggy Sue machine with the Cell Signalling D8H2 antibody. The top panel shows lysates that have been flash frozen as part of the lysate generation protocol, thawed, refrozen and thawed again. The bottom panel shows lysates that have been flash frozen and thawed before use. Blue and green lines are technical replicates. Y axis = chemiluminescence. X axis = pI.

Antibody Titration

An antibody titration was performed to establish the optimal concentration of antibody to give a strong signal without giving 'burn out'. Burn out can occur when too high a concentration of antibody or protein causes the peroxidase substrate to be rapidly exhausted and thus the limiting factor in the peroxidase reaction is the luminol (ProteinSimple, 2014). To test antibody titrations, PreB697 cell lysates treated with a 100nM dex were used. Lysates were used at a concentration of 0.1µg/µl. Figure 5.6 shows the results of the antibody titration. Peaks at all pls decreased proportionally to antibody concentration. There was no burn out observed, so the dilution of 1:25 was used as it gave the strongest signal.

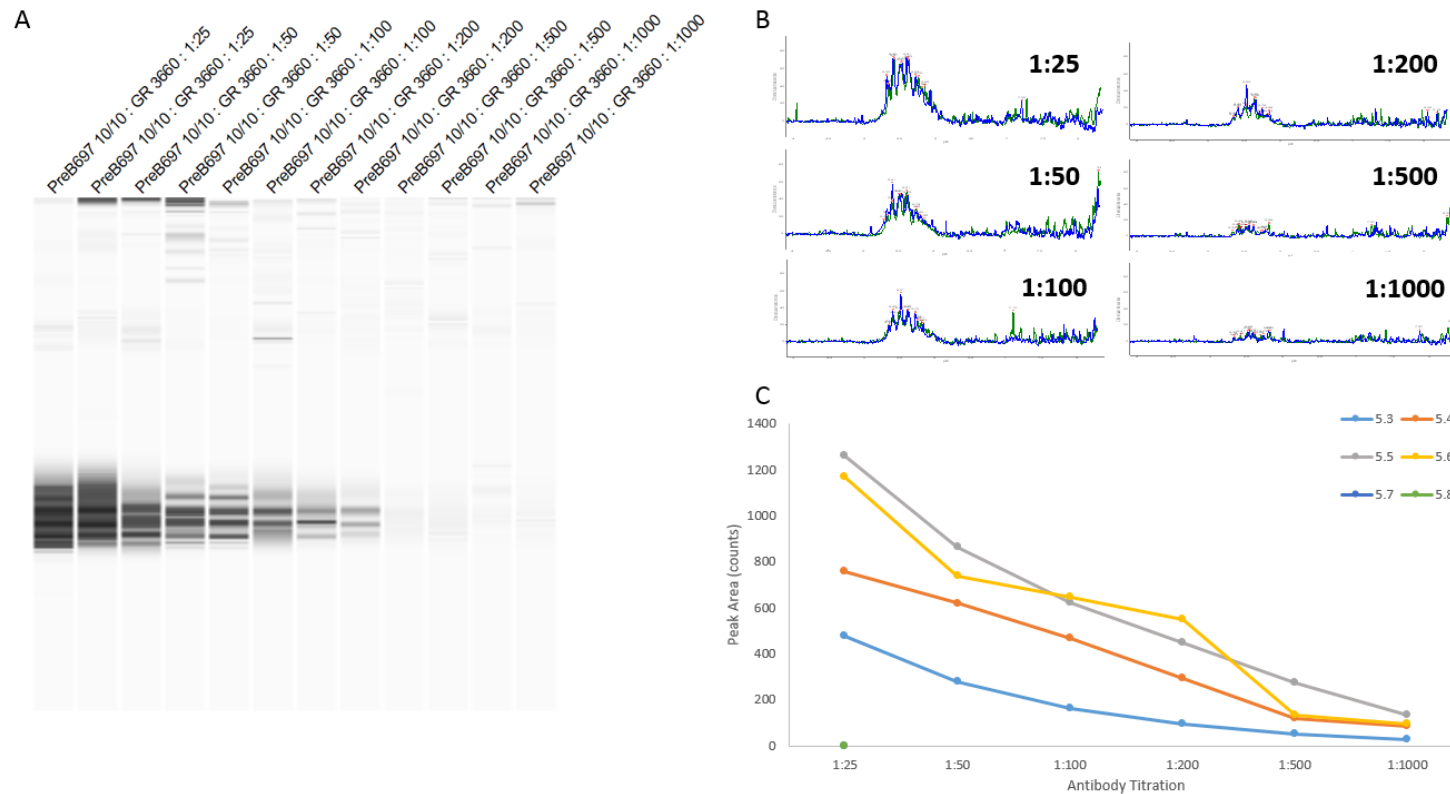


Figure 5.6 Peggy Sue D8H2 (Cell Signalling) antibody titration in PreB697 dex treated lysates.

Figures A, B, C show different representations of the same data. (A) The camera capture view of the chemiluminescent signal (inverted colours). The strength of chemiluminescent signal can be converted into a graphical representation, which is shown in (B). The stronger the signal, the larger the peak. The area under the peaks can be integrated, in this case dropped lines analysis was used. (C) Shows the area of the peaks (pI of peaks displayed in the legend) against antibody titration.

Lysate Titration

A lysate titration was also performed as having too high a protein concentration can also cause burn out. Cells were diluted to 0.8, 0.5, 0.2, 0.08, 0.05 and 0.02 $\mu\text{g}/\mu\text{l}$. Cell lysates were probed with Cell Signalling antibody D8H2 at a dilution of 1:25. As can be seen from Figure 5.7, there was no burn out and peak areas decreased with decreasing lysate concentration.

As there was no burn out, a concentration of 0.45 $\mu\text{g}/\mu\text{l}$ was selected for cell line analysis, as this was the highest concentration attainable from all cell line lysates. In primagraft samples, protein concentration estimation accuracy can vary due to mouse red cell contamination. Sample analysis was therefore performed on peaks relative to total area under the curve for each sample, rather than raw peak areas. As such, it was not essential to load identical amounts of protein for each sample. In previous experiments performed by Nicholson, it had been noted that occasionally not enough primagraft material was loaded to give sufficient signal as the protein concentration was lower than the estimate given by the Pierce assay. Therefore, the highest amount of primagraft material possible was used, which ranged between 0.4 and 0.8 $\mu\text{g}/\mu\text{l}$.

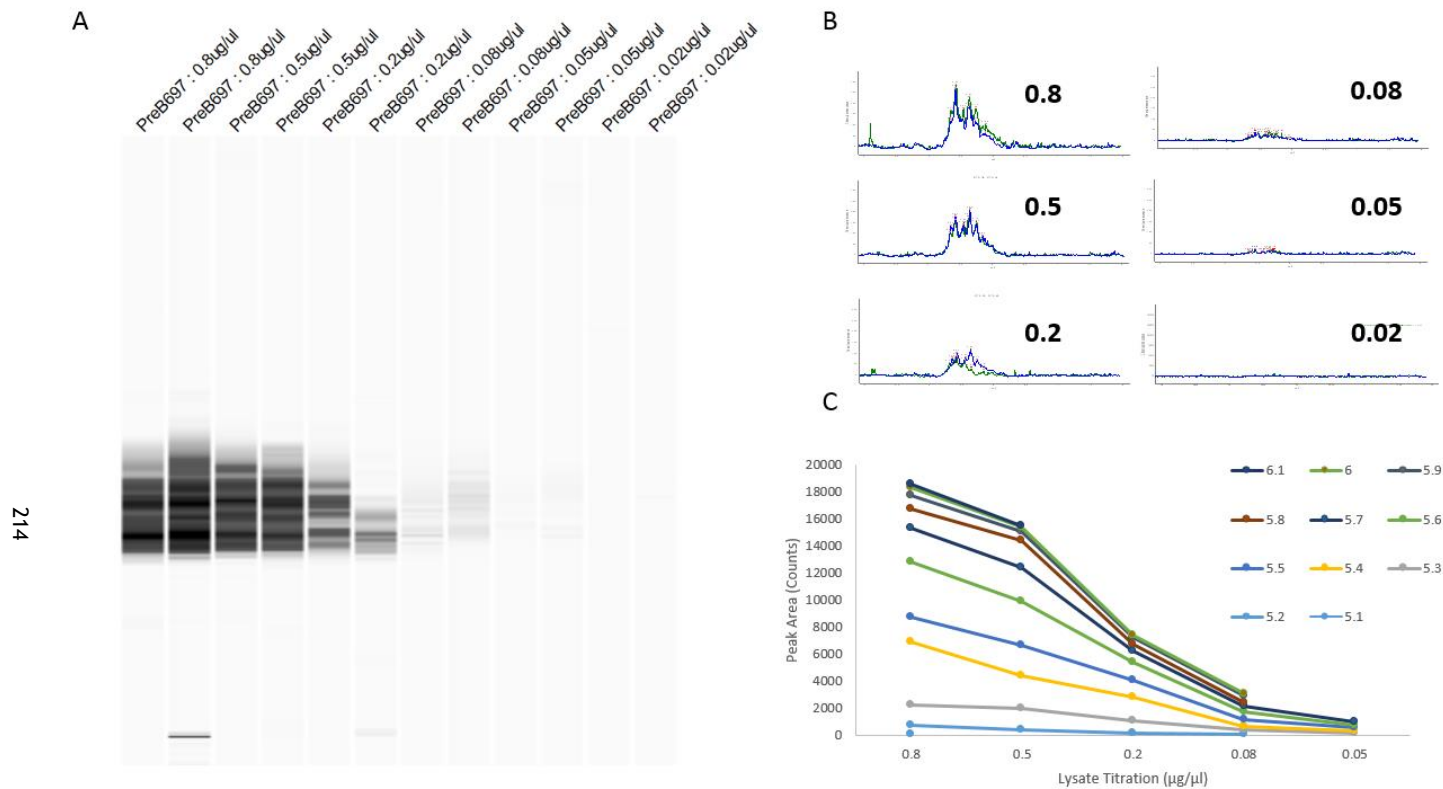


Figure 5.7 Peggy Sue lysate titration in PreB697 dex treated lysates probed with D8H2 (Cell Signalling) GR antibody.

Figures A, B, C show different representations of the same data. (A) The camera capture view of the chemiluminescent signal (inverted colours). The strength of chemiluminescent signal can be converted into a graphical representation, which is shown in (B). The stronger the signal, the larger the peak. The area under the peaks can be integrated, in this case dropped lines analysis was used. (C) Shows the area of the peaks (pI of peaks displayed in the legend) against antibody titration.

Inter and intra assay variability

To account for technical variability between capillaries leading to intra assay variability, each sample was run in triplicate (three separate capillaries). If samples are not mixed fully, or the proteins do not separate properly, there can be differences between technical replicates. However, in this assay, there was little variation between technical replicates, as is shown in Figure 5.8 (A) and (B). Each line on the electropherogram represents the trace from an individual capillary. The mean intra assay coefficient of variation for individual peaks in this sample was 16.8%.

To assess inter assay variability, three PreB697 lysates generated on three separate occasions were run on the Peggy Sue on the same day. The data is displayed in Figure 5.8 (C) and (D). The mean inter assay coefficient of variation for individual peaks in the three samples was 13.4%.

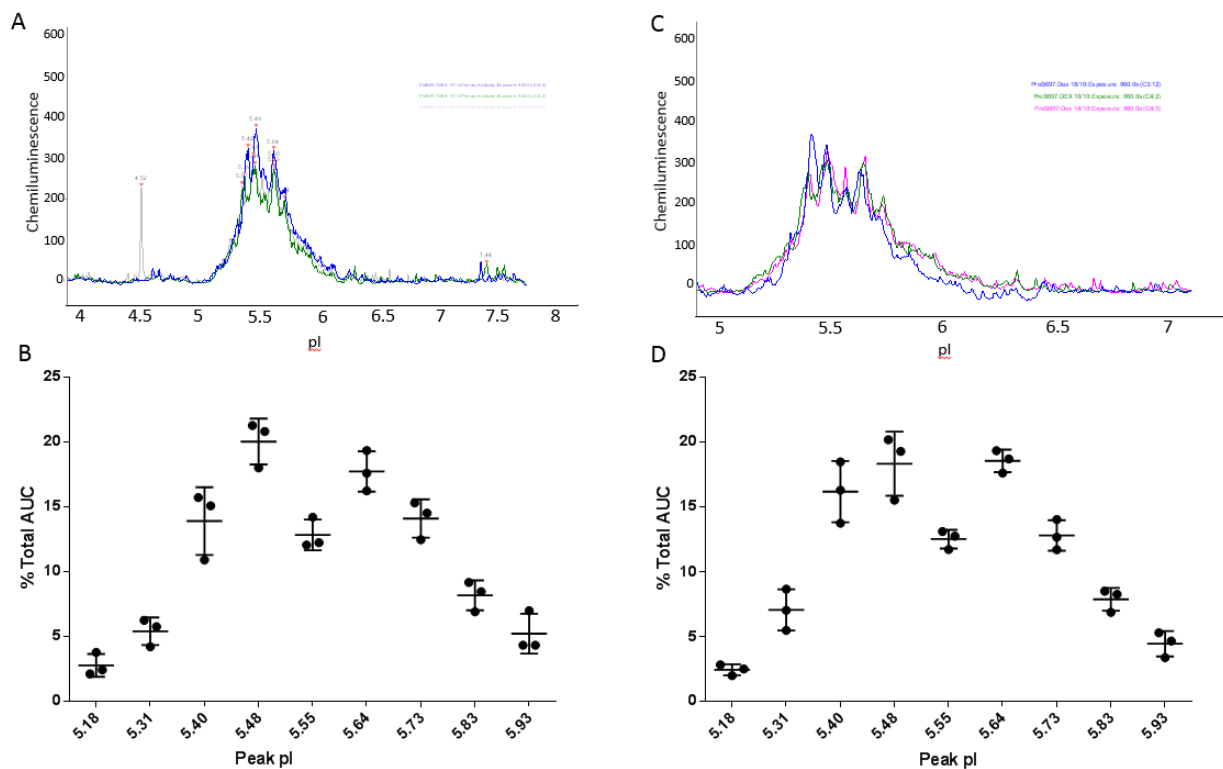


Figure 5.8 Variation between technical and biological replicates

(A and B) Technical replicates of PreB697 lysate (A) Electropherogram; blue green and grey lines represent each technical replicate (B) Percentage of the total area under the curve comprised by each peak for technical replicates.

(C and D) Lysates were generated on three separate occasions and run on the same day on the Peggy Sue. (C) shows an electropherogram of a lysates; green line, pink and blue lines represent samples generated on the 10th, 14th and 18th of October, 2016, respectively. (D) Percentage of the total area under the curve comprised by each peak for biological replicates.

(A and C) Y axis = chemiluminescence. X axis = pI. (B and D) Error bars show standard deviation.

5.3.4 Analysis of the GR by cIEF in ALL cell lines

Four cell lines were assessed by charge assay using cIEF; PreB697, R3F9, R3D11 and REH cells (Figure 5.9). Lysates were analysed untreated, and treated with control vehicle or 100nM dex for 3 hours. Surprisingly, untreated and CV treated lysates showed little to no signal. This was unexpected as a pan specific GR antibody was used; untreated and control vehicle treated cells still have GR even if it is not stimulated or phosphorylated. Furthermore, all lysates used in cIEF analysis were also assessed by western blot to check for normal phosphorylation at serine 211 of the GR. In these western blots, a clear band for GR was seen, of equal magnitude to the dex treated lysates (Figure 5.1). This is further investigated in 5.3.6.

There was a smaller signal observed in the R3D11 cell line, which is consistent with previous reports that R3D11 has a reduced amount of GR compared to PreB697 cells (Nicholson *et al.*, 2010). There was a small signal observed in the REH cell lysates, a cell line which was selected as a negative control for functional GR. Although one GR allele is deleted, the other is truncated in REH cells, and the low signal is likely to be due to binding of the antibody to the truncated GR allele. This truncated allele is also seen in the western blot in Figure 5.4, depicted by a lower molecular weight band in REH cell lysates.

Despite the signal difference between PreB697 and R3F9 lysates and R3D11 lysates, the composition of the GR profile is similar between the cell lines. Figure 5.10 shows the proportion of the total area under the curve represented by individual peaks. There was no statistical difference between any of the cell line full cIEF GR profiles. Multiple comparisons revealed that R3F9 had larger peak percentages of 5.4 and 5.47 than PreB697 (2 way ANOVA with Bonferroni's multiple comparisons test; $p=0.01$ for peaks 5.40 and 5.47).

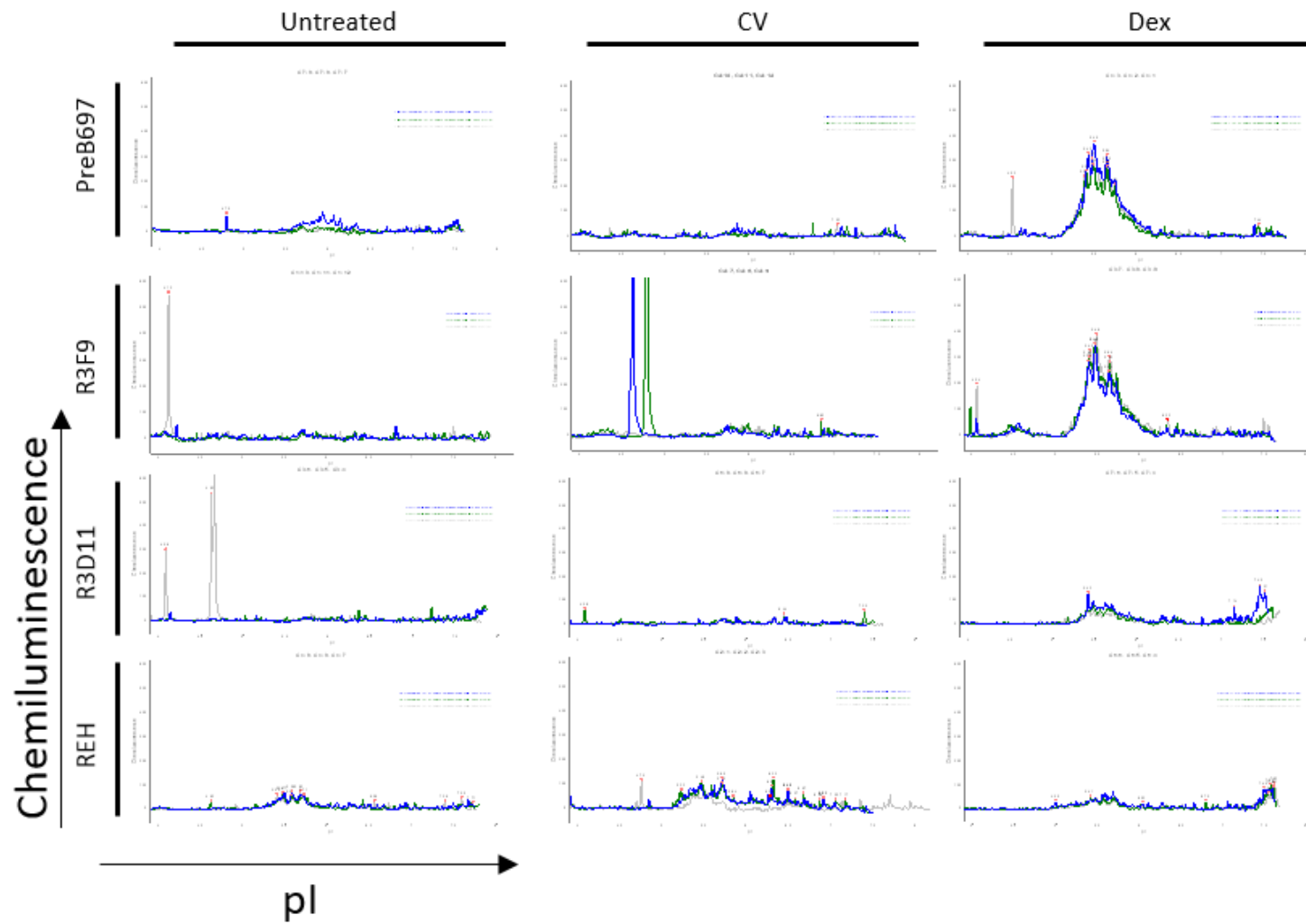


Figure 5.9 Electropherograms generated by cIEF of PreB697, R3F9, R3D11 and REH cell lines with D8H2 (Cell Signalling) GR antibody.

Cell line lysates are shown measured by cIEF with the cell signalling D8H2 antibody. Untreated = untreated lysate. CV = control vehicle treated lysate and Dex= dex treated lysate. Y axis = Chemiluminescence (0-600). X axis = pI (4-8).

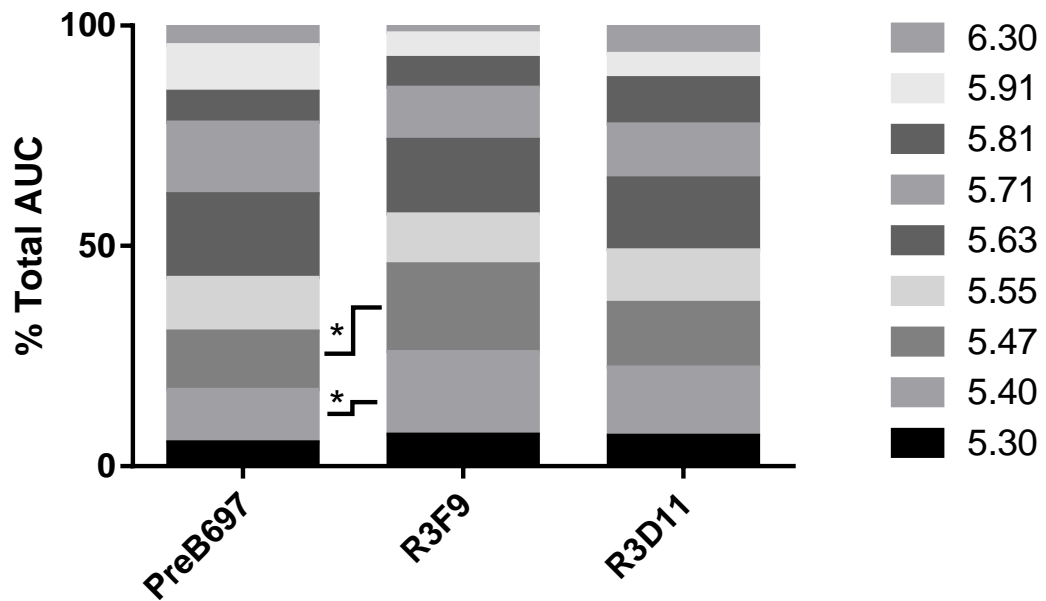


Figure 5.10 Proportion of total electropherogram area under the curve comprised of individual electropherogram peaks for PreB697, R3F9 and R3D11 cell lines.

Bars show percentage of the total electropherogram AUC comprised by each individual peak, an average of three technical replicates. There was no statistical difference between any of the cell lines in full GR profile. There was a statistical difference between the size of peaks 5.40 and 5.47 between PreB697 and R3F9 (2 way ANOVA with Bonferroni's multiple comparisons test; $p=0.01$ for peaks 5.40 and 5.47, depicted by *).

5.3.5 Analysis of the GR by cIEF in primagraft ALL cells

The control vehicle and dex treated primagraft lysates were analysed using cIEF. Primagraft electropherograms are displayed in Figure 5.11. All samples displayed peaks at similar pIs to cell lines, for dex treated samples this was between pI 5 and 6 with multiple individual peaks. Samples also displayed a much smaller signal in control vehicle treated samples. In all cases, the GR profile shifted to a lower pI from control vehicle treated lysates to dex treated lysates, indicating an increase in post-translational modifications such as phosphorylation in the dex treated sample.

Samples were analysed using peak areas as a percentage of total area under the curve of the GR profile. Analysis was performed in this way to account for signal differences caused by different amounts of lysate loaded, and variation in protein estimation due to mouse red cell contamination. Figure 5.12 shows individual peaks from primagraft samples as a percentage of total AUC. The control vehicle treated samples were more variable due to the smaller signal size and therefore peak size. However, the dex treated lysates displayed a consistent ratio of peaks across the range of pI values.

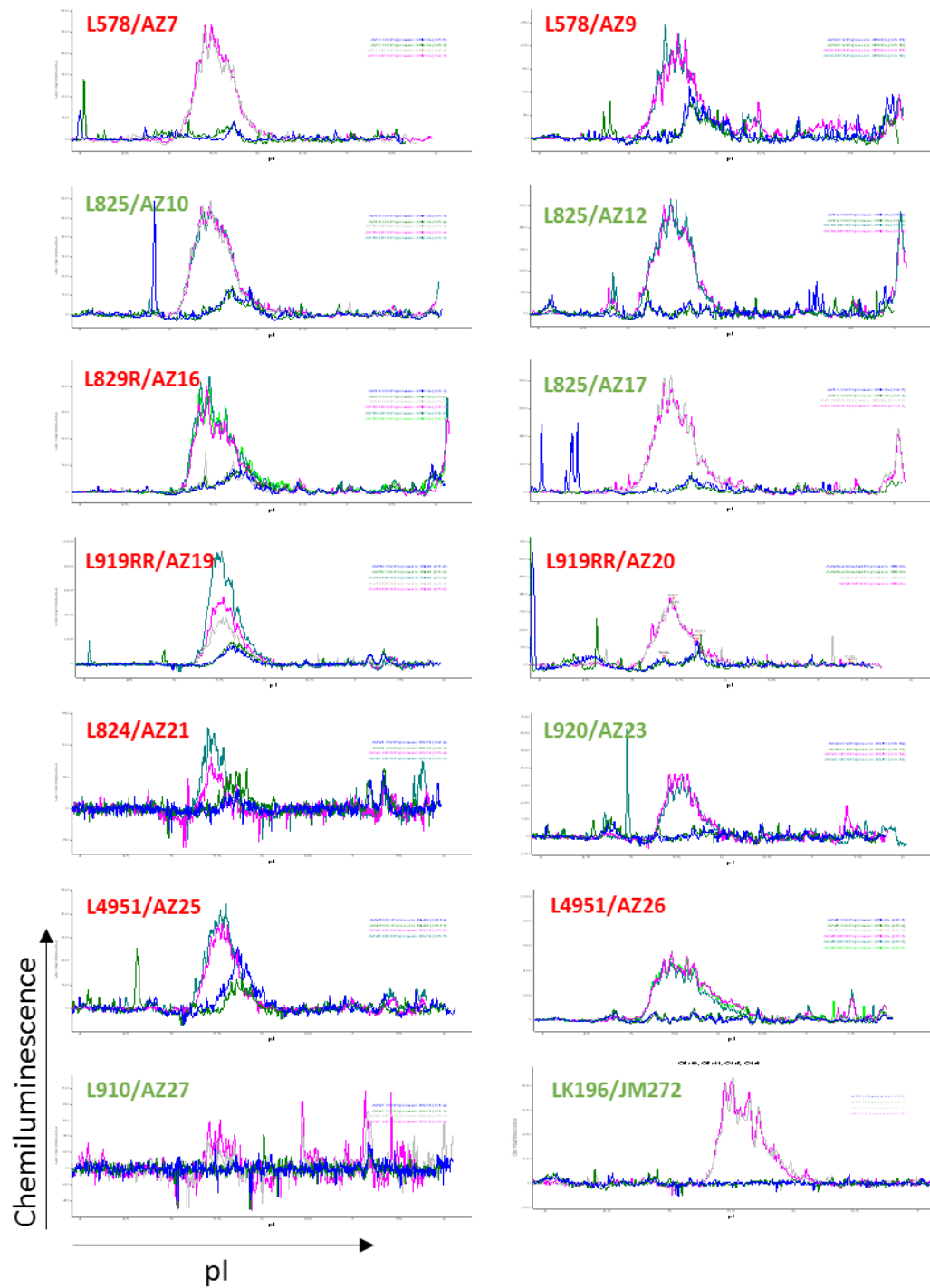


Figure 5.11 Electropherograms of primagraft lysates by CIEF probed with D8H2 (Cell Signalling) GR antibody.

Samples shown are control vehicle treated (dark green/blue lines) and dex treated (pink/grey/green lines). Samples were treated with control vehicle or 100nM dex for 3 hours before cell lysis. Multiple traces are technical replicates. Sample names annotated in green are dex sensitive and red are dex resistant.

One of the aims of this chapter was to assess whether the GR posttranslational modifications, as assessed by cIEF, differed in dex sensitive and dex resistant samples. In order to assess whether the peak distribution was related to dex sensitivity, outliers were identified visually (shown by red circles in Figure 5.12). However, as illustrated in Table 5.1, outlier groups contain a mix of dex-sensitive and resistant samples. Although there are two groups that contain just resistant samples, this is likely to be due to the larger number of dex-resistant samples used in this study.

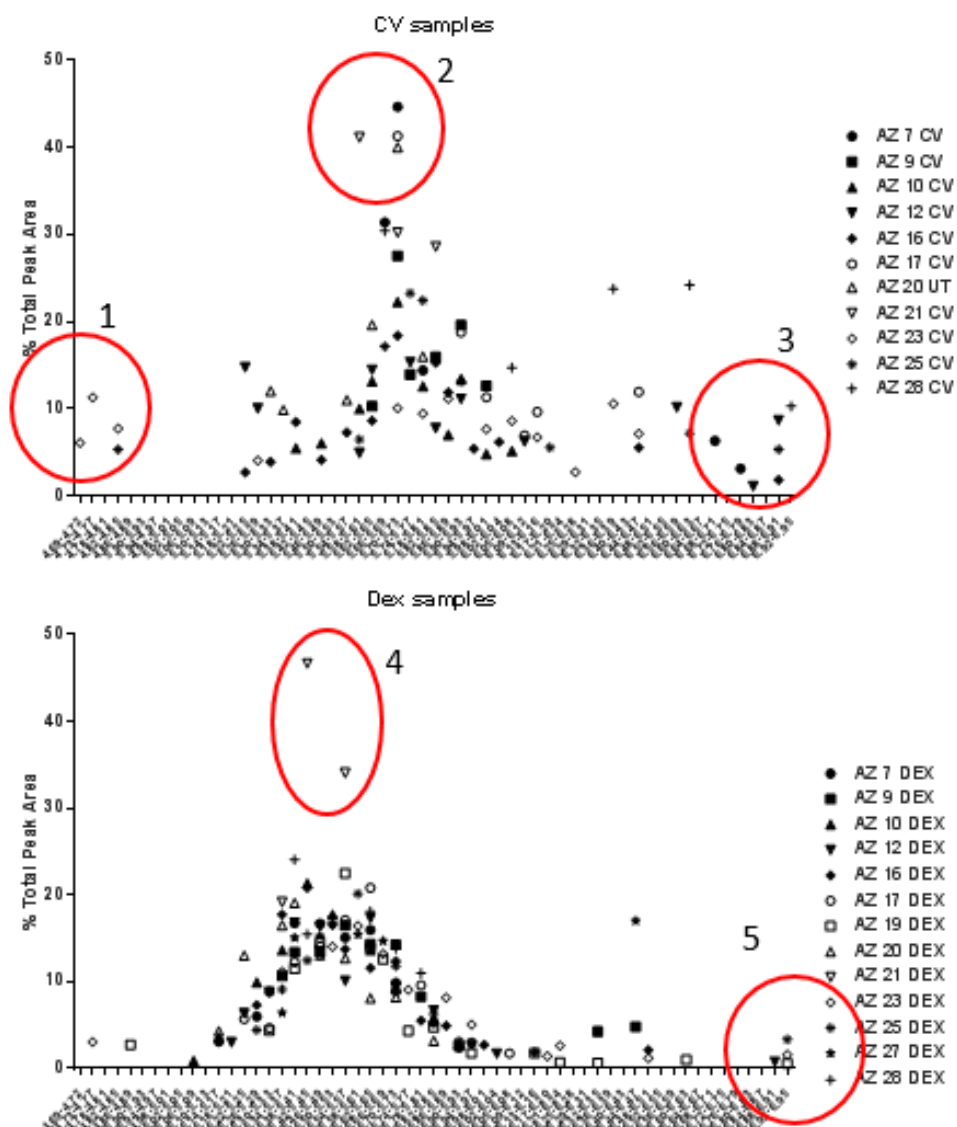


Figure 5.12 Electropherogram peak areas displayed relative to the total area under the curve of the GR profile for control vehicle and dex treated primagraft samples.

Percentage were calculated by determining the proportion of individual peak areas of the total AUC of GR profile for each individual sample. Numbered circles (1-5) identify outlying peaks and are assessed in Table 5.1. X axis shows increasing pI values. Y axis is % tptal peak AUC.

Outlier group	Dex-sensitive samples	Dex Resistant samples
1		L920/AZ23, L4591/AZ25
2	L825/AZ17	L578R/AZ7, L919RR/AZ20, L824/AZ21
3	L825/AZ12, AZ28	L578R/AZ7, L4951/AZ25, L829R/AZ16
4		L824/AZ21
5	L825/AZ12, L825/AZ17	AZ19, L4951/AZ25

Table 5.1 Identification of samples in outlier groups shown in Figure 5.12.

Each outlier group represents a circle numbered in Figure 5.12. The dex sensitivity of the samples with peaks within the circles were recorded in the table.

The samples were analysed to assess whether there was any difference between peak areas relative to total AUC in relation to dex sensitivity. Although there were differences in the peak composition of the total AUC, there was no difference in any of the peak areas between sensitive and resistant samples (Figure 5.13, student's t test).

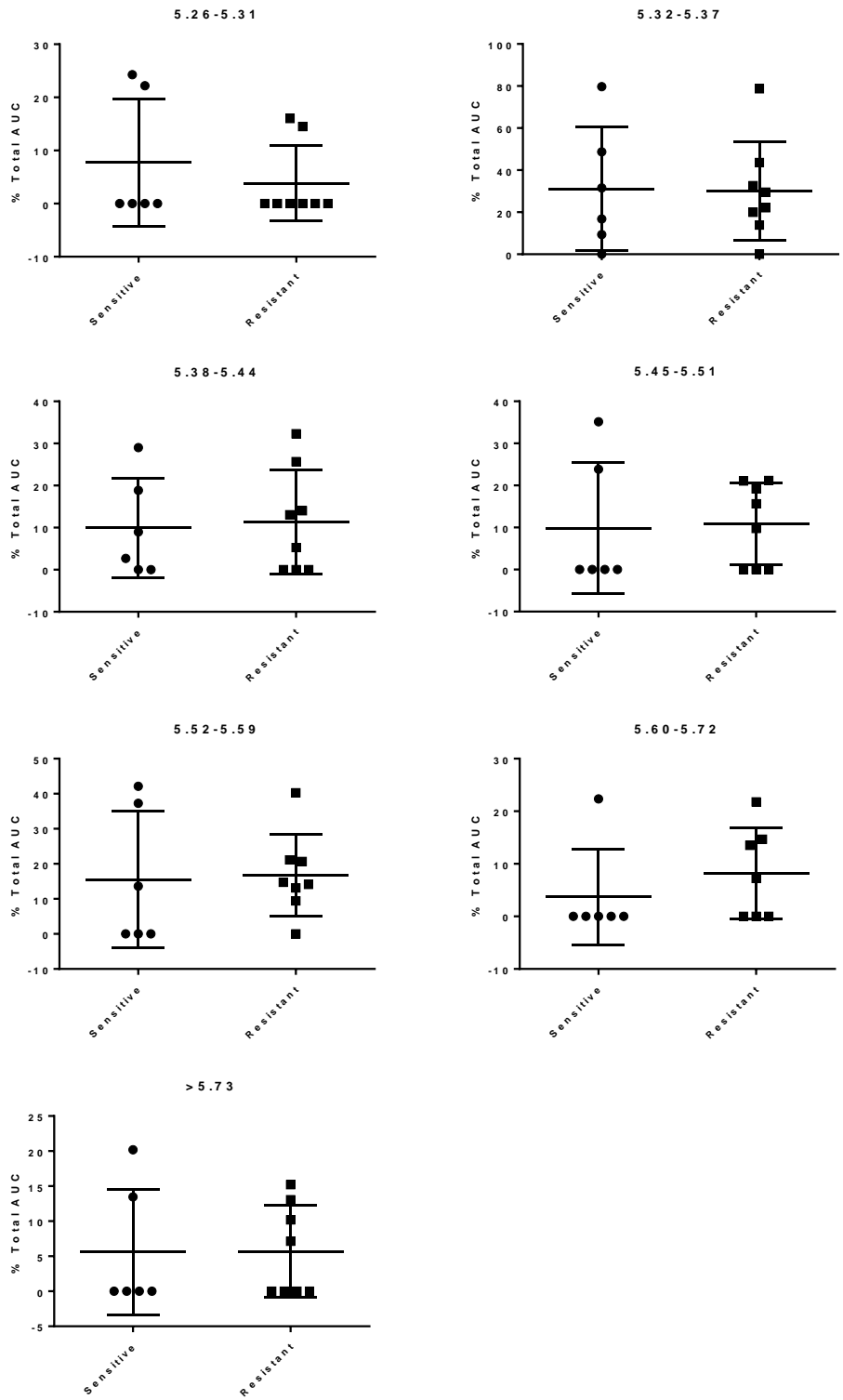


Figure 5.13 Comparison of peak composition of GR profiles between sensitive and resistant primagraft samples.

Graphs show the percentage of the total AUC comprised by peaks within the range indicated above the graph. There was no difference in AUC composition between sensitive and resistant primagraft samples (student's t-test). Error bars show mean \pm standard deviation.

5.3.6 Investigation into reduced signal in untreated samples

As identified in 5.3.4 and 5.3.5, untreated and control vehicle treated samples exhibited a much smaller signal than dex treated samples. This is surprising as a pan specific GR antibody was used, which is able to detect normal GR as well as phosphorylated GR. Furthermore, all samples analysed using cIEF were shown to have a similar amount of GR in control vehicle and dex treated samples by western blot (Figure 5.1).

One potential explanation for this phenomenon lies in the difference in denaturing capacity of cIEF compared to western blotting. In its unstimulated form, the GR is held in complex with a number of proteins, such as chaperone heat shock proteins (HSP) 90 and 70, and immunophilins (Pratt, 1993; Nicolaides *et al.*, 2010). As cIEF is less denaturing than western blotting, which incorporates several steps to denature samples, it is possible that the proteins in the cIEF assay are still in complex with the GR during charge analysis. This could potentially mask the binding site of the D8H2 GR antibody. Upon dex treatment, the GR is released from this complex, and therefore the antibody will be able to bind, thus why a signal was seen in dex treated samples.

To test this hypothesis, a western blot under non-denaturing conditions was performed using the Cell Signalling D8H2 antibody used in the cIEF analysis. This uses all the same principles as a conventional western blot, but denaturing steps, such as heating of samples, and use of beta mercaptoethanol and sodium dodecyl sulphate are omitted. Figure 5.14 shows the results of this western blot. REH samples were used as a negative control. It is not possible to determine protein size in a western blot under non denaturing conditions, as there is no SDS present to give the proteins charge. The GR band in the dex treated samples has migrated further down the gel, which is likely to be a result of an increased negative charge due to a higher level of phosphorylation in dex treated samples. This could be tested by treating the sample with phosphatases and assessing whether sample migration is still altered in dex treated samples. However, importantly the dex treated band in the neutral non-denaturing gel is stronger than the untreated and control vehicle treated samples. This supports the above mentioned hypothesis that in a non-denatured setting, the GR is held in complex with other proteins which may explain why there is a reduced signal in untreated and control treated samples in cIEF analysis.

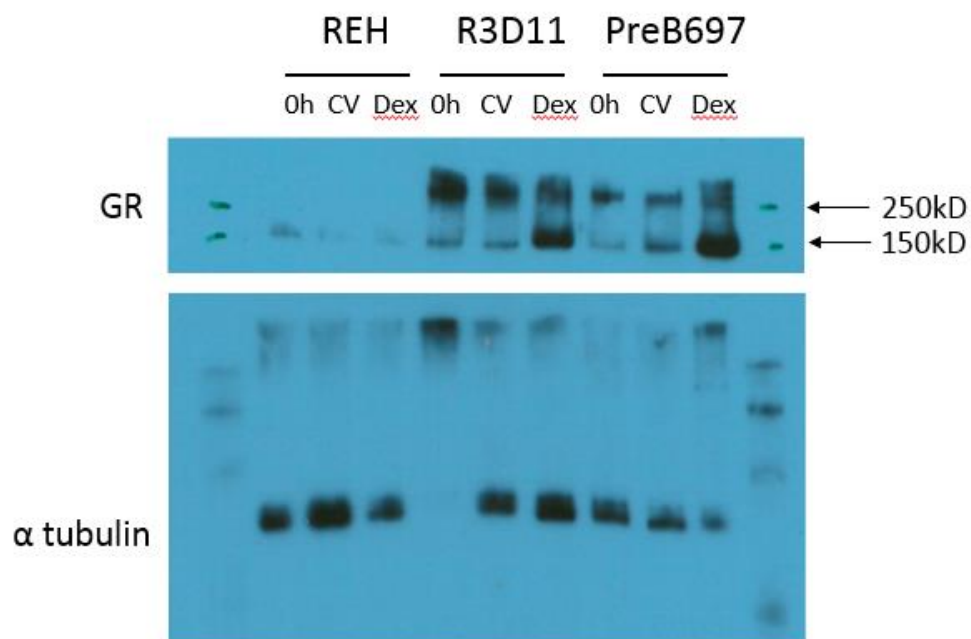


Figure 5.14 Analysis of GR lysates by western blot under non-denaturing conditions.

REH, R3D11 and PreB697 lysates were used untreated (0h) and treated with control vehicle (CV) and 100nM dex (Dex). Lysates were probed with the GR D8H2 antibody (Cell Signalling).

5.4 Discussion

The aim of this project was to assess differences in GR posttranslational modifications in dex sensitive and resistant ALL cells and to determine whether these differences account for variations in dex cell sensitivity in ALL cells. Determining the interactors critical to GC response may lead to potential therapeutic targets to reverse GC resistance or serve as response biomarkers. In this chapter, an assay has been developed to study the GR posttranslational modifications and a clear difference in GR profile between control vehicle treated and dex treated lysates was observed. Little difference was seen in the GR profile with the D8H2 antibody between dex sensitive and resistant samples.

Samples were first assessed for GR status. All samples similarly expressed GR, irrespective of GC sensitivity status. There was also no difference seen in the functionality of the GR, as all samples displayed phosphorylation at serine 211, an indication that the GR has translocated to the nucleus and is transcriptionally active (Wang *et al.*, 2002). This is consistent with other observations in the literature. Although GR deletions and mutations are seen in relapsed ALL (Irving *et al.*, 2005b), they are rare and in this project no evidence of GR deletion was seen. This indicates that the GC resistance mechanism does not directly relate to the GR itself in these samples, and therefore provide a good model to study GC resistance in ALL.

The Sigma antibody used for the generation of the pilot data (by L. Nicholson using NanoPro1000 platform, detailed in Appendix E, did not transfer to the Peggy Sue machine. It was therefore necessary to establish a new assay on the Peggy Sue using a different GR antibody. With the Cell Signalling GR D8H2 antibody, a good signal above the baseline was generated. No burn out was observed in the antibody and lysate titration, and variation between technical and biological replicates was low. The assay was therefore accepted as valid and used for analysis of cell line and primagraft lysates.

GR profiles in PreB697 and dex resistant sub line, R3F9, showed very similar GR profiles. R3D11, also a dex resistant sub line of PreB697, displayed a lower signal, however the proportion of the peaks comprising the GR profile was similar to that observed in PreB697 and R3F9 cell lines. The cell line used as a negative functional GR

control, REH, had a small GR signal. This is likely to be due to REH expressing one truncated GR allele of 528 amino acids (Grausenburger *et al.*, 2016). This truncated allele is also seen as a lower molecular weight band in the western blot in Figure 5.4, with a molecular weight of ~70kDa, consistent with the size of the truncated allele. The signal was not deemed problematic as it was lower than that displayed in the PreB697 and R3F9 electropherograms. Furthermore, despite differences between the pilot data and data generated here (discussed later), a small signal is also seen with REH cells with the Sigma Aldrich antibody at a lower molecular weight by western blot (Figure E.9A, Appendix E) and with the NanoPro 1000 machine (Figure E.9B, Appendix E). Therefore this phenomenon is not antibody or platform specific so did not affect validation of the assay.

Despite the use of a pan specific GR antibody in the generation of both the data in this project, and the pilot data, there were differences in the displayed cell line GR profiles. Firstly, the shape of the electropherograms differed between the samples. The electropherogram for dex treated PreB697 lysates in this project displayed a number of narrow peaks between approximately pI 5 and pI 6.5 whereas the data generated by Nicholson showed peaks starting at approximately pI 4 with a strong peak displayed around pI 4.75. Secondly, Nicholson saw differences between PreB697 and R3F9 both basally, and in response to dex stimulation. In this project, there was only a slight difference in peaks 5.4 and 5.47 between PreB697 and R3F9 in response to dex. It was not possible to ascertain if there were differences basally due to low signal.

The differences seen between Nicholson's data and the data generated here may be due the binding site of the two antibodies used. The human GR alpha sub form is 777 amino acids long (Hollenberg *et al.*, 1985). The HPA004248 antibody used by Nicholson binds to amino acids 2 – 49 at the n terminus of the protein. In contrast, the Cell Signalling antibody used in this project binds to amino acids surrounding Leucine 378, close to the DNA binding domain. A schematic of the functional human GR is shown in Figure 5.15. Antibody variation in peak shape and cell line GR profiles could be due to differences in post-translational modifications around the binding site of the two antibodies. GR post-translational modification locations, taken from Blast ('Database Resources of the National Center for Biotechnology Information,' 2017) are displayed in Figure 5.16.

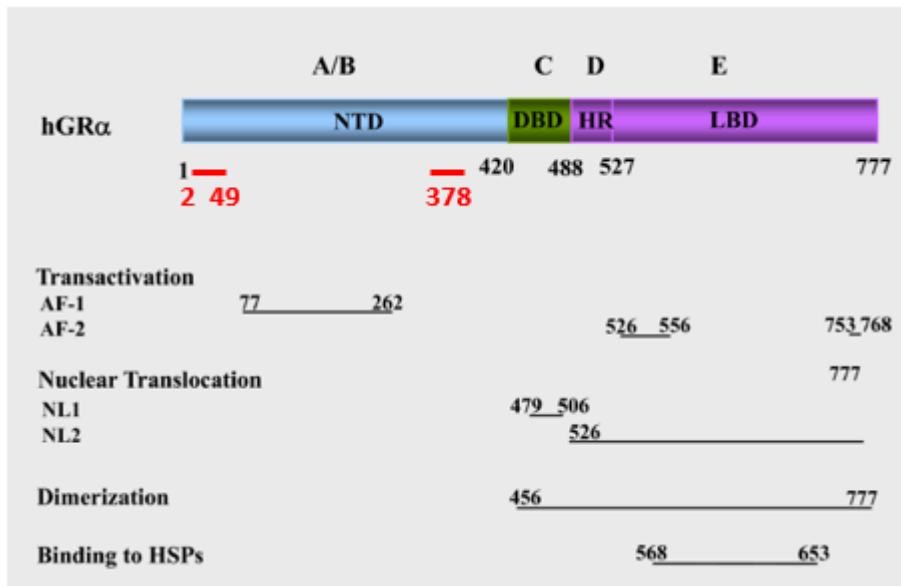


Figure 5.15 NR3C1 alpha amino function domain.

Adapted from (Nicolaidis *et al.*, 2010) The binding sites of the two antibodies are shown in red. HPA004248 antibody binds amino acids 2 – 49 and D8H2 binds to amino acids surrounding leucine 378.

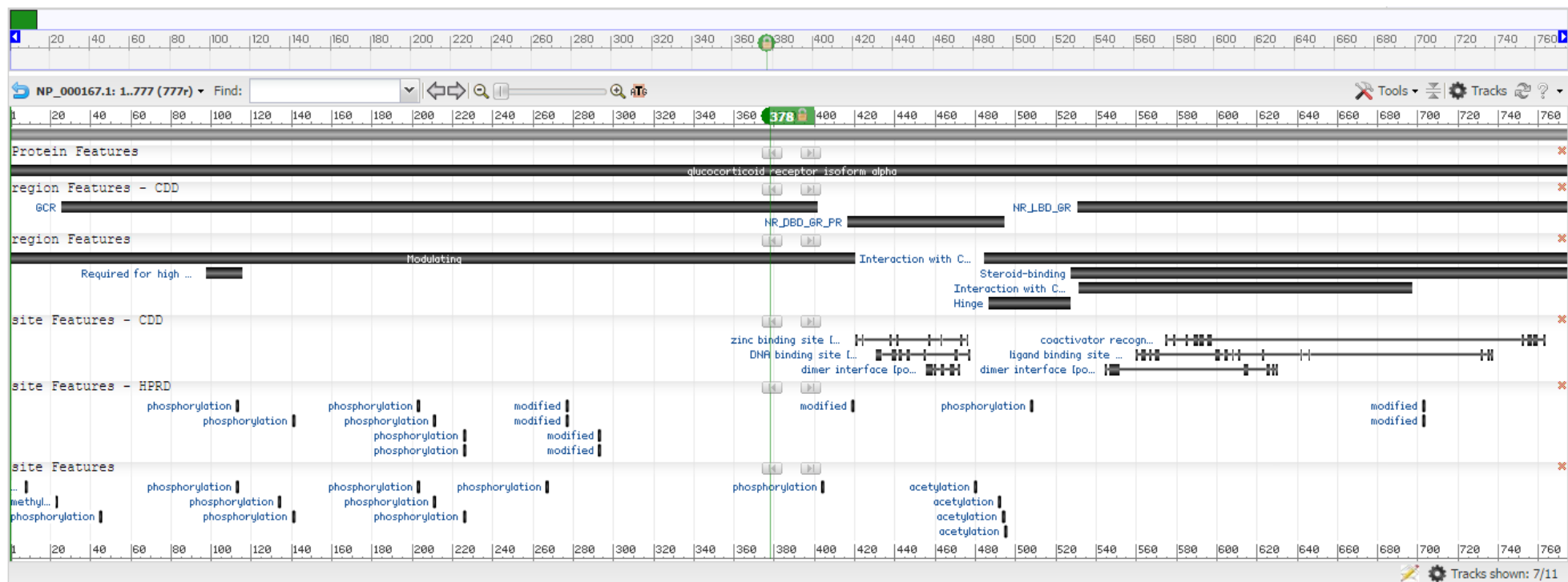


Figure 5.16 Position of NR3C1 post translational modifications.

Taken from ('Database Resources of the National Center for Biotechnology Information,' 2017). HPA004248 antibody binds amino acids 2 – 49 and D8H2 antibody binds amino acids surrounding leucine 378.

Furthermore, data generated here using the D8H2 antibody suggests that amino acids surrounding leucine 378 may be involved in the interaction of unstimulated GR with the heterodimeric complex in the cytoplasm. This might also further explain differences seen between the data generated in this chapter, and that by Nicholson. Despite control vehicle and dex treated samples displaying a similar amount of GR by western blot when probed with the Cell Signaling D8H2 antibody, there was a very low signal in control vehicle treated samples when analysed using cIEF. As cIEF is less denaturing than western blotting, it was hypothesised that the target epitope of the D8H2 antibody may be being masked by the heterodimeric complex.

To test this hypothesis, a western blot under non-denaturing conditions was performed. As shown in Figure 5.14, all GR bands were at a higher molecular weight suggesting that all GR probed was held in complex with some protein. Of particular interest, the dex treated GR band was stronger in comparison to the untreated and the control vehicle treated samples. This supports the hypothesis that the epitope is unmasked by disassociation with some element of the protein complex. This could be checked further by probing the neutral non-denatured blot for putative binding proteins, such as HSP90. If the hypothesis is correct, the untreated and control vehicle treated samples would have stronger expression of these proteins. Pull down or co-immunoprecipitation assays could also be performed using a GR antibody to identify stable protein-protein interactions. These would allow assessment, for example by LC/MS, of proteins interacting with the GR in dex treated and untreated samples.

It is possible that the antibody binding site was masked by a post translational modification such as a phosphorylation. However, this is unlikely as the level of GR post translational modification is increased on GC stimulation, which would mean that the dex treated samples would have a masked antibody binding site, the opposite of what has been observed. Supporting this, the cIEF data showed a decrease in pI for dex treated samples, an indication of increased phosphorylation in the dex treated samples, once again suggesting that it would be the dex samples which would have decreased antibody binding, as opposed to the untreated samples, seen in this project. Therefore the masking of the binding site uniquely in untreated samples is unlikely to be caused by posttranslational modification.

This potential epitope unmasking can also be seen in the primagraft electropherogram traces, shown in Figure 5.11. In 13 of the 14 samples, there was an increase in signal in the dex treated sample compared to the control vehicle treated sample. As the difference in signal between control vehicle and dex treated samples is seen in cell lines and primagrafts derived from multiple patients, it suggests that the area surrounding leucine 378 in the GR is masked constitutively.

cIEF data suggest that there is an increased number of phosphorylation events in the dex treated samples. In all electropherogram traces, peaks shift to the left, representing a lower pI value. When a protein is phosphorylated, neutral hydroxyl groups are substituted on serine, threonine and tyrosines with phosphate groups, which are negatively charged. This results in an acidic shift and therefore a decrease in pI. It is not possible to compare the shift in pI with phosphorylations on other proteins, as the exact effect on pI of phosphorylation depends on the original pI of the protein and the number of phosphorylation events (Halligan *et al.*, 2004; Zhu *et al.*, 2005).

PhosphoSitePlus®, an online resource for information on post-translational modifications, predicts the basal pI of the GR to be 6, and calculates the effect of phosphorylation residues on pI. For example, 10 and 17 phosphorylation residues to reduce the pI to 5.29 and 5.0 respectively (PhosphoSitePlus, 2017). The pIs of peaks in control vehicle treated samples ranges between 5.5 and 6, which is expected as unstimulated GR is phosphorylated (Ismaili and Garabedian, 2004), albeit to a lesser extent than stimulated GR. Furthermore, dex treated samples displayed multiple peaks between pI 5 and 6 representing hyperphosphorylation pI consistent with the PhosphoSitePlus® database. The GR is also, to a lesser extent, acetylated (Figure 5.16). However, acetylation generally has a much smaller effect on pI, with an average acidic shift in pH of 0.2 (Bjellqvist *et al.*, 1993; Zhu *et al.*, 2005) and would therefore be of minimal contribution to any observed changes in the GR electropherogram.

One of the aims of this chapter was to determine whether there was a difference in GR posttranslational modifications between dex sensitive and resistant samples. Although there was a range in GR peak composition, when the peaks were displayed as a proportion of the AUC, there was no difference between sensitive and resistant samples.

As there were no consistent differences in GR profiles between samples, it is not possible to further analyse differences in electropherogram traces. However, as a potential epitope unmasking event was uncovered, it may be beneficial to further analyse the interaction between the GR and the heteromeric complex. To further investigate the differences in GR cIEF profiles found in Nicholson's pilot data, an antibody should be used that is specific to the N terminus of the protein. It may also be of use to assess samples using phospho specific antibodies by cIEF, and separately to pre-treat the samples with phosphatases and proteases. This would allow a better understanding of the relative contribution of individual phosphorylations and other posttranslational modifications to the electropherograms observed using a pan specific GR antibody.

The heteromeric complex could be further analysed using approaches to isolate the complex before and after dex treatment. This would allow the molecular constituents of the complex to be studied in dex sensitive and resistant samples, as studies previously performed in this area were published a nearly two decades ago (Pratt and Toft, 1997; Jibard *et al.*, 1999). Furthermore, variation in different elements of the heteromeric complex have been associated with alterations in GC response. For example, a number of studies has identified that changes in or modulation of HSP90 affects GR activity (Picard *et al.*, 1990; Cadepond *et al.*, 1991; Cadepond *et al.*, 1993; Segnitz and Gehring, 1997; Lauten *et al.*, 2003a; Shen *et al.*, 2010). Of particular interest, Tago *et al.* (2004) found that two separate inhibitors of HSP90 diminished the effects of dex on transcription factors NF κ B and AP-1 *in vitro*. Similarly, the ratio of FKBP51 to FKBP52, complex immunophilins which play a role in GR signalling, have been implicated in GC resistance in primates (Denny *et al.*, 2000; Davies *et al.*, 2002b).

New techniques such as subcellular fractionation of the nucleus and cytosol such as LOPIT (localisation of organelle proteins by isotope tagging) may allow all constituents and phosphorylations of the GR and the heteromeric complex to be identified (Dunkley *et al.*, 2006; Hall *et al.*, 2009; Christoforou and Lilley, 2012; Mulvey *et al.*, 2017). Likewise, to further unravel the members of the multiprotein complex, iPAC (interactomics using Parallel Affinity Capture) could be utilised (Rees *et al.*, 2011).

In summary, data generated in this project using cIEF has shown that antibody selection is important when assessing post-translational modifications. Importantly, a new potential area of interaction has been identified between unstimulated GR, and the heteromeric complex it is held in, which may affect GC response. Further analysis of this complex interaction using new proteomic techniques could lead to a better understanding of the effect on GC response, and potentially provide new avenues for resensitisation of dex therapy.

Chapter 6. B cell maturation and GC sensitivity

6.1 Introduction

Cell development is a highly orchestrated process which consists of a continuum of cell types and stages leading from stem cells to more mature terminally differentiated cells. A deeper comprehension of these processes aids our understanding of what happens when these systems are perturbed and create disease states such as cancer (Bendall *et al.*, 2012). Furthermore, cell maturation state has been implicated as a therapy resistance mechanism in ALL (Rhein *et al.*, 2007; Nicholson *et al.*, 2015).

In the past, experimental platforms have broadly allowed the analysis of many aspects of a few cells, or a few aspects of many cells (Spitzer and Nolan, 2016). For example, flow cytometry permits a very high throughput of cells, but it is still only commonly possible to look at 12 markers simultaneously, due to spectral overlap of fluorochromes. This restricts the ability to look at cell development holistically, which requires a high cell throughput in combination with single cell resolution and multiple markers to characterise complex samples, rare cell populations and biological processes. The use of mass cytometry (CyTOF) a new technology combining the principles of flow cytometry with mass spectrometry, can overcome this problem. Mass cytometry is able to assess over 40 simultaneous parameters in cells, with a throughput of millions of cells from one sample (Bandura *et al.*, 2009; Ornatsky *et al.*, 2010; Bendall *et al.*, 2011).

There are some caveats to mass cytometry. Firstly, metals are not as sensitive as fluorochromes (Ornatsky *et al.*, 2006; Bendall *et al.*, 2011) due to limitations of the chelating polymer (Lou *et al.*, 2007; Majonis *et al.*, 2010). However this may not present a substantial problem as the background in mass cytometry is low, due to the natural absence of lanthanide metals in cells (unlike the phenomenon of cell autofluorescence in flow cytometry). Similarly, there is less variability in the sensitivity of lanthanides, meaning it is not necessary to remedy issues caused by the large variation between fluorochrome sensitivity. Secondly, although there is no spectral overlap, it is still possible to get spill over from isotopic impurities and oxidations (plus and minus 1 Da, and plus 16 Da) (Ornatsky *et al.*, 2008a). However, perhaps the biggest challenge faced in mass cytometry is the complex interpretation and processing of the multiple dimension data produced.

However, many of the challenges surrounding mass cytometry are overshadowed by its capacity to measure multiple cellular processes at different levels (Bendall *et al.*, 2012; Bjornson *et al.*, 2013). This is exemplified in a recent study characterising B cell development in healthy bone marrow, where new 'coordination points' of cell signalling, proliferation and cell death in distinct maturation stages were identified. The authors used a panel of 44 markers to determine B cell trajectory and characterise novel cell populations. Eighteen of these markers were used to develop a graph based algorithm, called Wanderlust, which constructs trajectories from early haematopoietic stem cells through to naïve B cells. Despite B cell development being studied for decades, Bendall uncovered and characterised a new precursor B cell subset using mass cytometry with expression of CD34, CD38, CD24 and terminal deoxynucleotidyl transferase (TdT). This is significant as previously, the earliest known markers of B cell identification were CD10 and CD19.

This study opens the opportunity to investigate the relationship between B cell development in BCP ALL and GC resistance. The potential importance of B cell development was firstly highlighted by Rhein *et al.* (2007) using genome wide gene expression analysis. They found that persisting blasts in ALL bone marrow undergoing induction treatment had a more mature phenotype. Secondly, Nicholson *et al.* showed that increasing GC resistance in the PreB697 GC resistant sub lines used in this project were associated with a more mature cell state using gene set enrichment analysis (2015). Although this change was relatively subtle, it may have important phenotypic significance in terms of GC response.

A greater understanding of B cell development, including the developmental relationships of cells and mechanisms that govern their differentiation, in addition to investigating whether maturation state is linked to sensitivity, may enable us to establish ways to treat these cases pharmacologically. In this project, the dex sensitivities of numerous cell lines, primagraft and patient samples were characterised as described in (Chapter 4). These samples were used in the current chapter to assess the developmental stage of ALL cells by mass cytometry and the Wanderlust algorithm, to investigate potential links between cell maturation and GC sensitivity.

6.2 Chapter specific aims:

- To create and validate a Wanderlust CyTOF panel
- To assess the relationship between B cell maturation and dex sensitivity in cell lines, primagraft and patient samples.

6.3 Results

6.3.1 Gating strategy

All cell lines, primagraft and primary patient cells were gated on 'non-beads' to eliminate EQ normalisation beads and bead-cell conjugates. Viable cells were then gated using cisplatin uptake, as low concentration cisplatin is more readily taken up by dead or dying cells after short incubations. Therefore live cells will have low cisplatin levels. Singlets were finally isolated by gating on iridium uptake, a DNA intercalator. Events with low iridium content are debris so are excluded. Aggregates of cells can be excluded as they have both a high intensity of iridium and also a higher event length, which is a measure of signal duration. This leaves the population of single cells. A summary of this gating strategy is shown in Figure 6.1.

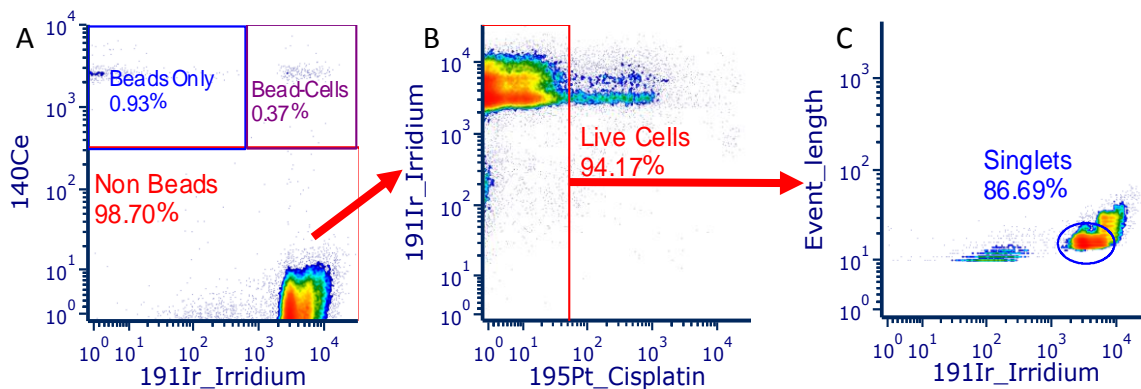


Figure 6.1 Gating strategy for all samples to isolate live, single cells in all cell lines, primagraft and patient samples.

Plot A: The 140Ce channel measures EQ beads. The DNA intercalator iridium is used to identify cells. High 140Ce and low 191Ir events are beads, low 140Ce and high 191Ir are cells, and high 140Ce and high 191Ir identifies bead-cell conjugates. Plot B is made up of the 'Non Beads' gate from plot A. Live cells are identified by low cisplatin uptake. Plot C is made up of the 'Live Cells' gate from plot B. Singlets are gated based on iridium content (low iridium events are debris, high iridium events are cell aggregates).

6.3.2 Panel design

The panel was designed based on the published panel in Bendall *et al.* (2014). The mass cytometry antibodies in the published panel had been mostly conjugated in house. It was not feasible to replicate the exact antibody panel using in house conjugation for all antibodies, due to both time and financial constraints. Therefore, the antibody targets and clones were kept the same as the Bendall panel, however the metal tags differed from that described in the original paper. This meant it was possible to purchase 16 of the antibodies commercially, and only two antibodies needed to be conjugated in house. The final panel is detailed in Table 2.7.

6.3.3 Validation of antibody-metal conjugation

There are two validation steps required when conjugating metals to antibodies which ensure successful conjugation. Firstly, it is necessary to verify that there is metal conjugated to the antibody using BD CompBeads (anti-mouse Ig κ). These beads are polystyrene microparticles which contain anti-mouse Ig κ particles and therefore bind any mouse κ light chain antibody. If signal is generated in a metal channel when using these beads, it shows that the metal has conjugated successfully to the antibody. Secondly, a titration of the antibody with a positive cell line for the marker is performed to check that the antibody still recognises the epitope of interest. The titration also allows an appropriate assessment of the amount of antibody to use when staining cells.

In this project, a CD34 antibody was conjugated to 164Dy, and IgM heavy chain (IgH) was conjugated to 176Yb. To validate that the metal was successfully conjugated to the antibody, 1 μ l of the antibody was added to 1ml PBS containing 2 drops BD comp beads and incubated for 30 minutes at room temperature, before washing and analysis by mass cytometry. The results are shown in Figure 6.2. There was a positive expression of both 164Dy (Figure 6.2A, conjugated to CD34) and 176Yb (Figure 6.2B, conjugated to IgH).

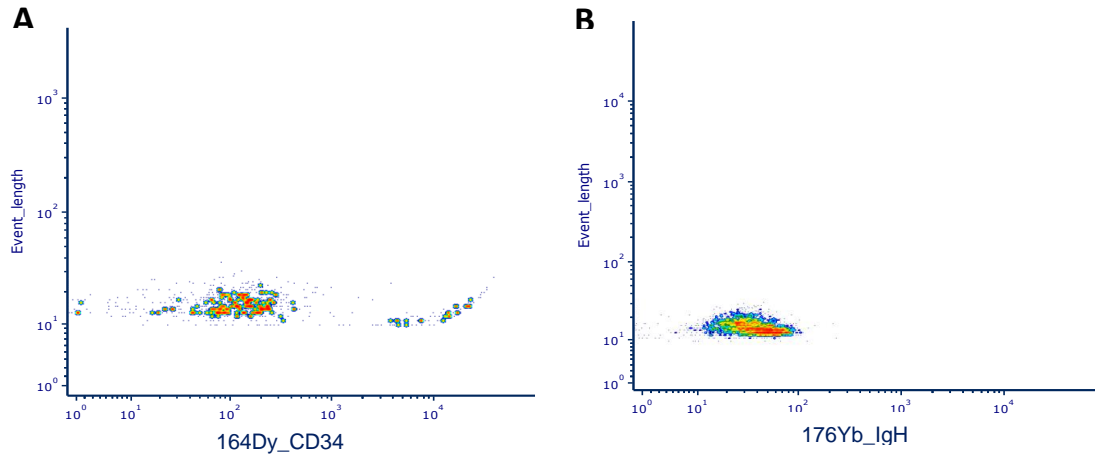


Figure 6.2 Antibody conjugation validation with BD beads.

Antibodies (1µl) were added to 1ml PBS containing 2 drops BD comp beads and incubated for 30 minutes at room temperature, before washing and analysis by mass cytometry. Y axis: event length. X axis (A) expression of 164Dy (conjugated to CD34 antibody) (B) expression of 176Yb (conjugated to IgH).

To assess that the antibody still recognised the epitope of interest (CD34 and IgH), an antibody titration was performed with cells positive for the epitopes. The antibodies were titrated in cell stain buffer to final dilutions of 1:250 to 1:5000. Kasumi and Ramos cells were used which are positive for CD34 and IgH, respectively. The cells were used in a 1:1 ratio for the titration so each cell line served as an internal negative control for the other marker. The staining index of the antibody can be calculated, which represents a measure of how strong the antibody staining is specific to the positive cell population.

$$\text{Staining index} = \frac{\text{median of positive population} - \text{median of negative population}}{2 * \text{standard deviation of negative population}}$$

The CD34 antibody showed clear separation between the CD34 positive and negative populations, in terms of 164Dy expression, at a dilution of 1:250, which diminished with increasing dilutions (Figure 6.3A). This is reflected in a high staining index value of 533, which reduces to 10 with a 1:5,000 dilution (Figure 6.3B). This confirms that the conjugation of the CD34 antibody to 164Dy was successful. The titration can also be used to assess an appropriate staining concentration. Due to the high staining index value with 1:250 dilution, this was used for all future experiments.

The IgH antibody showed a less clear separation between the IgH positive and negative populations (176Yb expression) at a dilution of 1:250, however this did not diminish with subsequent dilutions (Figure 6.3B). This is similarly reflected in the staining index values, which are much lower than those of CD34_164Dy (Figure 6.3B). The staining index reduces from 12.4 to 3.7 between dilutions 1:250 and 1:500. Beyond this dilution, the staining index does not decrease further, which is due to the very low metal mass intensity (MMI). However, a decrease in staining index from 1:250 to 1:500, in combination with the beads experiment (Figure 6.2) confirms that the conjugation of the IgH antibody to 176Yb was successful. Due to the low staining intensity of this antibody, a dilution of 1:100 was chosen, which although has not been shown here, is the concentration commonly used for commercially purchased antibodies.

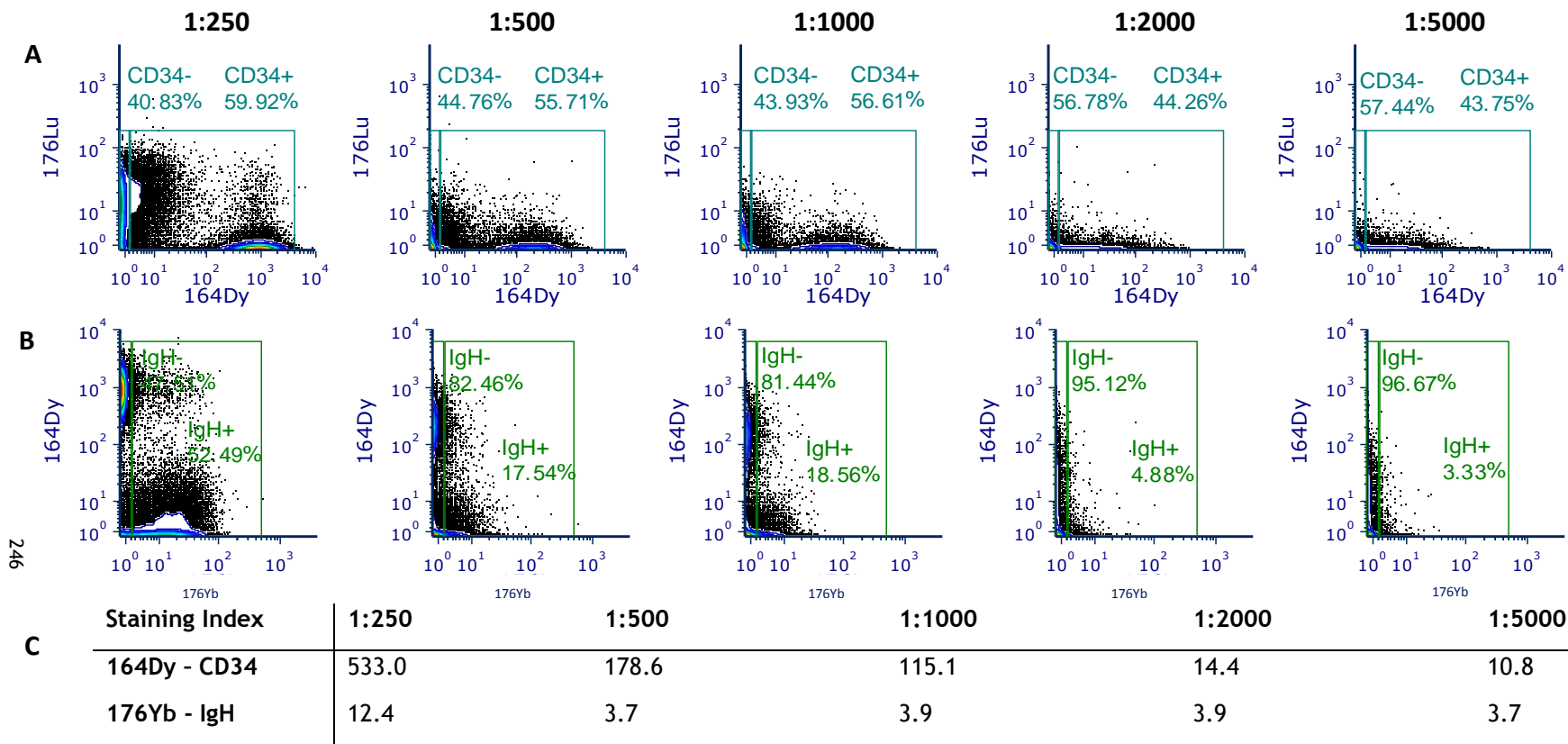


Figure 6.3 Titration of conjugated antibodies CD34 and IgH and staining index values.

The antibodies were titrated in cell stain buffer to final concentrations of 1:250 to 1:5000. Kasumi and Ramos cells were used which are positive for CD34 and IgH, respectively. The cells were used in a 1:1 ratio for the titration. All cells were gated on live single cells. (A) Shows the staining of the CD34 antibody conjugated to 164Dy (X axis); (B) Shows the staining of the CD34 antibody conjugated to 176Yb (X axis); (C) Staining index values ($\text{Staining index} = \frac{\text{median of positive population} - \text{median of negative population}}{2 * \text{standard deviation of negative population}}$).

6.3.4 Antibody panel validation

The quality and specificity of the antibodies is equally as important in mass cytometry as in flow cytometry. It is also essential to assess the combination of the metal markers. To validate the specificity of the antibodies, several steps were performed. Firstly, a cell line with known expression of markers was used. This allowed validation of both antibody specificity and also metal markers expression. Secondly, patient remission samples were assessed using the Wanderlust panel and compared with historical flow cytometry data, and data from the Bendall paper. Finally, T cell patient samples were assessed using the mass cytometry panel, which serves as a negative control for B cell specific markers. These steps will be described in the following sections.

As the metal markers had been changed from the original Wanderlust panel published by Bendall *et al.*, it was necessary to validate the full Wanderlust panel. For example, it is important to assess whether there is any spill over into the ± 1 or +16 channels, as a result of isotope impurity or oxidisation (Takahashi *et al.*, 2017).

Firstly, 1×10^6 PreB697 were stained with the full Wanderlust panel and acquired on the Helios mass cytometer to evaluate spill over. PreB697 contour plots from each channel used in the Wanderlust panel are shown in Figure 6.4. These plots clearly showed expression of markers consistent with PreB697 cells, including CD19, Igk (light chain), and high expression of HLA-DR and Ki67. Contour plots can also be used to assess for spill over. There was concern that there was spill over from the strong signals in the 169Tm channel (CD19) into 168Er (Ki67) and 167Er (CD38) into 166Er (CD24). This can be seen by the bulge in the contour plot indicated by the arrow in Figure 6.5.

To further investigate this potential signal overlap, a 'mass minus many' (MMM) experiment was performed. Briefly, this involves staining cells with a full panel of markers minus the channels where spill over is occurring. If there is a signal in these channels, it will therefore be a result of signal overlap from another channel. The full panel was run with PreB697 cells minus CD24_166Er and Ki67_168Er. The 166Er and 168Er channels are shown in Figure 6.6. There was spill over into both channels, as there was a small signal with a MMI of 0.95 in 166Er_CD24 and 3.2 in 168Er_Ki67.

However, this was not deemed to be problematic, as the MMI of stained PreB697 cells with the antibodies was 26.7 in the 166Er_CD24 channel and 142.4 in 168Er_Ki67 channel. There would therefore be no interference of the spill over signal on the staining signal.

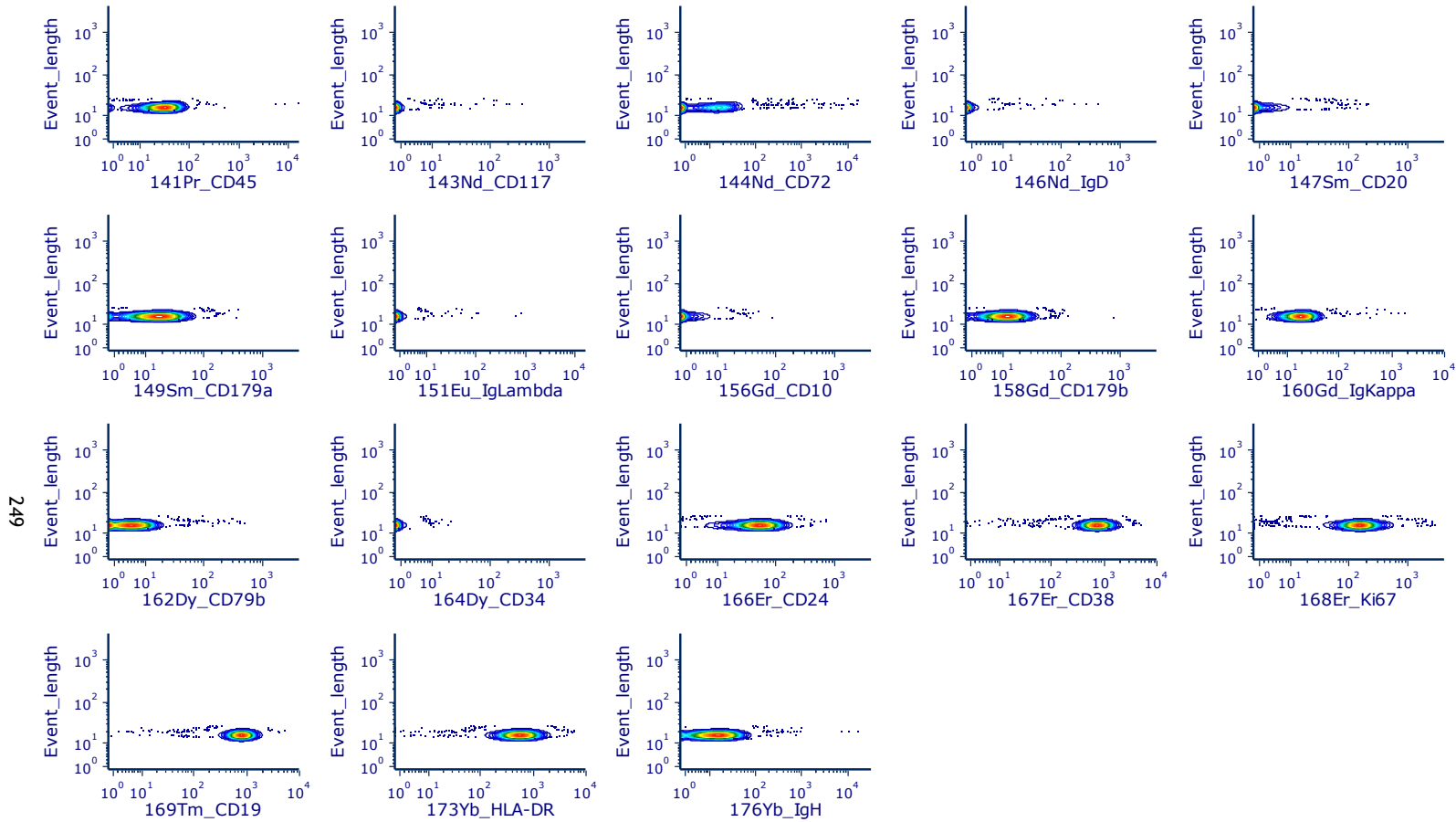


Figure 6.4 Full Wanderlust antibody panel with PreB697 cells.

PreB697 cells (1×10^6) were stained with the Wanderlust antibody panel before being acquired on the Helios mass cytometer. Y axis = event length. X axis = metal channel.

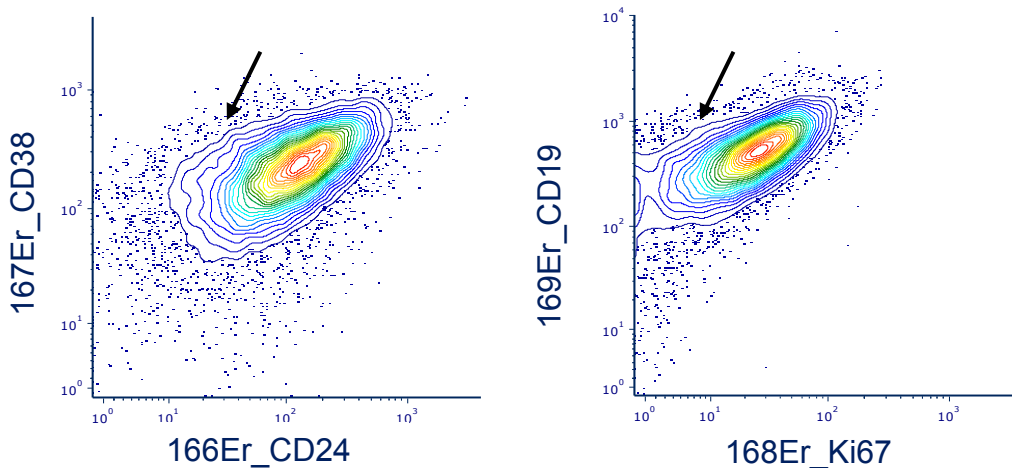


Figure 6.5 Contour plots indicating potential spill over from 167Er into 166Er, and 169Er into 168Er.

The full Wanderlust antibody panel was used to stain PreB697 cells before being acquired on the Helios mass cytometer. The contour plots of 167Er_CD38 and 166Er_CD24 (left), and 169Er_CD19 and 168Er_Ki67 (right) suggests that there may be spill over from the 167 channel into the 166 channel and from the 169 channel into the 168 channel. This is seen by a bulging shape on the plots indicated by the black arrows.

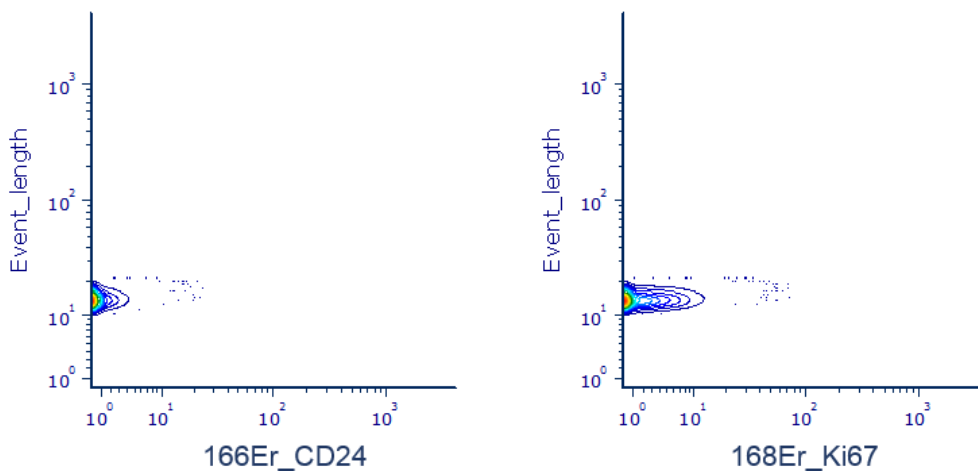


Figure 6.6 Mass Minus Many experiment to determine spillover.

The full panel of Wanderlust markers was used, minus 166Er_CD24 and 168Er_Ki67 to stain PreB697 cells before being acquired on the Helios mass cytometer, to determine if there was spill over into these channels. Both channels show a small signal (left: 166Er MMI= 0.95, right: 168Er MMI = 3.2).

6.3.5 Remission bone marrow samples

Next, four remission ALL bone marrow samples were stained; L826 (week 40), L835 (week 23), L837 (end of treatment) and L940 (week 23). As these samples had already been assessed using flow cytometry, it was possible to validate the mass cytometry Wanderlust panel using the flow cytometry data.

6.3.5.1 Gating strategy

Cells were first gated to isolate singlets, as described in 6.3.1 and Figure 6.1. To isolate different populations of B cells, further gating was performed, which is shown in Figure 6.7. Gating was not performed to isolate whole cell populations, but to identify small numbers of cells at discrete stages of development. For Wanderlust gates, used for start cell selection in 6.3.11, a final gate was needed that contained a maximum of thirty cells. Therefore Wanderlust gates were kept to a size that included a maximum of thirty cells. CD19 positive and negative cells were first selected. CD19 negative cells were then gated on CD34 and CD38 positivity to identify an early cell population (Wanderlust 0.1 stage, or maturation gate 1). CD19 positive cells were then gated on CD34 positivity. CD19 and CD34 positive cells formed maturation gate 2. Maturation gate 2 was then used to isolate cells at approximately Wanderlust 0.3 stage (pre pro B cells) by gating using high CD10 expression followed by low CD19 expression. CD19 positive, CD34 negative cells were divided into CD10 positive (maturation gate 3) and CD10 negative (maturation gate 4). Cells in maturation gate 4 were then gated using high CD20 expression to isolate the most mature cells.

For the historical flow cytometry analyses, cells were first gated using forward and side scatter to isolate lymphoblasts. Cells were then gated using CD19 positivity and CD34 positivity/negativity.

6.3.5.2 Comparison to flow cytometry data

All flow cytometry data was from the same stage of treatment as the mass cytometry data except L837, which was analysed using flow cytometry at week 15. To compare flow cytometry and mass cytometry data, CD19 positive, CD34 positive and negative cells were isolated, as previously detailed (Figure 6.7). Cells were then gated using the same strategy as the flow cytometry analysis to assess whether marker expression was

the same using both methods. Data for patient L829 is shown in Figure 6.8 and Figure 6.9, and other patients results are shown in Appendix F . Although far fewer events were acquired by mass cytometry, all patients showed similar marker expression using the Wanderlust panel to those shown in the flow cytometry data, which serves as a good validation for the panel.

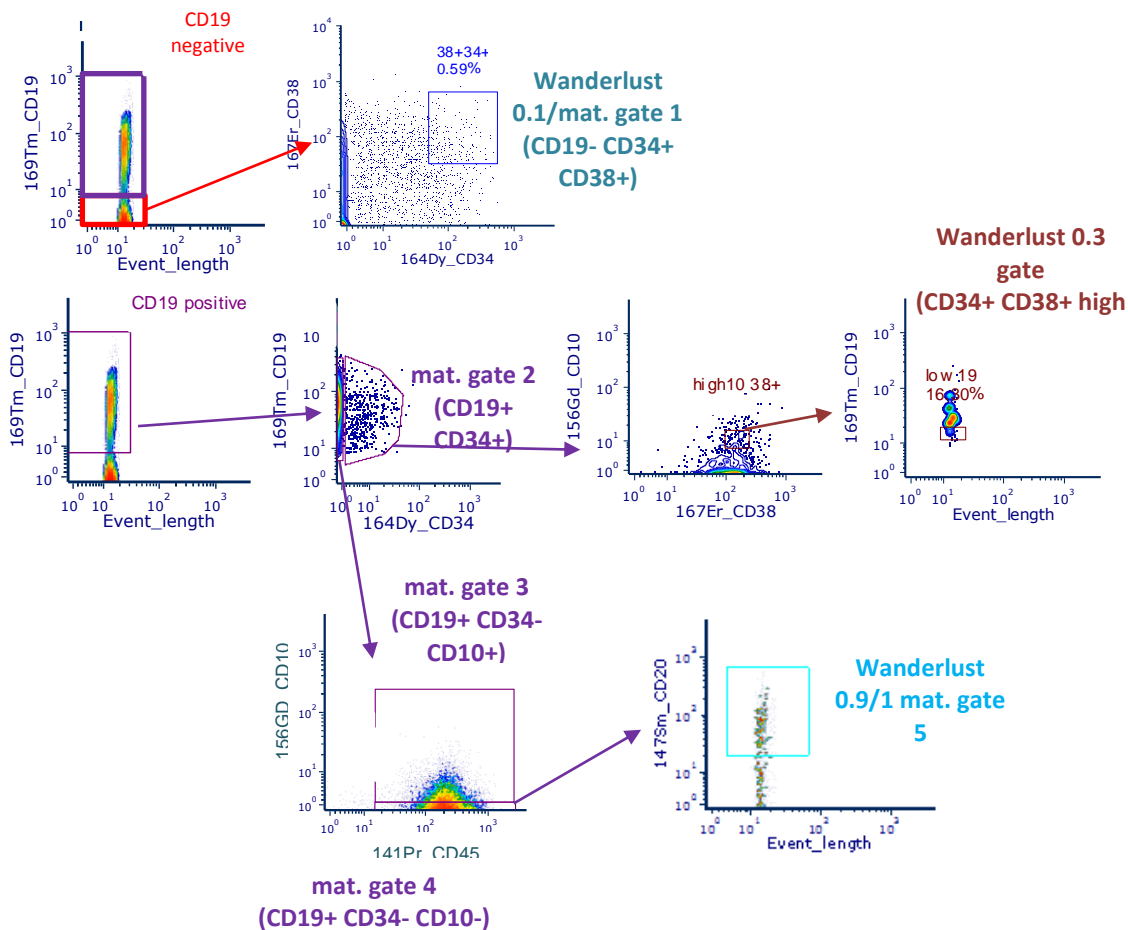


Figure 6.7 Gating strategy to isolate different B cell populations in remission bone marrow samples using mass cytometry.

Cells were first gated to isolate singlets, as described in Figure 6.1. CD19 positive and negative cells were then selected. CD19 negative cell were then gated on CD34 and CD38 positivity to give the least mature population (Wanderlust 0.1 stage of maturation gate 1). CD19 positive cells were then gated by CD34 positivity. CD19 and CD34 positive cells formed maturation gate 2. Maturation gate 2 was then used to isolate cells at approximately Wanderlust 0.3 stage (pre pro B cells) by gating on high CD10 followed by low CD19 expression.

CD19 positive, CD34 negative cells were divided into CD10 positive (maturation gate 3) and CD10 negative (maturation gate 4). Cells in maturation gate 4 were then gated on high CD20 expression to isolate the most mature cells.

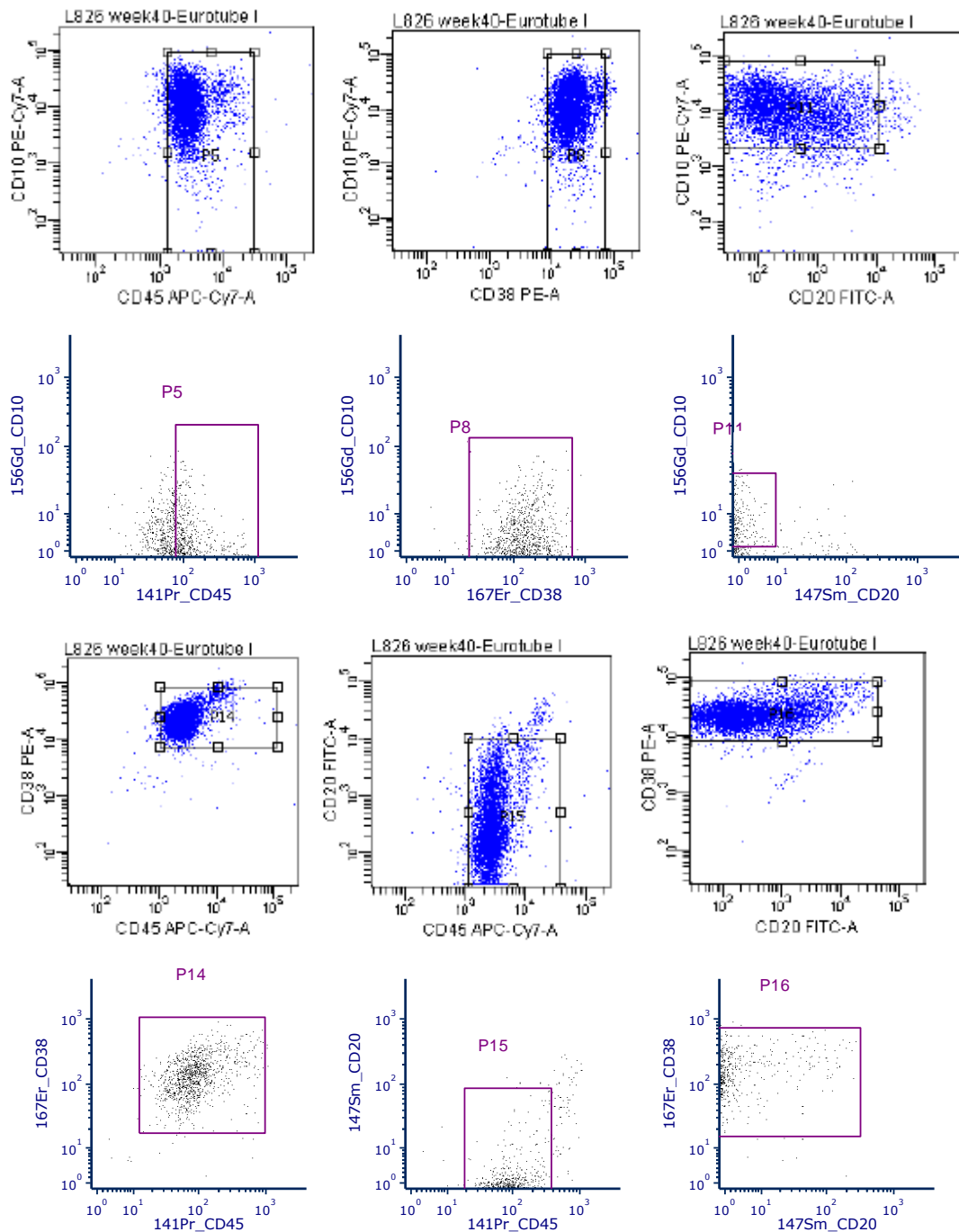


Figure 6.8 Comparison of Wanderlust antibody panel data generated by mass cytometry to historical flow cytometry data; CD34 positive cells.

Patient L826 (week 40) historically assessed using the Eurotubes I panel by flow cytometry (black outline with blue dots) and (end of treatment) assessed using the Wanderlust panel on the Helios by mass cytometry (navy axes with black dots). Each flow cytometry dot plot is a direct comparison of the mass cytometry dot plot beneath it.

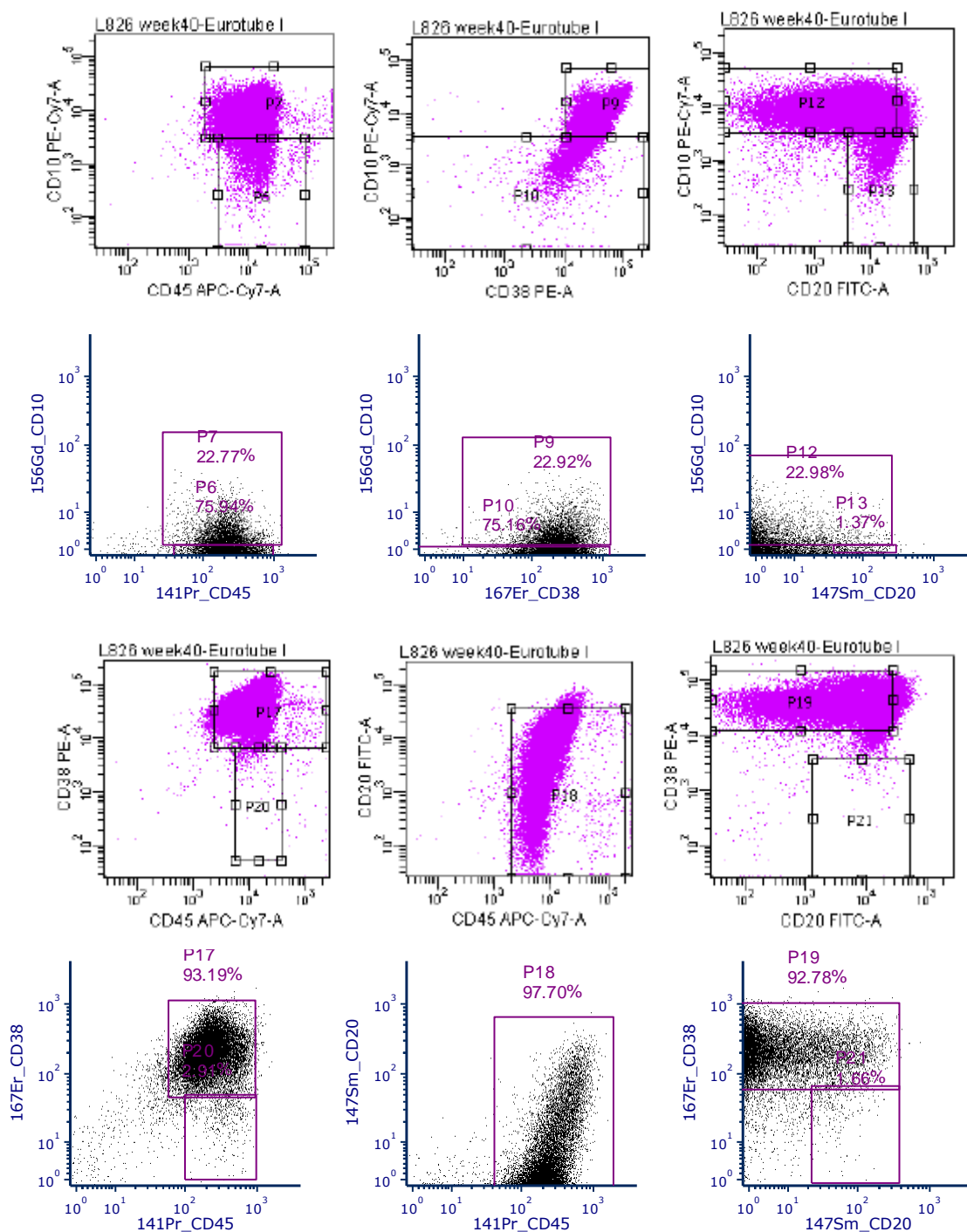


Figure 6.9 Comparison of Wanderlust antibody panel data generated by mass cytometry to historical flow cytometry data; CD34 negative cells.

Patient L826 (week 40) historically assessed using the Eurotubes I panel by flow cytometry (black outline with pink dots) and (end of treatment) assessed using the Wanderlust panel on the Helios by mass cytometry (navy axes with black dots). Each flow cytometry dot plot is a direct comparison of the mass cytometry dot plot beneath it.

6.3.5.3 Comparison to Wanderlust panel

To further validate the Wanderlust panel, a comparison was made to the published data in Bendall *et al.* (2014). The paper presents a figure showing the expression of several key markers representing different B cell maturation states. To replicate this, the remission bone marrow samples were broadly separated into five maturation gates, gate 1 (CD19 negative, CD34 and CD38 positive) gate 2 (CD19 and CD34 positive), gate 3 (CD19 positive, CD34 negative, CD10 positive) gate 4 (CD19 positive, CD34 and CD10 negative) and gate 5 (CD19 positive, CD34 and CD10 negative, high expression of CD20). These gates are shown in Figure 6.7. These five groups were compared to the Bendall paper in terms of expression of various markers of these maturation points (Figure 6.10). The markers showed a similar expression pattern to that displayed in the paper. Patient L829 is shown in Figure 6.10 and all other patients are displayed in Appendix F.

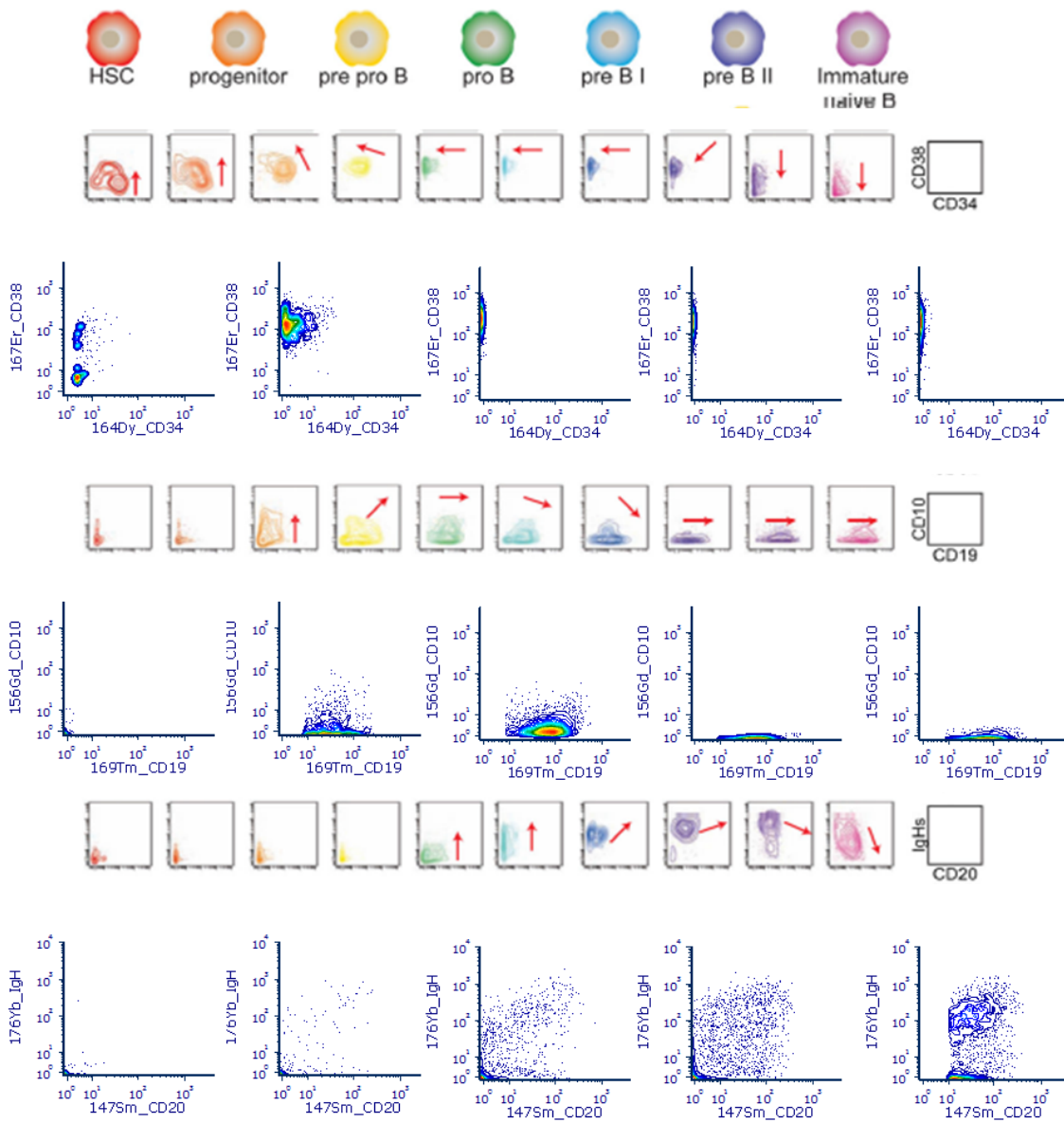


Figure 6.10 Comparison of data generated using the metal-altered Wanderlust panel across B cells of different maturation stages to that published in Bendall *et al.* (2014).

Patient L826 (week 40) was stained using the Wanderlust antibody panel and compared to data published by Bendall *et al.* (2014). Each row of 10 plots is from the Bendall paper, and the rows beneath them represent data generated at similar cell development stages in this project. The red arrows on the Bendall plots show the two dimensional progression of cellular marker expression through maturation taken in segments of 0.1 on the Wanderlust scale.

Finally, three T cell patient samples (L705, L809 and LK203) were analysed as a negative control for B cell specific markers. These T-ALL samples were all negative for B cell markers including CD10, CD19 and CD20, and were positive for markers commonly expressed by T-ALL including CD45, CD38 and Ki67 (Figure 6.11).

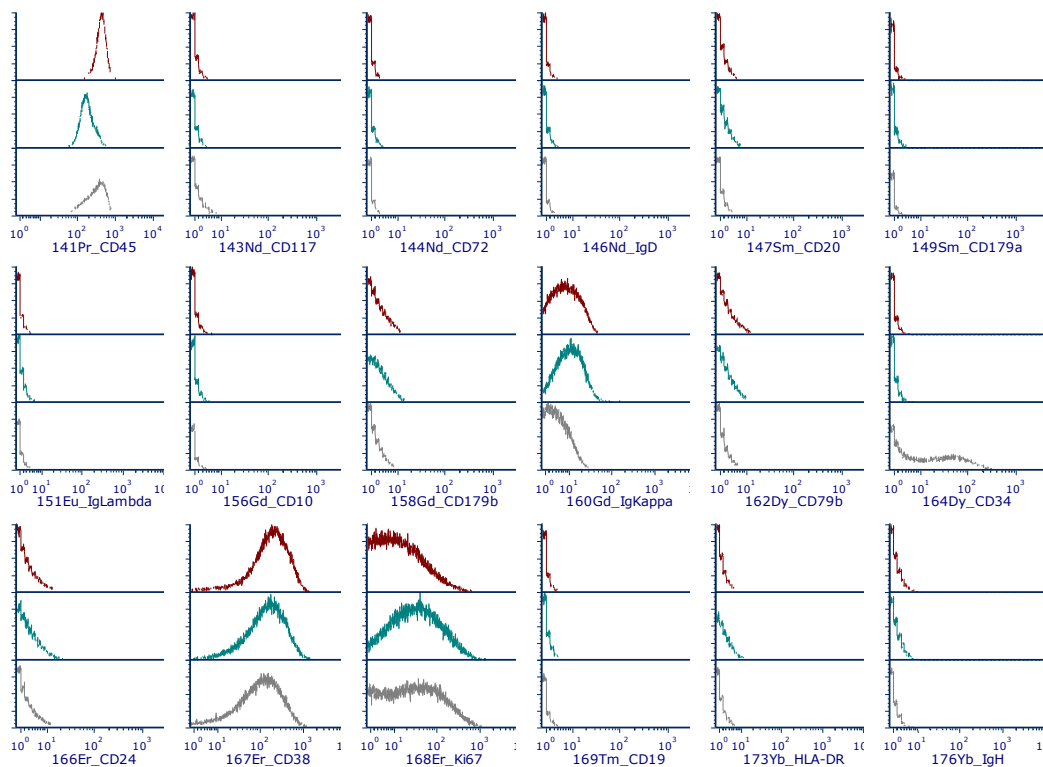


Figure 6.11 Histograms of T-ALL patient samples stained with the Wanderlust Panel.

Histograms show patients L705, L809 and LK203 (top to bottom). Patients have negative expression of B cell specific markers including CD10, CD19 and CD20. All samples were stained with the Wanderlust antibody panel and acquired on the Helios mass cytometer. Histograms are gated on live singlets. X axis: Marker expression. Y axis: counts.

6.3.6 Cell Lines

PreB697 and resistant sub lines R3F9, R3D11, R4C10, R3C3 and R3G7 were all stained with the Wanderlust antibody panel, and acquired on the Helios mass cytometer. Although the majority of the markers showed a similar MMI, there were some differences in CD72, CD179a (also known as vPreB, a subunit of the PreB cell receptor) and IgKappa between cell lines (Figure 6.12). For example, R4C10 had a lower expression of CD179a and increased expression of IgKappa. This indicates an increase in maturation state of this cell line compared to other resistant sub lines and PreB697.

Cell lines PreB697, R3F9 and R3D11 were also run on a further two occasions, and R4C10, R3C3 and R3G7 on one further occasion. Interassay variability is further discussed in 6.3.10.

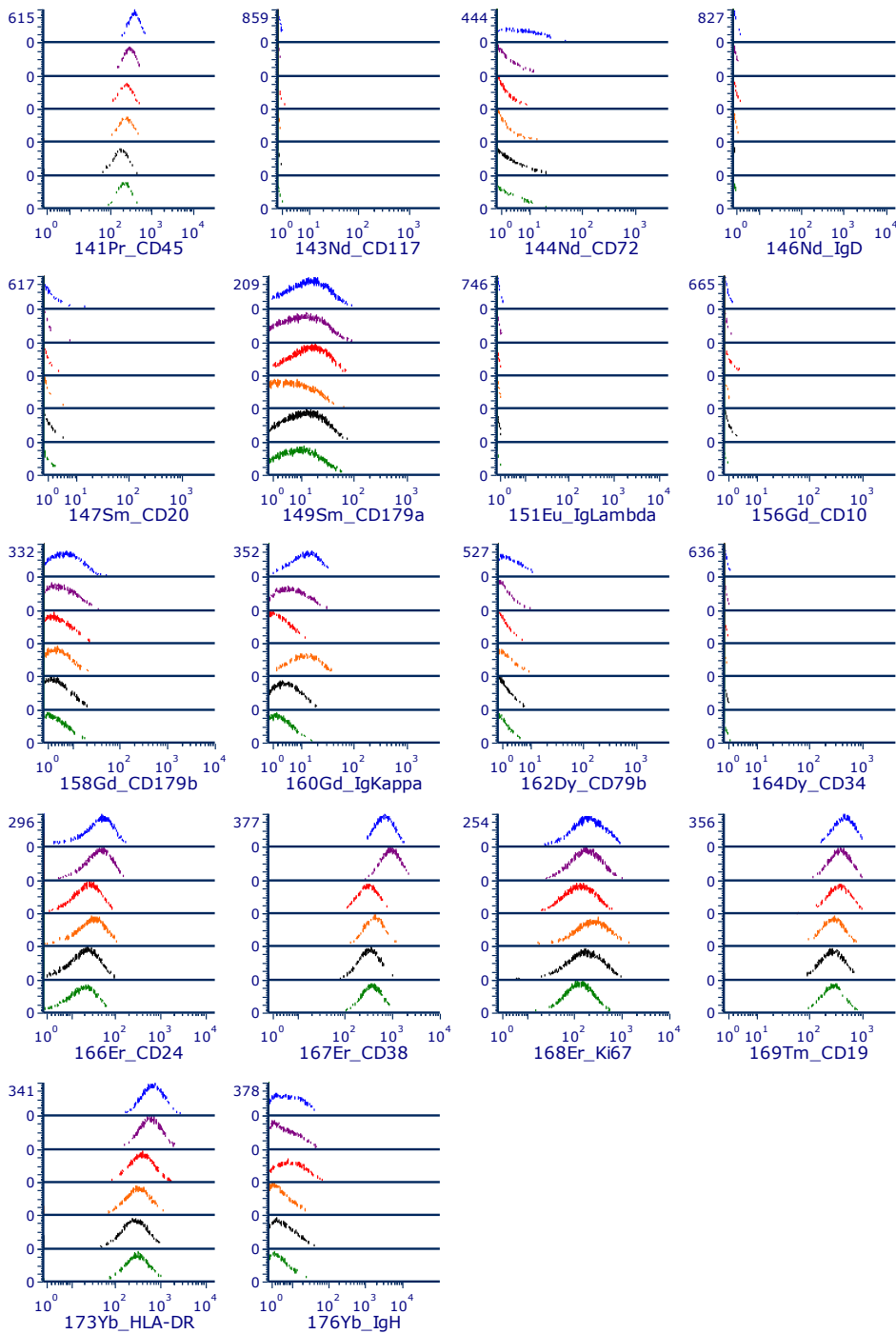


Figure 6.12 Histograms of Wanderlust markers for PreB697 and GC resistant sub lines.

PreB697, R3F9, R3D11, R4C10, R3C3 and R3G7 (order top to bottom of each histogram) were all stained with the Wanderlust antibody panel and acquired on the Helios mass cytometer. Cell lines were all stained simultaneously, and

acquired on the Helios on the same day. Cells were gated on live singlets. X axis: Marker expression. Y axis: counts.

6.3.7 Primagraft samples

Primagraft samples were stained, and acquired on the mass cytometer on the same day as other primagrafts derived from the same patient. For the majority of samples, primagrafts derived from the same patient shows very similar expression of markers (Figure 6.13A, and Appendix F). The exceptions to this were the two primagraft samples, AZ2 and AZ3, derived from patient L829 (Figure 6.13B). However, when all samples were assessed using MDS plots in the Pre Wanderlust analysis, L829/AZ2 appeared to be a distinct outlier, with clear separation from all other samples (Figure 6.18). As this sample was so different from all other primagraft samples, it may be that something may have gone wrong during staining or acquisition of this sample.

There was one patient for whom primagrafts were created at the point of first and second relapse. The expression of markers changed from first relapse to the second relapse (Figure 6.14). This was particularly noticeable for CD10, CD24, CD34 and CD38. Interestingly, the 2nd relapse samples were also more resistant to dexamethasone (first relapse GI50 ~26nM, second relapse GI50>1,000nM).

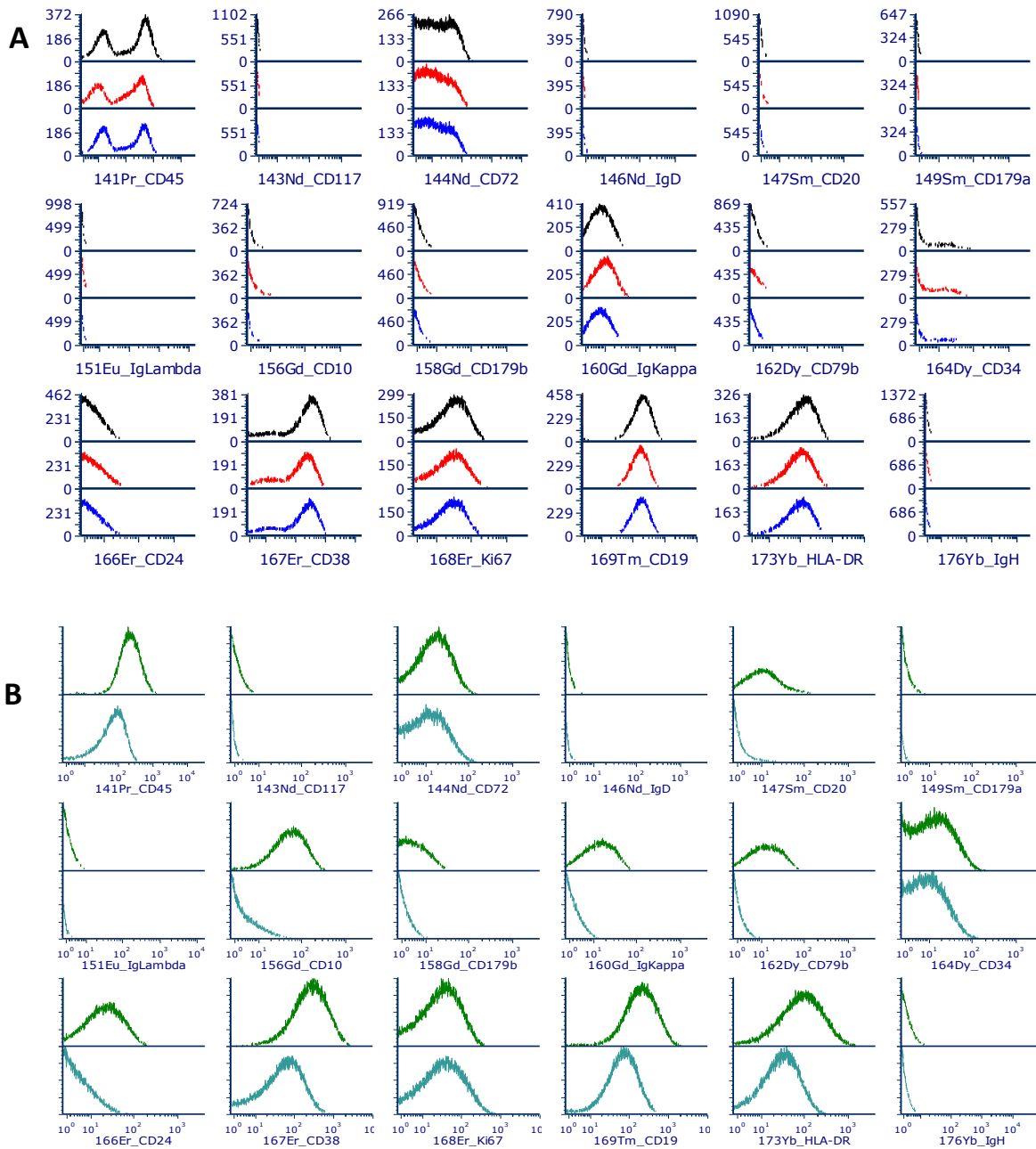


Figure 6.13 Histograms of primagraft samples, stained with the Wanderlust panel, derived from the same patient.

All samples were stained with the Wanderlust antibody panel acquired on the Helios mass cytometer and are gated on live singlets. (A) Similar histograms are seen for primagrafts derived from the same patient including patient L578 2nd relapse (mice AZ7, AZ8 and AZ9, top to bottom on each histogram). Further examples are shown in appendix F (B) Differences in histograms between primagrafts derived from patient L829 1st relapse, (mice AZ2 and AZ3, top and bottom on each histogram). X axis: marker expression. Y axis: counts.

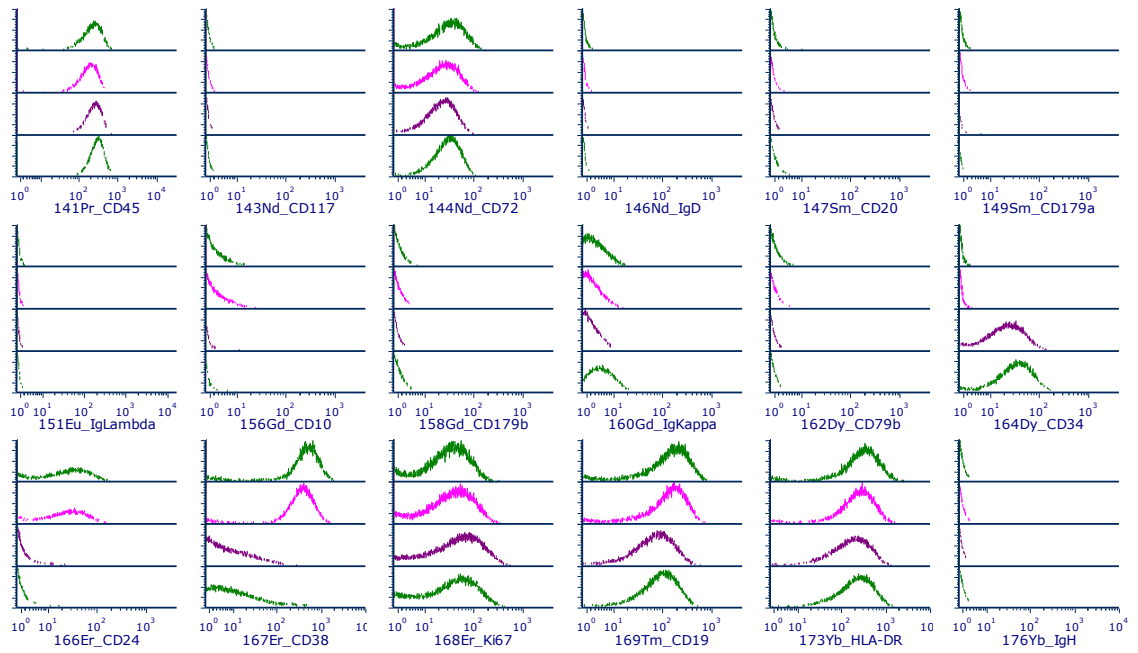


Figure 6.14 Histograms of primagraft samples from L919 first relapse and second relapse, stained with the Wanderlust panel, show differences in key markers.

The top two samples of each histogram show primagrafts JM267 and JM268, derived from a bone marrow sample of the first relapse of patient L919. The bottom two samples of each histogram show primagrafts AZ19 and AZ20, derived from a bone marrow sample of the second relapse of patient L919. All samples were stained with the Wanderlust antibody panel and acquired on the Helios mass cytometer and are gated on live singlets. X axis: marker expression. Y axis: counts.

6.3.8 Patient samples

Primary patient samples were also stained using the Wanderlust antibody panel, the histograms are shown in Figure 6.15. The expression of CD19 and CD10 and/or CD34 confirmed the B lineage immunophenotype of these samples. Several samples (L733, LK213, LK220 and LK221) had a bimodal distribution of CD45. The minor peak with a high CD45 expression is likely to be composed of normal cells. Further analysis of these cells confirmed that they had negative CD34 and CD10 expression, which alongside a high CD45 expression, is concordant with non-ALL cells. This population of normal cells was also seen in flow cytometric analysis of the same samples, verifying this observation.

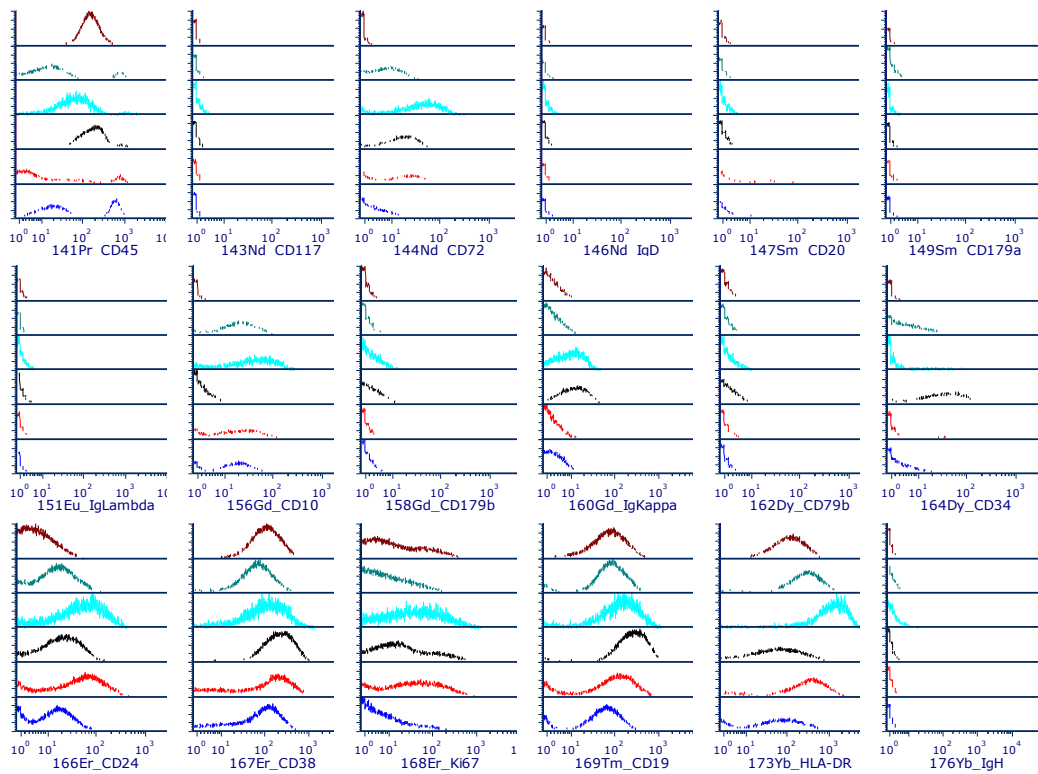


Figure 6.15 Histograms of patient samples stained with the Wanderlust panel.

Each histogram shows top to bottom: L715, L733, LK209, LK213, LK220, LK221. All samples were stained with the Wanderlust antibody panel and acquired on the Helios mass cytometer and are gated on live singlets. X axis: marker expression. Y axis: counts.

6.3.10 Pre Wanderlust analysis

The analyses described in this section were performed by Dr. Rachel Queen, Institute of Genetic Medicine, Newcastle University.

Prior to Wanderlust analysis, a number of analysis steps were performed to check the mass cytometry data. Initially a heat map was created to show expression of all Wanderlust markers in samples (Figure 6.17). The heat map also clusters samples by similarity so it is possible to assess whether primagrafts derived from the same patient grouped together, and displayed a similar expression of the Wanderlust markers.

Interestingly, sensitive and resistant cells seem to group together in blocks based on expression of Wanderlust markers. The groups also comprised samples stained and acquired on different occasions, discounting any possible batch effect in this clustering.

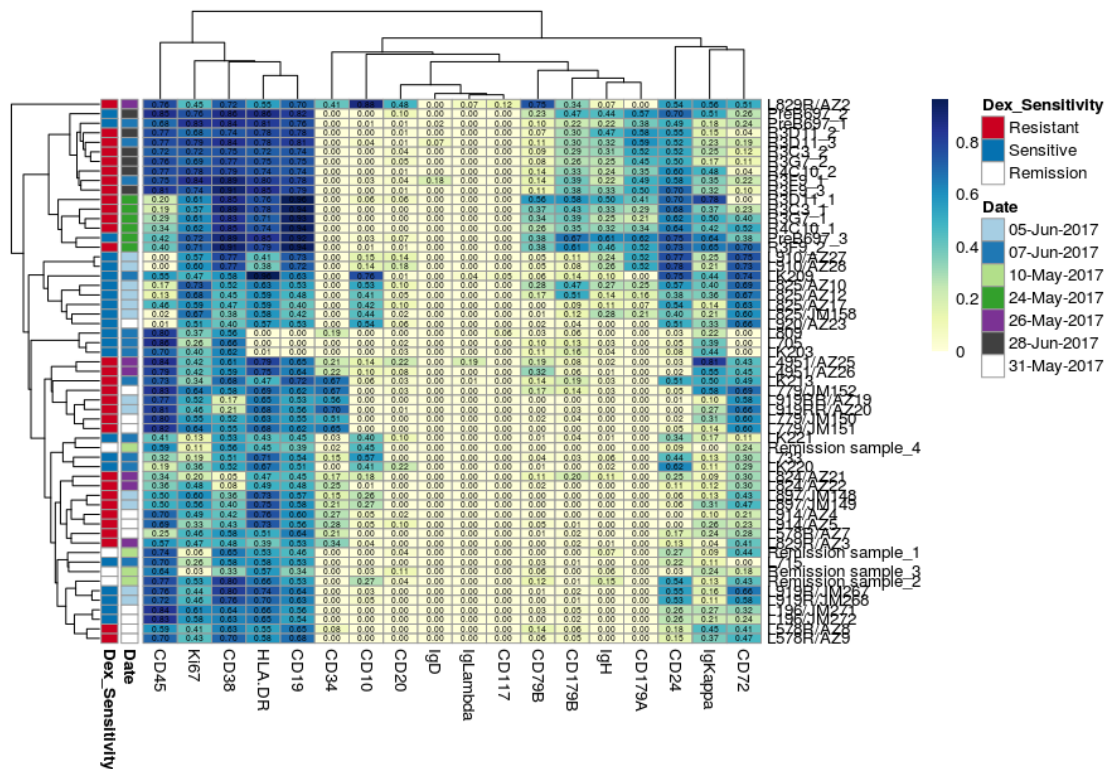


Figure 6.17 Heat map showing expression of all the Wanderlust markers.

Each row represents an individual sample indicated by the far right column. Dex sensitivity of samples is shown in the first column (red = resistant, blue = sensitive, white = remission sample). The date of the sample run is shown in the second column. Expression of markers is shown in the middle panel (blue = highest expression, pale yellow = lowest expression). Figure created in R by Dr. Queen.

MDS plots, a way of showing similarity between samples using distance, were also used to assess the data. For example, cells which are very similar to each other will be plotted close together, whereas cells which have many differences will be plotted far away from each other on an MDS plot. Firstly, MDS plots allow assessment of any batch effect, for example by date or sample type. Although EQ normalisation beads are included when samples are being assessed by mass cytometry, variability can still occur on different days.

As previously noted in 6.3.6, the cell lines PreB697, R3F9 and R3D11 were run on three separate occasions, and R4C10, R3C3 and R3G7 were run on two separate occasions with the Wanderlust panel, which enables assessment of interassay variation. Two of the assays were very similar to each other, but one assay was different. This is seen when all samples were plotted on MDS plots (Figure 6.18A). The cell lines acquired on the 24th May were clustered apart from those acquired on the 7th of June and 28th June. As there were two replicates of cell lines that did cluster together, the cell lines from the 24th May were removed from analysis. As mentioned previously, despite using EQ normalisation beads, it is possible to get day to day variation on the mass cytometer and during the staining process. Therefore the variation seen here may be, in part, due to this.

The primagraft sample AZ2, derived from patient L829, exhibited a different expression of markers to L829/AZ3, which was observable in the comparison of the histogram plots (Figure 6.13). These differences were reflected in an MDS analysis of all primagraft samples, AZ2 clustered at a distance from all other primagraft samples (Figure 6.18). This extreme separation may be due to an anomaly in the staining of acquisition of the sample, and it was therefore not included in the final Wanderlust analysis.

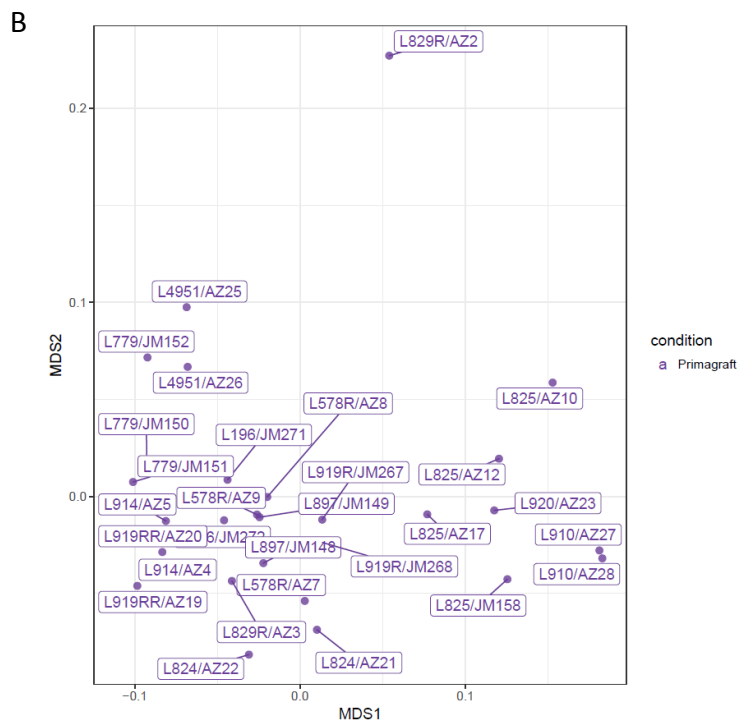
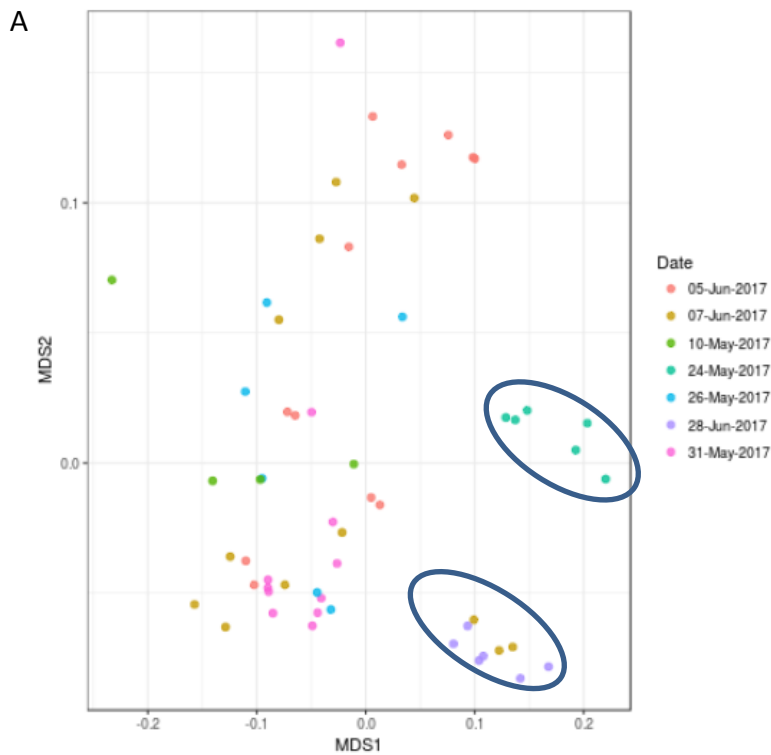


Figure 6.18 MDS plot of all of all cell samples colour coded by date (A) and primagraft samples (B).

Each dot represents an individual sample. (A) Cell lines, indicated by the navy ovals, cluster more closely by date; cell lines were run on 24/05/17, 07/06/17 and 28/06/17. (B) L829R/AZ2 clusters separately to all other primagraft samples. Figures created in R by Dr. Queen.

The MDS plot of all samples stained, after removal of the cell lines analysed on the 24th May, is shown below in Figure 6.19. Interestingly, the majority of the dex sensitive samples clustered together at the top of the plot, shown by green diamonds. Importantly, these samples were stained and acquired on multiple days so this is not an effect caused by interassay variation.

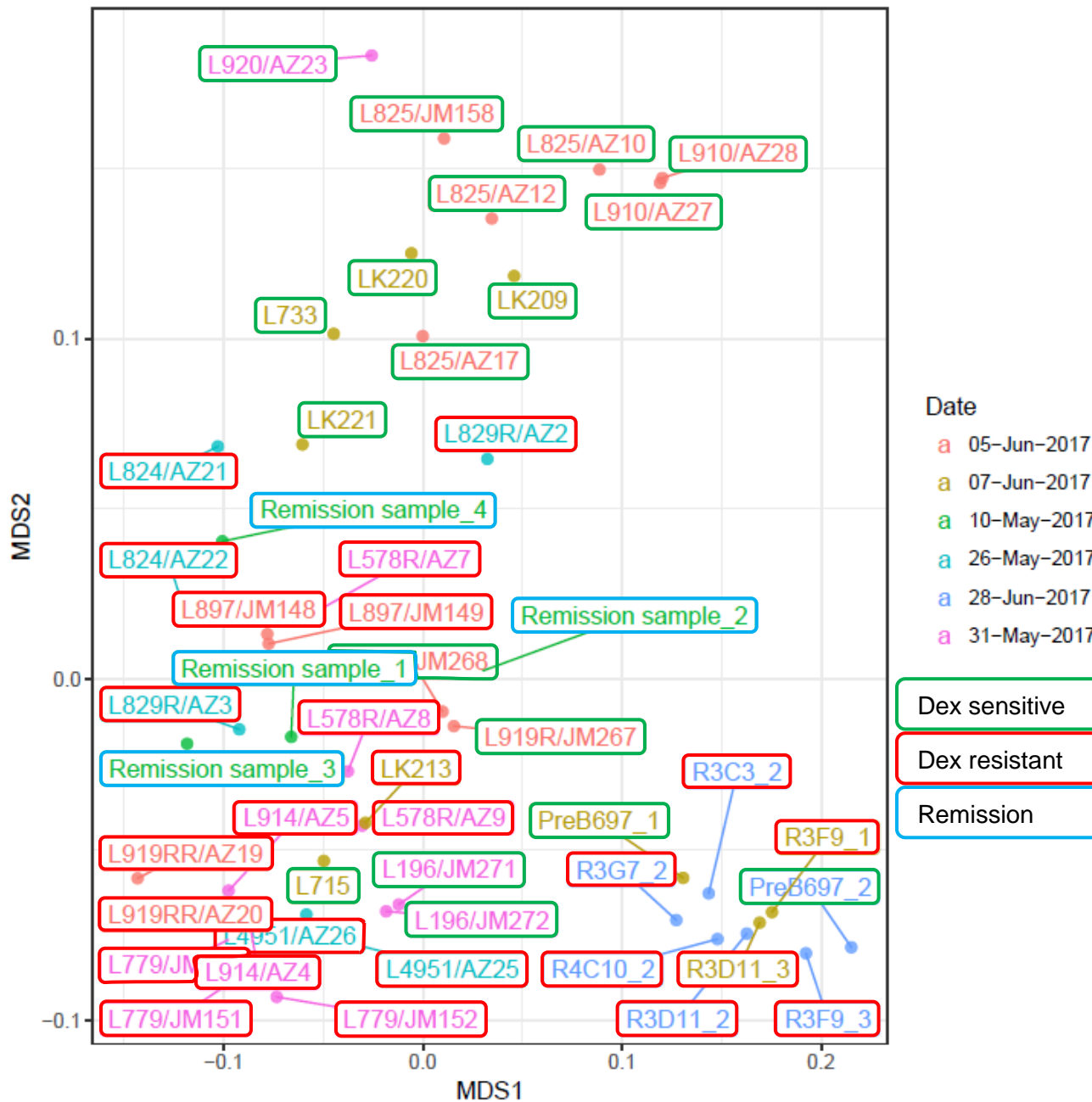


Figure 6.19 MDS plot displaying all samples after removal of cell lines acquired on the 24th May.

Each labelled circle shows an individual sample. The different colour circles and labels represent the date the sample was acquired. Box outline colour indicates dex sensitivity (green = sensitive, red = resistant). Figure created in R by Dr. Queen.

6.3.11 Selection of Wanderlust start cell.

All gating was performed by myself and the Wanderlust algorithm was executed by Dr. Queen in MATLAB.

In order to run the Wanderlust algorithm, it is necessary to identify a start cell, or group of start cells, from which the trajectory can begin mapping. In Bendall *et al.* (2014), a very early start cell was chosen (Wanderlust stage 0.1, equivalent to a haematopoietic stem cell). Therefore initially, a group of start cells were selected in the remission bone marrow samples that were approximately at this Wanderlust level (CD34 and CD38 positive, CD19, CD20, CD10, and IgH negative, Figure 6.20A, box 1). Gating is shown in Figure 6.7 (mat. gate 1). However, this generated a Wanderlust trajectory that was different to that published in Bendall *et al.*, and to known expression patterns of these markers (Figure 6.20B, graph 1). The main differences to the Bendall trajectory were a large dip in expression of all markers approximately half way along the trajectory, and a high expression of CD20 at the start of the trajectory. These differences may be due insufficient numbers of very immature cells, which hampers the ability of the algorithm to create an accurate trajectory. The low cell numbers in the remission samples is shown in Figure 6.16. The differences may also be due to a dissimilarity in cell populations, as Bendall *et al.* lineage depleted their bone marrow samples to rid them of T cells, however, this lineage depletion step was not performed in this study. The presence of T cells may therefore have skewed the trajectory.

Bendall *et al.* assessed the effect of using trajectory start cells from different Wanderlust stages, and observed that the trajectory was still generated when a start cell of up to Wanderlust stage 0.3 (approximately equivalent to a pre pro B cells) was chosen. They also observed that when a very mature start cell was selected, the trajectory ran backwards, from the most mature cells to the least mature. Therefore, both start cell gates at 0.3 and 0.9/1 wanderlust stages (immature naïve B cells) were selected and tested with the Wanderlust algorithm (Figure 6.20A, boxes 2 and 3, respectively). The 0.3 start cell gate was created using cells which had CD34 and CD38 positivity, high CD10 expression, mid CD19 expression and CD20 and IgH negativity (gating shown in Figure 6.7, Wanderlust 0.3 gate). As all B cells are CD19 positive by Wanderlust stage 0.3, by using a start cell gate at this point, it was possible create the

trajectory using remission samples gated on CD19 positivity, thus removing the influence of T cells. The trajectory created by a 0.3 start cell gate was very similar to the original Wanderlust trajectory Figure 6.20B2. However, the CD38 trajectory was different to that expected, as it seemed to follow the trajectory of the CD19. These differences may once again be due to the significantly smaller cell numbers used to create the trajectory in this project.

To establish whether the trajectory was able to map backwards (from the most mature to least mature cells) a gate was created using cells which were at the Wanderlust stage of 0.9/1.0 (equivalent to immature naïve B cells). These cells were CD19, CD20 and IgH positive and CD10, CD34 and CD38 negative (gating shown in Figure 6.7, mat. gate 5). The trajectory created by this start cell did mirror some of the marker trajectories, for example low expression of CD34 and CD10 in the more mature B cells which increased as cells became more immature (Figure 6.20B3). However, other markers such as CD19 did not reverse their trajectory as well.

As the trajectory created using start cell gates of Wanderlust stage 0.3 recreated the Bendall trajectory the most faithfully, this start cell gate was used for further analyses.

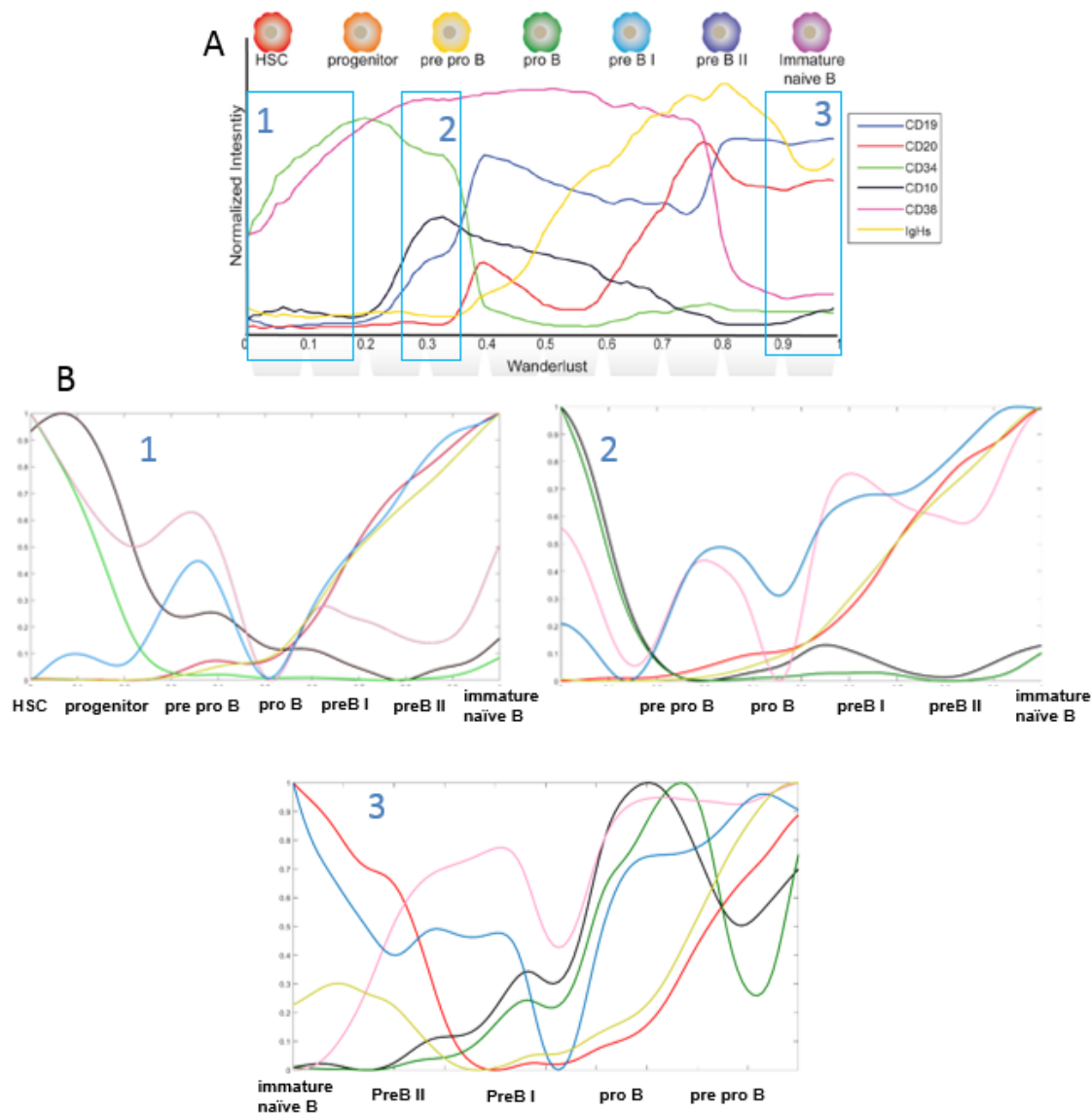


Figure 6.20 Start cell selection, adapted from Bendall *et al.* (2014) (A) and trajectories created in this project (B).

(A) Shows the selection of the start gates. Boxes denote start cell selections. In all cases 10-20 cells were gated and used to define the start of the trajectory. (B) Shows the resultant trajectories from these start gates outlines in (A).

1. A very early start cell was selected that had CD34 and CD38 positivity, but was negative for CD19, CD20, CD10, and IgH.
2. A start cell of approximately 0.3 on the Wanderlust scale was selected which was positive for CD34 and CD38, had high CD10 expression, mid CD19 expression and was CD20 and IgH negative.
3. A very mature start cell was selected which was CD19, CD20 and IgH positive and CD10, CD34 and CD38 negative.

6.3.12 Wanderlust

The Wanderlust trajectory was run with each remission ALL bone marrow individually to assess the interpatient variability in trajectories (Figure 6.21). The individual trajectories varied markedly from one another. This may be for two reasons; firstly, the remission samples were taken from different points of treatment. Some of the samples were taken whilst patients were still undergoing treatment for ALL, for example at week 23, whilst others were taken at the end of treatment.

Secondly, there were different numbers of cells in each sample. Due to clumping of the cells during the permeabilisation step of antibody labelling, a number of cells were lost. In particular, two samples (L835 and L837) only had ~2,600 events after gating (Figure 6.16). This is compared to L826, which had 29,400 cells after gating.

Therefore, in the remission samples with fewer cells, there may not have been enough cells at the different maturation stages to as accurately create the trajectory as the sample with nearly 30,000 events. However, as has shown in Figure 6.20, when the remission samples are combined, the trajectory is similar to that published by Bendall.

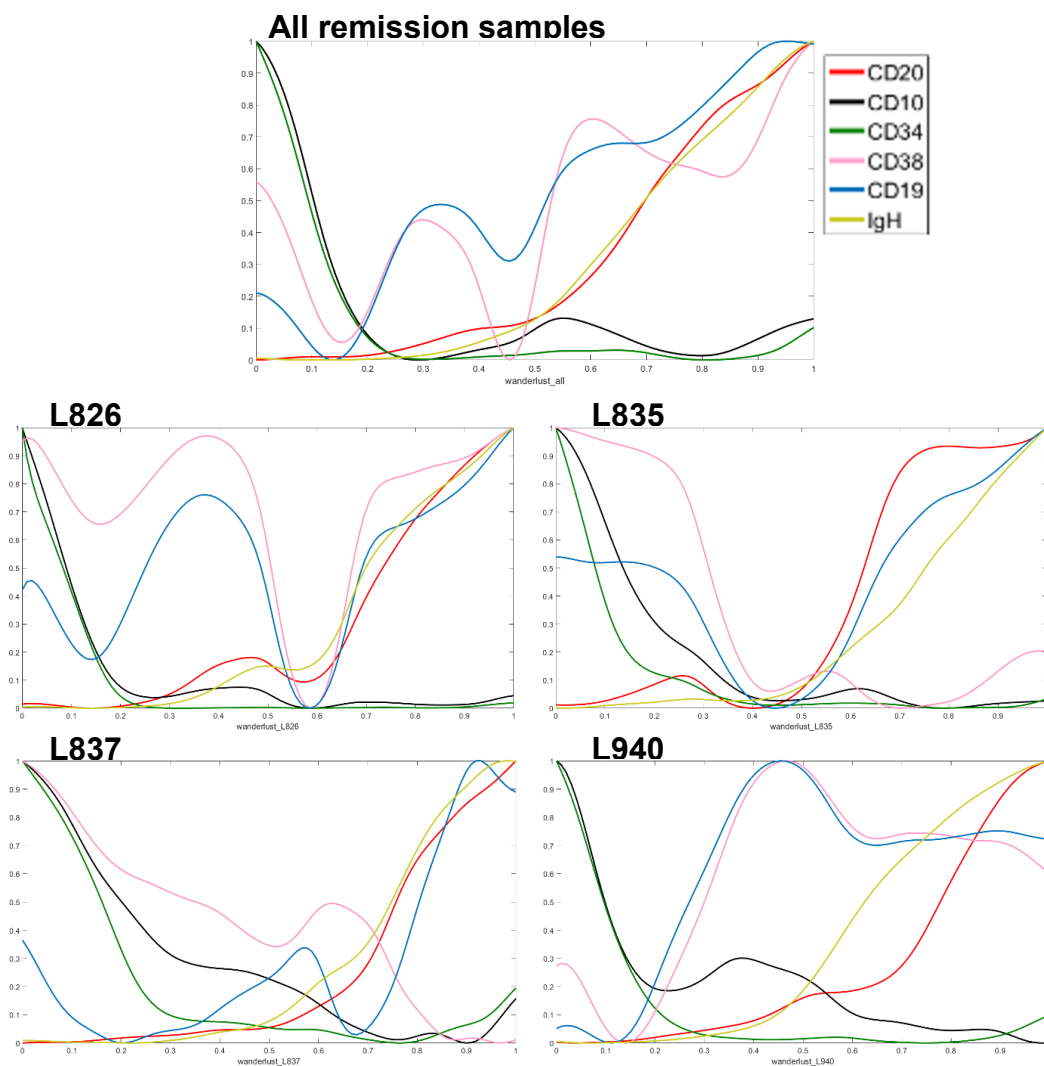


Figure 6.21 Wanderlust trajectories resulting from four individual remission bone marrow samples.

Trajectories were created by Dr Queen with the Wanderlust algorithm in MATLAB using the 0.3 start cell gate. Trajectories: red = CD20, blue = CD19, black = CD10, green = CD34, pink = CD38, yellow = IgH. X axis = maturation. Y axis = normalised marker expression.

In order to assess the maturation stage of the ALL cell lines and patient samples, cell numbers needed to be reduced in order to not skew the trajectory. This would easily happen due to the small number of cells in the remission samples (total approximately 44,000) compared to other samples (Figure 6.16). Therefore, for patient samples, 1000 cells were selected at random (using the Wanderlust software in MATLAB). For primagraft samples, primagrafts from the same patient were grouped together and 1,000 cells were selected at random from this group. However, primagrafts L825/AZ2, L578/AZ7 and L825/JM158 were excluded from this grouping as they clustered too far away from other primagrafts derived from the same patient sample (Figure 6.23).

Interestingly, in the cluster dendrogram of primagrafts, samples segregate broadly into sensitive and resistant cells, with the exception of primagraft samples from patient LK196, and L919 (first relapse) based on the expression of markers in the Wanderlust panel. Despite both samples being dex sensitive, both had a poor outcome. The sample for LK196 was taken at second relapse, and they subsequently died from their disease. L919 (first relapse) went on to relapse a second time.

Figure 6.24 shows the effect of adding ALL cells to the into the Wanderlust algorithm to create the trajectory. On one occasion all ALL samples were included in the algorithm, on a second only dex sensitive ALL samples were included and on the third occasion only dex resistant samples were included (A, B and C, respectively). Even after reduction of cell numbers to 1000 per sample, it can be seen that addition of ALL samples still skews the trajectory compared to the trajectory created with remission samples alone (Figure 6.21). This is once again likely due to be a result of a limited number of cells in the remission bone marrow samples.

A heat map for all Wanderlust markers through cell development, as ordered by the Wanderlust trajectory is shown in Figure 6.22. This has been generated using all samples (remission and patient/primagraft samples). Although some marker expression is as expected, some markers show a different pattern of expression. For example, the trajectory shows cells expressing CD34 after the pre b I cell stage, when physiologically, CD34 expression at this point in development should be minimal. This is once again an indication that the ALL cells have skewed the trajectory and that a greater number of normal B cells are needed to anchor the trajectory.

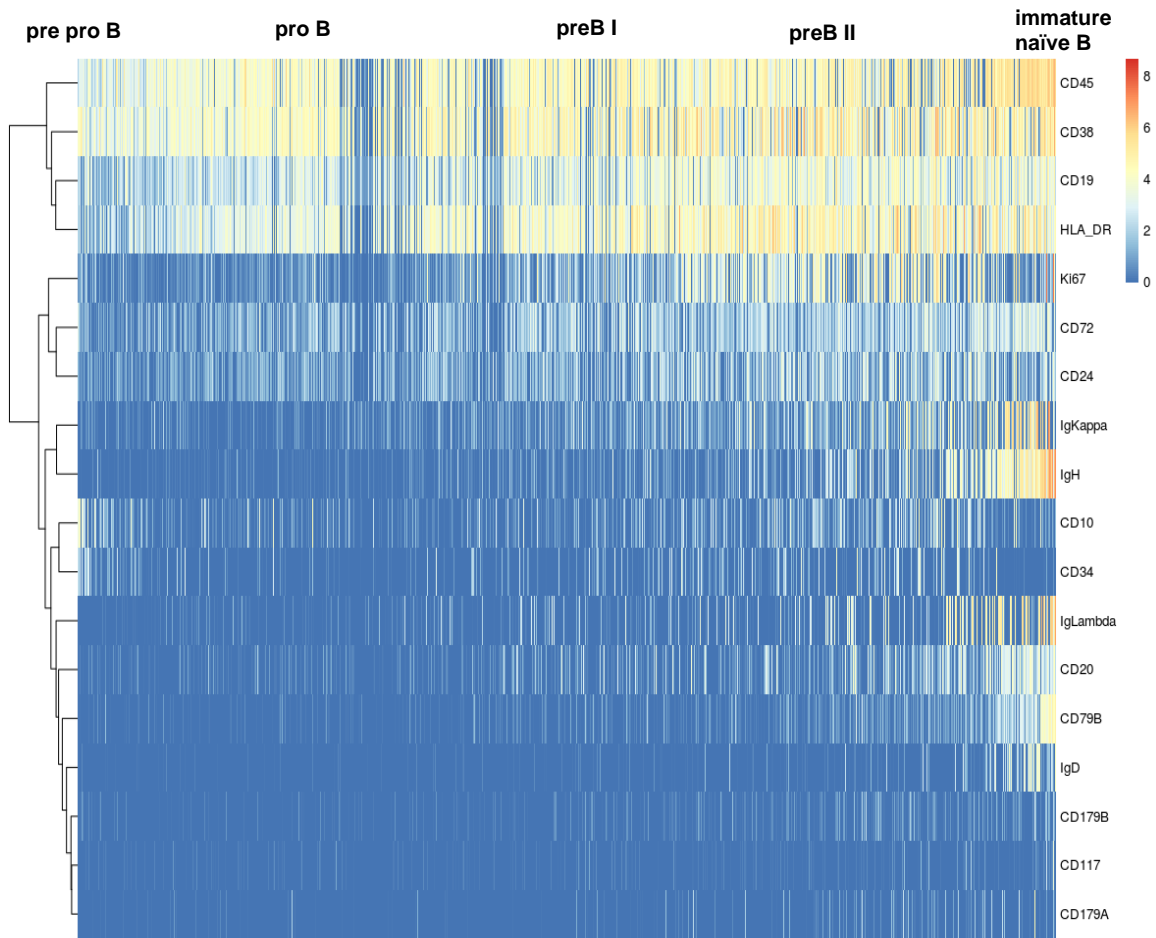


Figure 6.22 Summary of Wanderlust marker expression throughout B cell development as ordered by the Wanderlust trajectory.

Each row represents an individual marker. X axis shows maturation (left least mature, right most mature), approximate cell stages are shown above heat map. Highest expression is shown by red and lowest expression is shown by blue. Figure created in R by Dr. Queen.

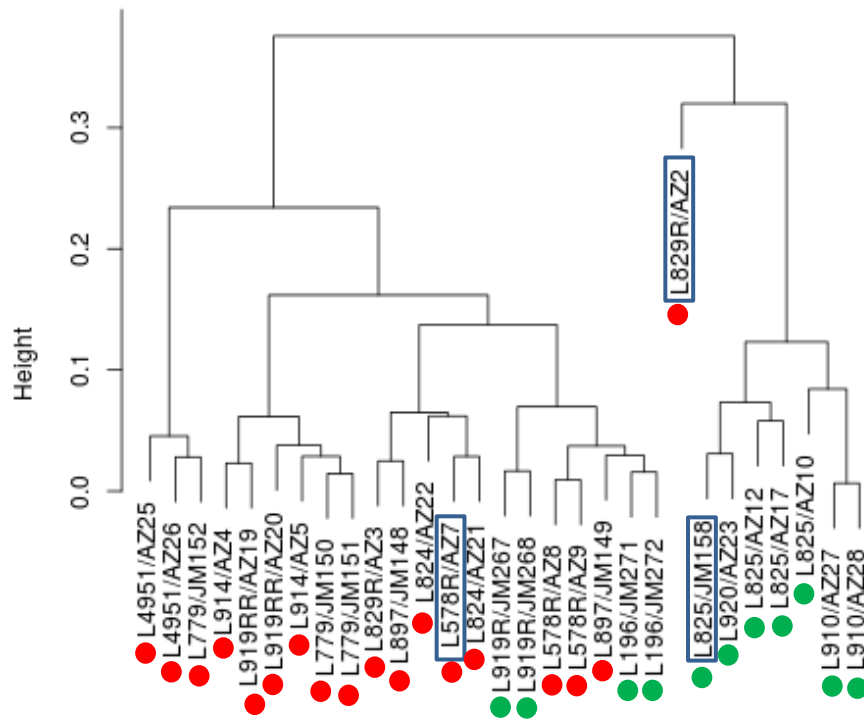


Figure 6.23 Cluster dendrogram of primagraft samples.

Primagraft samples were clustered according to their most similar sample. Most primagraft samples clustered close to other primagrafts derived from the same patient. Exceptions are denoted by a blue box and are L829/AZ2, L578R/AZ7 and L825/JM158. Dex sensitivity is indicated by a green circle. Dex resistance is indicated by a red circle.

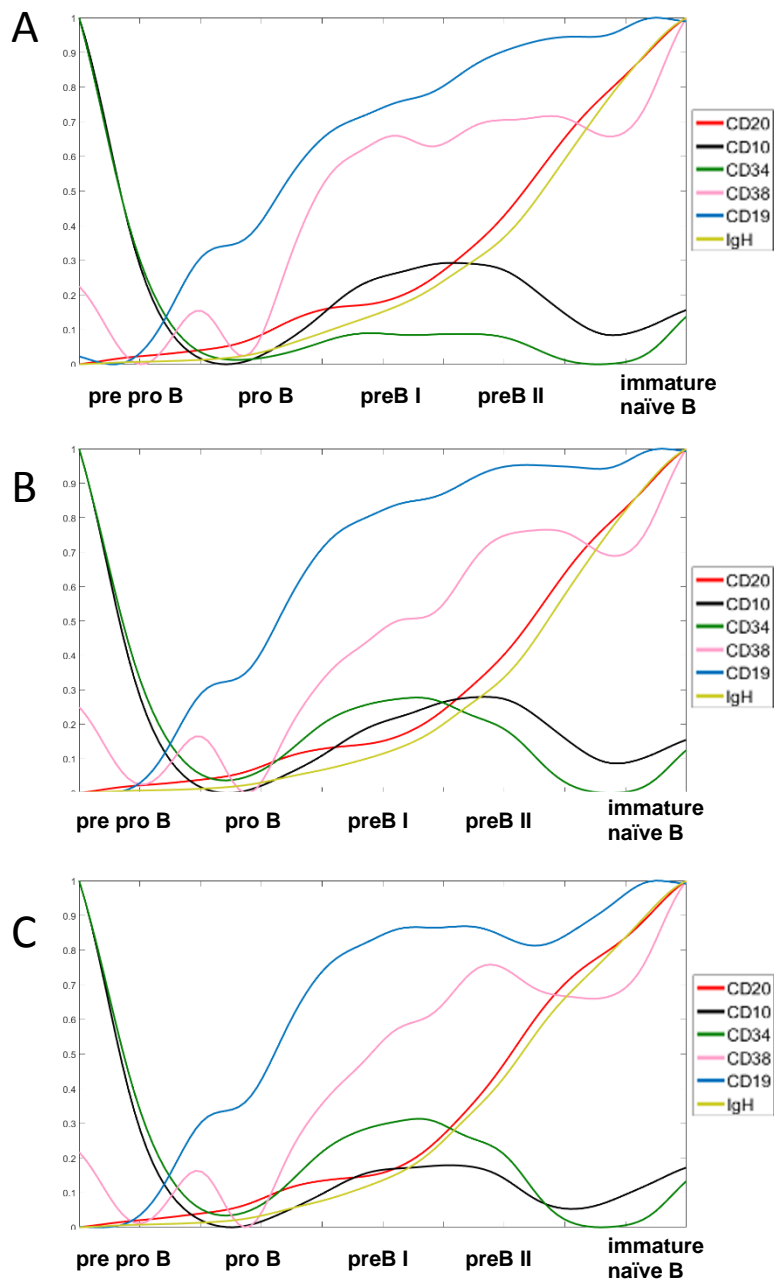


Figure 6.24 Wanderlust trajectories created after the addition of all ALL samples (A), dex sensitive ALL samples (B) and dex resistant ALL samples (C).

Trajectories were created using the four remission samples with the addition of (A) all ALL samples, (B) all dex sensitive ALL samples and (C) all dex resistant ALL samples. ALL cells were gated on live singlets and 1,000 cells were selected at random for each patient (including patients used to create primagrafts). Figure created in MATLAB by Dr. Queen.

6.3.13 Post Wanderlust analysis

Although the Wanderlust trajectory shown in Bendall *et al.* was not accurately reconstructed due to a limited number of normal B cells in the remission samples, and a distorting influence of ALL cells, an initial density analysis was performed by Dr. Rachel Queen to assess the Wanderlust results generated (Figure 6.25). As expected, the remission samples, shown in red, displayed the broadest maturation range of cells. This is also reflected in the Wanderlust values for individual samples shown in Figure 6.26. The remission samples show differing average maturation scores, however the standard deviation is larger than seen in ALL samples (remission: 0.16-0.20, ALL: 0.08-0.16), reflecting the range of maturation of cells in these 'normal' bone marrow samples. The variation in the average maturation of the remission samples may be due to the small number of events in some samples or the different cell populations resulting from the samples being obtained at different stages of treatment.

The Wanderlust density plot indicates that dex resistant cells have a less mature phenotype than dex sensitive ALL cells, the opposite of what has been observed by previous groups. However, the maturation scores generated using this algorithm are likely not to be accurate due to the inaccurate trajectory. When the Wanderlust trajectory has been replicated exactly, there is likely to be a reordering of marker expression which will likely affect the maturation values assigned to the cells. Therefore, further work should be performed to refine the algorithm and these analyses repeated to reassess the relationship between cell maturation and dex resistance.

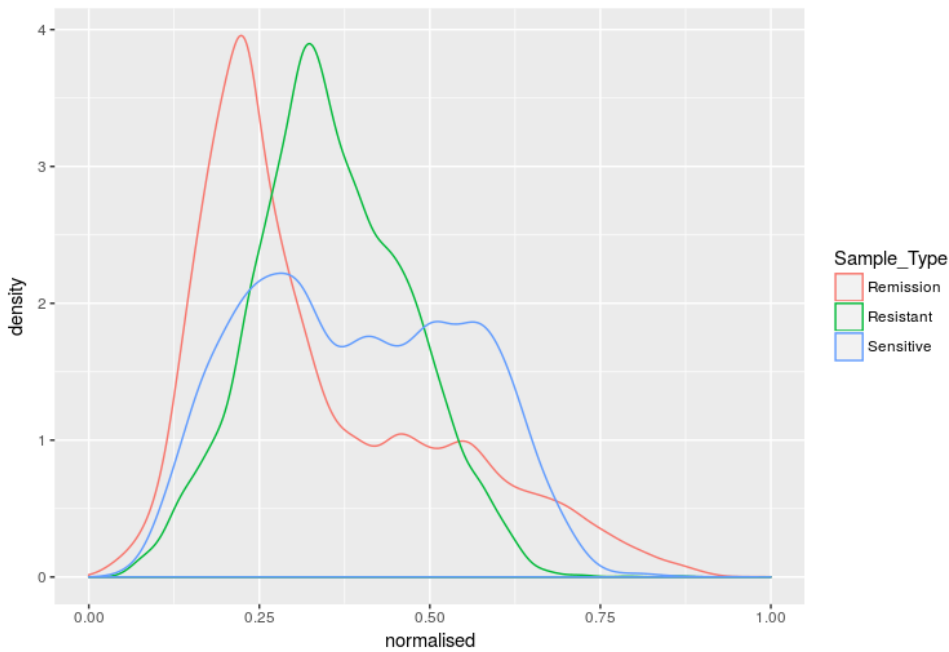


Figure 6.25 Density plot showing the normalised maturation of cells in remission, resistant, and sensitive cells.

Y axis shows the cell density and X axis shows the normalised maturation of cells based on values generated from the Wanderlust trajectory. Figure created by Dr. Rachel Queen in R.

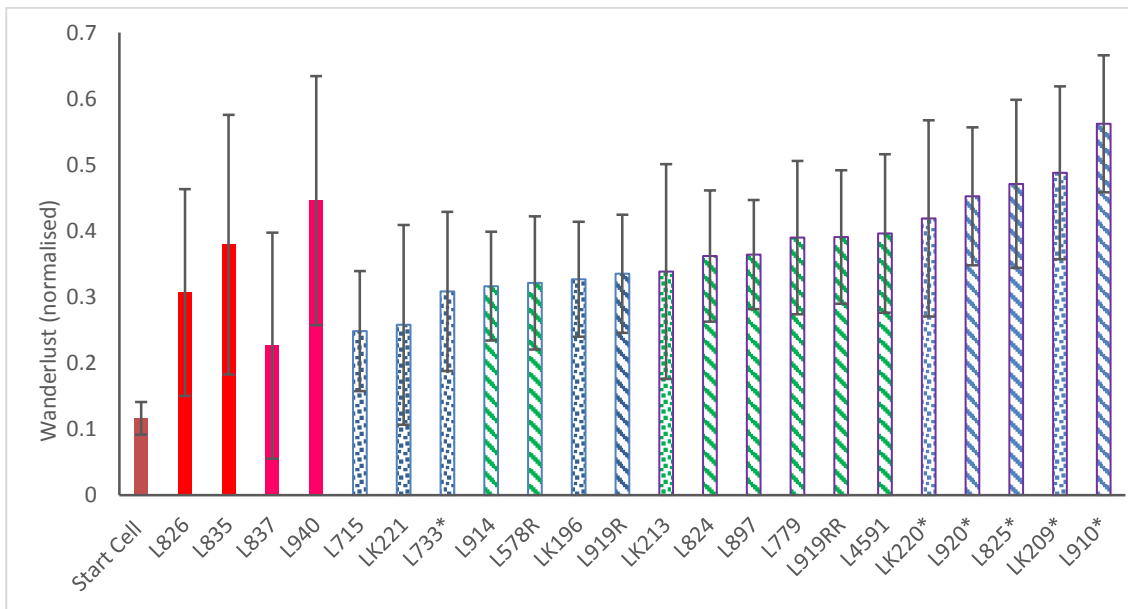


Figure 6.26 Average Wanderlust maturation value of cells in each patient sample.

Each bar represents the mean Wanderlust maturation score for each sample. Error bars show standard deviation. Orange = start cell, red = remission samples, green = dex resistant samples, blue = dex sensitive samples. Dashed bars = primagraft sample, spotted bars = primary patient sample. *Indicates samples which clustered together in Figure 6.19.

6.4 Discussion

This chapter aimed to characterise the maturation phenotype of ALL samples, and determine whether the level of maturation of ALL samples is linked to GC resistance. Cell maturation has been previously implicated in GC resistance, both in ALL (Rhein *et al.*, 2007; Nicholson *et al.*, 2015), and healthy B cells (Lill-Elghanian *et al.*, 2002). In order to investigate this association further, a deeper understanding of B cell development is needed. However, this is a highly complex process and previous studies have been limited by techniques which are not able to assess the developmental course as a whole. A recent study has developed a mass cytometry based approach coupled with a graph based algorithm, called Wanderlust, to study the development of healthy B cells. This has opened up the possibility to assess B cell development in ALL samples, as during this project, the dex sensitivity for a range of primagraft and patient cells had been characterised in Chapter 4.

Despite using the same antibody targets and clones as the published Wanderlust panel (Bendall *et al.*, 2014), it was necessary to alter the metal tags. Altering the metal labels on the mass cytometry antibodies is the same concept as a fluorochrome change on a flow cytometry antibody; the antibody will still bind to the cellular target, but the data are reported in a different channel. A change of metal should therefore not affect the end data generated, however validation of certain aspects of the altered metal panel is still necessary. This included validation of the two antibodies conjugated in house; both metals were successfully conjugated to the antibodies, and the antibody still recognised the epitope of interest in cell lines. The CD34 antibody had a stronger signal than the IgH antibody, although the IgH signal was still sufficient for use. A validation of the panel as a whole was also performed, to check for events such as spill over between channels. A full panel stain with the PreB697 cell line indicated that there was possible spill over from channel 169 (CD19) into 168 (Ki67) and 167 (CD38) into 166 (CD24) which was confirmed in an MMM experiment, however this was not deemed to be problematic as the signal was considerably lower than would be produced by a cell which was positive for these markers.

The full panel was also used to stain four remission bone marrow samples, from ALL patients at week 23, week 40 and end of treatment. Remission samples were used to

firstly validate the panel against historical flow cytometry data and data presented in Bendall *et al.* (2014), and secondly to create a trajectory from which to assess the maturation state of the ALL samples. Comparison of the results generated by flow cytometry and mass cytometry allowed validation of antibodies CD10, CD19, CD20, CD34, CD38 and CD45 within the mass cytometry panel. Although a lower number of events were collected by mass cytometry compared to flow cytometry, the results generated between the two experimental approaches are similar.

The remission sample mass cytometry data were divided broadly into five maturation stages, using gating to enable a comparison to the data published in Bendall *et al.* (2014). The expression patterns through the maturation stages of markers imitated those seen by Bendall *et al.* Finally, as a negative control, three T-ALL samples were stained using the Wanderlust panel. As would be expected, the T-ALL samples showed no expression of any B-cell markers including CD10, CD19 and CD20, but did show expression for markers that are expressed by both B and T cells including CD38 and CD45. This validates that the Wanderlust panel is recognising true expression of B cell markers.

The panel was therefore accepted as valid and used to stain cell lines, primagraft and patient samples. For the majority of primagraft samples, there was more than one primagraft derived from the same patient, and these represent a biological replicate of sorts. Most primagrafts derived from the same patient displayed a similar expression of Wanderlust markers. As a reduction of cell numbers was needed for Wanderlust analysis, primagraft samples derived from the same patient were merged, and 1,000 cells were selected at random for use in the trajectory. Primagraft samples from patient L829 had a differential expression of Wanderlust markers. On MDS analysis of all samples, one of the two L829 primagraft samples, AZ2, clustered away from all other samples. This suggests that there was a problem in the staining or acquisition of this sample, and it was therefore not included in Wanderlust analysis. Similarly, clustering approaches also identified that primagraft samples L825/JM158 and L578/AZ7 did not cluster closely with their patient derivatives, although this was not as extreme as the case of L829/AZ2. These samples were therefore also not included in the sample merging. It may be that a different ALL clone engrafted in these primagraft samples, causing a difference in marker expression, rather than the difference being

created experimentally. However, a larger number of cells in the normal B cell developmental trajectory would be needed to allow analysis of individual primagraft samples to assess inter primagraft variation.

MDS plots, used to check clustering of replicates, also identified inter assay variation between cell lines. Three replicates of cell lines PreB697, R3D11 and R3F9 were run on three separate days. Samples clustered more strongly on date than sample cell line, and cell lines acquired on one day clustered away from those acquired on the two separate occasions. Although EQ beads are used to account for variability in machine performance, machine variability between days can still occur. Mass cytometry is a relatively new technology and therefore problems encountered with methodology such as this are not surprising. There are several techniques that could be used in the future to help control such variation. Firstly, an internal control could be spiked into each sample before staining, which could be used for data normalisation. This approach would not only account for day to day fluctuation of the mass cytometer sensitivity, but also variation produced during the antibody staining component of the protocol. Secondly, a technique called 'barcoding' could be employed. In this approach, samples are barcoded, and then stained and acquired together. Barcoding can be achieved using different approaches, but commonly involved labelling cells with different combinations of isotopes (for example palladium) to achieve a unique barcode, before combination of samples and subsequently staining and acquisition (Behbehani *et al.*, 2014; Zunder *et al.*, 2015). Such approaches would require validation, but would aid the integrity of the resultant data.

For patient L919, primagraft samples were available from the patient's first and second relapse. Interestingly, primagraft samples from the first relapse were sensitive to dex, and samples from the second relapse were resistant to dex. The samples showed differential expression of markers such as CD10, CD24, CD34 and CD38 by mass cytometry. This indicates that this sample has a slightly more mature phenotype, although it is not possible to determine this using the Wanderlust algorithm until an accurate trajectory has been created. Samples from the first relapse also clustered away from the other sensitive samples and were closer to the dex resistant samples. This may mean that expression of Wanderlust markers are able to predict prognosis as well as potentially being associated with dex sensitivity. Similarly, primagrafts derived

from the LK196 patient sample at second relapse, also dex sensitive, clustered with the dex resistant primagrafts. This patient unfortunately went on to die from their disease. Within the cluster of dex sensitive patients, no patients died from their disease, although one patient died post infection. However, this association between Wanderlust marker expression and outcome had been proposed based on a small number of patients, and would need to be replicated in a larger cohort.

The choice of start cell was investigated for the Wanderlust trajectory. Bendall *et al.* found that the choice of start cell between Wanderlust stages 0.1 and 0.3 did not affect the algorithm's ability to reproduce the B cell developmental trajectory, however this was not the case in this project. This is most likely to be a result of a difference in protocols between Bendall *et al.* and this project. Bendall *et al.* used lineage depletion to remove T cells from bone marrow samples, however this was not done here. Therefore, when a very early start cell was selected, it was not possible to run the algorithm without discounting T cells, which may have skewed the trajectory. However, a start cell gate of cells at 0.3 maturation stage enabled the algorithm to be executed on CD19 positive cells only, as B cells have gained CD19 by this point of development. This meant that the influence of T cells were removed and consequently the trajectory produced replicated that published in Bendall *et al.* much more faithfully.

However, the 0.3 start cell gate still did not exactly mirror the trajectory published by Bendall *et al.*, with key differences seen in the trajectory of CD38. This may be due to the very low cell number in the remission samples used to create the trajectory, and therefore not enough cells in rare populations to create an accurate trajectory. The trajectory may therefore be improved through staining and acquisition of more 'normal' B cell samples, if possible with T-lineage depletion. A greater number of B cells may allow a more accurate trajectory to be created.

The low number of cells used to create the trajectory has also hampered the ability to accurately assess the maturation state of the individual primagraft samples, as when the ALL samples were added into the pool of cells to execute the algorithm, the trajectory was distorted, which meant it differed to a greater extent to the original trajectory published by Bendall *et al.* This means the maturation levels assigned to

cells may not be accurate due to incorrect ordering of Wanderlust marker expression. For example, although an initial post Wanderlust analysis suggested that remission samples had the broadest range of cell maturation phenotypes, as expected, it also indicated that dex resistant samples had less mature phenotype than sensitive samples. This is the opposite to that observed in studies such as Dworzak *et al.* (2008), who observed an increased expression of CD20, and antigen of differentiation, in residual blasts after GC treatment, and those by Nicholson *et al.* (2015) and Rhein *et al.* (2007), which have already been discussed. Furthermore, it is well characterised that B cell maturation state in normal B cell development has an inverse relationship to endogenous GC sensitivity, with a higher amount of apoptosis in early B cells compared to more mature cells (Lill-Elghanian *et al.*, 2002; Igarashi *et al.*, 2005a). This may be a mechanism to control steady state lymphopoiesis. Therefore, as previously indicated, it would be beneficial to run additional 'healthy' bone marrow samples, to generate an accurate trajectory. Having a high event number of healthy bone marrow events would also anchor the trajectory, and prevent distortion when ALL samples are added in. It may be useful to consider the use of healthy bone marrow samples from a non ALL source, for example from total hip replacement surgery. These samples will not have been subjected to the effects of prior or ongoing chemotherapy and may therefore be a more accurate representation of the B cell subtypes.

However, despite difficulties in creating an accurate B cell trajectory, the pre wanderlust analysis shows encouraging associations. An analysis of all samples showed that samples clustered in broad groups based on their dex sensitivity and resistance. Furthermore, these samples were stained and acquired on different days, eliminating any role of a batch effect in creating this outcome. When just primagraft cells were clustered using a cluster dendrogram, samples clustered strongly based on dex sensitivity. As previously discussed, two groups of sensitive samples clustered with the dex resistant samples, however these patients both had poor outcomes. Similarly, all other dex sensitive samples clustered together based on their expression of the Wanderlust markers.

Together, these data show that ALL samples clustered by dex sensitivity based on their expression of Wanderlust markers. However, an inability to recreate an accurate B cell trajectory thus far has meant it has not been possible to accurately determine whether

resistant samples are more or less mature than dex sensitive samples. More remission or healthy bone marrow samples are needed to enable the Wanderlust algorithm to create a more accurate and anchored B cell trajectory allowing the maturation stage of samples to be determined. This will open the opportunity for therapeutic targeting of this more, or less, mature phenotype to resensitise patients to dex.

Chapter 7. General discussion

Over the last few decades, outcome in ALL has improved significantly, with 5 year EFS in the UK increasing from 35% in 1972, to 87.2% in the most recently closed UKALL trial, UKALL 2003 (Working Party on Leukaemia, 1986; Vora *et al.*, 2013b). This dramatic improvement has largely been due to the augmentation and intensification of ALL therapies, including the use of GCs. However, this has also brought with it an increase in toxicity. The UKALL 2003 trial reported a 5 year overall survival of around 91%, and greater than 3% treatment related mortality (TRM) (O'Connor *et al.*, 2014). Therefore, TRM makes up approximately a third of trial deaths, which is extremely high in a disease with such a good event free survival.

A key question is whether this treatment intensification is necessary in all patients, when around 50% of patients were cured on the much less intensive protocols of the 1980s. Furthermore, there are a proportion of patients still not cured, and who therefore do not benefit from intensified treatment and its associated adverse effects. Although modern day therapy is stratified based on a number of factors, there is clearly still a need for further treatment personalisation, to combat both the problems of under- and overexposure of treatment, including dex, in ALL patients. The aim of this project has therefore been to explore variables in dex therapy and response, to better understand how dex personalisation may be achieved. Key areas included dex pharmacokinetics, and cellular determinants of GC response, which may include intracellular dex accumulation, GR posttranslational modifications and B cell maturation state.

Personalisation using pharmacokinetics

Dose adjustment is of particular interest in guiding treatment of anticancer drugs, due to the narrow therapeutic window that exists between clinically effective and toxic drug exposures for the majority of cancer therapeutics (Paci *et al.*, 2014). Indeed wide pharmacokinetic variability is seen in many other cancer therapeutics, and successful therapeutic dose monitoring (TDM) approaches have been implemented with drugs such as carboplatin, methotrexate and 13-cis-retinoic acid (Stoller *et al.*, 1977; Chevreau *et al.*, 2005; Veal *et al.*, 2013). With dex, there are a number of points to consider before dose individualisation can be seen as a viable treatment option. In order to effectively develop a personalisation of dex dosing, factors such as disease heterogeneity and inter- and inpatient variability need to be considered.

The substantial pharmacokinetic variation seen in the study by Yang *et al.* (2008) has been replicated in this patients on the UKALL 2011 trial; extensive inter-patient variability was seen in dex exposure, as defined by AUC_{0-12h} and clearance, on both the short ($10mg/m^2 \times 14$ days) and standard ($6mg/m^2 \times 28$ days) arms of the trial's first randomisation, R1. Furthermore, although dex exposure was significantly higher on the short arm after a single dose of dex, there was substantial overlap between the two arms. A number of patients on the standard arm displayed higher exposures than those on the short arm, despite having a longer duration of treatment. Importantly, this pharmacokinetic variability was reflected in the results of UKALL2011 R1. A futility analysis performed in April 2017, with a median follow up time of 20.4 months, found that there was no statistically significant difference between the arms in terms of MRD response, steroid-related toxicity or relapse free survival (Goulden *et al.*, unpublished).

In this study, a relationship was seen between dex exposure and day 8 blast count, with patients exhibiting a blast count of $<5\%$ having a statistically higher exposure to dex AUC_{0-12h} . However, there was no difference in day 8 blast count between the two treatment arms of R1. This highlights the impact that such extensive variation in dex pharmacokinetics can have. The longer term effect of such an early dex response would have to be assessed. If early dex exposure was associated with a benefit in terms of long term outcome, the measurement of dex plasma concentrations could enable the modification of dex dose in those patients achieving potentially sub therapeutic or particularly high exposures to dex. However, in some high exposure, high-risk groups, it may not be appropriate to reduce treatment. Knowledge regarding the relationship between pharmacokinetics and toxicity from a longer follow up, however, could still be useful for the prediction and consequentially better detection of toxicity, allowing prompt and effective treatment.

Inpatient variability can affect TDM strategies, and in this study, a certain degree of inpatient variability was seen. However, if a cause for such variability is determined, this can be appropriately factored into a TDM equation. Several potential reasons for inpatient variability were identified in the current study, such as the concomitant administration of asparaginase and other concomitant medications. In this study, patients who had received two doses of asparaginase had a greater inpatient variability in terms of AUC_{0-12h} and blood albumin concentrations.

Asparaginase administration was also highlighted as a source of inpatient variability in the trial by Yang *et al.* (2008).

Future studies in this area should focus on clarifying the source of inpatient variability, particularly focusing on the proposed relationship between dex and asparaginase. The inclusion of later sampling points during the delayed intensification phase of therapy, or international equivalent, would facilitate this and enable a more direct comparison to data generated by Yang *et al.* (2008). If inpatient variation was attributed to concomitant administration of asparaginase in an independent study, the decrease in dex clearance associated with asparaginase treatment would need to be factored into any proposed dex dose adjustment approach utilised for individual patients (Jackson *et al.*, 2016).

A TDM approach would be strengthened if a therapeutic window for dex was defined, and correlations between plasma dex concentrations, and apoptosis in ALL cells were determined. However, ALL is a heterogeneous disease, with multiple subtypes displaying different molecular characteristics and prognoses. It may well be that the therapeutic window for dex is different in defined patient subpopulations, and investigation of ALL as one disease may not allow the effects of variables in different patient subgroups to be identified. Therefore, future studies may generate more valuable data through evaluation of these groups individually. This would be challenging based on the numbers of patients at a national level, and sub-group specific research would be facilitated if there was a common therapy backbone worldwide. Comparisons would then be possible across an international cohort of patients. This would require carefully planned prospective studies to further elucidate relationships between dex pharmacokinetics and clinical outcome and toxicity in large patient populations (Jackson *et al.*, 2016).

Consideration should also be given to the feasibility of TDM approaches for children with ALL, as other paediatric cancers which utilise TDM, such as high risk neuroblastoma, have a much lower incidence. The assay utilised in this project would not be practical for use with over 400 new patients a year, for reasons including the high demand on research nurses, dry ice shipment of samples and a lengthy extraction process. A possible alternative would be the use of dried spots collected with Guthrie

Cards or Mitra blood sampling devices, which would allow transport at room temperature and sample collection at home. For example, the Newcastle Cancer Centre Pharmacology Group has been testing Mitra blood sampling devices with dex in blood spots, and has developed a linear and robust method with a limit of quantification of 2ng/ml. The extraction process is simple and it is easy to process over 100 samples simultaneously.

Personalisation using pharmacogenetics

Although no pharmacogenetic studies have been included in this project, this still represents an important avenue of investigation as a way of personalising therapy, particularly as a number of the genes involved in both the pharmacokinetics and mechanism of action of dex exhibit polymorphisms. A clinically important example of personalisation of an anticancer drug using pharmacogenetic information is the administration of azathioprine and 6-mercaptopurine in relation to TPMT genotype (McLeod *et al.*, 2000; Relling *et al.*, 2013).

To date there have been contradictory reports from pharmacogenetic studies regarding the effects of different SNPs on GC response. This may, in part, be due to a limited amount of research in relatively small groups of patients. As discussed for pharmacokinetics, it would be beneficial to confirm these findings in larger cohorts, which would allow evaluation of whether such relationships are consistent across different ALL subgroups. Analysis of patient data from previous trials has been limited by the incomplete collection of high quality clinical data. Future studies should therefore endeavour to gather detailed clinical information alongside DNA to facilitate powerful genetic analyses, such as genome-wide association studies (GWAS). This will enable the collection of meaningful datasets relating to the potential impact of pharmacogenetic variation on clinical parameters, such as the incidence and severity of osteonecrosis associated with dex treatment (Karol *et al.*, 2015).

Looking forward, with regards to this project, it would be useful to perform two types of studies. Firstly, to continue to take a global approach and analyse the effect of genetic variation on pharmacokinetics as well as outcome, as this might provide an explanation for the extent of pharmacokinetic variation seen in ALL patients. As DNA samples have been collected as part of the UKALL 2011 trial, a candidate gene analysis

could be performed to assess the impact of variation in key genes relating to dex pharmacokinetic and mechanism of action. However, in the current project it has been shown that dex may not be a strong substrate for MDR1, therefore this would not need to be included in the panel of candidate genes to be investigated.

Secondly, a case control study could be performed, investigating the impact of pharmacogenetic variation on steroid induced toxicity. It would be sensible to use experience of hypertension as a measure of steroid induced toxicity. Hypertension is a frequently measured and objective parameter, which cannot be attributed to other drugs used in induction therapy. This would allow identification of SNPs relevant to steroid toxicity rather than experience of toxicity overall.

If any associations were found, the impact and costs of such a test would need to be evaluated. Although genetic testing is currently relatively expensive, the cost and ease of genetic testing is advancing all the time. Similarly, if a SNP was associated with increased toxicity, it may not be that therapy is reduced, but that increased vigilance is taken with these patients to identify and treat the associated toxicity effectively.

Personalisation using molecular oncology

There are a number of approaches to explore for stratification of dex based on current knowledge of its molecular pharmacology. One well-investigated option is using *in vitro* dex sensitivity to adjust dosing. Several studies have highlighted a correlation between *in vitro* dex sensitivity and dex response, even in low risk groups (Hongo *et al.*, 1997; Kaspers *et al.*, 1997; Frost *et al.*, 2003). Den Boer *et al.* (2003) proposed that such an approach could be used as a way of identifying patients who may benefit from a therapy reduction, for example those with multiple low risk variables including low MRD and high drug sensitivity.

However, this approach to dose stratification would only be appropriate for patients who are highly sensitive to dex. It is also essential to consider the treatment personalisation strategy for patients who display dex resistance. In this project, many patients who displayed resistance to dex had GI_{50s} that were greater than any patient on either arm of the UKALL 2011 trial. Those patients exhibiting high dex GI₅₀ values would be less likely to obtain a clinical benefit from dex at a dose equivalent to that

used in the UKALL 2011 trial, but may still suffer toxicity. Several molecular variables have therefore been investigated in this project to better understand decreased dex sensitivity and ways in which this can be reversed.

In the past, studies have focused on deletion or mutation of the GR as a mechanism of resistance. However, although slightly more common at relapse, GR deletion and mutations are rare in patient samples (Irving *et al.*, 2005b; Irving *et al.*, 2016). In this project, all patients appeared to have normal GR levels which and underwent phosphorylation at serine 211 on stimulation with dex, a sign of activation associated with nuclear translocation. This is a further indication of the rarity of GR deletions and mutations a cause of GC resistance.

Nevertheless, as would be expected, patients with deletions at relapse have been associated with an increased risk of induction failure, second relapse, and also have a reduced overall survival (Irving *et al.*, 2016). Therefore, in patients with GR deletions and mutations, it may be sensible to avoid treatment with dex, in order to limit dex exposure and subsequent unnecessary toxicity. Treatment in these situations could be focussed on other core chemotherapeutics, such as vincristine, or targeted therapies, as will be discussed below. Testing for GR is possible using MLPA (multiplex ligation-dependent probe amplification) or FISH (fluorescence in situ hybridisation), two tests commonly used to detect other genetic changes in ALL. However, due to the infrequency of this situation, a cost-benefit analysis would need to be performed to establish the feasibility of testing ALL patients for a GR deletions, even at relapse.

However, as GR mutation and deletion do not explain the majority of dex resistance in ALL, other mechanisms were assessed as potential approaches of personalising therapy. Firstly, intracellular drug accumulation in sensitive and resistant ALL cells was measured, including the role within this of the multidrug transporter, MDR1. While pharmacokinetics and cellular response were shown to be hugely variable, variations in drug accumulation did not appear to be caused by MDR1 substrate specificity. Consequently, personalisation approaches involving genotyping for *MDR1* polymorphisms, or testing ALL cells for mutations in *MDR1*, are unlikely to be useful. Although the extent of variation in intracellular accumulation was comparable to that observed in dex pharmacokinetics, variation in intracellular accumulation does not

appear to play a key role in dex response in ALL cells, and therefore does not provide a strategy for dex personalisation.

Secondly, variation in the GR cIEF profiles (comprising GR post-translational modifications and GR interacting proteins), was also studied as a potential stratification approach. Although previous work had identified differences between sensitive and resistant cells, these differences were not seen here. In this project, a novel epitope unmasking event was possibly identified. This could be further studied through analysis of the interaction between the GR and its heteromeric complex, however there were no consistent differences observed between sensitive and resistant cells in the epitope unmasking event. Moreover, alteration in epitope unmasking would likely affect the ability of the GR to bind GC and translocate to the nucleus. As resistant cells are generally able to translocate successfully to the nucleus, it is likely this is not a cause of resistance and it would thus be better to focus research aimed at re-sensitising ALL cells to dex on post-GR mechanisms of resistance.

Finally, B cell maturation state was investigated as a cause of dex resistance in ALL cells. Previous studies have highlighted a role of maturation state as a way of evading GC therapy in ALL (Rhein *et al.*, 2007; Nicholson *et al.*, 2015). Furthermore, non ALL studies have reported an inverse relationship of maturation with sensitivity to both synthetic and endogenous GCs (Lill-Elghanian *et al.*, 2002). In this project, ALL cells clustered together by dex sensitivity based on their expression of Wanderlust markers. Although it was not possible to accurately order cells in terms of maturation state due to problems reconstructing the B cell developmental trajectory, resistant cells appeared to have a different maturation phenotype to sensitive cells. This was based on their differential expression of Wanderlust markers, although further work is needed to ascertain whether dex resistant cells were more or less mature than sensitive cells.

If dex resistant cells are found to have a more mature phenotype, consistent with previous studies, the maturation state of ALL cells could be targeted as a way to re-sensitise therapy using phenotypic differences of more mature cells. For example, Nicholson *et al.* (2015) showed that increased maturation was associated with altered PAX5 levels and JNK activation. Therefore, approaches like JNK inhibition could be

used in these cells, as JNK inhibition was shown to increase dex sensitivity 30-fold in cell lines, to a GI₅₀ value that would be clinically achievable (Nicholson *et al.*, 2015). Similarly, Rhein *et al.*, (2007) found more mature cells had a change of expression of molecules related to the JAK-STAT pathway, and therefore this also provides a potential avenue for re-sensitisation.

As there will likely not be a single way to re-sensitise all patients to dex therapy, some approaches not explored as part of this project will be briefly discussed. Studies in the literature have mainly focused on combinations with other drugs as a way of re-sensitising cells to GCs. These include BCL2 antagonists (Miyashita and Reed, 1993) and mechanistic target of rapamycin (mTOR) inhibitor rapamycin, which is thought to modulate MCL1 (Wei *et al.*, 2006; Zhang *et al.*, 2011; Guo *et al.*, 2013). Due to the high incidence of *RAS* mutations in ALL, a role for MEK inhibitors has been identified by several groups (Irving *et al.*, 2014; Aries *et al.*, 2015; Jones *et al.*, 2015). This has been confirmed by the sensitisation of B ALL cell lines to dex by the MEK1/2 inhibitor, selumetinib (Polak *et al.*, 2016). Other possible drugs include arsenic trioxide (Bornhauser *et al.*, 2007), MAPK inhibitors (Garza *et al.*, 2009), and the glycolysis inhibitor 2-deoxyglucose (Eberhart *et al.*, 2009; Hulleman *et al.*, 2009) all of which have been shown to restore sensitivity in GC-resistant ALL cells. As much of this data has been generated in cell lines, further work is needed to validate these findings in primary patient cells.

Combined approach

Potentially one of the most useful approaches to achieving therapy personalisation would be a combined approach of targeted investigation, as previous research has generally focussed on individual areas of dex pharmacology.

For example, a pharmacokinetics-based personalisation approach does give not consideration to the response and sensitivity of the individual cancer cell. Conversely, using drug sensitivity assays or similar strategies to personalise therapy do not take into account the exposure of the leukaemic cells to dex. This combined approach could be achieved in future studies by assessing pharmacokinetics, pharmacogenetics and drug sensitivity simultaneously in an individual patient, and considering their combined effects on toxicity and outcome.

Similarly, in the situation of reduced cellular dex sensitivity, a combined approach could be taken to study the molecular pharmacology of dex. Published studies have used numerous experimental approaches to identify markers of resistance. In the clinical setting, in order to personalise dex therapy, it would be useful to have one method that could identify an appropriate dex re-sensitising agent. The further development of mass cytometry approaches would aid this, as mass cytometry can assess up to 40 parameters simultaneously in individual cells. Multi-purpose metal conjugated antibody panels could be designed to incorporate CD-antigens to detect MRD, maturation markers, and phospho-antibodies to investigate pathway activation as therapeutic targets. This would enable the appropriate dex re-sensitisation agent to be used at an individual patient level. For example, if a change in MAPK signalling was identified, a MEK inhibitor such as selumetinib could be used. Similarly if cells of a more mature phenotype were seen, a JAK inhibitor could be prescribed in an attempt to re-sensitise patients to dex.

However, there is clearly more work and validation that needs to be done before this situation becomes a realistic possibility. For example, a TDM approach may not be possible if intra-patient variability is too high. Similarly, the feasibility of using drug sensitivity assays to predict cellular dex response, and subsequent mass cytometry tests to establish a potential cause of resistance, would have to be evaluated in a clinical setting. In terms of finance, the additional cost of stratifying therapy would also need to be justified (Jackson *et al.*, 2016).

Conclusions

Although a large focus of cancer research is directed at novel targeted therapies, for the majority of cancers, old drugs still form a fundamental component of treatment. As a result, patients are subjected to both long and short-term toxicities. It is therefore important, where feasible, to personalise these therapies to achieve the best possible clinical outcome for patients whilst reducing the chances of treatment related morbidity and mortality. This is particularly relevant in ALL, as, while the majority of children are now treated successfully, there are significant problems associated with the levels of toxicity experienced by children.

Dex is a central component of treatment in childhood ALL and patients display wide inter-patient dex pharmacokinetic variability. At a cellular level, there are also clearly differences in dex response, with a wide range of dex sensitivities seen between patients. For the future optimisation of therapy, it would be useful to define an optimal exposure to dex, which results in minimal toxicity and maximum cancer cell death. The aim of personalised treatment would be better achieved through prospective studies focused on defining the source of both inter- and intra-patient variability, and the effect of ALL subtype within this. A strategy of targeted investigation would help to achieve this aim more efficiently, as there is still much to be learned about the clinical and molecular pharmacology of dex.

There is a broad spectrum of causes for reduced sensitivity to dex, however this project has highlighted a role for altered maturation state as a way of evading dex cytotoxicity in some resistant ALL cells. All-encompassing approaches like mass cytometry provide opportunities to ask many questions simultaneously about the foundation of dex resistance, and how therefore to best re-sensitise the patient to dex.

Despite advances in targeted therapy, the excellent outcome for patients with ALL means that conventional chemotherapy is unlikely to be replaced in the foreseeable future. Optimisation of therapies such as dex is therefore important, to lessen the considerable short and long term impact of toxicity on patient quality of life. While other drugs also contribute to the successful treatment of childhood ALL, the generation of additional knowledge regarding dex personalisation may enable novel approaches and improvement to treatment.

Bibliography

- Abrams, M.T., Robertson, N.M., Yoon, K. and Wickstrom, E. (2004) 'Inhibition of glucocorticoid-induced apoptosis by targeting the major splice variants of BIM mRNA with small interfering RNA and short hairpin RNA', *J Biol Chem*, 279(53), pp. 55809-17.
- Amacher, D.E. (2012) 'The primary role of hepatic metabolism in idiosyncratic drug-induced liver injury', *Expert Opin Drug Metab Toxicol*, 8(3), pp. 335-47.
- Anderer, G., Schrappe, M., Brechlin, A.M., Lauten, M., Muti, P., Welte, K. and Stanulla, M. (2000) 'Polymorphisms within glutathione S-transferase genes and initial response to glucocorticoids in childhood acute lymphoblastic leukaemia', *Pharmacogenetics*, 10(8), pp. 715-26.
- Andrews, E. and Daly, A.K. (2008) 'Flucloxacillin-induced liver injury', *Toxicology*, 254(3), pp. 158-63.
- Antakly, T., O'Donnell, D. and Thompson, E.B. (1990) 'Immunocytochemical localization of the glucocorticoid receptor in steroid-sensitive and -resistant human leukemic cells', *Cancer Res*, 50(4), pp. 1337-45.
- Anthony, V.M., Hazel, R., Claire, S., Sue, M.R., Jeremy, H., Christopher, D.M., Nicholas, G., Ajay, V. and Christine, J.H. (2013) 'Risk-Directed Treatment Intensification Significantly Reduces the Risk of Relapse Among Children and Adolescents With Acute Lymphoblastic Leukemia and Intrachromosomal Amplification of Chromosome 21: A Comparison of the MRC ALL97/99 and UKALL2003 Trials', *Journal of Clinical Oncology*, 31(27), pp. 3389-3396.
- Aries, I.M., van den Dungen, R.E., Koudijs, M.J., Cuppen, E., Voest, E., Molenaar, J.J., Caron, H.N., Pieters, R. and den Boer, M.L. (2015) 'Towards personalized therapy in pediatric acute lymphoblastic leukemia: RAS mutations and prednisolone resistance', *Haematologica*, 100(4), pp. e132-6.
- Armstrong, S.A. and Look, A.T. (2005) 'Molecular genetics of acute lymphoblastic leukemia', *J Clin Oncol*, 23(26), pp. 6306-15.
- Arseniev, L., Pickerd, N., Goudeva, L., Hertenstein, B. and Ganser, A. (1999) 'Comparative evaluation of commonly used clones and fluorochrome conjugates of monoclonal antibodies for CD34 antigen detection', *J Hematother Stem Cell Res*, 8(5), pp. 547-59.
- Asselin, B.L. (2012) 'The right dose for the right patient', *Blood*, 119(7), pp. 1617-8.
- Bachmann, P.S., Gorman, R., Mackenzie, K.L., Lutze-Mann, L. and Lock, R.B. (2005) 'Dexamethasone resistance in B-cell precursor childhood acute lymphoblastic leukemia occurs downstream of ligand-induced nuclear translocation of the glucocorticoid receptor', *Blood*, 105(6), pp. 2519-26.
- Bachmann, P.S., Gorman, R., Papa, R.A., Bardell, J.E., Ford, J., Kees, U.R., Marshall, G.M. and Lock, R.B. (2007) 'Divergent mechanisms of glucocorticoid resistance in

experimental models of pediatric acute lymphoblastic leukemia', *Cancer Res*, 67(9), pp. 4482-90.

Balamurugan, S., Sugapriya, D., Shanthi, P., Thilaka, V., Venkatesilalu, S., Pushpa, V. and Madhavan, M. (2007) 'Multidrug resistance 1 gene expression and AgNOR in childhood acute leukemias', *Indian J Hematol Blood Transfus*, 23(3-4), pp. 73-8.

Balis, F.M., Lester, C.M., Chrousos, G.P., Heideman, R.L. and Poplack, D.G. (1987) 'Differences in cerebrospinal fluid penetration of corticosteroids: possible relationship to the prevention of meningeal leukemia', *J Clin Oncol*, 5(2), pp. 202-7.

Bandura, D.R., Baranov, V.I., Ornatsky, O.I., Antonov, A., Kinach, R., Lou, X., Pavlov, S., Vorobiev, S., Dick, J.E. and Tanner, S.D. (2009) 'Mass cytometry: technique for real time single cell multitarget immunoassay based on inductively coupled plasma time-of-flight mass spectrometry', *Anal Chem*, 81(16), pp. 6813-22.

Bartram, J., Wade, R., Vora, A., Hancock, J., Mitchell, C., Kinsey, S., Steward, C., Moppett, J. and Goulden, N. (2016) 'Excellent outcome of minimal residual disease-defined low-risk patients is sustained with more than 10 years follow-up: results of UK paediatric acute lymphoblastic leukaemia trials 1997-2003', *Arch Dis Child*, 101(5), pp. 449-54.

Beck, J., Niethammer, D. and Gekeler, V. (1996) 'MDR1, MRP, topoisomerase II α /beta, and cyclin A gene expression in acute and chronic leukemias', *Leukemia*, 10 Suppl 3, pp. S39-s45.

Behbehani, G.K., Thom, C., Zunder, E.R., Finck, R., Gaudilliere, B., Fragiadakis, G.K., Fantl, W.J. and Nolan, G.P. (2014) 'Transient partial permeabilization with saponin enables cellular barcoding prior to surface marker staining()', *Cytometry. Part A : the journal of the International Society for Analytical Cytology*, 85(12), pp. 1011-1019.

Bendall, S.C., Davis, K.L., Amir el, A.D., Tadmor, M.D., Simonds, E.F., Chen, T.J., Shenfeld, D.K., Nolan, G.P. and Pe'er, D. (2014) 'Single-cell trajectory detection uncovers progression and regulatory coordination in human B cell development', *Cell*, 157(3), pp. 714-25.

Bendall, S.C., Nolan, G.P., Roederer, M. and Chattopadhyay, P.K. (2012) 'A deep profiler's guide to cytometry', *Trends Immunol*, 33(7), pp. 323-32.

Bendall, S.C., Simonds, E.F., Qiu, P., Amir el, A.D., Krutzik, P.O., Finck, R., Bruggner, R.V., Melamed, R., Trejo, A., Ornatsky, O.I., Balderas, R.S., Plevritis, S.K., Sachs, K., Pe'er, D., Tanner, S.D. and Nolan, G.P. (2011) 'Single-cell mass cytometry of differential immune and drug responses across a human hematopoietic continuum', *Science*, 332(6030), pp. 687-96.

Bercovich, D., Ganmore, I., Scott, L.M., Wainreb, G., Birger, Y., Elimelech, A., Shochat, C., Cazzaniga, G., Biondi, A., Basso, G., Cario, G., Schrappe, M., Stanulla, M., Strehl, S., Haas, O.A., Mann, G., Binder, V., Borkhardt, A., Kempski, H., Trka, J., Bielorei, B., Avigad, S., Stark, B., Smith, O., Dastugue, N., Bourquin, J.P., Tal, N.B., Green, A.R. and Izraeli, S. (2008) 'Mutations of JAK2 in acute lymphoblastic leukaemias associated with Down's syndrome', *Lancet*, 372(9648), pp. 1484-92.

- Bhojwani, D., Pei, D., Sandlund, J.T., Jeha, S., Ribeiro, R.C., Rubnitz, J.E., Raimondi, S.C., Shurtleff, S., Onciu, M., Cheng, C., Coustan-Smith, E., Bowman, W.P., Howard, S.C., Metzger, M.L., Inaba, H., Leung, W., Evans, W.E., Campana, D., Relling, M.V. and Pui, C.H. (2012) 'ETV6-RUNX1-positive childhood acute lymphoblastic leukemia: improved outcome with contemporary therapy', *Leukemia*, 26(2), pp. 265-70.
- Bjellqvist, B., Hughes, G.J., Pasquali, C., Paquet, N., Ravier, F., Sanchez, J.C., Frutiger, S. and Hochstrasser, D. (1993) 'The focusing positions of polypeptides in immobilized pH gradients can be predicted from their amino acid sequences', *Electrophoresis*, 14(10), pp. 1023-31.
- Bjornson, Z.B., Nolan, G.P. and Fantl, W.J. (2013) 'Single-cell mass cytometry for analysis of immune system functional states', *Curr Opin Immunol*, 25(4), pp. 484-94.
- Bodwell, J.E., Webster, J.C., Jewell, C.M., Cidlowski, J.A., Hu, J.M. and Munck, A. (1998) 'Glucocorticoid receptor phosphorylation: overview, function and cell cycle-dependence', *J Steroid Biochem Mol Biol*, 65(1-6), pp. 91-9.
- Bokemeyer, A., Eckert, C., Meyr, F., Koerner, G., von Stackelberg, A., Ullmann, R., Turkmen, S., Henze, G. and Seeger, K. (2014) 'Copy number genome alterations are associated with treatment response and outcome in relapsed childhood ETV6/RUNX1-positive acute lymphoblastic leukemia', *Haematologica*, 99(4), pp. 706-14.
- Bonapace, L., Bornhauser, B.C., Schmitz, M., Cario, G., Ziegler, U., Niggli, F.K., Schafer, B.W., Schrappe, M., Stanulla, M. and Bourquin, J.P. (2010) 'Induction of autophagy-dependent necroptosis is required for childhood acute lymphoblastic leukemia cells to overcome glucocorticoid resistance', *J Clin Invest*, 120(4), pp. 1310-23.
- Bornhauser, B.C., Bonapace, L., Lindholm, D., Martinez, R., Cario, G., Schrappe, M., Niggli, F.K., Schafer, B.W. and Bourquin, J.P. (2007) 'Low-dose arsenic trioxide sensitizes glucocorticoid-resistant acute lymphoblastic leukemia cells to dexamethasone via an Akt-dependent pathway', *Blood*, 110(6), pp. 2084-91.
- Bostrom, B.C., Sensel, M.R., Sather, H.N., Gaynon, P.S., La, M.K., Johnston, K., Erdmann, G.R., Gold, S., Heerema, N.A., Hutchinson, R.J., Provisor, A.J. and Trigg, M.E. (2003) 'Dexamethasone versus prednisone and daily oral versus weekly intravenous mercaptopurine for patients with standard-risk acute lymphoblastic leukemia: a report from the Children's Cancer Group', *Blood*, 101(10), pp. 3809-17.
- Buemann, B., Vohl, M.C., Chagnon, M., Chagnon, Y.C., Gagnon, J., Perusse, L., Dionne, F., Despres, J.P., Tremblay, A., Nadeau, A. and Bouchard, C. (1997) 'Abdominal visceral fat is associated with a BclI restriction fragment length polymorphism at the glucocorticoid receptor gene locus', *Obes Res*, 5(3), pp. 186-92.
- Burke, G.A., Estlin, E.J. and Lowis, S.P. (1999) 'The role of pharmacokinetic and pharmacodynamic studies in the planning of protocols for the treatment of childhood cancer', *Cancer Treat Rev*, 25(1), pp. 13-27.
- Cadepond, F., Binart, N., Chambrud, B., Jibard, N., Schweizer-Groyer, G., Segard-Maurel, I. and Baulieu, E.E. (1993) 'Interaction of glucocorticosteroid receptor and wild-type or mutated 90- kDa heat shock protein coexpressed in baculovirus-infected

Sf9 cells', *Proceedings of the National Academy of Sciences of the United States of America*, 90(22), pp. 10434-10438.

Cadepond, F., Schweizer-Groyer, G., Segard-Maurel, I., Jibard, N., Hollenberg, S.M., Giguère, V., Evans, R.M. and Baulieu, E.E. (1991) 'Heat shock protein 90 as a critical factor in maintaining glucocorticosteroid receptor in a nonfunctional state', *Journal of Biological Chemistry*, 266(9), pp. 5834-5841.

Cairo, M.S. (1982) 'Adverse reactions of L-asparaginase', *Am J Pediatr Hematol Oncol*, 4(3), pp. 335-9.

Cancer Research UK. Available at: <http://www.cancerresearchuk.org/health-professional/cancer-statistics/childrens-cancers/incidence#heading-Four> (Accessed: 19/07/17).

Cario, G., Zimmermann, M., Romey, R., Gesk, S., Vater, I., Harbott, J., Schrauder, A., Moericke, A., Izraeli, S., Akasaka, T., Dyer, M.J., Siebert, R., Schrappe, M. and Stanulla, M. (2010) 'Presence of the P2RY8-CRLF2 rearrangement is associated with a poor prognosis in non-high-risk precursor B-cell acute lymphoblastic leukemia in children treated according to the ALL-BFM 2000 protocol', *Blood*, 115(26), pp. 5393-7.

Casale, F., D'Angelo, V., Addeo, R., Caraglia, M., Crisci, S., Rondelli, R., Di Tullio, M.T. and Indolfi, P. (2004) 'P-glycoprotein 170 expression and function as an adverse independent prognostic factor in childhood acute lymphoblastic leukemia', *Oncol Rep*, 12(6), pp. 1201-7.

Case, M., Matheson, E., Minto, L., Hassan, R., Harrison, C.J., Bown, N., Bailey, S., Vormoor, J., Hall, A.G. and Irving, J.A. (2008) 'Mutation of genes affecting the RAS pathway is common in childhood acute lymphoblastic leukemia', *Cancer Res*, 68(16), pp. 6803-9.

Cass, C.E., Janowska-Wieczorek, A., Lynch, M.A., Sheinin, H., Hindenburg, A.A. and Beck, W.T. (1989) 'Effect of duration of exposure to verapamil on vincristine activity against multidrug-resistant human leukemic cell lines', *Cancer Res*, 49(21), pp. 5798-804.

Cave, H., van der Werff ten Bosch, J., Suci, S., Guidal, C., Waterkeyn, C., Otten, J., Bakkus, M., Thielemans, K., Grandchamp, B. and Vilmer, E. (1998) 'Clinical significance of minimal residual disease in childhood acute lymphoblastic leukemia. European Organization for Research and Treatment of Cancer--Childhood Leukemia Cooperative Group', *N Engl J Med*, 339(9), pp. 591-8.

Chen, C.L., Liu, Q., Pui, C.H., Rivera, G.K., Sandlund, J.T., Ribeiro, R., Evans, W.E. and Relling, M.V. (1997) 'Higher frequency of glutathione S-transferase deletions in black children with acute lymphoblastic leukemia', *Blood*, 89(5), pp. 1701-7.

Chen, Y.L., Jiang, X.Y. and Weng, N.D. (2002) 'A liquid chromatographic-tandem mass spectrometric method for the quantitative analysis of dexamethasone in human plasma', *Journal of Liquid Chromatography & Related Technologies*, 25(9), pp. 1317-1334.

Chessells, J.M., Bailey, C. and Richards, S.M. (1995) 'Intensification of treatment and survival in all children with lymphoblastic leukaemia: results of UK Medical Research Council trial UKALL X. Medical Research Council Working Party on Childhood Leukaemia', *Lancet*, 345(8943), pp. 143-8.

Chessells, J.M., Harrison, G., Richards, S.M., Gibson, B.E., Bailey, C.C., Hill, F.G. and Hann, I.M. (2002) 'Failure of a new protocol to improve treatment results in paediatric lymphoblastic leukaemia: lessons from the UK Medical Research Council trials UKALL X and UKALL XI', *Br J Haematol*, 118(2), pp. 445-55.

Chevreau, C., Thomas, F., Couteau, C., Dalenc, F., Mourey, L. and Chatelut, E. (2005) 'Ototoxicity of high-dose carboplatin', *J Clin Oncol*, 23(15), pp. 3649-50; author reply 3650-1.

Chiaretti, S., Zini, G. and Bassan, R. (2014) 'Diagnosis and subclassification of acute lymphoblastic leukemia', *Mediterr J Hematol Infect Dis*, 6(1), p. e2014073.

Christoforou, A.L. and Lilley, K.S. (2012) 'Isobaric tagging approaches in quantitative proteomics: the ups and downs', *Anal Bioanal Chem*, 404(4), pp. 1029-37.

Cole, S.P., Bhardwaj, G., Gerlach, J.H., Mackie, J.E., Grant, C.E., Almquist, K.C., Stewart, A.J., Kurz, E.U., Duncan, A.M. and Deeley, R.G. (1992) 'Overexpression of a transporter gene in a multidrug-resistant human lung cancer cell line', *Science*, 258(5088), pp. 1650-4.

Conter, V., Bartram, C.R., Valsecchi, M.G., Schrauder, A., Panzer-Grumayer, R., Moricke, A., Arico, M., Zimmermann, M., Mann, G., De Rossi, G., Stanulla, M., Locatelli, F., Basso, G., Niggli, F., Barisone, E., Henze, G., Ludwig, W.D., Haas, O.A., Cazzaniga, G., Koehler, R., Silvestri, D., Bradtke, J., Parasole, R., Beier, R., van Dongen, J.J., Biondi, A. and Schrappe, M. (2010) 'Molecular response to treatment redefines all prognostic factors in children and adolescents with B-cell precursor acute lymphoblastic leukemia: results in 3184 patients of the AIEOP-BFM ALL 2000 study', *Blood*, 115(16), pp. 3206-14.

Costlow, M.E., Pui, C.H. and Dahl, G.V. (1982) 'Glucocorticoid receptors in childhood acute lymphocytic leukemia', *Cancer Res*, 42(11), pp. 4801-6.

Daly, A.K. (2003) 'Pharmacogenetics of the major polymorphic metabolizing enzymes', *Fundam Clin Pharmacol*, 17(1), pp. 27-41.

'Database Resources of the National Center for Biotechnology Information', (2017) *Nucleic Acids Res*, 45(D1), pp. D12-d17.

Davies, S.M., Bhatia, S., Ross, J.A., Kiffmeyer, W.R., Gaynon, P.S., Radloff, G.A., Robison, L.L. and Perentesis, J.P. (2002a) 'Glutathione S-transferase genotypes, genetic susceptibility, and outcome of therapy in childhood acute lymphoblastic leukemia', *Blood*, 100(1), pp. 67-71.

Davies, T.H., Ning, Y.M. and Sanchez, E.R. (2002b) 'A new first step in activation of steroid receptors: hormone-induced switching of FKBP51 and FKBP52 immunophilins', *J Biol Chem*, 277(7), pp. 4597-600.

- Demeule, M., Jodoin, J., Beaulieu, E., Brossard, M. and Beliveau, R. (1999) 'Dexamethasone modulation of multidrug transporters in normal tissues', *FEBS Lett*, 442(2-3), pp. 208-14.
- Den Boer, M.L., Harms, D.O., Pieters, R., Kazemier, K.M., Gobel, U., Korholz, D., Graubner, U., Haas, R.J., Jorch, N., Spaar, H.J., Kaspers, G.J., Kamps, W.A., Van der Does-Van den Berg, A., Van Wering, E.R., Veerman, A.J. and Janka-Schaub, G.E. (2003) 'Patient stratification based on prednisolone-vincristine-asparaginase resistance profiles in children with acute lymphoblastic leukemia', *J Clin Oncol*, 21(17), pp. 3262-8.
- Den Boer, M.L., Pieters, R., Kazemier, K.M., Janka-Schaub, G.E., Henze, G., Creutzig, U., Kaspers, G.J., Kearns, P.R., Hall, A.G., Pearson, A.D. and Veerman, A.J. (1999) 'Different expression of glutathione S-transferase alpha, mu and pi in childhood acute lymphoblastic and myeloid leukaemia', *Br J Haematol*, 104(2), pp. 321-7.
- den Boer, M.L., Pieters, R., Kazemier, K.M., Rottier, M.M., Zwaan, C.M., Kaspers, G.J., Janka-Schaub, G., Henze, G., Creutzig, U., Scheper, R.J. and Veerman, A.J. (1998) 'Relationship between major vault protein/lung resistance protein, multidrug resistance-associated protein, P-glycoprotein expression, and drug resistance in childhood leukemia', *Blood*, 91(6), pp. 2092-8.
- Den Boer, M.L., van Slegtenhorst, M., De Menezes, R.X., Cheok, M.H., Buijs-Gladdines, J.G., Peters, S.T., Van Zutven, L.J., Beverloo, H.B., Van der Spek, P.J., Escherich, G., Horstmann, M.A., Janka-Schaub, G.E., Kamps, W.A., Evans, W.E. and Pieters, R. (2009) 'A subtype of childhood acute lymphoblastic leukaemia with poor treatment outcome: a genome-wide classification study', *Lancet Oncol*, 10(2), pp. 125-34.
- Denny, W.B., Valentine, D.L., Reynolds, P.D., Smith, D.F. and Scammell, J.G. (2000) 'Squirrel monkey immunophilin FKBP51 is a potent inhibitor of glucocorticoid receptor binding', *Endocrinology*, 141(11), pp. 4107-13.
- Dhaini, H.R., Thomas, D.G., Giordano, T.J., Johnson, T.D., Biermann, J.S., Leu, K., Hollenberg, P.F. and Baker, L.H. (2003) 'Cytochrome P450 CYP3A4/5 expression as a biomarker of outcome in osteosarcoma', *J Clin Oncol*, 21(13), pp. 2481-5.
- Dhooge, C., De Moerloose, B., Laureys, G., Ferster, A., De Bacquer, D., Philippe, J., Leroy, J. and Benoit, Y. (2002) 'Expression of the multidrug transporter P-glycoprotein is highly correlated with clinical outcome in childhood acute lymphoblastic leukemia: results of a long-term prospective study', *Leuk Lymphoma*, 43(2), pp. 309-14.
- Dobson, M.G., Redfern, C.P., Unwin, N. and Weaver, J.U. (2001) 'The N363S polymorphism of the glucocorticoid receptor: potential contribution to central obesity in men and lack of association with other risk factors for coronary heart disease and diabetes mellitus', *J Clin Endocrinol Metab*, 86(5), pp. 2270-4.
- Domenech, C., Suci, S., De Moerloose, B., Mazingue, F., Plat, G., Ferster, A., Uyttebroeck, A., Sirvent, N., Lutz, P., Yakouben, K., Munzer, M., Rohrlich, P., Plantaz, D., Millot, F., Philippet, P., Dastugue, N., Girard, S., Cave, H., Benoit, Y., Bertrandfor, Y., Children's Leukemia Group of European Organisation for, R. and Treatment of, C. (2014) 'Dexamethasone (6 mg/m²/day) and prednisolone (60 mg/m²/day) were

equally effective as induction therapy for childhood acute lymphoblastic leukemia in the EORTC CLG 58951 randomized trial', *Haematologica*, 99(7), pp. 1220-7.

Dordelmann, M., Reiter, A., Borkhardt, A., Ludwig, W.D., Gotz, N., Viehmann, S., Gadner, H., Riehm, H. and Schrappe, M. (1999) 'Prednisone response is the strongest predictor of treatment outcome in infant acute lymphoblastic leukemia', *Blood*, 94(4), pp. 1209-17.

Dumitrescu, L., Brown-Gentry, K., Goodloe, R., Glenn, K., Yang, W., Kornegay, N., Pui, C.H., Relling, M.V. and Crawford, D.C. (2011) 'Evidence for age as a modifier of genetic associations for lipid levels', *Ann Hum Genet*, 75(5), pp. 589-97.

Dunkley, T.P.J., Hester, S., Shadforth, I.P., Runions, J., Weimar, T., Hanton, S.L., Griffin, J.L., Bessant, C., Brandizzi, F., Hawes, C., Watson, R.B., Dupree, P. and Lilley, K.S. (2006) 'Mapping the Arabidopsis organelle proteome', *Proceedings of the National Academy of Sciences*, 103(17), pp. 6518-6523.

Dworzak, M.N., Schumich, A., Printz, D., Potschger, U., Husak, Z., Attarbaschi, A., Basso, G., Gaipa, G., Ratei, R., Mann, G. and Gadner, H. (2008) 'CD20 up-regulation in pediatric B-cell precursor acute lymphoblastic leukemia during induction treatment: setting the stage for anti-CD20 directed immunotherapy', *Blood*, 112(10), pp. 3982-8.

Eberhart, K., Renner, K., Ritter, I., Kastenberger, M., Singer, K., Hellerbrand, C., Kreutz, M., Kofler, R. and Oefner, P.J. (2009) 'Low doses of 2-deoxy-glucose sensitize acute lymphoblastic leukemia cells to glucocorticoid-induced apoptosis', *Leukemia*, 23(11), pp. 2167-70.

Eden, O.B., Lilleyman, J.S., Richards, S., Shaw, M.P. and Peto, J. (1991) 'Results of Medical Research Council Childhood Leukaemia Trial UKALL VIII (report to the Medical Research Council on behalf of the Working Party on Leukaemia in Childhood)', *Br J Haematol*, 78(2), pp. 187-96.

Eiser, C., Stride, C.B., Vora, A., Goulden, N., Mitchell, C., Buck, G., Adams, M. and Jenney, M.E.M. (2017) 'Prospective evaluation of quality of life in children treated in UKALL 2003 for acute lymphoblastic leukaemia: A cohort study', *Pediatr Blood Cancer*.

Elens, L., Nieuweboer, A., Clarke, S.J., Charles, K.A., de Graan, A.J., Haufroid, V., Mathijssen, R.H. and van Schaik, R.H. (2013a) 'CYP3A4 intron 6 C>T SNP (CYP3A4*22) encodes lower CYP3A4 activity in cancer patients, as measured with probes midazolam and erythromycin', *Pharmacogenomics*, 14(2), pp. 137-49.

Elens, L., van Gelder, T., Hesselink, D.A., Haufroid, V. and van Schaik, R.H. (2013b) 'CYP3A4*22: promising newly identified CYP3A4 variant allele for personalizing pharmacotherapy', *Pharmacogenomics*, 14(1), pp. 47-62.

Evans, A.E., Gilbert, E.S. and Zandstra, R. (1970) 'The increasing incidence of central nervous system leukemia in children. (Children's Cancer Study Group A)', *Cancer*, 26(2), pp. 404-9.

Evans, W.E. and McLeod, H.L. (2003) 'Pharmacogenomics--drug disposition, drug targets, and side effects', *N Engl J Med*, 348(6), pp. 538-49.

Fernandez, C.A., Smith, C., Yang, W., Date, M., Bashford, D., Larsen, E., Bowman, W.P., Liu, C., Ramsey, L.B., Chang, T., Turner, V., Loh, M.L., Raetz, E.A., Winick, N.J., Hunger, S.P., Carroll, W.L., Onengut-Gumuscu, S., Chen, W.M., Concannon, P., Rich, S.S., Scheet, P., Jeha, S., Pui, C.H., Evans, W.E., Devidas, M. and Relling, M.V. (2014) 'HLA-DRB1*07:01 is associated with a higher risk of asparaginase allergies', *Blood*, 124(8), pp. 1266-76.

Fienberg, H.G., Simonds, E.F., Fantl, W.J., Nolan, G.P. and Bodenmiller, B. (2012) 'A platinum-based covalent viability reagent for single-cell mass cytometry', *Cytometry A*, 81(6), pp. 467-75.

Finck, R., Simonds, E.F., Jager, A., Krishnaswamy, S., Sachs, K., Fantl, W., Pe'er, D., Nolan, G.P. and Bendall, S.C. (2013) 'Normalization of mass cytometry data with bead standards', *Cytometry A*, 83(5), pp. 483-94.

Findley, H.W., Jr., Cooper, M.D., Kim, T.H., Alvarado, C. and Ragab, A.H. (1982) 'Two new acute lymphoblastic leukemia cell lines with early B-cell phenotypes', *Blood*, 60(6), pp. 1305-9.

Fleury, I., Primeau, M., Doreau, A., Costea, I., Moghrabi, A., Sinnett, D. and Krajcinovic, M. (2004) 'Polymorphisms in genes involved in the corticosteroid response and the outcome of childhood acute lymphoblastic leukemia', *Am J Pharmacogenomics*, 4(5), pp. 331-41.

Fojo, A.T., Ueda, K., Slamon, D.J., Poplack, D.G., Gottesman, M.M. and Pastan, I. (1987) 'Expression of a multidrug-resistance gene in human tumors and tissues', *Proc Natl Acad Sci U S A*, 84(1), pp. 265-9.

Foley, G.E., Lazarus, H., Farber, S., Uzman, B.G., Boone, B.A. and McCarthy, R.E. (1965) 'Continuous Culture of Human Lymphoblasts from Peripheral Blood of a Child with Acute Leukemia', *Cancer*, 18, pp. 522-9.

French, D., Hamilton, L.H., Mattano, L.A., Jr., Sather, H.N., Devidas, M., Nachman, J.B. and Relling, M.V. (2008) 'A PAI-1 (SERPINE1) polymorphism predicts osteonecrosis in children with acute lymphoblastic leukemia: a report from the Children's Oncology Group', *Blood*, 111(9), pp. 4496-9.

Frost, B.M., Nygren, P., Gustafsson, G., Forestier, E., Jonsson, O.G., Kanerva, J., Nygaard, R., Schmiegelow, K., Larsson, R. and Lonnerholm, G. (2003) 'Increased in vitro cellular drug resistance is related to poor outcome in high-risk childhood acute lymphoblastic leukaemia', *Br J Haematol*, 122(3), pp. 376-85.

Gagne, V., Rousseau, J., Labuda, M., Sharif-Askari, B., Brukner, I., Laverdiere, C., Ceppi, F., Sallan, S.E., Silverman, L.B., Neuberg, D., Kutok, J.L., Sinnett, D. and Krajcinovic, M. (2013) 'Bim polymorphisms: influence on function and response to treatment in children with acute lymphoblastic leukemia', *Clin Cancer Res*, 19(18), pp. 5240-9.

Gale, K.B., Ford, A.M., Repp, R., Borkhardt, A., Keller, C., Eden, O.B. and Greaves, M.F. (1997) 'Backtracking leukemia to birth: Identification of clonotypic gene fusion sequences in neonatal blood spots', *Proceedings of the National Academy of Sciences*, 94(25), pp. 13950-13954.

- Garza, A.S., Miller, A.L., Johnson, B.H. and Thompson, E.B. (2009) 'Converting cell lines representing hematological malignancies from glucocorticoid-resistant to glucocorticoid-sensitive: signaling pathway interactions', *Leuk Res*, 33(5), pp. 717-27.
- Goasguen, J.E., Lamy, T., Bergeron, C., Ly Sunaram, B., Mordelet, E., Gorre, G., Dossot, J.M., Le Gall, E., Grosbois, B., Le Prise, P.Y. and Fauchet, R. (1996) 'Multifactorial drug-resistance phenomenon in acute leukemias: impact of P170-MDR1, LRP56 protein, glutathione-transferases and metallothionein systems on clinical outcome', *Leuk Lymphoma*, 23(5-6), pp. 567-76.
- Goulden, D.N. (2012) *United Kingdom National Randomised Trial for Children and Young Adults with Acute Lymphoblastic Leukaemia and Lymphoma 2011*. Clinical Trial Protocol. Cancer Research UK Clinical Trials Unit.
- Grausenburger, R., Bastelberger, S., Eckert, C., Kauer, M., Stanulla, M., Frech, C., Bauer, E., Stoiber, D., von Stackelberg, A., Attarbaschi, A., Haas, O.A. and Panzer-Grumayer, R. (2016) 'Genetic alterations in glucocorticoid signaling pathway components are associated with adverse prognosis in children with relapsed ETV6/RUNX1-positive acute lymphoblastic leukemia', *Leuk Lymphoma*, 57(5), pp. 1163-73.
- Greaves, M. (2005) 'In utero origins of childhood leukaemia', *Early Hum Dev*, 81(1), pp. 123-9.
- Greaves, M. (2006) 'Infection, immune responses and the aetiology of childhood leukaemia', *Nat Rev Cancer*, 6(3), pp. 193-203.
- Greaves, M.F., Maia, A.T., Wiemels, J.L. and Ford, A.M. (2003) 'Leukemia in twins: lessons in natural history', *Blood*, 102(7), pp. 2321-33.
- Gregers, J., Green, H., Christensen, I.J., Dalhoff, K., Schroeder, H., Carlsen, N., Rosthøj, S., Lausen, B., Schmiegelow, K. and Peterson, C. (2015) 'Polymorphisms in the ABCB1 gene and effect on outcome and toxicity in childhood acute lymphoblastic leukemia', *Pharmacogenomics J*.
- Griaud, F., Williamson, A.J., Taylor, S., Potier, D.N., Spooncer, E., Pierce, A. and Whetton, A.D. (2012) 'BCR/ABL modulates protein phosphorylation associated with the etoposide-induced DNA damage response', *J Proteomics*, 77, pp. 14-26.
- Gruber, G., Carlet, M., Turtscher, E., Meister, B., Irving, J.A., Ploner, C. and Kofler, R. (2009) 'Levels of glucocorticoid receptor and its ligand determine sensitivity and kinetics of glucocorticoid-induced leukemia apoptosis', *Leukemia*, 23(4), pp. 820-3.
- Guo, X., Zhou, C.Y., Li, Q., Gao, J., Zhu, Y.P., Gu, L. and Ma, Z.G. (2013) 'Rapamycin sensitizes glucocorticoid resistant acute lymphoblastic leukemia CEM-C1 cells to dexamethasone induced apoptosis through both mTOR suppression and up-regulation and activation of glucocorticoid receptor', *Biomed Environ Sci*, 26(5), pp. 371-81.
- Haber, M., Norris, M.D., Kavallaris, M., Bell, D.R., Davey, R.A., White, L. and Stewart, B.W. (1989) 'Atypical multidrug resistance in a therapy-induced drug-resistant human leukemia cell line (LALW-2): resistance to Vinca alkaloids independent of P-glycoprotein', *Cancer Res*, 49(19), pp. 5281-7.

- Hall, A.G., Autzen, P., Cattan, A.R., Malcolm, A.J., Cole, M., Kernahan, J. and Reid, M.M. (1994) 'Expression of mu class glutathione S-transferase correlates with event-free survival in childhood acute lymphoblastic leukemia', *Cancer Res*, 54(20), pp. 5251-4.
- Hall, S.L., Hester, S., Griffin, J.L., Lilley, K.S. and Jackson, A.P. (2009) 'The organelle proteome of the DT40 lymphocyte cell line', *Mol Cell Proteomics*, 8(6), pp. 1295-305.
- Halligan, B.D., Ruotti, V., Jin, W., Laffoon, S., Twigger, S.N. and Dratz, E.A. (2004) 'ProMoST (Protein Modification Screening Tool): a web-based tool for mapping protein modifications on two-dimensional gels', *Nucleic Acids Res*, 32(Web Server issue), pp. W638-44.
- Hama, Y., Urano, Y., Koyama, Y., Bernardo, M., Choyke, P.L. and Kobayashi, H. (2006) 'A comparison of the emission efficiency of four common green fluorescence dyes after internalization into cancer cells', *Bioconjug Chem*, 17(6), pp. 1426-31.
- Hanahan, D. and Weinberg, R.A. (2000) 'The hallmarks of cancer', *Cell*, 100(1), pp. 57-70.
- Hanahan, D. and Weinberg, R.A. (2011) 'Hallmarks of cancer: the next generation', *Cell*, 144(5), pp. 646-74.
- Hansch C., L.A., Hoekman D. (1995) 'Exploring QSAR - Hydrophobic, Electronic, and Steric Constants', *Washington, DC: American Chemical Society.*, p. 192.
- Harrison, C.J. (2015) 'Blood Spotlight on iAMP21 acute lymphoblastic leukemia (ALL), a high-risk pediatric disease', *Blood*, 125(9), pp. 1383-6.
- Harrison, C.J., Moorman, A.V., Barber, K.E., Broadfield, Z.J., Cheung, K.L., Harris, R.L., Jalali, G.R., Robinson, H.M., Strefford, J.C., Stewart, A., Wright, S., Griffiths, M., Ross, F.M., Harewood, L. and Martineau, M. (2005) 'Interphase molecular cytogenetic screening for chromosomal abnormalities of prognostic significance in childhood acute lymphoblastic leukaemia: a UK Cancer Cytogenetics Group Study', *Br J Haematol*, 129(4), pp. 520-30.
- Hasle, H., Clemmensen, I.H. and Mikkelsen, M. (2000) 'Risks of leukaemia and solid tumours in individuals with Down's syndrome', *Lancet*, 355(9199), pp. 165-9.
- Hill, C.R., Cole, M., Errington, J., Malik, G., Boddy, A.V. and Veal, G.J. (2014) 'Characterisation of the clinical pharmacokinetics of actinomycin D and the influence of ABCB1 pharmacogenetic variation on actinomycin D disposition in children with cancer', *Clin Pharmacokinet*, 53(8), pp. 741-51.
- Hill, C.R., Jamieson, D., Thomas, H.D., Brown, C.D., Boddy, A.V. and Veal, G.J. (2013) 'Characterisation of the roles of ABCB1, ABCC1, ABCC2 and ABCG2 in the transport and pharmacokinetics of actinomycin D in vitro and in vivo', *Biochem Pharmacol*, 85(1), pp. 29-37.
- Hill, F.G., Richards, S., Gibson, B., Hann, I., Lilleyman, J., Kinsey, S., Mitchell, C., Harrison, C.J. and Eden, O.B. (2004) 'Successful treatment without cranial radiotherapy of children receiving intensified chemotherapy for acute lymphoblastic leukaemia:

results of the risk-stratified randomized central nervous system treatment trial MRC UKALL XI (ISRC TN 16757172)', *Br J Haematol*, 124(1), pp. 33-46.

Hogan, L.E., Meyer, J.A., Yang, J., Wang, J., Wong, N., Yang, W., Condos, G., Hunger, S.P., Raetz, E., Saffery, R., Relling, M.V., Bhojwani, D., Morrison, D.J. and Carroll, W.L. (2011) 'Integrated genomic analysis of relapsed childhood acute lymphoblastic leukemia reveals therapeutic strategies', *Blood*, 118(19), pp. 5218-26.

Holleman, A., Cheok, M.H., den Boer, M.L., Yang, W., Veerman, A.J., Kazemier, K.M., Pei, D., Cheng, C., Pui, C.H., Relling, M.V., Janka-Schaub, G.E., Pieters, R. and Evans, W.E. (2004) 'Gene-expression patterns in drug-resistant acute lymphoblastic leukemia cells and response to treatment', *N Engl J Med*, 351(6), pp. 533-42.

Hollenberg, S.M., Weinberger, C., Ong, E.S., Cerelli, G., Oro, A., Lebo, R., Brad Thompson, E., Rosenfeld, M.G. and Evans, R.M. (1985) 'Primary structure and expression of a functional human glucocorticoid receptor cDNA', *Nature*, 318(6047), pp. 635-641.

Homo, F., Duval, D., Harousseau, J.L., Marie, J.P. and Zittoun, R. (1980) 'Heterogeneity of the in vitro responses to glucocorticoids in acute leukemia', *Cancer Res*, 40(7), pp. 2601-8.

Hongo, T., Yajima, S., Sakurai, M., Horikoshi, Y. and Hanada, R. (1997) 'In vitro drug sensitivity testing can predict induction failure and early relapse of childhood acute lymphoblastic leukemia', *Blood*, 89(8), pp. 2959-65.

Howard, S.C., Jones, D.P. and Pui, C.-H. (2011) 'The Tumor Lysis Syndrome', *The New England journal of medicine*, 364(19), pp. 1844-1854.

Huizenga, N.A., Koper, J.W., De Lange, P., Pols, H.A., Stolk, R.P., Burger, H., Grobbee, D.E., Brinkmann, A.O., De Jong, F.H. and Lamberts, S.W. (1998) 'A polymorphism in the glucocorticoid receptor gene may be associated with an increased sensitivity to glucocorticoids in vivo', *J Clin Endocrinol Metab*, 83(1), pp. 144-51.

Hulleman, E., Kazemier, K.M., Holleman, A., VanderWeele, D.J., Rudin, C.M., Broekhuis, M.J., Evans, W.E., Pieters, R. and Den Boer, M.L. (2009) 'Inhibition of glycolysis modulates prednisolone resistance in acute lymphoblastic leukemia cells', *Blood*, 113(9), pp. 2014-21.

Hunger, S.P. (1996) 'Chromosomal translocations involving the E2A gene in acute lymphoblastic leukemia: clinical features and molecular pathogenesis', *Blood*, 87(4), pp. 1211-24.

Hunger, S.P., Lu, X., Devidas, M., Camitta, B.M., Gaynon, P.S., Winick, N.J., Reaman, G.H. and Carroll, W.L. (2012) 'Improved survival for children and adolescents with acute lymphoblastic leukemia between 1990 and 2005: a report from the children's oncology group', *J Clin Oncol*, 30(14), pp. 1663-9.

Hunger, S.P. and Mullighan, C.G. (2015) 'Acute Lymphoblastic Leukemia in Children', *N Engl J Med*, 373(16), pp. 1541-52.

Igarashi, H., Medina, K.L., Yokota, T., Rossi, M.I., Sakaguchi, N., Comp, P.C. and Kincade, P.W. (2005a) 'Early lymphoid progenitors in mouse and man are highly sensitive to glucocorticoids', *Int Immunol*, 17(5), pp. 501-11.

Igarashi, S., Manabe, A., Ohara, A., Kumagai, M., Saito, T., Okimoto, Y., Kamijo, T., Isoyama, K., Kajiwara, M., Sotomatsu, M., Sugita, K., Sugita, K., Maeda, M., Yabe, H., Kinoshita, A., Kaneko, T., Hayashi, Y., Ikuta, K., Hanada, R. and Tsuchida, M. (2005b) 'No advantage of dexamethasone over prednisolone for the outcome of standard- and intermediate-risk childhood acute lymphoblastic leukemia in the Tokyo Children's Cancer Study Group L95-14 protocol', *J Clin Oncol*, 23(27), pp. 6489-98.

Inaba, H., Greaves, M. and Mullighan, C.G. (2013) 'Acute lymphoblastic leukaemia', *Lancet*, 381(9881), pp. 1943-55.

Inaba, H. and Pui, C.H. (2010) 'Glucocorticoid use in acute lymphoblastic leukaemia', *Lancet Oncol*, 11(11), pp. 1096-106.

Inoue, H., Takemura, H., Kawai, Y., Yoshida, A., Ueda, T. and Miyashita, T. (2002) 'Dexamethasone-resistant human Pre-B leukemia 697 cell line evolving elevation of intracellular glutathione level: an additional resistance mechanism', *Jpn J Cancer Res*, 93(5), pp. 582-90.

Irving, J., Matheson, E., Minto, L., Blair, H., Case, M., Halsey, C., Swidenbank, I., Ponthan, F., Kirschner-Schwabe, R., Groeneveld-Krentz, S., Hof, J., Allan, J., Harrison, C., Vormoor, J., von Stackelberg, A. and Eckert, C. (2014) 'Ras pathway mutations are prevalent in relapsed childhood acute lymphoblastic leukemia and confer sensitivity to MEK inhibition', *Blood*, 124(23), pp. 3420-30.

Irving, J.A. (2016) 'Towards an understanding of the biology and targeted treatment of paediatric relapsed acute lymphoblastic leukaemia', *Br J Haematol*, 172(5), pp. 655-66.

Irving, J.A., Enshaei, A., Parker, C.A., Sutton, R., Kuiper, R.P., Erhorn, A., Minto, L., Venn, N.C., Law, T., Yu, J., Schwab, C., Davies, R., Matheson, E., Davies, A., Sonneveld, E., den Boer, M.L., Love, S.B., Harrison, C.J., Hoogerbrugge, P.M., Revesz, T., Saha, V. and Moorman, A.V. (2016) 'Integration of genetic and clinical risk factors improves prognostication in relapsed childhood B-cell precursor acute lymphoblastic leukemia', *Blood*, 128(7), pp. 911-22.

Irving, J.A., Minto, L., Bailey, S. and Hall, A.G. (2005a) 'Loss of heterozygosity and somatic mutations of the glucocorticoid receptor gene are rarely found at relapse in pediatric acute lymphoblastic leukemia but may occur in a subpopulation early in the disease course', *Cancer Res*, 65(21), pp. 9712-8.

Irving, J.A.E., Minto, L., Bailey, S. and Hall, A.G. (2005b) 'Loss of Heterozygosity and Somatic Mutations of the Glucocorticoid Receptor Gene Are Rarely Found at Relapse in Pediatric Acute Lymphoblastic Leukemia but May Occur in a Subpopulation Early in the Disease Course', *Cancer Research*, 65(21), pp. 9712-9718.

Ishibashi, T., Yaguchi, A., Terada, K., Ueno-Yokohata, H., Tomita, O., Iijima, K., Kobayashi, K., Okita, H., Fujimura, J., Ohki, K., Shimizu, T. and Kiyokawa, N. (2016) 'Ph-

like ALL-related novel fusion kinase ATF7IP-PDGFRB exhibits high sensitivity to tyrosine kinase inhibitors in murine cells', *Exp Hematol*, 44(3), pp. 177-88 e5.

Ismaili, N. and Garabedian, M.J. (2004) 'Modulation of glucocorticoid receptor function via phosphorylation', *Ann N Y Acad Sci*, 1024, pp. 86-101.

Ito, C., Evans, W.E., McNinch, L., Coustan-Smith, E., Mahmoud, H., Pui, C.H. and Campana, D. (1996) 'Comparative cytotoxicity of dexamethasone and prednisolone in childhood acute lymphoblastic leukemia', *J Clin Oncol*, 14(8), pp. 2370-6.

Iwata, S., Hori, T., Sato, N., Hirota, K., Sasada, T., Mitsui, A., Hirakawa, T. and Yodoi, J. (1997) 'Adult T cell leukemia (ATL)-derived factor/human thioredoxin prevents apoptosis of lymphoid cells induced by L-cystine and glutathione depletion: possible involvement of thiol-mediated redox regulation in apoptosis caused by pro-oxidant state', *J Immunol*, 158(7), pp. 3108-17.

Jackson, R. (2014) *Investigating the Clinical Pharmacology of Dexamethasone in Acute Lymphoblastic Leukaemia*. Newcastle University.

Jackson, R.K., Irving, J.A. and Veal, G.J. (2016) 'Personalization of dexamethasone therapy in childhood acute lymphoblastic leukaemia', *Br J Haematol*, 173(1), pp. 13-24.

Jakubowska-Pietkiewicz, E., Mlynarski, W., Klich, I., Fendler, W. and Chlebna-Sokol, D. (2012) 'Vitamin D receptor gene variability as a factor influencing bone mineral density in pediatric patients', *Mol Biol Rep*, 39(5), pp. 6243-50.

Jamroziak, K., Mlynarski, W., Balcerczak, E., Mistygacz, M., Trelinska, J., Mirowski, M., Bodalski, J. and Robak, T. (2004) 'Functional C3435T polymorphism of MDR1 gene: an impact on genetic susceptibility and clinical outcome of childhood acute lymphoblastic leukemia', *Eur J Haematol*, 72(5), pp. 314-21.

Jibard, N., Meng, X., Leclerc, P., Rajkowski, K., Fortin, D., Schweizer-Groyer, G., Catelli, M.G., Baulieu, E.E. and Cadepond, F. (1999) 'Delimitation of two regions in the 90-kDa heat shock protein (Hsp90) able to interact with the glucocorticosteroid receptor (GR)', *Experimental Cell Research*, 247(2), pp. 461-474.

Jing, D., Bhadri, V.A., Beck, D., Thoms, J.A., Yakob, N.A., Wong, J.W., Knezevic, K., Pimanda, J.E. and Lock, R.B. (2015) 'Opposing regulation of BIM and BCL2 controls glucocorticoid-induced apoptosis of pediatric acute lymphoblastic leukemia cells', *Blood*, 125(2), pp. 273-83.

Johansson, B., Moorman, A.V., Haas, O.A., Watmore, A.E., Cheung, K.L., Swanton, S. and Secker-Walker, L.M. (1998) 'Hematologic malignancies with t(4;11)(q21;q23)--a cytogenetic, morphologic, immunophenotypic and clinical study of 183 cases. European 11q23 Workshop participants', *Leukemia*, 12(5), pp. 779-87.

Jones, B., Freeman, A.I., Shuster, J.J., Jacquillat, C., Weil, M., Pochedly, C., Sinks, L., Chevalier, L., Maurer, H.M., Koch, K. and et al. (1991) 'Lower incidence of meningeal leukemia when prednisone is replaced by dexamethasone in the treatment of acute lymphocytic leukemia', *Med Pediatr Oncol*, 19(4), pp. 269-75.

Jones, C.L., Bhatla, T., Blum, R., Wang, J., Paugh, S.W., Wen, X., Bourgeois, W., Bitterman, D.S., Raetz, E.A., Morrison, D.J., Teachey, D.T., Evans, W.E., Garabedian, M.J. and Carroll, W.L. (2014) 'Loss of TBL1XR1 disrupts glucocorticoid receptor recruitment to chromatin and results in glucocorticoid resistance in a B-lymphoblastic leukemia model', *J Biol Chem*, 289(30), pp. 20502-15.

Jones, C.L., Gearheart, C.M., Fosmire, S., Delgado-Martin, C., Evensen, N.A., Bride, K., Waanders, A.J., Pais, F., Wang, J., Bhatla, T., Bitterman, D.S., de Rijk, S.R., Bourgeois, W., Dandekar, S., Park, E., Burleson, T.M., Madhusoodhan, P.P., Teachey, D.T., Raetz, E.A., Hermiston, M.L., Muschen, M., Loh, M.L., Hunger, S.P., Zhang, J., Garabedian, M.J., Porter, C.C. and Carroll, W.L. (2015) 'MAPK signaling cascades mediate distinct glucocorticoid resistance mechanisms in pediatric leukemia', *Blood*, 126(19), pp. 2202-12.

Jones, T.S., Kaste, S.C., Liu, W., Cheng, C., Yang, W., Tantisira, K.G., Pui, C.H. and Relling, M.V. (2008) 'CRHR1 polymorphisms predict bone density in survivors of acute lymphoblastic leukemia', *J Clin Oncol*, 26(18), pp. 3031-7.

Jugert, F.K., Agarwal, R., Kuhn, A., Bickers, D.R., Merk, H.F. and Mukhtar, H. (1994) 'Multiple cytochrome P450 isozymes in murine skin: induction of P450 1A, 2B, 2E, and 3A by dexamethasone', *J Invest Dermatol*, 102(6), pp. 970-5.

Kakihara, T., Tanaka, A., Watanabe, A., Yamamoto, K., Kanto, K., Kataoka, S., Ogawa, A., Asami, K. and Uchiyama, M. (1999) 'Expression of multidrug resistance-related genes does not contribute to risk factors in newly diagnosed childhood acute lymphoblastic leukemia', *Pediatr Int*, 41(6), pp. 641-7.

Kamps, M.P. (1997) 'E2A-Pbx1 induces growth, blocks differentiation, and interacts with other homeodomain proteins regulating normal differentiation', *Curr Top Microbiol Immunol*, 220, pp. 25-43.

Kanerva, J., Saarinen-Pihkala, U.M., Niini, T., Riikonen, P., Mottonen, M., Makipernaa, A., Salmi, T.T., Vettenranta, K. and Knuutila, S. (2004) 'Favorable outcome in 20-year follow-up of children with very-low-risk ALL and minimal standard therapy, with special reference to TEL-AML1 fusion', *Pediatr Blood Cancer*, 42(1), pp. 30-5.

Kanerva, J., Tiirikainen, M., Makipernaa, A., Riikonen, P., Mottonen, M., Salmi, T.T., Krusius, T. and Saarinen-Pihkala, U.M. (1998) 'Multiple drug resistance mediated by P-glycoprotein is not a major factor in a slow response to therapy in childhood ALL', *Pediatr Hematol Oncol*, 15(1), pp. 11-21.

Kanerva, J., Tiirikainen, M.I., Makipernaa, A., Riikonen, P., Mottonen, M., Salmi, T.T., Krusius, T. and Saarinen-Pihkala, U.M. (2001) 'Initial P-glycoprotein expression in childhood acute lymphoblastic leukemia: no evidence of prognostic impact in follow-up', *Pediatr Hematol Oncol*, 18(1), pp. 27-36.

Karol, S.E., Mattano, L.A., Jr., Yang, W., Maloney, K.W., Smith, C., Liu, C., Ramsey, L.B., Fernandez, C.A., Chang, T.Y., Neale, G., Cheng, C., Mardis, E., Fulton, R., Scheet, P., San Lucas, F.A., Larsen, E.C., Loh, M.L., Raetz, E.A., Hunger, S.P., Devidas, M. and Relling, M.V. (2016) 'Genetic risk factors for the development of osteonecrosis in children under age 10 treated for acute lymphoblastic leukemia', *Blood*, 127(5), pp. 558-64.

Karol, S.E., Yang, W., Van Driest, S.L., Chang, T.Y., Kaste, S., Bowton, E., Basford, M., Bastarache, L., Roden, D.M., Denny, J.C., Larsen, E., Winick, N., Carroll, W.L., Cheng, C., Pei, D., Fernandez, C.A., Liu, C., Smith, C., Loh, M.L., Raetz, E.A., Hunger, S.P., Scheet, P., Jeha, S., Pui, C.H., Evans, W.E., Devidas, M., Mattano, L.A., Jr. and Relling, M.V. (2015) 'Genetics of glucocorticoid-associated osteonecrosis in children with acute lymphoblastic leukemia', *Blood*, 126(15), pp. 1770-6.

Kaspers, G.J., Veerman, A.J., Pieters, R., Van Zantwijk, C.H., Smets, L.A., Van Wering, E.R. and Van Der Does-Van Den Berg, A. (1997) 'In vitro cellular drug resistance and prognosis in newly diagnosed childhood acute lymphoblastic leukemia', *Blood*, 90(7), pp. 2723-9.

Kaspers, G.J., Veerman, A.J., Popp-Snijders, C., Lomecky, M., Van Zantwijk, C.H., Swinkels, L.M., Van Wering, E.R. and Pieters, R. (1996) 'Comparison of the antileukemic activity in vitro of dexamethasone and prednisolone in childhood acute lymphoblastic leukemia', *Med Pediatr Oncol*, 27(2), pp. 114-21.

Kawedia, J.D., Kaste, S.C., Pei, D., Panetta, J.C., Cai, X., Cheng, C., Neale, G., Howard, S.C., Evans, W.E., Pui, C.H. and Relling, M.V. (2011) 'Pharmacokinetic, pharmacodynamic, and pharmacogenetic determinants of osteonecrosis in children with acute lymphoblastic leukemia', *Blood*, 117(8), pp. 2340-7; quiz 2556.

Kawedia, J.D., Liu, C., Pei, D., Cheng, C., Fernandez, C.A., Howard, S.C., Campana, D., Panetta, J.C., Bowman, W.P., Evans, W.E., Pui, C.H. and Relling, M.V. (2012) 'Dexamethasone exposure and asparaginase antibodies affect relapse risk in acute lymphoblastic leukemia', *Blood*, 119(7), pp. 1658-64.

King, B.P., Leathart, J.B.S., Mutch, E., Williams, F.M. and Daly, A.K. (2003) 'CYP3A5 phenotype-genotype correlations in a British population', *British Journal of Clinical Pharmacology*, 55(6), pp. 625-629.

Kinlen, L.J. and Petridou, E. (1995) 'Childhood leukemia and rural population movements: Greece, Italy, and other countries', *Cancer Causes Control*, 6(5), pp. 445-50.

Kitzmiller, J.P., Luzum, J.A., Baldassarre, D., Krauss, R.M. and Medina, M.W. (2014) 'CYP3A4*22 and CYP3A5*3 are associated with increased levels of plasma simvastatin concentrations in the cholesterol and pharmacogenetics study cohort', *Pharmacogenet Genomics*, 24(10), pp. 486-91.

Klumper, E., Pieters, R., Veerman, A.J., Huismans, D.R., Loonen, A.H., Hahlen, K., Kaspers, G.J., van Wering, E.R., Hartmann, R. and Henze, G. (1995) 'In vitro cellular drug resistance in children with relapsed/refractory acute lymphoblastic leukemia', *Blood*, 86(10), pp. 3861-8.

Kofler, R. (2000) 'The molecular basis of glucocorticoid-induced apoptosis of lymphoblastic leukemia cells', *Histochem Cell Biol*, 114(1), pp. 1-7.

Kofler, R., Schmidt, S., Kofler, A. and Ausserlechner, M.J. (2003) 'Resistance to glucocorticoid-induced apoptosis in lymphoblastic leukemia', *J Endocrinol*, 178(1), pp. 19-27.

- Kovarik, J.M., Purba, H.S., Pongowski, M., Gerbeau, C., Humbert, H. and Mueller, E.A. (1998) 'Pharmacokinetics of dexamethasone and valspodar, a P-glycoprotein (mdr1) modulator: implications for coadministration', *Pharmacotherapy*, 18(6), pp. 1230-6.
- Kowalik, A., Kiernożek, E., Kulinczak, M., Brodaczevska, K., Kozłowska, E., Gieczewska, K., Riccardi, C. and Drela, N. (2013) 'Dexamethasone-FITC staining application for measurement of circadian rhythmicity of glucocorticoid receptor expression in mouse living thymocyte subsets', *J Neuroimmunol*, 261(1-2), pp. 44-52.
- Krajinovic, M., Labuda, D., Mathonnet, G., Labuda, M., Moghrabi, A., Champagne, J. and Sinnett, D. (2002) 'Polymorphisms in genes encoding drugs and xenobiotic metabolizing enzymes, DNA repair enzymes, and response to treatment of childhood acute lymphoblastic leukemia', *Clin Cancer Res*, 8(3), pp. 802-10.
- Kuiper, R.P., Schoenmakers, E.F., van Reijmersdal, S.V., Hehir-Kwa, J.Y., van Kessel, A.G., van Leeuwen, F.N. and Hoogerbrugge, P.M. (2007) 'High-resolution genomic profiling of childhood ALL reveals novel recurrent genetic lesions affecting pathways involved in lymphocyte differentiation and cell cycle progression', *Leukemia*, 21(6), pp. 1258-66.
- Kunkele, A., Grosse-Lordemann, A., Schramm, A., Eggert, A., Schulte, J.H. and Bachmann, H.S. (2013) 'The BCL2-938 C > A promoter polymorphism is associated with risk group classification in children with acute lymphoblastic leukemia', *BMC Cancer*, 13, p. 452.
- Kuster, L., Grausenburger, R., Fuka, G., Kaindl, U., Krapf, G., Inthal, A., Mann, G., Kauer, M., Rainer, J., Kofler, R., Hall, A., Metzler, M., Meyer, L.H., Meyer, C., Harbott, J., Marschalek, R., Strehl, S., Haas, O.A. and Panzer-Grumayer, R. (2011) 'ETV6/RUNX1-positive relapses evolve from an ancestral clone and frequently acquire deletions of genes implicated in glucocorticoid signaling', *Blood*, 117(9), pp. 2658-67.
- Labuda, M., Gahier, A., Gagne, V., Moghrabi, A., Sinnett, D. and Krajinovic, M. (2010) 'Polymorphisms in glucocorticoid receptor gene and the outcome of childhood acute lymphoblastic leukemia (ALL)', *Leuk Res*, 34(4), pp. 492-7.
- Lal, S., Wong, Z.W., Sandanaraj, E., Xiang, X., Ang, P.C., Lee, E.J. and Chowbay, B. (2008) 'Influence of ABCB1 and ABCG2 polymorphisms on doxorubicin disposition in Asian breast cancer patients', *Cancer Sci*, 99(4), pp. 816-23.
- Lamba, V., Panetta, J.C., Strom, S. and Schuetz, E.G. (2010) 'Genetic predictors of interindividual variability in hepatic CYP3A4 expression', *J Pharmacol Exp Ther*, 332(3), pp. 1088-99.
- Lauten, M., Beger, C., Gerdes, K., Asgedom, G., Kardinal, C., Welte, K. and Schrappe, M. (2003a) 'Expression of heat-shock protein 90 in glucocorticoid-sensitive and -resistant childhood acute lymphoblastic leukaemia', *Leukemia*, 17(8), pp. 1551-6.
- Lauten, M., Cario, G., Asgedom, G., Welte, K. and Schrappe, M. (2003b) 'Protein expression of the glucocorticoid receptor in childhood acute lymphoblastic leukemia', *Haematologica*, 88(11), pp. 1253-8.

- Lemahieu, W.P., Maes, B.D., Verbeke, K. and Vanrenterghem, Y. (2005) 'Impact of gastric acid suppressants on cytochrome P450 3A4 and P-glycoprotein: consequences for FK506 assimilation', *Kidney Int*, 67(3), pp. 1152-60.
- Leschziner, G.D., Andrew, T., Pirmohamed, M. and Johnson, M.R. (2006) 'ABCB1 genotype and PGP expression, function and therapeutic drug response: a critical review and recommendations for future research', *Pharmacogenomics J*, 7(3), pp. 154-179.
- Li, Y., Schwab, C., Ryan, S.L., Papaemmanuil, E., Robinson, H.M., Jacobs, P., Moorman, A.V., Dyer, S., Borrow, J., Griffiths, M., Heerema, N.A., Carroll, A.J., Talley, P., Bown, N., Telford, N., Ross, F.M., Gaunt, L., McNally, R.J., Young, B.D., Sinclair, P., Rand, V., Teixeira, M.R., Joseph, O., Robinson, B., Maddison, M., Dastugue, N., Vandenberghe, P., Haferlach, C., Stephens, P.J., Cheng, J., Van Loo, P., Stratton, M.R., Campbell, P.J. and Harrison, C.J. (2014) 'Constitutional and somatic rearrangement of chromosome 21 in acute lymphoblastic leukaemia', *Nature*, 508(7494), pp. 98-102.
- Lieblich, M., Jackson, R.K., Irving, J.A.E., Veal, G.J. and Hempel, G. (2017) 'Modelling of Dexamethasone in Paediatric Leukaemia Patients using a Population Pharmacokinetic Approach', *PAGE 26 Abstracts of the Annual Meeting of the Population Approach Group in Europe*.
- Lill-Elghanian, D., Schwartz, K., King, L. and Fraker, P. (2002) 'Glucocorticoid-induced apoptosis in early B cells from human bone marrow', *Exp Biol Med (Maywood)*, 227(9), pp. 763-70.
- Liu, C., Janke, L.J., Kawedia, J.D., Ramsey, L.B., Cai, X., Mattano, L.A., Jr., Boyd, K.L., Funk, A.J. and Relling, M.V. (2016) 'Asparaginase Potentiates Glucocorticoid-Induced Osteonecrosis in a Mouse Model', *PLoS One*, 11(3), p. e0151433.
- Loew, D., Schuster, O. and Graul, E.H. (1986) 'Dose-dependent pharmacokinetics of dexamethasone', *Eur J Clin Pharmacol*, 30(2), pp. 225-30.
- Loh, M.L., Goldwasser, M.A., Silverman, L.B., Poon, W.M., Vattikuti, S., Cardoso, A., Neuberg, D.S., Shannon, K.M., Sallan, S.E. and Gilliland, D.G. (2006) 'Prospective analysis of TEL/AML1-positive patients treated on Dana-Farber Cancer Institute Consortium Protocol 95-01', *Blood*, 107(11), pp. 4508-13.
- Lou, X., Zhang, G., Herrera, I., Kinach, R., Ornatsky, O., Baranov, V., Nitz, M. and Winnik, M.A. (2007) 'Polymer-based elemental tags for sensitive bioassays', *Angew Chem Int Ed Engl*, 46(32), pp. 6111-4.
- Lu, J., Quearry, B. and Harada, H. (2006) 'p38-MAP kinase activation followed by BIM induction is essential for glucocorticoid-induced apoptosis in lymphoblastic leukemia cells', *FEBS Lett*, 580(14), pp. 3539-44.
- Mahmoudian, J., Hadavi, R., Jeddi-Tehrani, M., Mahmoudi, A.R., Bayat, A.A., Shaban, E., Vafakhah, M., Darzi, M., Tarahomi, M. and Ghods, R. (2011) 'Comparison of the Photobleaching and Photostability Traits of Alexa Fluor 568- and Fluorescein Isothiocyanate- conjugated Antibody', *Cell Journal (Yakhteh)*, 13(3), pp. 169-172.

- Maia, A.T., van der Velden, V.H., Harrison, C.J., Szczepanski, T., Williams, M.D., Griffiths, M.J., van Dongen, J.J. and Greaves, M.F. (2003) 'Prenatal origin of hyperdiploid acute lymphoblastic leukemia in identical twins', *Leukemia*, 17(11), pp. 2202-6.
- Majonis, D., Herrera, I., Ornatsky, O., Schulze, M., Lou, X., Soleimani, M., Nitz, M. and Winnik, M.A. (2010) 'Synthesis of a functional metal-chelating polymer and steps toward quantitative mass cytometry bioassays', *Anal Chem*, 82(21), pp. 8961-9.
- Manning, G., Plowman, G.D., Hunter, T. and Sudarsanam, S. (2002) 'Evolution of protein kinase signaling from yeast to man', *Trends Biochem Sci*, 27(10), pp. 514-20.
- Marchetti, P., Natoli, V., Ranelletti, F.O., Mandelli, F., De Rossi, G. and Iacobelli, S. (1981) 'Glucocorticoid receptor studies in human leukemia', *J Steroid Biochem*, 15, pp. 261-8.
- Martinelli, G., Iacobucci, I., Storlazzi, C.T., Vignetti, M., Paoloni, F., Cilloni, D., Soverini, S., Vitale, A., Chiaretti, S., Cimino, G., Papayannidis, C., Paolini, S., Elia, L., Fazi, P., Meloni, G., Amadori, S., Saglio, G., Pane, F., Baccarani, M. and Foa, R. (2009) 'IKZF1 (Ikaros) deletions in BCR-ABL1-positive acute lymphoblastic leukemia are associated with short disease-free survival and high rate of cumulative incidence of relapse: a GIMEMA AL WP report', *J Clin Oncol*, 27(31), pp. 5202-7.
- Martinez, C., Albet, C., Agundez, J.A., Herrero, E., Carrillo, J.A., Marquez, M., Benitez, J. and Ortiz, J.A. (1999) 'Comparative in vitro and in vivo inhibition of cytochrome P450 CYP1A2, CYP2D6, and CYP3A by H2-receptor antagonists', *Clin Pharmacol Ther*, 65(4), pp. 369-76.
- Mastrangelo, R., Malandrino, R., Riccardi, R., Longo, P., Ranelletti, F.O. and Iacobelli, S. (1980) 'Clinical implications of glucocorticoid receptor studies in childhood acute lymphoblastic leukemia', *Blood*, 56(6), pp. 1036-40.
- Matheson, E.C. and Hall, A.G. (2003) 'Assessment of mismatch repair function in leukaemic cell lines and blasts from children with acute lymphoblastic leukaemia', *Carcinogenesis*, 24(1), pp. 31-8.
- McHale, C.M., Wiemels, J.L., Zhang, L., Ma, X., Buffler, P.A., Feusner, J., Matthay, K., Dahl, G. and Smith, M.T. (2003a) 'Prenatal origin of childhood acute myeloid leukemias harboring chromosomal rearrangements t(15;17) and inv(16)', *Blood*, 101(11), pp. 4640-1.
- McHale, C.M., Wiemels, J.L., Zhang, L., Ma, X., Buffler, P.A., Guo, W., Loh, M.L. and Smith, M.T. (2003b) 'Prenatal origin of TEL-AML1-positive acute lymphoblastic leukemia in children born in California', *Genes Chromosomes Cancer*, 37(1), pp. 36-43.
- McLeod, H.L., Krynetski, E.Y., Relling, M.V. and Evans, W.E. (2000) 'Genetic polymorphism of thiopurine methyltransferase and its clinical relevance for childhood acute lymphoblastic leukemia', *Leukemia*, 14(4), pp. 567-72.
- McNeil, M.M., Weintraub, E.S., Duffy, J., Sukumaran, L., Jacobsen, S.J., Klein, N.P., Hambidge, S.J., Lee, G.M., Jackson, L.A., Irving, S.A., King, J.P., Kharbanda, E.O.,

- Bednarczyk, R.A. and DeStefano, F. (2016) 'Risk of anaphylaxis after vaccination in children and adults', *J Allergy Clin Immunol*, 137(3), pp. 868-78.
- Meikle, A.W. and Tyler, F.H. (1977) 'Potency and duration of action of glucocorticoids. Effects of hydrocortisone, prednisone and dexamethasone on human pituitary-adrenal function', *Am J Med*, 63(2), pp. 200-7.
- Mitchell, C., Richards, S., Harrison, C.J. and Eden, T. (2010) 'Long-term follow-up of the United Kingdom medical research council protocols for childhood acute lymphoblastic leukaemia, 1980-2001', *Leukemia*, 24(2), pp. 406-18.
- Mitchell, C.D., Richards, S.M., Kinsey, S.E., Lilleyman, J., Vora, A. and Eden, T.O. (2005) 'Benefit of dexamethasone compared with prednisolone for childhood acute lymphoblastic leukaemia: results of the UK Medical Research Council ALL97 randomized trial', *Br J Haematol*, 129(6), pp. 734-45.
- Miyashita, T. and Reed, J.C. (1993) 'Bcl-2 oncoprotein blocks chemotherapy-induced apoptosis in a human leukemia cell line', *Blood*, 81(1), pp. 151-7.
- Miyoshi, Y., Ando, A., Takamura, Y., Taguchi, T., Tamaki, Y. and Noguchi, S. (2002) 'Prediction of response to docetaxel by CYP3A4 mRNA expression in breast cancer tissues', *Int J Cancer*, 97(1), pp. 129-32.
- Moore, J.T. and Kliewer, S.A. (2000) 'Use of the nuclear receptor PXR to predict drug interactions', *Toxicology*, 153(1-3), pp. 1-10.
- Moorman, A.V. (2016) 'New and emerging prognostic and predictive genetic biomarkers in B-cell precursor acute lymphoblastic leukemia', *Haematologica*, 101(4), pp. 407-16.
- Moorman, A.V., Enshaei, A., Schwab, C., Wade, R., Chilton, L., Elliott, A., Richardson, S., Hancock, J., Kinsey, S.E., Mitchell, C.D., Goulden, N., Vora, A. and Harrison, C.J. (2014) 'A novel integrated cytogenetic and genomic classification refines risk stratification in pediatric acute lymphoblastic leukemia', *Blood*, 124(9), pp. 1434-44.
- Moorman, A.V., Ensor, H.M., Richards, S.M., Chilton, L., Schwab, C., Kinsey, S.E., Vora, A., Mitchell, C.D. and Harrison, C.J. (2010) 'Prognostic effect of chromosomal abnormalities in childhood B-cell precursor acute lymphoblastic leukaemia: results from the UK Medical Research Council ALL97/99 randomised trial', *Lancet Oncol*, 11(5), pp. 429-38.
- Mori, H., Colman, S.M., Xiao, Z., Ford, A.M., Healy, L.E., Donaldson, C., Hows, J.M., Navarrete, C. and Greaves, M. (2002) 'Chromosome translocations and covert leukemic clones are generated during normal fetal development', *Proc Natl Acad Sci U S A*, 99(12), pp. 8242-7.
- Mullighan, C.G. (2012) 'Molecular genetics of B-precursor acute lymphoblastic leukemia', *J Clin Invest*, 122(10), pp. 3407-15.
- Mullighan, C.G., Collins-Underwood, J.R., Phillips, L.A., Loudin, M.G., Liu, W., Zhang, J., Ma, J., Coustan-Smith, E., Harvey, R.C., Willman, C.L., Mikhail, F.M., Meyer, J., Carroll,

A.J., Williams, R.T., Cheng, J., Heerema, N.A., Basso, G., Pession, A., Pui, C.H., Raimondi, S.C., Hunger, S.P., Downing, J.R., Carroll, W.L. and Rabin, K.R. (2009a) 'Rearrangement of CRLF2 in B-progenitor- and Down syndrome-associated acute lymphoblastic leukemia', *Nat Genet*, 41(11), pp. 1243-6.

Mullighan, C.G., Goorha, S., Radtke, I., Miller, C.B., Coustan-Smith, E., Dalton, J.D., Girtman, K., Mathew, S., Ma, J., Pounds, S.B., Su, X., Pui, C.H., Relling, M.V., Evans, W.E., Shurtleff, S.A. and Downing, J.R. (2007) 'Genome-wide analysis of genetic alterations in acute lymphoblastic leukaemia', *Nature*, 446(7137), pp. 758-64.

Mullighan, C.G., Miller, C.B., Radtke, I., Phillips, L.A., Dalton, J., Ma, J., White, D., Hughes, T.P., Le Beau, M.M., Pui, C.H., Relling, M.V., Shurtleff, S.A. and Downing, J.R. (2008a) 'BCR-ABL1 lymphoblastic leukaemia is characterized by the deletion of Ikaros', *Nature*, 453(7191), pp. 110-4.

Mullighan, C.G., Phillips, L.A., Su, X., Ma, J., Miller, C.B., Shurtleff, S.A. and Downing, J.R. (2008b) 'Genomic analysis of the clonal origins of relapsed acute lymphoblastic leukemia', *Science*, 322(5906), pp. 1377-80.

Mullighan, C.G., Zhang, J., Harvey, R.C., Collins-Underwood, J.R., Schulman, B.A., Phillips, L.A., Tasian, S.K., Loh, M.L., Su, X., Liu, W., Devidas, M., Atlas, S.R., Chen, I.M., Clifford, R.J., Gerhard, D.S., Carroll, W.L., Reaman, G.H., Smith, M., Downing, J.R., Hunger, S.P. and Willman, C.L. (2009b) 'JAK mutations in high-risk childhood acute lymphoblastic leukemia', *Proc Natl Acad Sci U S A*, 106(23), pp. 9414-8.

Mulvey, C.M., Breckels, L.M., Geladaki, A., Britovsek, N.K., Nightingale, D.J.H., Christoforou, A., Elzek, M., Deery, M.J., Gatto, L. and Lilley, K.S. (2017) 'Using hyperLOPIT to perform high-resolution mapping of the spatial proteome', *Nat Protoc*, 12(6), pp. 1110-1135.

Nakayama, G.R., Caton, M.C., Nova, M.P. and Parandoosh, Z. (1997) 'Assessment of the Alamar Blue assay for cellular growth and viability in vitro', *J Immunol Methods*, 204(2), pp. 205-8.

Nebral, K., Denk, D., Attarbaschi, A., Konig, M., Mann, G., Haas, O.A. and Strehl, S. (2009) 'Incidence and diversity of PAX5 fusion genes in childhood acute lymphoblastic leukemia', *Leukemia*, 23(1), pp. 134-43.

Newell, E.W., Sigal, N., Bendall, S.C., Nolan, G.P. and Davis, M.M. (2012) 'Cytometry by time-of-flight shows combinatorial cytokine expression and virus-specific cell niches within a continuum of CD8+ T cell phenotypes', *Immunity*, 36(1), pp. 142-52.

Nicholson, L., Evans, C.A., Matheson, E., Minto, L., Keilty, C., Sanichar, M., Case, M., Schwab, C., Williamson, D., Rainer, J., Harrison, C.J., Kofler, R., Hall, A.G., Redfern, C.P., Whetton, A.D. and Irving, J.A. (2015) 'Quantitative proteomic analysis reveals maturation as a mechanism underlying glucocorticoid resistance in B lineage ALL and re-sensitization by JNK inhibition', *Br J Haematol*, 171(4), pp. 595-605.

Nicholson, L., Hall, A.G., Redfern, C.P. and Irving, J. (2010) 'NFkappaB modulators in a model of glucocorticoid resistant, childhood acute lymphoblastic leukemia', *Leuk Res*, 34(10), pp. 1366-73.

- Nicolaides, N.C., Galata, Z., Kino, T., Chrousos, G.P. and Charmandari, E. (2010) 'The human glucocorticoid receptor: molecular basis of biologic function', *Steroids*, 75(1), pp. 1-12.
- Nyla, A.H., Andrew, J.C., Meenakshi, D., Mignon, L.L., Michael, J.B., Julie, M.G.-F., Eric, C.L., Leonard, A.M., Jr., Kelly, W.M., Cheryl, L.W., Brent, L.W., Naomi, J.W., William, L.C., Stephen, P.H. and Elizabeth, A.R. (2013) 'Intrachromosomal Amplification of Chromosome 21 Is Associated With Inferior Outcomes in Children With Acute Lymphoblastic Leukemia Treated in Contemporary Standard-Risk Children's Oncology Group Studies: A Report From the Children's Oncology Group', *Journal of Clinical Oncology*, 31(27), pp. 3397-3402.
- O'Sullivan, B.T., Cutler, D.J., Hunt, G.E., Walters, C., Johnson, G.F. and Caterson, I.D. (1997) 'Pharmacokinetics of dexamethasone and its relationship to dexamethasone suppression test outcome in depressed patients and healthy control subjects', *Biol Psychiatry*, 41(5), pp. 574-84.
- O'Connor, D., Bate, J., Wade, R., Clack, R., Dhir, S., Hough, R., Vora, A., Goulden, N. and Samarasinghe, S. (2014) *Infection-related mortality in children with acute lymphoblastic leukemia: an analysis of infectious deaths on UKALL2003*.
- Oettgen, H.F., Stephenson, P.A., Schwartz, M.K., Leeper, R.D., Tallai, L., Tan, C.C., Clarkson, B.D., Golbey, R.B., Krakoff, I.H., Karnofsky, D.A., Murphy, M.L. and Burchenal, J.H. (1970) 'Toxicity of E. coli L-asparaginase in man', *Cancer*, 25(2), pp. 253-78.
- Olson, D.P., Taylor, B.J., La, M., Sather, H., Reaman, G.H. and Ivy, S.P. (2005) 'The prognostic significance of P-glycoprotein, multidrug resistance-related protein 1 and lung resistance protein in pediatric acute lymphoblastic leukemia: a retrospective study of 295 newly diagnosed patients by the Children's Oncology Group', *Leuk Lymphoma*, 46(5), pp. 681-91.
- Onciu, M. (2009) 'Acute lymphoblastic leukemia', *Hematol Oncol Clin North Am*, 23(4), pp. 655-74.
- Ornatsky, O., Bandura, D., Baranov, V., Nitz, M., Winnik, M.A. and Tanner, S. (2010) 'Highly multiparametric analysis by mass cytometry', *J Immunol Methods*, 361(1-2), pp. 1-20.
- Ornatsky, O., Baranov, V.I., Bandura, D.R., Tanner, S.D. and Dick, J. (2006) 'Multiple cellular antigen detection by ICP-MS', *J Immunol Methods*, 308(1-2), pp. 68-76.
- Ornatsky, O.I., Kinach, R., Bandura, D.R., Lou, X., Tanner, S.D., Baranov, V.I., Nitz, M. and Winnik, M.A. (2008a) 'Development of analytical methods for multiplex bio-assay with inductively coupled plasma mass spectrometry', *J Anal At Spectrom*, 23(4), pp. 463-469.
- Ornatsky, O.I., Lou, X., Nitz, M., Schafer, S., Sheldrick, W.S., Baranov, V.I., Bandura, D.R. and Tanner, S.D. (2008b) 'Study of cell antigens and intracellular DNA by identification of element-containing labels and metallointercalators using inductively coupled plasma mass spectrometry', *Anal Chem*, 80(7), pp. 2539-47.

Paci, A., Veal, G., Bardin, C., Leveque, D., Widmer, N., Beijnen, J., Astier, A. and Chatelut, E. (2014) 'Review of therapeutic drug monitoring of anticancer drugs part 1-- cytotoxics', *Eur J Cancer*, 50(12), pp. 2010-9.

Panarelli, M., Holloway, C.D., Fraser, R., Connell, J.M., Ingram, M.C., Anderson, N.H. and Kenyon, C.J. (1998) 'Glucocorticoid receptor polymorphism, skin vasoconstriction, and other metabolic intermediate phenotypes in normal human subjects', *J Clin Endocrinol Metab*, 83(6), pp. 1846-52.

Patel, P., Tanna, S., Mulla, H., Kairamkonda, V., Pandya, H. and Lawson, G. (2010) 'Dexamethasone quantification in dried blood spot samples using LC-MS: The potential for application to neonatal pharmacokinetic studies', *J Chromatogr B Analyt Technol Biomed Life Sci*, 878(31), pp. 3277-82.

Paugh, S.W., Bonten, E.J., Savic, D., Ramsey, L.B., Thierfelder, W.E., Gurung, P., Malireddi, R.K., Actis, M., Mayasundari, A., Min, J., Coss, D.R., Lauder milk, L.T., Panetta, J.C., McCorkle, J.R., Fan, Y., Crews, K.R., Stocco, G., Wilkinson, M.R., Ferreira, A.M., Cheng, C., Yang, W., Karol, S.E., Fernandez, C.A., Diouf, B., Smith, C., Hicks, J.K., Zanut, A., Giordanengo, A., Crona, D., Bianchi, J.J., Holmfeldt, L., Mullighan, C.G., den Boer, M.L., Pieters, R., Jeha, S., Dunwell, T.L., Latif, F., Bhojwani, D., Carroll, W.L., Pui, C.H., Myers, R.M., Guy, R.K., Kanneganti, T.D., Relling, M.V. and Evans, W.E. (2015) 'NALP3 inflammasome upregulation and CASP1 cleavage of the glucocorticoid receptor cause glucocorticoid resistance in leukemia cells', *Nat Genet*, 47(6), pp. 607-14.

Pavek, P., Merino, G., Wagenaar, E., Bolscher, E., Novotna, M., Jonker, J.W. and Schinkel, A.H. (2005) 'Human breast cancer resistance protein: interactions with steroid drugs, hormones, the dietary carcinogen 2-amino-1-methyl-6-phenylimidazo(4,5-b)pyridine, and transport of cimetidine', *J Pharmacol Exp Ther*, 312(1), pp. 144-52.

Persson, E.M., Nordgren, A., Forsell, P., Knutson, L., Öhgren, C., Forssén, S., Lennernäs, H. and Abrahamsson, B. (2008) 'Improved understanding of the effect of food on drug absorption and bioavailability for lipophilic compounds using an intestinal pig perfusion model', *European Journal of Pharmaceutical Sciences*, 34(1), pp. 22-29.

Pession, A., Barbieri, E., Santoro, N., Paolucci, P., Porta, F. and Locatelli, F. (2005) 'Efficacy and safety of recombinant urate oxidase (rasburicase) for treatment and prophylaxis of hyperuricemia in children undergoing chemotherapy', *Haematologica*, 90(1), pp. 141-2.

PhosphoSitePlus (2017) *GR (human)*. Available at: <http://www.phosphosite.org/proteinAction.action?id=1310&showAllSites=true> (Accessed: 29/06/17).

Picard, D., Khursheed, B., Garabedian, M.J., Fortin, M.G., Lindquist, S. and Yamamoto, K.R. (1990) 'Reduced levels of hsp90 compromise steroid receptor action in vivo', *Nature*, 348(6297), pp. 166-8.

Pierce, A., Whetton, A.D., Owen-Lynch, P.J., Tavernier, J., Spooncer, E., Dexter, T.M. and Heyworth, C.M. (1998) 'Ectopic interleukin-5 receptor expression promotes

proliferation without development in a multipotent hematopoietic cell line', *J Cell Sci*, 111 (Pt 6), pp. 815-23.

Pierce, A., Williamson, A., Jaworska, E., Griffiths, J.R., Taylor, S., Walker, M., Aspinall-O'Dea, M., Spooncer, E., Unwin, R.D., Poolman, T., Ray, D. and Whetton, A.D. (2012) 'Identification of nuclear protein targets for six leukemogenic tyrosine kinases governed by post-translational regulation', *PLoS One*, 7(6), p. e38928.

Piovan, E., Yu, J., Tosello, V., Herranz, D., Ambesi-Impiombato, A., Da Silva, A.C., Sanchez-Martin, M., Perez-Garcia, A., Rigo, I., Castillo, M., Indraccolo, S., Cross, J.R., de Stanchina, E., Paietta, E., Racevskis, J., Rowe, J.M., Tallman, M.S., Basso, G., Meijerink, J.P., Cordon-Cardo, C., Califano, A. and Ferrando, A.A. (2013) 'Direct reversal of glucocorticoid resistance by AKT inhibition in acute lymphoblastic leukemia', *Cancer Cell*, 24(6), pp. 766-76.

Plant, N. (2007) 'The human cytochrome P450 sub-family: transcriptional regulation, inter-individual variation and interaction networks', *Biochim Biophys Acta*, 1770(3), pp. 478-88.

Plasschaert, S.L., Kamps, W.A., Vellenga, E., de Vries, E.G. and de Bont, E.S. (2004) 'Prognosis in childhood and adult acute lymphoblastic leukaemia: a question of maturation?', *Cancer Treat Rev*, 30(1), pp. 37-51.

Plasschaert, S.L., Vellenga, E., de Bont, E.S., van der Kolk, D.M., Veerman, A.J., Sluiter, W.J., Daenen, S.M., de Vries, E.G. and Kamps, W.A. (2003) 'High functional P-glycoprotein activity is more often present in T-cell acute lymphoblastic leukaemic cells in adults than in children', *Leuk Lymphoma*, 44(1), pp. 85-95.

Ploner, C., Schmidt, S., Presul, E., Renner, K., Schröcksnadel, K., Rainer, J., Riml, S. and Kofler, R. (2005) 'Glucocorticoid-induced apoptosis and glucocorticoid resistance in acute lymphoblastic leukemia', *The Journal of Steroid Biochemistry and Molecular Biology*, 93(2-5), pp. 153-160.

Polak, A., Kiliszek, P., Sewastianik, T., Szydłowski, M., Jabłonska, E., Białopiotrowicz, E., Gorniak, P., Markowicz, S., Nowak, E., Grygorowicz, M.A., Prochorec-Sobieszek, M., Nowis, D., Golab, J., Giebel, S., Lech-Maranda, E., Warzocha, K. and Juszczynski, P. (2016) 'MEK Inhibition Sensitizes Precursor B-Cell Acute Lymphoblastic Leukemia (B-ALL) Cells to Dexamethasone through Modulation of mTOR Activity and Stimulation of Autophagy', *PLoS One*, 11(5), p. e0155893.

Pratt, W.B. (1993) 'The role of heat shock proteins in regulating the function, folding, and trafficking of the glucocorticoid receptor', *Journal of Biological Chemistry*, 268(29), pp. 21455-21458.

Pratt, W.B. and Toft, D.O. (1997) 'Steroid receptor interactions with heat shock protein and immunophilin chaperones', *Endocr Rev*, 18(3), pp. 306-60.

ProteinSimple (2014) 'Simple Western Charge Assay Development Guide', [Online] (Accessed: 26/06/17).

- Pui, C.-H., Mullighan, C.G., Evans, W.E. and Relling, M.V. (2012) *Pediatric acute lymphoblastic leukemia: where are we going and how do we get there?*
- Pui, C.H., Campana, D., Pei, D., Bowman, W.P., Sandlund, J.T., Kaste, S.C., Ribeiro, R.C., Rubnitz, J.E., Raimondi, S.C., Onciu, M., Coustan-Smith, E., Kun, L.E., Jeha, S., Cheng, C., Howard, S.C., Simmons, V., Bayles, A., Metzger, M.L., Boyett, J.M., Leung, W., Handgretinger, R., Downing, J.R., Evans, W.E. and Relling, M.V. (2009) 'Treating childhood acute lymphoblastic leukemia without cranial irradiation', *N Engl J Med*, 360(26), pp. 2730-41.
- Pui, C.H., Carroll, W.L., Meshinchi, S. and Arceci, R.J. (2011) 'Biology, risk stratification, and therapy of pediatric acute leukemias: an update', *J Clin Oncol*, 29(5), pp. 551-65.
- Pui, C.H. and Costlow, M.E. (1986) 'Sequential studies of lymphoblast glucocorticoid receptor levels at diagnosis and relapse in childhood leukemia: an update', *Leuk Res*, 10(2), pp. 227-9.
- Pui, C.H., Dahl, G.V., Rivera, G., Murphy, S.B. and Costlow, M.E. (1984) 'The relationship of blast cell glucocorticoid receptor levels to response to single-agent steroid trial and remission response in children with acute lymphoblastic leukemia', *Leuk Res*, 8(4), pp. 579-85.
- Pui, C.H. and Evans, W.E. (2006) 'Treatment of acute lymphoblastic leukemia', *N Engl J Med*, 354(2), pp. 166-78.
- Pui, C.H. and Howard, S.C. (2008) 'Current management and challenges of malignant disease in the CNS in paediatric leukaemia', *Lancet Oncol*, 9(3), pp. 257-68.
- Pui, C.H., Relling, M.V. and Downing, J.R. (2004) 'Acute lymphoblastic leukemia', *N Engl J Med*, 350(15), pp. 1535-48.
- Pui, C.H., Robison, L.L. and Look, A.T. (2008) 'Acute lymphoblastic leukaemia', *Lancet*, 371(9617), pp. 1030-43.
- Qiu, P., Simonds, E.F., Bendall, S.C., Gibbs, K.D., Jr., Bruggner, R.V., Linderman, M.D., Sachs, K., Nolan, G.P. and Plevritis, S.K. (2011) 'Extracting a cellular hierarchy from high-dimensional cytometry data with SPADE', *Nat Biotechnol*, 29(10), pp. 886-91.
- Queckenberg, C., Wachall, B., Erlinghagen, V., Di Gion, P., Tomalik-Scharte, D., Tawab, M., Gerbeth, K. and Fuhr, U. (2011) 'Pharmacokinetics, pharmacodynamics, and comparative bioavailability of single, oral 2-mg doses of dexamethasone liquid and tablet formulations: a randomized, controlled, crossover study in healthy adult volunteers', *Clin Ther*, 33(11), pp. 1831-41.
- Ravandi, F., O'Brien, S., Thomas, D., Faderl, S., Jones, D., Garris, R., Dara, S., Jorgensen, J., Kebriaei, P., Champlin, R., Borthakur, G., Burger, J., Ferrajoli, A., Garcia-Manero, G., Wierda, W., Cortes, J. and Kantarjian, H. (2010) 'First report of phase 2 study of dasatinib with hyper-CVAD for the frontline treatment of patients with Philadelphia chromosome-positive (Ph+) acute lymphoblastic leukemia', *Blood*, 116(12), pp. 2070-7.

Rees, J.S., Lowe, N., Armean, I.M., Roote, J., Johnson, G., Drummond, E., Spriggs, H., Ryder, E., Russell, S., St Johnston, D. and Lilley, K.S. (2011) 'In vivo analysis of proteomes and interactomes using Parallel Affinity Capture (iPAC) coupled to mass spectrometry', *Mol Cell Proteomics*, 10(6), p. M110.002386.

Relling, M.V., Gardner, E.E., Sandborn, W.J., Schmiegelow, K., Pui, C.H., Yee, S.W., Stein, C.M., Carrillo, M., Evans, W.E., Hicks, J.K., Schwab, M., Klein, T.E. and Clinical Pharmacogenetics Implementation, C. (2013) 'Clinical pharmacogenetics implementation consortium guidelines for thiopurine methyltransferase genotype and thiopurine dosing: 2013 update', *Clin Pharmacol Ther*, 93(4), pp. 324-5.

Relling, M.V., Yang, W., Das, S., Cook, E.H., Rosner, G.L., Neel, M., Howard, S., Ribeiro, R., Sandlund, J.T., Pui, C.H. and Kaste, S.C. (2004) 'Pharmacogenetic risk factors for osteonecrosis of the hip among children with leukemia', *J Clin Oncol*, 22(19), pp. 3930-6.

Rhein, P., Scheid, S., Ratei, R., Hagemeyer, C., Seeger, K., Kirschner-Schwabe, R., Moericke, A., Schrappe, M., Spang, R., Ludwig, W.D. and Karawajew, L. (2007) 'Gene expression shift towards normal B cells, decreased proliferative capacity and distinct surface receptors characterize leukemic blasts persisting during induction therapy in childhood acute lymphoblastic leukemia', *Leukemia*, 21(5), pp. 897-905.

Richter, O., Ern, B., Reinhardt, D. and Becker, B. (1983) 'Pharmacokinetics of dexamethasone in children', *Pediatr Pharmacol (New York)*, 3(3-4), pp. 329-37.

Roberts, K.G., Li, Y., Payne-Turner, D., Harvey, R.C., Yang, Y.L., Pei, D., McCastlain, K., Ding, L., Lu, C., Song, G., Ma, J., Becksfort, J., Rusch, M., Chen, S.C., Easton, J., Cheng, J., Boggs, K., Santiago-Morales, N., Iacobucci, I., Fulton, R.S., Wen, J., Valentine, M., Cheng, C., Paugh, S.W., Devidas, M., Chen, I.M., Reshmi, S., Smith, A., Hedlund, E., Gupta, P., Nagahawatte, P., Wu, G., Chen, X., Yergeau, D., Vadodaria, B., Mulder, H., Winick, N.J., Larsen, E.C., Carroll, W.L., Heerema, N.A., Carroll, A.J., Grayson, G., Tasian, S.K., Moore, A.S., Keller, F., Frei-Jones, M., Whitlock, J.A., Raetz, E.A., White, D.L., Hughes, T.P., Guidry Auvil, J.M., Smith, M.A., Marcucci, G., Bloomfield, C.D., Mrozek, K., Kohlschmidt, J., Stock, W., Kornblau, S.M., Konopleva, M., Paietta, E., Pui, C.H., Jeha, S., Relling, M.V., Evans, W.E., Gerhard, D.S., Gastier-Foster, J.M., Mardis, E., Wilson, R.K., Loh, M.L., Downing, J.R., Hunger, S.P., Willman, C.L., Zhang, J. and Mullighan, C.G. (2014) 'Targetable kinase-activating lesions in Ph-like acute lymphoblastic leukemia', *N Engl J Med*, 371(11), pp. 1005-15.

Robey, R.W., Polgar, O., Deeken, J., To, K.W. and Bates, S.E. (2007) 'ABCG2: determining its relevance in clinical drug resistance', *Cancer Metastasis Rev*, 26(1), pp. 39-57.

Rose, L.I. and Sacchar, C. (1978) 'Choosing corticosteroid preparations', *Am Fam Physician*, 17(3), pp. 198-204.

Rosmond, R., Chagnon, Y.C., Holm, G., Chagnon, M., Perusse, L., Lindell, K., Carlsson, B., Bouchard, C. and Bjorntorp, P. (2000) 'A glucocorticoid receptor gene marker is associated with abdominal obesity, leptin, and dysregulation of the hypothalamic-pituitary-adrenal axis', *Obes Res*, 8(3), pp. 211-8.

Roussel, R., Reis, A.F., Dubois-Laforgue, D., Bellanne-Chantelot, C., Timsit, J. and Velho, G. (2003) 'The N363S polymorphism in the glucocorticoid receptor gene is associated with overweight in subjects with type 2 diabetes mellitus', *Clin Endocrinol (Oxf)*, 59(2), pp. 237-41.

Rubnitz, J.E., Wichlan, D., Devidas, M., Shuster, J., Linda, S.B., Kurtzberg, J., Bell, B., Hunger, S.P., Chauvenet, A., Pui, C.H., Camitta, B. and Pullen, J. (2008) 'Prospective analysis of TEL gene rearrangements in childhood acute lymphoblastic leukemia: a Children's Oncology Group study', *J Clin Oncol*, 26(13), pp. 2186-91.

Rushmore, T.H. and Kong, A.N. (2002) 'Pharmacogenomics, regulation and signaling pathways of phase I and II drug metabolizing enzymes', *Curr Drug Metab*, 3(5), pp. 481-90.

Russell, L.J., Capasso, M., Vater, I., Akasaka, T., Bernard, O.A., Calasanz, M.J., Chandrasekaran, T., Chapiro, E., Gesk, S., Griffiths, M., Guttery, D.S., Haferlach, C., Harder, L., Heidenreich, O., Irving, J., Kearney, L., Nguyen-Khac, F., Machado, L., Minto, L., Majid, A., Moorman, A.V., Morrison, H., Rand, V., Strefford, J.C., Schwab, C., Tonnie, H., Dyer, M.J., Siebert, R. and Harrison, C.J. (2009) 'Deregulated expression of cytokine receptor gene, CRLF2, is involved in lymphoid transformation in B-cell precursor acute lymphoblastic leukemia', *Blood*, 114(13), pp. 2688-98.

Sai, S., Nakagawa, Y., Sakaguchi, K., Okada, S., Takahashi, H., Hongo, T., Seckl, J.R., Chapman, K.E. and Ohzeki, T. (2009) 'Differential regulation of 11beta-hydroxysteroid dehydrogenase-1 by dexamethasone in glucocorticoid-sensitive and -resistant childhood lymphoblastic leukemia', *Leuk Res*, 33(12), pp. 1696-8.

Sakaeda, T., Nakamura, T. and Okumura, K. (2003) 'Pharmacogenetics of MDR1 and its impact on the pharmacokinetics and pharmacodynamics of drugs', *Pharmacogenomics*, 4(4), pp. 397-410.

Samuels, A.L., Beesley, A.H., Yadav, B.D., Papa, R.A., Sutton, R., Anderson, D., Marshall, G.M., Cole, C.H., Kees, U.R. and Lock, R.B. (2014) 'A pre-clinical model of resistance to induction therapy in pediatric acute lymphoblastic leukemia', *Blood Cancer J*, 4, p. e232.

Sanchez, R., St-Cyr, J., Lalonde, M.E., Healy, J., Richer, C., Gagne, V., Laverdiere, C., Silverman, L.B., Sallan, S.E., Neuberg, D., Kutok, J.L., Kritikou, E.A., Krajcinovic, M. and Sinnett, D. (2014) 'Impact of promoter polymorphisms in key regulators of the intrinsic apoptosis pathway on the outcome of childhood acute lymphoblastic leukemia', *Haematologica*, 99(2), pp. 314-21.

Schaaf, M.J. and Cidrowski, J.A. (2002) 'Molecular mechanisms of glucocorticoid action and resistance', *J Steroid Biochem Mol Biol*, 83(1-5), pp. 37-48.

Schinkel, A.H. (1998) 'Pharmacological insights from P-glycoprotein knockout mice', *Int J Clin Pharmacol Ther*, 36(1), pp. 9-13.

Schinkel, A.H., Kemp, S., Dolle, M., Rudenko, G. and Wagenaar, E. (1993) 'N-glycosylation and deletion mutants of the human MDR1 P-glycoprotein', *J Biol Chem*, 268(10), pp. 7474-81.

Schinkel, A.H., Mol, C.A., Wagenaar, E., van Deemter, L., Smit, J.J. and Borst, P. (1995a) 'Multidrug resistance and the role of P-glycoprotein knockout mice', *Eur J Cancer*, 31A(7-8), pp. 1295-8.

Schinkel, A.H., Wagenaar, E., van Deemter, L., Mol, C.A. and Borst, P. (1995b) 'Absence of the *mdr1a* P-Glycoprotein in mice affects tissue distribution and pharmacokinetics of dexamethasone, digoxin, and cyclosporin A', *J Clin Invest*, 96(4), pp. 1698-705.

Schmidt, S., Irving, J.A., Minto, L., Matheson, E., Nicholson, L., Ploner, A., Parson, W., Kofler, A., Amort, M., Erdel, M., Hall, A. and Kofler, R. (2006a) 'Glucocorticoid resistance in two key models of acute lymphoblastic leukemia occurs at the level of the glucocorticoid receptor', *FASEB J*, 20(14), pp. 2600-2.

Schmidt, S., Irving, J.A.E., Minto, L., Matheson, E., Nicholson, L., Ploner, A., Parson, W., Kofler, A., Amort, M., Erdel, M., Hall, A. and Kofler, R. (2006b) 'Glucocorticoid resistance in two key models of acute lymphoblastic leukemia occurs at the level of the glucocorticoid receptor', *The FASEB Journal*, 20(14), pp. 2600-2602.

Schmiegelow, K., Forestier, E., Hellebostad, M., Heyman, M., Kristinsson, J., Soderhall, S., Taskinen, M., Nordic Society of Paediatric, H. and Oncology (2010) 'Long-term results of NOPHO ALL-92 and ALL-2000 studies of childhood acute lymphoblastic leukemia', *Leukemia*, 24(2), pp. 345-54.

Schrapppe, M., Reiter, A., Zimmermann, M., Harbott, J., Ludwig, W.D., Henze, G., Gadner, H., Odenwald, E. and Riehm, H. (2000) 'Long-term results of four consecutive trials in childhood ALL performed by the ALL-BFM study group from 1981 to 1995. Berlin-Frankfurt-Munster', *Leukemia*, 14(12), pp. 2205-22.

Schultz, K.R., Bowman, W.P., Aledo, A., Slayton, W.B., Sather, H., Devidas, M., Wang, C., Davies, S.M., Gaynon, P.S., Trigg, M., Rutledge, R., Burden, L., Jorstad, D., Carroll, A., Heerema, N.A., Winick, N., Borowitz, M.J., Hunger, S.P., Carroll, W.L. and Camitta, B. (2009) 'Improved early event-free survival with imatinib in Philadelphia chromosome-positive acute lymphoblastic leukemia: a children's oncology group study', *J Clin Oncol*, 27(31), pp. 5175-81.

Schultz, K.R., Carroll, A., Heerema, N.A., Bowman, W.P., Aledo, A., Slayton, W.B., Sather, H., Devidas, M., Zheng, H.W., Davies, S.M., Gaynon, P.S., Trigg, M., Rutledge, R., Jorstad, D., Winick, N., Borowitz, M.J., Hunger, S.P., Carroll, W.L. and Camitta, B. (2014) 'Long-term follow-up of imatinib in pediatric Philadelphia chromosome-positive acute lymphoblastic leukemia: Children's Oncology Group study AALL0031', *Leukemia*, 28(7), pp. 1467-71.

Seckl, J.R. (2004) '11 β -hydroxysteroid dehydrogenases: changing glucocorticoid action', *Current Opinion in Pharmacology*, 4(6), pp. 597-602.

Segnitz, B. and Gehring, U. (1997) 'The function of steroid hormone receptors is inhibited by the hsp90- specific compound geldanamycin', *Journal of Biological Chemistry*, 272(30), pp. 18694-18701.

Shen, H.Y., Zhao, Y., Chen, X.Y., Xiong, R.P., Lu, J.L., Chen, J.F., Chen, L.Y. and Zhou, Y.G. (2010) 'Differential alteration of heat shock protein 90 in mice modifies glucocorticoid

receptor function and susceptibility to trauma', *Journal of Neurotrauma*, 27(2), pp. 373-381.

Shou, M., Hayashi, M., Pan, Y., Xu, Y., Morrissey, K., Xu, L. and Skiles, G.L. (2008) 'Modeling, prediction, and in vitro in vivo correlation of CYP3A4 induction', *Drug Metab Dispos*, 36(11), pp. 2355-70.

Shultz, L.D., Ishikawa, F. and Greiner, D.L. (2007) 'Humanized mice in translational biomedical research', *Nat Rev Immunol*, 7(2), pp. 118-30.

Shultz, L.D., Lyons, B.L., Burzenski, L.M., Gott, B., Chen, X., Chaleff, S., Kotb, M., Gillies, S.D., King, M., Mangada, J., Greiner, D.L. and Handgretinger, R. (2005) 'Human lymphoid and myeloid cell development in NOD/LtSz-scid IL2R gamma null mice engrafted with mobilized human hemopoietic stem cells', *J Immunol*, 174(10), pp. 6477-89.

Silverman, L.B., Gelber, R.D., Dalton, V.K., Asselin, B.L., Barr, R.D., Clavell, L.A., Hurwitz, C.A., Moghrabi, A., Samson, Y., Schorin, M.A., Arkin, S., Decker, L., Cohen, H.J. and Sallan, S.E. (2001) 'Improved outcome for children with acute lymphoblastic leukemia: results of Dana-Farber Consortium Protocol 91-01', *Blood*, 97(5), pp. 1211-8.

Spitzer, M.H. and Nolan, G.P. (2016) 'Mass Cytometry: Single Cells, Many Features', *Cell*, 165(4), pp. 780-91.

Stam, R.W., Den Boer, M.L., Schneider, P., de Boer, J., Hagelstein, J., Valsecchi, M.G., de Lorenzo, P., Sallan, S.E., Brady, H.J., Armstrong, S.A. and Pieters, R. (2010) 'Association of high-level MCL-1 expression with in vitro and in vivo prednisone resistance in MLL-rearranged infant acute lymphoblastic leukemia', *Blood*, 115(5), pp. 1018-25.

Stoller, R.G., Hande, K.R., Jacobs, S.A., Rosenberg, S.A. and Chabner, B.A. (1977) 'Use of plasma pharmacokinetics to predict and prevent methotrexate toxicity', *N Engl J Med*, 297(12), pp. 630-4.

Sun, C., Chang, L. and Zhu, X. (2017) 'Pathogenesis of ETV6/RUNX1-positive childhood acute lymphoblastic leukemia and mechanisms underlying its relapse', *Oncotarget*, 8(21), pp. 35445-35459.

Tago, K., Tsukahara, F., Naruse, M., Yoshioka, T. and Takano, K. (2004) 'Hsp90 inhibitors attenuate effect of dexamethasone on activated NF- κ B and AP-1', *Life Sciences*, 74(16), pp. 1981-1992.

Takahashi, C., Au-Yeung, A., Fuh, F., Ramirez-Montagut, T., Bolen, C., Mathews, W. and O'Gorman, W.E. (2017) 'Mass cytometry panel optimization through the designed distribution of signal interference', *Cytometry A*, 91(1), pp. 39-47.

Takanashi, M., Morimoto, A., Yagi, T., Kuriyama, K., Kano, G., Imamura, T., Hibi, S., Todo, S. and Imashuku, S. (2003) 'Impact of glutathione S-transferase gene deletion on early relapse in childhood B-precursor acute lymphoblastic leukemia', *Haematologica*, 88(11), pp. 1238-44.

Teuffel, O., Kuster, S.P., Hunger, S.P., Conter, V., Hitzler, J., Ethier, M.C., Shah, P.S., Beyene, J. and Sung, L. (2011) 'Dexamethasone versus prednisone for induction therapy in childhood acute lymphoblastic leukemia: a systematic review and meta-analysis', *Leukemia*, 25(8), pp. 1232-8.

Thakur, A., Kadam, R.S. and Kompella, U.B. (2011) 'Influence of drug solubility and lipophilicity on transscleral retinal delivery of six corticosteroids', *Drug Metab Dispos*, 39(5), pp. 771-81.

Tissing, W.J., den Boer, M.L., Meijerink, J.P., Menezes, R.X., Swagemakers, S., van der Spek, P.J., Sallan, S.E., Armstrong, S.A. and Pieters, R. (2007) 'Genomewide identification of prednisolone-responsive genes in acute lymphoblastic leukemia cells', *Blood*, 109(9), pp. 3929-35.

Tissing, W.J., Meijerink, J.P., Brinkhof, B., Broekhuis, M.J., Menezes, R.X., den Boer, M.L. and Pieters, R. (2006) 'Glucocorticoid-induced glucocorticoid-receptor expression and promoter usage is not linked to glucocorticoid resistance in childhood ALL', *Blood*, 108(3), pp. 1045-9.

Tissing, W.J., Meijerink, J.P., den Boer, M.L., Brinkhof, B. and Pieters, R. (2005a) 'mRNA expression levels of (co)chaperone molecules of the glucocorticoid receptor are not involved in glucocorticoid resistance in pediatric ALL', *Leukemia*, 19(5), pp. 727-33.

Tissing, W.J., Meijerink, J.P., den Boer, M.L., Brinkhof, B., van Rossum, E.F., van Wering, E.R., Koper, J.W., Sonneveld, P. and Pieters, R. (2005b) 'Genetic variations in the glucocorticoid receptor gene are not related to glucocorticoid resistance in childhood acute lymphoblastic leukemia', *Clin Cancer Res*, 11(16), pp. 6050-6.

Tissing, W.J.E., Meijerink, J.P.P., den Boer, M.L., Brinkhof, B., van Rossum, E.F.C., van Wering, E.R., Koper, J.W., Sonneveld, P. and Pieters, R. (2005c) 'Genetic Variations in the Glucocorticoid Receptor Gene Are Not Related to Glucocorticoid Resistance in Childhood Acute Lymphoblastic Leukemia', *Clinical Cancer Research*, 11(16), pp. 6050-6056.

Tissing, W.J.E., Meijerink, J.P.P., den Boer, M.L. and Pieters, R. (2003) 'Molecular determinants of glucocorticoid sensitivity and resistance in acute lymphoblastic leukemia', *Leukemia*, 17(1), pp. 17-25.

Tomlinson, E.S., Lewis, D.F., Maggs, J.L., Kroemer, H.K., Park, B.K. and Back, D.J. (1997) 'In vitro metabolism of dexamethasone (DEX) in human liver and kidney: the involvement of CYP3A4 and CYP17 (17,20 LYASE) and molecular modelling studies', *Biochem Pharmacol*, 54(5), pp. 605-11.

Tricot, S., Meyrand, M., Samiccheli, C., Elhmouzi-Younes, J., Corneau, A., Bertholet, S., Malissen, M., Le Grand, R., Nuti, S., Luche, H. and Cosma, A. (2015) 'Evaluating the efficiency of isotope transmission for improved panel design and a comparison of the detection sensitivities of mass cytometer instruments', *Cytometry A*, 87(4), pp. 357-68.

U.S. Food and Drug Administration (2017) *Drug Development and Drug Interactions: Table of Substrates, Inhibitors and Inducers*. Available at:

<https://www.fda.gov/drugs/developmentapprovalprocess/developmentresources/druginteractionslabeling/ucm093664.htm> (Accessed: 14/08/17).

van den Heuvel-Eibrink, M.M., Wiemer, E.A., de Boevere, M.J., van der Holt, B., Vossebeld, P.J., Pieters, R. and Sonneveld, P. (2001) 'MDR1 gene-related clonal selection and P-glycoprotein function and expression in relapsed or refractory acute myeloid leukemia', *Blood*, 97(11), pp. 3605-11.

van Dongen, J.J., Seriu, T., Panzer-Grumayer, E.R., Biondi, A., Pongers-Willemse, M.J., Corral, L., Stolz, F., Schrappe, M., Masera, G., Kamps, W.A., Gadner, H., van Wering, E.R., Ludwig, W.D., Basso, G., de Bruijn, M.A., Cazzaniga, G., Hettinger, K., van der Does-van den Berg, A., Hop, W.C., Riehm, H. and Bartram, C.R. (1998) 'Prognostic value of minimal residual disease in acute lymphoblastic leukaemia in childhood', *Lancet*, 352(9142), pp. 1731-8.

van Galen, J.C., Kuiper, R.P., van Emst, L., Levers, M., Tijchon, E., Scheijen, B., Waanders, E., van Reijmersdal, S.V., Gilissen, C., van Kessel, A.G., Hoogerbrugge, P.M. and van Leeuwen, F.N. (2010) 'BTG1 regulates glucocorticoid receptor autoinduction in acute lymphoblastic leukemia', *Blood*, 115(23), pp. 4810-9.

Veal, G.J., Errington, J., Rowbotham, S.E., Illingworth, N.A., Malik, G., Cole, M., Daly, A.K., Pearson, A.D. and Boddy, A.V. (2013) 'Adaptive dosing approaches to the individualization of 13-cis-retinoic acid (isotretinoin) treatment for children with high-risk neuroblastoma', *Clin Cancer Res*, 19(2), pp. 469-79.

Veerman, A.J., Hahlen, K., Kamps, W.A., Van Leeuwen, E.F., De Vaan, G.A., Solbu, G., Suci, S., Van Wering, E.R. and Van der Does-Van der Berg, A. (1996) 'High cure rate with a moderately intensive treatment regimen in non-high-risk childhood acute lymphoblastic leukemia. Results of protocol ALL VI from the Dutch Childhood Leukemia Study Group', *J Clin Oncol*, 14(3), pp. 911-8.

Veerman, A.J., Kamps, W.A., van den Berg, H., van den Berg, E., Bokkerink, J.P., Bruin, M.C., van den Heuvel-Eibrink, M.M., Korbijn, C.M., Korthof, E.T., van der Pal, K., Stijnen, T., van Weel Sipman, M.H., van Weerden, J.F., van Wering, E.R., van der Does-van den Berg, A. and Dutch Childhood Oncology, G. (2009) 'Dexamethasone-based therapy for childhood acute lymphoblastic leukaemia: results of the prospective Dutch Childhood Oncology Group (DCOG) protocol ALL-9 (1997-2004)', *Lancet Oncol*, 10(10), pp. 957-66.

Vora, A., Goulden, N., Mitchell, C., Hancock, J., Hough, R., Rowntree, C., Moorman, A.V. and Wade, R. (2014) 'Augmented post-remission therapy for a minimal residual disease-defined high-risk subgroup of children and young people with clinical standard-risk and intermediate-risk acute lymphoblastic leukaemia (UKALL 2003): a randomised controlled trial', *Lancet Oncol*, 15(8), pp. 809-18.

Vora, A., Goulden, N., Wade, R., Mitchell, C., Hancock, J., Hough, R., Rowntree, C. and Richards, S. (2013a) 'Treatment reduction for children and young adults with low-risk acute lymphoblastic leukaemia defined by minimal residual disease (UKALL 2003): a randomised controlled trial', *Lancet Oncol*, 14(3), pp. 199-209.

- Vora, A., Goulden, N., Wade, R., Mitchell, C., Hancock, J., Hough, R., Rowntree, C. and Richards, S. (2013b) 'Treatment reduction for children and young adults with low-risk acute lymphoblastic leukaemia defined by minimal residual disease (UKALL 2003): a randomised controlled trial', *The Lancet Oncology*, 14(3), pp. 199-209.
- Vrooman, L.M., Stevenson, K.E., Supko, J.G., O'Brien, J., Dahlberg, S.E., Asselin, B.L., Athale, U.H., Clavell, L.A., Kelly, K.M., Kutok, J.L., Laverdiere, C., Lipshultz, S.E., Michon, B., Schorin, M., Relling, M.V., Cohen, H.J., Neuberg, D.S., Sallan, S.E. and Silverman, L.B. (2013) 'Postinduction dexamethasone and individualized dosing of Escherichia Coli L-asparaginase each improve outcome of children and adolescents with newly diagnosed acute lymphoblastic leukemia: results from a randomized study--Dana-Farber Cancer Institute ALL Consortium Protocol 00-01', *J Clin Oncol*, 31(9), pp. 1202-10.
- Walsh, C., Bonner, J.J., Johnson, T.N., Neuhoff, S., Ghazaly, E.A., Gribben, J.G., Boddy, A.V. and Veal, G.J. (2016) 'Development of a physiologically based pharmacokinetic model of actinomycin D in children with cancer', *Br J Clin Pharmacol*, 81(5), pp. 989-98.
- Wang, Z., Frederick, J. and Garabedian, M.J. (2002) 'Deciphering the phosphorylation "code" of the glucocorticoid receptor in vivo', *J Biol Chem*, 277(29), pp. 26573-80.
- Wang, Z., Malone, M.H., He, H., McColl, K.S. and Distelhorst, C.W. (2003) 'Microarray analysis uncovers the induction of the proapoptotic BH3-only protein Bim in multiple models of glucocorticoid-induced apoptosis', *J Biol Chem*, 278(26), pp. 23861-7.
- Wei, G., Twomey, D., Lamb, J., Schlis, K., Agarwal, J., Stam, R.W., Opferman, J.T., Sallan, S.E., den Boer, M.L., Pieters, R., Golub, T.R. and Armstrong, S.A. (2006) 'Gene expression-based chemical genomics identifies rapamycin as a modulator of MCL1 and glucocorticoid resistance', *Cancer Cell*, 10(4), pp. 331-42.
- Wiemels, J. (2012) 'Perspectives on the causes of childhood leukemia', *Chem Biol Interact*, 196(3), pp. 59-67.
- Wiemels, J.L., Cazzaniga, G., Daniotti, M., Eden, O.B., Addison, G.M., Masera, G., Saha, V., Biondi, A. and Greaves, M.F. (1999) 'Prenatal origin of acute lymphoblastic leukaemia in children', *Lancet*, 354(9189), pp. 1499-503.
- Wiemels, J.L., Xiao, Z., Buffler, P.A., Maia, A.T., Ma, X., Dicks, B.M., Smith, M.T., Zhang, L., Feusner, J., Wiencke, J., Pritchard-Jones, K., Kempfski, H. and Greaves, M. (2002) 'In utero origin of t(8;21) AML1-ETO translocations in childhood acute myeloid leukemia', *Blood*, 99(10), pp. 3801-5.
- Woiterski, J., Ebinger, M., Witte, K.E., Goecke, B., Heininger, V., Philippek, M., Bonin, M., Schrauder, A., Rottgers, S., Herr, W., Lang, P., Handgretinger, R., Hartwig, U.F. and Andre, M.C. (2013) 'Engraftment of low numbers of pediatric acute lymphoid and myeloid leukemias into NOD/SCID/IL2R γ manu mice reflects individual leukemogenicity and highly correlates with clinical outcome', *Int J Cancer*, 133(7), pp. 1547-56.
- Woo, M.H., Hak, L.J., Storm, M.C., Evans, W.E., Sandlund, J.T., Rivera, G.K., Wang, B., Pui, C.H. and Relling, M.V. (1998) 'Anti-asparaginase antibodies following E. coli

asparaginase therapy in pediatric acute lymphoblastic leukemia', *Leukemia*, 12(10), pp. 1527-33.

Working Party on Leukaemia (1986) 'Improvement in treatment for children with acute lymphoblastic leukaemia. The Medical Research Council UKALL trials, 1972-84. Report to the Council by the Working Party on Leukaemia in Childhood', *Lancet*, 1(8478), pp. 408-11.

Xu, C., Li, C.Y. and Kong, A.N. (2005) 'Induction of phase I, II and III drug metabolism/transport by xenobiotics', *Arch Pharm Res*, 28(3), pp. 249-68.

Yang, L., Panetta, J.C., Cai, X., Yang, W., Pei, D., Cheng, C., Kornegay, N., Pui, C.H. and Relling, M.V. (2008) 'Asparaginase may influence dexamethasone pharmacokinetics in acute lymphoblastic leukemia', *J Clin Oncol*, 26(12), pp. 1932-9.

Zhang, J., Mullighan, C.G., Harvey, R.C., Wu, G., Chen, X., Edmonson, M., Buetow, K.H., Carroll, W.L., Chen, I.M., Devidas, M., Gerhard, D.S., Loh, M.L., Reaman, G.H., Relling, M.V., Camitta, B.M., Bowman, W.P., Smith, M.A., Willman, C.L., Downing, J.R. and Hunger, S.P. (2011) 'Key pathways are frequently mutated in high-risk childhood acute lymphoblastic leukemia: a report from the Children's Oncology Group', *Blood*, 118(11), pp. 3080-7.

Zhu, K., Zhao, J., Lubman, D.M., Miller, F.R. and Barder, T.J. (2005) 'Protein pI shifts due to posttranslational modifications in the separation and characterization of proteins', *Anal Chem*, 77(9), pp. 2745-55.

Zunder, E.R., Finck, R., Behbehani, G.K., Amir, E.-a.D., Krishnaswamy, S., Gonzalez, V.D., Lorang, C.G., Bjornson, Z., Spitzer, M.H., Bodenmiller, B., Fantl, W.J., Pe'er, D. and Nolan, G.P. (2015) 'Palladium-based mass tag cell barcoding with a doublet-filtering scheme and single-cell deconvolution algorithm', *Nat. Protocols*, 10(2), pp. 316-333.

Appendices

Appendix A. UKALL 2011 inclusion and exclusion criteria

Taken directly from UKALL 2011 Protocol version 6.0

Main Inclusion and Exclusion Criteria

Inclusion Criteria

UKALL 2011 is open to all patients from age 1 (first birthday) to 24 years 364 days (at time of diagnosis) with a first diagnosis of acute lymphoblastic leukaemia or lymphoblastic lymphoma (T-NHL or Smlg negative precursor B-NHL) diagnosed using standard criteria. Written informed consent is required for all patients and a negative pregnancy test within 2 weeks prior to starting treatment for female patients of childbearing potential.

Exclusion Criteria

The following patients are excluded from entering the trial

- Infants less than a year old at diagnosis. It is recommended that these patients be entered onto the relevant Interfant ALL study.
- Patients diagnosed with mature B-ALL (Burkitt-like, t(8;14), or C-MYC re-arranged regardless of morphology or phenotype). Patients with this disease should be treated as mature-B-ALL on a suitable protocol for this condition.
- Patients diagnosed with Philadelphia-positive ALL (t(9;22) or BCR/ABL positive). If randomised patients are subsequently found to have Philadelphia-positive ALL they will be withdrawn from the UKALL 2011 protocol treatment and transferred to a suitable alternative protocol for further therapy.
- Patients in whom written informed consent has not been obtained from parents and/or patients prior to trial entry.
- Patients who are sexually active and are unwilling to use adequate contraception during therapy and for one month after last trial treatment.
- All patients must be registered within 7 days of starting induction treatment.

Appendix B. Validation of plasma dexamethasone assay transfer

Introduction

This report is documenting the validation of the assay to measure dexamethasone in human plasma by LC/MS on the Agilent HPLC coupled to a PE4000 MS. The assay was originally validated on the QTrap LC/MS but had to be transferred as the QTrap LC/MS was being decommissioned. The original method was validated in February 2014 and the details can be found in the report version 1. As the validation is covering an LC/MS change, a full validation is not necessary, as sample specific validation is still applicable from the original validation. Therefore only instrument specific validation needs performing.

During the course of this validation, several small changes were made to the validation performed on the QTrap LC/MS, and these changes are:

- The range of the standard curve was changed from 1 to 100ng/ml because of the range of linearity. From the previous data collected, we know that samples taken 1 and 2 hours post dexamethasone administration are likely to have dexamethasone concentrations above 100ng/ml. Therefore, samples taken 1 and 2 hours after administration of dexamethasone will be diluted 1:2 in blank plasma.
- The quality control sample concentrations were also altered to match the new standard curve range. These were 2, 45 and 90 ng/ml.

Abbreviations

SD	Standard deviation
%CV	Coefficient of variation expressed as a percentage
v/v	Volume/volume
w/v	Weight/volume
M	Molar solution

Limit of detection / quantitation (LOD / LOQ)

This was not performed, as we know from previous data collected that the lowest standard needed is 1ng/ml. Therefore, it was only necessary to verify that concentrations of 1ng/ml were above the limit of quantitation.

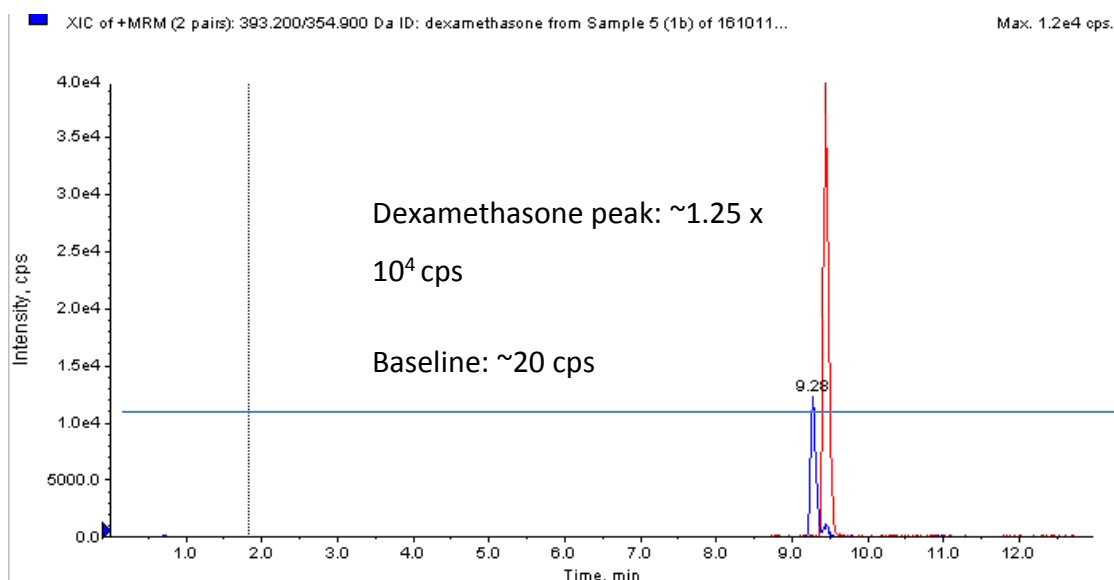


Figure B.1 Limit of detection/quantitation.

The assay performed on 11/10/16 proves this (LB299/13)

Linear range of assay

Lab book ref: LB299/013

Spiked plasma containing dex at concentrations of 0, 1, 5, 10, 50, 100, 150, 200 and 250ng/ml were extracted in triplicate according to the method described in appendix 1 and injected onto the LC/MS/MS system.

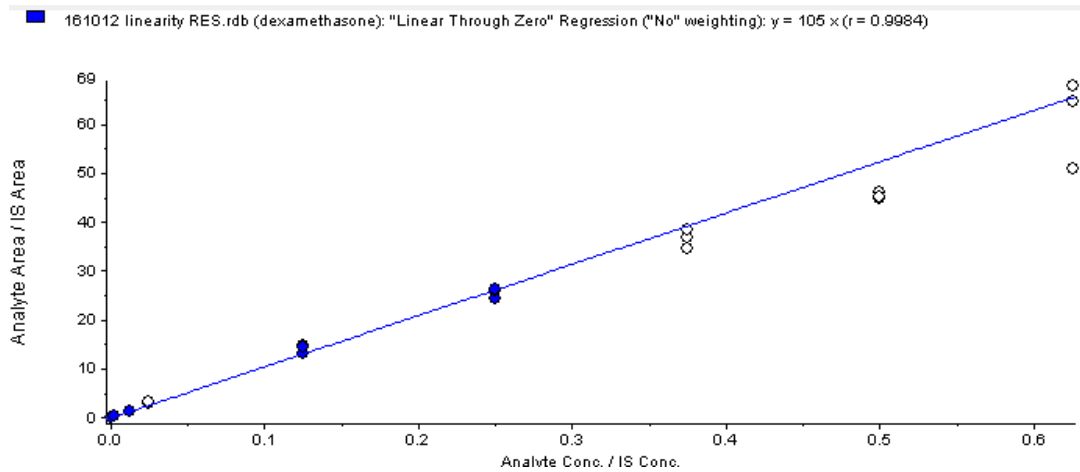
Standard curves using a variety of curve fits and weighting were constructed and the linear range of the assay and best curve fit were determined.

See Figure B.2 for curve types

The assay is linear between 1 and 100 ng/ml.

The proposed range for the assay is 1 to 100ng/ml.

The most appropriate curve fit was 'linear through zero', 'no weighting'

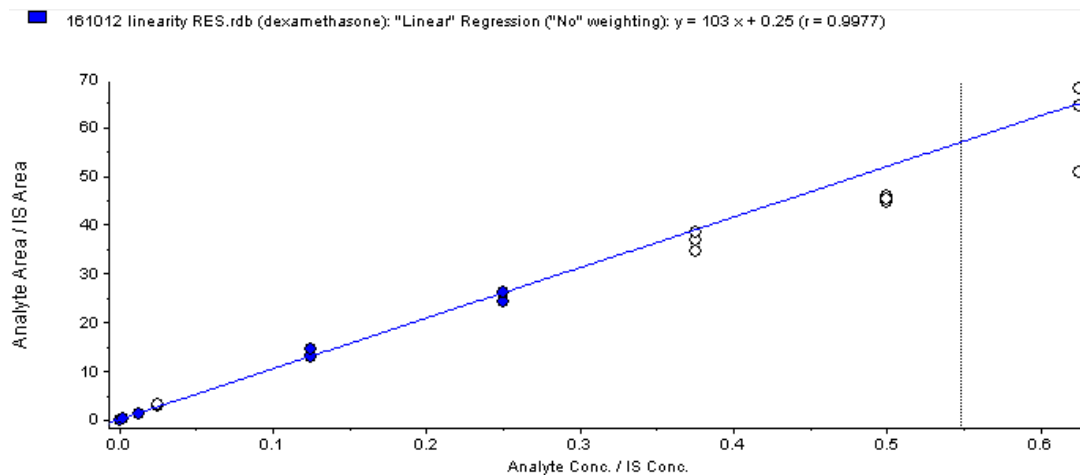


Weighting: Linear through zero, no weighting

Range 1-100ng.ml

Curve: $y=105x$

Correlation: $r = 0.9984$



Weighting: Linear

Range: 1-100ng/ml

Curve: $y=103x+0.25$

Correlation $r=0.9977$

Figure B.2 Curve fits for dex standard curve.

Specificity

Not applicable. For specificity validation see original validation report.

Recovery Data

Not applicable. For specificity validation see original validation report.

Intra assay precision

Lab book ref: LB299/018

Blank plasma was spiked with 2, 45 and 90ng/ml dex and 9 aliquots were extracted, according to the method described in appendix 1, alongside a standard curve of 0 to 100 ng/ml. Extracts were then injected onto the LC/MS/MS system.

The mean, SD and %CV for dexamethasone at each concentration was then determined.

See Table B.2 for results.

INTRA - ASSAY VARIATION													
	Dexamethasone calculated concentration ng/ml												
	1	2	3	4	5	6	7	8	9	Mean	SD	CV (%)	% Accuracy
QC 2	2.28	2.3	2.52	2.28	2.58	2.11	2.14	1.98	2	2.24	0.21	9.4	112.2
QC 45	45.7	49.6	44.2	47	50.5	41	47.4	41.9	37.6	45.0	4.22	9.4	100.0
QC 90	82.8	83.2	82.2	83.3	85.1	78.3	82.8	90.1	81.2	83	3.17	3.8	92.5

Table B.2 Intra assay precision.

Intra assay precision was good with a mean %CV for dexamethasone of 7.5%. Acceptable CV is less than 10%.

Inter assay precision

Lab book refs: LB299/019, 021, 026, 030, 035, 038, 043, 047, 059.

Blank plasma was spiked with 2, 45 and 90 ng/ml dexamethasone and between 3 and 9 aliquots were extracted, according to the method described Chapter 2, alongside a standard curve of 0 to 100 ng/ml. Extracts were then injected onto the LC/MS/MS system.

This was performed on 10 separate occasions.

The mean inter assay variation for each compound at each concentration was then determined.

See Table B.2 for results.

INTER - ASSAY VARIATION													
QC 2ng/ml													
Date	Results file (.rdb)	Calculated concentration ng/ml										Mean	
		Rep 1	Rep 2	Rep 3	Rep 4	Rep 5	Rep 6	Rep 7	Rep 8	Rep 9	Rep 10		
17/10/2016	161017 intraassay 24h RES	2.28	2.3	2.52	2.28	2.58	2.11	2.15	1.98	2		2.24	
19/10/2016	161019 KW1591 CA1594 RES	2.14	2.32	2.19								2.22	
24/10/2016	161024 KM1608 GM1612 LB1620 RES	2.63	2.26	2.2								2.36	
24/10/2016	161031 KM1501 HC1451 WC1644 RES	2.91	2.08	1.94								2.31	
01/11/2016	161101 New QCs JH 1702 RES	1.98	1.91	1.82	2.07	2.1	2.01					1.98	
24/11/2016	161124 SR1696 RES	2.16	2.36	2.26								2.26	
05/12/2016	161205 AG1482 SM1516 LR1528 JG1549 RES	2.11	2.05	2.13								2.10	
06/12/2016	161212 LA1607 BR1541 HP1517 RES	2.26	2.23	2.02								2.17	
11/01/2017	170111 new std test RES	2.26	2.13	1.95								2.11	
03/02/2017	170203 AW1768 new QCs RES	2.28	2.18	2.33	2.25	2.54	2.24					2.30	
												MEAN	2.21
												STD	0.12
												CV %	5.3
QC 45ng/ml													
Date	Results file (.rdb)	Calculated concentration ng/ml										Mean	
		Rep 1	Rep 2	Rep 3	Rep 4	Rep 5	Rep 6	Rep 7	Rep 8	Rep 9	Rep 10		
17/10/2016	161017 intraassay 24h RES	45.7	49.6	44.3	47	50.5	41	47.6	41.9	37.7		45.0	
19/10/2016	161019 KW1591 CA1594 RES	44.4	47.0	44.4								45.3	
24/10/2016	161024 KM1608 GM1612 LB1620 RES	43.4	45.9	45.0								44.8	
24/10/2016	161031 KM1501 HC1451 WC1644 RES	39.1	39.5	42.1								40.2	
01/11/2016	161101 New QCs JH 1702 RES	41.9	42.8	40.9	45.4	46	45.8					43.8	
24/11/2016	161124 SR1696 RES	47.1	43.5	47.4								46.0	
05/12/2016	161205 AG1482 SM1516 LR1528 JG1549 RES	39.8	43.1	44.8								42.6	
06/12/2016	161212 LA1607 BR1541 HP1517 RES	41.2	39.9	40.0								40.4	
11/01/2017	170111 new std test RES	43.5	44.6	42.1								43.4	
03/02/2017	170203 AW1768 new QCs RES	40.4	41.8	43.6	46.3	45.9	44.9					43.8	
												MEAN	43.5
												STD	2.0
												CV %	4.5
QC 90ng/ml													
Date	Results file (.rdb)	Calculated concentration ng/ml										Mean	
		Rep 1	Rep 2	Rep 3	Rep 4	Rep 5	Rep 6	Rep 7	Rep 8	Rep 9	Rep 10		
17/10/2016	161017 intraassay 24h RES	83.3	83.3	82.4	83.4	85.4	78.3	83.4	90.6	81.2		83	
19/10/2016	161019 KW1591 CA1594 RES	79.9	84.5	78.4								81	
24/10/2016	161024 KM1608 GM1612 LB1620 RES	75.2	78.7	18.3								57	
24/10/2016	161031 KM1501 HC1451 WC1644 RES	72.7	79.4	91.7								81	
01/11/2016	161101 New QCs JH 1702 RES	83.3	77.7	86.7	90.5	88.7	88.9					86	
24/11/2016	161124 SR1696 RES	81.0	81.0	82.4								81	
05/12/2016	161205 AG1482 SM1516 LR1528 JG1549 RES	80.5	77.5	82.4								80	
06/12/2016	161212 LA1607 BR1541 HP1517 RES	79.1	79.1	73.4								77	
11/01/2017	170111 new std test RES	83.6	76.7	81.3								81	
03/02/2017	170203 AW1768 new QCs RES	78.7	78.3	81.6	81.2	85.0	90.0					82	
												MEAN	79
												STD	8.0
												CV %	10.1
									Without 18.3 value			MEAN	81
												STD	2.7
												CV %	3.3
										mean CV			6.6

Table B.2 Interassay precision.

Values greater than +/- 15% (20% for QC2). Inter assay precision was good with a mean CV for dex of 6.6%. Acceptable CV is less than 10%.

Stability data

- Experimental stability
- Freeze/Thaw stability – Not applicable, see original validation report
- Long Term Storage stability – Not applicable, see original validation report

Experimental stability - Lab book ref: LB299/018 & 020

Blank plasma was spiked with 2, 45 and 90ng/ml dex and 5 aliquots were extracted, according to the method described in appendix 1, alongside a standard curve of 0 to 100 ng/ml.

50µl of all replicates of each extracted spiked plasma sample were injected immediately onto the LC/MS/MS alongside the standard curve.

The remainder of the extracted spiked plasma samples were stored at 4°C (in the auto sampler) for 24 hours.

After 24 hours, 50µl of the remainder of the sample of all replicates of each extracted spiked plasma sample were injected onto the LC/MS/MS.

The percentage difference in mean peak area for the samples stored for 24 hours was calculated against the mean peak area for those samples injected at time 0 to determine the experimental stability of the assay.

See Table B.3 for results.

QC 2 ng/ml

Calculated concentration ng/ml							
Time	Rep 1	Rep 2	Rep 3	Rep 4	Rep 5	Mean	% change from Time 0
0 - 4oC	2.58	2.11	2.15	1.98	2	2.16	
24h - 4oC	2.56	2.17	2.17	1.96	2	2.17	100.4

QC 45 ng/ml

Calculated concentration ng/ml							
Time	Rep 1	Rep 2	Rep 3	Rep 4	Rep 5	Mean	% change from Time 0
0 - 4oC	49.6	44.3	47	50.5	41	46.48	
24h - 4oC	51.5	47.4	49.2	51.4	42.3	48.36	104.0

QC 90 ng/ml

Calculated concentration ng/ml							
Time	Rep 1	Rep 2	Rep 3	Rep 4	Rep 5	Mean	% change from Time 0
0 - 4oC	83.2	82.2	83.3	85.1	78.3	82.42	
24h - 4oC	90.9	87.3	87.2	93.8	86.4	89.12	108.1

Table B.3 Dex experimental stability.

There was no loss of stability of dex when stored at either room temperature or 4°C on the autosampler.

Appendix C. LC/MS advanced settings

QTrap Settings for quantification of dex concentrations in human plasma

Mass Spec parameters:

Scan Type:	MRM	Duration:	5.002mins
Polarity:	Positive	Delay time:	0
Total Scan Time:	0.3100	Cycles:	968

ID	Time (msecs)	DP (volts)	EPstart (volts)	CE (volts)	CEPstart (volts)	CXPstart (volts)
Dex	150.0	76.000	12.000	33.000	30.000	6.000
Bec	150.0	71.000	10.000	39.000	32.000	6.000

Table C.1 QTrap mass spectrometer settings

Ion Source parameters:

CAD:	-2.000
Ihe:	1.000
GS2:	80.00
GS1:	40.00
TEM:	550.00
IS:	5500
CUR:	40.00

Advanced MS parameters:

Resolution Q1:	Unit
Resolution Q2:	Unit
Intensity threshold:	0
Settling time:	0 ms
Pause:	5.007 ms

Autosampler parameters:

Syringe size (μl):	250
Injection volume (μl):	50
Pre inject Flushes (#):	2
Post inject flushes (#):	2
Air cushion (μl):	10
Excess volume (μl):	10
Sample speed:	Medium
Needle level (%):	10
Inject delay time:	0 min
Replicate injections:	1
Analysis time:	0 min
Vial vent mode:	Off
Loop mode:	Partial
Loop volume (μl):	200
Flush volume (μl):	250
Flush speed:	Medium
Temperature control:	Enable
Set point:	4 °C

Pump settings:

	Total Time (min)	Flow Rate (µl/min)	Gradient Profile	A (%)	B (%)
0	0.0	300.000	1.0	60.0	40.0
1	0.5	300.000	1.0	60.0	40.0
2	1.5	300.000	1.0	0.0	100.0
3	2.0	300.000	1.0	60.0	40.0
4	5.0	300.000	1.0	60.0	40.0

Table C.2 QTrap pump settings.

Limits:

Minimum Pressure: 0.0 psi

Maximum Pressure: 6100.0 psi

Shutdown time: 60 min

Valco valve settings

Position name for Step0: Waste

	Total Time (min)	Position
0	1.4	B
1	3.2	Waste

Table C.3 QTrap Valco Valve settings.

Agilent Settings for quantification of dex concentrations in human plasmaLC/MS Conditions

Flow Rate: 300µl/min

Column: Gemini 3µ C18 110A (50x3mm) (Phenomenex,008-4439-YO)

Injection volume: 50µl

Run Time: 13 min

Column temperature: Ambient

Sample temperature: 4°C

Dexamethasone Q1 Mass: 393.27

Dexamethasone Q3 Mass: 354.90

Beclomethasone Q1 Mass: 409.114

Beclomethasone Q3 Mass: 147.1

Retention time of Dexamethasone ~9.36mins

Retention time of Beclomethasone ~9.60 mins

Mass Spec parameters:

Scan Type: MRM Duration: 13.000mins
Polarity: Positive Delay time: 0
Total Scan Time: 0.3100seconds Cycles: 2516

ID	Time (msecs)	DP (volts)	EP (volts)	CE (volts)	CXP (volts)
Dex	150.0	46.000	10.000	19	12.000
Bec	150.0	56.000	10.000	43	10.000

Table C.4 Mass spectrometer settings.

Ion Source parameters:

CAD: 5.00
Ihe: ON
GS2: 40.00
GS1: 60.00
TEM: 600.00
IS: 5500
CUR: 20.00

Advanced MS parameters:

Resolution Q1: Unit
Resolution Q2: Unit
Intensity threshold: 0
Settling time: 0 ms
Pause: 5.007 ms

Autosampler parameters:

Sampler 1 (G7167A): "Multisampler"
Draw Speed: 100.0
Eject Speed: 400.0
Wait Time After Drawing: 1.2
Needle Wash Mode: Flush Port
Duration: 3
Needle Wash Mode: Standard
Wash
Injection Volume: 50.00
Overlap Injection Enabled: No

Injection Valve to Bypass for Delay Volume

Reduction: No
Sample Flush-Out Factor: 5.0
Draw Position Offset: 0.0
Use Vial/Well Bottom Sensing: Yes
Stoptime Mode: No Limit
Posttime Mode: Off
Column Comp. 1 (G1316A): "Column Comp."
Enable Analysis Left Temperature On: No
Temperature Control Mode: Not Controlled
Enable Analysis Right Temperature On: No
Right temperature Control Mode: Not Controlled
Stoptime Mode: As
pump/injector
Posttime Mode: Off
Autosampler temperature 4°C

	Total Time (min)	Flow Rate (µl/min)	A (%)	B (%)
0	0.0	300.000	100	0
1	0.5	300.000	100	0
2	7.0	300.000	30.0	70.0
3	9.0	300.000	30.0	70.0
4	10.0	300.000	100.0	0
5	13	300.000	100.0	0

Table C.5 Pump settings.

Limits

Minimum Pressure: 0.0 bar

Maximum Pressure: 400 bar

Shutdown time: 60 min

Valco valve settings

Position name for Step B: Waste

	Total Time (min)	Position
1	0.0	B
2	8.0	A
3	11.0	B

Table C.6 Valco Valve settings.

Appendix D. Validation of LC/MS method to quantify dex concentrations in cell lysates

Data submitted for the degree of Masters by Research in 2014 (Jackson, 2014):

The validated method for the measurement of dexamethasone in human plasma was adapted to measure dexamethasone concentrations in cell lysates. In order to ensure compatibility of the two methods, a number of checks were made. First, it was investigated whether there was a matrix effect of RF10 culture media. There was no difference in dexamethasone retention time between plasma, mobile phase (the matrix cell lines were reconstituted in) and RF10 media (Figure D.1)

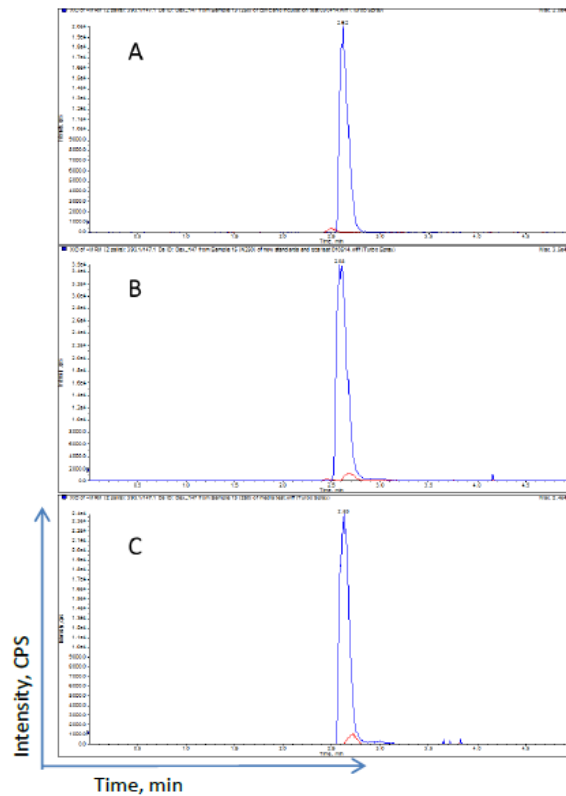


Figure D.1 Chromatograms of dexamethasone in (A) spiked mobile phase (B) spiked plasma and (C) Spiked RF10.

All matrices show a comparable retention time of ~2.5 minutes. X axis: time (Minutes) Y axis: Intensity of peak (CPS)

Second, the stability of dexamethasone in media for the duration of the intracellular accumulation experiments was established.

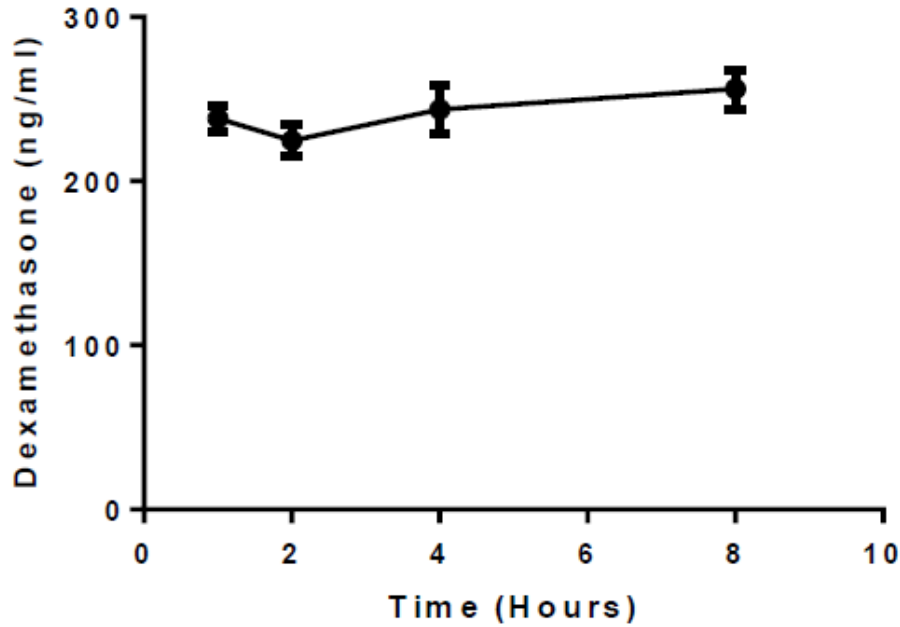


Figure D.2 Dexamethasone is stable in RF10 culture media for at least eight hours.

Aliquots of spiked media were extracted up to eight hours following incubation of PreB697 cells with 500nM dexamethasone. Data is from four independent experiments (\pm SEM)

Appendix E. Pilot GR interactome data

This data was generated by Dr. Lindsay Nicholson with Prof. Julie Irving in collaboration with Prof. Tony Whetton and Prof. David Ray at Manchester University.

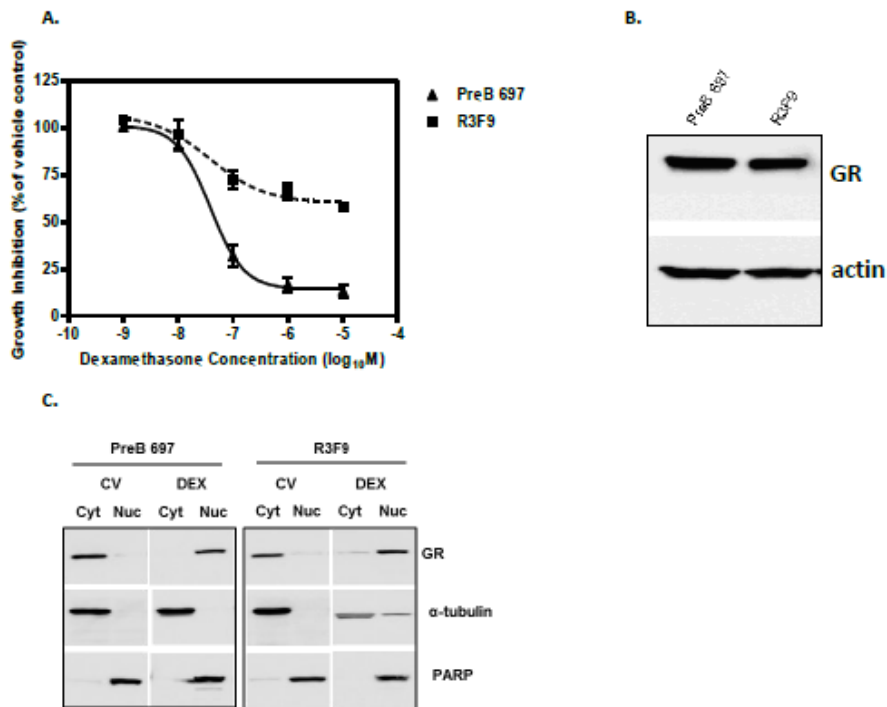


Figure E.1 Characterisation of the GC-sensitive PreB 697 cell line and a GC-resistant sub-clone, R3F9.

A : Response of PreB697 and R3F9 to dexamethasone *in vitro*. The cells were cultured for 96 hours with a range of dexamethasone concentrations (1 -10,000 nM) and growth inhibition was determined by the addition of MTS reagent (Promega, Southampton, UK) which assesses the capacity of cells to reduce formazan and thus is a measure of metabolically active cells. The growth inhibition at each drug concentration was calculated relative to vehicle-control treated cells and expressed as a percentage. Data are the mean \pm S.E.M. of at least three independent experiments. B. Basal GR protein expression in the PreB697 cell lines was assessed by western blotting, with actin as a loading control. C. Nuclear translocation of the GR was assessed in both cell lines by exposing cells to a control vehicle (CV; 0.05% ethanol) or 0.1 μ M dexamethasone (DEX), harvested after 4 hours, followed by subcellular fractionation and immunoblot analysis. Equal amounts of protein from cytosolic (Cyt) and nuclear (Nuc) fractions were separated by SDS-PAGE and membranes probed using antibodies against GR, α -tubulin (cytosolic control) and PARP (nuclear control).

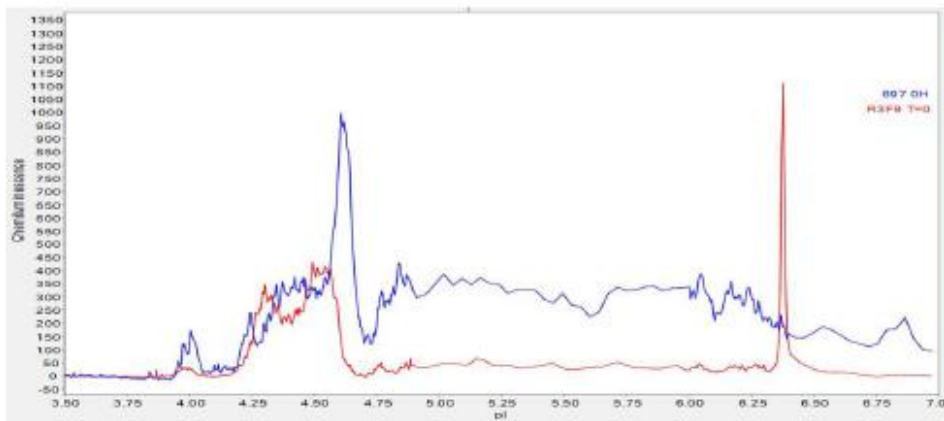


Figure E.2 NanoPro technology shows differences in GR profiles in a GC-sensitive cell line, PreB 697, and a GC-resistant sub-clone, R3F9.

Bicine/CHAPs lysates from untreated PreB 697 (blue line) and R3F9 (red line) cells were separated according to optimised assay conditions and probed with a human-specific pan-GR antibody (Sigma-Aldrich, St Louis, MO, USA). Differences in GR profiles, both in peak intensity and pI positions were found between the cell lines, indicative of distinct post-translational modification events and/or GR interactants.

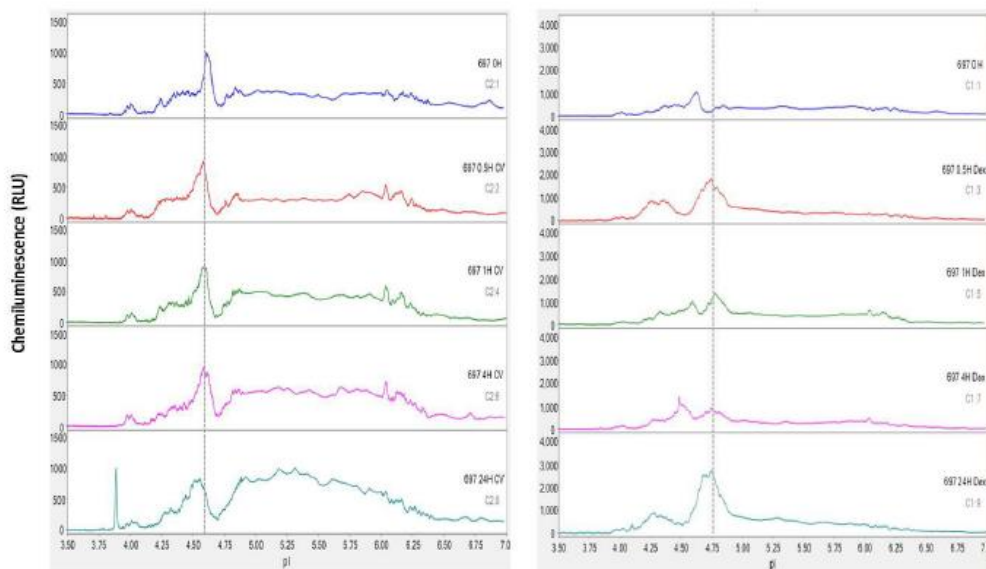


Figure E.3 Nanopro detection of changes in GR profiles in response to dexamethasone-treatment in the GC-sensitive cell line, PreB 697.

Cells were exposed to either control vehicle (CV; 0.05% ethanol) or Dex (0.1 μ M dexamethasone) over a time-course and harvested for protein at the indicated time-points. Bicine/CHAPs lysates were separated according to optimised assay conditions and probed with a human-specific pan-GR antibody (Sigma-Aldrich).

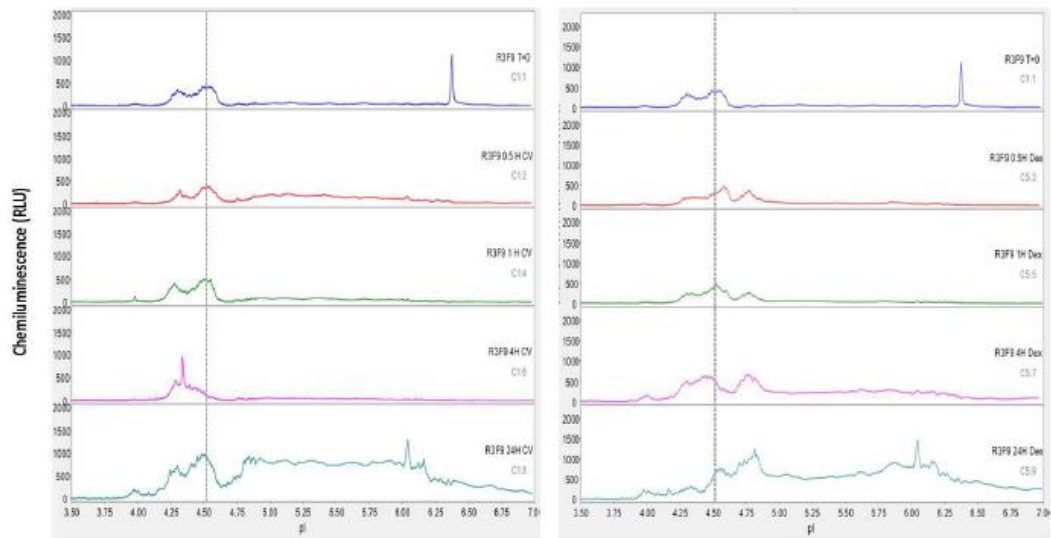


Figure E.4 Nanopro detection of changes in GR profiles in response to dexamethasone-treatment in the GC-resistant cell line, R3F9.

Cells were exposed to either control vehicle (CV; 0.05% ethanol) or Dex (0.1 μ M dexamethasone) over a time-course and harvested for protein at the indicated time-points. Bicine/CHAPs lysates were separated according to optimised assay conditions and probed with a human-specific pan-GR antibody (Sigma-Aldrich).

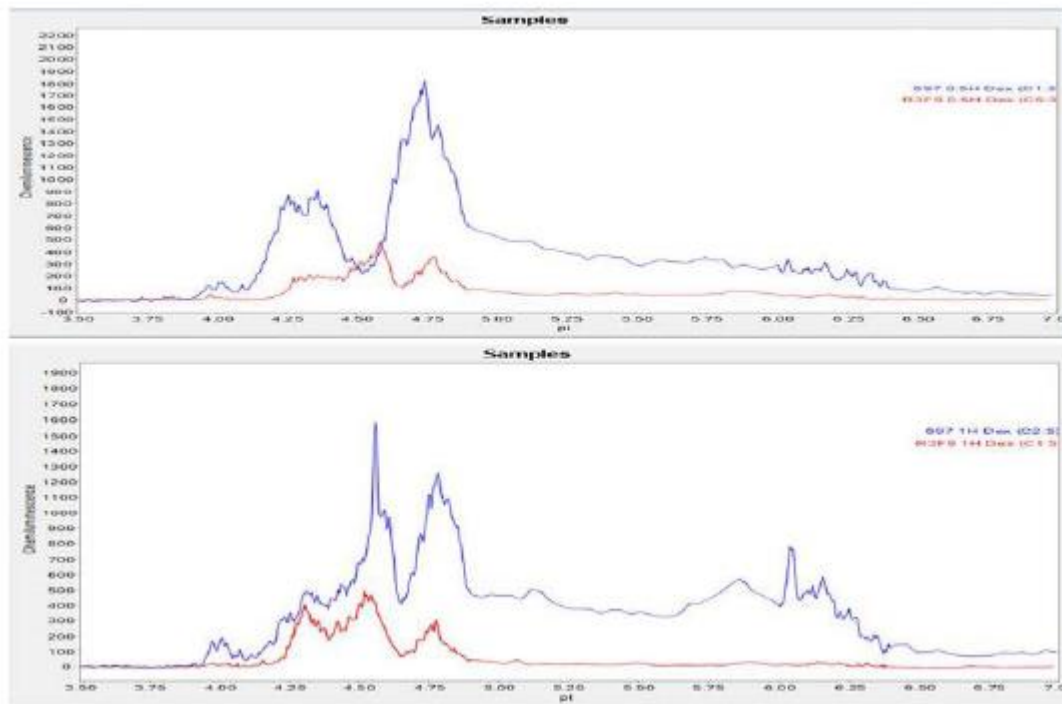


Figure E.5 Nanopro detection of changes in GR profiles in response to dexamethasone-treatment in the GC-sensitive, PreB697, and GC-resistant, R3F9, cell lines after 30 min (upper plot) and 1 hr (lower plot) exposure to 0.1 μ M dexamethasone.

Bicine/CHAPs lysates were separated according to optimised assay conditions and probed with a human-specific pan-GR antibody (Sigma-Aldrich). Differences in GR profiles, both in peak intensity and pI positions were found between the cell lines, indicative of distinct post-translational modification events and/or GR interactants in response to GC-exposure.

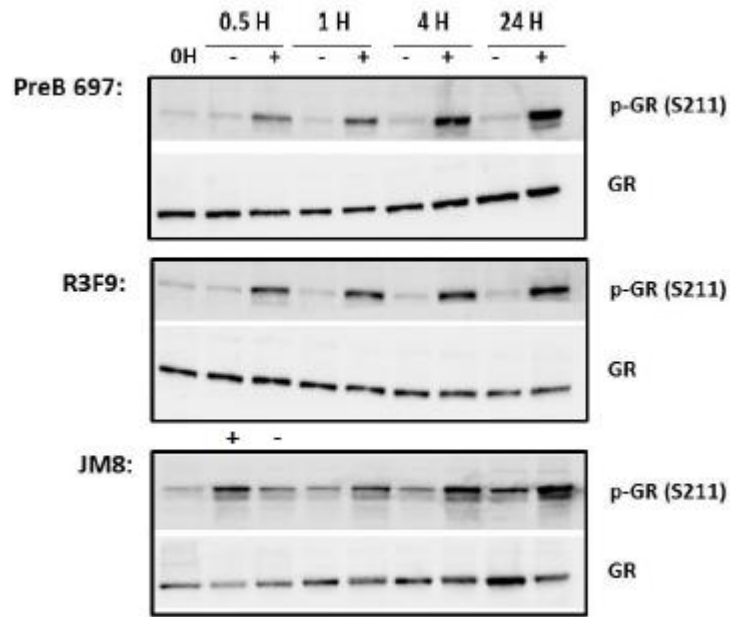


Figure E.6 Glucocorticoid receptor phosphorylation at Serine residue S211 does not differ in a GC-sensitive, PreB697, and a GC-resistant cell line, R3F9, or a GC-resistant primagraft, JM8, in response to GC-exposure.

Cells were exposed to either control vehicle (-; 0.05% ethanol) or GC (+; 0.1 μ M dexamethasone) over a time-course and harvested for protein at the indicated time-points. Equal amounts of protein were loaded and analysed by immunoblotting using antibodies directed to GR phospho-S211 (Cell Signaling Technology) or total GR (Santa Cruz Biotechnology).

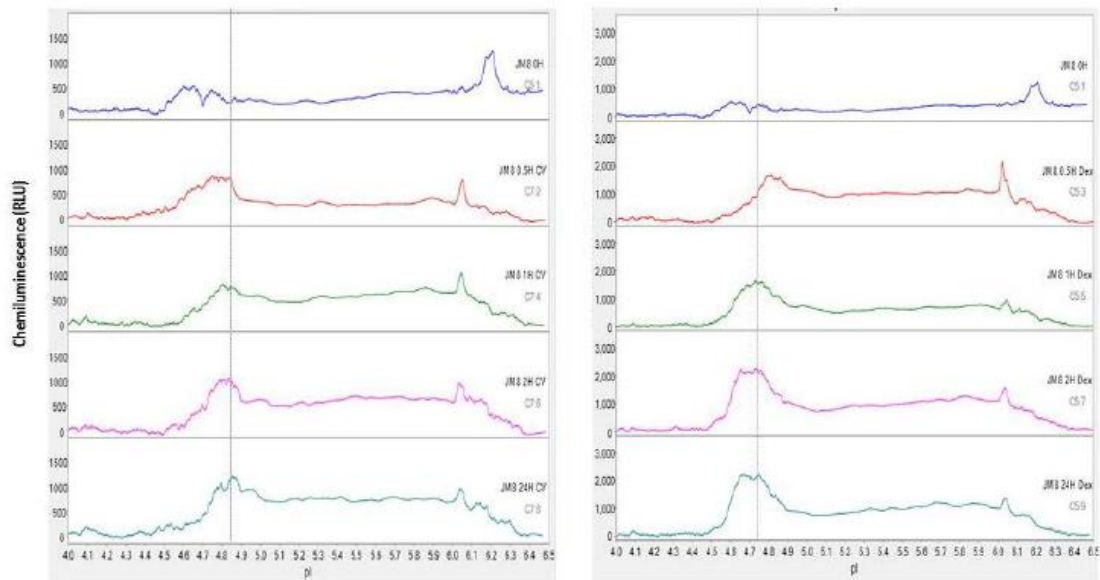


Figure E.7 Nanopro detection of changes in GR profile in response to dexamethasone-treatment in the GC-resistant primagraft, JM8.

Mouse splenic cells with 97.5% engraftment were exposed to either control vehicle (CV; 0.05% ethanol) or Dex (0.1 μ M dexamethasone) over a time-course and harvested for protein at the indicated time-points. Bicine/CHAPs lysates were separated according to optimised assay conditions and probed with a human-specific pan-GR antibody (Sigma-Aldrich).

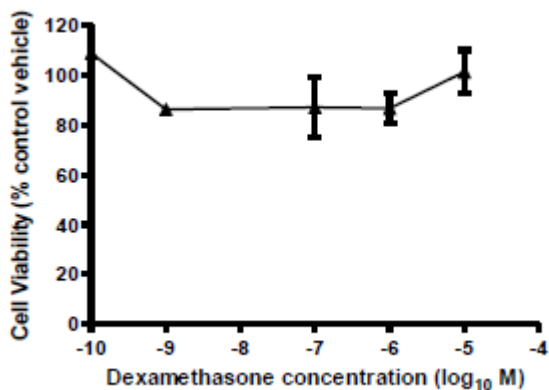


Figure E.8 Response of a xenograft, JM8, to dexamethasone exposure in vitro.

Cells were dosed with 0.1 – 10,000 nM dexamethasone and cell viability was assessed using the MTS assay after a 96 hour drug exposure. The viable cell number at each drug concentration was calculated relative to vehicle-control treated cells, data are mean \pm S.E.M. of at least three wells from a single experiment.

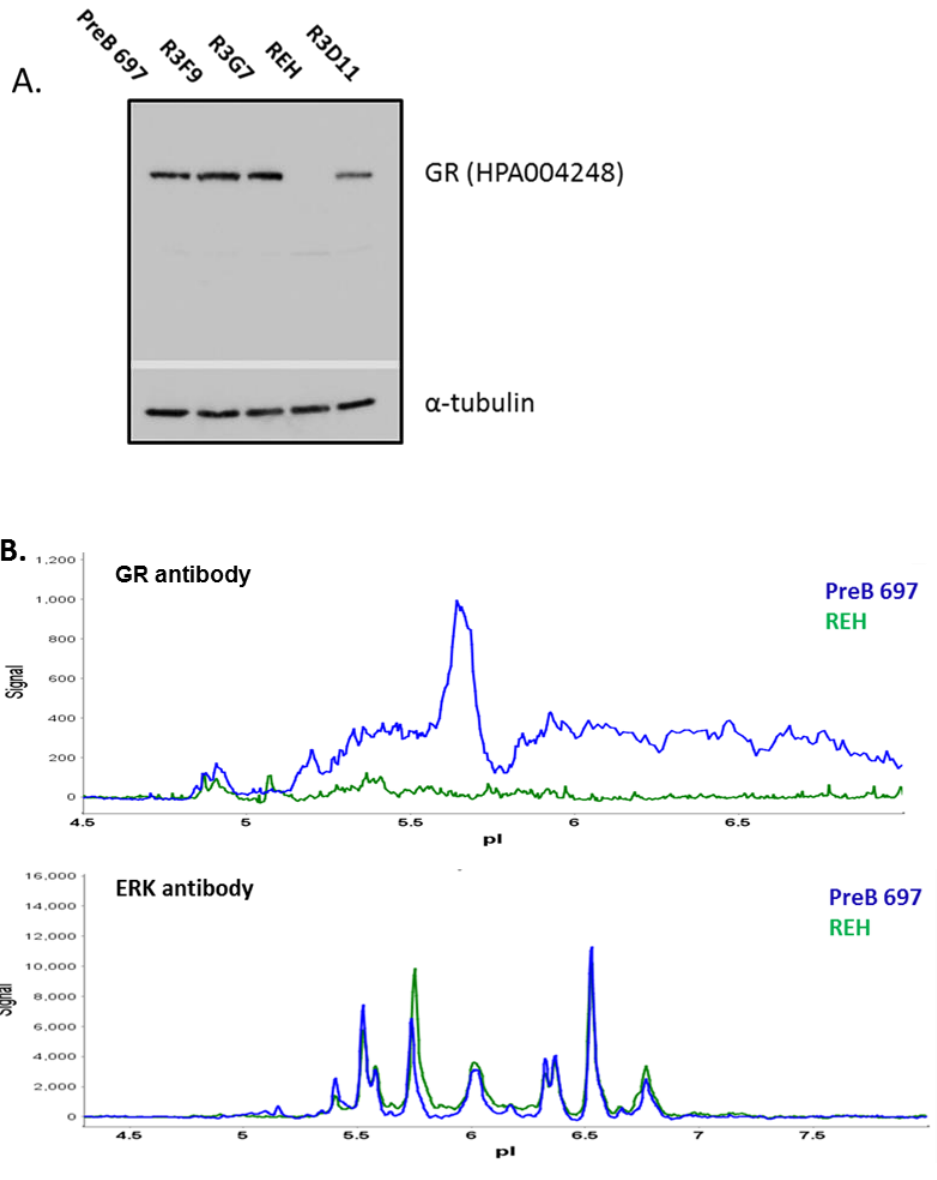
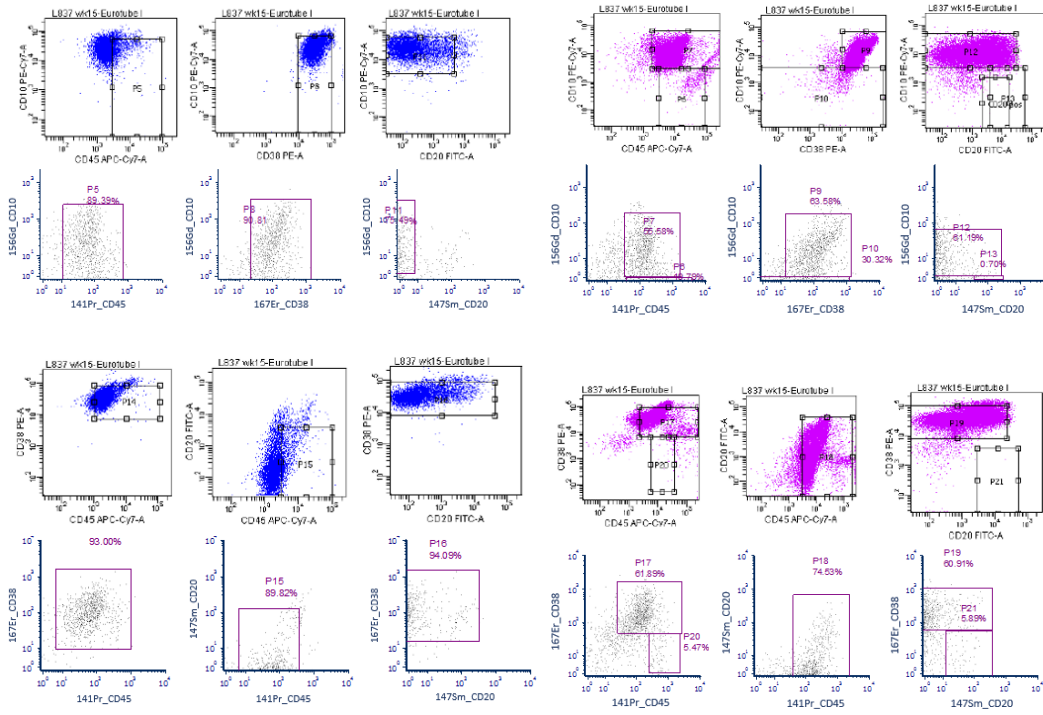


Figure E.9 (A) Glucocorticoid Receptor Expression in Cell lines (B) Nanoprofiles of PreB697 and REH cells with GR and ERK antibodies.

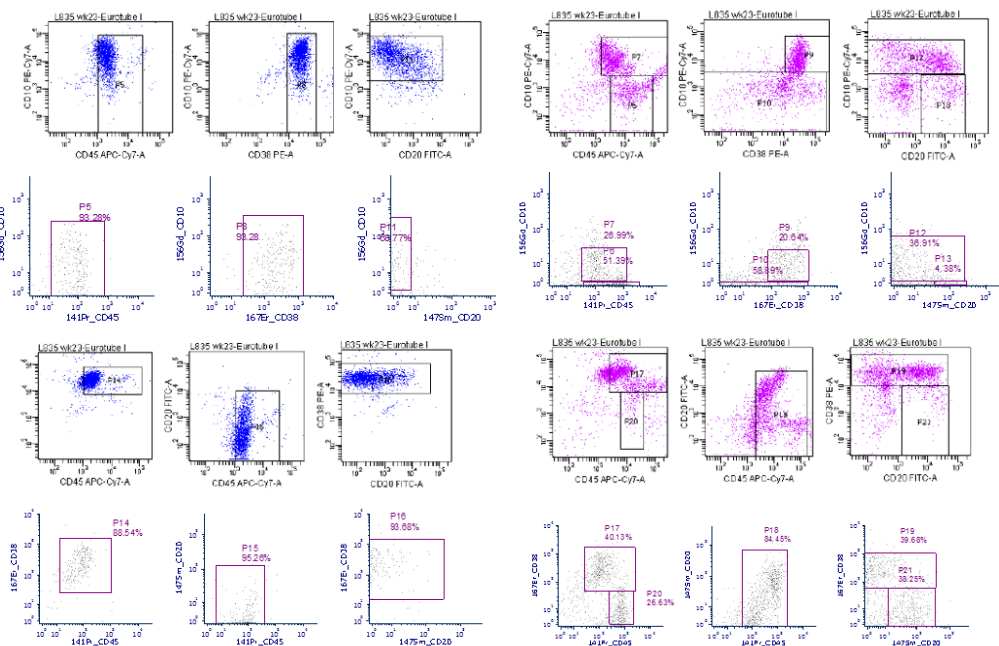
Appendix F. Additional mass cytometry figures

Remission bone marrow samples – comparison to FACS data

A. L837: Blue/Pink = flow cytometry data (week 15). Grey = mass cytometry data (end of treatment)



B. L835 week 23: Blue/Pink = flow cytometry data. Grey = mass cytometry data



C. L940 (week 23): Blue/Pink = flow cytometry data. Grey = mass cytometry data

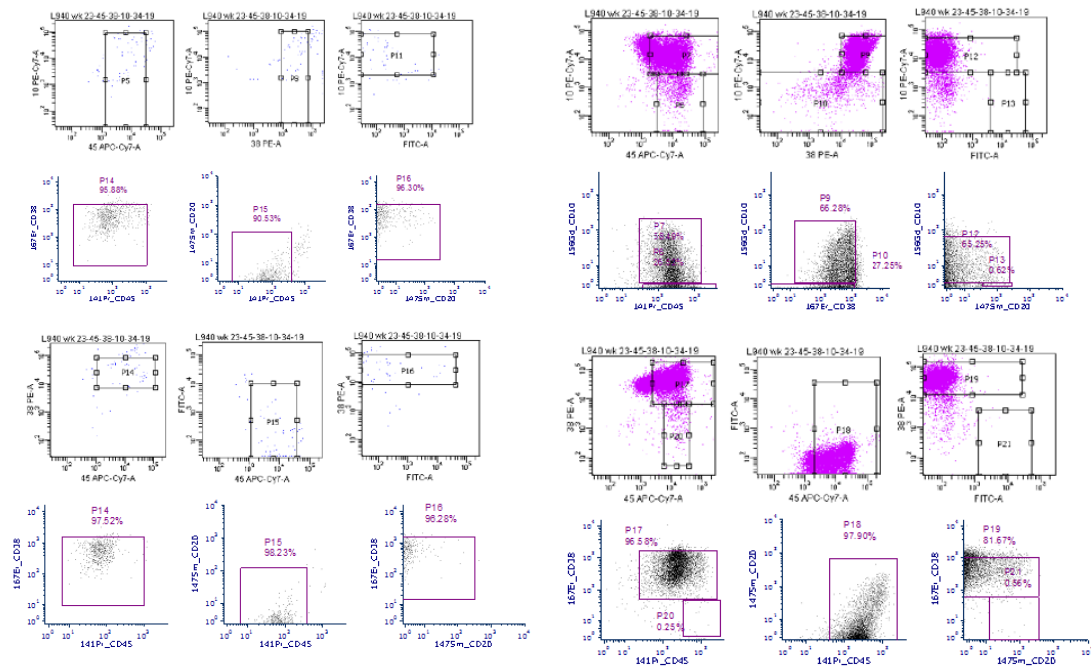
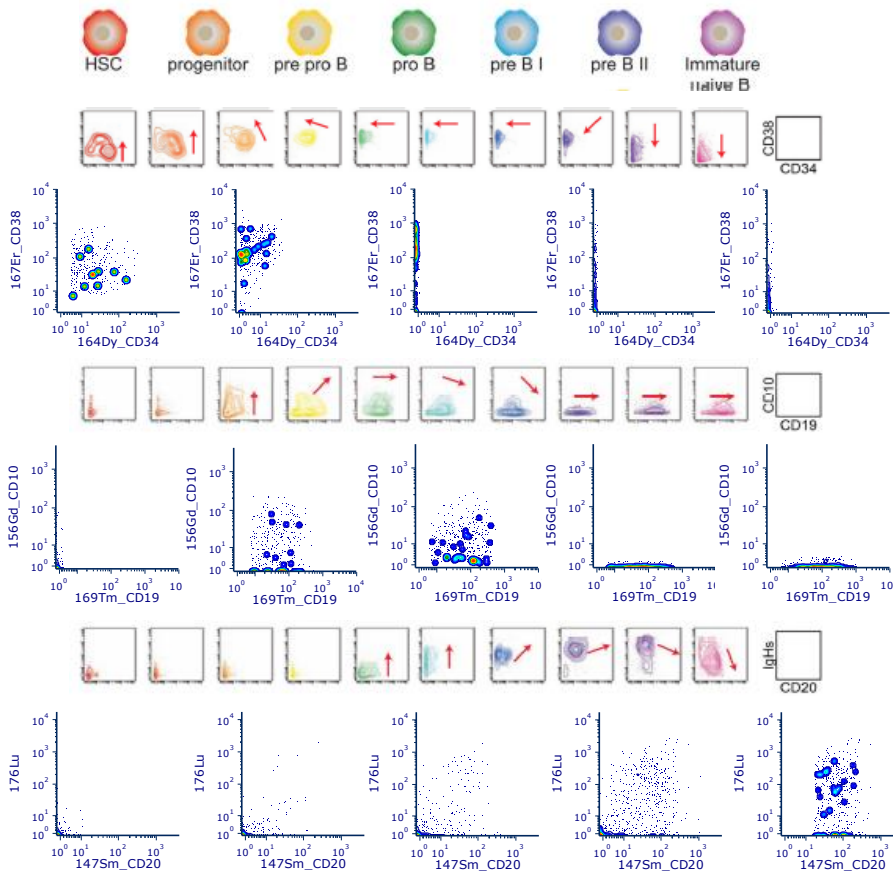


Figure F.1 Comparison of Wanderlust antibody panel data generated using the Helios mass cytometer to historical flow cytometry data; CD34 positive (blue) and negative (pink) cells.

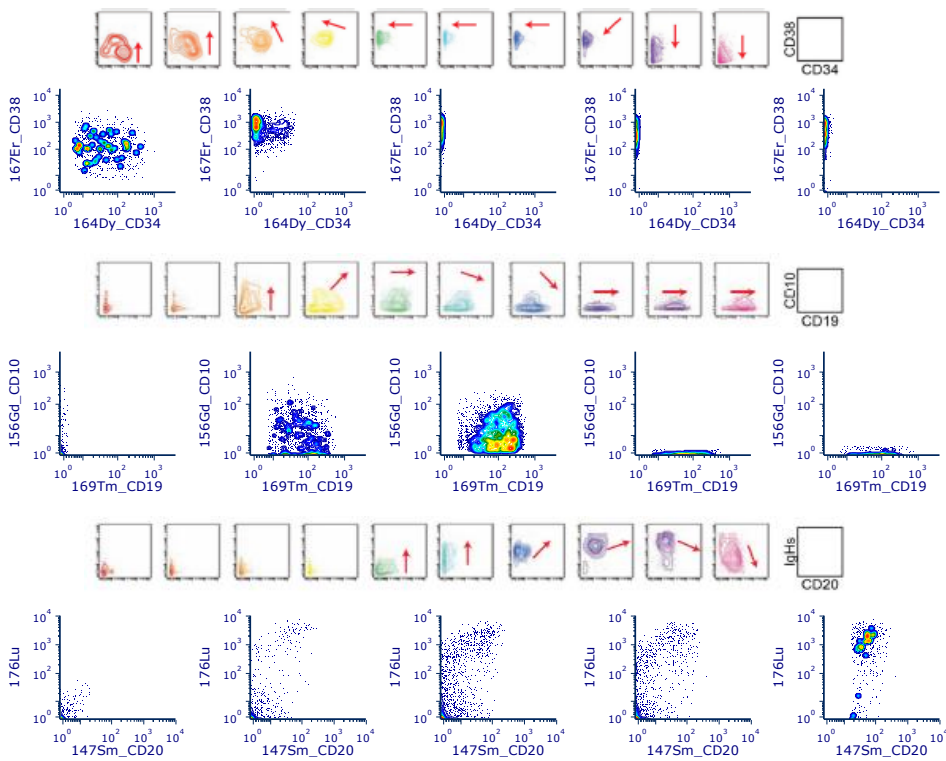
A. Patient L837 (week 15) historically assessed using the Eurotubes I panel by flow cytometry (black outline with blue/pink dots) and (end of treatment) assessed using the Wanderlust panel on the Helios by mass cytometry (navy axes with black dots). B. Patient L835 (week 23) historically assessed using the Eurotubes I panel by flow cytometry (black outline with blue/pink dots) and using the Wanderlust panel on the Helios by mass cytometry (navy axes with black dots). C. Patient L940 (week 23) historically assessed by flow cytometry (black outline with blue/pink dots) and using the Wanderlust panel on the Helios by mass cytometry (navy axes with black dots).

Each flow cytometry dot plot is a direct comparison of the mass cytometry dot plot beneath it.

A. L835 week 23



B. L940 week 23



C. L837 end of treatment

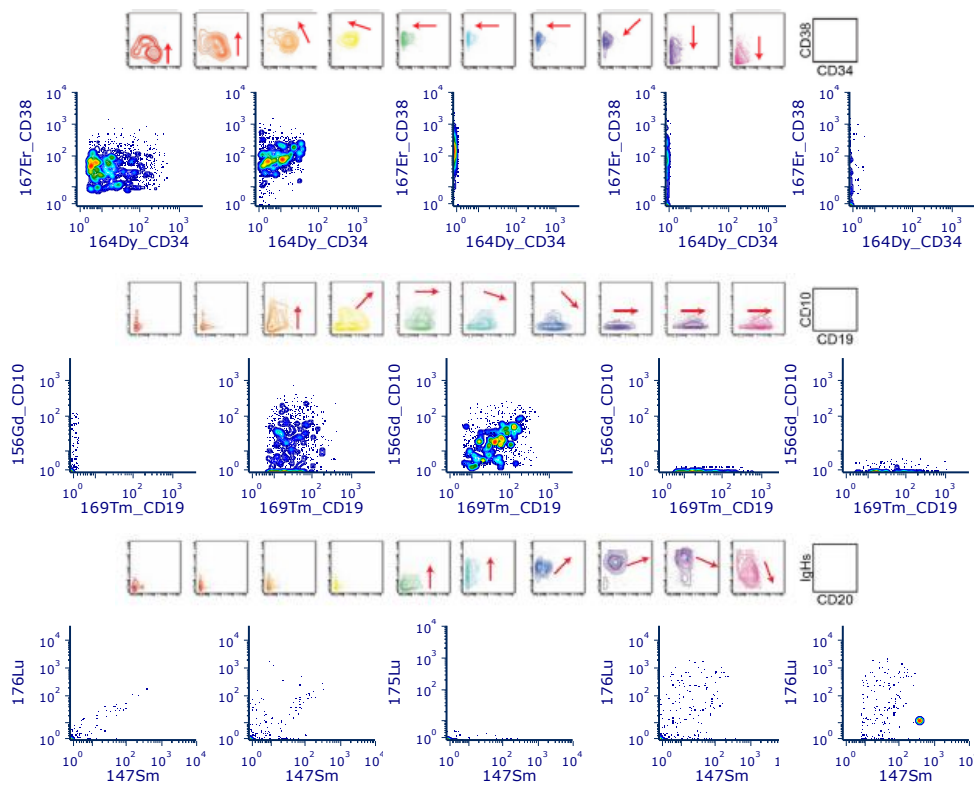
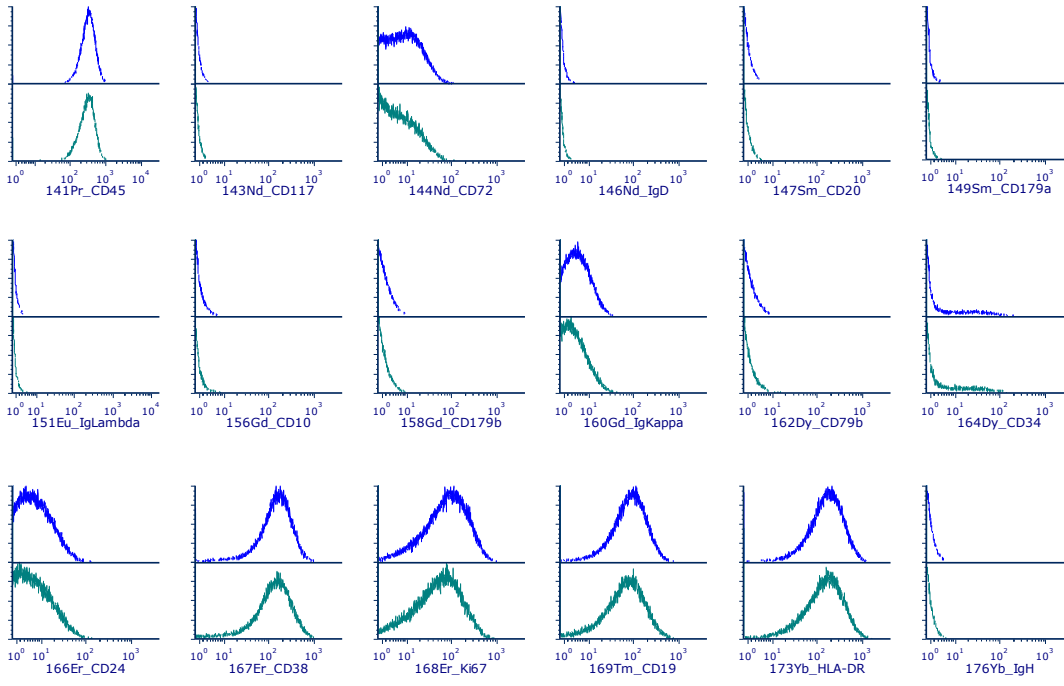


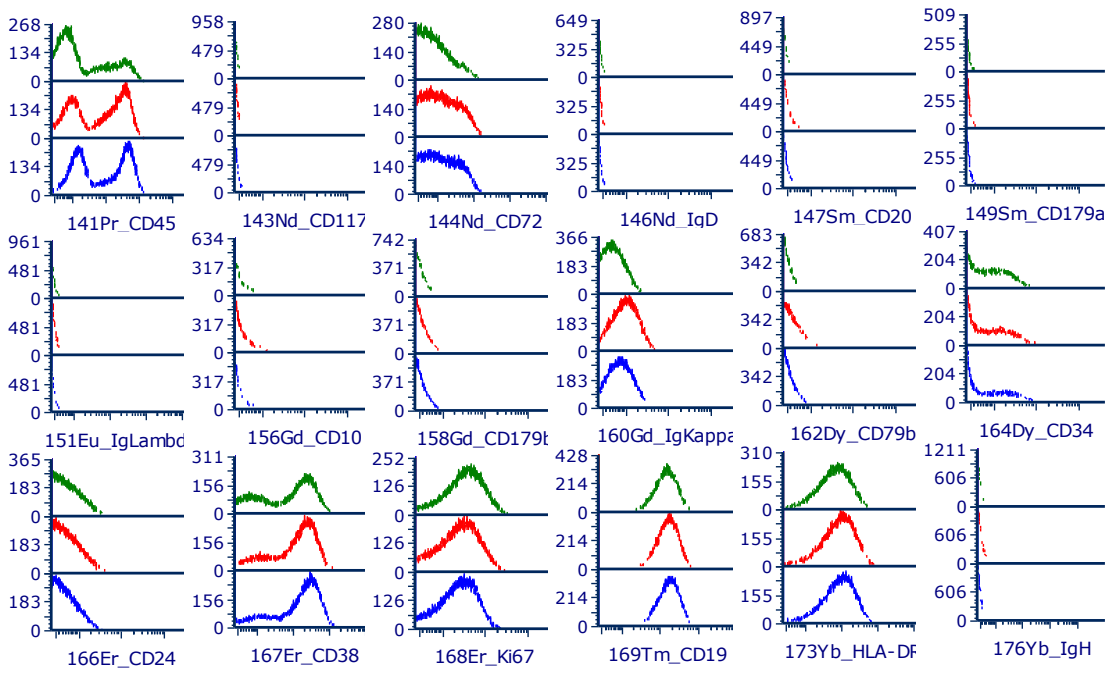
Figure F.2 Comparison of data generated using the metal-altered Wanderlust panel across B cells of different maturation stages compared to that published in Bendall *et al.* (2014).

(A) Patient L835 (week 23) (B) L940 week 23 and (C) L837 end of treatment samples were stained using the Wanderlust antibody panel and compared to data published by Bendall *et al.* (2014). Each row of 10 plots is from the Bendall paper, and the rows beneath them represent data generated at similar cell development stages in this project.

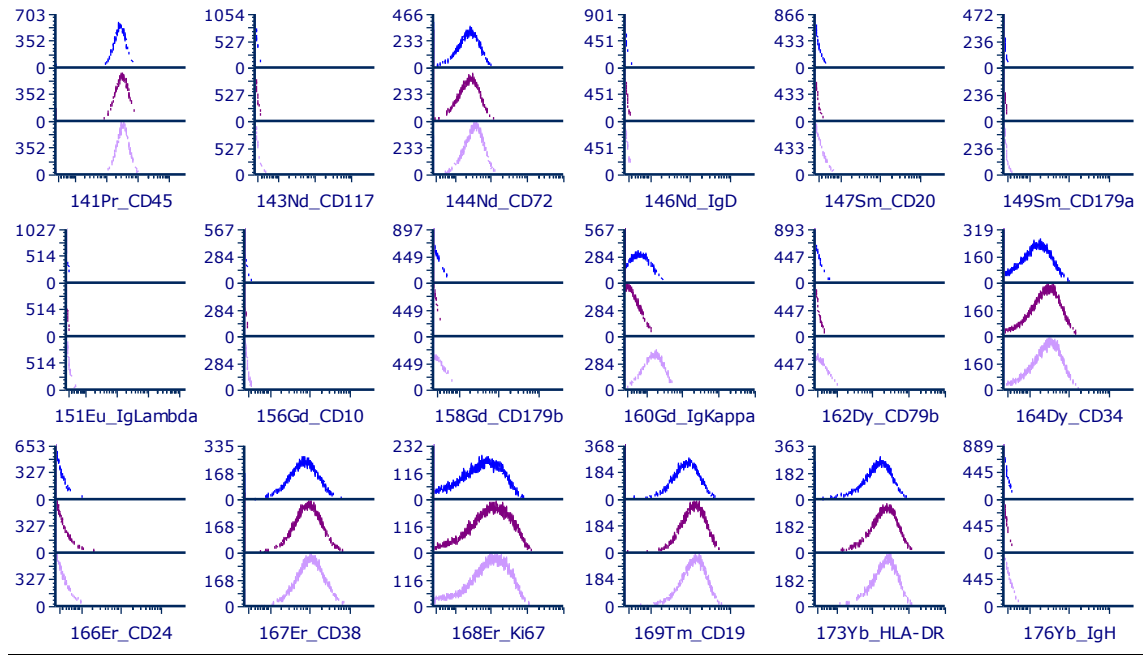
L196



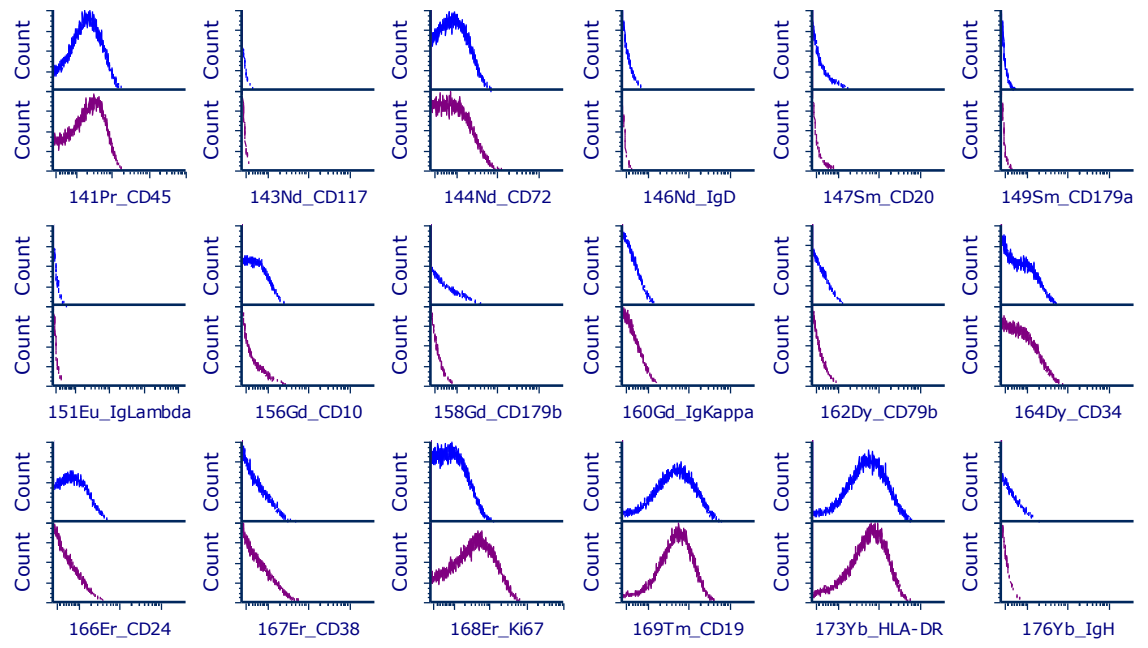
L578



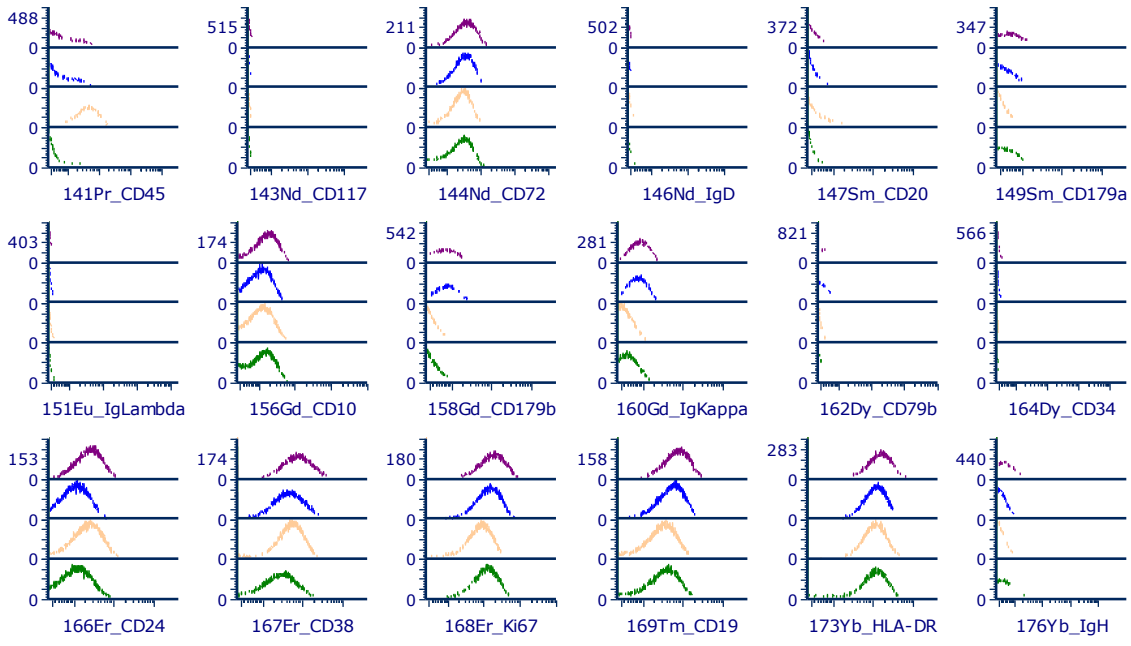
L779



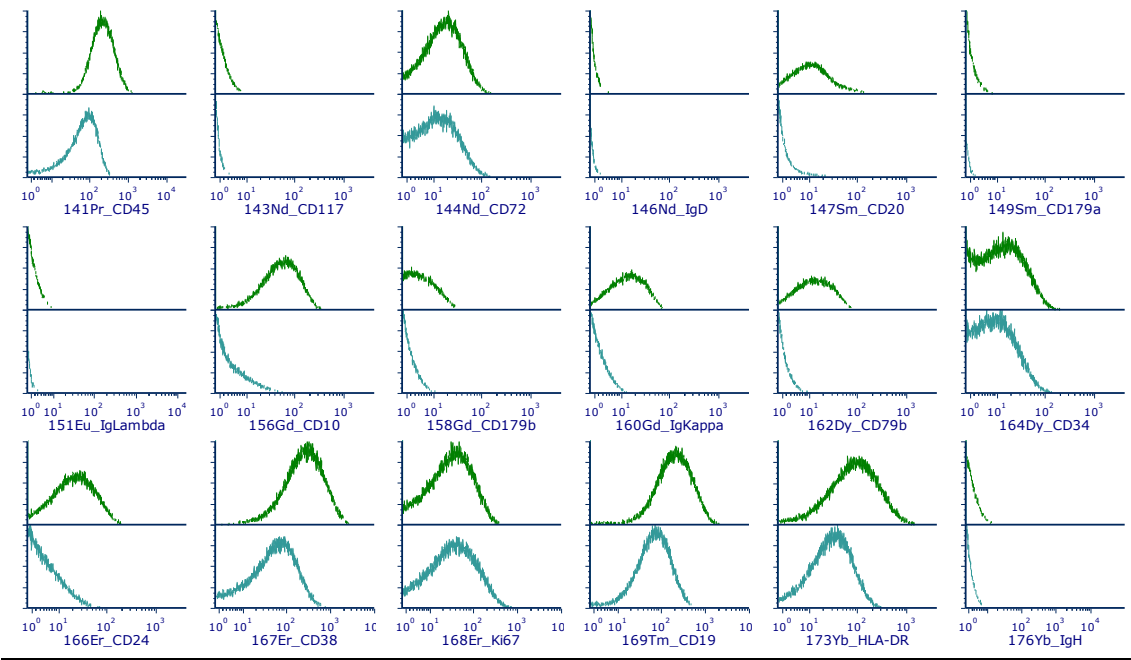
L824



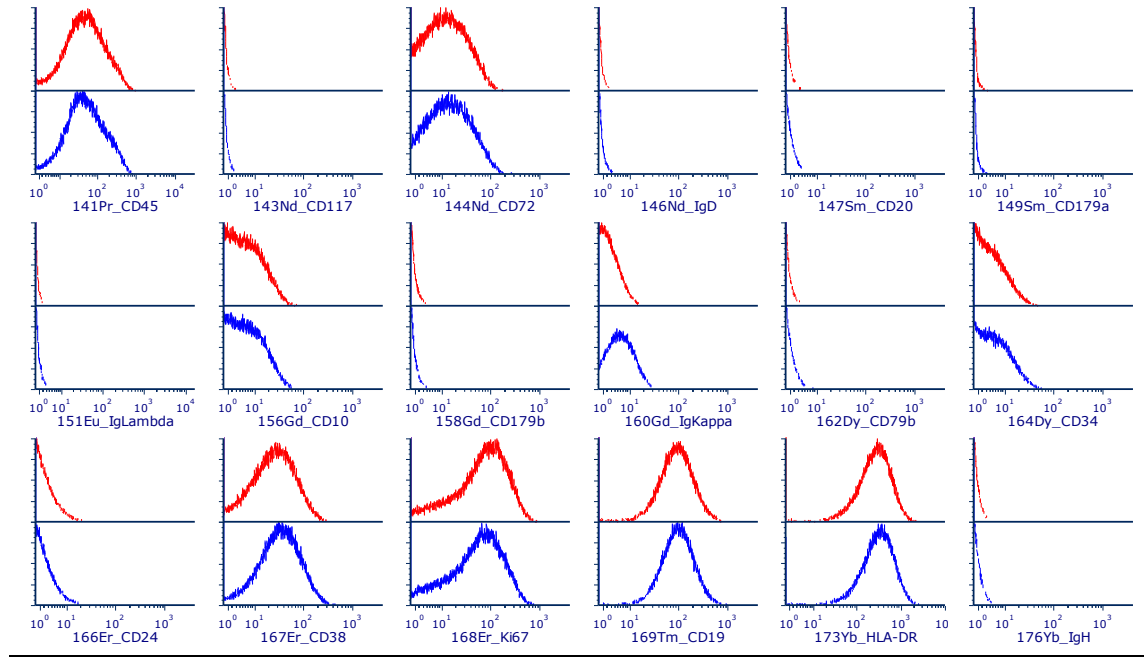
L825



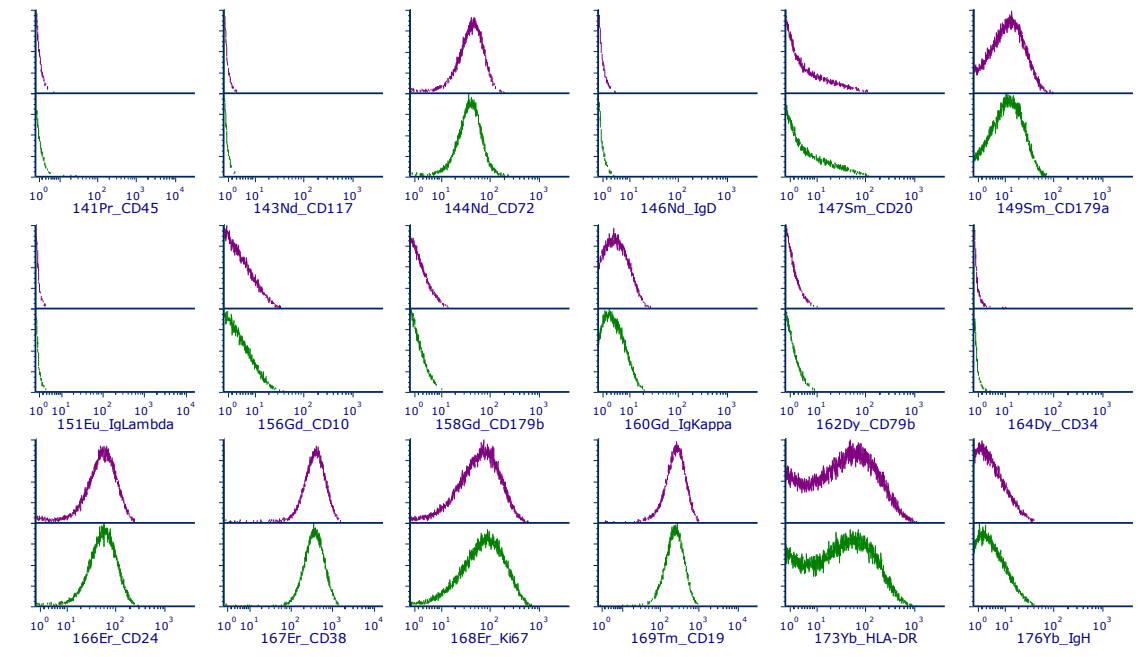
L829



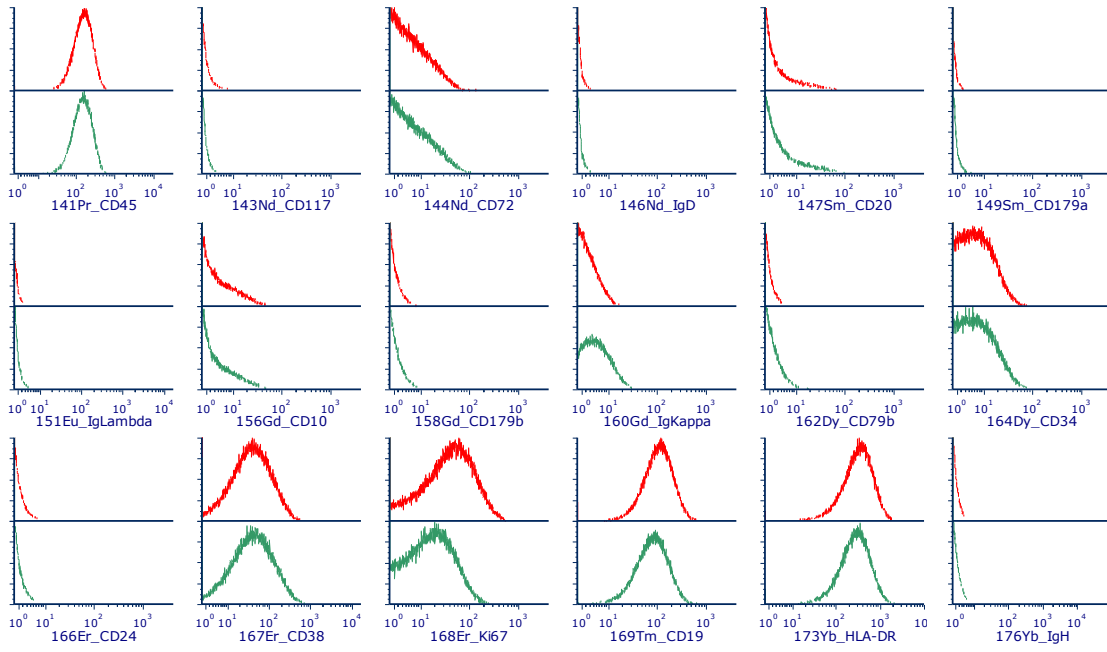
L879



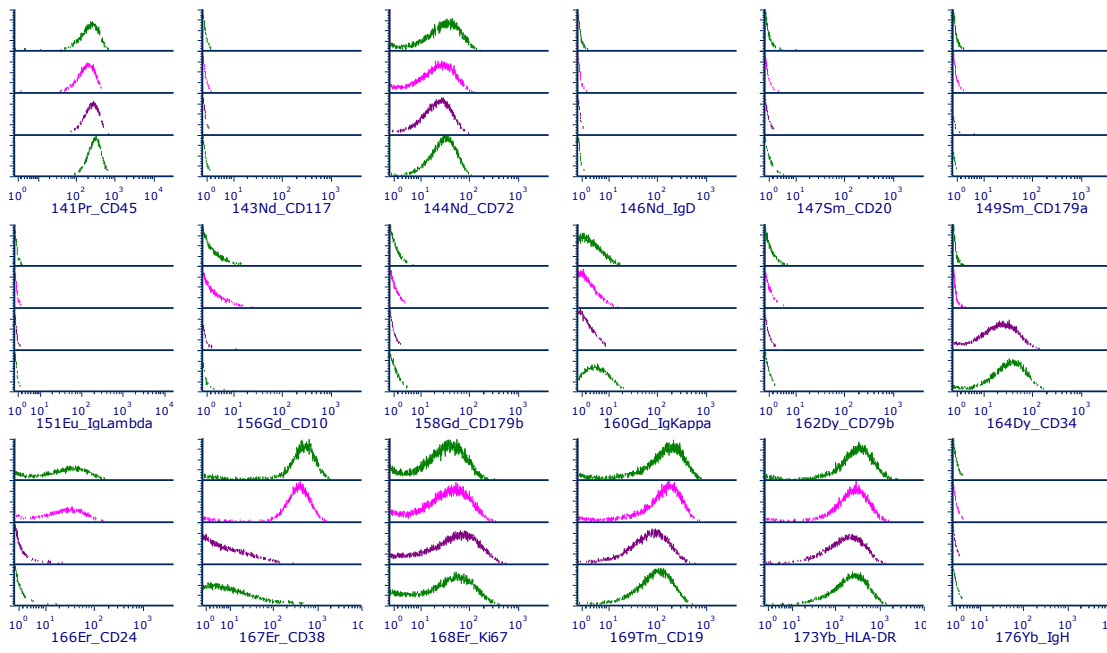
L910



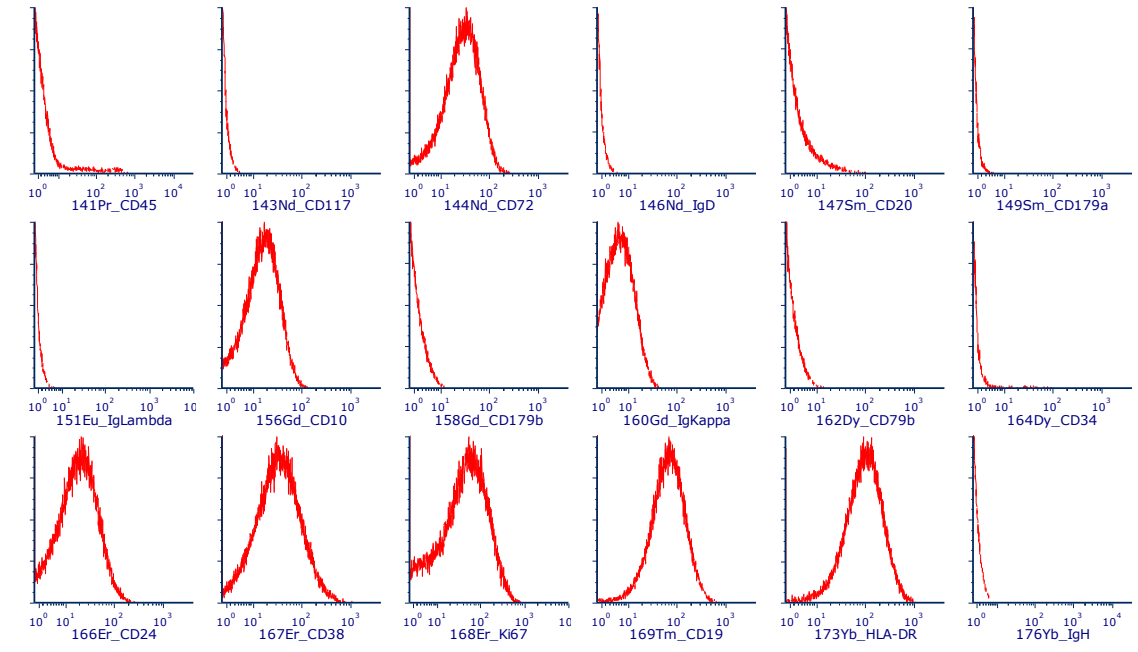
L914



L919



L920



L4951

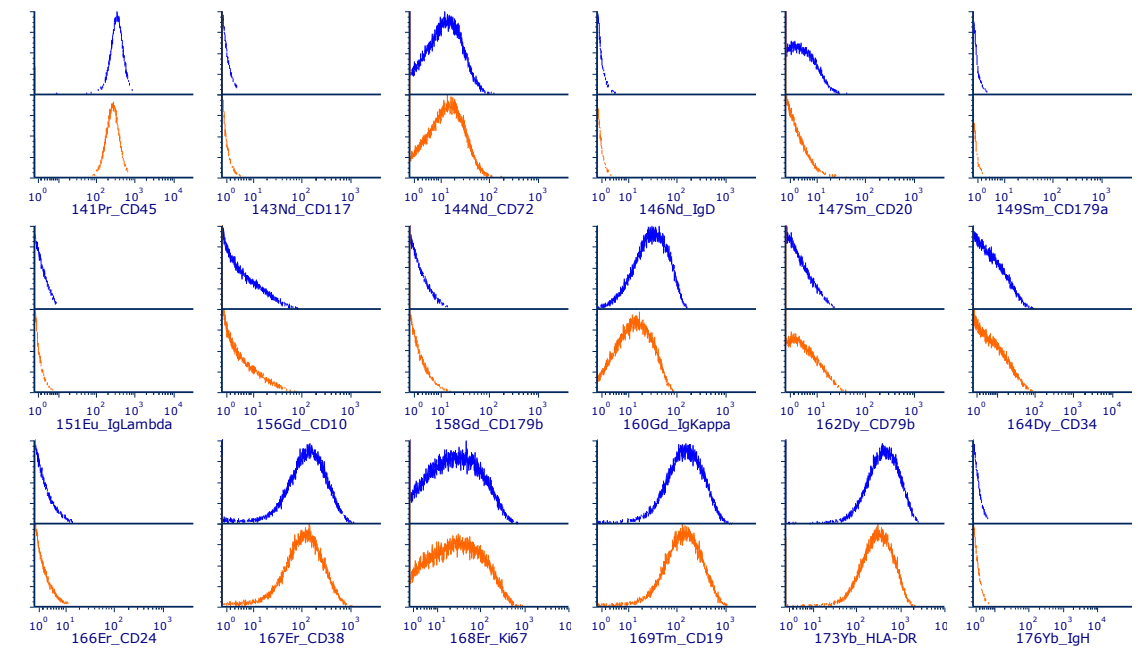


Figure F.3 Histograms of primagraft samples stained by the Wanderlust panel and acquired on the Helios mass cytometer.

Primagrafts are grouped by patient they were derived from. L919: top two panels of each histogram show primagraft samples created from first relapse and bottom two panels of each histogram show primagraft samples created from the second relapse. X axis: marker expression. Y axis: counts.

Appendix G. Conference abstracts

NCRI annual meeting 2014, Liverpool, UK - Poster Presentation

Development and validation of an analytical method for the quantitation of dexamethasone plasma concentrations in clinical samples obtained as part of the UKALL 2011 trial

Rosanna Jackson, Julie Errington, Philip Berry, Julie A.E. Irving, Gareth J. Veal

Background: Due to its ability to induce apoptosis in cells of lymphoid lineage, the corticosteroid dexamethasone plays a key role in the treatment of childhood acute lymphoblastic leukaemia (ALL). However, despite dexamethasone therapy being integral to the substantial improvements observed in prognosis of children diagnosed with ALL in recent decades, it also contributes to a wide range of side effects. Given its wide clinical use, surprisingly few studies investigating dexamethasone pharmacokinetics in children have been performed. A recently published study in childhood ALL found large inter and intra-patient variability in systemic exposure to dexamethasone (1). Investigating the relationships between pharmacokinetic variation, drug scheduling and clinical response/toxicity may facilitate continued improvement in ALL treatment.

Methods: Validation of a method to measure dexamethasone concentrations in human plasma samples was performed in accordance with GCP guidelines. Dexamethasone was extracted from plasma using methyl-t-butyl-ether and analysis performed on an API QTRAP LC/MS/MS using beclomethasone as an internal standard. Initial patient samples collected following dexamethasone treatment as part of the UKALL 2011 trial have been analysed.

Results: A quantitation limit of 1ng/ml was determined, allowing measurement of dexamethasone in clinical trial samples. The method demonstrated good linearity and reproducibility over the calibration curve range of 1-375ng/ml ($r^2 > 0.996$), with inter- and intra-assay precision CVs of 5.3% and 8.1%, respectively. Dexamethasone was shown to be stable in plasma for >12 months, allowing time for transport and analysis of patient samples collected at clinical centres across the UK. Preliminary patient data showed considerable variation in dexamethasone pharmacokinetics following treatment at doses of 6mg/m² and 10mg/m².

Conclusion: We have validated a reliable and accurate assay to enable the measurement of plasma dexamethasone concentrations in patients treated on the UKALL 2011 trial, facilitating the generation of data to guide future dosing of dexamethasone in childhood ALL.

References (1) Yang L, Panetta JC, Cai X, Yang W, Pei D, Cheng C, et al. Asparaginase may influence dexamethasone pharmacokinetics in acute lymphoblastic leukemia. *Journal of clinical oncology : official journal of the American Society of Clinical Oncology*. 2008 Apr 20;26(12):1932-9. PubMed PMID: 18421047.

AACR annual meeting 2016, New Orleans, US - Poster Presentation

Pharmacokinetics of standard versus short high-dose dexamethasone therapy in childhood acute lymphoblastic leukemia: results from the UKALL 2011 trial

Rosanna Jackson, Julie A.E. Irving, Gareth J. Veal

Dexamethasone (Dex) is a key component of ALL therapy, with glucocorticoid sensitivity strongly linked to prognosis. However, it also contributes to life threatening toxicities. The ongoing UKALL 2011 trial is investigating a new schedule of Dex (10mg/m² × 14 days vs 6mg/m² × 28 days), in an attempt to bring about a more rapid cytoreduction whilst limiting toxicities associated with long term steroid exposure. There are limited data regarding Dex pharmacokinetics, however large variability has been reported in children with ALL (Yang et al. 2008).

For Dex pharmacokinetic studies, blood samples were collected up to 8h post oral administration on one of the first and last three days of induction chemotherapy. Plasma Dex levels were analysed using a validated LC-MS method, with a range of 5-250ng/ml, and non-compartmental pharmacokinetic analysis was performed.

Pharmacokinetic parameters from day one sampling are shown below. Exposure, as defined by AUC_{0-12h}, and C_{max} were significantly higher on the short arm ($p = 0.0002$ and 0.0007 , respectively). However there was substantial overlap between the two arms, with a number of patients on the standard arm exhibiting higher exposures than those on short therapy, despite having a longer duration of treatment. This is reflected in the AUC_{0-12h} ranges observed on the two arms (short: 202-1606; standard: 38-1009 hr*ng/mL). Pharmacokinetic profiles also differed between the two days of treatment, with AUC_{0-12h} being significantly higher at the end of induction chemotherapy ($n = 37$, study day 1: 655 ± 322 ; study day 2: 894 ± 496 hr*ng/mL, $p = 0.003$).

Pharmacokinetic Parameters (mean ± SD)	Half-life (hr)	T _{max} (h)	C _{max} (h)	Clearance (l/h/m ²)	AUC _{0-12h} (hr*ng/ml)
Short (n=43)	3.96 ± 3.2	1.9 ± 1.0	128 ± 55	8.1 ± 5.3	692 ± 325
Standard (n=33)	3.68 ± 2.1	1.7 ± 1.1	87 ± 41	9.2 ± 12.7	443 ± 202

Based on these preliminary data it will be important to consider pharmacokinetic variability when analysing the results generated from the UKALL 2011 trial. Further evaluation of relationships between pharmacokinetic variation, dose scheduling and clinical outcome may enable better stratification of Dex therapy for future patients.

Children with Cancer UK annual meeting, London, UK - Poster Presentation

Pharmacokinetics of Standard versus Short High Dose Dexamethasone Therapy in Childhood Acute Lymphoblastic Leukaemia – Results from the UKALL 2011 Trial

Rosanna K Jackson, Julie AE Irving, Vaskar Saha, Gareth J Veal

Dexamethasone (Dex) is a key component of Acute Lymphoblastic Leukaemia (ALL) therapy, with glucocorticoid sensitivity strongly linked to prognosis. However, it is associated with significant toxicities. The ongoing UKALL 2011 trial is investigating a new schedule of Dex (10mg/m² x 14 days vs 6mg/m² x 28 days), in an attempt to bring about a more rapid cytoreduction whilst limiting toxicities associated with long term steroid exposure. The limited published data regarding Dex pharmacokinetics suggest substantial interpatient variability. Dex pharmacokinetics have also been shown to correlate with serum albumin concentration, which is thought to be due to asparaginase (ASNase) activity (Yang et al., 2008). The current study is therefore also aiming to investigate potential interactions between Dex and ASNase pharmacokinetics in children with ALL.

For Dex pharmacokinetic studies, blood samples were collected up to 8h post oral administration on one of the first and last three days of induction chemotherapy, allowing measurement of Dex pre- and post-ASNase exposure. Plasma Dex levels were analysed using a validated LC-MS method, with a range of 5-250ng/ml, and non-compartmental pharmacokinetic analysis was performed. ASNase levels are being measured at Manchester University by Vaskar Saha's laboratory.

Day one sampling Dex pharmacokinetic parameters are shown in the table below. Exposure, as defined by AUC_{0-12h} and C_{max}, were significantly higher on the short arm compared to the standard arm (p=0.0003 and 0.0006, respectively). However there was substantial overlap between the two arms, with a number of patients on the standard arm exhibiting higher exposures than those on short therapy, an important finding bearing in mind the different durations of treatment between the two arms. This is reflected in the AUC_{0-12h} ranges observed on the two arms (short: 202-1606; standard: 142-1009 hr*ng/mL). Pharmacokinetic profiles also differed significantly between the two days of treatment, with AUC_{0-12h} being significantly higher at the end of induction chemotherapy (n=28, p=0.0016). A decrease in clearance was also observed, alongside a drop in serum albumin concentration. This is a key indication that ASNase is affecting Dex pharmacokinetics.

	Half-life (hr)	Tmax (hr)	Cmax (ng/mL)	Clearance (L/hr/m ²)	AUC0-12h (hr*ng/mL)
Short (n=44)	3.0 (1.7-20.6)	1.5 (0.8-2.7)	122 (13-265)	8.1 (1.6-30.8)	564 (202-1606)
Standard (n=36)	3.0 (1.8-9.4)	1.1 (1.0-4.2)	89 (10-196)	6.6 (2.7-19.3)	408 (142-1009)

Comparison of pharmacokinetic parameters between short (10mg/m²) and standard (6mg/m²) groups. Data shown is median and range.

To date, high inter- and intra-patient variability in Dex pharmacokinetics has been observed. The UKALL 2011 trial is currently investigating the potential clinical benefit of a modified Dex dosing regimen. However, large inter-patient pharmacokinetic variability observed may mask any potential impact of the change in dosing regimen. Therefore, based on these preliminary data, it will be important to consider pharmacokinetic variability when analysing the results generated from the UKALL2011 trial. With more data generated, further elucidation of the relationship between drug scheduling, clinical response and toxicity may enable better stratification of Dex and ASPase in childhood ALL.

Childhood Leukaemia Research – UK (CLRUK) annual meeting 2016, oral presentation – Glasgow, UK

No abstract available.

AACR annual meeting 2017, Washington D.C., US - Poster Presentation

Personalization of dexamethasone in acute lymphoblastic leukemia

Rosanna K. Jackson, Ali Alhammer, Zach Dixon, Gareth J. Veal, Julie AE Irving

Synthetic glucocorticoids, such as dexamethasone (Dex), are pivotal in the treatment of childhood acute lymphoblastic leukemia (ALL) but are associated with significant variability, both in terms of toxicity and efficacy. We investigated three key variables to better understand how Dex personalization may be achieved: pharmacokinetics (PK), intracellular Dex accumulation, and cellular response, following Dex binding to the glucocorticoid receptor (GR).

For Dex PK studies, blood samples were collected post oral administration on one of the first three days of induction chemotherapy in 99 patients on the UKALL 2011. Plasma Dex levels were analysed using a validated LC/MS method, and a non-compartmental pharmacokinetic analysis. To assess intracellular Dex levels, cell lines, primagraft and primary patient samples were studied. The plasma Dex LC/MS method was optimized to quantify Dex in ALL cell lysates. Dex accumulation was also assessed using flow cytometric analysis of Dex-FITC. Dex sensitivity was assessed using Alamar Blue assays.

There was a wide Dex PK variability, with AUC_{0-12h} , and C_{max} significantly higher on the short compared to the standard arm; 564 (202-1606) versus 408 (142-1009), median (range), $p=0.0003$ and 0.0006 , respectively. However there was substantial overlap between the two arms, with a number of patients on the standard arm exhibiting higher exposures than those on short therapy.

Dex GI50 values ranged from 37 - > 1000 nM and 2 - > 1000 nM in cell lines and patient samples respectively. Western blotting indicated wildtype GR in all samples, with R3D11 and REH cell lines serving as hemizygous deleted and GR negative controls. Dex accumulation in cell lines was 2.1 and 1.8 (range 1.2 - 2.1) pmol/ 10^6 cells in PreB697 and Dex resistant sub-lines, respectively. While patient samples exhibited greater variability, Dex accumulation was not significantly different between sensitive and resistant cells; mean of 1.0 versus 1.4 (range 0.1-2.3, 0.4-4.4 pmol/ 10^6 cells, $p=0.17$). Flow cytometry Dex FITC accumulation confirmed these data, with a mean fluorescence intensity of 4.2 versus 4.1 (range 1.5-5.9, 2.0 - 9.1, respectively; $p=0.97$).

These data suggest that while PK and cellular response are hugely variable, variations in drug accumulation do not appear to play a key role in Dex response in ALL cells. Importantly, 62% of patient cell samples had Dex GI50 values greater than plasma concentrations observed in any patient, on both arms on the UKALL 2011 trial. A combined approach incorporating PK assessments and cellular response in ALL cells should be further investigated, to allow a comprehensive understanding of Dex pharmacology with a view to optimizing its clinical utility.

Appendix H. Publications

Jackson, R.K., Irving, J.A. and Veal, G.J. (2016) 'Personalization of dexamethasone therapy in childhood acute lymphoblastic leukaemia', *Br J Haematol*, 173(1), pp. 13-24.